EDO Principal Correspondence Control

FROM: DUE: / / EDO CONTROL: G20000280
DOC DT: 06/02/00
FINAL REPLY:

John F. Groth
Consolidated Edison Company
of New York, Inc.

TO:

Travers, EDO

FOR SIGNATURE OF : ** GRN ** CRC NO:

DESC:

2000 Refueling Outage Steam Generator Inspection Condition Monitoring and Operational Assessment Reports - Indian Point Unit 2

ROUTING:

(Ltr. Only):
Travers
Paperiello
Miraglia
Norry
Craig
Burns/Cyr
Miller, RI

DATE: 06/06/00

ASSIGNED TO: CONTACT:

NRR Collins

SPECIAL INSTRUCTIONS OR REMARKS:

Appropriate Action.

Template: SECY-017

E-RIDS: SECY-01

OFFICE OF THE SECRETARY
CORRESPONDENCE CONTROL TICKET

Date Printed: Jun 07, 2000 15:59

PAPER NUMBER:	LTR-00-0370	**LOGGING DATE:**	06/07/2000
ACTION OFFICE:	EDO		
AUTHOR:	JOHN GROTH		
AFFILIATION:	CENY		
ADDRESSEE:			
SUBJECT:	2000 REFUELING OUTAGE STEAM GENERATOR INSPECTION CONDITION MONITORING AND OPERATIONAL ASSESSMENT REPORTS - INDIAN PT.		
ACTION:	Appropriate		
DISTRIBUTION:	CHAIRMAN, COMRS, SECY/RAS		
LETTER DATE:	06/02/2000		
ACKNOWLEDGED	No		
SPECIAL HANDLING:			
NOTES:			
FILE LOCATION:	ADAMS		
DATE DUE:		**DATE SIGNED:**	

John F. Groth
Senior Vice President, Nuclear Operations

Consolidated Edison Company of New York, Inc.
Indian Point Station
Broadway & Bleakley Avenue, Buchanan, NY 10511
Telephone (914) 734-5713, Fax (914) 734-5718
E-mail: grothj@coned.com

June 2, 2000

Re: Indian Point Unit No. 2
Docket No. 50-247

Dr. William Travers
Executive Director for Operations
US Nuclear Regulatory Commission
Mail Stop O-16 E15
Washington, DC 20555-0001

Subject: 2000 Refueling Outage Steam Generator Inspection Condition Monitoring and Operational Assessment Reports

Dear Dr. Travers:

The enclosed "Condition Monitoring and Operational Assessment" reports pertaining to the steam generator inspections conducted at Indian Point Unit 2 during the 2000 refueling outage, are hereby submitted for your review. The reports consist of an executive summary, a specific report concerning Primary Water Stress Corrosion Cracking (PWSCC) in the U-bend, and a report discussing the remaining degradation mechanisms. Also included is a report that compares the corrosion performance of the Indian Point 2 steam generators to industry experience with Model 44 and Model 51 steam generators.

As the NRC staff is aware, and as referenced in our current submittal, in several instances certain limited follow-up and verification activities are continuing. Although it is unlikely that there would be any substantive changes to this submittal, we will promptly notify the NRC of related information as necessary to assure that the materials submitted to the NRC relating to the 2000 Refueling Outage examination of the IP-2 steam generators remains complete and accurate in all material respects.

As noted in the attached reports, Con Edison has concluded that continued operation of the installed steam generators will require more frequent inspection such that mid cycle outages will be needed. Additionally, as electric power production of the plant is currently limited by steam flow to the turbine with the throttle valves fully open, the increased number of tubes requiring plugging will result in a 3 to 4 percent output reduction. Con Edison has therefore concluded that the installed steam generators are nearing the end of economic life and that replacement will begin by the end of this year.

EDO --G20000280

Should you or your staff have any concerns regarding this matter, please contact Mr. John McCann, Manager, Nuclear Safety & Licensing.

Sincerely,

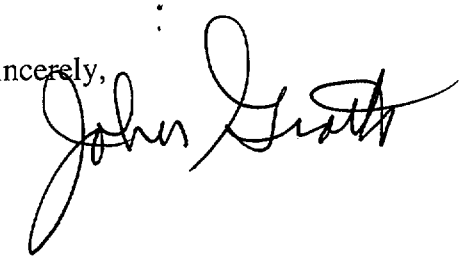

Enclosure

C: W/O Enclosure

Mr. Richard A. Meserve, Chairman
Office of the Chairman
US Nuclear Regulatory Commission
Mail Stop O16 C1
Washington, DC 20555

Greta Joy Dicus, Commissioner
Office of the Commissioners
US Nuclear Regulatory Commission
Mail Stop O16 C1
Washington, DC 20555

Mr. Nils J. Diaz, Commissioner
Office of the Commissioners
US Nuclear Regulatory Commission
Mail Stop O16 C1
Washington, DC 20555

Mr. Edward McGaffigan, Jr., Commissioner
Office of the Commissioners
US Nuclear Regulatory Commission
Mail Stop O16 C1
Washington, DC 20555

Mr. Jeffrey S. Merrifield, Commissioner
Office of the Commissioners
US Nuclear Regulatory Commission
Mail Stop O16 C1
Washington, DC 20555

With Enclosure

Mr. Samuel J. Collins, Director
Office of Nuclear Reactor Regulation
US Nuclear Regulatory Commission
Mail Stop O-5 E7
Washington, DC 20555

Mr. Hubert J. Miller
Regional Administrator-Region I
US Nuclear Regulatory Commission
475 Allendale Road
King of Prussia, PA 19406

Mr. Jefferey F. Harold, Project Manager
Project Directorate I-1
Division of Reactor Projects I/II
US Nuclear Regulatory Commission
Mail Stop 14B-2
Washington, DC 20555

Senior Resident Inspector
US Nuclear Regulatory Commission
PO Box 38
Buchanan, NY 10511

Document Control Desk
US Nuclear Regulatory Commission
Mail Station P1-137
Washington, DC 20555-0001

Mr. J. T. Rhodes
Chairman, President and Chief Executive Officer
Institute of Nuclear Power Operations
700 Galleria Parkway, SE, Ste. 100
Atlanta, GA 30339-5957

Ted Marston, Vice President
Nuclear Power Division
Electric Power Research Institute
3412 Hillview Avenue
Palo Alto, CA 94304

Mr. Ralph Beedle
Senior Vice President and Chief Nuclear Officer
Office of Nuclear Generation
Nuclear Energy Institute
Suite 400
1776 "I" Street, NW
Washington, DC 20006-3708

Executive Summary

May 31, 2000

Thomas C. Esselman, Ph.D.
President
ALTRAN Corporation

S. D. Rupprecht
Vice President, Engineering Services
Nuclear Services Business Unit
Westinghouse Electric Company, LLC

J. S. Baumstark
Vice President, Nuclear Engineering
Consolidated Edison Company of New York

Executive Summary

The attached two Condition Monitoring and Operational Assessment Reports (CMOA's) conclude that the Indian Point Unit 2 steam generators will meet all applicable safety requirements for operation during the next cycle of operation. The CMOA's have been conducted for the Indian Point 2 steam generators in accordance with guidelines developed by the Nuclear Energy Institute (NEI) and the Electric Power Research Institute (EPRI). The period of operation until another inspection is to be performed has been calculated in the CMOA's to be 1.0 EFPY (effective full power year) with the limiting degradation mode being primary water stress corrosion cracking (PWSCC) in the low row U-bends. However, the operating time to a mid-cycle point is 0.85 EFPY. Therefore, the recommended operating cycle to the next inspection has been shortened to 0.85 EFPY (310 EFPD).

The safety requirements referred to above are the criteria included in NEI-97-06, revision 1B. These performance criteria govern structural integrity and accident induced leakage performance. "Meeting the performance criteria provides reasonable assurance that the steam generator tubing remains capable of fulfilling its specific safety function of maintaining reactor coolant pressure boundary integrity." [1] The criteria are as follows:

- Structural Performance Criteria:

  A margin of 3.0 against burst under normal steady state full power operation and a margin of 1.4 against burst under the limiting design basis accident occurring with a safe shutdown earthquake. The limiting design basis accident for Indian Point 2 is a steam line break (SLB).

- Accident Induced Leakage Performance Criteria:

  Primary to secondary accident induced leakage for the limiting design basis accident shall not exceed the leakage rate used in the accident analysis in terms of total leakage rate and leakage rate for all steam generators. This is typically a leakage rate not to exceed 1 gpm per steam generator except for specific types of degradation where the tubes are confined and the NRC has approved an alternate repair criteria.

- Operational Leakage Performance Criteria:

  The operational primary to secondary leakage through one steam generator is normally limited to the more conservative of the values given in the plant's technical specification or the EPRI PWR Primary to Secondary Leakage Guidelines. For Indian Point 2 this is recommended to be 30 gpd. The EPRI guideline is 75 gpd.

[1] NEI-97-06, Rev. 1B, p.6

The CMOA's are organized into one for U-bend PWSCC, reference 1, and one for the other degradation mechanisms active in the Indian Point 2 steam generators, reference 2. Reference 2 specifically addresses degradation in the sludge pile region, tubesheet crevices, roll transition expansion zone, pitting and volumetric indications at the top of the tubesheet, wear at anti-vibration bars intersections, and wear due to foreign objects. In addition to the CMOA's, a document discussing the corrosion performance of the tubing in all Westinghouse manufactured Model 44 and 51 steam generators, reference 3, is attached. Reference 3 is provided to aid in placing the Indian Point 2 steam generators in a context with similar steam generators in the industry. The NDE program that was implemented is in conformance with the current industry guidelines. For critical areas of the steam generators such as the low row U-bends and the sludge pile region, the inspection exceeded industry guidelines by utilizing multiple inspection techniques and various independent reviews of the data to improve confidence in the results.

Based on a review of operating experience in the Model 44 and 51 steam generators (Reference 3), the degradation mechanisms active in the Indian Point Unit 2 steam generator tubes are similar to those which are occurring elsewhere in the industry. The comparison was made to the Model 44 and 51 steam generators because they were manufactured with tubing that is metallurgically similar to that at Indian Point 2, they have similar design features and they employed manufacturing methods of a similar vintage. The types of corrosion experienced in the Indian Point 2 steam generators are mainly axially oriented PWSCC and ODSCC in the tubesheet and sludge pile region, and pitting. The occurrence of Row 2 U-bend PWSCC, the cause of the leaker outage, is limited in number, which is consistent with industry experience. The possibility of a recurrence of PWSCC in row 2 has been eliminated since Indian Point 2 plugged all row 2 tubes this outage. No indications of PWSCC in the Row 3 U-bends have been detected at Indian Point 2 or elsewhere in Model 44 and 51 steam generators, and the incidence of ODSCC in the low row U-bends at other plants has been extremely limited. Degradation at tube support plate intersections at Indian Point 2 has been previously confirmed to be intergranular attack, and tubes with indications at this location were plugged this outage. Since the application of stricter plugging limits for dented tubes at support plate intersections and the implementation of more stringent chemistry control, the activity of denting has subsided to a very low level and no forced shutdowns due to steam generator leakage from dented tubes has occurred since 1988. The occurrence of free span degradation has also been limited (which is comparable to other steam generators of similar design).

In general, the current condition of the Indian Point Unit 2 steam generators compares favorably with all Model 44 and 51 steam generators. The Indian Point 2 steam generators have been in service for 16.8 EFPY. The longest length of service for a Model 44 steam generator prior to replacement was 18.9 EFPY and the next longest was 18.8 EFPY. Both of these plants replaced steam

generators as a result of the occurrence of SCC with a significantly greater number of tubes either plugged or repaired than are currently plugged due to SCC at Indian Point Unit 2. However, both of these plants operated at the higher temperatures of 601F and 597F, respectively. Converting the longest running plant to the operating temperature of Indian Point 2, 589F, this would be equivalent to an operating period of approximately 29.3 EFPY. It should be noted that Indian Point 2 currently operates at 589F but ran at the lower temperature of 574F in the early years of operation. This may account in part for the reason that Indian Point 2 Model 44 steam generators are the last Model 44 steam generators remaining in service.

The occurrence of SCC in the Indian Point Unit 2 steam generators has also been compared to industry experience with Model 51 steam generators. The occurrence of SCC at Indian Point is less than other Model 51steam generators remaining in service that have operated for a similar time period. Eleven plants with Model 51 steam generators have been replaced. For these plants, the longest length of service to replacement was 16.4 EFPY operating at 607F. The steam generators at this plant were just recently replaced. At the 589F operating temperature of Indian Point 2, this would be equivalent to approximately 31.7 EFPY. A total of 12 plants remain in service with Model 51 steam generators. Similar to Indian Point 2, each of these plants has added boric acid to the secondary side of the steam generators. Some have operated longer than Indian Point 2 and at higher temperature, which should provide leading indicators of the Indian Point 2 performance.

The most important element in maintaining steam generator tube integrity during plant operation is the performance of the steam generator tube inservice inspection (ISI) process and the associated reliability of the nondestructive examination (NDE) systems. Current recommendations relative to ISI effectiveness are based on conformance to EPRI Report NP-6201, Revision 5, "PWR Steam Generator Examination Guidelines". These guidelines provide reliable NDE strategies for the diversity of degradation types occurring in the field: to minimize the likelihood of forced outages due to tube leaks during each operating cycle; to ensure that established regulatory requirements are met relative to the maintenance of steam generator tube integrity; and to minimize unnecessary plugging and sleeving. The ISI strategies implemented during the current outage either met or exceeded current EPRI-Guidelines to detect the presence of tube degradation mechanisms. Several additional examinations with alternate techniques and additional independent reviews of the data were conducted to increase the confidence in the detection of structurally significant indications. Based on the inspection results obtained during the current outage, it is judged that the condition of the steam generator tube bundles at Indian Point 2 remains comparable to the 12 plant sites with Model 51 steam generators remaining in service

A three phased approach has been used to demonstrate the integrity of the tubes for the upcoming operating cycle. This consists of inspection conducted to detect and size degradation, in-situ pressure and leak testing to verify the NDE sizing of detected indications and to verify that the largest indications detected are not structurally significant, and structural analysis to determine that potential undetected and new indications will not grow to a size to challenge structural integrity before the next inspection. It should be noted that many more indications were in-situ pressure tested than required by the EPRI guidelines including tubes with no detectable degradation (NDD). Tubes that were in-situ tested, were pressure tested for their full length. This paper will review the methods used to justify structural integrity and provide a "roadmap" though the various attached reports, which provide the detailed justification for restart. The discussion is organized by the active degradation mechanisms detected during this outage.

Low Row U-Bends

Inspection Program

The low row U-bend inspection program (Section 3 of reference 1) was conducted in two phases. The first phase employed the normal +Point probe, which utilized the standard mid-range coil. This inspection discovered 3 tubes with indications in row 2 and no indications in row 3 or row 4. Interpretation of the mid-range coil inspection data was difficult due to the low signal to noise (S/N) ratio obtained during inspection of these low row tubes. To address this situation, inspection guidelines were revised on two occasions and the analysts were retrained to these revised guidelines. In addition, an independent team of analysts (tertiary review) reanalyzed all low row tubes. This tertiary review identified many tubes with low S/N ratio that made data difficult to interpret. Continuing difficulty in data interpretation due to a low S/N ratio led to the initial qualification and use of a new probe, the high frequency +Point, which significantly improved the S/N ratio in the low row U-bend tubes. The problem with the low S/N ratio was attributed to deposits on the tube outside surface. All row 2 and 3 tubes and those with a low S/N ratio in row 4 were re-inspected with this probe. Only 5 tubes were classified as having too low a S/N ratio with this probe and were plugged. This inspection identified a total of 4 new indications (3 in tubes with low S/N ratio and one in a restricted tube that could not be inspected with the mid-range plus point). No indications were detected in row 3 or row 4. Both the primary and secondary analysts detected all 7 indications identified in this inspection.

In-situ Testing Program

The in-situ testing program for the U-bends consisted of testing all tubes with indications, two row 2 tubes without any detectable degradation (NDD), and an

NDD tube in row 3, for a total of 10 tubes. All were tested full length. As discussed in Sections 3.5 and 8.2 of Reference 1, all tubes tested met the condition monitoring criteria. Five of the indications withstood the $3\Delta P_{NO}$ (3 times normal operating primary to secondary pressure differential) burst margin with no leakage, one indication exceeded the $3\Delta P_{NO}$ with a small leak rate starting at 4800 psi which is far above the steam line break limit, and one indication leaked at the steam line break pressure but at levels below the criteria and did not burst at the $3\Delta P_{NO}$ pressure. This tube, R2C71, in steam generator 24 met the EPRI criteria for in-situ testing.

Condition monitoring criteria was not met for the R2C5 tube, which ultimately leaked and led to the forced outage. Many of the tubes were tested to the capacity of the equipment, which is above the $3\Delta P_{NO}$ requirement. These tests were also used to verify the NDE sizing methods and to demonstrate additional structural integrity margin. The calculations performed to predict the in-situ test results utilizing the 400 kHz Profiles, correlated well with the actual test results supporting the reasonableness of the actual crack sizing (Sections 3.4, 3.5, and 6.1 of Reference 1). All sizing and indication profile determinations were performed by the same experienced senior analyst for consistency of the results. The testing of NDD tubes, the testing of tubes above the $3\Delta P_{NO}$ pressure requirement, and the calculations performed to predict the in-situ test results from the eddy current profiles, also gives confidence in the probability of detecting structurally significant flaws in these low row U-bends.

Analysis to Justify the Upcoming Operational Cycle

The operational assessment was based on independent analyses performed by Westinghouse, E-Mech Technologies, and Altran. The approach taken was to base the operational period on the indications discovered in row 2 and assume that they existed in row 3. This is a very conservative assumption since: no indications were detected in row 3 at Indian Point 2; no PWSCC has been detected in row 3 U-bends in Model 44 or 51 steam generators; and row 3 has a reduced sensitivity to PWSCC due to the lower residual stresses (larger bending radius, different bending process) and the reduced sensitivity to bending of the straight legs due to hourglassing of the TSPs. The row 2 tubes were taken out of service by plugging. In order to project an operating cycle it is necessary to show that all structurally significant degradation has been detected and that which may be undetected will not grow to be structurally significant during the next operating cycle. This relies on a probability of detection (POD) of these indications, projected growth rate, and NDE sizing.

The ability to size the U-bend flaws was accomplished by being able to calculate the performance of the R2C5 indication which leaked in service and the predicted performance of the 10 tubes which were in-situ tested based on the NDE profiles. Several methods were employed to determine POD as discussed in Section 5.3 of Reference 1. The first method was based on the smallest indications detected

by the 800 kHz probe. Another method compared this POD with other POD's for PWSCC that were developed for other regions of the generators at other plants. The comparison was made with the POD for PWSCC induced in tubes by denting at support plates and denting at eggcrate supports and the POD for low row U-bends determined from the EPRI NDE qualification primarily based on EDM notches. These different methods were expected to envelop the range of POD's anticipated for PWSCC. The POD for denting at eggcrate supports was found to envelop that for Indian Point 2 and was, therefore, used for the operational assessment. The probability of missing a structurally significant defect in row 3 was calculated to be very small (Section 5.3.3 of Reference 1). Hence, the basic approach of the operational assessment is very conservative.

The growth rates were determined from taking the indications discovered in 2000 by the high frequency probe and comparing the mid-range probe results from 1997 and 2000 as discussed in Section 5.4 of Reference 1. This is a valid technique since the high frequency probe with the higher S/N ratio was used for detection. Knowing that an indication is present, the analyst can usually find the indication at a prior cycle. The S/N ratio in some of the tubes was too low in the 1997 inspection to accurately determine a profile measurement. However, a total of 9 indications were able to be sized. Nine data points is not a very large statistical sample, so the ensuing growth rate distribution was enlarged to account for the small sample size in accordance with Bernard's median ranking.

The same "senior" analyst was used for all sizing for growth rates. He was not a production analyst and was not subjected to the same schedule of analyzing data as at the site. Another important point is that any growth rates that were used based on Indian Point 2 data were then compared to others in the industry as a confirmatory check and to show consistency. Unfortunately, there is no growth rate data for U-Bend PWSCC in the industry as indications were always plugged on detection and events of row 2 indications have been very infrequent. The approach used was to compare the Indian Point 2 growth rates to that for PWSCC, the same phenomenon, at other locations where large sample sizes of growth rates had been obtained. This was the dented support plate program for Westinghouse plants and the dented eggcrate program for CE plants where an accurate set of growth rate measurements for axial PWSCC was obtained.
When the growth rates from these programs are corrected to the Indian Point 2 operating temperature, it is seen that the conservatively developed Indian Point 2 U-bend growth rates exceeds that found for dented TSP intersections for depth and length growth. In part, this difference may be due to the small population of growth values for the U-bend data. Since the growth rates developed from the Indian Point 2 data for row 2 U-bends were slightly larger, these were used in the operational assessment. For a sensitivity evaluation, the growth rates were then increased by 25% with the result being that the tubes were found to meet the performance criteria at the end of the limited operating cycle.

All row 2 U-bends were plugged prior to the return to power for Cycle 15. As discussed in Section 7 and Attachment 1 of Reference 1, both the initiation rates and growth rates for row 3 U-bends would be expected to be smaller than for row 2 U-bends. Based on consideration of industry experience with low row U-bend cracking, stress analysis of the low row U-bends, and manufacturing considerations, the following conclusions can be drawn with regard to row 3 U-bend susceptibility to apex axial PWSCC at Indian Point 2:

1. No apex axial PWSCC has been observed in any row 3 U-bend in any Westinghouse model 44 or 51 steam generator to date.

2. Based on analyses of the total stresses in the U-bends including hourglassing effects, it is concluded that cracks are not expected to exist in row 3. The difference between the row 2 and row 3 tube stress levels shows that the time to crack initiation in row 3 would be at least approximately 2.5 times the time required for row 2 crack initiation. This is consistent with the fact that no indications were seen in row 3.

3. The time to initial observation of row 2 cracking at Indian Point 2 has been greater than for other operating plants, consistent with the lower operating temperature of Indian Point 2. The initiation of cracking in the row 2 U-bends as influenced by denting and hourglassing effects is compensated by the lower operating temperatures at Indian Point 2. A like relationship is expected to apply for potential row 3 cracking. Since none of the plants with mill annealed Alloy 600 tube have heat treated the row 3 and larger U-bends, plants operating at higher temperatures are lead indicator plants for potential row 3 cracking at Indian Point 2.

4. The effect of "hourglassing" of the support plates in raising the stress at the apex of the low row U-bends has already occurred as discussed in Attachment 1 to Reference 1. Minimal increase in the stress would result from small increases in the extent of hourglassing. As discussed in Appendix A of reference 2, the overall denting trend of the tubes has subsided in recent cycles.

5. Accelerated corrosion laboratory tests with prototypic U-bends in polythionic acid have shown that row 3 tubes did not crack in the time that row 2 U-bends cracked, confirming that the manufacturing process differences have significant influence on the cracking behavior of the low row U-bends.

6. Manufacturing differences (different bending processes) between the row 2 and row 3 tubes may result in residual stress states that may increase row 2 susceptibility to PWSCC while reducing the susceptibility of the row 3 tubes to cracking. Tests performed on a prototypic row 3 tube (Attachment 1 to Reference 1) indicate that the residual circumferential stress state at the inside diameter at the row 3 U-bend apex is compressive. This effect reduces the susceptibility of the row 3 U-bends to PWSCC.

The U-bend operational cycle length was calculated by two independent analyses, the reference single cycle axial profile (Section 9.3 of Reference 1) and the multi-cycle analysis method (Section 9.4 of reference 1). These results support Cycle 15 operation of 1.0 EFPY. However, the operating time to a mid-cycle point is 0.85 EFPY. Therefore, the recommended operating cycle until the next inspection is 0.85 EFPY (310 EFPD).

Acceptability of the 0.85 EFPY operating period is based upon:

- All row 2 tubes have been preventively plugged.
- No indications were found in row 3 tubes during the EOC-14 inspection with either the midrange or high frequency +Point probes. Based on historical operating experience for other Westinghouse model 44 and 51 steam generators, no row 3 indications have been found and no PWSCC would be expected in row 3 tubes at Indian Point 2 during Cycle 15.
- Independent Monte Carlo analysis techniques (reference single cycle analyses using crack profiles and independent multi-cycle analyses based upon crack initiation rates) support Cycle 15 operation in excess of 1.0 EFPY. The analyses support the recommended cycle length even if it would be assumed that all row 2 tubes were not preventively plugged (i.e., equivalent to assuming that the row 2 indications occurred in row 3).
- The reference cycle length analyses show that the $3\Delta P_{NO}$ = 4668 psi burst margin requirement for Cycle 15 is satisfied for a > 1.0 EFPY operating period between inspections. The projected limiting indication burst pressure is 4840 psi at 1.0 EFPY and 4937 psi at 0.85 EFPY. No SLB leakage is expected for cycle lengths in excess of one year. The projected SLB tube burst probability after 1.0 EFPY of operation is 3.2×10^{-3} compared to an acceptance guideline of 1.0×10^{-2}. Sensitivity analyses to growth, POD and NDE profile depths show that the limiting indication burst pressures do not change significantly when more conservative assumptions are made on these key parameters for cycle length evaluations. The 1.0 EFPY operating period is acceptable for a 25% increase in growth and the use of the more conservative 800 kHz +Point profiles rather than the 400 kHz profiles supported by benchmark analyses. The effect of POD uncertainty was addressed by looking at the effect of a 5% depth shift to improve the POD and a 5% depth shift to reduce the POD. This resulted in a limiting indication burst pressure increase of about 600 psi. and a burst pressure decrease of only about 345 psi., respectively.
- Independent analyses were performed with the multi-cycle methodology developed by E-Mech technologies using parameters conservatively benchmarked against EOC-14 inspection results for row 2. If it is conservatively assumed that one indication was detected in row 3 at the

EOC-14 inspection, the SLB burst probability is 2.2×10^{-3} and no leakage is predicted at SLB conditions even after 1.9 EFPY or full cycle operation. Under the very conservative assumption that row 2 tubes were not preventively plugged, the probability of burst at SLB conditions would be about 4.5×10^{-3} after 1.0 EFPY of operation and the probability of burst at $3\Delta P_{NO}$ is only 5.8×10^{-2}. These results are consistent with the Westinghouse reference single cycle axial profile analysis. Benchmarking of the multi-cycle analyses against the EOC-14 inspection results required a low crack initiation rate over multiple prior cycles. An adequate benchmarking could not be obtained for a high initiation rate that could have resulted in a large number of undetected indications at EOC-14.

As an additional defense in depth measure, the Indian Point 2 operating leak rate limit is being administratively set at 30 gpd to enhance the potential for detection of a large leaking flaw prior to the flaw growing to a structurally unacceptable size. Although the operating leakage at Indian Point 2 was only a few gpd prior to the R2C5 leakage event and this leakage level may not have been due to the R2C5 indication, the reduced leakage limit provides additional margin against an unexpected flaw. The set point alarm on the Nitrogen-16 radiation monitors will be adjusted to match the administrative limit.

A laboratory test program is being initiated to develop +Point POD and NDE sizing uncertainty information for axial PWSCC in rows 2 and 3 U-bends. Accelerated cracking will be performed on prototypically fabricated U-bends. Differences in the time to crack between row 2 and row 3 U-bends will be evaluated as a part of this test program. NDE data will be obtained with and without deposits simulating the noise levels found in the Indian Point 2 U-bends. "Blind" (without knowledge of destructive exam results) analyses of the NDE data by field analysts will be used to develop POD and NDE uncertainty distributions. It is expected that these tests will demonstrate POD and NDE uncertainty distributions less conservative than the values used in this operational assessment.

Sludge Pile

Inspection Program

The inspection program for the sludge pile region as discussed in Section 3 of Reference 2 involved an inspection of 100% of the tubes with the Cecco and bobbin probes, a re-inspection of tubes with the +Point probe, and a sample ultrasonic inspection. The Cecco-bobbin inspections were performed in the sludge pile region were part of the base program. The +Point expansion program was performed as a result of finding a tubesheet crevice indication following a retest after in-situ testing of an indication above the top of the tubesheet. This expansion program encompassed a 100% inspection of the hot

leg tubes in all four steam generators; 20% of the cold leg tubes in steam generators 21 and 22; and 40% of the cold leg tubes in steam generators 23 and 24. Twenty percent of the hot leg tubes were inspected from tube end hot to a height of 48" above the top of tubesheet and the remaining hot leg tubes were inspected from tube end hot to 24" above the top of tubesheet. The cold leg program was conducted from tube end cold to 24" above the top of tubesheet, with the exception of steam generator 23 where the upper extent was 48" for 20% of the tubes. This program identified a number of additional indications beyond those reported in the base scope sludge pile program. The inspections in the hot leg to a height of 48" were performed in the kidney region, an area where the sludge was judged to have the largest potential to affect eddy current results. Based on the absence of indications at heights ~10" above the top of tubesheet, the remaining tubes were inspected from tube end to 24" above the top of tubesheet.

Ultrasonic examinations were also conducted with the Westinghouse UTEC system on a sample of tubes in steam generator 22 to support the eddy current program in place during 2R14 for detection and disposition of axial ODSCC in the free span sludge pile regions. Ultrasonic inspections were selected because they are not affected by copper-bearing sludge in the same manner as eddy current inspections. Steam generator 22 was selected for this investigation because it had the largest number of single and multiple axial indications confirmed by +Point during the 2R13 inspection outage in 1997. A total of 39 tubes were examined: 16 were locally inspected where indications had been reported by Cecco-bobbin for which confirmation +Point testing had been performed, and 23 others (including 6 with known indications, the remainder with no reported degradation) were inspected from just above the 1st TSP to the top of the tubesheet. Three tubes that had been subjected to in-situ testing were also included in this sample.

The agreement between results from the eddy current program and the investigation by ultrasonic testing tends to validate the effectiveness of the eddy current protocol in place at Indian Point 2. Despite the observation that eddy current signal-to-noise ratios in the sludge pile region tend to vary according to the degree to which copper-bearing sludge and deposits are present, the inspections performed provide confidence that no structurally significant indications remain. This conclusion is supported by the following:

- Three independent eddy current test methods were applied
- The +Point expansion program identified five new axial indications above the top of the tubesheet, two others reported earlier were ultimately classified as deposits
- Analyst performance on axial indications in the sludge pile and crevice regions was on the order of 85% for primary analysts and 84% for secondary analysts which is above the industry standard.

- Results of the ultrasonic sample program correlate well with the eddy current results
- All OD axial indications (SAI and MAI) confirmed by +Point were confirmed by UTEC.
- No additional axial indications were found by ultrasonic inspection in areas where +Point did not confirm the Cecco and/or bobbin calls as OD axial degradation.
- Cecco and/or bobbin indications not confirmed by +Point were also reported as NDD by UTEC.
- There was general agreement between +Point and UTEC on volumetrics (VOL) and pits (PIT).

In-situ Testing Program

All sludge pile ODSCC indications detected during the EOC-14 inspection were in situ pressure tested. All pressure tests were conducted over the full tube length. Except for tube R34C51, none of the other sludge pile ODSCC flaws experienced either leakage or depressurization at steamline break pressure differential (2560 psi) or even at the maximum test pressure of 5173 psi which significantly exceeds the $3\Delta P_{NOP}$ structural margin requirement. Tube R34C51 met the $3\Delta P_{NO}$ burst margin requirement prior to experiencing significant leakage. Thus, since no sludge pile indication leaked at the $3\Delta P_{NO}$ margin requirement, all sludge pile indications met the structural margin requirement.

Satisfaction of condition monitoring requirements for pits and volumetric indications was demonstrated by in-situ testing of the bounding indications. None of the indications tested leaked at applied pressures equal to the $3\Delta P_{NO}$.

In situ test data were used to benchmark profiles and analysis methodology used for the tube integrity analyses. The results (Section 5.2 of reference 2) show that the deterministic and Monte-Carlo analysis methods used for tube structural integrity evaluations yield conservative results. The analysis correctly predicted R34C51 to be the limiting indication with even the nominal burst pressure (at nominal properties) at less than the pressure attained in the in situ test.

Analysis to Justify the Upcoming Operational Cycle

For Sludge Pile ODSCC, both the reference analyses and sensitivity analyses support Cycle 15 operation in excess of 1.0 EFPY (Section 6.1 of Reference 2). The reference analyses show that the $3\Delta P_{NO}$ = 4668 psi burst margin requirement for Cycle 15 is satisfied for an operating period approximately equal to the full cycle operation of 1.7 EFPY. The projected limiting indication burst pressure at 1.7 EFPY is only 6 psi below the 4668 psi acceptance limit and 5093 psi at 1.0 EFPY. No steam line break (SLB) leakage is expected for cycle

lengths in excess of one year. The projected SLB tube burst probability after 1.0 EFPY of operation is 3.5x10-4 compared to an acceptance guideline of 1.0x10-2. Sensitivity analyses to growth, POD and NDE uncertainties show that substantial margins would still exist in the limiting indication burst pressures after 1.0 EFPY operation.

The minimum acceptable cycle length for Pitting and Volumetric indications above the tubesheet is 436 EFPD, based on an assumed 40% through wall (TW) indication retained in service, and 95% confidence limit (CL) growth rate based on Indian Point 2 observed indications (Section 6.4 of Reference 2). Since all confirmed pits and volumetric indications were plugged, the assumption of a 40% TW indication retained in service is based on a conservative evaluation of the EPRI database which indicates a detection level of approximately 20%TW.

The POD was developed from Indian Point 2 specific data and from pulled tube data from plants with similar signal to noise ratios in their sludge pile tubes. This is detailed in Section 4.3 of reference 2. The Indian Point 2 specific POD was found to be consistent with that from the pulled tube database.

All crack-like indications detected in the hot leg +Point expansion program were identified in the zone from 3" above tube end hot. These indications were assessed in terms of analyst statistics for "hits" and "misses" by primary and secondary analysts. These data support an 85.7% success rate for the primary analysts and an 84.5% success rate for secondary analysts in the +Point expansion program. This results in a global POD for this expansion program of 97.8%.

Growth rate distributions for axial ODSCC in the sludge pile have been developed from +Point profile analyses for another plant with 7/8 inch diameter tubing as discussed in Section 4.5 of Reference 2. Consecutive +Point inspections are not available for Indian Point 2 to obtain growth distributions. However, an Indian Point 2 maximum depth growth distribution can be obtained from analyses of the bobbin coil indications. For indications confirmed by +Point in the 2000 inspection, the bobbin data were evaluated for maximum depth at the 2000, 1997 and 1995 inspections to obtain a database for maximum depth growth. Based on knowledge of the indication from the 2000 inspection, reevaluation of the 1997 and 1995 bobbin data indicated that signals representative of axial ODSCC could be observed for all flaws found by the bobbin coil in the 2000 inspection. These results support a conclusion that the growth period for these indications is greater than two full cycles of operation. For R34C51, the structurally most limiting indication found in the 2000 inspection, the presence of a 1.1 bobbin volt signal in 1995 suggests that the growth period for this indication extends at least over three operating cycles. From the bobbin data reevaluation, the bobbin voltage growth trends were obtained for 11 indications including R34C51. R34C51 had the largest voltage growth of about 1.5 volts from 1995 to 1997. Other than this growth, all indications show modest

growth in voltage with about equal growth over the two cycles. This review of the bobbin data shows that the flaws experienced in the sludge pile region do not initiate and grow to significant average depths and lengths in less than one cycle. The minimum estimated burst pressure for R34C51 is consistent with the trend from the pulled tubes. Since R34C51 had a 2.6 bobbin voltage at EOC-13 in 1997, the decrease in burst pressure is only about 400 psi over Cycle 14, again supporting modest growth.

The cumulative probability distribution, adjusted for the small population, of the Indian Point 2 average depth growth was compared with a sludge pile growth distribution obtained from +Point data from another plant and with a growth distribution obtained from bobbin analyses for free span ODSCC at another plant. The data from the other plants were corrected to the Indian Point 2 T_{hot} of 590 °F. The Indian Point 2 data show the smallest growth rates of the three plants, which is consistent with the above evaluation indicating that these indications have been present for about three cycles. The +Point based growth distribution for sludge pile indications shows the largest growth rates. Since these data bound the Indian Point 2 data, this distribution was conservatively applied for the evaluation of Indian Point 2 growth used in the sludge pile operational assessment contained in Section 6.1 of Reference 2. The average growth rate for the recommended growth distribution is 3.45%/EFPY compared to the 3.30%/EFPY for the Indian Point 2 data developed from bobbin measurements.

Tubesheet Crevice

Inspection Program

The inspection program for the tubesheet crevices was part of the program for the sludge pile cited above, i.e. inspection of 100% of the tubesheet crevices by Cecco-bobbin, and supplemented by +Point inspection. Approximately seventy-five tubes were identified among the 4 steam generators as exhibiting +Point axial indications of OD origin below the top of the hot leg tubesheet (TSH) and above the expansion zone roll transition (RT). Tubesheet crevice ODSCC is a phenomenon that has been observed in Westinghouse SGs since 1971, in SGs assembled with partial expansion of the tubes into the tubesheet bore. With respect to the tubesheet crevice, the Indian Point 2 steam generators are typical of all Model 44 steam generators.

Historically, the morphology of crevice ODSCC has been most strongly associated with plants operating on fresh water sites such as Point Beach, Robinson, and Ginna. Plants like Turkey Point and Indian Point, which use brackish cooling water, have experienced degradation associated mainly with acid chloride environments, like pitting and denting. Indian Point 2 was operated successfully for many years after denting was first observed, and pitting did not

reach the level where condition monitoring and operational assessment requirements would not be met. Thus for about 20 years there was essentially no reported incidence of ODSCC. This extended period of resistance ended during Cycle 12 or 13.

In-Situ Testing Program

Tubesheet crevice cracks cannot burst due to the restraint provided by the tubesheet; thus the potential condition monitoring concern is limited to leakage. The largest tubesheet crevice cracks were sized using profiling techniques to determine the need for in-situ testing according to the criteria for in-situ test selection. None of the cracks met the criteria that would have required in-situ testing. Nevertheless, six of the largest crevice cracks were in-situ tested at the SLB pressure differential (Section 5.2.2 of Reference 2). None of the cracks tested resulted in any leakage; thus, condition monitoring requirements are met for tubesheet crevice cracks. None of the 6 tubes with crevice ODSCC that were subjected to in-situ testing at SLB conditions exhibited leakage related to crevice indications during the testing, repeating the experience for the limiting 1997 crevice indication (3.64 +Point volts, 85% peak depth). Several of the tubes were also pressure tested at 5173 psi without leakage.

Analysis to Justify the Upcoming Operational Cycle

Tubesheet crevice indications are not subject to burst because of the restraint provided by the tubesheet. The potential for leakage was shown to be acceptable for the 2R15 operating interval by leak-free results returned from in-situ testing of the most severe crevice ODSCC indications. It is expected that no indications with unacceptable leakage potential at SLB conditions will exist during Cycle 15. Similar indications detected during the next scheduled eddy current inspection would also not be expected to leak at SLB conditions, particularly since the population of detected indications includes significantly smaller indications in 2000 than in 1997. As no changes are anticipated in operating temperatures at Indian Point 2 for Cycle 15 and the anticipated cycle length is less than the Cycle 14 length of 436 days, a more extensive crevice degradation condition is not anticipated. Therefore, it can be reasonably concluded, as discussed in Section 6.2 of Reference 2, that tubesheet crevice ODSCC would not be expected to be a source of significant primary to secondary leakage during a postulated SLB event. Thus, since tubesheet crevice ODSCC is not a burst potential and the leakage is expected to be negligible, the operational assessment requirements for tubesheet crevice ODSCC are satisfied for a cycle length of 436 EFPD.

Expansion Zone

Inspection Program

The inspection program consisted of a 100% inspection of all tubes with the Cecco-bobbin probe. Indications were then profiled with a combination bobbin/rotating pancake probe to determine if the crack tip is below the F* region. If re-rolling was employed to restore this tube to service, the combination bobbin/rotating pancake probe was used to re-inspect the tube after re-rolling.

In-situ testing Program

Expansion zone cracks cannot burst due to the restraint provided by the tubesheet; thus, only potential leakage of these cracks need be considered for condition monitoring as discussed in Section 5.2.3 of Reference 2. The reported cracks, both axial and circumferential, were found in the original hardroll region or below F*, licensed at Indian Point 2. An in-situ leak test performed in 1997 on a 0.56" long crack in the original hardroll resulted in no leakage. Pullout of tubes due to presumed circumferential separation of tubes is prevented by F* criteria since circumferential cracks were observed only below the F* length. Therefore, since tube rupture is not an issue, absence of leakage has been confirmed by in-situ testing (in 1997), and pull-out potential of the tubes is addressed by F*, condition monitoring requirements for expansion zone cracks were satisfied.

Analysis to Justify the Upcoming Operational Cycle

Expansion zone (EZ) cracks are constrained from rupture by the reinforcement provided by the tubesheet; thus operational concerns are limited to leakage from EZ cracks. Leakage from roll transition cracks is limited to small values due to the flow restriction provided by the tubesheet crevice. Expansion zone cracks are repaired according to the criteria of F* licensed for Indian Point 2. Tubes failing to meet the F* criteria are plugged. The potential leakage anticipated from expansion zone SCC under SLB conditions is acceptable based on the provisions of F* and the leak-free result for the worst case crack tested in 2R13 as discussed in Section 6.2 of Reference 2.

Wear at Anti-Vibration Bars, Wear due to Loose Parts, and Potential Indications at TSP Intersections

Inspection Program

Wear at anti-vibration bars (AVB's), wear due to loose parts, and potential indications at TSP intersections were inspected by the 100% Cecco-bobbin inspection program. Any wear indications were then profiled by a +Point probe. TSP's, which were not fully inspected by the Cecco probe due to restrictions,

were inspected by a smaller +Point probe. Cecco indications at the TSP's were also inspected by the +Point probe and were plugged even if not confirmed by +Point.

Condition Monitoring

Observed indications of AVB wear meet condition monitoring requirements as discussed in Section 5.2.5 of Reference 2. The maximum indication found was 38% TW (SG-24, tube R35/C42-AVB3). When the NDE sizing uncertainties of 14.6% (95% CL) are added, the resulting 52.6% TW degradation is well below the structural limit of 71%.

No tubes with foreign object wear were found with significant wear depth. For loose parts wear analyses, a conservative structural limit of 60% TW was assumed, although the structural limit for uniform thinning is greater than 80% TW. Sizing of wear resulting from loose parts utilizes the same technique as AVB wear sizing; thus, the sizing uncertainties are the same as for AVB wear, that is 14.6% (95% CL). No tubes are projected to exceed the structural limit during the next operating cycle when sizing uncertainties are included. Thus, condition monitoring requirements are satisfied. A single tube, R30C13, SG 22 , with observable growth from 2R13 to 2R14 was plugged. Neighboring tubes that had not previously been plugged were also plugged to provide a buffer zone against potential wear propagation in the unlikely event that the tube should sever due to the continuing wear. The wear of this tube was judged to be active based on a <20% TW signal in 2000 and zero reported depth in 1997 (See Section 5.2.6 of Reference 2).

No ID or OD cracks were identified at dented TSPs; i.e., none of the Cecco-5 "SPI" indications were confirmed as flaws by +Point examination. All tubes with "SPI" indications were administratively plugged.

Operational Assessment

The acceptable cycle length for AVB wear is 925 EFPD (2.53 years, assuming 100% availability). This is based on a 38% TW maximum indication retained in service, NDE uncertainties for the qualified NDE technique (ETSS #96004), and 95%CL growth rates based on the Indian Point 2 reported AVB wear as discussed in Section 6.5 of Reference 2.

Known foreign objects residing in the SGs were evaluated for the potential to wear a tube beyond the acceptable limit (60% TW), assuming that these objects are located at the worst case location for wear against the tubes (i.e., high cross flow region). The data from the 2000 inspection confirmed that there were no star pieces missing from the TSPs. A star is a portion of the TSP that is linked by the thinnest ligaments around a flow hole. A minimum acceptable operating cycle length of 2 years was confirmed for the known foreign objects. Therefore,

operational assessment requirements are satisfied for known loose parts as discussed in Section 6.6 of Reference 2.

Tubes with possible loose part (PLP) indications were examined for historical growth rates. Only one tube was found to have potentially excessive growth of the wear. This tube was plugged, and its neighboring tubes were plugged to provide a buffer zone around the tube to eliminate the potential for propagation in the extremely unlikely event that the tube should sever due to continuing wear. It was judged that this conservative action will provide a minimum of one full cycle of operation. It is anticipated that the Indian Point 2 steam generators will be replaced at the next outage. Therefore, operational assessment requirements are satisfied for tubes with PLP indications.

References

1. SG-00-05-008, Indian Point 2 U-bend PWSCC Cycle 14 Condition Monitoring and Cycle 15 Operational Assessment, dated May 2000.

2. SG-00-05-010, Indian Point 2 Cycle 14 Condition Monitoring Assessment and Cycle 15 Operational Assessment for degradation Mechanisms Other than U-bend PWSCC, dated May 2000.

3. Attachment to NSD-RLE-00-165, Model 44 and 51 Steam Generator Tube Corrosion Performance Comparison to Indian Point 2, dated May 2000

Indian Point Unit 2 (IP2)

Cycle 14 Condition Monitoring Assessment and Cycle 15 Operational Assessment for Degradation Mechanisms Other than U-bend PWSCC

May 30, 2000

Prepared By

Westinghouse Electric Company LLC

Indian Point Unit 2

Cycle 14 Condition Monitoring Assessment and Cycle 15 Operational Assessment for Degradation Mechanisms Other than U-bend PWSCC

May 2000

Authors

D.D. Malinowski
Consultant

H.O.Lagally
Fellow Engineer

T.A.Pitterle
Consulting Engineer

D. Adamonis
Manager, SG NDE Applications

W.K. Cullen
Principal Engineer

S.Orbon
Fellow Engineer

A.Sagar
Consultant,NDE

Verification

This document has been independently reviewed and verified by personnel competent in the preparation of Condition Monitoring and Operational Assessments. Verifiers may also be authors; however, in no case was work authored and verified by the same person; thus, independence of the verification was maintained. The review was performed to assure inputs to the assessments were correctly selected, and that assessment outputs are reasonable compared to the inputs. The reviews also assured that appropriate assessment methods were used, that the inputs to the assessments were correctly used in the assessments, and that necessary assumptions are adequately described, are reasonable and are identified.

Verifier: V. Srinivas
Principal Engineer

Verified sections 1.0 , 2.0 and all subsections, 3.0 and all subsections, 5.1 and all subsections, 5.3 and all subsections, 5.2.4 through 5.2.7 and all subsections, 6.2 through 6.7 and all subsections .

Verifier: H.O. Lagally
Fellow Engineer

Verified sections 4.0 and all subsections, 5.2 and all subsections, and 6.1 and all subsections.

Approved: W.B. Middlebrooks
Manager, Steam Generator Design and Analysis

Indian Point Unit 2

Cycle 14 Condition Monitoring Assessment and Cycle 15 Operational Assessment for Degradation Mechanisms Other than U-bend PWSCC

Table of Contents

Section			Page
1.0	Introduction		1
2.0	Summary and Conclusions		1
2.1	Inspections		1
2.2	EC Database		2
2.3	Analysis Methods		2
2.4	Condition Monitoring		2
2.5	Operational Assessment		3
2.6	Open Issues		5
3.0	Inspections		6
3.1	Summary		6
3.2	Expansion of Sludge Pile and Tubesheet Inspections		7
	3.2.1	Hot Leg RPC Program	7
	3.2.2	Cold Leg RPC Program	8
	3.2.3	Results	9
3.3	UTEC Inspections		10
	3.3.1	Inspection Program Phase 1	11
	3.3.2	Inspection Program Phase 2	11
	3.3.3	Conclusions	12
3.4	Other Inspections		12
3.5	Identified Steam Generator Degradation Modes		15
	3.5.1	2R14 Degradation Findings	15
	3.5.2	Tubes Plugged Due to Various Degradation Modes	16
4.0	Inputs for Integrity Analysis		19
4.1	Operating Parameters		19
4.2	Structural and Leakage Requirements		19
4.3	Probability of Detection for Sludge Pile Indications		20
4.4	Sizing Methods and Uncertainties for Sludge Pile Indications		22
4.5	Growth Rates for Sludge Pile Indications		32
4.6	Sludge Pile Tube Integrity Analysis Methods		34

5.0 Condition Monitoring 43
5.1 In-situ Testing Recommendations 43
5.1.1 IP-2 In-situ Testing Screening for Axial Cracks 43
5.1.2 IP-2 In-situ Testing Screening for Circumferential Cracks 45
5.1.3 IP-2 In-situ Testing Screening for Non-crack Indications 45
5.1.4 Summary of Tests Performed and Results 46
5.2 Cycle 14 Condition Monitoring Assessment 60
5.2.1 Sludge Pile Cracking 60
5.2.2 Tubesheet Crevice 67
5.2.3 PWSCC in the Roll Expansion Region 70
5.2.4 TTS Pitting/Volumetric 72
5.2.5 AVB Related Wear 80
5.2.6 Foreign Objects 80
5.2.7 Condition Monitoring Conclusions 80
6.0 Operational Assessment 85
6.1 Sludge Pile/Free Span Cracking 85
6.1.1 Reference Analysis 85
6.1.2 Sensitivity Analysis 85
6.1.3 Operational Assessment Conclusions 85
6.2 Operational Assessment Evaluations for Tubesheet Crevice 90
6.3 Axial and Circumferential PWSCC/ODSCC in Expansion Zone – Roll Transition Zone 91
6.4 TTS Pitting/Volumetric Indications 92
6.5 AVB Wear 93
6.6 Foreign Objects 95
6.7 Operational Assessment Conclusions 97
7.0 Glossary of Abbreviations 98
8.0 References 100

Appendix A – Secondary Side Condition Monitoring and Operational Assessment A-1
Appendix B – Verification of Eddy Current Database B-1

1.0 Introduction

This report provides the condition monitoring and operational assessment (CMOA) for the Indian Point (IP2) Steam Generator (SG) tube indications found, except for the axial Primary Water Stress Corrosion Cracking (PWSCC) U-bends of low row tubes, during the March/April 2000 inspection. A SG leak in the U-bend of SG 24 tube R2C5 led to a forced outage in February 2000 with a subsequent SG inspection and end of cycle (EOC-14) refueling outage. The CMOA for the axial PWSCC U-bends of low row tubes is provided in a separate report (Reference 1).

The condition monitoring assessment evaluates the structural and leakage integrity of the tubes at the time of the inspection, and thus reflects EOC-14 conditions. The operational assessment is performed to determine an acceptable plant operating period up to the next SG inspection, and thus reflects a look-ahead evaluation. The principal objective of this report is to establish an operating period such that burst margin and accident condition requirements would be satisfied at the end of the operating period. The tube integrity analysis methods applied in this report are established techniques used in prior alternate repair criteria (ARC) analyses and/or operational assessments. Input data for the analyses are developed from IP2 data and supplemented by data from other evaluations.

Section 2 provides the summary and conclusions of this report. The inspections performed and the results of the inspection are discussed in Section 3. The tube integrity analysis methods and essential inputs are described in Section 4. The Condition Monitoring Assessment, including the results of in-situ tests performed are provided in Section 5. The operational assessment to determine an acceptable Cycle 15 operating period to the next SG inspection is provided in Section 6.

2.0 Summary and Conclusions

2.1 Inspections

The planned eddy current inspection program for IP2 was based principally on the use of the Cecco/bobbin probe for the tubesheet region and the tube straight legs. A bobbin probe was planned for the row 4 to 11 U-bends, and a Cecco/bobbin probe (with the bobbin as the active probe) for U-bends beyond Row 11; a midrange frequency +Point probe was planned for the row 2 and row 3 U-bends.

The leakage from R2C5 resulted in adding application of the mid-range frequency +Point in the row 4 U-bends to the program base scope. A further expansion of the U-bend inspection utilized a high frequency +Point probe in all active row 2 and row 3 tubes and row 4 tubes with bad mid-range +Point data (BDA) to provide inspection detail beyond that provided by the mid-range +Point probe. Specific details of the base and expanded program scope are included in Table 3.1-1. The details of the U-bend inspections are contained in Reference 1.

As a result of finding a tubesheet crevice indication following a retest after in-situ testing of an indication above the top of the tubesheet, the sludge pile and crevice region inspection program was further expanded to include mid-range +Point examination of 100% of the hot leg tubes. In addition, 20% of the cold leg tubes were inspected with the +Point probe in all 4 SGs. In SGs 23 and 24, the cold leg sample was expanded to 40% due to finding pit indications exceeding the projected condition monitoring repair limit (28% through wall (TW) – Section 5.2.4). The 28% repair limit was

determined from a structural limit of 85% TW, based on a uniform thinning model, minus the NDE sizing uncertainty applicable to pits (32%TW, maximum), minus the growth rate for pits based on 2R14 IP2 data.

Ultrasonic examinations (UTEC) were conducted in SG-22 to show that copper bearing sludge deposits were not masking the EC signal, since UTEC is not affected by such deposits. Thirty-nine tubes were examined. The results of the ultrasonic inspections were consistent with those of the Cecco/bobbin and +Point confirmation eddy current program. Based on this UTEC inspection, additional assurance is provided that an acceptable EC inspection was performed.

2.2 Eddy Current Database

The certification of the eddy current database utilized for this CMOA is contained in Appendix B. The files noted on the certification are the files from which the summary EC data contained in this CMOA were compiled.

2.3 Analysis Methods

The analysis methods utilized for the sludge pile degradation tube integrity analysis are the same as utilized in Reference 1, IP2 U-bend Operational Assessment. Documentation of these methods is contained in Westinghouse WCAP-15128, Revision 2. The methods utilize a Monte Carlo technique and inputs for Probability of Detection (POD), Non Destructive Examination (NDE) uncertainties and growth rates to predict the limiting indication burst pressure at the end of the operating cycle. The Westinghouse burst correlations applied for burst pressure analysis and the ligament-tearing model (developed by Argonne National Laboratories - ANL) is applied for leakage analysis.

2.4 Condition Monitoring

Condition monitoring assessments were completed for all identified degradation mechanisms. The condition monitoring evaluation for U-bend PWSCC is detailed in reference 1. Specific conclusions for all other identified degradation mechanisms are provided below:

- All sludge pile Outside Diameter Stress Corrosion Cracking (ODSCC) indications detected during the EOC-14 inspection were in- situ pressure tested. Except tube R34C51, none of the other sludge pile ODSCC flaws experienced either leakage or depressurization at steamline break (SLB) pressure differential (2560 psi at operating conditions, 2782 psi corrected to room temperature conditions) or even at the maximum test pressure of 5173 psi which significantly exceeds $3\Delta P_{NOP}$, (3 times normal operating primary to secondary SG differential pressure) which is the structural margin requirement. Tube R34C51 met the $3\Delta P_{NO}$ burst margin requirement prior to experiencing significant leakage. Thus, since no sludge pile indication leaked at the $3\Delta P_{NO}$ margin requirement, all sludge pile indications met the structural margin requirement.

- Tubesheet crevice cracks cannot burst due to the restraint provided by the tubesheet; thus the potential condition monitoring concern is limited to leakage. The largest tubesheet crevice cracks were sized using profiling techniques to determine the need for in-situ testing according to the

criteria for in-situ test selection (Section 5.1). None of the cracks met the criteria that would have required in-situ testing. Nevertheless, three of the largest crevice cracks were in-situ tested at the SLB pressure differential. None of the cracks tested resulted in any leakage; thus, condition-monitoring requirements are met for tubesheet crevice cracks.

- Expansion zone (EZ) cracks cannot burst due to the restraint provided by the tubesheet; thus, only potential leakage of these cracks need be considered for condition monitoring. The reported cracks, both axial and circumferential, were found in the original hardroll region or below F*, Alternate Repair Criteria (ARC) licensed at IP2. None of the EZ cracks detected in 2000 required in-situ testing . An in-situ leak test performed in 1997 on a 0.56" long crack in the original hardroll resulted in no leakage. No operational leakage issues due to EZ cracks were encountered during Cycle 14; therefore, it is concluded that condition-monitoring requirements are met.

- Pullout of tubes due to presumed circumferential separation of tubes is prevented by application of the F* criteria since circumferential cracks were observed only below the F* length. Therefore, since tube rupture is not an issue, absence of leakage has been confirmed by in-situ testing in 1997, and pull-out potential of the tubes is addressed by F*, condition monitoring requirements for expansion zone cracks are satisfied.

- Satisfaction of condition monitoring requirements for pits and volumetric indications was demonstrated by in-situ testing of the bounding indications. None of the indications tested leaked at applied pressures equal to the $3\Delta P_{NO}$.

- Observed indications of Anti-vibration Bar (AVB) wear meet condition monitoring requirements. The maximum indication found was 38% TW (SG-24, tube R35/C42-AV3). When the NDE sizing uncertainties of 14.6% (95% Confidence Level (CL)) are added, the resulting 52.6%TW degradation is well below the structural limit of 71%.

- No tubes with foreign object wear were found that exhibited excessive wear depth. A single tube, R30C13, SG-22 , with observable growth from 2R13 to 2R14 was plugged, along with its neighboring tubes that had not previously been plugged, to provide a buffer zone against potential wear propagation in the unlikely event that the tube should sever due to the continuing wear. Based on the observed wear depths plus the sizing uncertainties, no tubes exceeded the structural limit; thus condition monitoring requirements are satisfied for wear resulting from loose parts.
- No ID or OD cracks were identified at dented TSPs; i.e., none of the Cecco-5 "SPI" indications were confirmed as flaws by +Point examination. All tubes with "SPI" indications were administratively plugged.

2.5 Operational Assessment

Operational assessments were completed for all identified degradation mechanisms. The operational assessment for U-bend PWSCC is detailed in reference 1. A recommended operational cycle of 0.85 Effective Full Power Years (EFPY) is identified for U-bend PWSCC; thus, this represents the minimum cycle length objective for all other degradation mechanisms. Specific conclusions for all other identified degradation mechanisms are provided below:

- For Sludge Pile ODSCC, the operational assessment analyses show that the $3\Delta P_{NO}$ = 4668 psi burst margin requirement for Cycle 15 is satisfied for an operating period of 1 EFPY. The total freespan burst probabilities, that include contributions of both U-bend PWSCC indications and sludge pile ODSCC indications, at 90/50 are 3.22×10^{-3} and 6.58×10^{-2}, respectively, at ΔP_{SLB} and $3\Delta P_{NO}$, and they are below their respective acceptance guideline values (0.04 at ΔP_{SLB} and 0.08 at $3\Delta P_{NO}$. The projected limiting indication burst pressure at 1.7 EFPY is only 6 psi below the 4668 psi acceptance limit. No SLB leakage is expected for cycle lengths in excess of one year.

- Sensitivity analyses for Sludge Pile ODSCC support Cycle 15 operation in excess of 1.0 EFPY. Sensitivity analyses to growth, POD and NDE uncertainties show that substantial margins would still exist in the limiting indication burst pressures after 1.0 EFPY operation.

- Tubesheet crevice indications are not subject to burst because of the restraint provided by the tubesheet. The 2R14 inspection results from the CECCO probe are approximately the same as they were from the 2R13 results. The expanded inspection using the +Point probe identified additional indications that were smaller than those identified by the CECCO probe. All tubes with crevice indications were plugged. The potential for leakage was shown to be acceptable for the 2R15 operating interval by leak-free results returned from in-situ testing of the most severe crevice ODSCC indications. The operating temperature and primary to secondary pressure differentials are essentially the same for cycle 15 as they were for cycle 14. Since there is no potential for burst, and in-situ testing and cycle 14 performance show that no indications with unacceptable leakage potential at SLB conditions will exist during Cycle 15, the operational assessment requirements are met for a full operating cycle of at least 1.48 EFPY.

- Expansion zone (EZ) cracks are constrained from rupture by the reinforcement provided by the tubesheet; thus, operational concerns are limited to leakage from EZ cracks. Leakage from roll transition cracks is limited to small values due to the flow restriction provided by the tubesheet crevice. Expansion zone cracks are repaired according to the criteria of F* licensed for IP2. Tubes failing to meet the F* criteria are plugged. The potential leakage anticipated from expansion zone PWSCC under SLB conditions is acceptable based the absence of indications above the bottom of the roll transition that required leak testing and the leak-free result for the worst-case crack tested in 2R13.

- The minimum acceptable cycle length for Pitting and Volumetric indications above the tubesheet is 1.4 EFPY, based on an assumed 40% TW indication retained in service. The database for ETSS #96005 indicates a detection level of approximately 20%TW. The 95% CL growth rate for pits is 32%/ 1.2 EFPY based on IP2 observed indications. No NDE uncertainty applies since all detected pits were plugged. The structural limit for pits , 85% TW, was calculated based on a uniform thinning assumption. Thus, operation for a cycle of at least 2.1 EFPY is justified.

- The acceptable cycle length for AVB wear is 3.1 EFPY. This is based on a 38% TW maximum indication retained in service, NDE uncertainties for the qualified NDE technique (ETSS #96004), and 95%CL growth rates based on the IP2 reported AVB wear.

- Known foreign objects residing in the SGs were evaluated for the potential to wear a tube beyond a lower bound structural limit of 60% TW. Analyses of wear due to foreign objects assume that these objects are located at the worst case location for wear against the tubes (i.e., high cross flow region). The data from the 2000 inspection confirmed that there were no star pieces missing from the Tube Support Plates (TSPs). A minimum acceptable operating cycle length of 1.2 EFPY was confirmed for the known foreign objects. Therefore, operational assessment requirements for a cycle length of at least 2.48 EFPY are satisfied for known loose parts.

- Tubes with possible loose part (PLP) indications were examined for historical growth rates; only one tube was found to have active growth of the wear. R30C13, SG-22 , with observable growth (from 2R13 to 2R14) of wear resulting from impingement of a foreign object was plugged, along with its neighboring tubes that had not previously been plugged to provide a buffer zone against potential wear propagation in the unlikely event that the tube should sever due to the continuing wear. The wear of this tube was judged to be active based on a <20% TW signal in 2000 and zero reported depth in 1997 (See Section 5.2.6). Stabilization of tube R30C13 was judged not to be required for the next operating cycle due to the plugging of the surrounding tubes. No tubes are projected to exceed the structural limit during the next operating cycle. Thus, operational requirements for tubes with PLP indications are satisfied for the next operating cycle.

2.6 Open Items

As of the date of issue, the following open items exist .

a) Appendix A makes reference to a Degradation Assessment that is not finalized as of the date of this report.
b) A computer code utilized for these analyses, AUTOAXPROFILE, is a modification of a code documented in WCAP-15218 to increase the flexibility of on input data compared to the original code. Although the changes to the coded have been checked, final configuration control and documentation are in process at the time of this report.
c) Computer spreadsheets were utilized in the preparation of some of the supporting data in this report, which have not been completely verified. These spreadsheets were used for the following information:
    a. Development of Figures 5.1-1 and 5.1-2
    b. Development of Figures 4.3-1 and 4.3-2
    c. Development of Figures 4.5-4, 4.5-5 and 4.5-6

    Verification is in process.

3.0 Inspections

3.1 Summary

The IP 2 primary side steam generator inspection plan for the 2R14 outage was developed in accordance with Section 3 of the EPRI PWR Steam Generator NDE Guidelines.

Inspection requirements were selected based on identification of forms of degradation considered active or having the potential to occur in the IP2 steam generators. During the course of the inspection program, additional testing was deemed necessary to achieve better data quality for the U-bend examination program and to verify results from inspections in the sludge pile.

Table 3.1 provides the details for the base scope and additional scope for the IP 2 steam generator inspection program.

Table 3.1 -Eddy Current Test Program RFO 14 - Base Scope vs. Actual

Location	Base Scope RFO14		Additional Scope RFO14
	Detection	Disposition	Detection and Disposition
U-bend R2-3	+Point MR		+Point HF
U-bend R4	+Point MR		+Point HF on +Point MR BDA
U-bend R5 to R11	Bobbin		
U-bend > R11	(Cecco-)Bobbin		
AVB	(Cecco-)Bobbin		
TSP Pass ≥ .640	Cecco-Bobbin		
TSP Pass < .640	+Point MR DIP	+Point MR DIP	
Dent Gage .610	Bobbin		
Free Span	(Cecco-)Bobbin	+Point MR	
Free Span Sludge Pile	Cecco-Bobbin	+Point MR	
TE to TTS+24	--		+Point MR
Top of TS	Cecco(-Bobbin)		+Point MR
TS Crevice	Cecco(-Bobbin)	+Point MR	+Point MR
Re-Roll F*	Cecco-Bobbin, Combo	Combo, Bobbin	+Point MR/Combo
Roll Transition	Cecco-Bobbin Combo	Combo, Bobbin	+Point MR/Combo
Tube End	Cecco-Bobbin	Cecco	+Point MR

Note: Probe designation in parentheses indicates that the probe module on a combination probe was either inactive or un-qualified for the application.

3.2 Expansion of Sludge Pile and Tubesheet Inspections

During "post-in-situ" eddy current inspections of R34C51 in steam generator 22, an axial indication was detected in the crevice region which had not been reported during the Cecco/bobbin inspection program After considering several options, including reanalysis of the Cecco data, the IP2 steam generator inspection program was expanded to include a +Point program to provide a complementary inspection of the sludge pile and tubesheet crevice regions. The program consisted of two elements, one for the SG hot legs and one for the cold legs.

3.2.1 Hot Leg RPC Program

A +Point RPC inspection program was performed in the hot leg sludge pile region of all four steam generators. The logic for the +Point inspection program, based on Revision 5 of the EPRI PWR Steam Generator NDE Guidelines, was as follows:

1. A sample of 20% of the tubes in steam generators 21, 22, 23 and 24 was inspected from tube end hot (TEH) to just below the first hot leg support plate (TSP1), a distance of approximately 48" above the top of tubesheet. This sample was concentrated in the sludge pile "kidney region".

2. Results from this 20% sample were analyzed to establish the maximum elevation above the tubesheet at which axial indications were found, identify the height of the sludge pile, and define the upper boundary for +Point inspections of the remaining tubes in each steam generator. The highest axial indication reported in the four steam generators was 12.89" above the top of tubesheet. The mean sludge pile height using data concentrated in the steam generator kidney regions fell into a range from 3.8" to 6.2".

3. To add conservatism to the program the inspection height for the remaining tubes was defined as 20" plus a 20% buffer, or 24" above the top of tubesheet.

4. The remaining 80% of the hot leg tubes in all steam generators were examined from TEH to a height of 24" above the top of tubesheet.

5. The need for expansion of the hot leg inspection program was based on paragraphs 3.5 and 3.6 of Revision 5 of the EPRI PWR Steam Generator NDE Guidelines.

    - If less than 5% of the total tubes inspected are degraded, with none defective, a C-1 condition exists

    - If between 5% and 10% of the total tubes inspected are degraded, or one or more tubes, but not more than 1% of the total tubes inspected are defective, a C-2 condition exists

    - If more than 10% of the total tubes inspected are degraded or more than 1% of the inspected tubes are defective, a C-3 condition exists

- For cracks:

  In the event crack indications were found in the upper 4" of the inspection zone, the upper extent of the inspection zone would be extended to a distance just below the first hot leg support plate for 100% of the tubes in that steam generator.

- For non-cracks:

  In the event non-crack indications, classified as defective (exceeding the plugging limit of 28% through-wall as measured by bobbin), were found in the upper 4" of the inspection zone the upper extent of the inspection zone would be extended to a height equal the original height plus 20% for all tubes in that steam generator.

3.2.2 Cold Leg RPC Program

A +Point RPC inspection program was performed in the cold leg region of all four steam generators. The logic for the +Point inspection program, based on Revision 5 of the EPRI PWR Steam Generator NDE Guidelines, was as follows:

1. A random sample of 20% of the tubes in steam generator 23 was inspected from tube end cold (TEC) to just below the first cold leg support plate (TSP1) and analyzed to establish the maximum elevation above the tubesheet at which indications were found and to identify the height of the sludge pile. This sample focused on the "kidney region" and fell into the same range as that found in the hot leg RPC program. No evidence of ODSCC was identified, however there were some "pit-like" indications with maximum elevation of 7.62" above the top of the cold leg tubesheet.

2. The remaining three steam generators; 21, 22 and 24 were inspected to a height of 24" above the top of tubesheet. A 20% sample of SGs 21 and 22 CL tubes were inspected, and a 40% sample of the tubes in SGs 23 and 24 was inspected.

3. Expansion of the cold leg inspection program was based on paragraphs 3.5 and 3.6 of Revision 5 of the EPRI PWR Steam Generator NDE Guidelines, identical to the expansion criteria for the hot leg program.

   - For cracks:

     If crack indications were found in the cold leg of a given steam generator, expand the inspection sample from 20% to 100% of that steam generator cold leg.

   - For non-cracks:

     In the event non-crack indications, classified as defective (exceeding the plugging limit of 28% through-wall as measured by bobbin), were found within the zone bounded by 20" above the top of tubesheet, expand the inspection sample from 20% to 40% of the tubes in that steam generator.

In the event non-crack indications, classified as defective (exceeding the plugging limit of 28% through-wall as measured by bobbin), were found in the upper 4" of the inspection zone, 1) the upper extent of the inspection zone would be extended to a height equal the original height plus 20% and 2) expand the inspection sample from 20% to 40% of the tubes in that steam generator.

3.2.3 Results

Steam Generator 21 Hot Leg

The steam generator 21 hot leg RPC program involved +Point inspection of 603 tubes from tube end hot (TEH) to just below the first hot leg support plate (TSP 1H), a distance of approximately 48" above the top of tubesheet. Examinations of the remaining 2344 tubes were conducted from tube end hot (TEH) to a distance of 24" above the top of tubesheet. One indication of ODSCC and 13 pit-like indications were identified, none requiring expansion of the inspection program.

Steam Generator 21 Cold Leg

The steam generator 21 cold leg RPC program involved +Point inspection of 589 tubes from tube end cold (TEC) to a distance of 24" above the top of tubesheet. No evidence of cracking was identified in this sample. Eleven new pits were identified, none requiring an expansion of the program.

Steam Generator 22 Hot Leg

The steam generator 22 hot leg RPC program involved +Point inspection of 619 tubes from tube end hot (TEH) to just below the first hot leg support plate (TSP 1H), or to a distance of approximately 48" above the top of tubesheet. Examinations of the remaining 2235 tubes were conducted from tube end hot (TEH) to a distance of 24" above the top of tubesheet. Four new ODSCC indications and 77 pit-like indications were identified, none requiring expansion of the inspection program.

Steam Generator 22 Cold Leg

The steam generator 22 cold leg RPC program involved +Point inspection of 571 tubes from tube end cold (TEC) to a distance of 24" above the top of tubesheet. No evidence of cracking was identified in this sample. Eight new pits were identified none requiring expansion of the program.

Steam Generator 23 Hot Leg

The steam generator 23 hot leg RPC program involved +Point inspection of 620 tubes from tube end hot (TEH) to just below the first hot leg support plate (TSP 1H), or to a distance of approximately 48" above the top of tubesheet. Examinations of the remaining 2339 tubes were conducted from tube end hot (TEH) to a distance of 24" above the top of tubesheet. One new ODSCC indication and 20 pit-like indications were identified, none requiring expansion of the inspection program.

Steam Generator 23 Cold Leg

The steam generator 23 cold leg RPC program involved +Point inspection of 592 tubes from tube end cold (TEC) to just below the first cold leg support plate (TSP 1C), or to a distance of approximately 48" above the top of tubesheet. No evidence of ODSCC was identified in this sample. However, six new pits were identified. One of the pits had a depth in excess of the plugging limit of 28%, thus it was necessary to expand the program. The expansion program involved inspection of an additional sample of 591 cold leg tubes from TEC to a distance of 24" above the top of the tubesheet. Eighteen pit-like indications were identified in the expanded program, none requiring further expansion.

Steam Generator 24 Hot Leg

The steam generator 24 hot leg RPC program involved +Point inspection of 626 tubes from tube end hot (TEH) to just below the first hot leg support plate (TSP 1H), or to a distance of approximately 48" above the top of tubesheet. Examinations of the remaining 2271 tubes were conducted from tube end hot (TEH) to a distance of 24" above the top of tubesheet. One new ODSCC indication and 2 pit-like indications were identified, none requiring expansion of the inspection program.

Steam Generator 24 Cold Leg

The steam generator 24 cold leg RPC program involved +Point inspection of 581 tubes from tube end cold (TEC) to a distance of approximately 24" above the top of tubesheet. No evidence of cracking was identified in this sample. However, two new pits were identified. One of the pits had a depth in excess of the plugging limit of 28%, thus it was necessary to expand the program. The expansion program involved inspection of an additional sample of 581 cold leg tubes from TEC to a distance of approximately 24" above the top of the tubesheet. Fifteen pit-like indications were identified in the expanded program, none requiring further expansion.

3.3 UTEC Inspections

Ultrasonic examinations were conducted with the Westinghouse UTEC system on a sample of tubes in IP 2 steam generator 22 to support the eddy current program in place during 2R14 for detection and disposition of axial ODSCC in the freespan sludge pile regions. Ultrasonic inspection was selected because it is not affected by copper-bearing sludge.

The system was calibrated and examinations performed by qualified personnel in accordance with Westinghouse Nuclear Services Division Field Service Procedure STD-FP-1995-7281, Rev. 3, "Generic UTEC Inspection With ROSA III Delivery".

The ultrasonic testing program was conducted in two phases. The first phase involved inspection of localized areas of sixteen tubes in the hot leg where Cecco and/or bobbin eddy current examinations had identified indications and where +Point examinations were used for confirmation. The second phase of the ultrasonic testing program involved inspections of twenty-three tubes, some containing known eddy current indications and others with no reported eddy current signals. The UTEC

examinations during the second phase were performed from just above the first support plate to the top of tubesheet on the hot leg side. Three tubes subject to full-length in-situ pressure testing were included in this population.

Steam generator 22 was identified for this investigation because it had 3 axial indications confirmed by +Point, the most in any of the steam generators

3.3.1 Inspection Program Phase 1

Cecco and/or bobbin indications reported in the 2R14, 2000 sludge pile inspection program for steam generator 22 were identified as candidates for the first UTEC investigation. Twenty-two tubes containing Cecco and/or bobbin sludge pile indications fell into this category. Of that total, axial indications (MAIs and SAIs) were confirmed with +Point in 3 tubes. The objective of this inspection was to confirm the adequacy of the +Point coil for confirmation in the presence of deposits and that the CECCO probe was conservatively overcalling indications.

Six of the tubes in the original population of 22 were peripheral tubes, or otherwise not accessible to the UTEC end effector. Sixteen tubes were accessible for the ultrasonic examination program, including the 3 tubes with axial indications confirmed by +Point.

Scan lengths were 4.5" for each area. For top of tubesheet scans, the extents were generally from 3.0" above the top of tubesheet to 1.5" below the top of tubesheet. For the elevated scans, the 4.5" scan distance was generally centered about the eddy current indication location.

Results for the Cecco, +Point and ultrasonic inspections (UTEC) are summarized in Table 3.3-1. In instances where the bobbin probe originally identified the indication and a re-review of Cecco data revealed a Cecco call, the Cecco result is listed.

Consistent with the results of the eddy current program, UTEC identified axial ODSCC in three tubes, and there was general agreement regarding pits and volumetric indications and tubes with no detectable degradation. The UTEC data were used for information only; UTEC was not the probe of record that was used for determining tube plugging requirements.

3.3.2 Inspection Program Phase 2

Twenty-three tubes in steam generator 22 were identified as candidates for the second UT investigation. All twenty-three tubes were examined from one inch above the first hot leg support plate to one inch below the top of tubesheet, with the exception of R3C24. Denting of R3C24 at support plate 1 limited the start position of the UTEC probe to a point slightly below the first support plate elevation.

Of the population of twenty-three tubes, seven had indications confirmed with +Point and sixteen had no detectable degradation. Three of the twenty-three tubes had been subject to full-length in-situ pressure testing prior to these ultrasonic tests. The three tubes inspected after pressure testing included R3C24, R33C51 and R35C51.

Results for the +Point and ultrasonic inspections (UTEC) are summarized in Table 3.3-2. Consistent with the +Point confirmation results, seven of the twenty-three tubes inspected showed reportable indications with the UTEC probe. Four tubes had multiple axial indications, two tubes had indications typical of pitting and one tube showed evidence of thinning and/or wear. The remaining sixteen tubes were identified as no detectable degradation (NDD).

3.3.3 Inspection Program Conclusions

Results of the ultrasonic investigation are consistent with those of the eddy current program where Cecco and bobbin probes are used for detection in the sludge pile region. All indications reported by Cecco and or bobbin were examined using the rotating +Point probe. Cecco and/or bobbin indications confirmed by +Point are repaired. Those not confirmed by +Point are dispositioned "no detectable degradation" (NDD).

The agreement between results from the eddy current program and the investigation by ultrasonic testing support the eddy current protocol in place at IP 2. Despite the observation that eddy current signal-to-noise ratios in the sludge pile region tend to vary due to the presence of copper-bearing sludge and deposits, the Cecco/bobbin combination and +Point tend to provide a conservative result. This conclusion is supported by the following See Table 3.5-1 for definitions):

- All OD axial indications (SAI and MAI) confirmed by +Point were confirmed by UTEC.
- No additional axial indications were found by ultrasonic inspection in areas where +Point did not confirm the Cecco and/or bobbin calls as OD axial degradation.
- Cecco and/or bobbin indications not confirmed by +Point were also reported as NDD by UTEC.
- There was general agreement between +Point and UTEC on volumetrics (VOL) and pits (PIT).

3.4 Other Inspections

Visual inspections of the SGs were performed with the objectives of assessing the condition of the TSPs, specifically flow slot hourglassing of the lower three and uppermost support plate, and to survey the periphery of the tube bundle for foreign objects. The inspections were recorded on video tape for review and analysis. The results of the examinations of the bundle and TSP structure are discussed in Appendix A, "Secondary Side Condition Monitoring and Operational Assessment". The survey for foreign objects resulted in removal of a number of them from the SGs. In addition, an inventory of objects that could not be removed was provided for evaluation of the damage potential from these objects (see Section 5.2.6).

During visual examination of the secondary side, a previously plugged tube was identified with a fishmouth rupture. The cause of this rupture was identified as a flow diode effect; water ingress into the tube occurs at cold conditions at an apparently leaking plug, subsequent heating of the tube causes pressurization of the tube and eventual burst. This condition does not challenge either structural or leakage requirements since the tube is already plugged, and leakage does not occur at operating conditions. If leakage occurred at operating conditions, pressurization of the tube would not have occurred. Also, this is not considered a degradation mechanism since the tube was previously plugged.

Table 3.3-1
Comparison of Cecco, +Point and UTEC Results for Steam Generator 22

Cecco				+Point	UTEC
Tube	**Volts**	**Location**	**Code**		
R18C83	13.92	TSH +1.40	PI	NDD	NDD
R19C83	2.52	TSH + 0.85	PI	NDD	NDD
R21C83	16.79	TSH + 0.74	PI	NDD	NDD
R27C26	1.98	TSH + 12.97	PI	NDD	NDD
R30C43	8.68	TSH + 3.2	PI	PIT	PIT
R33C51	7.98	TSH + 0.61	PI	MAI	MAI
R33C51	6.31	TSH + 0.68	PI	SAI	MAI
R34C28	55.29	TSH + 1.19	PI	PIT	NDD/DEPOSIT
R34C28	30.12	TSH + 0.63	PI	PIT	NDD/DEPOSIT
R34C28	14.22	TSH + 17.71	PI	NDD	NDD
R34C51	24.35	TSH + 0.17	PI	MAI	MAI
R34C51	13.19	TSH + 0.62	PI	MAI	MAI
R35C27	118.4	TSH + 1.41	PI	PIT	NDD/DEPOSIT
R35C40	11.55	TSH + 4.37	PI	VOL	NDD/DEPOSIT
R35C50	17.32	TSH + 0.27	PI	VOL	PIT
R35C50	0.67	TSH - 0.19	PI	NDD	NDD
R35C51	10.61	TSH + 0.60	PI	MAI	MAI
R35C51	13.66	TSH + 0.93	PI	MAI	MAI
R38C64	122.3	TSH + 16.63	PI	VOL	NDD/DEPOSIT
R39C43	8.09	TSH + 9.96	PI	NDD	NDD
R39C43	6.02	TSH + 9.69	PI	NDD	NDD
R39C59	13.87	TSH + 8.68	PI	VOL	NDD/DEPOSIT
R43C53	16.29	TSH + 1.26	PI	VOL	PIT/WEAR
R43C53	14.88	TSH + 1.29	PI	NDD	PIT/WEAR

Table 3.3-2
UTEC Results on Steam Generator 22
TSP 1H to TTS

Tube	Post In-situ	+Point	Location	UTEC
R3C24	YES	NDD	NA	NDD
R7C66	NO	NDD	NA	NDD
R9C18	NO	NDD	NA	NDD
R11C81	NO	NDD	NA	NDD
R15C32	NO	NDD	NA	NDD
R15C77	NO	NDD	NA	NDD
R15C80	NO	NDD	NA	NDD
R17C72	NO	NDD	NA	NDD
R18C76	NO	NDD	NA	NDD
R22C75	NO	NDD	NA	NDD
R22C78	NO	NDD	NA	NDD
R25C37	NO	NDD	NA	NDD
R25C49	NO	PIT	TSH +6.48	PIT
R26C76	NO	NDD	NA	NDD
R29C63	NO	NDD	NA	NDD
R31C41	NO	NDD	NA	NDD
R32C48	NO	SAI	TSH + 0.73	WEAR
R33C51	YES	MAI	TSH + 1.07	MAI
R34C54	NO	MAI	TSH + 0.57	MAI
R35C50	NO	VOL	TSH + 0.38	PIT
R35C51	YES	MAI	TSH + 0.65	MAI
R35C52	NO	MAI	TSH +0.75	MAI
R35C56	NO	NDD	NA	NDD

3.5 Identified Steam Generator Tube Degradation Modes

3.5.1 2R14 Degradation Findings:

This assessment examines the identified degradation mechanisms and categorizes them according to their contributions to the IP 2 repair activities and their impact on tube integrity. The following degradation mechanisms were identified at IP 2 during the 2R14 In Service Inspection (ISI); there are no degradation mechanisms that were not previously identified in an assessment of IP2 active or potential mechanisms:

Degradation Mechanism	Location
Axial PWSCC and ODSCC (default)	Dented TSPs (Unconfirmed C-5 calls)
Axial ODSCC	HL tubesheet crevice
Axial ODSCC	Above tubesheet sludge pile, free span
OD Pitting	HL and CL sludge pile
Axial PWSCC	Row 2 U-bends
Axial/Circumferential ODSCC/PWSCC	Partial depth expansion transition, down to F*
Tube ID Restrictions	TSPs
Tube wear	AVB
Tube Wear (loose parts)	TTS periphery

Table 3.5-1 summarizes the degradation mechanisms found during the Spring 2000 (2R14) inspection. This table summarizes the indications reported and their definitions during 2R14 regardless if there were multiple indications on the same tube. Consequently, the number of tubes affected by degradation is smaller, and there is not a direct correlation between tube plugging and the indications summary. Plugging attributions are discussed below.

The dominant degradation mechanism was PWSCC (primary water stress corrosion cracking) at or below the partial depth expansion transition. About 97% of the indications were axially oriented, and all of the circumferential indications had phase angles indicative of ID flaws. As in previous inspections, expansion zone cracking – predominantly axial PWSCC – was observed in the partial expansion length at the base of the tubesheet; a few tubes were reported with expansion zone cracks in the cold leg tube ends, more than 98% of the indications were found in the hot leg tubes. Approximately 300 tubes were re-rolled to re-establish sound tube wall above the crack tips, thereby permitting these tubes to be continued in service under the provisions of the F* alternate repair criteria.

SCC was attributed to unconfirmed Cecco-5 calls found at dented TSP (tube support plate) intersections; widespread denting at the TSP intersections required the use of Cecco 5 T/R (transmit/receive) inspection technology. None of the intersections tested by +Point exhibited signals interpreted as cracks. Eight row 2 tubes with U-bend PWSCC indications were plugged in Row 2; these are discussed in reference 1. The balance of the Row 2 tubes were preventively plugged as conservative measure to provide additional margin against a recurrence of the Row 2 U-bend leakage event that precipitated the 2R14 outage 2 months ahead of schedule. Section 3.5.2 lists the prioritization of plugging attributions. In Table 3.5-3, row 2 tubes with cracks in other locations were

given priority over "preventive" as the attribution for plugging; e.g., SAI in expansion zone attributed to F* instead of row 2 preventive. Four row 2 tubes and 1 row 3 tube were plugged due low signal to noise ratio that reduced the POD for potential cracks, but no tubes were identified with PWSCC indications in any of the Row 3 tubes. One row 3 tube (R3C87 in SG 21) was plugged after it was subjected to pressure testing at 3 times normal operating pressure differential (see Section 5.1.4). Additional tubes (4) were plugged preventively when tube ID restrictions caused by denting did not permit examination with the probe qualified for detection in the obstructed region.

Outside diameter corrosion mechanisms encountered included pitting above the tubesheet, predominantly a cold leg phenomenon of long standing at IP 2, and ODSCC above the hot leg tubesheet as well as within the hot leg unexpanded portion of the tubesheet. None of the signals attributed to wear at AVB (anti-vibration bar) locations was repairable; the maximum depth indication was 38%. Several peripheral tubes were plugged for observed wear – usually as a volumetric +Point indication that corroborated a C-5 or bobbin indication; when a loose part was found either visually or by detection of a low frequency eddy current signal (PLP), the tube at issue was subjected to a "loose parts tube integrity evaluation". This also could result in the preventive plugging of tubes in contact with the loose part even though no wear was detected.

A quantity of tubes (82) with signals derived from the Cecco-5 probe (SPI, TSI, PI) were repaired in spite of the finding that some of them exhibited no degradation detectable with the rotating +Point probe; this was done pursuant to the 1997 agreement with the NRC staff that flaws detected in regions where the C-5 demonstrated superior POD would not be subject to cancellation based on +Point examination. Tube sections that could not be inspected with the appropriate probe were also plugged; in these cases plugging is attributed to tube ID restriction (RST) or the unacceptable data (BDA).

3.5.2 Tubes Plugged Due to Various Degradation Modes

Plugging attributions were prioritized according to the logic shown in Table 3.5-2

Table 3.5-3 summarizes the number of tubes plugged in each SG along with the attributed cause of plugging.

Table 3.5-1
IP-2: Summary of Degradation Found in the 2R14 Inspection
(Number of Indication Records Reported)

Indication	SG 21	SG 22	SG 23	SG 24	ALL	Definition
DRI	151	10	1693	71	1925	Distorted Roll Transition Indication
DRN	72	21	130	9	232	Distorted Roll Transition Indication Not Confirmed
DTN	1	2	1	0	4	Distorted Tubesheet Indication Not Confirmed
MAI	163	141	382	100	786	Multiple Axial Indications
MCI	14	10	24	1	49	Multiple Circumferentially Oriented Indications
MMI	0	0	2	0	2	Mixed Mode Indications
NQI	3	70	31	6	110	Non-Quantifiable Indication
NQN	121	162	50	53	386	Non-Quantifiable Indication Not Confirmed
PCT	115	93	47	124	379	Percent (Depth) Indication
PI	8	94	22	19	143	Possible Indication
PIN	115	333	47	69	564	Possible Indication Not Confirmed
PIT	126	183	82	66	457	Pitting
PLP	26	12	19	22	79	Possible Loose Part
PVN	1	1	1	0	3	Permeability Variation
RST	1628	1581	1834	1772	6815	Restricted Tube
SAI	131	133	258	183	705	Single Axial Indication
SCI	9	17	21	4	51	Single Circumferentially Oriented Indications
SPI	30	4	22	23	79	Support Plate Indication
TSI	6	6	8	8	28	Tubesheet Indication
VOL	5	19	5	10	39	Volumetric Indication
Total	2725	2892	4679	2540	12836	

Note: This table is an indication summary; there are many redundancies of indications on tubes. Therefore, the number of tubes affected by indications is a significantly smaller number.

Table 3.5-2
Prioritization of Plugging Attribution

Priority	Degradation Mechanism	Rationale
1	U-bend PWSCC	Cause of leakage event (R2C5)
2	Sludge Pile ODSCC	In situ test leak (R34C51)
3	Pitting/Volumetric Indications	No barrier to leakage
4	Wear due to Foreign Objects	No barrier to leakage
5	TSP Cecco Indications (SPI)	NRC Commitment; unconfirmed
6	TS Crevice ODSCC	No burst potential; small potential leakage
7	Roll transition PWSCC and Circ. ODSCC/PWSCC	No burst potential; very small potential for leak
8	TSP Restrictions and Bad Data	Preventive
9	Row 2 U-bend	Preventive
10	In-situ test; Discretionary	Preventive

Table 3.5-3
IP 2 Spring 2000 SG Tube Plugging Summary

SG		ATTRIBUTED CAUSES FROM PLUG FILES									
	Tubes Plugged	U-bend PWSCC	Sludge Pile ODSCC	Sludge Pile Pitting	Loose Parts Wear	C-5 Calls	Crevice ODSCC	EZ PWSCC	BDA RST	Row 2 U-bend Preventive	Customer Discretion
21	190	1	1	71	1	30	4	9	2	70	1
22	237	0	9	119	1	5	58	9	2	33	1
23	192	1	5	66	0	23	13	37	5	42	0
24	172	6	2	44	0	24	25	17	2	51	1
ALL	**791**	**8**	**17**	**300**	**2**	**82**	**100**	**72**	**11**	**196**	**3**

- **U-bend PWSCC**: Cracks found in small radius U-bends
- **Sludge pile ODSCC**: Cracks found at or above the tubesheet below TSP#1
- **Sludge pile pitting**: Pit-like volumetric indications (PIT) at or above the tubesheet below TSP#1
- **Loose parts wear**: Volumetric indications (VOL) on peripheral tubes, sometimes with loose parts (PLP)
- **C-5 calls**: Cecco probe indications at TSPs (SPI), top of dented tubesheet (TSI), or in tubesheet crevice (PI)
- **Crevice ODSCC**: +Point signals (MAI, SAI) found below top of the tubesheet above roll transition (RT)
- **EZ PWSCC**: All +Point SCC signals (MAI, SAI, MCI, SCI, MMI) at or below RT not satisfying F*
- **BDA, RST**: Incomplete or unacceptable data
- **Preventive plugging**: Row 2 tubes, tubes from in situ tests, or tubes near active loose parts with no detectable flaws. See section 3.5.2 for prioritization of plugging attributions.

4.0 Inputs for Integrity Analysis

4.1 Operating Parameters

IP2 operates at a T-hot of 590°F based on previously lowering T-hot to reduce the potential for tube degradation. This temperature applies to Cycle 14 and is expected to be maintained for Cycle 15.

To establish if tubes meet the $3\Delta P_{NO}$ integrity requirement, the reported steam pressure, RCS pressure, and internal SG pressure losses are considered. The measured range of dome steam pressures for Cycle 14 was 702.3 psia for SG-21, 701.3 psia for SG-22, 699.2 psia for SG-23 and 697.2 psia for SG-24 (Reference 4). A 700 psia value adequately spans the 4 SGs. The maximum pressure drop across the SG tubes occurs at the top of the tubesheet where the primary pressure including static head is about 2250 psia. The SG pressure drop from the top of the tubesheet to the dome of the SG is calculated to be 11 psi for the IP2 SGs. The use of the pressure drop across the tube at the top of the tubesheet defines a ΔP_{NO} that can be applied for all SG tube degradation. At the top of the tubesheet location, the maximum pressure drop across the tubes under normal operating conditions (ΔP_{NO}) at EOC-14 is 2250 – 700 - 11 = 1539 psi. It is noted that large-scale denting in the IP-2 TSPs has caused flow slot hourglassing, and it is reasonable to assume that flow hole deformation would also be encountered, thus resulting in larger losses through the SG bundle, and subsequently, a lower pressure differential. No credit is taken for this effect, and the 1539 psi ΔP is applied for the condition monitoring assessment.

For Cycle 15, the steam pressure is reduced due to plugging of additional tubes while maintaining T-hot at 590°F. Based on an upper estimate for the increase in tube plugging of about 6%, the steam pressure would be reduced by up to about 17 psi. Then, ΔP_{NO} = 1556 psi for Cycle 15.

4.2 Structural and Leakage Requirements

The structural requirement for freespan indications is to satisfy a burst margin requirement of $3\Delta P_{NO}$ per the requirements of the EPRI SG integrity guidelines (Reference 2. For EOC-14, $3\Delta P_{NO}$ is 4617 psi (3 x 1539 psi) at operating temperature for condition monitoring assessments. At room temperature, for acceptance of in situ test pressures, the burst margin must be increased by 9% to correct for the changes in U-bend material properties (see Section 5.6), and $3\Delta P_{NO}$ = 5032 psi at. For Cycle 15 with reduced steam pressure due to tube plugging, $3\Delta P_{NO}$ = 4668 psi at operating temperature for operational assessments.

Under accident conditions, the freespan leakage limit as the sum of all leaking tubes in a SG must be less than 1 gpm/SG per the requirements of the EPRI SG integrity guidelines (Reference 2). The limiting accident condition is the steam line break (SLB) for which the applicable pressure difference across the tubes is ΔP_{SLB} = 2560 psi at operating conditions.

The above structural and leakage monitoring requirements must be satisfied at a specified probability and confidence level. Per the EPRI SG integrity guidelines, the required values are 90% probability

and 50% confidence (referenced as 90/50).). The more conservative requirements of 95/50 and 95/95 confidence limits for condition monitoring and operational assessment, respectively, were applied for these evaluations

Since the deterministic $3\Delta P_{NO}$ burst margin requirement is applied for the condition monitoring and operational assessment analyses, no explicit requirements are necessary for burst probability at $3\Delta P_{NO}$ or ΔP_{SLB} conditions. Burst probabilities provide supplemental information on tube integrity due to their sensitivity to the entire population of indications rather than the single most limiting indication satisfying the deterministic $3\Delta P_{NO}$ burst margin. The EPRI SG integrity guidelines define satisfying a burst probability of < 0.1 for the burst of one or more tubes at $3\Delta P_{NO}$ pressure differential as equivalent to satisfying the deterministic burst margin requirement at 90/50 probability. The conditional probability of burst criterion at ΔP_{SLB} in the EPRI guidelines is $< 5x10^{-2}$ for the burst of one or more tubes. These burst probability should include known and unknown degradation mechanisms. Applying an allowance of 20% of the criterion for unknown degradation mechanisms, the burst probability guidelines become 0.08 for burst at $3\Delta P_{NO}$ and 0.04 for burst at ΔP_{SLB} at 90/50 probability when summed over all known degradation mechanisms. The $3\Delta P_{NO}$ guideline would generally be expected to be more limiting than the ΔP_{SLB} guideline for IP2. The two known freespan degradation mechanisms that could contribute significantly to a burst probability are the U-bend axial PWSCC indications and the sludge pile ODSCC axial indications.

4.3 Probability of Detection for Sludge Pile Indications

For sludge pile indications, the probability of detection (POD) can be developed principally from pulled tube information. The following data is applied herein to develop a POD as a function of maximum depth:

- ETSS 96402 and 96404: Only pulled tube data for axial ODSCC from the EPRI detection qualification for +Point ODSCC are applied, which includes a total of 14 indications of which 4 were NDD. For the ETSS detection qualification, detection is based on the peer group performing the qualification.
- EPRI NP-7480-L Addenda 2 and 3 for axial ODSCC at TSP intersections: Addenda 2 and 3 provide pulled tube data for + Point detection. A total of 25 indications are included of which 11 were NDD. Detection for these data is based on the field inspection and includes the normal field resolution process.
- Pulled tubes for sludge pile axial ODSCC: These pulled tubes include 8 indications of which 1 was NDD. The field inspection for the 1996 NDD indication was based on a 115 mil pancake coil, but is conservatively included in the POD evaluation as a plus point NDD indication at a maximum depth of 52%. Detection is based on the field inspection since the indication was called by both the 115 mil pancake and +Point coils in the post-pull laboratory inspection.
- Pulled tubes for freespan axial ODSCC: These pulled tubes include 23 indications of which 4 were NDD. Detection is based on the field inspection.
- IP2 1997 +Point NDD indications: Although not pulled tubes, these indications were called in 2000 but called NDD in the 1997 inspection, and identifiable as flaws from reanalysis of the 1997 data knowing an indication was found in the 2000 inspection. These indications are included to reflect plant specific data for IP2. Since destructive exam data is not available, the best estimate of the

maximum depths of the indications was obtained from the reanalysis of the +Point data. The maximum depths for these indications were 30%, 33% and 40%.

The above data represent dominantly field inspection results and conservatively include the 115-mil pancake coil NDD and the IP2 1997 inspection results. The data were evaluated by fitting a log logistic function to the data as shown in Figure 4.3-1 where non-detected indications are show at POD = 0 and the detected indications at POD = 1. At 50% POD, indications > 37% maximum depth are detected, and at 95% POD, indications > 55% depth are detected.

The maximum depth POD is applied for leakage analyses and an average depth POD is required for burst pressure analyses. The most representative average depth POD would be based upon the burst effective average depth (depth over length resulting in the lowest burst pressure) for the indications. The burst effective lengths are not available for all the indications in the database used to develop the POD of Figure 4.3-1. The average depth POD can be obtained from the maximum depth POD by dividing the maximum depths by the ratio of maximum to burst effective average depth for IP2 data as developed in Section 4.4 below. The correlation of maximum to burst effective average depth results in a ratio of 1.257. The resulting average depth POD is shown in Figure 4.3-2.

Figure 4.3-2 shows the burst effective average depth (plotted at POD=1) of indications detected in the EOC-14 inspection as developed in Section 4.4 below. This comparison indicates that the recommended POD may be too low below 30% average depth. A total of 15 of the 25 sludge pile indications sized by +Point were found have less than 30% average depth where the POD varies from about 0.03 to about 0.40

Figure 4.3-2 also includes a comparison of the +Point average depth POD to a bobbin coil POD developed from pulled tubes and field analyses for freespan axial ODSCC. In general, the +Point POD would be expected to be shifted a few percent toward lower depths compared to the bobbin coil POD of Figure 4.3-2. This would result if the 115 mil pancake coil NDD at 52% maximum depth was excluded from the POD database. However, the intent herein is to apply a conservative POD estimate for the IP2 sludge pile analyses. The average and maximum depth PODs of Figure 4.3-2 are applied for the sludge pile axial ODSCC operational assessment given in Section 6.1.

An overall estimate of a global POD is provided in reference 8.

To assess the adequacy of the pulled tube data of Table 4.4-1 as representative of the IP2 data, the signal-to-noise data for pulled tubes used in the POD and NDE uncertainty analyses were evaluated and compared with IP2 sludge pile indications. For rotating probes, both the flaw signal and the noise signals are constantly changing for each scan line along the entire crack length. The signal at any location is really a vector sum of the flaw signal and the noise. The noise contribution comes from such sources as sludge/copper deposits on the tube OD, geometry effects (dents, ovality, etc.), permeability variation in the tube material, etc. In the absence of a better approximation available, all signals are treated as scalar quantities for estimating signal-to-noise ratio (S/N). Since the flaw signal and the noise are constantly changing, a wide range of S/N values can be obtained from different scan lines. This assessment estimated the maximum S/N value encountered along a crack length. First, a peak-to-peak voltage measurement was made at a location producing the maximum signal; the measurement represents the sum of flaw signal and noise. The voltage for the portion of the signal

judged as representing the flaw only was subtracted from the overall signal voltage to obtain an estimate for the noise contribution. An estimate of the noise can also be obtained from a region slightly away from the flaw signal. Generally the two noise values are quite close. An average of the two values was used for obtaining the maximum S/N value for a given crack. The S/N values thus obtained are shown in Table 4.3-1.

It is seen from Table 4.3-1 that the IP2 S/N ratios range from about 1 for the shallow flaws to about 5.5 for the deep flaws in R34C51. The S/N ratios for the pulled tube data are primarily in the range of 1 to 2 for sludge pile and free span indications with some higher values obtained for some of the deep indications at the tube support plate intersections. Overall, the S/N ratios for the pulled tubes tend to be conservatively towards the lower end of the IP2 data. The pulled tubes adequately represent the IP2 S/N ratios, and can be applied for IP2 POD and NDE uncertainty estimates.

4.4 Sizing Methods and NDE Uncertainties for Sludge Pile Indications

NDE +Point Sizing Techniques

The NDE sizing techniques applied for the sludge pile axial ODSCC are based upon extending techniques applied for axial PWSCC to axial ODSCC indications. A senior NDE analyst with extensive experience in evaluating pulled tube data was used for analyses of pulled tube data to develop NDE uncertainties and for analyses of the most limiting IP2 sludge pile indications. This use of the same analyst for sizing and NDE uncertainties provides a consistent database for the sludge pile tube integrity analyses. Two sizing techniques were evaluated as part of the NDE uncertainty study: (1) The depths from phase analyses can be evaluated as the phase angle for the peak to peak response, or (2) The depth can be evaluated as the part of the peak to peak response that yields the maximum depth. The pulled tube database used for the NDE sizing uncertainties was evaluated using both techniques. The smallest uncertainty was obtained using the local maximum depth analysis technique (part of phase response with maximum depth) and this technique was applied to define the NDE sizing uncertainties for IP2. For indications with low signal to noise ratios, the best estimate of the maximum depth has been found in previous sizing analyses, and in this study, to be the depth at maximum voltage. Prior sizing evaluations for axial ODSCC have shown that the maximum depth from phase analysis at maximum voltage should be applied for indications with maximum +Point voltages <0.6 volt. This cutoff voltage was applied for the IP2 analyses of this report. For indications below the 0.6 volt cutoff, sizing techniques using the depth profile from phase analyses and from the voltage profile were compared. It was found that both techniques for defining the axial profile of the indications yielded about the same sizing uncertainties. For general consistency with techniques applied for axial PWSCC, the profile based on phase angle analyses (maximum local depth) with the profile adjusted to the depth at maximum voltage was applied for the IP2 analyses.

+Point Sizing Uncertainties

This section describes the development of NDE uncertainties for application in the Monte Carlo analyses to support condition monitoring and operational assessments. Specifically, NDE uncertainties associated with average depth, maximum depth and length of depth profiles obtained by sizing +Point coil signals are presented. Since IP2 specific pulled tube data applicable to sludge pile indications are

not available, pulled tube data from other plants are used to develop the +Point sizing uncertainties. Available data for pulled tubes with sludge pile indications are supplemented with data for ODSCC indications in the freespan and at TSP intersections. NDE uncertainties are developed considering the burst effective length corresponding to the partial crack length that results in the lowest burst pressure. For axial ODSCC indications, NDE uncertainties for the burst effective length are used for the tube integrity analyses. ODSCC cracks can be long with shallow tails that have no influence on tube integrity, and the principal objective for the NDE analyses must be to predict the structurally significant length and depth for the indications.

Table 4.4-1 provides the length, average depth and maximum depth data from the NDE analysis and destructive examination for each of the pulled tube indications included in the NDE uncertainty evaluation. The last columns of the table provide the errors for each NDE parameter given as destructive exam value minus NDE value. Although linear correlations are used for the NDE uncertainties in this report, the mean error, and standard deviation are given at the end of the table to provide a general basis for assessing the uncertainties.

Figures 4.4-1 to 4.4-3 provide the linear regression correlations for the +Point coil sizing uncertainties on the burst effective length, average depth and maximum depth. The parameters for the regression correlations are given in Table 4.4-2. The linear correlations for the NDE uncertainties are used in the operational assessment analyses as described in Section 6.1. Each of the correlations and standard deviations are given below:

Average Depth, %

$$Davg(\%) = 15.7 + 0.738 \times Davg,NDE$$
$$\sigma = 8.7\%$$

Maximum Depth, %

$$Dmax(\%) = 8.6 + 0.866 \times Dmax,NDE$$
$$\sigma = 10.7\%$$

Length, inch

$$L = 0.217 + 0.633 \times LNDE$$
$$\sigma = 0.163 \text{ inch}$$

EOC-14 Sludge Pile Indication Profiles

Table 4.4-3 shows a summary of the EOC-14 crack depth profiles from sizing +Point data for sludge pile indications. For each profile, length of crack, maximum depth and average depth values are shown. These profiles parameters are shown for the as measured profiles as well as the adjusted profiles and burst-adjusted profiles. The techniques for adjusting as-measured profiles are discussed above. The adjusted profiles are used for the condition monitoring evaluations in Section 5.1 and the operational assessment in Section 6.1.

Sludge Pile Maximum to Average Depth Ratio

Evaluations of both pulled tube and field NDE profile data have shown that the ratio of maximum depth to the burst effective average depth is nearly constant from cycle to cycle and approximately the same for axial PWSCC and ODSCC. The ratio is typically between 1.23 and about 1.3 with a 1.25 ratio being most common. Based on the EOC-14 +Point profiles of Table 4.4-3, a correlation was developed for the maximum to average depth ratio for use in the tube integrity evaluations. Burst adjusted data were used since they represent the part of the crack that controls the burst pressure. The resulting correlation of maximum to average depth is shown in Figure 4.4-4. The resulting ratio of 1.257 from the IP2 +Point sizing of the 2000 inspection sludge pile indications is consistent with that found from many other sizing studies and supports the consistency of the sizing evaluations. The 1.257 ratio of Figure 4.4-4 was applied in Section 4.3 above to obtain the average depth POD from the maximum depth POD developed from pulled tube data and in Section 4.5 to obtain average depth growth from maximum depth data.

Table 4.3-1 Signal to Noise Ratios (S/N) for Pulled Tubes and IP2 Data					
Plant	**Row**	**Col.**	**Location**	**Crack No.**	**Signal to Noise Ratio**
Pulled Tube Data					
ALA	6	28	TTS +10"	1	~2
			TTS + 23.7"	2	~2
			TTS +39.3"	3	~2
			TTS +47"	4	~1
	6	10	TTS +9"	2	~1
			TTS + 22.3"	4	~3
CAE	20	102	3H	1	~3.5
			5H	1	< 0.5
CCE	42	44	5H	1	~3
			3H	1	~4
	37	34	5H	1	~10
			3H	1	~ 0.5
DLW	12	45		2	~1.5
				4	~0.5
				5	~1
	16	28		1	~1
				2	~1
	18	30		1	~1.5
	18	36		1	~1
PGE	37	32	3H	1	> 6
IP2 Data					
IP-2	34	51		1	~5
				2	~5.5
	33	51			~5
	34	54		1	~3
	35	52			~1.6
	3	88			~1
	44	36			< 1

Table 4.4 - 1

IP2 Sludge Pile ODSCC Indications

Data Used to Develop NDE Uncertainty Correlations

Plant	Ins. Year	SG	Row	Col	Loc	Crack No.	NDE				NDE				DESTRUCTIVE EXAM			DESTRUCTIVE EXAM			Burst DE minus Burst NDE		
							Unadjusted NDE				Burst Adjusted NDE				Unadjusted DE			Burst Adjusted DE					
							Length (in.)	Max. Depth (%)	Avg. Depth (%)	Max. Volts	Length (in.)	Max. Depth (%)	Avg. Depth (%)	Max. Volts	Length (in.)	Max. Depth (%)	Avg. Depth (%)	Length (in.)	Max. Depth (%)	Avg. Depth (%)	Length (in.)	Max. Depth (%)	Avg. Depth (%)
ALA	1996	2	6	28	TTS	1	3.800	67.0	27.0	0.26	0.560	28.0	23.2	0.2	2.080	40.5	29.8	1.110	40.5	33.2	0.550	12.46	10.01
ALA	1996	2	6	28	TTS	2	1.090	77.0	17.6	0.14	0.130	30.0	23.5	0.1	0.640	38.0	29.5	0.420	38.0	34.2	0.290	8.00	10.77
ALA	1996	2	6	28	TTS	3	2.200	56.0	16.6	0.16	0.280	37.7	30.1	0.2	1.150	39.7	24.8	0.540	39.7	33.4	0.260	1.97	3.28
ALA	1996	2	6	28	TTS	4	0.480	73.0	33.8	0.14	0.380	48.0	29.5	0.1	1.040	31.6	17.0	0.290	31.6	25.7	-0.090	-16.36	-3.76
ALA	1996	2	28	35	TTS	1	0.730	72.0	39.2	0.25	0.500	30.0	20.7	0.3	0.800	46.1	29.5	0.430	46.1	37.9	-0.070	16.09	17.17
ALA	1997	1	29	47	TSH	1	1.140	100.0	77.3	10.53	0.580	100.0	91.6	10.3	1.690	100.0	44.8	0.580	100.0	79.6	0.000	0.00	-12.08
ALA	1998	3	6	10	TTS	2	2.120	81.0	51.2	0.76	0.860	81.0	60.1	0.4	2.100	70.7	50.0	0.690	70.7	58.9	-0.170	-10.28	-1.18
ALA	1998	3	6	10	TTS	4	1.590	67.0	29.8	0.51	0.520	59.0	48.9	0.4	1.668	59.0	30.9	0.670	59.0	46.6	0.150	0.04	-2.29
CAE	1995	3	20	102	03H	1	0.390	91.0	63.4	1.99	0.270	90.0	67.2	1.7	0.380	92.7	61.0	0.320	92.7	69.9	0.050	2.70	2.71
CAE	1995	3	20	102	05H	1	0.440	51.0	29.5	0.56	0.200	51.0	45.6	0.6	0.410	61.3	45.9	0.270	61.3	53.6	0.070	10.27	8.01
CCE	1995	1	42	44	03H	1	0.510	94.0	78.8	3.39	0.510	94.0	78.8	3.4	0.520	95.1	74.4	0.470	95.1	78.2	-0.040	1.10	-0.57
CCE	1995	1	42	44	05H	1	0.430	90.0	64.8	1.54	0.340	90.0	73.71	1.54	0.530	95.5	57.7	0.360	95.5	72.4	0.020	5.53	-1.35
CCE	1995	4	37	34	03H	1	0.300	99.0	75.5	0.82	0.240	73.0	60.53	0.55	0.470	52.9	43.6	0.350	52.9	48.5	0.110	-20.09	-12.05
CCE	1995	4	37	34	05H	1	0.580	99.0	80.9	6.69	0.380	100.0	86.31	6.69	0.460	100.0	81.0	0.460	100.0	81.0	0.080	0.00	-5.33
DLW	1996	2	12	45	TSH	2	1.260	78.0	51.1	0.37	0.910	66.0	49.10	0.37	1.360	69.7	45.3	0.670	69.7	62.5	-0.240	3.75	13.42
DLW	1996	2	12	45	TSH	4	0.680	85.0	58.8	0.18	0.590	62.6	46.12	0.17	0.566	76.9	58.9	0.390	76.9	67.4	-0.200	14.31	21.33
DLW	1996	2	12	45	TSH	5	1.220	97.0	54.4	0.24	0.430	89.0	72.57	0.24	1.150	88.0	54.5	0.520	88.0	76.9	0.090	-1.00	4.36
DLW	1996	3	16	28	TSH	1	0.980	74.0	50.3	0.2	0.770	57.0	47.1	0.2	1.195	35.7	28.3	0.810	35.7	32.7	0.040	-21.29	-14.39
DLW	1996	3	16	28	TSH	2	0.430	78.0	48.8	0.18	0.340	61.0	53.7	0.2	0.535	47.6	36.2	0.340	47.6	44.0	0.000	-13.43	-9.72
DLW	1996	3	18	30	TSH	1	1.320	81.0	49.0	0.2	0.410	36.7	29.17	0.19	1.280	52.0	41.9	0.660	52.0	48.1	0.250	15.33	18.94
DLW	1996	3	18	36	TSH	1	0.270	84.0	38.3	0.25	0.220	49.8	36.18	0.20	0.411	47.2	35.4	0.310	47.2	39.3	0.090	-2.65	3.10
PGE	1997	2	37	32	03H	1	0.420	72.0	46.5	0.68	0.300	71.0	59.7	0.7	0.654	66.8	36.9	0.280	66.8	58.1	-0.020	-4.15	-1.65
																			Mean		0.055	0.10	2.21
																			Standard Dev.		0.173	10.69	9.90

Table 4.4 -2
IP2 Sludge Pile ODSCC Indications
NDE Uncertainties Applied in the Monte Carlo Analyses

$$l_{true} = a_0 + a_1 \times l_{nde}$$

Correlation Parameter	Length (inches)	Max. Depth (%)	Average Depth (%)
Intercept (a_0)	0.2174	8.65	15.71
Slope (a_1)	0.6336	0.8662	0.7381
Std. Error (σe)	0.1633	10.742	8.711
Mean	0.442	63.86	51.51
Sum of Squares	0.9219	11647.1	9287.0
No. of Data Pairs	22	22	22

Table 4.4 -3
IP2 EOC-14 Sludge Pile Indications

				Unadjusted NDE				Adjusted NDE				Burst Adjusted NDE				Burst Pressure (ksi)
SG	Row	Col.	Crack No.	Length (in.)	Maximum Depth (%)	Average Depth (%)	Max. Volts	Length (in.)	Maximum Depth (%)	Average Depth (%)	Max. Volts	Length (in.)	Maximum Depth (%)	Average Depth (%)	Max. Volts	
1	34	41	1	0.520	66.0	46.12	0	0.540	56.5	38.24	0.26	0.410	56.5	43.91	0.26	7.852
2	32	48	1	0.280	71.0	40.13	0	0.280	62.0	35.29	0.16	0.230	62.0	37.80	0.16	8.855
2	33	49	1	0.400	56.0	32.49	0	0.400	38.0	22.05	0.18	0.310	38.0	25.85	0.18	9.610
2	33	51	1	0.770	67.0	44.16	0	0.770	47.0	34.31	0.39	0.530	47.0	42.07	0.39	7.841
2	33	54	1	0.260	73.0	38.35	0	0.260	30.0	15.76	0.33	0.130	30.0	22.68	0.25	10.353
2	33	54	2	0.130	42.0	24.69	0	0.130	30.0	17.64	0.28	0.100	30.0	20.46	0.28	10.637
2	34	51	1	1.260	91.0	63.48	1	1.260	84.0	63.48	0.88	1.160	84.0	65.79	0.88	4.962
2	34	51	2	1.330	90.0	66.12	1	1.350	88.0	65.34	0.89	0.540	88.0	77.41	0.89	4.405
2	34	51	3	0.590	93.0	75.29	1	0.590	75.0	60.72	0.55	0.490	75.0	65.90	0.55	5.639
2	34	54	1	0.170	40.0	18.74	1	0.190	40.0	18.87	0.75	0.140	40.0	24.32	0.75	10.202
2	34	54	2	0.070	25.0	20.93	0	0.110	30.0	20.24	0.19	0.090	30.0	22.47	0.19	10.592
2	34	54	3	0.270	48.0	26.94	1	0.270	30.0	16.84	0.56	0.150	30.0	26.27	0.47	10.028
2	35	51	1	0.590	80.0	52.70	1	0.590	62.0	44.15	0.51	0.390	62.0	54.74	0.51	6.917
2	35	52	1	0.420	80.0	25.77	1	0.420	30.0	11.29	0.55	0.220	30.0	17.52	0.55	10.438
3	3	88	1	2.280	75.0	30.39	0	2.280	30.0	12.16	0.18	0.740	30.0	21.34	0.12	9.693
3	29	46	1	0.270	50.0	35.19	0	0.270	44.0	31.59	0.47	0.205	44.0	37.14	0.47	9.008
3	29	46	2	0.370	40.0	22.61	0	0.370	30.0	16.96	0.27	0.160	30.0	23.55	0.21	10.168
3	29	46	3	0.290	30.0	20.27	0	0.305	30.0	19.57	0.34	0.260	30.0	21.93	0.34	10.020
3	30	46	1	0.750	40.0	26.69	0	0.750	33.0	22.88	0.32	0.490	33.0	27.92	0.32	9.206
3	31	46	1	1.080	81.0	53.34	1	1.080	62.5	46.30	0.56	0.930	62.5	48.93	0.56	6.848
3	31	47	1	0.570	32.0	19.68	1	0.585	30.0	18.03	0.56	0.315	30.0	23.98	0.56	9.759
3	31	47	2	0.270	49.0	32.83	0	0.270	47.5	31.83	0.46	0.210	47.5	38.24	0.46	8.903
3	31	47	3	0.210	45.0	23.60	0	0.210	45.0	23.60	0.31	0.170	45.0	27.38	0.31	9.865
4	30	27	1	2.350	44.0	18.80	1	2.350	30.0	12.82	0.51	0.460	26.6	17.45	0.41	10.186
4	42	43	1	0.330	93.0	36.22	0	0.350	30.0	17.60	0.22	0.350	30.0	17.60	0.22	10.257

Figure 4.3-1. Indian Point-2 Sludge Pile POD vs. Maximum Depth + Point Coil, Log Logistic Function

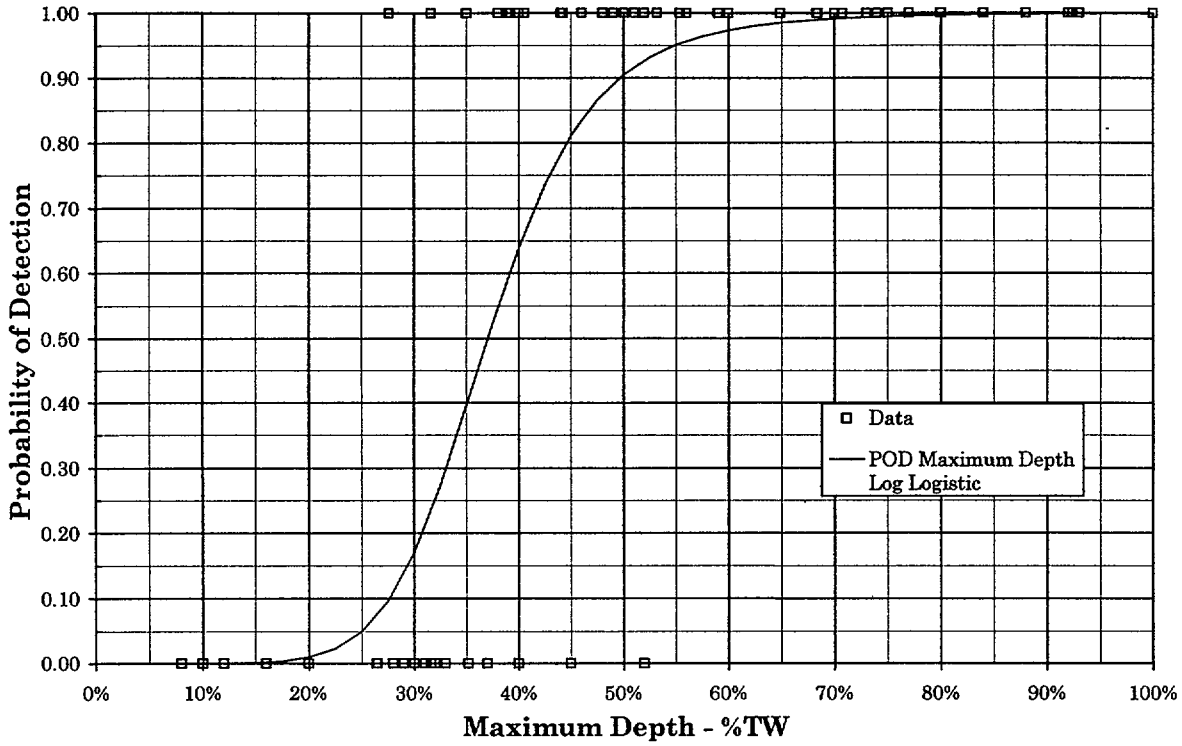

Figure 4.3-2. Indian Point-2 Sludge Pile PODs for Max. and Avg. Depth + Point Coil, Log Logistic Function Comparison with Bobbin Coil Freespan ODSCC Average Depth POD

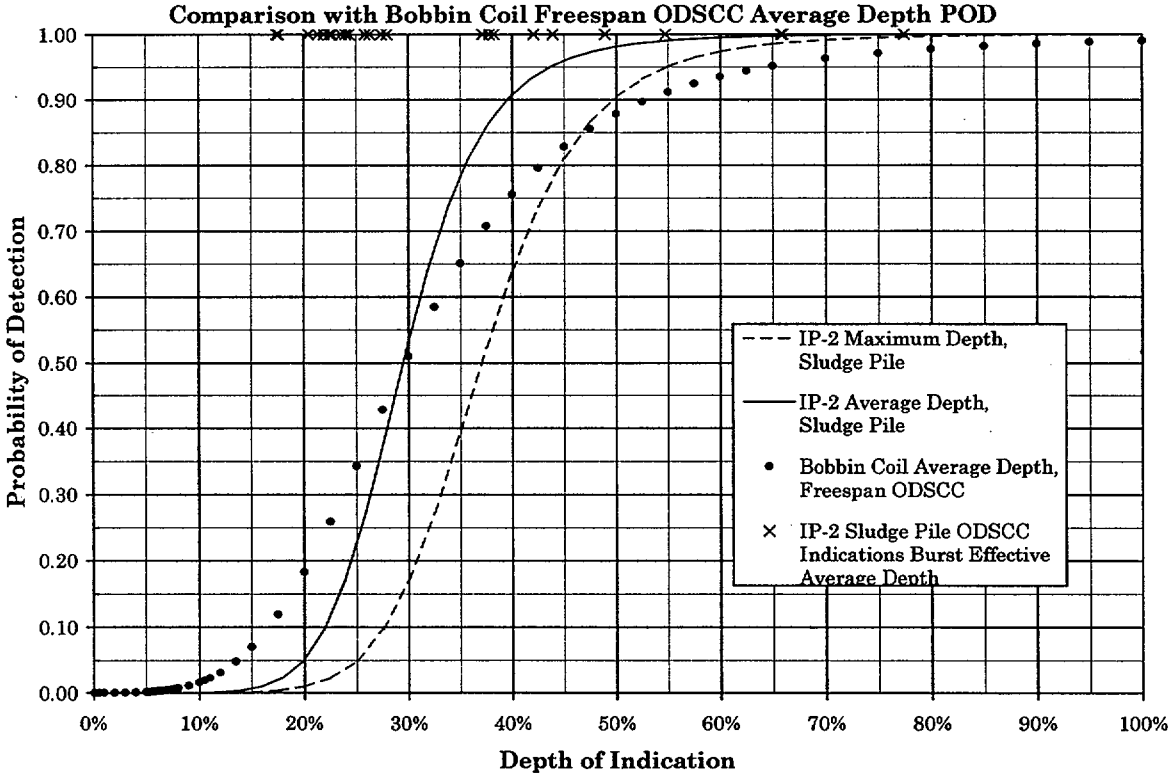

Figure 4.4 -1

Indian Point-2 Sludge Pile ODSCC – NDE Sizing Uncertainties
Destructive Exam vs. Burst Adjusted NDE Trends - Axial Length

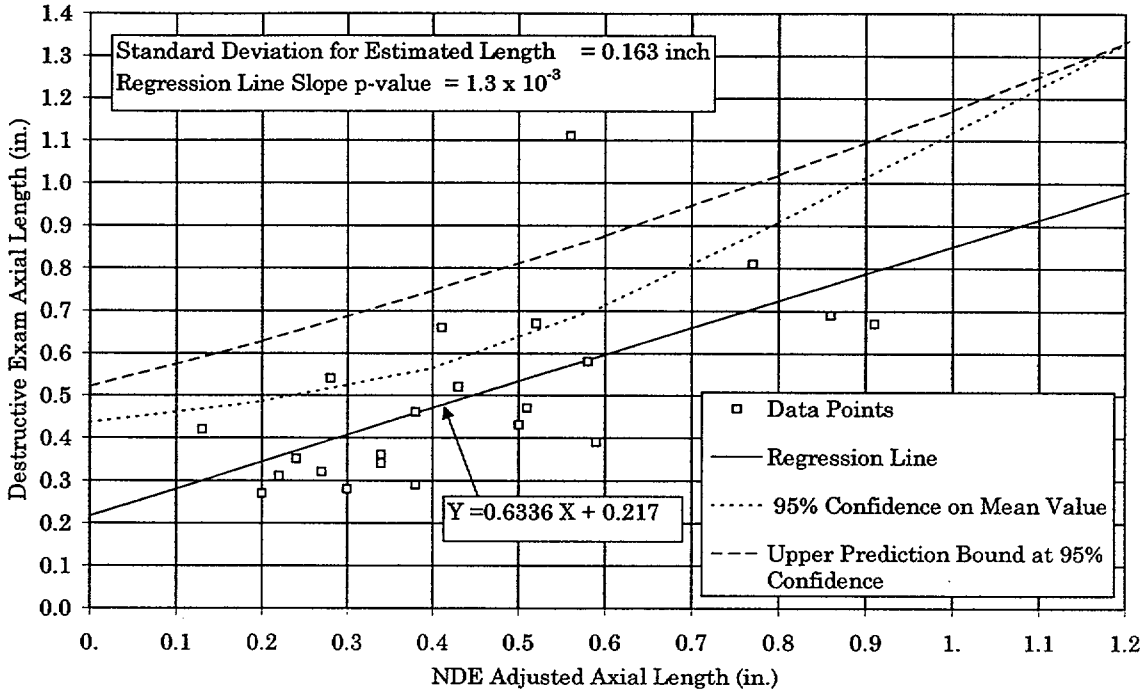

Figure 4.4 -2

Indian Point-2 Sludge Pile ODSCC – NDE Sizing Uncertainties
Destructive Exam vs. Burst Adjusted NDE Trends - Maximum Depth

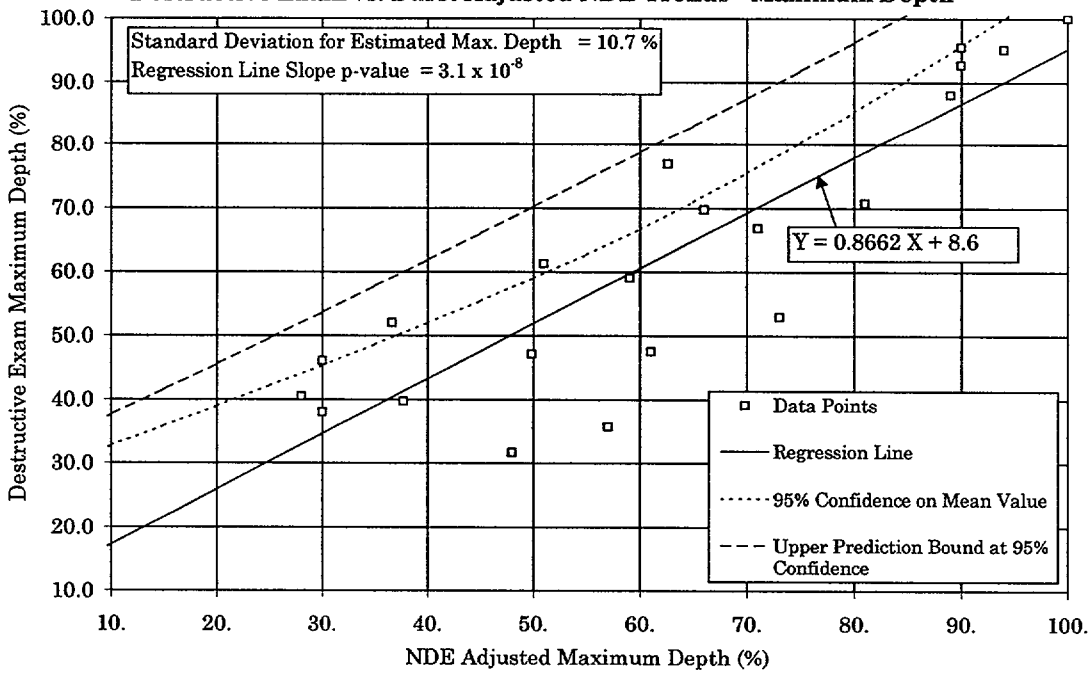

Figure 4.4 -3

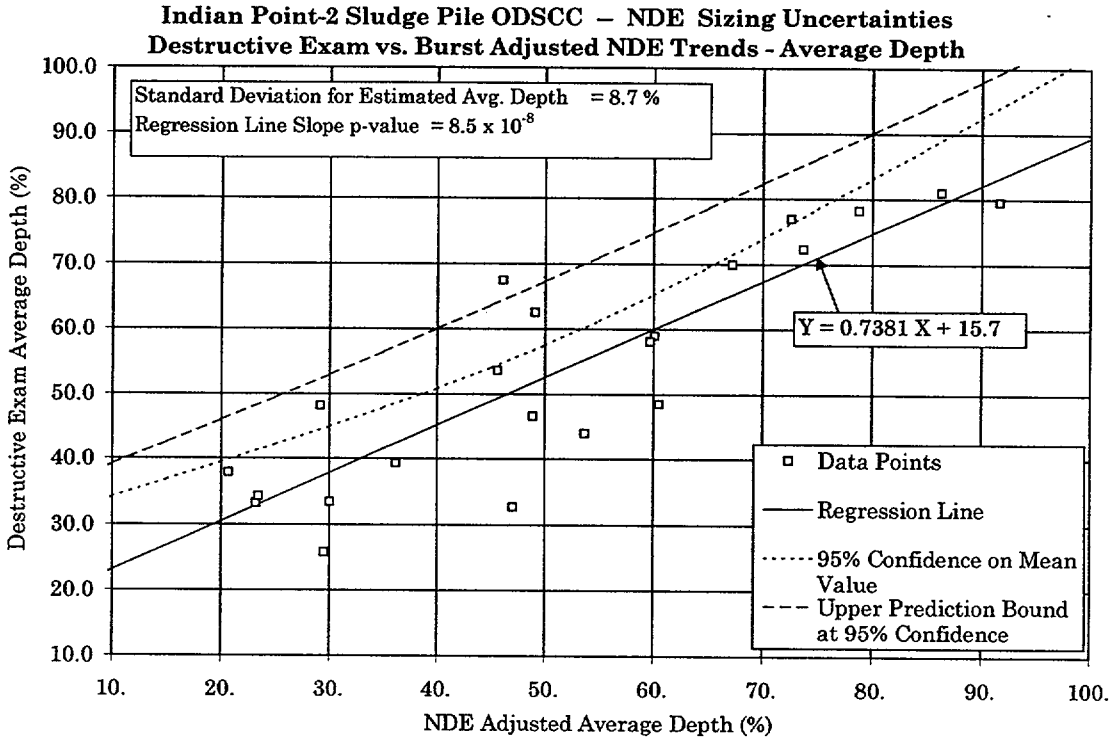

Figure 4.4 -4

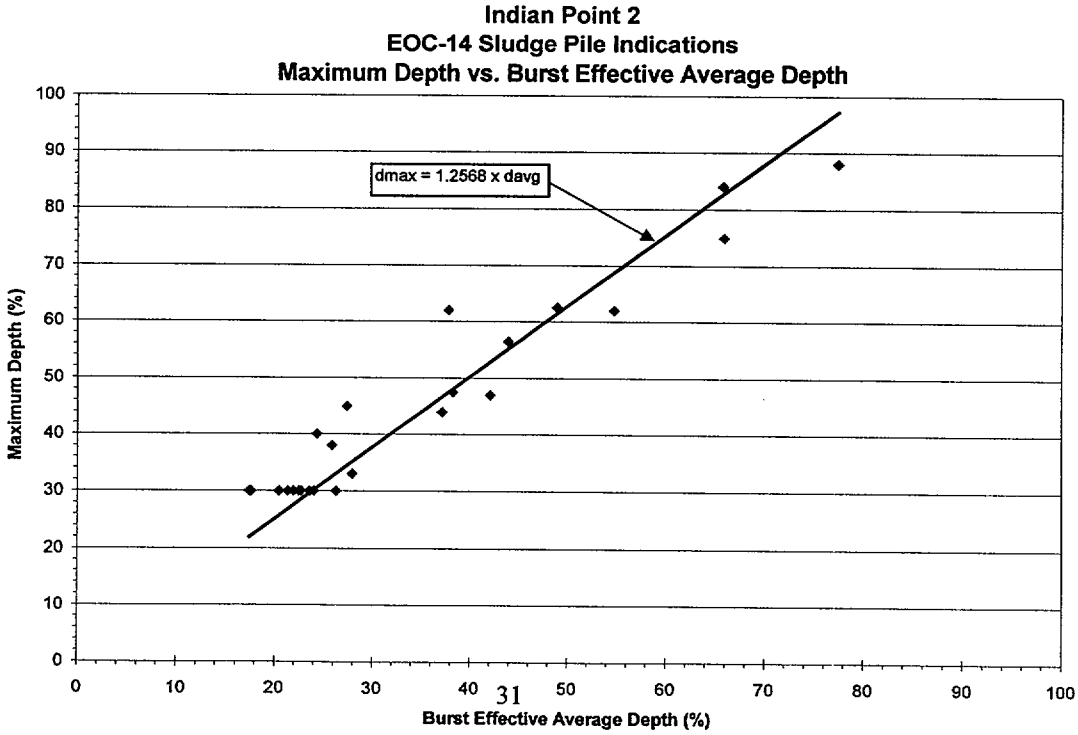

4.5 Growth Rates for Sludge Pile Indications

Growth rate distributions for axial ODSCC in the sludge pile have been developed from +Point profile analyses for another plant with 7/8 inch diameter tubing. Consecutive +Point inspections are not available for IP2 to obtain growth distributions. However, an IP2 maximum depth growth distribution can be obtained from analyses of the bobbin coil indications. For indications confirmed by +Point in the 2000 inspection, the bobbin data were evaluated for maximum depth at the 2000, 1997 and 1995 inspections to obtain a database for maximum depth growth. Based on knowledge of the indication from the 2000 inspection, reevaluation of the 1997 and 1995 bobbin data indicated that signals representative of axial ODSCC could be observed for all flaws found by the bobbin coil in the 2000 inspection. These results support a conclusion that the growth period for these indications is greater than two full cycles of operation. For R34C51, the structurally most limiting indication found in the 2000 inspection, the presence of a 1.1 bobbin volt signal in 1995 suggests that the growth period for this indication extends for at least over three operating cycles. From the bobbin data reevaluation, the bobbin voltage growth trends of Figure 4.5-1 were obtained for 11 indications including R34C51. R34C51 had the largest voltage growth of about 1.5 volts from 1995 to 1997. Other than this growth, all indications show modest growth in voltage with about equal growth over the two cycles. This review of the bobbin data shows that the flaws experienced in the sludge pile region do not initiate and grow to significant average depths and lengths in less than one cycle. Figure 4.5-2 shows the burst pressure versus bobbin voltage trend for six sludge pile pulled tube indications and the data point for R34C51 assuming the indication burst in the in situ test (indication had ligament tearing with an implied higher burst pressure). The minimum estimated burst pressure for R34C51 is consistent with the trend from the pulled tubes. Since R34C51 had a 2.6 bobbin voltage at EOC-13 in 1997, the decrease in burst pressure implied by Figure 4.5-1 is only about 400 psi over Cycle 14, again supporting modest growth.

The IP2 bobbin growth data are given in Table 4.5-1. From the bobbin coil analyses, maximum depth growth values were obtained for 12 indications for Cycle 14 (1997 to 2000) and for 9 points for Cycle 13 (1995 to 1997). Of the six sludge pile indications reported in the +Point inspection of all hot leg intersections, only one indication at SG 22 R33C49 exhibited a bobbin flaw signal in 2000 based on reevaluation of the data applying knowledge of a flaw from the +Point inspection. This signal could be observed in the 1997 and 1995 data. This indication was the only one found in the supplemental +Point program with a predicted nominal burst pressure <10000 psi (9185 psi). For some of the indications in Table 4.5-1, bobbin coil depths were obtained at two elevations of the indication. The data were evaluated for the largest growth value at either elevation when multiple depths were reported. Maximum depth growth per EPPY was obtained by dividing the measured growth by 1.48 EFPY for Cycle 14 and 1.64 EFPY for Cycle 13. The IP2 bobbin growth data are maximum depth values, and average depth growth is obtained by dividing the depths by the maximum to average depth ratio of 1.257

developed in Section 4.4. The average growth rates are 4.26%/EFPY for maximum depth and 3.39%/EFPY for average depth.

The cumulative probability distribution, adjusted for the small population, of the IP2 average depth growth is shown in Figure 4.5-3 by the open square symbols. This figure compares the IP2 data with a sludge pile growth distribution obtained from +Point data from another plant and with a growth distribution obtained from bobbin analyses for freespan ODSCC at another plant. The data from the other plants are corrected to the IP2 T_{hot} of 590 °F. The IP2 data show the smallest growth rates of the three plants above 5% growth per EFPY, which is consistent with the above evaluation indicating that these indications have been present for about three cycles. The +Point based growth distribution for sludge pile indications in Figure 4.5-3 shows the largest growth rates. Since these data bound the IP2 data, this distribution is conservatively applied for the evaluation of IP2 growth given below. The average growth rate for the recommended growth distribution is 3.45%/EFPY compared to the 3.39%/EFPY for the IP2 data developed from bobbin measurements.

Since the +Point based growth distribution provides an adequate database for growth evaluations, the data can be used to develop the "true" growth distribution. The true growth can be estimated by applying corrections for NDE uncertainties. The NDE uncertainties can be represented by a mean error with a standard deviation. Since a difference between two cycles is used to obtain growth, the mean error is essentially eliminated from the NDE uncertainties influencing growth. Since the NDE uncertainty on growth is then equally distributed between positive and negative corrections, the average growth rate of the measured data is maintained when the data are corrected for NDE sizing uncertainties to obtain the true growth. Figure 4.5-4 shows the +Point based measured sludge pile growth as the open square symbols. A log normal distribution is applied to represent the true growth with an average growth equal to the measured distribution. The unknowns in obtaining the true growth are then the standard deviations of the log normal true growth and NDE uncertainty distributions. These values are estimated by requiring that the statistical application of the NDE uncertainties to the true log normal distribution reproduce the measured growth distribution. The results of this iterative process are shown in Figure 4.5-4 where the predicted measured and actual measured distributions are in good agreement except for the larger negative growths of the measured distribution. Since the negative growths appear to be somewhat larger than expected from the statistical analysis, the average growth rate for the true growth (corrected avg. depth growth in Figure 4.5-4) was increased to obtain the results of Figure 4.5-4. The NDE uncertainties applied in Figure 4.5-4 are a mean error of 0% and a standard deviation of 4.0%. The measured average growth rate is 3.45%/EFPY and the average of the log normal distribution is 4.0%/EFPY. The corrected or true average depth growth distribution of Figure 4.5-3 is applied for the operational assessment of Section 6.1 for sludge pile indications.

For sensitivity analyses in the sludge pile operational assessment, an upper bound log normal growth distribution can be obtained by bounding the measured data as shown in Figure 4.5-5. In this case, a log normal distribution bounding the data is selected with an

average growth that exceeds the measured data and the NDE uncertainty is conservatively assumed to include a negative mean error to compensate the increased average depth for the log normal distribution. Given these conservative assumptions, the data are iterated to obtain good agreement between the predicted measured and actual measured distributions as shown in the Figure. The NDE uncertainties applied in Figure 4.5-5 are a mean error of –1.5% and a standard deviation of 2.0%. The average growth for the resulting conservative log normal distribution is 5.75% compared to the true growth average of 4.0% developed above. The upper bound growth distribution of Figure 4.5-5 is used for sensitivity analyses in the operational assessment of Section 6.1.

The NDE uncertainty for length measurements can be obtained from the +Point based sludge pile growth data in the same manner as applied above for average depth growth. The number of growth data points in length is smaller than obtained for average depth as length growth was evaluated only for the last cycle for this plant. The length growth data are shown as the measured length growth in Figure 4.5-6. For the length growth data, the NDE uncertainties required to fit the data were found to be small with little difference between the true growth and a bound growth. The bounding growth evaluation obtained conservatively assuming a mean NDE error of –0.01 inch with a 0.015 inch standard deviation is shown in Figure 4.5-6. The average growth for the bounding log normal distribution is 0.065 inch compared to the average of the measured data of 0.052 inch.

A review of IP2 chemistry data shows a trend of decreasing contaminant concentrations over time. This trend is a positive indication of the improvements that have been made in secondary chemistry at the plant. The copper reduction plan initiated in the '80s will have resulted in all the major copper-containing feedwater systems components having been changed out by the end of the current outage. Boric acid, as indicated in the "Strategic Secondary Water Chemistry Plan" , will continue to be used through Cycle 15. No changes to secondary chemistry are anticipated that would adversely affect ODSCC growth, and growth rates obtained for Cycle 14 are applicable to cycle 15.

4.6 Sludge Pile Tube Integrity Analysis Methods

The Monte Carlo analysis methods used for the sludge pile tube integrity analyses are the same as applied for the IP2 U-bend operational assessment and in Westinghouse report WCAP-15128, Revision 2. These analysis methods utilize the +Point depth profiles, POD, NDE uncertainties and growth rates developed in the above sections. The Westinghouse burst correlation is applied for burst pressure analyses and the ANL ligament tearing model is applied for leakage analyses. For the operational assessment, the limiting indication burst pressure at the end of the operating cycle is computed for comparison with the $3\Delta P_{NO}$ burst margin requirement and the SLB leak rate is calculated for comparison with the 1 gpm freespan leak rate limit. The tube burst probability at SLB conditions is also calculated at the end of the operating cycle.

Table 4.5-1. IP2 Sludge Pile ODSCC Growth Rates from Bobbin Coil Analysis

SG	Tube	Bobbin Coil Analysis						Maximum Depth Growth					Average Depth Growth % Per EFPY[3]
								2000-1997		1997-1995		All Data % Per EFPY	
		1995 Volts	1997 Volts	2000 Volts	1995 Max. Depth %	1997 Max. Depth %	2000 Max. Depth %	Growth %	Growth per EFPY[1]	Growth %	Growth per EFPY[2]		
22	R34C51	1.1	2.6	2.94	65	60	78	18	12.16	-5	-3.05	12.16	9.67
			0.61	0.95		40	46					-3.05	-2.43
22	R35C51		0.8	1.55		66	65	4	2.70			2.70	2.15
		0.57	0.99	1.23	67[4]	58	62						
22	R33C51	0.31	0.77	1.06		26	25	27	18.24	5	3.05	18.24	14.51
			0.38	0.72		5	32					3.05	2.43
22	R35C52	0.47	0.66	1.44	37	41	50	9	6.08	4	2.44	6.08	4.84
												2.44	1.94
22	R33C49	0.21	0.27	0.28	18	32	29	-3	-2.03	14	8.54	-2.03	-1.61
												8.54	6.79
22	R32C48	0.74	0.59	0.69	0	8	8	0	0.00	8	4.88	0.00	0.00
												4.88	3.88
22	R34C54	0.38	0.82	1.05	42	52	52	0	0.00	10	6.10	0.00	0.00
												6.10	4.85
23	R29C46	0.64	1.33	1.76	60[4]	33	44	11	7.43			7.43	5.91
23	R30C46	0.49	1.17	1.66	39	34	36	2	1.35	-5	-3.05	1.35	1.07
												-3.05	-2.43
23	R31C46	0.41	2.63	1.39	28	38	42	20	13.51	10	6.10	13.51	10.75
		1.22	1.45	1.52	33	12	32					6.10	4.85
23	R31C47	0.55	0.70	1.28	16	21	33	12	8.11	5	3.05	8.11	6.45
												3.05	2.43
22	R33C49	0.21	0.35	0.25	59[4]	47	38	-9	-6.08			-6.08	-4.84
											Average	4.26	3.39

Notes:

1. Cycle 14 length = 1.48 EFPY
2. Cycle 13 length = 1.64 EFPY
3. Average depth growth obtained from maximum depth growth by dividing by maximum to burst effective average depth ratio of 1.257
4. Data not used due to implied large negative growth. Negative growth data were conservatively excluded from the database for growth rate.

Figure 4.5 - 1

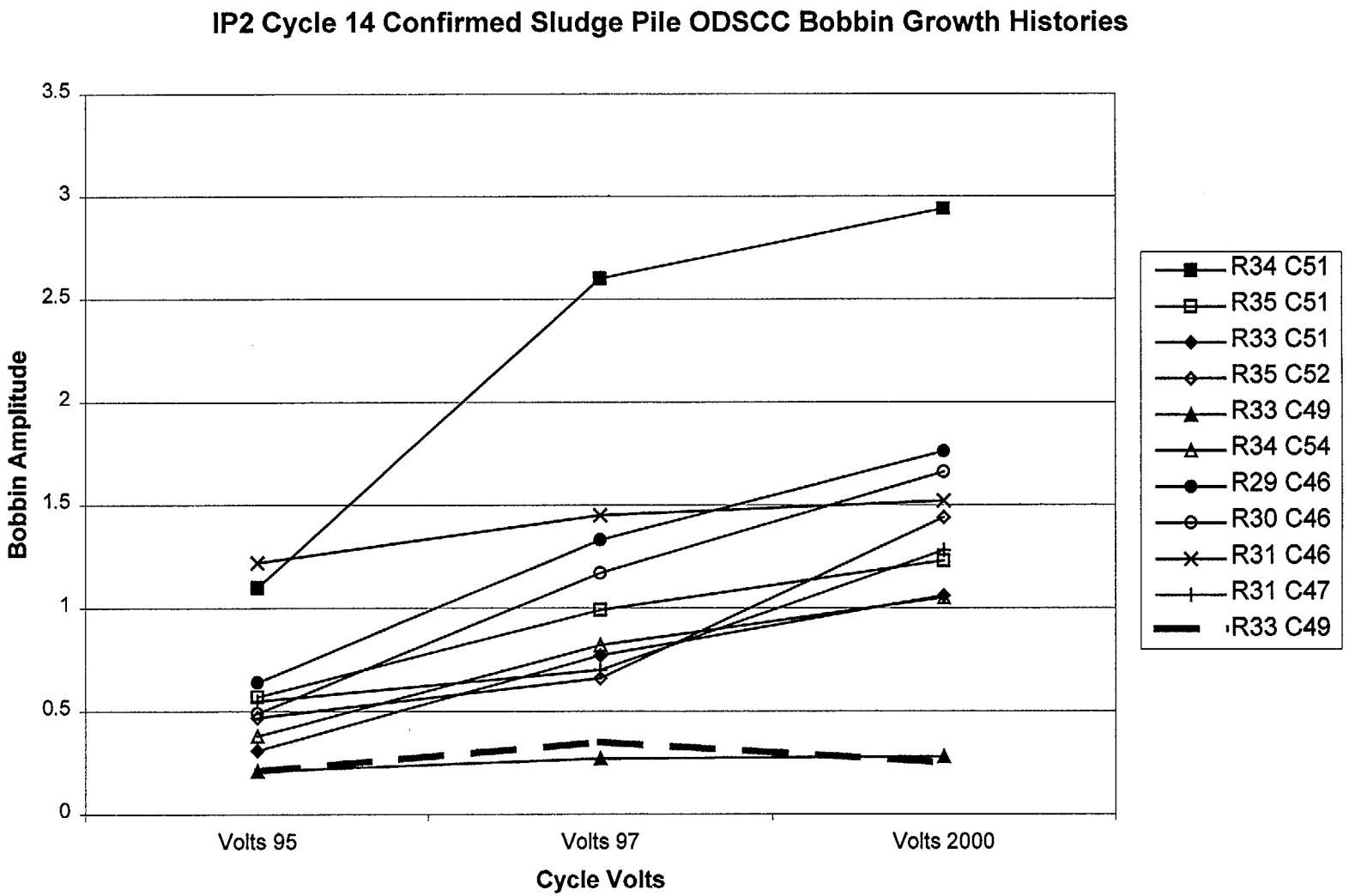
IP2 Cycle 14 Confirmed Sludge Pile ODSCC Bobbin Growth Histories
Bobbin Amplitude
3.5
3
2.5
2
1.5
1
0.5
0
Volts 95
Volts 97
Volts 2000
Cycle Volts
R34 C51
R35 C51
R33 C51
R35 C52
R33 C49
R34 C54
R29 C46
R30 C46
R31 C46
R31 C47
R33 C49

Figure 4.5 - 2

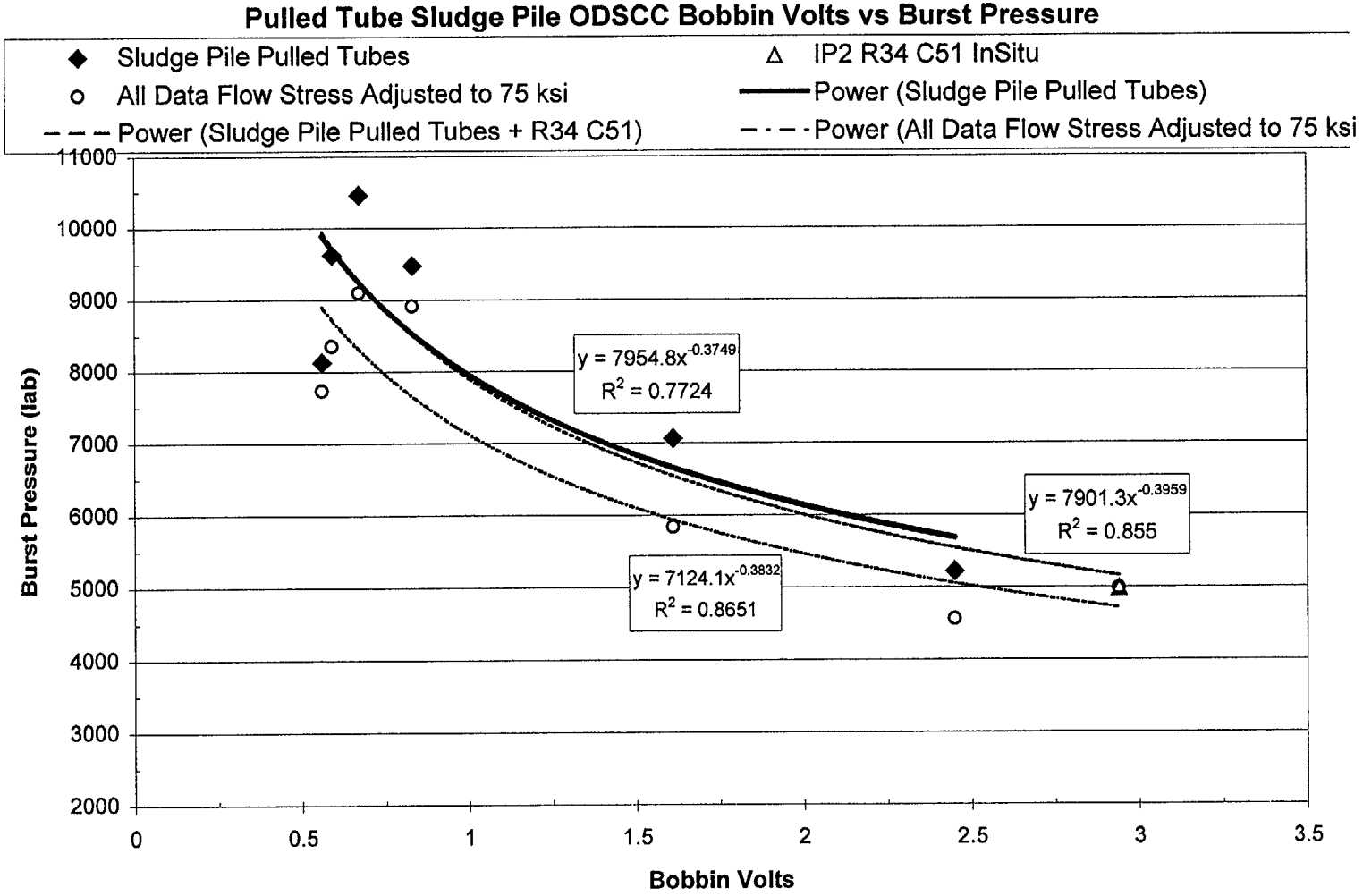
Pulled Tube Sludge Pile ODSCC Bobbin Volts vs Burst Pressure
Sludge Pile Pulled Tubes
IP2 R34 C51 InSitu
All Data Flow Stress Adjusted to 75 ksi
Power (Sludge Pile Pulled Tubes)
Power (Sludge Pile Pulled Tubes + R34 C51)
Power (All Data Flow Stress Adjusted to 75 ksi
y = 7954.8x^-0.3749
R2 = 0.7724
y = 7901.3x^-0.3959
R2 = 0.855
y = 7124.1x^-0.3832
R2 = 0.8651
Burst Pressure (lab)
Bobbin Volts
11000
10000
9000
8000
7000
6000
5000
4000
3000
2000
0
0.5
1
1.5
2
2.5
3
3.5

Figure 4.5-3
Sludge Pile ODSCC Average Depth Growth Rate per EFPY
Thot = 590 Degrees

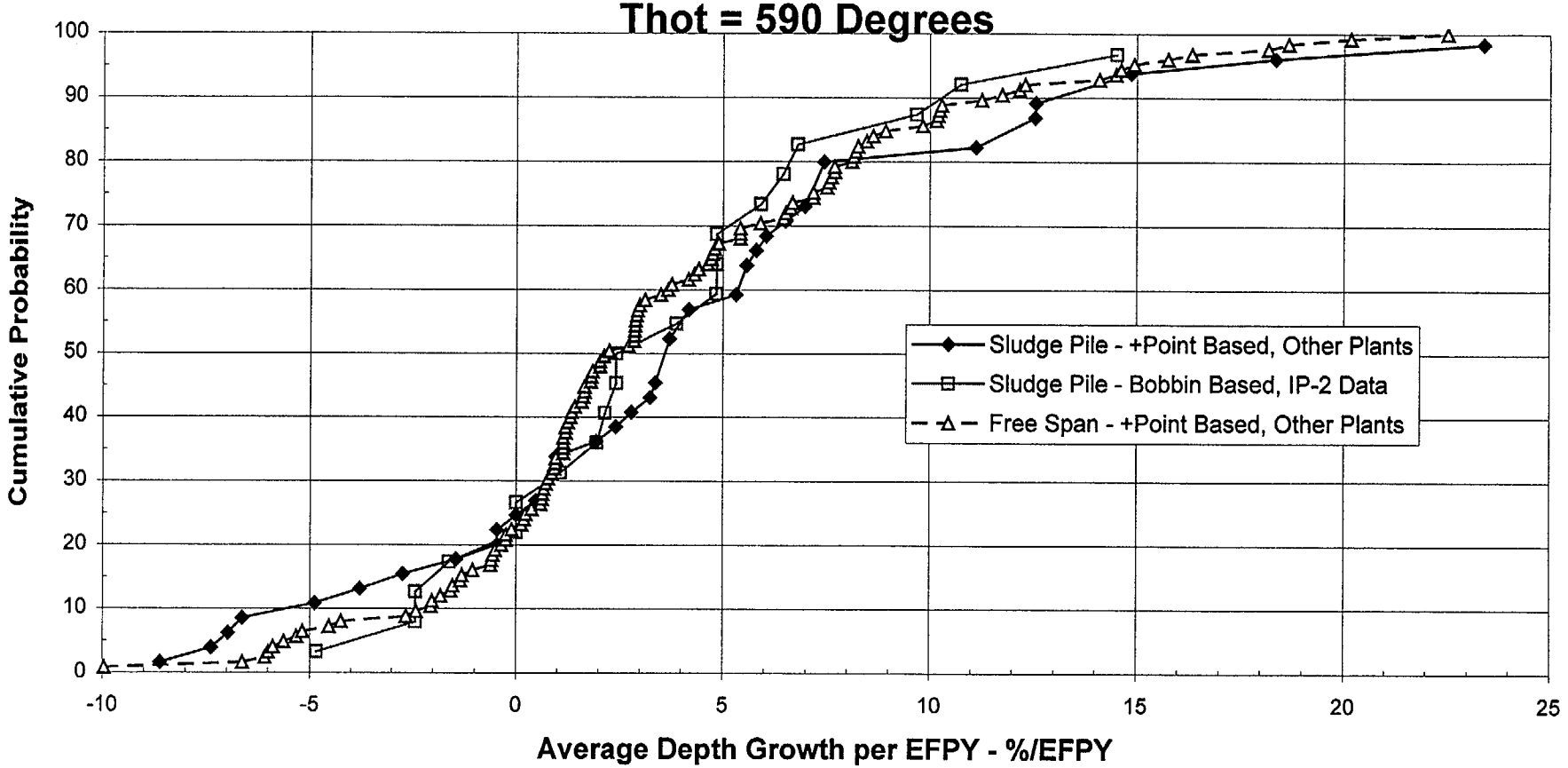

Figure 4.5-4. Indian Point-2 Sludge Pile ODSCC Average Depth True Growth Distribution

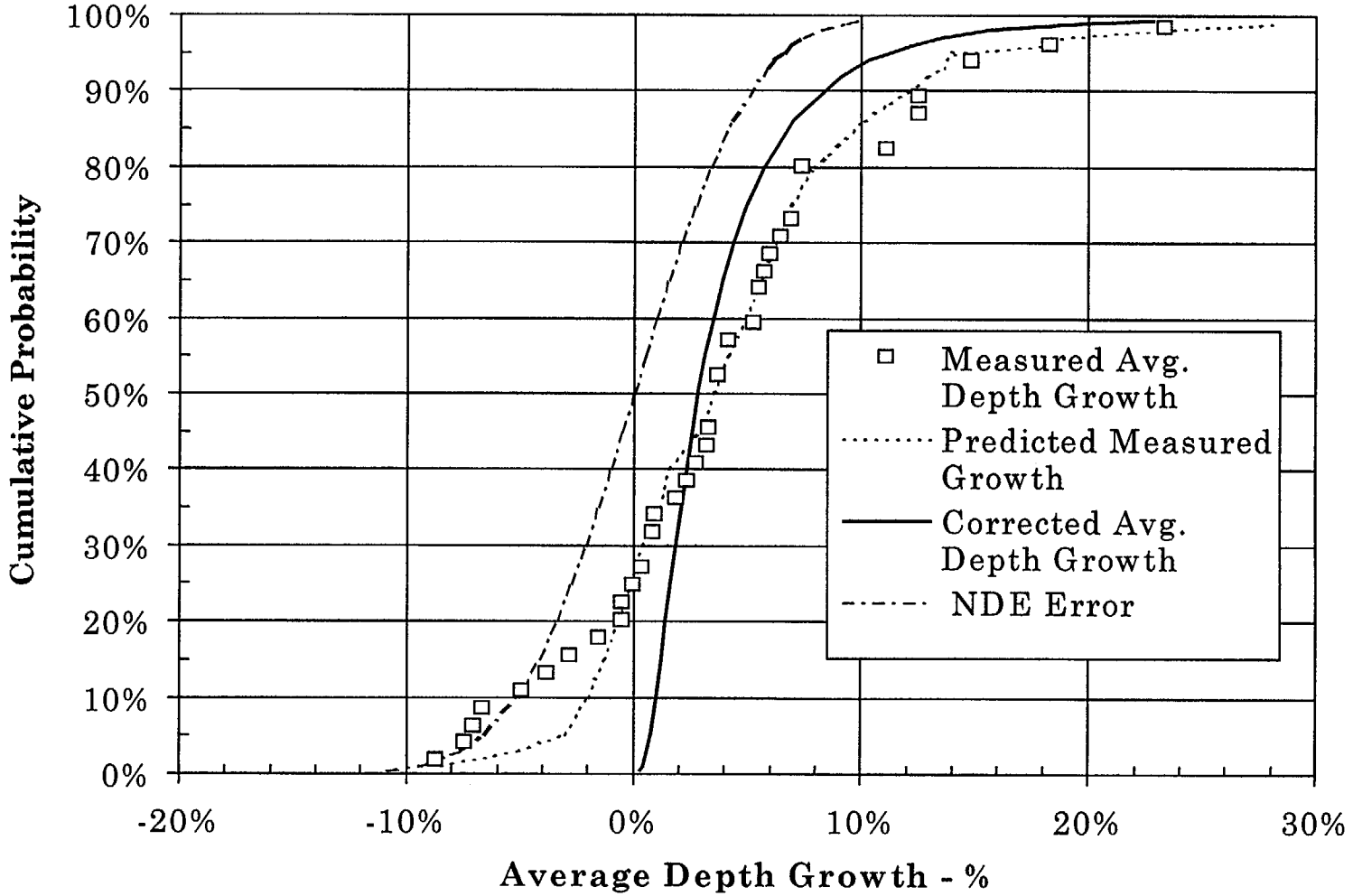

Figure 4.5-5. Indian Point-2 Sludge Pile Average Depth Growth Data and Bounding Distribution

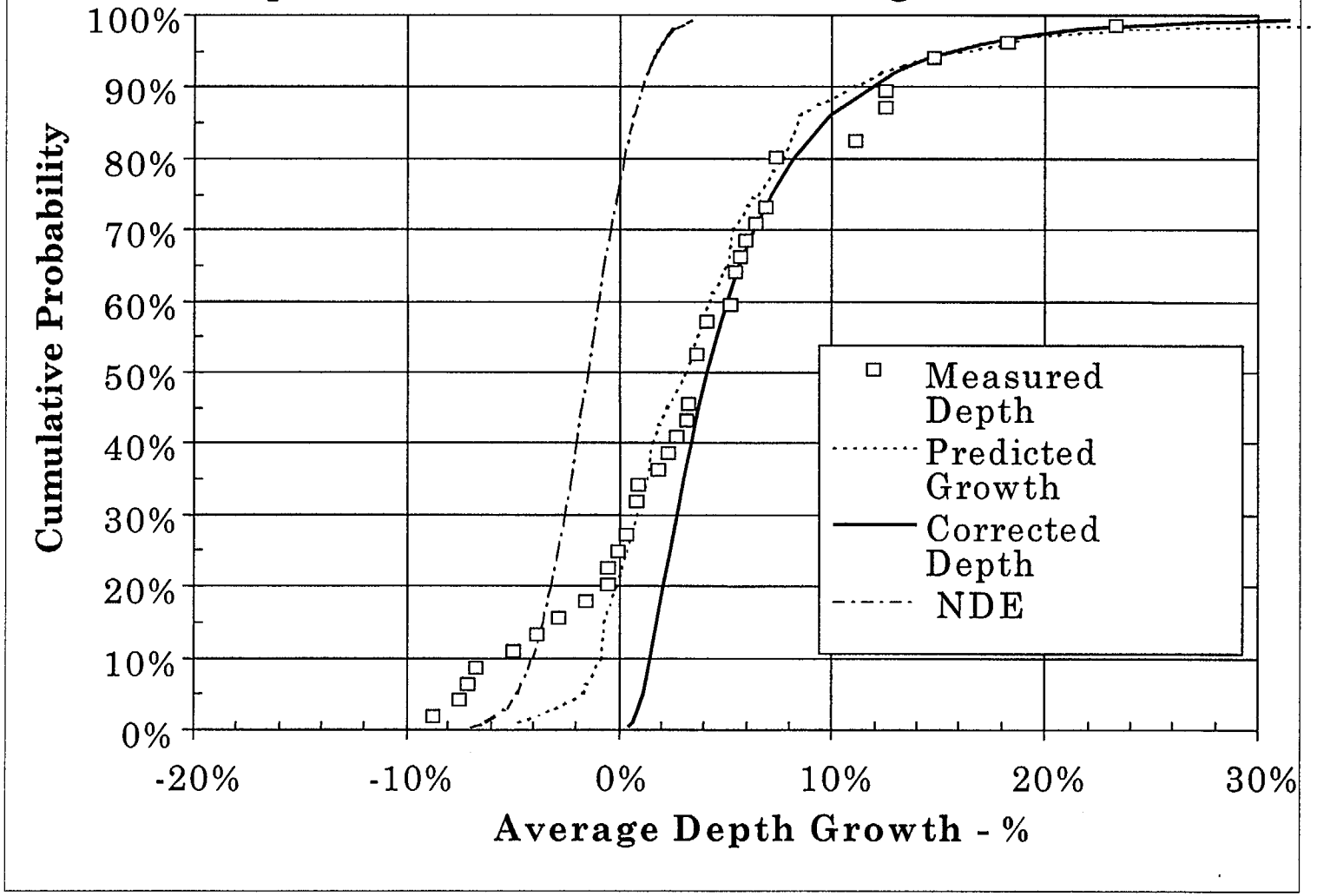

Figure 4.5-6. Indian Point-2 Sludge Pile Length Growth Data and Bounding Distribution

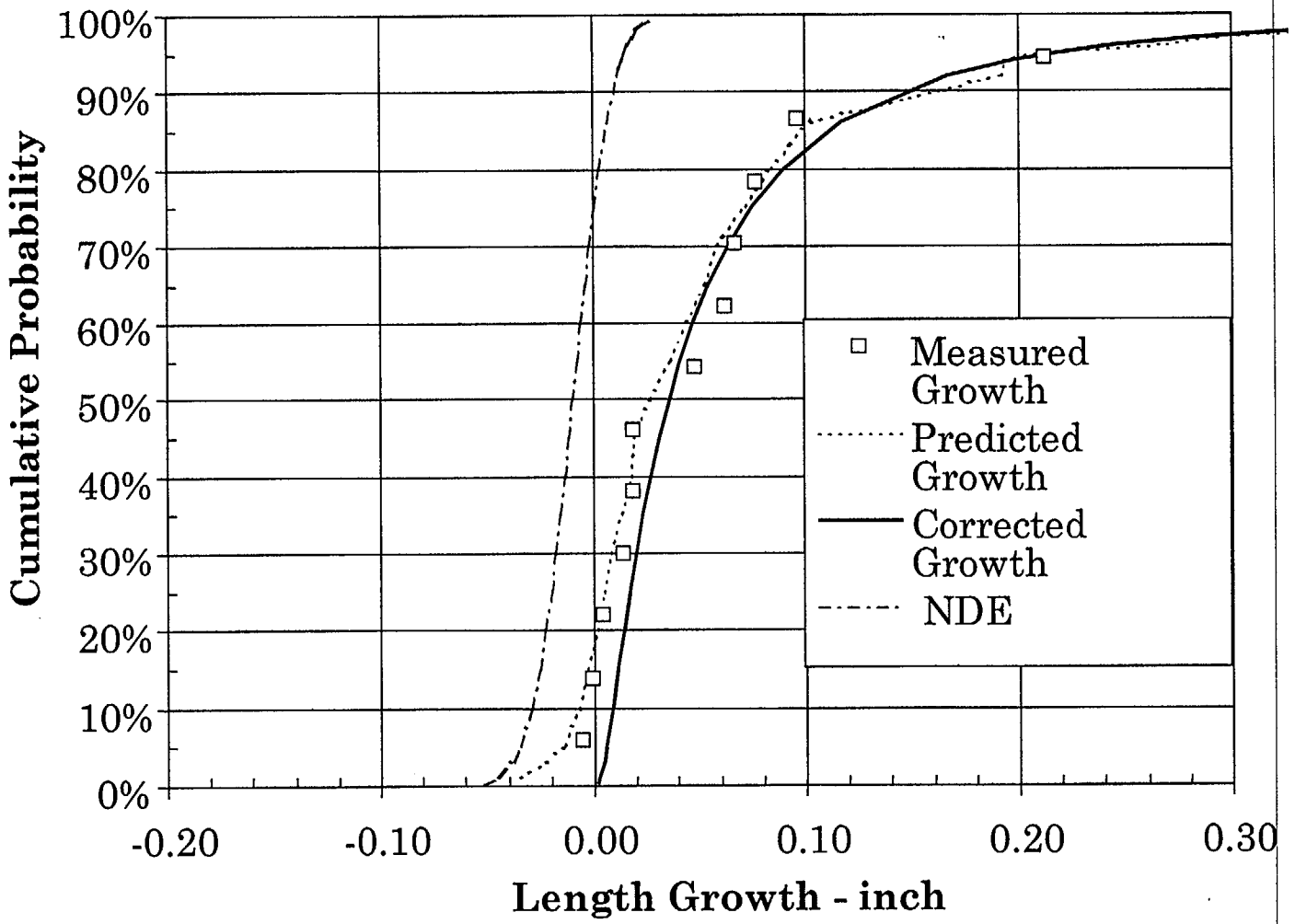

5 Condition Monitoring for Degradation Mechanisms Excluding U-bend PWSCC

The condition monitoring evaluations below apply only to indications below the U-bend region of the SGs. A separate Condition Monitoring and Operational Assessment for the U-bends is provided by Reference 1.

5.1 In-situ Testing Recommendations

Tubes considered for in-situ testing are identified using the guidelines outlined in EPRI TR-107620-R1 "Steam Generator In-Situ Pressure Test Guidelines", Revision 1 (June 1999). Tables were prepared for the specific conditions at IP2. The criteria for selecting tubes with cracks are well-defined and explicitly stated, while those for pitting, wear, and other volumetric indications are based on the expected NDE responses for simulated flaws, such as ASME drilled holes, uniform thinning, and wear scars of pertinent geometries. For tubes with U-bend or straight-length non-through-wall cracks above the tubesheet, graphical relationships (see Figures 5-1 and 5-2) were defined to determine which tubes exceed the threshold depth-length combination for burst.

Since the Spring 2000 outage was initiated as a forced outage associated with a leaking Row 2 U-bend (SG24 R2/C5), all tubes that were identified as exhibiting cracks in the small radius U-bends as well as several tubes without crack indications but in close proximity to tubes with U-bend cracks were subjected to whole tube in-situ pressure testing; the latter group included 1 Row 3 tube in SG 21that was adjacent to a cracked Row 2 tube (2/87). The CMOA for the U-bend cracking was issued as a separate report (Indian Point 2 U-bend PWSCC Cycle 14 Condition Monitoring and Cycle 15 Operational Assessment, Reference 1).

5.1.1 IP2 SG 22 In-Situ Testing Screening for Axial Cracks

In-situ Screening Process (Proof of Pressure)

1.Length: Does the field reported length exceed the structural limit (L_{STR} = 0.42")?

2. Depth: Does the maximum depth of the indication (MD) as reported from the profile analysis exceed the threshold maximum depth (adjusted for NDE uncertainty) for burst pressure (MD_{THR-P} = 62% for ODSCC, 59% for PWSCC)?

3. Average depth: Did the average depth (AD) for the burst effective crack length[1] as determined from profile evaluation of the indication exceed the length - specific average depth threshold as given in Figures 5.1-1 (ODSCC) and 5.1-2 (PWSCC)?

In-situ Screening Process (Leak Testing)

1. Voltage: Does the maximum +Point signal amplitude (VM) as reported from the profile analysis exceed the threshold amplitude criterion (V_{THR} = 2.00V for PWSCC, 1.50V for ODSCC)?

2. Depth: Does the maximum depth of the indication (MD) as reported from the profile analysis exceed the threshold maximum depth for leakage (MD_{THR-L} = 80% for PWSCC, 75% for ODSCC)?

Based on the process described above, tubes with maximum length, depth and voltage were selected for profiling; the tubes with the maximum depth voltage, length, and average depth based on the profile analysis were considered for in situ testing, subject to the following feasibility limitations: Tubes that could not be accessed by the in-situ test equipment and those with cracks below the sealing height limit (~ 6" above the tube end) for full tube testing gear were not tested. Based on the adjusted NDE profiles, no tubes exceeded the requirements for proof-of pressure in-situ testing; however when burst effective length vs depth relationships were derived from the adjusted profiles, 1 tube (SG22 R34C51-TSH+0.89") in the population outside of the small radius U-bend sections of Rows 2 and 3 satisfied the proof of pressure screening criteria identifying tubes required to be tested. All tubes identified with sludge pile cracks (and U-bend cracks) were subjected to in-situ proof of pressure testing.

Tubes with crack indications in the tubesheet crevices were exempted from proof of pressure testing, since the tubesheet restrains burst in that geometry. Several tubes with tubesheet cracks were tested for leakage at Steam Line Break pressure differentials (Section 5.2.2) with no leakage observed. These tubes were chosen based on maximum depth and maximum voltage, since the burst effective length was not a determining factor. None of those with sufficient amplitude (see bullet item 1 above for leak testing) were required to be tested, since their lengths at depths exceeding the depth criteria for leakage (see bullet item 2 for leak testing) did not exceed 0.1", the depth screening criteria.

[1] Burst Effective Crack Length is the partial flaw length that provides the lowest predicted burst pressure.

5.1.2 IP2 SG 22 In-Situ Testing Screening for Circumferential Cracks

Circumferential cracks were observed in the lower reaches of the tubes, at or below the roll transitions. Given their location in the partially expanded region of the tubesheet, there was no requirement for proof of pressure testing. All the tubes so affected were subject to evaluation for repair by re-rolling; in this process the establishment of a sufficient length of expanded sound tubing above these cracks removed them from consideration for leak testing, since they were governed by the provisions of the F* alternate repair criteria. The screening criteria for circumferential cracking are shown in Table 5.1-1. The criteria for leak testing, maximum voltage ≥ 3.0 volts for both PWSCC and ODSCC, which would have warranted the in-situ testing of several tubes, could not be applied because of the proximity of the tube end to the location of the indications on those tubes.

5.1.3 IP2 SG 22 In-Situ Testing Screening for Non-crack Indications

The criteria for repair of tubes with volumetric indications, such as pitting (PIT), Intergranular Attack (IGA), AVB wear, and loose parts wear, are based on the bobbin and +Point responses to such indications compared to the expected responses from uniform thinning and/or ASME 100% drilled hole flaws. Table 5.1-2 details the selection logic for volumetric indications. None of the confirmed PIT indications satisfied both the bobbin and +Point depth screens.
The largest deepest and longer volumetric indications were reviewed to permit selection of "worst case" indications for discretionary in-situ testing; none of the tubes tested (see Section 5.2.4) exhibited leakage during the tests. Section 5.2.4 also lists the tubes found with VOL (volumetric) indications that were in-situ tested. It is likely that most of the VOL indications represented pitting indications. There was no positive assessment that any of the indications observed were representative of IGA. Since all the sludge pile crack indications – except SG22 R34/C51, were tested and found to be leak-free, there is no unresolved issue relative to tube integrity arising from IGA.

It should be noted that SG22 R31/C15 was originally tested as one of the sludge pile crack indications; however, profile analysis indicated that the tube was in reality a wear scar. Comparison of the eddy current data with the Table 5.1-2 criteria suggest that this tube might not have required testing since there was no bobbin call; the selection rules did not regard as credible that a significant volumetric degradation indication in the freespan could escape identification with the bobbin probe. The burst effective length (0.9") of the wear scar exceeded 0.7" and the width was less than 53° azimuthal extent, representing a scar dimensionally more like a crack than elliptical wastage. +Point depth estimates (based on crack depth sizing) and average depth (53.6%) were sufficient to warrant testing had both depth screens been satisfied. The voltage measurement (1.8V) did not exceed 80% of equivalent voltage for a 100% ASME drilled hole. As the in-situ test result established, a wear scar of these dimensions does not pose a challenge to structural integrity.

There were no tubes with AVB wear scars that exceeded the repair limit; therefore none qualified for in-situ testing and none were tested.

5.1.4 Summary of In-situ Tests Performed and Results

Table 5.1-3 summarizes the in-situ tests that were performed for all degradation mechanisms in all four SGs. The low row U-bend tests are included in this table; however, discussion of the U-bend tests is provided by Reference 1. Fifty-one tubes were in-situ tested: 8 tubes in SG-21, 16 tubes in SG-22, 11 tubes in SG 23, and 16 tubes in SG-24. Figure 5.1-3 illustrates the results of those sludge pile indications whose structural evaluation gave results near the in-situ testing criteria as taken from Figure 5.1-1. Among these 51 tubes tested, only one with indications unrelated to U-bend PWSCC, SG-22, R34C51, met the screening criteria for in-situ testing as noted above; there were 3 indications that satisfied the testing criteria on this tube, representing all of the points above the curve in figure 5.1-3. All other tests were conservatively performed to support demonstration of tube integrity.

Three low row U-bends, R2C84, R3C87 and R2C88 in SG 21, were tested that were NDD during the inspection in an attempt to open potentially missed indications. No leakage was observed during the tests of these three tubes, and no indications were observed during posttest NDE of these tubes. The details of these tests are discussed in Reference 1.

The test pressure applied for indications tested to $3\Delta P_{NO}$ was at 5173 psi or greater. As noted in section 4.1, the normal operating pressure differential is 1539 psi. Application of the temperature correction factor, 1.0921, to account for the material property differences between operating temperature and room temperature, the room temperature equivalent $3\Delta P_{NO}$ pressure is 5042 psi. Thus, the applied in-situ test pressure for $3\Delta P_{NO}$ was conservative. Similarly, to simulate SLB pressure differential, an in-situ test pressure of 2844 psi was applied for constrained cracks (i.e., tubesheet crevice cracks). Except for tube R34C51 in SG-22, and several U-bend indications discussed in Reference 1, all indications tested exhibited no leakage at the applied test pressures, either $3\Delta P$ or SLB pressure differentials as appropriate. Tube R34C51 is discussed in detail in Section 5.2, below.

All in-situ tests performed were full tube length tests, not tests confined to a local area of the tube. Among the 51 tubes tested, the only reported leakage was in R34C51, and three U-bends tested. None of the other tubes leaked at either the indication for which the test was performed or at any other location along the tube. Thus, the full tube in-situ tests provide added confidence that no significant indications were missed during the SG inspections.

Post in-situ test visual examination was performed for Tube R34C51 utilizing a video camera to visualize the crack opening. Figure 5.1-4 shows photographs of the crack opening, including a closeup of the crack tip. The bottom of the crack opening is not visible due to an apparent bulge in the tube (possible dent at the top of the tubesheet); however, the observable characteristics of the crack opening are consistent with ligament tearing coalescing parallel cracks in a network of cracks. The torn ligaments are clearly visible in the closeup of the crack tip. Analysis of the photograph of the crack opening indicates that the crack opening is approximately 0.16 inch.

Table 5.1-1

Updated Table E-4 – EPRI Circumferential Guidelines for In Situ Testing In-Situ Screening Parameters (EPRI TR-107620) IP 2 Specific Values for 3ΔP = 4617 psi (operating conditions)		
Parameter	**Westinghouse 7/8" OD, 0.050" Wall Thickness Tubing**	
	PWSCC	**ODSCC**
Crack Angle: CA_{TWSL}	**216°(1)**	**216°(1)**
PDA • **PDA_{SL}** • **PDA_{THR}**	**71%** (3) **23%**	**71%** (3) **23%**
Avg. Volts; +Point(2) • **AV_{SL}** • **AV_{THR}**	**Undefined** **0.3**	**Undefined** **0.3**
Max. Volts; +Point(2) • **VM_{THR}** • **VM_{PLL}**	**1.5** **3.0**	**1.00** **3.0**
Max. Depth • **DM_{THR}**	**75%**	**70%**

Notes:

1. Represents a conservative threshold angle compared to structural limit of about 237° for a throughwall crack.
2. Voltages given are vertical amplitudes obtained using EDDYNET95 voltage integral software.
3. Based on lower 95% structural limit at LTL material properties. OD and ID are the same since throughwall crack is assumed

Table 5.1-2

In-situ Leak and Proof Pressure Test Screening Criteria for IP 2: Volumetric Indications

<table>
<tr><td>Bobbin Maximum Depth</td><td>AVB Wear: 65%
Pitting: 53%
IGA: 50%</td><td>If the observed bobbin maximum depth does not exceed these values, leak test only if the signal voltage exceeds 4.5 volts (80% of single 100% through wall ASME hole.</td></tr>
<tr><td>MRPC Maximum Depth

(+Point depth sizing should be based on ASME FBH standard or other volumetric (e.g., wear) standards.</td><td>AVB Wear: 65%
Pitting: 53%
IGA: 50%</td><td>If the observed +Point maximum depth does not exceed these values, leak test if the signal voltage exceeds 80% of +Point response for a single 100% through wall ASME hole.</td></tr>
<tr><td rowspan="3">+Point Axial Length:

(For indications that satisfy both bobbin and +Point depth criteria.)</td><td>If the axial length > 0.7”</td><td>Perform leak test and proof pressure test.</td></tr>
<tr><td rowspan="2">If the axial length is not > 0.7”</td><td>Compare to length/depth table; if indications exceeds criteria, perform leak test and proof pressure test.</td></tr>
<tr><td>If indication does not exceed criteria in length/depth table, leak test in the signal voltage exceeds 80% of +Point response for a single 100% through wall ASME hole.</td></tr>
<tr><td colspan="3">Average Depth Vs Axial Length

<table>
<tr><th rowspan="2">Axial Length</th><th rowspan="2">AVB Wear</th><th colspan="2">IGA</th><td rowspan="3">Pitting:

Structural Limit: 85% (NSD-E-SGDA-99-448); with NDE error @ 32%, leak test if voltage > 80% of +Point or bobbin response for a single 100% through wall ASME hole.</td></tr>
<tr><th>Elliptical Wastage</th><th>Uniform Thinning</th></tr>
<tr><th>< 100°</th><th>≥ 100°</th></tr>
<tr><td>Up to 0.375”</td><td>N/A</td><td>55%</td><td>49%</td><td></td></tr>
<tr><td>0.376” to 0.500”</td><td>64%</td><td>54%</td><td>44%</td><td></td></tr>
<tr><td>0.501” to 0.625”</td><td>N/A</td><td>53%</td><td>40%</td><td></td></tr>
<tr><td>0.626” to 0.750”</td><td>N/A</td><td>52%</td><td>38%</td><td></td></tr>
</table>
</td></tr>
<tr><td colspan="3">If any indication fails the proof pressure test, proof pressure test at least 5 additional indications per each failed indication as follows:
(1) Indications exceeding maximum bobbin and +Point depth with the largest average depth;
(2) Indications with bobbin depths > above criteria with largest average depth but with +Point depths < above criteria;
(3) Indications with largest lengths</td></tr>
</table>

Table 5.1-3
In-situ Test Results

Steam Generator 21

SG	Row	Col	Probe	I_typ	Per	Loc	Inch1	Volts	Deg	Tape	Axial (in)	C-5/ Bobbin Call	Indication #	Max. Volts	Max. % TWD	Length (in)	PDA (%TWD)	Burst Effective Length (in)	PDA For Burst Indication	In-situ test required?	Leak	Test Pressure
21	16	6	720-ZP	VOL		TSH	0.94	0.32	98	441	0.24	1.53V NQI	1	0.45	55	0.38	39.1	0.30	42.4	No	0	5173
21	10	17	720-ZP	PIT		TSH	0.25	0.56	102	421	0.57		1	0.54	53	0.22	38.3	0.18	42.1	No	0	5173
21	34	41	720-ZP	SAI		TSH	0.47	0.29	107	531	0.21		1	0.26	56.5	0.54	38.2	0.41	43.9	No	0	5173
21	4	67	720-ZP	SAI		TEH	9.92	1.81	94	453	2.18		1	1.93	79	3.89	42.7	0.71	64.6	No	0	2844
21	2	84	620-ZPUHF	NDD								NA	U-bend Tube; see Reference 1									5223
21	2	87	620-ZPUHF	SAI		6H	7.13	1.03	27	54	0.307	NA	U-bend Tube; see Reference 1								0	5500
				SAI		6H	6.92	1.04	24	54	0.285	NA										
				SAI		6H	6.31	1.01	23	54	0.329	NA										
21	3	87	620-ZPUHF	NDD								NA	U-bend Tube; see Reference 1								0	5173
21	2	88	620-ZPUHF	NDD									U-bend Tube; see Reference 1								0	5173

Table 5.1-3 (continued)
In-situ Test Results

Steam Generator 22

SG	Row	Col	Probe	I_typ	Per	Loc	Inch1	Volts	Deg	Tape	Axial (in)	C-5/ Bobbin Call	Indication #	Max. Volts	Max. % TWD	Length (in)	PDA (%TWD)	Burst Effective Length (in)	PDA For Burst Indication	In-situ test required?	Leak	Test Pressure
22	30	13	680-ZP	VOL		TSH	0.33	0.89	124	261	0.28	74%, 3.15V	1	1.44	37	0.35	25.6	0.19	32.4	No	0	5173
22	31	15	700-ZPANM	VOL		TSH	0.58	1.85	95	509	0.96		1	1.8	63	2.32	35.0	0.9	56.5	No	0	5173
				VOL		TSH	0.58						2	1.02	62	0.44	52.1	0.38	56.1	No		
22	37	20	700-ZP	PIT		TSH	4.2	1.8	104	511	0.58	37%, 4.66V	1	1.64	61	0.57	42.9	0.29	56.3	No	0	5173
22	3	24	680-ZP	MAI	78	TEH	10.49	3.36	73	261	2.11	5.24V PI	7	2.91	75	1.96	33.2	0.4	62.9	No	0	2481
				MAI	58	TEH	8.74	0.37	101	261	1.01	0.57V NQI	6	0.6	60	1.03	41.1	0.82	46.8			
				MAI	58	TEH	8.74					O.34V NQI	5	0.60	48	0.57	19.9	0.31	29.9			
				MAI	77	TEH	5.52	3.81	75	261	1.52	0.74V NQI	4	2.67	68	0.87	47.1	0.47	58			
				MAI	77	TEH	5.52					5.65V NQI	3	0.51	35	0.99	21.4	0.28	28.0			
				MAI	62	TEH	4.64	1.27	96	261	0.18	2.39V PI	2	1.21	57	0.32	41.1	0.24	49.1			
				MAI	60	TEH	4.28	1.21	99	261	0.43	2.3V NQI	1	0.96	52	0.33	29.4	0.19	41.6			
22	13	26	700-ZP	PIT		TSH	16.76	1.18	41	523	0.36		1	0.33	73	0.18	43.8	0.18	43.8	No	0	5173
				PIT		TSH	17.25	1.48	108		0.29		2	0.25	30	0.08	15	0.08	15			
22	32	48	680-ZP	SAI		TSH	0.73	0.16	135	305	0.44	0.8V NQI	1	0.16	62	0.28	35.29	0.23	37.80	No	0	5173
22	33	49	720-ZP	SAI		TSH	1.24	0.19	114	509	0.44	1.42V NQI	1	0.18	38	0.4	22.05	0.31	25.85	No	0	5173
22	33	51	680-ZP	SAI	48	TSH	1.08	0.4	98	293	1.27	7.98V PI	1	0.39	47	0.77	34.3	0.53	42.1	No	0	5173
				SAI	48	TSH	1.08						2	0.69	51	0.69	35.5	0.49	43.3	No		
				SAI	48	TSH	1.08					0.99V NQI	3	0.47	47.5	0.7	30.8	0.46	36.6	No		
22	34	51	680-ZP	MAI	66	TSH	0.89	0.69	90	259	1.67	0.52V NQI	1	0.88	68	1.26	63.5	1.16	65.8	Yes		4678*
				MAI	66	TSH	0.89						2	0.89	69	1.35	65.3	0.54	77.4	Yes	.0027 gpm	
				MAI	66	TSH	0.89						3	0.55	75	0.59	60.7	0.49	65.9	Yes		
22	35	51	680-ZP	MAI	54	TSH	0.44	0.54	101	259	0.75	65.3V PI	1	0.59	62	0.51	44.2	0.39	62.0	No	0	5173
				MAI	54	TSH	0.35						2	0.46	62	0.67	31.1	0.58	33.5	No		
22	35	52	680-ZP	MAI		TSH	0.75	0.4	71	259	0.4	1.42V NQN	1	0.55	30	0.42	11.3	0.22	17.5	No	0	5173
22	33	54	720-ZP	SAI		TSH	0.81	0.81	116	473	0.42		1	0.33	30	0.26	15.8	0.13	22.7	No	0	5173

* Pressure at initial leakage; Leakage of .0089 gpm at 4985 psi, with sudden depressurization above 4985 psi.

Table 5.1-3 (continued)
In-situ Test Results

Steam Generator 22 (continued)

SG	Row	Col	Probe	I_typ	Per	Loc	Inch1	Volts	Deg	Tape	Axial (in)	C-5/ Bobbin Call	Indication	Max. Volts	Max. % TWD	Length (in)	PDA (%TWD)	Burst Effective Length	PDA For Burst Indicatio	In-situ test	Leak	Test Pressure
22	34	54	680-ZP	MAI MAI		TSH	0.87	0.43	139	259	0.72	5.28V PI	1	0.75	40	0.19	18.9	0.14	24.3	No	0	5173
						TSH	0.87						2	0.19	30	0.11	20.2	0.09	22.5	No		
						TSH	0.87					1.03V NQI	3	0.56	30	0.27	16.8	0.15	26.3	No		
22	5	55	680-ZP	PIT		TSC	1.45	0.72	127	226	0.22	1%, 3.62V	1	0.83	33	0.22	15.3	0.1	23.7	No	0	5173
22	41	61	720-ZP							487										No	0	5173

Table 5.1-3 (continued)
In-situ Test Results

Steam Generator 23

23	2	85	620-ZPUHF	SAI		6H	5.93	1.36	27	240	0.197	NA	U-bend Tube; see Reference 1							No	0	5500
SG	Row	Col	Probe	I_typ	Per	Loc	Inch1	Volts	Deg	Tape	Axial (in)	C-5/ Bobbin Call	Indication #	Max. Volts	Max. % TWD	Length (in)	PDA (%TWD)	Burst Effective Length (in)	PDA For Burst Crack	In-situ test required?	Leak	Test Pressure
23	20	34	720-ZP	PIT		TSC	0.64	0.41	58	340	0.22		1	0.47	30	0.14	8.9	0.06	17.2	No	0	5173
23	29	46	680-ZP	MAI	40	TSH	0.97	0.47	106	227	0.18		1	0.47	44	0.27	31.6	0.21	37.1	No	0	5173
				MAI	17	TSH	1.27	0.21	118	227	0.19		2	0.27	30	0.37	17	0.16	23.6			
				MAI	17	TSH	1						3	0.34	30	0.31	19.6	0.26	21.9			
23	30	46	680-ZP	MAI	72	TSH	0.46	0.11	88	227	1.03		1	0.32	33	0.75	22.9	0.49	27.9	No	0	5173
23	31	46	680-ZP	MAI	42	TSH	0.5						2	0.46	31.3	0.49	20.8	0.35	24.5	No	0	5173
				MAI	42	TSH	1.35	0.66	109	227	1.05		1	0.56	62.5	1.08	46.3	0.93	48.9			
23	31	47	680-ZP	SAI	31	TSH	0.52	0.56	112	227	0.54		1	0.56	30	0.59	18.0	0.32	24	No	0	5173
				SAI	31	TSH	0.9						2	0.46	47.5	0.27	31.8	0.21	38.2			
				SAI	85	TSH	1.59	0.2	73	227	0.21		3	0.31	45	0.21	23.6	0.17	27.4			
23	8	61	680-ZP	PIT		TSC	3.75	0.53	83	86	0.18	59%,	1	0.31	51.3	0.20	35.1	0.15	42.5	No	0	5173
23	10	72	720-ZP	PIT		TSC	1	0.62	113	350	0.19	3%, 2.79V	1	0.74	75.5	0.26	45.2	0.20	50.4	No	0	5173
				PIT		TSC		0.74	101	350	0.13		2	0.9	57	0.15						
23	19	73	720-ZP	MAI		TEH	6.23	0.29	112	561	0.432		1	0.2	30	0.350.	16.7	0.25	22	No	0	2841
				MAI		TEH	7.31	0.32	115	561	1.047		2	0.2	30	0.54	22.6	0.17	23.8			
				MAI		TEH	8	0.17	118	561	0.585		3	0.22	31	0.43	23.5	0.20	25.7			
				MAI		TEH	8.59	0.09	127	561	0.77		4	0.14	30	0.29	22.8	0.23	26.4			
				MAI		TEH	8.59						5	0.11	30	0.26	22	0.23	25			
				MAI		TEH	12	0.27	81	505	3.28		6	0.38	30	3.10	21	0.74	23.6			
				MAI		TEH	12.4						7	0.4	30	2.8	22.6	0.60	26.4			
23	33	77	720-ZP	VOL		TSH	18.7	0.72	108	507	0.56		1	0.84	32	0.34	10.8	0.23	14.3	No	0	5173
23	3	88	700-ZP	SAI		TSH	9.84	0.13	116	529	3.77		1	0.18	30	2.28	12.2	0.74	21.3	No	0	5173

Table 5.1-3 (continued)
In-situ Test Results

Steam Generator 24

SG	Row	Col	Probe	I_typ	Per	Loc	Inch1	Volts	Deg	Tape	Axial (in)	C-5/ Bobbin Call	Indication #	Max. Volts	Max. % TWD	Length (in)	PDA (%TWD)	Burst Effective Length (in)	PDA For Burst Crack	In-situ test required?	Leak	Test Pressure
24	2	4	620-ZPUHF	SAI		6H	5.88	1.46	24	218	0.119	NA	U-bend Tube; see Reference 1							No	0	5173
24	8	23	720-ZP	VOL		TSC	0.25	0.56	56	320	0.36	0%, 0.97V	1	0.23	52	0.20	28.1	0.14	38.5	No	0	5173
24	30	27	720-ZP	SAI		TSH	10.1	0.74	130	359	2.3		1	0.51	30	2.35	12.8	0.46	17.5	No	0	5173
24	26	31	680-ZPANM	MAI	61	TEH	3.9	1.37	91	225	1.34	5.75V PI	1	1.23	50.4	0.55	38.5	0.42	43.7	No	0	2841
				MAI	28	TEH	7.73	0.24	102	225	4.62	2.48V PI	2	0.17	30	0.22	19.9	0.18	22.6			
						TEH	7.4						3	0.13	30	0.18	17.7	0.14	21.0			
				MAI	1	TEH	9.3	0.17	108	225	1.11		5	0.28	30	0.95	16.5	0.35	23.2			
			720-ZMAGR	MAI		TEH	9.85	0.18	151	221			4	0.15	30	0.48	23.0	0.38	26.1			
24	24	34	680-ZP	VOL	6	TSH	12.11	0.13	118	203	0.218	4.75V		0.17	0	0.35				No	0	5173
				VOL	3	TSH	10.2	0.44	119	203	0.368	4.53V		0.13	0	0.27						
				VOL	6	TSH	8.3	0.21	118	203	0.288	17.38V		0.14	10	0.23						
				VOL	3	TSH	8.03	0.36	119	203	0.3	10.88V		0.1	0	0.32						
				VOL	3	TSH	6.39	0.36	119	203	0.323	14.83V		0.15	7	0.34						
24	21	42	680-ZP	VOL		TSC	3.28	0.14	94	180	0.34	34%, 1.33V	1	0.77	61	0.34	34.1	0.21	46.9	No	0	5173

Table 5.1-3 (continued)
In-situ Test Results

Steam Generator 24 Continued

SG	Row	Col	Probe	I_typ	Per	Loc	Inch1	Volts	Deg	Tape	Axial (in)	C-5/ Bobbin Call	Indication	Max. Volts	Max. % TWD	Length (in)	PDA (%TWD)	Burst Effective Length	PDA For Burst	In-situ	Leak	Test Pressure
24	42	43	680-ZP	SAI	18	TSH	0.39	0.09	116	211	0.38	2.98V TSI	1	0.22	30	0.35	17.6	0.35	17.6	No		5173
24	45	51	700-ZP	PIT		TSH	0.47	0.17	107	211	0.28	0.59V 78%		0.21	70	0.26				No	0	5173
				PIT		TSH	-0.1	0.21	118	211	0.17			0.15	33	0.22						
24	8	59	680-ZP	PIT		TSC	4.13	0.24	93	182	0.3	38%, 2.41V	1	0.23	51.5	0.20	28.1	0.14	36.5	No	0	5173
24	8	60		PIT	51	TSC	4.96	0.16	101	182	0.26	0.77V 28%		0.14	45	0.16				No	0	5173
24	17	63	680-ZP	PIT		TSH	4.7	0.27	98	217	0.31	1.06V 12%	1	0.30	53	0.15	36.6	0.13	41.0	No	0	5173
				PIT		TSH	5.54	0.32	116	217	0.22		2	0.37	30	0.11	15.5	0.08	19.9			
24	2	69	620-ZPUHF	SAI	75	6H	7.15	0.6	29	220	0.144	NA	U-bend Tube; see Reference 1									
				SAI	75	6H	5.93	1.74	29	220	0.781	NA										
24	2	71	620-ZPUHF	SAI		6H	6.12	3.62	25	220	0.263	NA	U-bend Tube; see Reference 1									
24	2	72	620-ZPUHF	NDD								NA	U-bend Tube; see Reference 1									
24	2	74	620-ZPUHF	SAI	51	6H	6.92	0.85	18	240	0.195	NA	U-bend Tube; see Reference 1									
24	10	87	720-ZP							461										No	0	5173
										509				54								

Figure 5.1-1

Condition Monitoring Burst Resistance Acceptance Limits

ODSCC of 7/8" x 0.050" Alloy 600 MA SG Tubes at 650°F

3DPno = 4.655 ksi, 95/50 Probability/Confidence

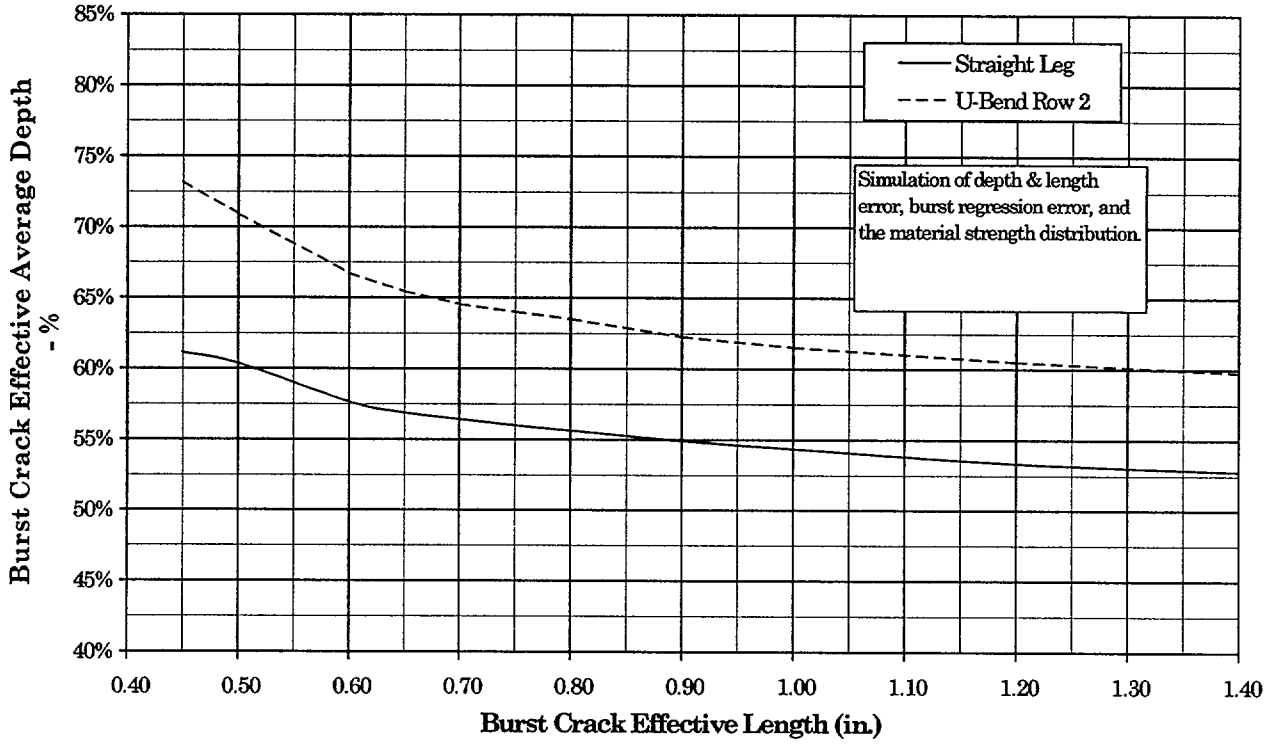

Notes:

1. These curves are based on a conservative pre-outage anticipated $3\Delta P_{NO}$ value of 4655 psi, rather than the actual IP2 value of 4617 psi.

Figure 5.1-2

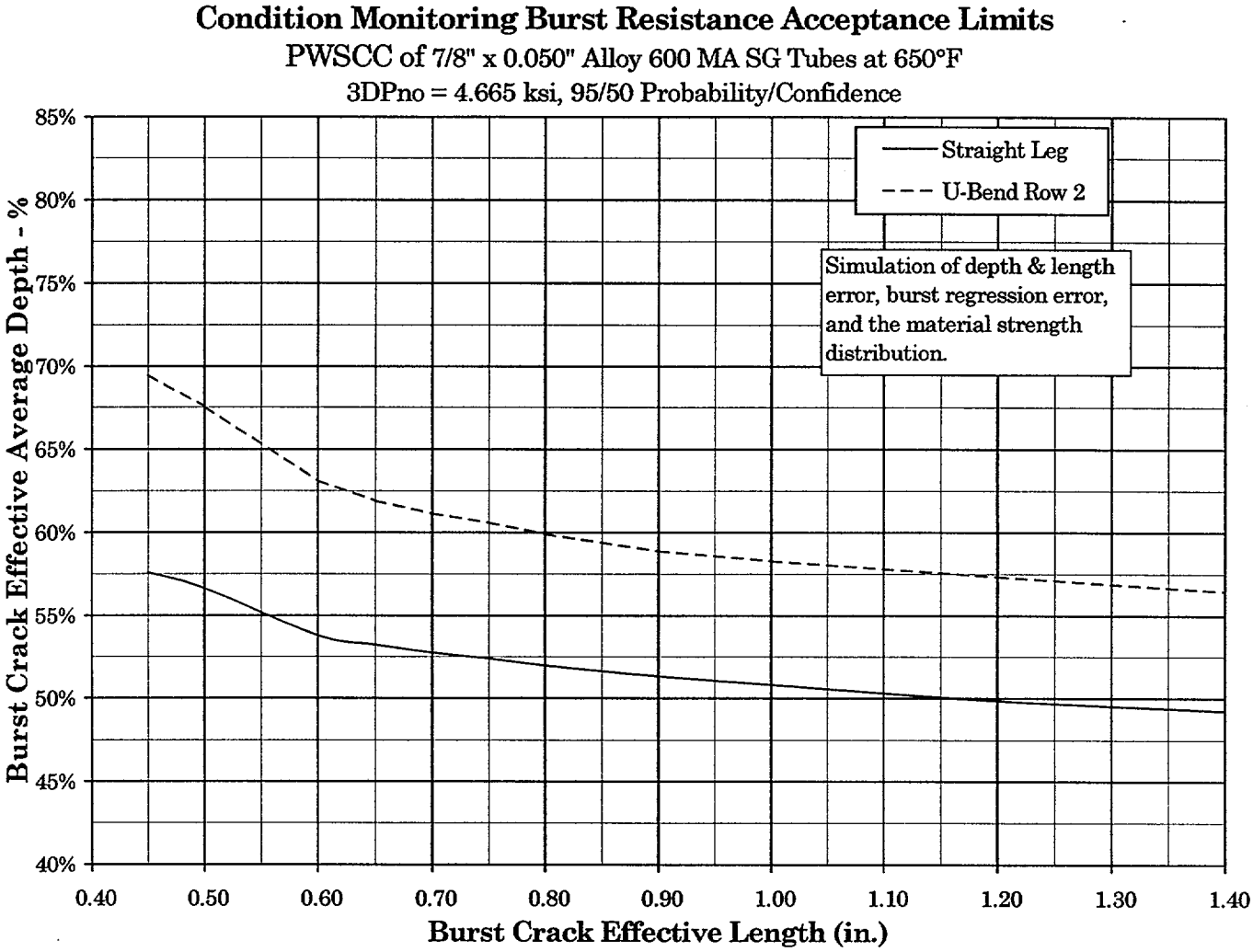

Notes:

1. These curves are based on a conservative pre-outage anticipated $3\Delta P_{NO}$ value of 4655 psi, rather than the actual IP2 value of 4617 psi.

Figure 5.1.3

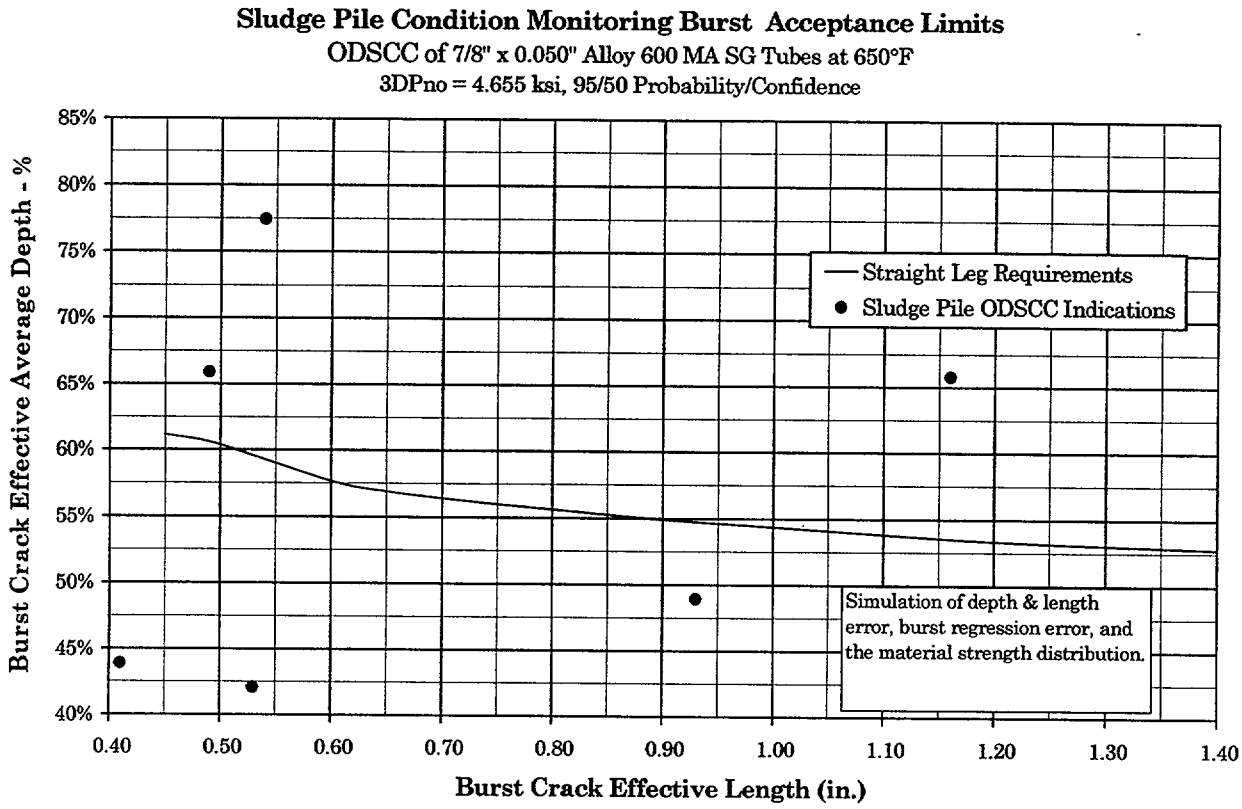

Notes:

1. This curve is based on a conservative pre-outage anticipated $3\Delta P_{NO}$ value of 4655 psi, rather than the actual IP2 value of 4617 psi.

Figure 5.1-4 Post-In-situ Visual Examination of R34C51, SG-22

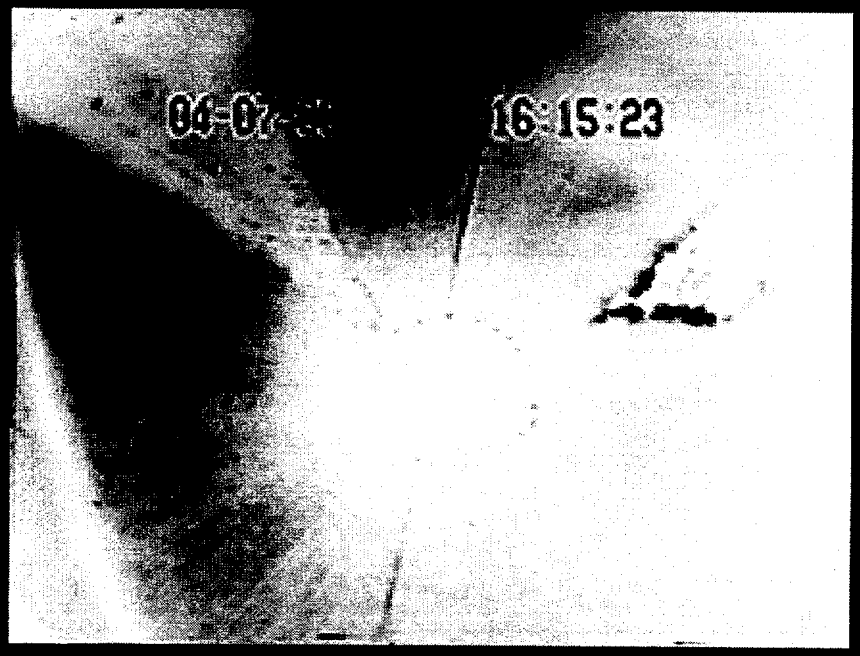

(a) Top Portion of the opening is visible; bottom portion is shielded by tubing. The opening appears to be located in a bulge.

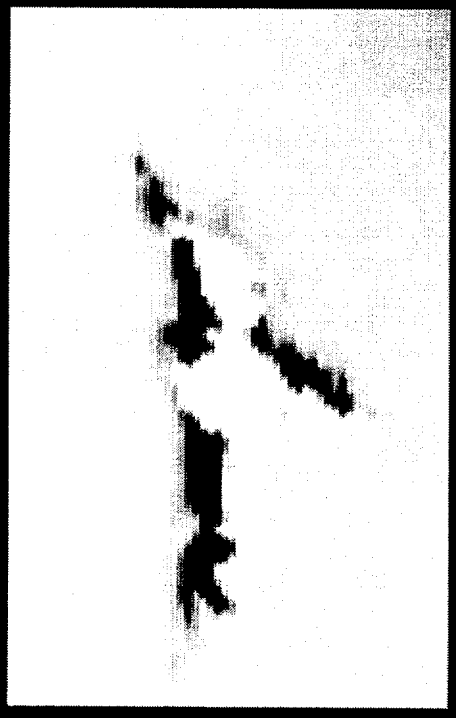

(b) Close-up of upper crack tip. Edge characteristics typically displayed by opened, partial through wall corrosion cracks; typical of ligament tearing linking parallel crack network.

5.2 Cycle 14 Condition Monitoring Assessment

5.2.1 Sludge Pile Cracking

5.2.1.1 Limiting Flaw Evaluation (R34C51)

Structural integrity of axial ODSCC indications is dependent upon the flaw length and the flaw average depth. The flaw maximum depth has little impact upon structural integrity unless 100% TW lengths > about 0.2" are present. No sludge pile indication detected during the EOC-14 inspection exhibited such characteristics. The sludge pile axial ODSCC indication lengths ranged from 0.19" to 1.4", based on +Pt depth profile results. The limiting sludge pile axial ODSCC flaw was observed in tube R34C51, SG 22, at approximately 1" above the Top of Tube Sheet (TTS).

In situ pressure testing was used to establish structural and leakage integrity of sludge pile ODSCC flaws detected during the EOC-14 inspection. All tubes with sludge pile axial ODSCC indications were in situ pressure tested. All tubes except tube R34C51 in SG-22 were tested to a pressure of 5173 psi without observing any leakage. With tube R34C51, rapid depressurization occurred when the differential pressure across the tube during the in situ pressure test reached 4985 psi. All test were conducted with the full tube pressurization setup; thus, no bladder or localized tool was used.

The normal operating pressure differential across the tube during Cycle 14 (ΔP_{NO}) was 1539 psi. Flow stress at an operation temperature of 590°F is about 92.1% of that at room temperature. Therefore, the margin-to-burst demonstrated by the in situ pressure test for tube R34C51 when it experienced a rapid depressurization at a pressure differential of 4985 psi. is:

$$\frac{4985 \times 0.921}{1539} = 3.0$$

Thus, tube R34C51 did meet the $3\Delta P_{NO}$ structural margin. No other sludge pile ODSCC flaws experienced either leakage or depressurization during in situ testing up to a maximum pressure of 5173 psi. Even though all indications satisfied structural and leakage requirements, the sludge pile inspection was expanded to include 100% of the hot sludge pile region as described in Section 3.2.

No significant leakage was observed prior to the depressurization of tube R34C51, indicating that maximum depth was less than about 95% throughwall prior to the test, and the failure likely occurred due to a ligament tear. Tearing of any crack ligament could have resulted in tearing of the remaining radial ligament, thus leading to the depressurization of the tube. Moreover, ligament tearing could have resulted in a condition where the resultant average depth over the affected length between crack

sections now joined by the ligament tear could not support the internal pressure, thus resulting in a failure over a longer crack front length.

The second large crack (labeled as Crack 1 in NDE data) in tube R34C51 did not open during the in situ test, and the post in situ data can be used to estimate the depth of the indication. Figure 5.2.1-1 shows a comparison of the pre and post in situ for R34C51 Crack 1. The post in situ sizing results are shown as solid squares symbols where the data was not distorted, and by open symbols where the signal is distorted and sizing is less reliable. Post in situ voltages increased to improve the signal-to-noise ratio. For the crack depths between 1.4 and 1.6 inch, the signal-to-noise ratio is less than one, and neither the pre nor the post in situ sizing results are considered reliable. The crack depths do not show a significant difference between pre and post in situ.

Using the crack profiles obtained by sizing the +Point data, predictions of burst pressures and ligament tearing probabilities were made at room temperature for the 3 indications identified in tube R34C51. The results are summarized in Table 5.2.1-1. The burst pressures shown were calculated 2 ways: 1) by a deterministic analysis at nominal material properties without considering measurement errors associated with the crack profiles used (nominal burst pressure), 2) by a Monte Carlo methodology that included measurement errors as well as uncertainties associated with burst correlation and material properties. The Monte Carlo methodology applied is the method used in lieu of in situ pressure testing for condition monitoring assessment. The methodology is similar to the operational assessment method described in Section 4.6, except no growth is considered and the probability of detection is take as unity. Both the deterministic and Monte Carlo analyses predicted bursting of 1 or 2 of the 3 indications detected in R34C51 at less than the in situ test pressure of 4985 psi. The definition of tube burst is that gross structural failure of the tube wall occurs accompanied by ductile tearing of the material at the crack tips. Analysis of the post-test eddy current test data indicates that tearing of the radial ligament was not accompanied by tearing of the material at the tips of the crack; hence, the tube did not burst. The fact that the predicted burst pressures are less than the maximum pressure reached during the in situ testing of R34C51 shows that the methodology used for burst prediction, especially the Monte Carlo methodology, is conservative. The nominal burst pressure prediction being less than the test pressure may be due to the crack depths being overestimated or to the material properties being higher than nominal.

Table 5.2.1-1 also shows the predicted ligament tearing pressures for all 3 cracks in R34C51 as well as the probabilities of ligament tearing for those cracks. The predicted nominal ligament tearing pressures at nominal properties (which do not include NDE measurement errors) for Cracks 1 and 2 are below the peak pressure reached during in situ testing, thus predicting a radial ligament tear. The Monte Carlo analysis yields ligament tearing probabilities between 62% to 73% for Cracks 1 and 2, depending on the confidence level, thus predicting a high likelihood of a ligament tear during the R34C51 in situ test.

In summary, a sludge pile ODSCC indication in tube R34C51 represents the limiting sludge pile flaw detected during the EOC-14 inspection. The tube met the 3□P_{NO} structural margin requirement. A comparison of the predicted burst pressures and ligament tearing probabilities with the in situ test data show that the +Point sizing and analysis methods yield conservative results.

5.2.1.2 Comparisons of Predictions and In Situ Tests for Sludge Pile Indications

All sludge pile ODSCC indications detected during the EOC-14 inspection were in situ pressure tested. Except tube R34C51, none of the other sludge pile ODSCC flaws experienced either leakage or depressurization at steamline break pressure differential (2560 psi) or even at the maximum test pressure of 5173 psi which significantly exceeds the $3\times\Delta P_{NOP}$ structural margin requirement. Thus, all sludge pile indications met the structural margin requirement.

As a benchmarking of the profiles and analytical methods used for tube integrity analysis, burst pressures were predicted for all tubes in situ pressure tested and the predictions compared against the test data. Both the deterministic and Monte Carlo methods used for comparison with R34C51 test data were applied. The results are summarized in Table 5.2.1-2. A comparison of the predicted burst pressures against the maximum in situ pressure of 5173 psi (for all indications except R34C51 for which the maximum pressure is 4985 psi) shows that the 95%/50% burst pressures from the Monte Carlo methodology for 3 tubes, R34C51 and R35C51 in SG-22 and tube R31C46 in SG-23, are below the maximum pressure reached during situ testing of those tubes. As these tubes did not burst during the in situ tests, their burst pressures are underpredicted. Burst pressures for the remaining tubes can also be expected to be underestimated. Thus, the Monte Carlo methodology applied for tube integrity analysis yields conservative results. The same methodology is applied to perform operational assessment analyses Cycle 15 presented in Section 6.1

5.2.1.3 Conclusions on Sludge Pile CM Evaluation

All sludge pile ODSCC indications detected during the EOC-14 inspection were in situ pressure tested. Except tube R34C51, none of the other sludge pile ODSCC flaws experienced either leakage or depressurization at steamline break pressure differential (2560 psi) or even at the maximum test pressure of 5173 psi which significantly exceeds $3\Delta P_{NOP}$ structural margin requirement. The R34C51 indication had ligament tearing and leakage exceeding test system capacity upon reaching $3\Delta P_{NO}$ burst margin requirement. Thus, all sludge pile indications met the structural margin requirement.

In situ test data were used to benchmark profiles and analysis methodology used for tube integrity analyses. The results show that the deterministic and Monte Carlo analysis methods used for tube structural integrity evaluations yield conservative results. The

analysis correctly predicted R34C51 to be the limiting indication with even the nominal burst pressure (at nominal properties) at less than the pressure attained in the in situ test.

Table 5.2.1-1

Indian Point-2 EOC-14 Inspection
Sludge Pile Indications in Tube R34C51
Predicted Ligament Tearing Pressures and Tearing Probabilities During In Situ testing

				As Measured NDE			Predicted Burst Pressure		Ligament Tearing		
SG	Row	Col.	Crack No.	Length (in.)	Maximum Depth (%)	Average Depth (%)	Nominal[1]	95% Prob./ 50% Conf.[2]	Nominal Ligament Tearing Pressure[1] (psi)	Ligament Tearing Probability at 95% Confidence	Ligament Tearing Probability at 50% Confidence
2	34	51	1	1.260	91.0	63.48	4,962	3,411	4,259	62%	64%
2	34	51	2	1.330	90.0	66.12	4,405	3,029	3,932	70%	73%
2	34	51	3	0.590	93.0	75.29	5,639	4,010	5,359	34%	37%

(1) Based on deterministic calculations at nominal material properties. Does not include NDE and burst/tearing pressure correlation uncertainties.

(2) Based on Monte Carlo calculations that include NDE and burst/tearing pressure correlation uncertainties

Table 5.2.1-2

Indian Point-2 EOC-14 Sludge Pile Indications
Predicted Ligament Tearing Pressures and Tearing Probabilities During In Situ testing

				As Measured NDE				Burst Pressure (psi)	
SG	Row	Col.	Crack No.	Length (in.)	Maximum Depth (%)	Average Depth (%)	Max. Volts	Nominal	95% Probability/ 50% Confidence
1	34	41	1	0.520	66.0	46.12	0.26	7,852	5,448
2	32	48	1	0.280	71.0	40.13	0.16	8,855	6,125
2	33	49	1	0.400	56.0	32.49	0.18	9,610	6,692
2	33	51	1	0.770	67.0	44.16	0.39	7,841	5,294
2	33	54	1	0.260	73.0	38.35	0.33	10,353	7,215
2	33	54	2	0.130	42.0	24.69	0.28	10,637	7,551
2	34	51	1	1.260	91.0	63.48	0.88	4,962	3,411
2	34	51	2	1.330	90.0	66.12	0.89	4,405	3,029
2	34	51	3	0.590	93.0	75.29	0.55	5,639	4,010
2	34	54	1	0.170	40.0	18.74	0.75	10,202	7,099
2	34	54	2	0.070	25.0	20.93	0.19	10,592	7,586
2	34	54	3	0.270	48.0	26.94	0.56	10,028	6,965
2	35	51	1	0.590	80.0	52.70	0.62	6,917	4,827
2	35	52	1	0.420	80.0	25.77	0.62	10,438	7,260
3	3	88	1	2.280	75.0	30.39	0.18	9,693	6,353
3	29	46	1	0.270	50.0	35.19	0.47	9,008	6,238
3	29	46	2	0.370	40.0	22.61	0.27	10,168	7,028
3	29	46	3	0.290	30.0	20.27	0.36	10,020	6,957
3	30	46	1	0.750	40.0	26.69	0.32	9,206	6,245
3	31	46	1	1.080	81.0	53.34	0.69	6,848	4,651
3	31	47	1	0.570	32.0	19.68	0.56	9,759	6,792
3	31	47	2	0.270	49.0	32.83	0.47	8,903	6,136
3	31	47	3	0.210	45.0	23.60	0.31	9,865	6,868
4	30	27	1	2.350	44.0	18.80	0.51	10,186	6,729
4	42	43	1	0.330	93.0	36.22	0.22	10257	7,034

Figure 5.2.1-1 Specimen SG 2 - R 34 - C 51 - TSH - Crack 1 - Year 2000
Comparison of Pre and Post In Situ Test Depth Profiles
Post Test Includes Non-Distorted and Distorted (Less Reliable) Data Points
NDE Depth vs. Axial Length

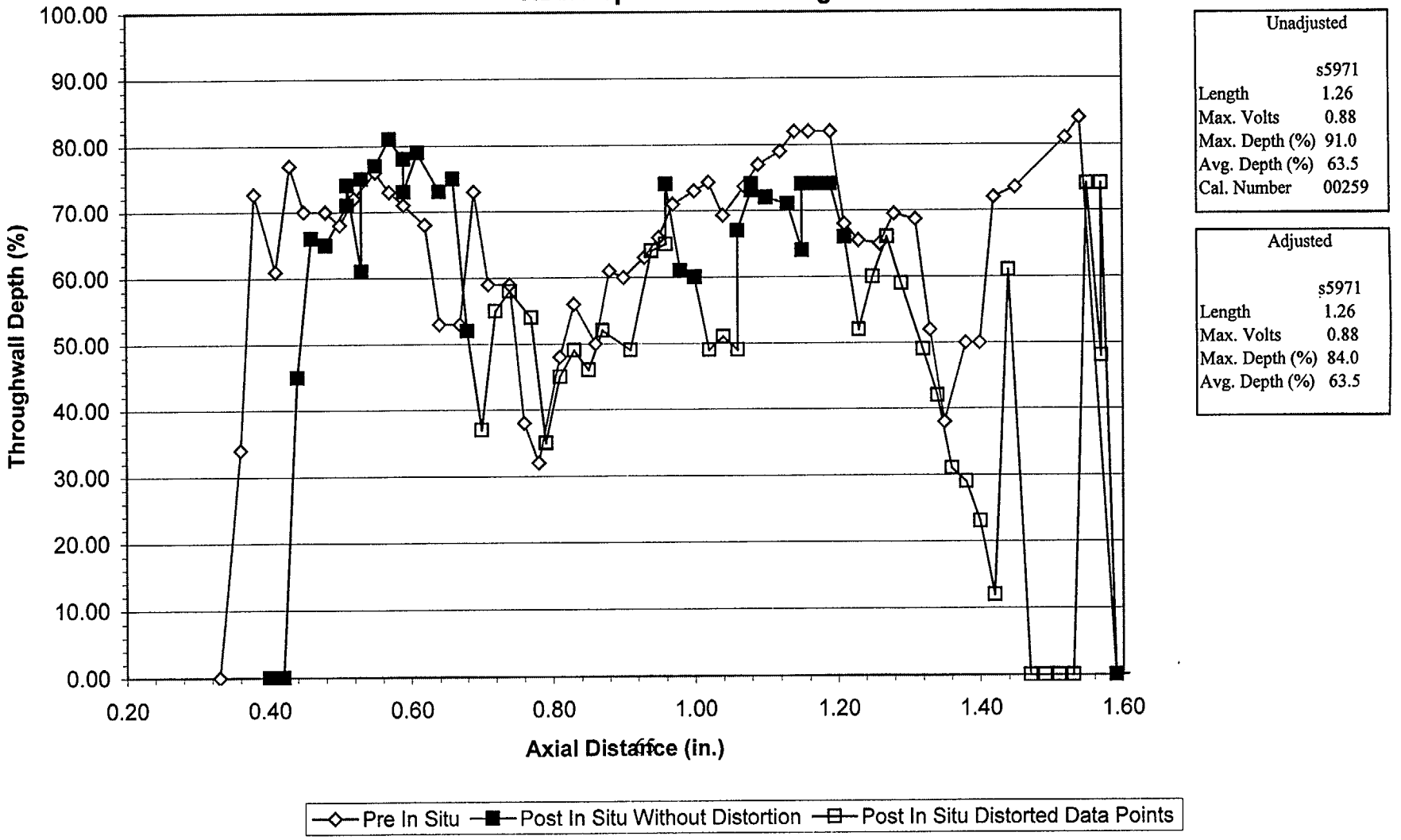

5.2.2 Tubesheet Crevice ODSCC

Approximately seventy-five tubes were identified among the 4 SGs as exhibiting +Point axial indications of OD origin below the top of the hot leg tubesheet (TSH) and above the expansion zone roll transition (RT); the location of the RT differs from the nominal 2.75" above the tube end (TEH, TEC) if the tube has previously been re-rolled. Tubesheet crevice ODSCC is a phenomenon that has been observed in Westinghouse SGs since 1971, in SGs assembled with partial expansion of the tubes into the tubesheet bore; the IP 2 SGs are typical of all Series 44 SGs, representing the last U.S. plant operating with the originally installed Series 44 SGs.

Historically the morphology of crevice ODSCC has been most strongly associated with plants operating on fresh water sites, such as Point Beach, Robinson, and Ginna. Plants like Turkey Point and IP2 were influenced by brackish water cooling and experienced degradation associated mainly with acid chloride environments, like pitting and denting. IP 2 was operated successfully for many years after denting was first observed, and pitting did not reach the level where condition monitoring and operational assessment requirements would not be met. Thus for about 20 years there was essentially no reported incidence of ODSCC. This extended period of resistance ended during Cycle 12 or 13, presumably accompanied by the alteration of the chemical environment in the hot leg tubesheet crevices, the hottest tube section in the tube bundles.

Four of the five tubes tested in 1997 for crevice ODSCC indications exhibited appreciable lengths with depths exceeding the 75% screen, as well as voltages ranging from 1.28V to 3.64 V; none of them leaked during tests up to the Steam Line Break ΔP. The 5th tube R35C54 in SG22 was tested to 3 ΔP; it also showed no leakage during the test.

The detection of ODSCC in the tubesheet crevice region during the 2000 forced outage was typified by small amplitude indications of varying length. The crevice indications observed were sorted first by length, then by depth and finally by amplitude to determine potential candidates for in-situ testing. As length is not a controlling factor for tubes with indications in the tubesheet, the latter 2 criteria were emphasized. All the tubes (6) with crevice ODSCC indications >1 volt (Table 5.2.2-1) were in-situ tested; the OD crack leak test screen for amplitude is 1.5 volts, if the corresponding leak test screen for ODSCC depth, at least 0.1" length with depth exceeding 75% is also exceeded. R3C24 (SG 22) had a portion of its profile that exceeded 75% (~ 0.1") and it was among the tubes tested to SLB ΔP (2841 psi), again without leakage. R4C67 in SG21 was found in the +Point expansion program; profile analysis indicated maximum depth exceeding 75% but the length of the tube at that depth was less than 0.1". The PDA for R4/C67 (64.6%) exceeded the structural limit for the burst effective length of 0.71" (59.5%), but this tube did not require testing because of the restraint provided by the tubesheet. As a conservative measure, this tube was included in the in-situ test program to demonstrate that those tubes in the crevice with the largest indications maintained structural integrity.

The field NDE data and the profiling analysis results for the 4 tubes selected for in-situ testing on the basis of their crevice ODSCC indications are presented in Table 5.2.2-2. Tubes with sludge pile ODSCC indications may also have had tubesheet crevice indications of lesser significance that were either not detected before in-situ testing or not profiled; R32C48, R34C51, and R35C51 (see table 5.2.2-2) fell into this category. No leakage was observed for 32/48 and 35/51, even at pressures up to 5173 psi; post-pressure test NDE for 34/51 indicates that the leakage observed was not attributable to the crevice ODSCC.

Table 5.2.2-1
IP 2 Tubesheet Crevice ODSCC Indications >1.0 Volts
Forced Outage (2R14) Spring 2000

SG	ROW	COL	VOLTS	DEG	CHN	IND	PER	LOCN	INCH1	INCH2	BEGT	ENDT	PDIA	PTYPE	CAL
21	4	67	3.28	75	3	SAI		TEH	8.16		TEH	TSH	0.72	ZPANM	551
21	4	67	1.81	94	3	SAI		TEH	9.92		TEH	TSH	0.72	ZPANM	453
22	3	24	3.93	71	3	MAI		TEH	5.9		TEH	TSH	0.68	ZPANM	305
22	3	24	3.81	75	3	MAI	77	TEH	5.52		TSH	TEH	0.68	ZPANM	261
22	3	24	3.36	73	3	MAI	78	TEH	10.49		TSH	TEH	0.68	ZPANM	261
22	3	24	1.27	96	3	MAI	62	TEH	4.64		TSH	TEH	0.68	ZPANM	261
22	3	24	1.21	99	3	MAI	60	TEH	4.28		TSH	TEH	0.68	ZPANM	261
22	32	48	1.6	99	2	MAI		TEH	3.03	12.45	TEH	TSH	0.7	ZPACC	569
22	34	51	4.18	85	3	MAI		TEH	8.02		TEH	TSH	0.68	ZPANM	305
22	34	51	1.3	107	3	MAI		TEH	6.85		TEH	TSH	0.68	ZPANM	315
22	35	51	1.12	112	3	SAI		TEH	6.13		TEH	1H	0.68	ZPANM	305
24	26	31	1.37	91	3	MAI	61	TEH	3.9		TEH	TEH	0.68	ZPANM	225

Table 5.2.2-2
IP2 In-situ Test of Tubes with Tubesheet Crevice Cracks
Forced Outage (2R14) Spring 2000

SG	Row	Col	Probe	I_typ	Per	Loc	Inch1	Volts	Deg	Tape	Axial (in)	C-5/ Bobbin Call	Crack #	Max. Volts	Max. % TWD	Length (in)	PDA (%TWD)	Burst Effective Length (in)	PDA For Burst Crack	In-situ test required?	Leak	Test Pressure (psi)
21	4	67	720-ZP	SAI		TEH	8.16	3.28	75	551	3.70		1							No	0	2844
				SAI		TEH	9.92	1.81	86	453	2.18		2	1.93	79	3.89	42.7	0.71	64.6			
22	3	24	680-ZP	MAI	78	TEH	10.49	3.36	73	261	2.11	5.24V PI	7	2.91	75	1.96	33.2	0.4	62.9	No	0	2841
				MAI	58	TEH	8.74	0.37	101	261	1.01	0.57V NQI	6	0.6	60	1.03	35.2	0.31	47.3			
				MAI	58	TEH	8.74					O.34V NQI	5	0.57	48	0.57	28.8	0.33	37.3			
				MAI	77	TEH	5.52	3.81	75	261	1.52	0.74V NQI	4	2.67	68	0.87	47.1	0.47	58			
				MAI	77	TEH	5.52					5.65V NQI	3	0.51	35	0.99	22.1	0.31	29.1			
				MAI	62	TEH	4.64	1.27	96	261	0.18	2.39V PI	2	1.21	57	0.32	41.1	0.24	49.1			
				MAI	60	TEH	4.28	1.21	99	261	0.43	2.3V NQI	1	0.96	52	0.33	29.4	0.19	41.6			
23	19	73	720-ZP	MAI		TEH	6.4						1	0.2	32	0.28				No	0	2841
				MAI		TEH	7.4						2	0.2	26	0.54						
				MAI		TEH	7.6						3	0.22	37	0.49						
				MAI		TEH	8.2						4	0.14	24	0.23						
				MAI		TEH	8.7						5	0.11	21	0.2						
				MAI		TEH	12	0.27	81	505	3.28		6	0.38	36	3.05						
				MAI		TEH	12.4						7	0.4	46	2.77						
24	26	31	680-ZPANM	MAI	61	TEH	3.9	1.37	91	225	1.34	5.75V PI	1	1.23	50.4	0.55	38.5%	0.42	43.7	No	0	2841
				MAI	28	TEH	7.73	0.24	102	225	4.62	2.48V PI	2	0.17	30	0.22	21.7%	0.18	24.4			
						TEH	7.4						3	0.13	30	0.18	21.5%	0.14	24.8			
				MAI	1	TEH	9.3	0.17	108	225	1.11		5	0.28	30	0.95	18.2%	0.39	24.8			
			720-ZMAGR	MAI		TEH	9.85	0.18	151	221			4	0.15	30	0.48	24.3%	0.38	26.5			

5.2.3 PWSCC in the Roll Expansion Region

The degradation mode responsible for the greatest number of +Point indications is expansion zone PWSCC. The contribution from indications in the expansion zone to potential leakage is low, since the presence of the tubesheet eliminates the possibility of tube burst under all circumstances. The potential for tube leakage from this mechanism is also reduced since most of the indications occur below the bottom of the roll transition. As there was no tube leakage attributed to the tubesheet crevice region of the IP 2 tube bundles, there was no in-situ testing performed for the EZ indications. Even if there was minor tube leakage from this type of indication, the leakage expected based on extrapolation of a truly small leakage rate at normal operating ΔP to Steam Line Break conditions at the time of the forced shutdown would result in a negligible contribution to projected leakage. Table 5.2.3-1 identifies the number of indications attributed to tubesheet PWSCC for the individual SGs. The same table also shows that most of the indications were retained in service rather than being plugged; the application of re-rolling in combination with the F* alternate repair criteria continues to preserve the service life of tubes that experience SCC in the partial expansion zone at the base of the tubesheet.

Table 5.2.3-1
Summary of Roll Expansion Region PWSCC
IP 2 2R14 Inspection

Degradation Mode	SG 21	SG 22	SG23	SG24
Tubesheet PWSCC (# of Indications)	290	150	1095	178
Tube Plugging Attributed to EZ PWSCC	9	36	73	19

During a secondary pressure test performed in SG 22, 3 tubes were identified with leakage; the examination of the tubes with +Point probes identified the source of leakage as "tube end" cracks. Identification of cracks of this sort was thereafter accomplished as part of the analysis of the 100% hot leg +Point examination of the tubesheet and the sludge pile region. The leaking tubes and other indications of this type are covered by the F* repair criteria; those tubes with no other reason for repair were re-rolled.

In 1997 tube R24 C77, SG 22, with a 4.13 volt 80 mil pancake coil voltage using the combination bobbin/RPC probe was in-situ tested at a maximum pressure of 2900 psi (corresponds to approximately 2636 psi at operating temperature). This tube had a 0.56" long axial indication located in the original hardroll flat region. No leakage was detected at SLB testing conditions. This indication was leak tested to show that indications typically re-roll repaired did not represent a leakage potential at EOC 13 conditions; this conclusion continues to apply to the EOC 14 circumstances.

None of the PWSCC indications with voltages >3 volts, identified in the expansion zone in the partially rolled region in the tubesheet, exhibited sufficient depth based on +Point phase angle analysis to warrant profiling for consideration as in-situ leak-testing candidates. The tubes listed in Table 5.3.2-2 below are those whose locations were above the roll transition and exceeded 3 volts. It should be noted that the indications satisfying these criteria in SG 21 and SG 22 were OD crevice indications that were in-situ tested, as were all ODSCC crevice indications exceeding 1 volt. The tubes in SG 23 and SG 24 were shallow (phase angles from 11 to 19 degrees equivalent to penetrations << 80% maximum depth) ID indications.

Since none of the tubes in this context present a challenge to tube integrity, and the F* repair criteria governed their disposition, no more of these tubes were in-situ tested.

Table 5.3.2-2
RT Zone Indication In-situ Test Summary

SG	ROW	COL	PROBE	IND	LOC	INCH1	CHAN	VOLT	DEG	TAPE	Length	DEG	In-situ Tested?
21	4	67	720-ZP	SAI	TEH	8.16	3	3.28	75	551	3.698	82	YES
22	34	51	680-ZP	MAI	TEH	8.02	3	4.18	85	305	7.137	236	YES
22	3	24	680-ZP	MAI	TEH	10.49	3	3.36	73	261	2.109	32	YES
22	3	24	680-ZP	MAI	TEH	5.52	3	3.81	75	261	1.523	40	
22	3	24	680-ZP	MAI	TEH	5.9	3	3.93	71	305	8.491	112	
23	31	33	720-ZP	SAI	TEH	2.89	1	4.43	11	375	0.113	85	NO
24	15	7	720-ZP	MAI	TEH	4.59	3	3.7	19	325	0.233	140	NO
24	26	33	720-ZP	SAI	TEH	3.18	3	3.13	18	255	0.517	53	NO

By far, the largest number of indications was detected in the original roll expanded regions. These indications however are located below the additional roll expansion repair performed as an extension of the F* tube repair criterion or below the F* distance in the original roll region. These indications do not represent a leakage potential under any condition since the sound roll length above the indication prevents primary to secondary leakage. As the primary mode of degradation was axially oriented PWSCC, the tube will continue to be able to transfer axial loads across the elevation of the flaws. This is not necessary in order for the tube to remain structurally sound since the length of the additional roll expansion provides sufficient restraint to prevent tube axial motion even for a tube postulated to be circumferentially separated at the F* distance.
Based on the 1997 in-situ testing result for R24 C77 and the eddy current responses for the 2000 (2R14) indications re-rolled or plugged due to roll region PWSCC, it is

concluded that SLB leakage would not be expected for the axial PWSCC indications in the hardroll expansions.

All of the 102 circumferential indications observed during 2R14 were detected in or below the roll transition from the roll-expanded region (see Table 3.4.1, SCI + MCI+MMI). This population is significantly larger than that reported in 1997 owing to the 100% +Point testing conducted in the hot legs of the SGs. The circumferential indications that were located at the elevation of the roll transition (RT) had arc lengths less than or equal to 100°; furthermore, all of these RT indications had amplitudes <1 volt. Profiling was not performed for any of the circumferential indications since those with a possible leak path were too small to present a challenge under the in-situ leak test criteria; the pertinent tube data are given in Table 5.2.3-3.

Table 5.2.3-3
Roll Transition Circumferential Indications
IP 2 2R14 Inspection

S_G	Row	Col	Probe	Stind	Loc	Inch1	Volts	Deg	Tape	Circ
44-2	23	66	720-ZP	MCI	TEH	2.82	0.56	92	413	79
44-4	39	42	720-ZM	SCI	TEH	3.07	0.81	64	223	63
44-4	38	39	720-ZP	SCI	TEH	3.22	0.53	104	391	100
44-4	3	20	720-ZP	SCI	TEH	2.92	0.26	38	341	24

Tube rupture type release rates due to a postulated circumferentially separated tube in the roll transition region are improbable due to the design configuration of a partial depth expanded steam generator tube. In order for tube rupture type release rates to be realized the separated location must be located above the TTS in order for sufficient flow area to be provided. Fixity at the TSPs (the tubes and TSPs are locked together by extensive denting), and design of the steam generator itself in the absence of TSP fixity preclude the separated location from being displaced above the TTS. Therefore, circumferentially oriented degradation in a partial depth expanded plant is not considered a potential tube rupture initiator.

5.2.4 TTS Pitting/Volumetric

Historically, the majority of freespan indications detected at IP2 were due to pitting of the tube OD in the sludge pile region, located immediately above the TTS. Twenty tubes were plugged due to pitting in 1997; a somewhat diminished effect based on previous inspection data. For all SGs 284 tubes were reported with either original PIT indications (+Point) not reported from the Cecco-5/bobbin examination or with +Point confirmed bobbin PCT indications in 2000; 16 of these tubes had bobbin indications ≥ 40% and would have been plugged under the Tech. Spec. plugging criteria.

Since it had been resolved that all confirmed HL pit indications would result in plugging the affected tube, a determination of the pitting growth rate allowance was made based on CL pitting indications; this review found that 25% allowance for growth (95% CL) would be appropriate for Cycle 15, assuming an operating interval equal to Cycle 14. This calculation resulted in a recommendation to lower the plugging limit for pitting to 28% after subtracting the growth and NDE uncertainty allowances from the structural limit of 85% for pitting.

On average for hot leg and cold leg pits reported as bobbin indications in both 1997 and 2000, the apparent growth rate was 2.4% for the operating interval ending with the forced shutdown; this compares to a slightly negative rate (-3.3%) calculated from the 1997 results compared to those reported for the same tubes in 1995. The uncertainties in the growth rates based on the distributions for Cycle 13 and Cycle 14 dominated the allowances necessary to meet the 95% confidence level. With the growth allowances ranging from 19% to 32% among the 4 SGs, the decision was taken to repair all confirmed pitting indications. Figure 5.2.4-1 presents side-by-side histograms for the 1997 and 2000 bobbin distributions corresponding to +Point confirmed PIT indications. Table 5.2.4-1 provides a per SG summary of the reported indications.

Table 5.2.4-1: IP2 Pitting Indications (Spring 2000)

SG	# of Tubes	Max. +P Voltage	Max. Bobbin % Depth	Max. Bobbin Voltage	# Tubes with ≥ 40% Depth
21	70	1.25	61	1.66	8
22	112	2.00	74	4.26	2
23	63	1.60	59	2.79	2
24	39	1.03	78	2.41	4
ALL	**284**	**2.00**	**78**	**4.26**	**16**

The pitting-related flaws detected appear to be normal for IP 2 and judged not to represent either a burst or leakage potential; nevertheless the licensee elected to plug all tubes with bobbin pitting indications that were confirmed by +Point testing regardless of the reported bobbin depth. This was done to provide conservatism in light of the large measurement uncertainty (32% @ 95% CL) associated with the bobbin technique (ETSS#96005). In addition, unconfirmed Cecco-5 indications reported in the sludge/deposit zone above the tubesheet were regarded as confirmed, and the tubes placed on the plug list. All tubes which exhibited numerical % depth bobbin calls or PI and TSI Cecco-5 calls at or above the tubesheet were re-examined with the +Point probe to establish the characterization that would permit determination of the relative severity of these indications.

A program of ultrasonic testing (UTEC) was implemented to determine whether deposit interference was suppressing the detection of flaws in the sludge pile zone. While the UTEC program was concerned with all types of flaws, the data on tubes with assessed by +Point examination as PITs or VOLs are excerpted from the UTEC report (Reference 3) and presented in Table 5.2.4-2. Eighteen locations cited with Cecco-5 PI calls were examined; 9 had been confirmed as either PITs or VOLs by +Point testing, while the remainder were reported as NDD by +Point. In 1 case (43/53-TSH+1.29) the UTEC result identified a flaw where the reported +Point result was NDD; however, immediately adjacent to the +Point "miss" was another VOL indication, the detection of either by Cecco-5 being sufficient to trigger +Point examination. In 6 cases wherein +Point analysis reported PIT or VOL indications, the UTEC system was unable to identify a flaw.

A second UTEC (see Table 5.2.4-3) program focused on the freespan tube section from the hot leg top of the tubesheet (TSH) to the 1st TSP; in this program 16 tubes with no reported +Point flaw and 2 tubes with either PIT or VOL indications were examined; the UTEC result was in agreement with the +Point analyses, i.e., only the 2 tubes with known indications were detected by UTEC, albeit both were characterized as pits on the basis of UTEC. Both these programs were conducted on tubes identified initially from the Cecco-5/bobbin program; thus the outcome supports the position that flaws detectable by EC testing are not being masked by the influence of conductive deposits such as copper. The influence of deposits on sizing of pit indications is reflected by the lack of correspondence between bobbin amplitudes and depths relative to those recorded from the +Point analyses. The large measurement uncertainty (~ 32%) associated with bobbin depth measurements results from the influence of deposits, viz., copper.

The largest bobbin response of 4.26 volts is ~71% of the voltage expected from a 100% deep ASME hole, ~6 volts. Since the largest pit response is less than 80% of the voltage expected for the 100% deep ASME standard hole, such an indication does not present a challenge with regard to tubing structural or leakage integrity. This is corroborated by the absence of leakage during the in-situ tests of 12 tubes selected for testing on the basis of confirmed pit indications. Compared to the ASME drilled-hole basis for comparison, none of these indications required in-situ testing to support tube integrity evaluation. The maximum bobbin depth for a confirmed pit was 78% (0.21 +Point-volts, SG24 45/51), and the maximum bobbin voltage for a confirmed pit was 4.26 volts (0.61 +Point-volts, SG22 37/20; these tubes were among the 12 tested for confirmed PITs. Results for all tubes designated for in-situ testing based on PIT indications are contained in Table 5.2.4-4; none of the tested tubes leaked.

Though not explicitly characterized as pitting indications, the category of +Point confirmed indications designated as VOL (volumetric) are included here, since they are regarded as similar in behavior with respect to the eddy current characteristics of the signals. Table 5.2.4 -5 gives the NDE data collected for the 7 in-situ tested tubes in this grouping. Tube R31/C15 in SG 22 was originally recommended for testing as an axial indication above the tubesheet; however, the profiling analysts re-assessed the indication as volumetric in character and attributed the indication to probable wear. This evaluation was consistent with the peripheral location of the tube and the proximity of apparent foreign objects adjacent to the tube. A similar conclusion can be drawn for R30/C13, given its location near R31/C15 and the presence of loose parts in the general area. The other tubes in the list of VOL indications are considered distant from the periphery and more likely to be affected by pitting; these indications are assessed as combinations of overlapping pits with respect to the resolution capability of the +Point coil. The largest, longest and deepest of this class of signals was recommended for in-situ testing even though none was considered large enough to challenge tube integrity; this is borne out by the zero leakage results for all of them.

Table 5.2.4-2: Comparison of Cecco, +Point and UTEC Results for SG 22 (C-5 PI Calls not confirmed as cracks by +Point)

Cecco				+Point	UTEC
Tube	**Volts**	**Location**	**Code**		
R18C83	13.92	TSH +1.40	PI	NDD	NDD
R19C83	2.52	TSH + 0.85	PI	NDD	NDD
R21C83	16.79	TSH + 0.74	PI	NDD	NDD
R27C26	1.98	TSH + 12.97	PI	NDD	NDD
R30C43	8.68	TSH + 3.2	PI	PIT	PIT
R34C28	55.29	TSH + 1.19	PI	PIT	NDD/DEPOSIT
R34C28	30.12	TSH + 0.63	PI	PIT	NDD/DEPOSIT
R34C28	14.22	TSH + 17.71	PI	NDD	NDD
R35C27	118.4	TSH + 1.41	PI	PIT	NDD/DEPOSIT
R35C40	11.55	TSH + 4.37	PI	VOL	NDD/DEPOSIT
R35C50	17.32	TSH + 0.27	PI	VOL	PIT
R35C50	0.67	TSH - 0.19	PI	NDD	NDD
R38C64	122.3	TSH + 16.63	PI	VOL	NDD/DEPOSIT
R39C43	8.09	TSH + 9.96	PI	NDD	NDD
R39C43	6.02	TSH + 9.69	PI	NDD	NDD
R39C59	13.87	TSH + 8.68	PI	VOL	NDD/DEPOSIT
R43C53	16.29	TSH + 1.26	PI	VOL	PIT/WEAR
R43C53	14.88	TSH + 1.29	PI	NDD	PIT/WEAR

Table 5.2.4-3: UTEC Results on Steam Generator 22
TSP 1H to TTS

Tube	+Point	Location	UTEC
R3C24	NDD	NA	NDD
R7C66	NDD	NA	NDD
R9C18	NDD	NA	NDD
R11C81	NDD	NA	NDD
R15C32	NDD	NA	NDD
R15C77	NDD	NA	NDD
R15C80	NDD	NA	NDD
R17C72	NDD	NA	NDD
R18C76	NDD	NA	NDD
R22C75	NDD	NA	NDD
R22C78	NDD	NA	NDD
R25C37	NDD	NA	NDD
R25C49	PIT	TSH +6.48	PIT
R26C76	NDD	NA	NDD
R29C63	NDD	NA	NDD
R31C41	NDD	NA	NDD
R35C50	VOL	TSH + 0.38	PIT
R35C56	NDD	NA	NDD

Table 5.2.4-4: IP 2 Spring 2000 Tubes with Pit Indications Subjected to In-situ Testing

SG	Row	Col	Probe	I_typ	Per	Loc	Inch1	Volts	Deg	Tape	Axial	C-5/Bobbin	Indication	Max. Volts	Max. %	Length (in)	In-situ test required?	Leak
21	10	17	720-ZP	PIT		TSH	0.25	0.56	102	421	0.57		1	0.54	53	0.14	No	0
22	37	20	700-ZP	PIT		TSH	4.2	1.8	104	511	0.58	37%, 4.66V	1	1.64	61	0.58	No	0
22	4	21	700-ZP	PIT		TSH	21.59	2	128	325	0.33		1	0.47	27	0.07	No	0
22	13	26	700-ZP	PIT		TSH	16.76	1.18	41	523	0.36		1	0.52	79	0.22	No	0
22	13	26	700-ZP	PIT		TSH	17.25	1.48	108	523	0.29		2	0.5	10	0.17		
22	5	55	680-ZP	PIT		TSC	1.45	0.72	127	226	0.22	1%, 3.62V	1	0.83	33	0.18	No	0
23	20	34	720-ZP	PIT		TSC	0.64	0.41	58	340	0.22		1	0.47	75	0.09	No	0
23	8	61	680-ZP	PIT		TSC	3.75	0.53	83	86	0.18	59%,	1	0.31	57	0.15	No	0
23	10	72	720-ZP	PIT		TSC	1	0.62	113	350	0.19	3%, 2.79V	1	0.57	89	0.21	No	0
23	10	72	720-ZP	PIT		TSC	1	0.74	101	350	0.13	3%, 2.79V	2	0.9	57	0.15		
24	45	51	700-ZP	PIT		TSH	0.47	0.17	107	211	0.28	0.59V 78%		0.21	70	0.26	No	0
24	45	51	700-ZP	PIT		TSH	-0.1	0.21	118	211	0.17			0.15	33	0.22		
24	8	59	680-ZP	PIT		TSC	4.13	0.24	93	182	0.3	38%, 2.41V	1	0.23	58	0.16	No	0
24	8	60	720-ZP	PIT	51	TSC	4.96	0.16	101	182	0.26	0.77V 28%		0.14	45	0.16	No	0
24	17	63	680-ZP	PIT		TSH	4.7	0.27	98	217	0.31	1.06V 12%					No	0
24	17	63	680-ZP	PIT		TSH	5.54	0.32	116	217	0.22							

Table 5.2.4-5: IP 2 Spring 2000 Tubes with VOL Indications Subjected to In-situ Testing

SG	Row	Col	Probe	I_typ	Per	Loc	Inch1	Volts	Deg	Tape	Axial	C-5/Bobbin	Indication	Max. Volts	Max. %	Length (in)	In-situ test required?	Leak
21	16	6	720-ZP	VOL	-	TSH	0.94	0.32	98	441	0.24	1.53V NQI	1	0.45	84	0.3	No	0
21	16	6	720-ZP	VOL	-	TSH	12.38	0.35	86	509	0.38		2	1.02	62	0.44	No	0
22	30	13	680-ZP	VOL	-	TSH	0.33	0.89	124	261	0.28	74%, 3.15V	1	1.44	37	30%	No	0
22	31	15	700-ZPANM	VOL	-	TSH	0.58	1.85	95	509	0.96		1	1.8	63	1.12	No	0
23	33	77	720-ZP	VOL	-	TSH	18.7	0.72	108	507	0.56		1	0.84	32	0.28	No	0
24	8	23	720-ZP	VOL	-	TSC	0.25	0.56	56	320	0.36	0%, 0.97V	1	0.47	52	0.08	No	0
24	24	34	680-ZP	VOL	6	TSH	12.11	0.13	118	203	0.218	4.75V		0.17	0.35	0%	No	0
24	24	34	680-ZP	VOL	3	TSH	10.2	0.44	119	203	0.368	4.53V		0.13	0.27	0%		
24	24	34	680-ZP	VOL	6	TSH	8.3	0.21	118	203	0.288	17.38V		0.14	0.23	10%		
24	24	34	680-ZP	VOL	3	TSH	8.03	0.36	119	203	0.3	10.88V		0.1	0.32	0%		
24	24	34	680-ZP	VOL	3	TSH	6.39	0.36	119	203	0.323	14.83V		0.15	0.34	7%		
24	21	42	680-ZP	VOL	-	TSC	3.28	0.14	94	180	0.34	34%, 1.33V	1	0.78	61	29%	No	0

Figure 5.2.4-1

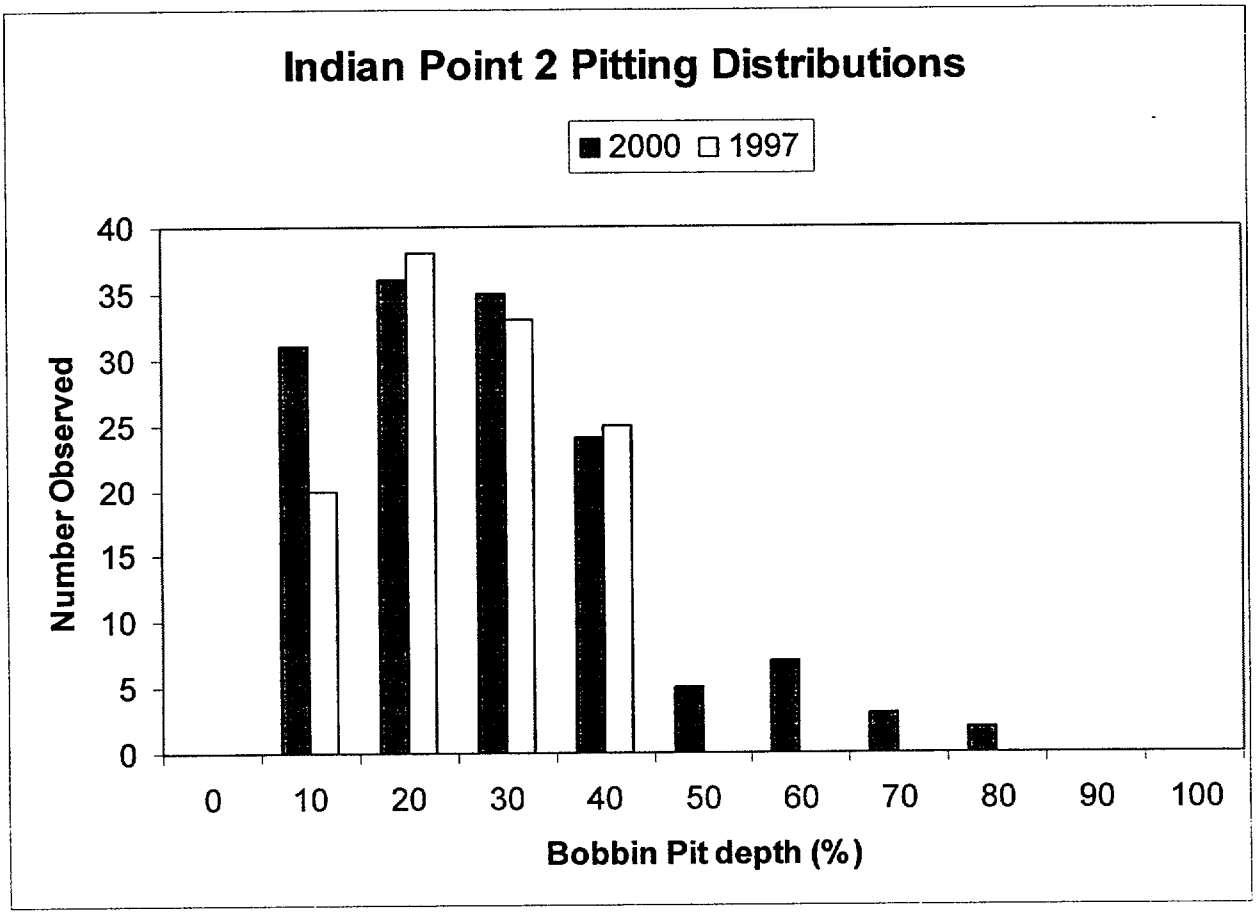
Indian Point 2 Pitting Distributions
2000
1997
Number Observed
0
5
10
15
20
25
30
35
40
0
10
20
30
40
50
60
70
80
90
100
Bobbin Pit depth (%)

5.2.5 AVB Related Wear

The AVB indications observed (Table 5.2.5-1) were consistent with expectations; none exceeded the 40% plugging criteria. The NDE sizing uncertainty for AVB wear is based on data in ETSS #96004 and is given as 14.6 % (95% CL). Therefore, none of the AVB wear indications exceeded the structural limit, and condition-monitoring requirements are met.

5.2.6 Foreign Objects

During the course of eddy current inspection, various potential loose part (PLP) signals were observed at locations near the top of the tubesheet. Some of the locations where the PLP signals were observed had indications of tube wear. Table 5.2.6-1 contains a summary of the tubes found with PLP indications during the current outage. Table 5.2.6-2 contains a summary of the tubes that were determined to require plugging due to PLP signals. Tube R31/C15 in SG 22 was found to have a wear depth of 52%TW. The NDE sizing uncertainty for foreign object wear is 14.6% (95% CL). Although a structural limit of 60% TW is conservatively used for analyses of foreign object wear, the actual structural limit for wear is approximately the same as for AVB wear, i.e., 71% TW. Since none of the indications exceeded the structural limit when NDE uncertainties are included, condition-monitoring requirements are met.

5.2.7 Condition Monitoring Conclusions

- All sludge pile ODSCC indications detected during the EOC-14 inspection were in situ pressure tested. Except tube R34C51, none of the other sludge pile ODSCC flaws experienced either leakage or depressurization at steam line break (SLB) pressure differential (2560 psi) or even at the maximum test pressure of 5173 psi which significantly exceeds $3\Delta P_{NOP}$ structural margin requirement. R34C51 was shown to meet the $3\Delta P_{NO}$ requirement by demonstrating that the depressurization occurred due to ligament tearing. When ligament tearing is taken into account, the burst pressure for a true burst with crack tip tearing was shown to exceed the $3\Delta P_{NO}$ requirement. Thus, all sludge pile indications met the structural margin requirement.

- Tubesheet crevice cracks cannot burst due to the restraint provided by the tubesheet; thus the potential condition monitoring concern is limited to leakage. The largest tubesheet crevice cracks were sized using profiling techniques to determine the need for in-situ testing according to the criteria for in-situ test selection. None of the cracks met the criteria that would have required in-situ testing. Nevertheless, three of the largest crevice cracks were in-situ tested at the SLB pressure differential. None of the cracks tested resulted in any leakage; thus, condition-monitoring requirements are met for tubesheet crevice cracks.

- Expansion zone cracks cannot burst due to the restraint provided by the tubesheet; thus, only potential leakage of these cracks need be considered for condition monitoring. The reported cracks, both axial and circumferential, were found in the original hardroll region or below

F*, licensed at IP2. An in-situ leak test performed in 1997 on a 0.56" long crack in the original hardroll resulted in no leakage. Since indications in this region do not present either burst or large leakage potential, none of the expansion zone cracks were in-situ tested in 2000. Pullout of tubes due to presumed circumferential separation of tubes is prevented by F* criteria since circumferential cracks were observed only below the F* length. Therefore, since tube rupture is not an issue, absence of leakage has been confirmed by in-situ testing (in 1997), and pull-out potential of the tubes is addressed by F*, condition monitoring requirements for expansion zone cracks are satisfied.

- Satisfaction of condition monitoring requirements for pits and volumetric indications was demonstrated by in-situ testing of the bounding indications. None of the indications tested leaked at applied pressures equal to the $3\Delta P_{NO}$.

- Observed indications of AVB wear meet condition monitoring requirements. The maximum indication found was 38% TW. When the NDE sizing uncertainties of 14.6% (95% CL) are added, the resulting 52.6 % is well below the structural limit of 71%.

- No tubes with foreign object wear were found that had average wear depth exceeding the conservative structural limit of 60% TW assumed, and no other tubes are projected to exceed this limit during the next operating cycle. Thus, condition-monitoring requirements are satisfied.

Table 5.2.5 - 1 IP2 2R14 AVB Wear Indication Summary				
SG	# IND	# ≥ 40%	Max. % Depth	Cycle 14 95% Cumulative Growth Rate*
21	0	0	0	-
22	3	0	31	Combined Data for 3 SGs: 8.67%
23	7	0	34	
24	71	0	38	

Table 5.2.6-1

PLP Indications – IP2 Spring 2000 Outage

S/G	Row	Col	Leg		S/G	Row	Col	Leg
21	18	7	H		22	28	12	H
21	8	9	H		22	29	12	H
21	9	9	H		22	30	13	H
21	20	14	H		22	31	15	H
21	21	14	H		22	30	16	H
21	31	15	H		22	31	16	H
21	32	17	H		22	30	17	H
21	33	35	H		22	31	17	H
21	3	45	C		22	32	17	H
21	38	62	C		22	33	17	H
21	29	79	H		22	30	18	H
21	30	79	H		22	31	18	H
21	8	96	C		22	35	79	H
21	9	87	C					
21	20	88	C					
21	8	89	C					

S/G	Row	Col	Leg		S/G	Row	Col	Leg
23	31	15	H		24	12	3	H
23	34	17	H		24	13	3	H
23	34	18	H		24	13	4	H
23	35	18	H		24	31	16	C
23	22	19	H		24	28	17	H
23	34	19	H		24	43	59	C
23	21	20	H		24	23	79	C
23	22	20	H		24	23	80	C
23	27	20	H		24	26	80	C
23	29	20	H		24	20	83	C
23	30	20	H		24	7	87	C
23	43	33	H		24	7	88	C
23	44	56	H		24	7	91	C
23	44	57	H					

Table 5.2.6 –2
Loose Part Plugging List – IP2 Spring 2000 Outage

No	Steam Generator	Tube Location	Comments
1	22	R31C15	Tube Has 52% TW Wear Indication
2	22	R30C12	Box Plug Tube (For R30C13)
3	22	R30C13	Tube Has PLP signal with <20% TW wear indication
4	22	R29C12	Box Plug Tube (For R30C13)
5	22	R29C13	Box Plug Tube (For R30C13)
6	22	R29C14	Box Plug Tube (For R30C13)

This list only includes tubes plugged due to loose objects.

6.0 Operational Assessment

6.1 Sludge Pile/Free Span Cracking

This section describes the analyses carried out to determine an acceptable operating period between inspections for axial Sludge Pile ODSCC indications. A conservative approach based on Monte Carlo methods is applied to perform structural and leakage assessment for sludge pile indications and is similar to the approach used for the analysis of U-bend indications. The methodology entails application of Monte Carlo methods to project crack depth profiles to the end of operating period and comparing the burst pressures calculated at 95% probability and 95% confidence (95/95) with the deterministic structural limit ($3\Delta P_{NO}$). The limiting EOC burst pressures are also calculated at 90% probability at 50% confidence (90/50) as required by the EPRI SG integrity guidelines. The Monte Carlo analyses included allowances for POD, NDE uncertainties and growth. This methodology is described in Section 4.6.

Development of the input data needed to perform structural and leakage assessment is presented in Section 4.

6.1.1 Reference Analyses

The reference analyses for establishing an acceptable Cycle 15 operating cycle length are based on a total SG analysis applying the axial profile analysis methodology described in Section 4.6. This analysis applies Monte Carlo techniques to develop the limiting indication burst pressure distribution at the end of the period for comparison at 95/95 or 90/50 confidence with the $3\Delta P_{NO}$ = 4668 psi burst margin requirement for Cycle 15. The analysis methods also evaluate for SLB leakage including the ANL ligament tearing model in the analysis. The limiting SG for this analysis is SG 2, which had 13 of the 26 sludge pile indications in the EOC-14 inspection, including 6 out of the 8 indications with the lowest burst pressures in the condition monitoring analysis.

The input data for the total SG analysis are developed in Section 4 of this report as noted below:

- EOC-14 crack depth profiles from sizing +Point data (Section 4.4).
- POD distributions as functions of average and maximum depth of Figure 4.3-2 (Section 4.3).
- NDE uncertainties on average depth, maximum depth and length per Section 4.4.
- Growth rates for average depth, maximum depth and length per Section 4.5 and Figures 4.5-4 to 4.5-6.
- Westinghouse tube material flow stress distribution for 7/8 inch tubing with a nominal value of 68.28 ksi at operating temperature.
- Axial profile analysis methods, Westinghouse burst correlation and ANL ligament tearing model for leakage as described in Section 4.6.

In addition, data is also needed for total number of new indications, their shape and depth and length distributions. However, the limiting indication burst pressure, total SG burst probability and leak rate are not sensitive to the input describing new indications (since the limiting indications are determined by undetected indications modeled by POD application). Therefore,

new indication parameters used in the operational assessment of free span indications in another plant were used in the present analyses.

To establish an acceptable operating cycle length, analyses were carried for the Cycle 15 full operation duration of 1.7 EFPY as well as for 1.0 EFPY, the latter period bounds the operating period recommended based on the operational assessment for U-bend indications. The reference analysis results are shown in Table 6.1-1. For a 1.0 EFPY operating cycle, the limiting indication burst pressure at the end of the period is 5093 psi at 95/95 confidence calculated for SG-22 compared to the $3\Delta P_{NO}$ = 4668 psi burst margin requirement for Cycle 15. The corresponding minimum burst pressure for SG-23 is 5528 psi, and the minimum burst pressures for SGs 21 and 24 are even higher. The projected SG-22 SLB tube burst probability at 95/95 for a 1.0 EFPY operating period is 3.5×10-4.

The POD, NDE uncertainties and growth input data used to the sludge pile ODSCC integrity analyses are well defined; therefore, the confidence level requirements of the EPRI guidelines (90% probability at 50% confidence) are adequate to support the operating cycle. As discussed in Section 4.2, the burst probability criteria based on the EPRI SG integrity guidelines for all known degradation mechanisms are 0.08 for burst at $3\Delta P_{NO}$ and 0.04 for burst at ΔPSLB, at 90/50 probability. Total free span burst probability that includes contributions of U-bend axial PWSCC indications and sludge pile ODSCC indications should be compared against the acceptance guidelines. From Reference 1, burst probabilities predicted by the reference analysis for U-bend axial PWSCC indications in the limiting SG (SG-22) at ΔPSLB and $3\Delta P_{NO}$ are 2.97×10-3 and 4.07×10-2, respectively, at 90/50 probability. The corresponding burst probabilities at 90/50 for the sludge pile ODSCC indications are 2.50×10-4 and 2.51×10-2, respectively, at ΔPSLB and $3\Delta P_{NO}$. Thus, the total free span burst probabilities at 90/50 from the reference analyses are 3.22×10-3 and 6.58×10-2, respectively, at ΔPSLB and $3\Delta P_{NO}$, and they are both below their respective guideline (0.04 at ΔPSLB and 0.08 at $3\Delta P_{NO}$). No SLB leakage is expected over this operating period at 90/50 or 95/95 probability. Consequently, operation for a period of 1.0 EFPY would be acceptable from the standpoint of structural integrity of tubes with sludge pile indications.

The analyses for the full operating period of 1.7 EFPY show that the 95/95 minimum burst pressure for the limiting SG (SG-22) is only 7 psi below the 4668 psi burst margin requirement for Cycle 15, but the limiting burst pressure at 90/50 exceeds the burst margin requirement. The burst probabilities at 90/50 for the sludge pile indications in SG-22 are 1.00×10-3 and 4.95×10-2, respectively, at ΔPSLB and $3\Delta P_{NO}$. Total free span burst probabilities cannot be calculated as the U-bend indications contribution at 1.7 EFPY is not available.

6.1.2 Sensitivity Analyses

Analyses were performed to assess the sensitivity of the operating cycle length to growth rates, POD and NDE uncertainties. All sensitivity analyses were performed for a 1.0 EFPY operating period. For growth rate sensitivity, a bounding log-normal distribution was developed as described in Section 4.5. Results from the sensitivity analyses are shown in Table 6.1-2. For a one year operating period, the bounding growth reduces the limiting indication burst pressure at

95/95 probability by about 253 psi to 4840 psi, which still substantially exceeds the $3\Delta P_{NO}$ = 4668 psi burst margin requirement for Cycle 15. No leakage is predicted at the higher growth rate. The total free span burst probabilities for SG-22 at 90/50 (including the U-bend indications contribution), 3.57×10-3 and 7.91×10-2 respectively at ΔPSLB and $3\Delta P_{NO}$, are both below their respective guidelines.

The +Point POD for sludge pile indications presented in Section 4.3 was developed conservatively. Nevertheless, a sensitivity analysis was performed for the limiting SG by using an even more conservative POD distribution. The POD for an indication would decrease if the POD distribution curve in Figure 4.3-2 is shifted to the right. So, as a sensitivity analysis, a POD distribution with 5% depth increase (shift of distribution to deeper depths) was evaluated. This reduces the limiting indication burst pressure at 95/95 probability by about 333 psi to 4760 psi, which is still significantly higher than the $3\Delta P_{NO}$ = 4668 psi burst requirement. The total free span burst probabilities at 90/50 (including the U-bend indications contribution) are 3.06×10-3 and 8.25×10-2, respectively, at ΔPSLB and $3\Delta P_{NO}$. The burst probability at $3\Delta P_{NO}$ slightly exceeds the 8 ×10-2 guideline developed in Section 4.2. However, the burst probability limit recommended in the EPRI structural integrity guideline is 10-2 and this limit is met the POD sensitivity analysis.

To assess the sensitivity of the minimum calculated burst pressure to NDE uncertainties, the analysis for the limiting SG (SG-22) was repeated with a 25% increase in the standard deviation for errors in the measurement of crack length, average depth and maximum depth. The results show that the limiting indication burst pressure at 95/95 probability decreases by about 206 psi to 4887 psi for 1.0 EFPY operation, which still exceeds the 4668 psi requirement. The total 90/50 free span burst probabilities at ΔPSLB and $3\Delta P_{NO}$, 3.47×10-3 and 7.70×10-2 remain below their respective guidelines.

In summary, analyses to assess the sensitivity of the limiting indication burst pressure to growth rates, POD and NDE uncertainties show that the $3\Delta P_{NO}$ = 4668 psi burst margin requirement for Cycle 15 is satisfied for a 1.0 EFPY operating period between inspections. No SLB leakage is expected for cycle lengths in excess of one year. The total free span 90/50 burst probabilities at ΔPSLB and 3ΔPNO that include the U-bend indications contribution are below their respective guidelines. The sensitivity analyses are primarily performed to demonstrate that there is no sharp drop in the predicted burst pressure and burst probability and are not required to satisfy the burst margin requirement. Thus, a 1.0 EFPY operating period is acceptable for sludge pile axial ODSCC indications.

6.1.3 Operational Assessment Conclusions

The reference analyses show that the $3\Delta P_{NO}$ = 4668 psi burst margin requirement for Cycle 15 is satisfied for a 1.0 EFPY operating period. The projected limiting indication burst pressure at 1.7 EFPY satisfies the 4668 psi acceptance limit at the EPRI integrity guideline required confidence level of 90/50. Sensitivity analyses to growth, POD and NDE uncertainties show that predicted limiting indication burst pressures and the total free span burst probabilities for a 1.0 EFPY operation are not sensitive to the input data used.

Table 6.1-1.
Indian Point-2 Cycle 15 Sludge Pile Indications
Reference SG Cycle Length Analyses for Projected Burst Pressures and Leak Rates[1]

SG	No. of Indications (EOC-14 Inspection)	Operating Period (EFPY)	Limiting Burst Pressure (psi)	SLB Leak Rate (gpm)	SLB Burst Probability	$3\Delta P_{NO}$ Burst Probability
95% Probability/95% Confidence						
22	13	1.0	5093	0.0	3.49×10^{-4}	2.66×10^{-2}
23	9		5528	0.0	1.57×10^{-4}	1.56×10^{-2}
22	13	1.7	4661	0.0	1.19×10^{-3}	5.67×10^{-2}
23	9		5094	0.1	7.22×10^{-4}	4.56×10^{-2}
90% Probability/50% Confidence						
22	13	1.0	5615	0.0	2.50×10^{-4}	2.51×10^{-2}
23	9		5993	0.0	1.00×10^{-4}	1.01×10^{-2}
22	13	1.7	5240	0.0	1.00×10^{-3}	4.95×10^{-2}
23	9		5640	0.0	3.20×10^{-4}	2.57×10^{-2}

1. Acceptance criteria: $3\Delta P_{NO} = 4668$ psi at operating temperature, SLB leak rate = 1 gpm summed over all degradation mechanisms. Burst probability guidelines: $\Delta P_{SLB} = 4\times10^{-2}$, $3\Delta P_{NO} = 8\times10^{-2}$ summed for all degradation mechanisms in limiting SG.

Table 6.1-2. Indian Point-2 Cycle 15 Sludge Pile Indications
SG Sensitivity Analyses for Growth, POD and NDE Uncertainties
Projected Burst Pressures and Leak Rates[1] for Assumed Cycle Duration = 365 EFPD

SG	Growth Rate	NDE Uncertainty	POD	Limiting Burst Pressure (psi)	SLB Leak Rate (gpm)	SLB Burst Probability	$3\Delta P_{NO}$ Burst Probability
Sensitivity to Growth Rates							
22	Nominal	Reference	Reference	5093	0.0	3.49×10^{-4}	2.66×10^{-2}
	Bounding	Reference	Reference	4840	0.0	7.22×10^{-4}	4.25×10^{-2}
23	Nominal	Reference	Reference	5528	0.0	1.57×10^{-4}	1.56×10^{-2}
	Bounding	Reference	Reference	5290	0.0	2.55×10^{-4}	2.91×10^{-2}
Sensitivity to POD							
2	Nominal	Reference	Reference	5093	0.0	3.49×10^{-4}	2.66×10^{-2}
	Nominal	Reference	Shift +5%	4760	0.0	5.58×10^{-4}	6.88×10^{-2}
Sensitivity to NDE Uncertainty							
2	Nominal	Reference	Reference	5093	0.0	3.49×10^{-4}	2.66×10^{-2}
	Nominal	1.25× Ref. Std. Dev.[2]	Reference	4887	0.0	6.22×10^{-4}	4.06×10^{-2}

1. Acceptance criteria: $3\Delta P_{NO}$ = 4668 psi at operating temperature, SLB leak rate = 1 gpm summed over all degradation mechanisms. Burst probability guidelines: $\Delta P_{SLB} = 4\times10^{-2}$, $3\Delta P_{NO} = 8\times10^{-2}$ summed for all degradation mechanisms in limiting SG.
2. Standard deviation of NDE uncertainty associated for indication length, average depth and max. depth increased by 25%.

6.2 Operational Assessment Evaluation for Tubesheet Crevice ODSCC

Should axially oriented degradation occur in the unexpanded tube length within the tubesheet, tube burst is precluded by the presence of the tubesheet. The eddy current inspections performed during the 2000 forced outage/refueling and maintenance outage have identified significant indications that potentially could have resulted in primary to secondary leakage during a postulated SLB event. All tubes with identified indications in the tubesheet crevice region have been plugged. While the total population of tubes plugged for 2R14 tubesheet crevice ODSCC indications increased to >3 times the number plugged at 2R13, this rise is attributed to the implementation of +Point inspection of the full hot leg tubesheet length for 100% of the tubes. Table 6.2-1 shows that the number of confirmed CECCO-5 indications is essentially the same for the 1997 and 2000 inspections, the expansion of the inspection to 100% of the tubesheet using the +Point probe resulted in a significant increase in the number of indications.
While the numbers of indications reported increased, the maximum depths observed were less than had been found acceptable in the 2R13 data for crevice ODSCC, and the maximum +Point amplitude observed (2.91V and ~0.1" length > 75% - maximum depth =79%, on 3/24 in SG 22) was substantially lower than was observed on the limiting indication from 1997. All of the known crevice ODSCC indications reported in 1997 were plugged, and generally, only tubes with indications detected by the Cecco/Bobbin probe were examined with the +Point probe. Since no tubesheet ODSCC growth data from IP-2 was available to be evaluated for Cycle 14, and since the projected operating interval would be shorter than Cycle 14, no attempt is made to calculate the deterministic maximum depth for Cycle 15 for tubesheet ODSCC.

None of the 6 tubes with crevice ODSCC that were subjected to in-situ testing at SLB conditions exhibited leakage related to crevice indications during the testing, repeating the experience for the limiting 1997 crevice indication (3.64 +Point volts, 85% peak depth). Similar indications detected during the next scheduled eddy current inspection would also not be expected to leak at SLB conditions, particularly since the population of detected indications includes significantly smaller indications in 2000 than in 1997.

As no changes are anticipated in operating temperatures at IP 2 for Cycle 15 and the anticipated cycle length is less than the Cycle 14 length of 540 days, a more extensive crevice degradation condition is not anticipated. Therefore, it can be reasonably concluded that tubesheet crevice ODSCC would not be expected to be a source of significant primary to secondary leakage during a postulated SLB event. Thus, since tubesheet crevice ODSCC does not present a challenge to structural integrity, i.e., no burst potential, and the leakage is expected to be negligible, the operational assessment requirements for tubesheet crevice ODSCC are satisfied for a cycle length of 1.48 EFPY.

Table 6.2-1
Comparison of 1997 and 2000 Crevice ODSCC Indications

SG	21	22	23	24	ALL	Notes
Spring 2000	0	27	1	2	30	1
Spring 2000	6	52	30	27	115	2
Spring 1997	0	20	2	7	29	1

Notes:

1) Tubes with confirmed CECCO-5 Indications >40° and >3" from TEH
2) Tubes with RPC Indications>40° and >3" from TEH; includes both confirmed CECCO-5 indications and additional +Point indications.

6.3 Axial and Circumferential PWSCC/ODSCC in the Expansion Zone - Roll Transition Zone

For both axial and circumferential SCC occurring in the expansion zone, whether in the factory condition or after re-rolling, the structural integrity of the tubing is unaffected because of the presence of the surrounding collar formed by the tubesheet. For the indications that extend above the bottom of the roll transition (BRT), there is the potential that an axial ID crack with depth exceeding 80% TWD for more than 0.1" in length could leak under SLB conditions. Indications were screened for maximum amplitude > 3 volts with +Point and for maximum depth > 80%. Since no tubes passed both criteria, no profiling analysis was performed on axial PWSCC indications and no in-situ tests were required for this degradation mechanism. .
In cases where the roll transition is at the top of the tubesheet, the operational analysis has assumed the presence of small crack (0.06"), from which industry growth rates are applied, leading to the conclusion none of such cracks would be expected to grow to the limiting crack length during the projected interval of operation. This analysis assumed that the cracks could grow into the free span above the top of the tubesheet, but for the deep tubesheet expansion zone cracks at IP2 it is expected that no axial PWSCC indications will be present above the tubesheet at EOC-15 and therefore cannot challenge structural integrity.

Circumferential PWSCC and ODSCC indications in the roll transition region have been found at IP2 for more than 4 cycles. The increased number found during 2R14 as a result of the 100% hot leg +Point inspection program included only 4 tubes with indications in the roll transition (Table 5.2.3.2). These were shown to have been insufficient in amplitude to represent a leakage potential. Only 3 prior indications that were examined with +Point probes were reported in 1997; therefore there was insufficient information on which to base a growth rate determination. Since there was no reported operational leakage and the amplitudes of the 4 indications found above the BRT were so small (all < 1 volt), no basis existed to perform an deterministic calculation for an operational assessment using the 2R14 data. With all the tubes with observed circumferential indications either plugged or re-rolled in compliance with F* repair criteria, there are no known cracks continued in service that have the potential to produce leakage under SLB

conditions. Since the Cycle 15 operating period is smaller than that for Cycle 14, circumferential indications at EOC-15 would be expected to be no larger than found at the 2R14 inspection. Consequently, operational assessment burst and leakage requirements would be satisfied at EOC-15.

It is concluded that the IP2 axial and circumferential indications in the expansion transition region will satisfy structural and leakage requirements

6.4 TTS Pitting/Volumetric Indications

All pitting indications and volumetric indications confirmed by +Point inspections were conservatively plugged, regardless of the reported bobbin depth of the indication. Volumetric indications, other than confirmed wear indications, are considered to be probable pits and will be treated the same as pits for this assessment; even if treated as IGA, these indications did not exceed the screening criteria for consideration as in-situ testing candidates.

The database for ETSS #96005 shows that all indications >20% throughwall were detected; a single indication less than 20% TW was also detected. Thus the bobbin detection sensitivity for pitting is shown to be about 20% TW. Section 5.2.4 provides an upper limit growth rate for pitting of 32% for the 1.48 EFPY operating cycle 14. The structural limit for pitting was determined to be 85% TW based on a uniform thinning assumption. Uniform thinning is the case where the tube wall is assumed to be reduced circumferentially around a tube over a length that envelopes any of the indication lengths; applied to pitting this is a conservative evaluation, as even a 100% TWD pit would not present a structural challenge.

For the operational assessment, it is conservatively assumed that a 40% TW pit or volumetric indication is undetected. If the 1.48 EFPY maximum growth rate , 32%, is added to this assumed undetected indication, the end of cycle predicted indication depth is 72% TW. Since the predicted depth of the indication is significantly less than the structural limit of 85% TW, operational assessment requirements are met for pitting/volumetric indications for the next cycle of at least 1.48 EFPY.

Based on these values for a pitting indication left in service, growth rate, NDE sizing uncertainties and structural limit, the acceptable operating period for Cycle 15 is calculated from the following logic:

Indication left in service	40%
+ growth rate (95%CL) * Cycle 15 EFPD/Cycle 14 EFPD	32%
+ NDE uncertainty (95% CL)	0%
<= structural limit.	85%

Based on a 32%/1.48 EFPY growth rate, the acceptable operating period for pitting/volumetric degradation is approximately 2.1 EFPY. Therefore, the operational assessment requirements are demonstrated for the next operating cycle of IP2 for pitting/volumetric degradation.

6.5 AVB Wear

For those of the 81 indications reported in all the SGs that could be evaluated as to growth rate, based on actual comparisons of measured values, an average Cycle 14 growth rate of 1.36% was observed.

Growth determinations for 55 of the observed indications were available either from the as-reported 2R13 results or from re-analysis of the 2R13 eddy current tapes at the site reported in 2R14. The largest growth rate associated with prior indications was 11%, observed in both SG 22 and SG 24 (see Figure 5.2.5-1). Comparison of the AVB wear indications distributions for 2R13 and 2R14 show a slightly higher incidence of wear but essentially no change in the overall distribution (Figure 5.2.5.2).

The corresponding 95% cumulative distribution values for the Cycle 14 growth rate was 8.67% (95%CL) for the operating period of 1.48 EFPY. The maximum observed growth rate for the same operating period was 11% TW. The observed growth rates are consistent with the 95% cumulative distribution allowance (8.48%), determined on the basis of Cycle 13 growth. These numbers are subject to minor adjustments for actual cycle length completed for Cycle 14 and the cycle length anticipated until the end-of cycle (EOC) 15; Cycle 14 accrued 1.48 EFPY .

NDE uncertainties were developed with a value of 14.6% at 95% CL, based on the EPRI data base for Appendix H qualification of the bobbin inspection technique (ETSS # 96004). (More recent data that are not yet included in the EPRI database show that the sizing uncertainties for AVB wear are less than 7% at 95% CL). The structural limit for AVB wear was calculated at 71% TW.

Based on these values for indication left in service, growth rate, NDE sizing uncertainties and structural limit, the acceptable operating period for Cycle 15 is calculated from the following logic:

Indication left in service	38%
+ growth rate (95%CL) * Cycle 15 EFPY/Cycle 14 EFPY	18.4%
+ NDE uncertainty (95% CL)	14.6%
<= structural limit.	71%

Based on the 8.67%/1.48 EFPY growth rate, the acceptable operating period for AVB wear is 3.1 EFPY. Therefore, the operational assessment requirements are demonstrated for the next operating cycle of IP 2 for AVB wear.

Figure 5.2.5.1

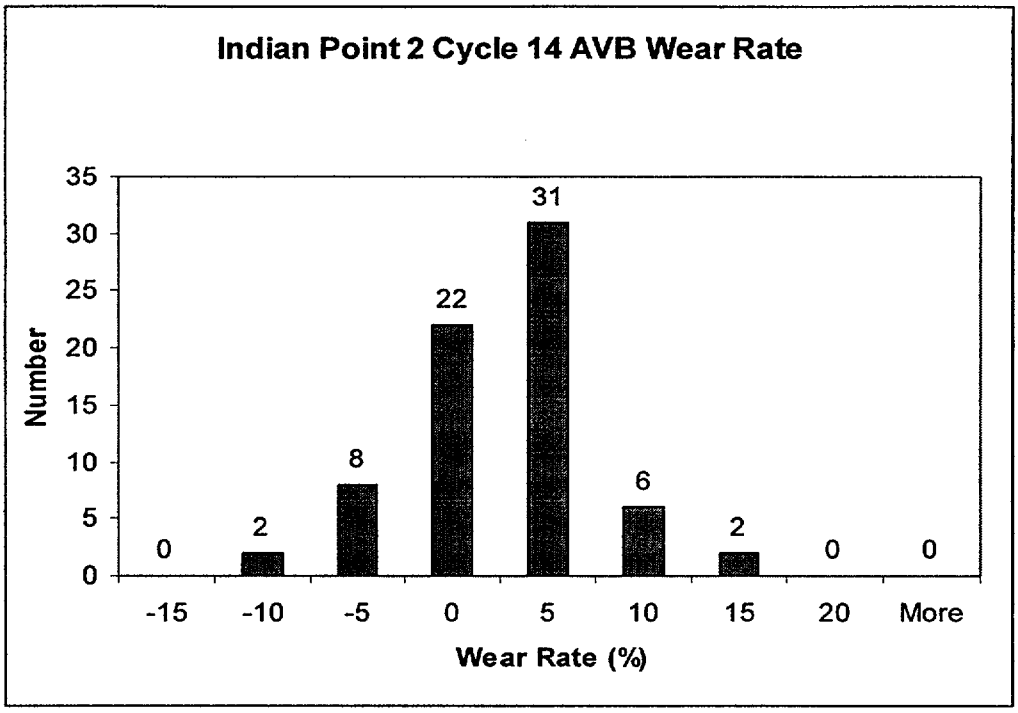

Figure 5.2.5.2

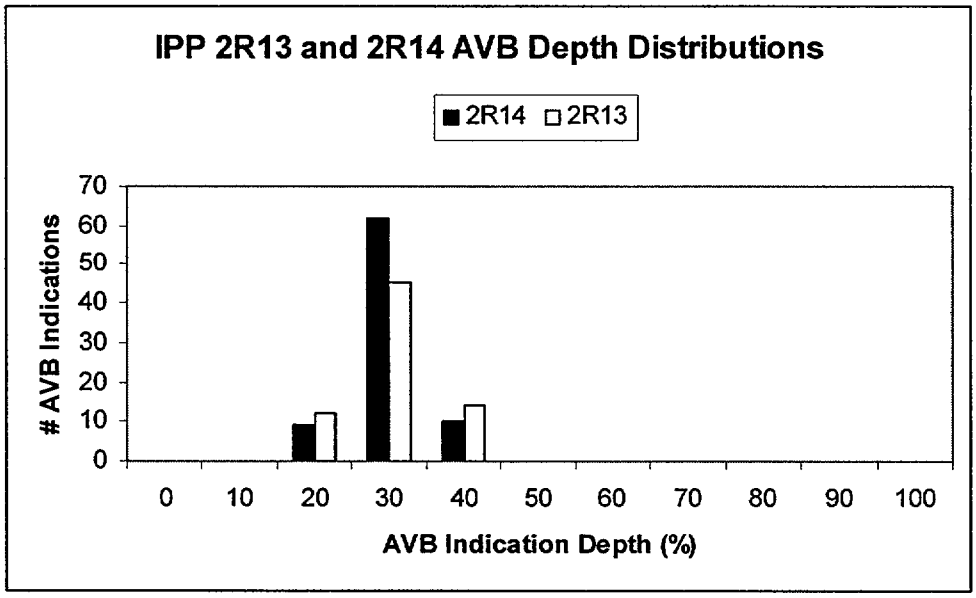

6.6 Foreign Objects

An analysis of the current and historic eddy current data was performed to generate a conservative estimate of the rate of tube wear that could be occurring at these locations (Reference 6). This analysis has determined that most of the locations had wear rates that were acceptable for continued operation for an additional 1.48 EFPY of operation. However, one of these tubes was found to have an active wear rate based on review of 2R13 and 2R14 inspection data. Since this tube was at a peripheral location, it was determined that this tube, along with its neighboring tubes should be plugged to provide a buffer zone against wear propagation in the bundle.

Visual examination of the SGs provided an inventory of foreign objects residing in the SGs that could not be removed. Evaluations were performed to determine the effects of these objects that are either known to be, or are presumed to be located in the secondary side of the S/Gs at IPP 2 (Reference 3). Object 1 through 12, as contained in 6.6-1, describes a list of objects that have been visually observed to be located in the S/Gs. Object 13 addresses machine chips that are believed to be present on the secondary side, and are a result of machining performed to provide access to the upper tube bundle region of S/G 24. Evaluations of all of these loose objects were performed assuming that the objects are located at the limiting location in the S/G with respect to tube wear. The analysis determined that none of these objects will wear a tube down to the minimum allowable tube wall thickness (60%TW) within the next 1.48 EFPY. Therefore, all of these objects can remain in the S/G for the next operating cycle.

An analysis of the current and historic eddy current data was performed for tubes with PLP indications to generate a conservative estimate of the rate of tube wear that could be occurring at these locations (Reference 7). This analysis has determined that most of the locations had wear rates that were acceptable for continued operation for an additional 2 years of operation. However, one of these tubes (R30/C13, SG- 22) was found to have a wear rate that could potentially be rapid. Since this tube was at a peripheral location it was determined that this tube, along with its neighboring tubes should be plugged to provide a buffer zone against wear propagation in the bundle. Table 5.2.6-2 contains a summary of the tubes that were determined to require plugging due to PLP signals.

A conservative structural limit of 60% TW was assumed for wear due to foreign objects. Conservatism is demonstrated by comparison with the structural limit for other volumetric indications such as AVB wear and Pits, for which structural limits are 71%TW and 85% TW respectively. Since none of the PLP indications had a depth that exceeded the structural limit when NDE uncertainties (14.6 % , 95% CL) and maximum growth found (20%TW/1.48 EFPY), operation for at least 1.48 EFPY is justified with regard to loose parts.

Table 6.6-1
Loose Object Inventory – IPP 2 Spring 2000 Outage

Object No	S/G	Foreign object	Description or Approx. Size	Location
1	21	Metal wedge	1.5" x ¾" x ½"	R14C3
2	21	Weld Rod/wire	1/8" dia. X > 4.0 " long	C51R45
3	21	Small Metal piece	1/3 "(t) x ¾ (h) x 2.5 " L	C57R44
4	21	strap	1/8"t x 2.0 h x 3.0" long	C58R44
5	21	All thread	~1/2" dia. x 3.5 " long	C47R1 TL
6	22	Metal Plate	.36" x 0.36 " x 0.75"	C53R45
7	23	Wire	1/8 " dia. x > 4.0 long	C18R36
8	23	round metal	½"dia x 2.8 " long	C16R34
9	24	Metal	7/8" (h) x 0.6"w x 0.6" L	C1R8
10	24	flex gasket	~0.14" wide x 2.8" long	C41R45
11	24	sludge rocks	Max 5/8" dia. x 1.0" long	Not defined
12	24	Wire	~0.1" dia. x ~ 0.5" long	C73R37
13	24	Machine Chips	0.2 Inch Curl	Unknown

6.7 Operational Assessment Conclusions

- For Sludge Pile ODSCC, both the reference analyses and sensitivity analyses support Cycle 15 operation in excess of 1.0 EFPY. The reference analyses show that the $3\Delta P_{NO}$ = 4668 psi burst margin requirement for Cycle 15 is satisfied for a operating period close to the full cycle operation of 1.7 EFPY. The projected limiting indication burst pressure at 1.7 EFPY is only 6 psi below the 4668 psi acceptance limit and 5093 psi at 1.0 EFPY. No SLB leakage is expected for cycle lengths in excess of one year. The total free span tube burst probabilities that includes contributions of U-bend indications after 1.0 EFPY of operation are 3.22×10^{-3} and 6.58×10^{-2} compared to an acceptance guidelines of 0.04 at ΔP_{SLB} and $3\Delta P_{NO}$, respectively. Sensitivity analyses to growth, POD and NDE uncertainties show that substantial margins would still exist in the limiting indication burst pressures after 1.0 EFPY operation.

- Tubesheet crevice indications are not subject to burst because of the restraint provided by the tubesheet. The potential for leakage was shown to be acceptable for the 2R15 operating interval by leak-free results returned from in-situ testing of the most severe crevice ODSCC indications. This projects that no indications with unacceptable leakage potential at SLB conditions will exist during Cycle 15.

- Expansion zone cracks are constrained from rupture by the reinforcement provided by the tubesheet; thus operational concerns are limited to leakage from EZ cracks. Leakage from roll transition cracks is limited to small values due to the flow restriction provided by the tubesheet crevice. Expansion zone cracks are repaired according to the criteria of F* licensed for IP 2. Tubes failing to meet the F* criteria are plugged. The potential leakage anticipated from expansion zone SCC under SLB conditions is acceptable based on the provisions of F* and the leak-free result for the worst case crack tested in 2R13.

- The minimum acceptable cycle length for Pitting and Volumetric indications above the tubesheet is 2.1 EFPY, based on an assumed 40% TW indication retained in service, and 95% CL growth rate based on IP 2 observed indications. Since all confirmed pits and volumetric indications were plugged, the assumption of a 40% TW indication retained in service is based on a conservative evaluation of the database for ETSS #96005 which indicates a detection level of approximately 20%TW.

- The acceptable cycle length for AVB wear is 3.1 EFPY. This is based on a 38% TW maximum indication retained in service, NDE uncertainties for the qualified NDE technique (ETSS #96004), and 95%CL growth rates based on the IP 2 reported AVB wear.

- Known foreign objects residing in the SGs were evaluated for the potential to wear a tube beyond the acceptable limit (60% TW), assuming that these objects are located at the worst case location for wear against the tubes (i.e., high cross flow region). A minimum acceptable operating cycle length of 1.48 EFPY was confirmed for these objects. Therefore, operational assessment requirements are satisfied for known loose parts.

- The 2000 inspection data confirm that there are no TSP segments ("star" pieces) missing from the TSPs; thus, since TSP cracking has been observed for many years, and analysis (Appendix A) shows that the plates are expected to remain intact, loose parts resulting from TSP degradation are not an operational issue.

- Tubes with PLP indications were evaluated for historical growth rates; only one tube was found to have potentially excessive growth of the wear. This tube was plugged, and its neighboring tubes were plugged to provide a buffer zone around the tube to eliminate the potential for propagation in the extremely unlikely event that the tube should sever due to continuing wear. It was judged that this conservative action will provide a minimum of one full cycle of operation. Therefore, operational assessment requirements are satisfied for tubes with PLP indications.

7.0 Glossary of Abbreviations

ANL	Argonne National Laboratories
ALA	Farley Nuclear Site
ARC	Alternate Repair Criteria
ASME	American Society of Mechanical Engineers
AVB	Anti-Vibration Bar
BDA	Eddy Current Data not useable due to low signal to noise ratio
BOC	Beginning of Cycle
C-5	CECCO 5 Inspection Probe
CAE	Byron Nuclear Station
CCE	Braidwood Nuclear Station
CDF	Cumulative Distribution Function
Circ.	Circumferential
CL	Confidence Level
CM	Condition Monitoring
CMOA	Condition Monitoring and Operational Assessment
CMTR	Certified Material Test Report
Col.	Column
CPD	Cumulative Probability Distribution
C-scan	Topographical Map Presentation of + Point and CECCO 5 EC Data
Dia	Diameter
DLW	Beaver Valley Nuclear Station
EC	Eddy Current
EOC	End of Cycle
EDM	Electro-Discharge Machining
EFPD	Effective Full Power Days (24 hours at 100% power)
EFPY	Effective Full Power Years (365 EFPD)
EPRI	Electric Power Research Institute
ETSS	Examination Technique Specification Sheet

EZ	Expansion Zone
FBH	Flat Bottom Hole
FEA	Finite Element Analysis
GPD	Gallons per Day
GPM	Gallons per Minute
HR	Hour
ID	Inside Diameter
IGA	Intergranular Attack
Ind.	Indication
IP2	Indian Point 2
ISI	In Service Inspection
I-typ	Indication Type
Kcal	Kilo (one thousand) calories
KHZ	Kilo (one thousand) hertz
Ksi	Thousands of Pounds per Square Inch
Loc.	Location
MA	Mil Annealed
MAI	Multiple Axial Indication
MCI	Multiple Circumferential Oriented Indications
MRPC	Motorized Rotating Pancake Coil
NDD	No Detectable Degradation
NDE	Non Destructive Examination
NOP	Normal Operating Pressure
NQI	Non Quantifiable Indication
NQN	Non Quantifiable Indication – Not Confirmed
NRC	Nuclear regulatory Commission
OA	Operational Assessment
OD	Outside Diameter
ODSCC	Outside Diameter Stress Corrosion Cracking
PDA	Percent Degraded Area
PGE	Diablo Canyon Site
POD	Probability of Detection
PI	Possible Indication
PLP	Potential Loose Part
PSI	Pounds per Square Inch
PSIA	Pounds per Square Inch Absolute
PWR	Pressurized Water Reactor
PWSCC	Primary Water Stress Corrosion Cracking
RAI	Request for Additional Information
R_C_	Row and Column in the SG Tube Bundle, R3 C85 = Row 3 Column 85
RPC	Rotating Pancake Coil
RST	Restricted Tube
RT	Roll Transition
SAI	Single Axial Indication
SCC	Stress Corrosion Cracking
SCI	Single Circumferential Oriented Indication

SG	Steam Generator
SLB	Steam Line Break
S/N	Signal to Noise Ratio
SPI	Support Plate Indication
Stind	Indication Identification (SUPERTUBIN INDICATION)
TEC	Tube End Cold
TEH	Tube End Hot
TSC	Tube Sheet Cold
TSH	Tube Sheet Hot
TSI	Tube Sheet Indication
TSP	Tube Support Plate
TTS	Top of Tube Sheet
TW	Through Wall
TWD	Through Wall Defect
UTEC	Ultra Sonic Eddy Current
V	Volts
VOL	Volumetric
2R14	Indian Point 2 Refueling Outage Number 14

8.0 References

1. Westinghouse Report SG-00-05-008, Indian Point 2 U-bend PWSCC Cycle 14 Condition Monitoring and Cycle 15 Operational Assessment; May 2000.
2. EPRI TR-107621, Rev 0; Steam Generator Integrity Assessment Guidelines ; November 1999.
3. NRC GL-95-05, "Voltage Based Repair Criteria for Westinghouse Steam Generator Tubes Affected by Outside Diameter Stress Corrosion Cracking", August 3, 1995.
4. Westinghouse MRS-TRC-1110, "UTEC Examinations of the Sludge Pile Region Steam Generator 22 Indian Point Unit 2, 2R14", May 15, 2000.
5. ConEd Letter , L.J.Burbige to R.R.Laubham (Westinghouse) dated 5/2/00
6. W Letter NSD-E-SGDA-00-71;"Evaluation of Foreign Objects in SGs at Indian Point Unit 2"; April 21, 2000.
7. W Letter LTR-SGDA-00-106; "Recommendations Resulting from Evaluation of PLP Signals at Indian Point Unit 2"; May 5, 2000.
8. W Report , "Analyst Performance and Data Quality; IP2, 2R14".

Appendix A
Secondary Side Condition Monitoring and Operational Assessment

Technical Report No. 00603-TR-004

Volume 1 of 1

Prepared for

Consolidated Edison Company of New York, Inc.
Indian Point Station, Unit 2

Prepared by

Altran Corporation
451 D Street
Boston, MA 02210

SECONDARY SIDE CONDITION MONITORING AND OPERATIONAL ASSESSMENT

Technical Report No. 00603-TR-004
Revision 0
Volume 1 of 1

Prepared for

Consolidated Edison Company of New York, Inc.
Indian Point Station, Unit 2

Originator: _____ Date: 5/26/00
F. Elsabee

Verifier: _____ Date: 5/26/00
for P. Habicht by Telecon.

Verifier: _____ Date: 5/26/00
for P. Skulte by telecon

Verifier: _____ Date: 5/26/00
T. Esselman

Project Manager: _____ Date: 5/26/00.
W. McBrine

TABLE OF CONTENTS

1.0	Purpose	3
2.0	Summary and Conclusions	3
3.0	Condition Monitoring Assessment	3
	3.1 Denting at Tube Intersections	4
	3.2 Flow Slot Deformations and Hourglassing	5
	3.3 Outward Plate Deformation	6
	3.4 Cracking and Plate Integrity	7
4.0	Operational Assessment	9
	4.1 Overall Plate Integrity/Deformation	10
	4.2 Tube Support Integrity	13
5.0	References	14

Secondary Side Condition Monitoring And Operational Assessment

1. Purpose

This report presents the Condition Monitoring and Operational Assessment of the secondary side components of the Indian Point 2 (IP2) steam generators (SGs) as they affect the integrity of the SG tubes. This assessment is based on the inspections performed in March 2000.

2. Summary and Conclusions

The Condition Monitoring Assessment concluded that the overall denting trend of the tubes in the SGs continues to "level off" from the previous years. Hourglassing at the lower support plates, where this has been monitored, continues to "level off" and is not significantly worsening. The hourglassing data indicates that any rate of continued hourglassing is very slow. Hourglassing of the top support plate has been measured in 2000 for the first time in SG 24 and SG 21. Based on the observations and evaluations performed, it is concluded that structural support integrity was provided by the tube support plates (TSPs) to the SG tubes during the last operating period (cycle 14).

The hourglassing at the sixth support plate of SG 24 caused a Primary Water Stress Corrosion Crack (PWSCC) that resulted in a leak near the apex of tube R2C5 U-bend tube (Ref. 1). As a result of the investigations performed after this event, all Row 2 tubes in all four SGs were plugged. The Operation Assessment evaluated the overall plate integrity during normal plant operation due to relative thermal growth and during accident conditions. The R2C5 event and these other mechanisms have been evaluated. These evaluations assure that continued proper support will be provided to the active tubes in the steam generators for the next cycle of operation.

3. Condition Monitoring Assessment

This condition monitoring assessment is intended to establish the structural integrity characteristics of the secondary components through the last operating cycle. Monitoring of the secondary side components whose failure could prevent the SG from fulfilling its intended safety function is required to assure that degradation of these components does not threaten the structural integrity of the primary pressure boundary. Various inspections, both visual and measured, have been undertaken of the affected components, followed by an assessment of their condition to assure support integrity is provided.

The secondary side assessments presented in this document are based on a 100% tube inspection program, using eddy current and ultrasonic examination techniques, and secondary side visual inspections using video equipment. The visual inspections provided detailed views of the lower three tube support plates as well as the top support plate of all SGs. Visual examination of the fourth and fifth plates of SGs 21 and 24 was also performed.

A sampling inspection of SG 22 J-tube wall thickness and an inspection of the upper internals was made. No change was observed since the previous inspection. The inspection of the transition cone girth welds and feedwater nozzles fall under the jurisdiction of the ASME Section XI inspection program and are not scheduled until the year 2002.

The following general observations of the conditions of the support plates were made based on the inspections:

- Four new tube restrictions at tube support plates, two at TSP 3 and two at TSP 4, were identified with the inability to pass 610 mil probes, resulting in the plugging of the subject tubes. However, the overall trend continues to show major decrease in tubes being plugged due to 610 mil probe restrictions after 1989 (see Figure 3.1).
- Denting and hourglassing at all support plates, noted during prior inspections and monitored during the current inspection, continue to "level off" and are not significantly worsening (see Fig 3.1 to Fig. 3.5).
- Measurement of the deformation of flow slot N-1 (at the location of tube R2C5) indicates the existence of approximately 0.5 inches of hourglassing at the top support plate in SG 24, and less in SG 21. Based on measurements and observations, it is clear that the hourglassing at the top plates is less than that observed in the lower plates.
- Cracked ligaments at some flow slots are noted. Some previous partial cracks have now been identified as full cracks from the flow slots to the first row tube holes. It is believed that this continued cracking is primarily from the continued effect of denting and stress levels that occurred in the early 1980s. No cracks in the flow slots were noted in the top TSPs.

3.1 Denting at Tube Intersections

Tube restrictions at the tube support plates are the direct result of denting caused by the corrosion build up of the carbon steel plates in the crevice between the tube and support plate. A detailed review of the tube restriction data from the March 2000 inspection results was performed. The inspection initially resulted in five new restrictions using the 610 mil probes for all four SGs. Four of these are located at TSP 3 and TSP 4. The fifth restriction, which was at the open end of a tube on the primary side of the tube sheet, was initially identified as an inability to inspect. A subsequent effort resulted in the opening of the tube and successful inspection.

The data associated with the twenty tubes that were plugged during the 1997 inspection due to restrictions using the 610 mil probes at the sixth plate and U-bend regions was re-evaluated. A careful examination of the 1997 inspection records showed the available data to be inconclusive for nineteen of the tubes as to the location and the reason of the restrictions. The tubes in question were not inspected with a plus-point probe after the operator had reported the restrictions and thus the exact location of the restrictions was not discernable.

The tubes were thus administratively plugged due to the inconclusive nature of the available data.

Figure 3.1 provides a comparison of all the tubes plugged due to restrictions of the 0.610" probe from year to year. As indicated by the figure, the overall decreasing trend from the mid 1980's is continuing with relatively few tubes being plugged after 1989.

Some restrictions noted during the 1997 inspection, which were identified while using probes larger than 610 mils were no longer identified as further restricted during the current inspection. Other restrictions noted in 1997 have slightly progressed and required a smaller probe during the current inspection. Also, new restrictions using the 640 and 620 mil probes were noted at TSP 6 of all SGs, especially SG22, in the vicinity of the tube lane. Note however, that this tube restriction data is not considered to be an accurate indication of the extent of tube denting, especially at TSP 6, due to differences in probe geometry, probe stiffness and operator response to resistances in the tube. Restrictions to 610 mil probes, resulting in plugging of the tubes (presented in Figure 3.1), are however considered a more reliable indication of denting.

Based on these observations, it is concluded that the overall denting trend of the tubes in the SGs continues to "level off" from the previous years. A discussion of the effects of the plate deformation, on the support integrity of the tubes, is further discussed in the Operational Assessment section below.

3.2 Flow Slot Deformations and Hourglassing

The videotapes from the March 2000 visual inspections were reviewed for progression and trending of the flow slot closures previously documented in the Secondary Side Integrity Assessment. The flow slots in the lower support plates visually appear much the same as observed during the May 1997 inspection.

Using the same process as that used for prior years, the total amount of closure of each flow slot was estimated from the videotape. Flow slot closure measurements were obtained for the lower three support plates. However, due to the angle of view and lighting limitations, the dimension of some of these slots could not be obtained.

The new measurement estimates are used to update the historical trending data previously reported in the Degradation Assessment. The updated data is presented in Figures 3-2 to 3-5. Due to the estimation required from the videotapes, this data is used for trending purposes only and is not considered to be an accurate measurement of the deformation of the flow slots.

A review of the figures indicates that the new flow slot closure measurements continue to follow the overall "leveling off" trend of hourglassing previously identified in the Degradation Assessment. Even though some of the estimated values have slightly increased

in magnitude from those estimated from prior inspections, the new values are still within the "leveling off" trend indicated by the prior inspections.

Visual inspection of the top support plates, in all four generators, was performed from the hillside ports of the generators. However, due to the camera angle and lighting, flow slot closure measurements could not be obtained from these videotapes.

Direct measurement of the hourglassing was obtained at the first nozzle-side slot (slot N-1 at the plate periphery) of TSP 6 in SG 24 (Ref. 1). Measurements were made by passing a gauge of known length between the Row 1 tubes and recording the length at which the gauge would just pass between the tubes at each specific column location. The measurements were taken for half of the slot and resulted in a maximum tube-to-tube dimension of 3.47 inches at the hard point (the region between the flow slots), and a minimum value of 3.03 inches at the middle of the slot. Considering the original Row 1 tube-to-tube spacing design value of 3.5 inches, these measurements indicate a maximum total flow slot closure of approximately 0.47 inch (Ref. 1).

A comparison of the flow slot closure at the manway-side slots of the top support plate of SG 21 to that measured at slot N-1 in SG 24 was performed. Although this comparison did not provide precise closure dimension in SG 21, it did indicate that the hourglassing of TSP 6 in SG 21 was less than that in SG 24.

This estimate of the extent of hourglassing at the top support plate is the first direct estimate of the slot deformation of the sixth plates in the Indian Point 2 steam generators. None of the previous visual inspections had provided a clear indication of deformation. Since the hourglassing measured at the top plate is less than that observed at the lower plates, it is concluded that the flow slots of the sixth support plates have been most likely deforming through the years in a similar manner to the lower plates but at a slower rate.

3.3 Outward Plate Deformation

The effect of corrosion build-up in the crevices between the tube holes and the tubes has resulted in in-plane compression loads in the plate and in-plane deformation. As has been documented and monitored by visual inspections through the years, the in-plane deformation is most evident around the flow slots, in the general vicinity of the tube lane and at the outer periphery of the plates, next to the wrapper. Deformation and cracking around the flow slots and in the general vicinity of the tube lane is further discussed below.

Outward deformation of the tube support plates at the periphery near the wrappers has been noted in the current video tapes taken during the March 2000 inspection at the sixth support plate of SGs 21, 22, and 24. This area was not inspected in SG 23 but is expected to be similar. Video observations have indicated that the support plates are in contact with the wrapper at the locations where clear images were available. At the wedge locations, the plate transitions over a length of several inches where a gap exists.

Contact with the wrapper was also noted at the periphery of the lower support plates in the tube lane region at the extremities of the flow slots. These regions were the only ones at the wrapper that are visually apparent on the videotapes for the lower plates.

Based on the above observations, it is concluded that radial restraint of the support plate is being provided by the wrapper for the sixth support plate. Although not specifically noted during the visual inspections, except at the tube lane, this condition is expected to also exist at the lower plates since the hourglassing is more severe than in the top TSP. Therefore, based on this assessment, it is concluded that radial restraint of TSP 6, and most likely of all the plates, is being provided by the outward deformation of the plates and their contact with the wrapper.

3.4 Cracking and Plate Integrity

The denting of the steam generators at Indian Point 2 resulted in ligament cracking in the TSPs. These cracks have been monitored since 1976 by visual inspections. Based on the observations provided below, it is concluded that the TSPs have maintained their integrity and adequately performed their safety function during the SG service conditions.

3.4.1 Cracking at Flow Slots

The videotapes from the March 2000 visual inspections were reviewed for progression and trending of the cracks at the flow slots previously documented in the Degradation Assessment. The new inspections are used to update the historical trending data previously reported in the Degradation Assessment. The updated data is presented in Figures 3.6 to 3.8. Note that even though the inspections covered up to the fourth and fifth support plates for some of the steam generators, the crack maps are only provided for the lower three plates. This is due to the fact that inspection of the fourth and fifth support plates was not as exhaustive and detailed as for the lower plates due to inaccessibility.

Figures 3.6 to 3.8 classify the cracks as "full' or "partial" and also indicate the year when the cracks were first noted. Some previous partial cracks have now been identified as full cracks. It is believed that this continued cracking is primarily from the continued effect of denting and stress levels which occurred in the early 1980s.

Identification of cracks during this inspection that were not previously recorded was also made. Due to changes in the photographic techniques used to record the inspections, the level of detail provided in the photographic recordings has varied from year to year. Therefore, it is likely that some of the cracks indicated to be new actually existed during previous inspections but were not detected. None of

the inspections of the top support plates have identified any cracks at the flow slots at these plates.

Inspection of the first nozzle-side flow slot on TSP 5 in SG 24 revealed a full ligament crack in the corner of the slot closest to the periphery of the support plate. This crack is believed to have existed in prior years. The crack extends to the R1C2 tube hole (located at the end of the flow slot). This crack in TSP 5 did not result in any apparent effect on the tubes at TSP 6 and the support plate has effectively supported the active tubes.

Based on these observations, it is concluded that cracking has not been fully arrested. Even with all the noted cracks around the flow slots, there has been no missing or dislocated ligaments noted around the flow slots. As a result, the tube support plates appear to have fully supported active tubes in their present condition. This conclusion is also supported by the results of the eddy current inspection which confirmed the presence of tube support capability at all active tube locations.

3.4.2 Cracking of Inner Ligaments

The March 2000 visual inspections, as well as previous inspections, have indicated the presence of cracks in the ligaments between the tube and flow holes in the vicinity of the flow slots. The recent inspections have documented cracks back to the Row 3 and Row 4 tubes.

Operation of the steam generators with cracked TSPs has been evaluated and analyzed since the 1970's. Integrity of the cracked TSPs has been demonstrated both analytically and through experience. The in-plane compressive forces that are necessary to cause ligament cracking are the same forces that preserve the geometry of the tube support plate when cracked. These forces lock the tubes and the plate firmly together even in the presence of TSP ligament cracking.

3.4.3 Cracking at Outer Plate Peripheries

As previously indicated, the outer periphery of the TSPs has been noted to be in contact with the wrapper and thus provides radial restraint of the plate.

During visual inspection of the outer periphery of TSP 6 in SG 24 on the nozzle side, a crack of the TSP was noted between a tube hole and the outer periphery edge of the plate, where the ligament is thinnest. Although the crack location could not be conclusively identified from the videotape, it is near tube R8C1, which has the smallest ligament to the outer edge of the TSP. This crack occurs at a location where the TSP is in direct contact with the wrapper. Review of other locations along the periphery indicates that there was only limited cracking and no

missing sections of the plate. Based on these visual examinations, the limited and localized cracking of the plates at their outer edges did not appear to affect the ability of the plates to support the tubes.

During the 2000 inspection, a review of the sixth TSP low frequency eddy current data was also undertaken to determine if there were any indications of missing sections of the tube support plate. A total of 1830 tubes (for all four SGs) at the 6th support plate intersections were reviewed. Of these, only two locations (involving four tubes) were identified that may have the potential for missing star segments. These two locations were further evaluated and it was concluded that although there are cracks in the ligaments around the tube of interest, there are no star segments of the plate missing. This conclusion is further supported by the evaluation of the four indications by an independent reviewer who reached the same conclusion.

3.5 TSP Wedge Supports and Wrapper Integrity

The March 2000 visual inspections included locations around the periphery of the sixth support plate of three generators. Inspection of these locations did not reveal any deterioration of the connections of the TSP to the wrapper at the welded intermediate wedges. All welds and wedges reviewed during the inspection were noted to be in good condition. Also, no visible deterioration of the wrapper was noted.

Proper insertion of the sludge lance equipment normally requires proper positioning of the wrapper. Thus, since no problems were encountered while positioning the equipment during the sludge lancing procedure, it is concluded that the wrapper is in its proper location and has not dropped.

Based on this assessment, it is concluded that the wedge supports of the tube support plates as well as the wrapper still maintain adequate structural integrity and have been properly performing their safety function.

4. Operational Assessment

The operational assessment is intended to establish the structural and leakage integrity characteristics of the components in their present condition for the upcoming cycle. As a result of the detailed investigations performed after the event of the R2C5 tube in SG 24, all Row 2 tubes were plugged in all four generators. Assessment of the secondary side components, whose failure could prevent the SG from fulfilling its intended safety function, has been performed to assure that degradation of these components does not threaten the structural integrity of the primary pressure boundary during the next operating cycle. Therefore, the following assessment, which is based on the condition that all Row 2 tubes are plugged, as well as the configurations noted during the March 2000 inspections, assures that tube support integrity is provided.

4.1 Overall Plate Integrity/Deformation

4.1.1 Relative Thermal Deflections

Based on the number of tubes exhibiting denting and the numerous visual inspections of the support plates performed since 1978, many or all of the tubes are fixed in the support plates by oxide wedging. Denting of the tubes is also prevalent throughout all the support plates. This fixity allows the tubes to exert out-of-plane loads into the support plate. Because the tubes are essentially anchored at the tube sheet and the support plates are independently supported by stay rods and wedges anchored to the wrapper at the perimeter, an evaluation of the differential thermal movement of these components was performed. The difference in vertical thermal growth between the active tubes, plugged tubes, stay rods, and the perimeter support wedges and wrapper will result in relative vertical movements.

The oxide growth and denting occurs during periods of hot operation. The larger temperature change of the active tubes during cooldown will pull the support plate down, while the slightly cooler plugged tubes, stay rods and support wedges will provide equal and opposite upward force on the plate. This condition was evaluated for the potential to cause damage to the support plates, in particular dislodging a "star" from between cracked ligaments.

The evaluation considered three categories of tubes:

- Active Tubes - These tubes are considered to have been locked to the TSP during operation and are exposed to the temperature gradient through the active tubes between the hot and the cold legs.
- Post-Denting Plugged Tubes - These tubes have been plugged after they were dented and thus were locked to the plate during operation of the steam generator when the tubes were functional. These tubes are presently not active and are only exposed to the secondary side temperature.
- Pre-Denting Plugged Tubes - These tubes were plugged prior to putting the steam generators into service (Row 1) or before denting occurred. These tubes were then subsequently dented and thus were locked to the plate during operation of the steam generator while the tubes were inactive. These tubes are presently still inactive and are only exposed to the secondary side temperature.

The evaluation concentrated on the relative thermal movement between each of these three categories of tubes and the stay rods. The thermal expansions and contractions for the different components were calculated for each of the tube support spans starting from the tubesheet and ending with the sixth support plate.

Cool down from the operating condition to a shutdown temperature of 70°F was considered. Relative movements were then compared to obtain the maximum possible thermal differential movements.

It is important to note that these thermally induced loads are displacement limited since any small amount of out-of-plane-movement at the support plate location will result in an associated thermal load reduction. Any damage caused by thermal expansion loads would be most visible in the cold condition since this is when relative thermal expansion movements will be the highest. Resulting damage from this loading condition would be evident by "step" displacements across plate cracks, stars partially dislodged in the vertical direction, and deformation at plate support points such as at dented tubes, support rods, and wedges. None of these conditions were noted.

The following observations were noted from this evaluation:

- Very small relative movements result from thermally induced loads. The maximum relative motion was calculated to be approximately 0.077 inch between adjacent support plates. This relative movement is considered small in comparison to the 0.75 inch thickness of the tube support plate and will not affect its ability to carry any applied loads.
- The small thermal movements are likely to be absorbed by local deformation of the tube support plate around the tube holes that could be cracked. This could result in relative displacements at the cracks on the order of the calculated 0.077 inch.
- The maximum effects of the thermally induced expansions should be observed when the steam generators are cold and the plant is in the shutdown condition and thus any deformations in the SG internals will have minimal or no effect on safety.

The inspections performed show that the support plates are flat with no apparent step dislocations across ligament cracks. Dislodged stars have not been found during any of the routine foreign object search and retrieval (FOSAR) activities. Any progression of damage due to thermal differences between tubes and support structures would appear as crack offsets and out of plane deformation, which is not observed. This would be most apparent in the region around the flow slots where there are stay rods, pre-dented plugged tubes, and post-denting plugged tubes. No evidence of axial disturbance across ligament cracks has been noted.

This evaluation demonstrated that thermally induced relative displacements between any type of tube and the wrapper or stay rods are not of sufficient magnitude to impact the integrity of the tube support plates. Any relative movements will be absorbed through local deformation of the tube support plate around the tube hole. The small local deformations of the plate, in the order of

0.077 inch will not result in failure of the tube support plate or the dislocation of a "star" through the 0.75 inch thick support plates.

Therefore, based on this assessment, it is concluded that the integrity of the support plates will be maintained and is not expected to be compromised by the relative thermal expansion between the tubes and stay rods.

4.1.2 Accident Conditions

Corrosion product accumulation at the tube-plate intersections produces in-plane compressive loads in the TSPs that result in the cracking of the ligaments. These forces are capable of locking the tubes and the plate firmly together even in the presence of TSP ligament cracking. The in-plane compressive forces that are necessary to cause ligament cracking are the same forces that preserve the geometry of the tube support plates when cracked.

Finite element analyses were previously performed to show that the cracked ligaments in the Indian Point 2 TSPs are fully constrained and will not become free, even with cracking in four adjacent ligaments, during a pipe break combined with an earthquake. A steam line break or feed line break would apply upward differential pressures across the TSP that can cause the TSP to bend. This bending applies loads at the cracked ligaments that "pinch" the "star" segments, formed by the ligaments between the tube and flow holes, and tend to hold them in place. The loads trying to push a star section out of position due to the differential pressure across the TSP are far less than the loads that are restraining the star due to the plate bending. The analyses demonstrated that an interior star segment would not come free, even during the most severe accident condition. Integrity of the TSP was also demonstrated by parametric studies with up to two adjacent stars missing, and with no initial compressive preload.

A pipe break event combined with an earthquake could also result in loads being applied in-plane to the plate. These loads have the potential to plastically deform the plate in the wedge areas due to the in-plane dynamic reaction forces. However, noting that the visual inspections indicated the plates to be in contact with the wrapper at locations around its periphery, the reaction loads at the end of the plates would be more evenly distributed around the circumference and continue to maintain the plate in a high state of compression. The in-plane load distribution at the wedges will not be significantly affected by the presence of cracked ligaments and thus "unloading" or dislodging of star sections in these regions is not expected.

Thus, given the present cracked configuration of the TSPs without any, or at worst case only a few missing or dislodged stars, it is concluded that the conditions and configurations considered in the previous analysis, along with the

conclusions reached, are valid and applicable to the next cycle of service. The tube support plates are still considered adequate to meet their design functions for the upcoming service cycle.

4.2 Tube Support Integrity

4.2.1 Effect of Hourglassing on U-Bend Tubes

Alloy 600 mill annealed (MA) SG tubes are susceptible to Stress Corrosion Cracking (SCC) at locations of high stress. One such location is the small radius U bends. The Row 2 and, to a lesser degree, the Row 3 U-bend tubes can experience stresses due to the combined effect of residual stresses from fabrication, normal operating stresses, and the stress caused by the hour-glassing deformation of the flow slots at the top support plate. This condition would increase the susceptibility of the low radius tubes to SCC in the U-bend region.

Deformation of the top support plate around the flow slots, results in the "squeezing" of the legs of the U-bend tubes. This deformation of the legs results in tensile stresses in the inside diameter of the extrados at the apex, which when added to the residual stresses, make the small radius U-bend tubes susceptible to PWSCC. Analysis of the tube support plates has shown that the in-plane plate deformation due to denting and hourglassing decreases as the distance from the flow slots increases outward. Analyses have also shown that the hoop stress at the ID apex extrados of the U-bend, due to the lateral "squeezing" of the tube legs, decreases as the radius of the U-bend increases. The effect is a decrease of the hoop stress for the Row 3 U-bend tubes from that in the Row 2 tubes. This is discussed in greater detail elsewhere in this CMOA.

4.2.2 Relative Tube Support Plate Displacements

As previously indicated in the Condition Monitoring section, cracks next to flow slots propagating back to the flow holes and possibly the next row of tubes have been noted to result in a shift of a series of tubes towards the slot. This shift results in partially supported tubes and a displacement of these tubes at one plate relative to the next higher plate. The tubes that may be so affected are all inactive tubes.

The condition of a partially supported tube has been evaluated for flow induced vibration loads and has been shown to be acceptable. The possible effect of a relative tube displacement between the fifth and sixth support plates affecting the U-bend stress has also been considered. Considering the case where the top plate is partially supported, the tube would be fixed at the fifth plate and allowed to rotate at the sixth plate, the hoop stress conditions developed at the apex of the U-bend, where the PWSCC condition is of most concern, will be reduced.

Therefore, based on this assessment, it is concluded that the condition of a partially supported tube at a tube support plate will not result in any worse case configuration or loads than when considering a fully supported and restrained tube. Also, note that circumferential SCC indications due to axial stress in the tubes at the support plates or at the tube sheet have not been observed during the inspection programs.

4.2.3 Tube Wear

In the unlikely event that a star segment of a tube support plate breaks free and becomes a loose part, wear of adjacent tubes due to the vibration of the part against the tube becomes a concern. A loose part analysis is performed for such items to insure that damage to active tubes will not occur. If the loose part of the plate is broken off the tube lane area, protection of the active tubes will be provided by the plugged Row 1 and Row 2 tubes.

5. References

1. Westinghouse, Indian Point 2 - Root Cause Evaluation for SG-24, R2C5 Leakage

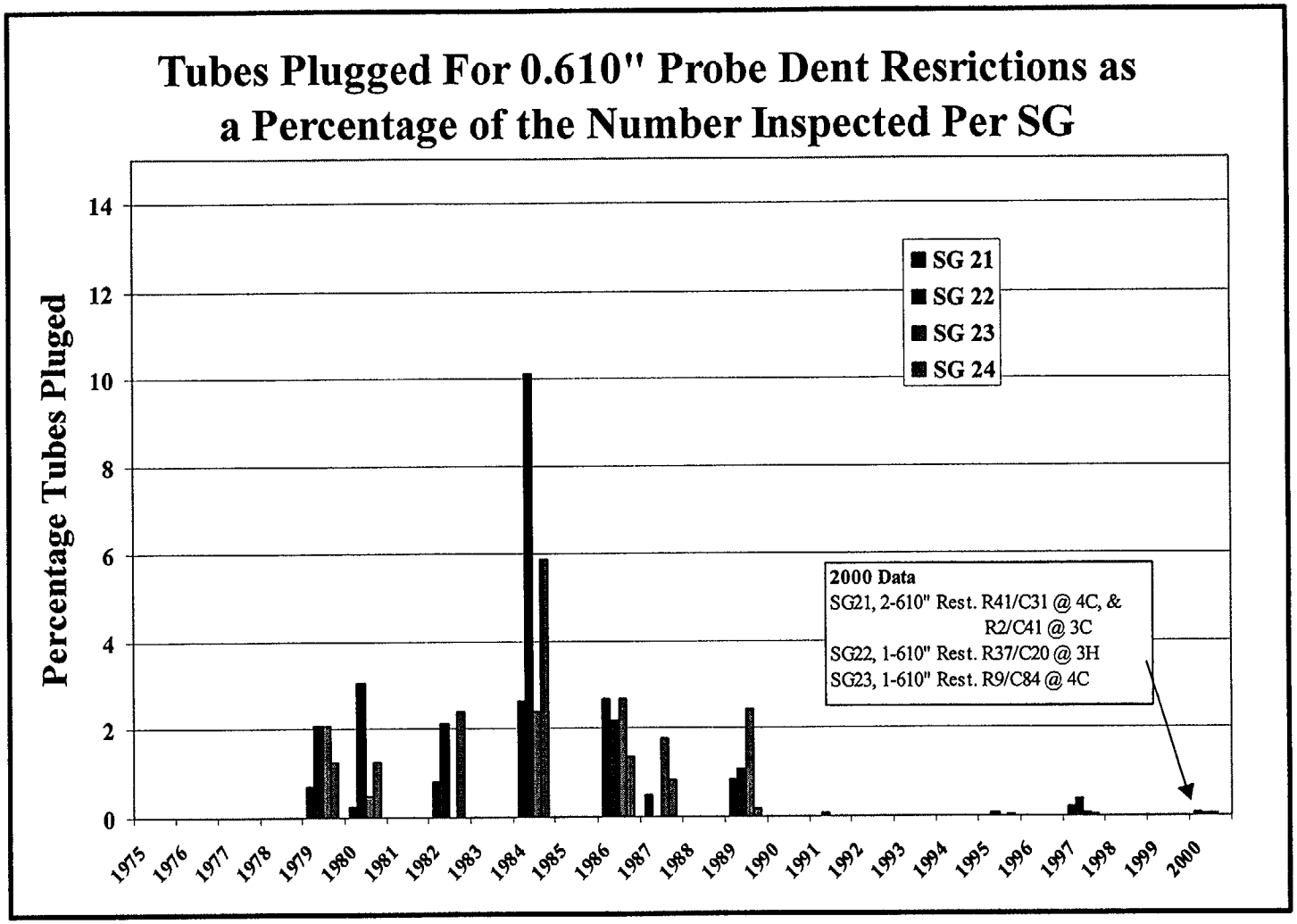
Tubes Plugged For 0.610" Probe Dent Resrictions as a Percentage of the Number Inspected Per SG
Percentage Tubes Pluged
0
2
4
6
8
10
12
14
1975
1976
1977
1978
1979
1980
1981
1982
1983
1984
1985
1986
1987
1988
1989
1990
1991
1992
1993
1994
1995
1996
1997
1998
1999
2000
SG 21
SG 22
SG 23
SG 24
2000 Data
SG21, 2-610" Rest. R41/C31 @ 4C, & R2/C41 @ 3C
SG22, 1-610" Rest. R37/C20 @ 3H
SG23, 1-610" Rest. R9/C84 @ 4C

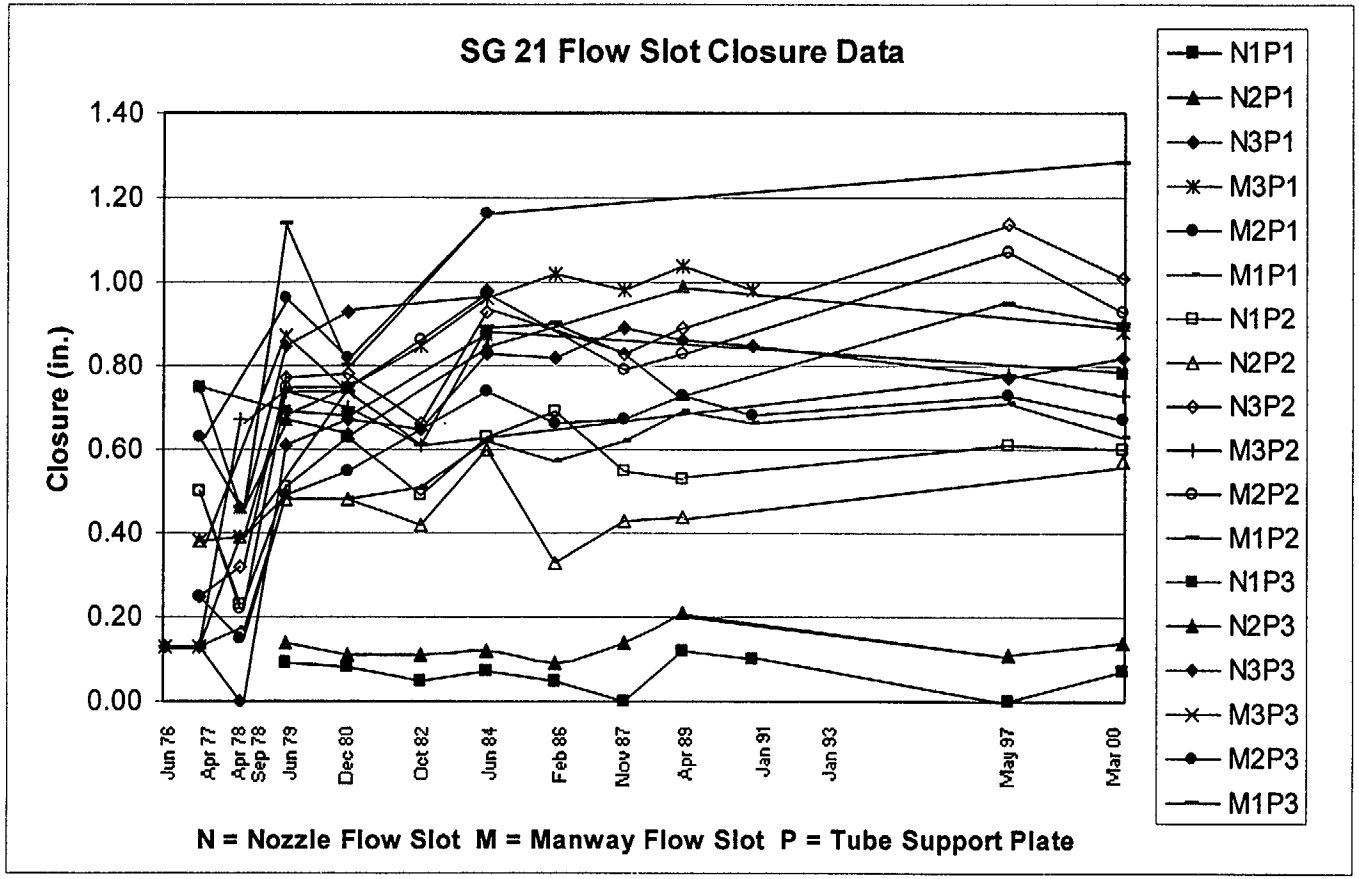

FIGURE 3.2: Updated SG 21 Flow Slot Closure History

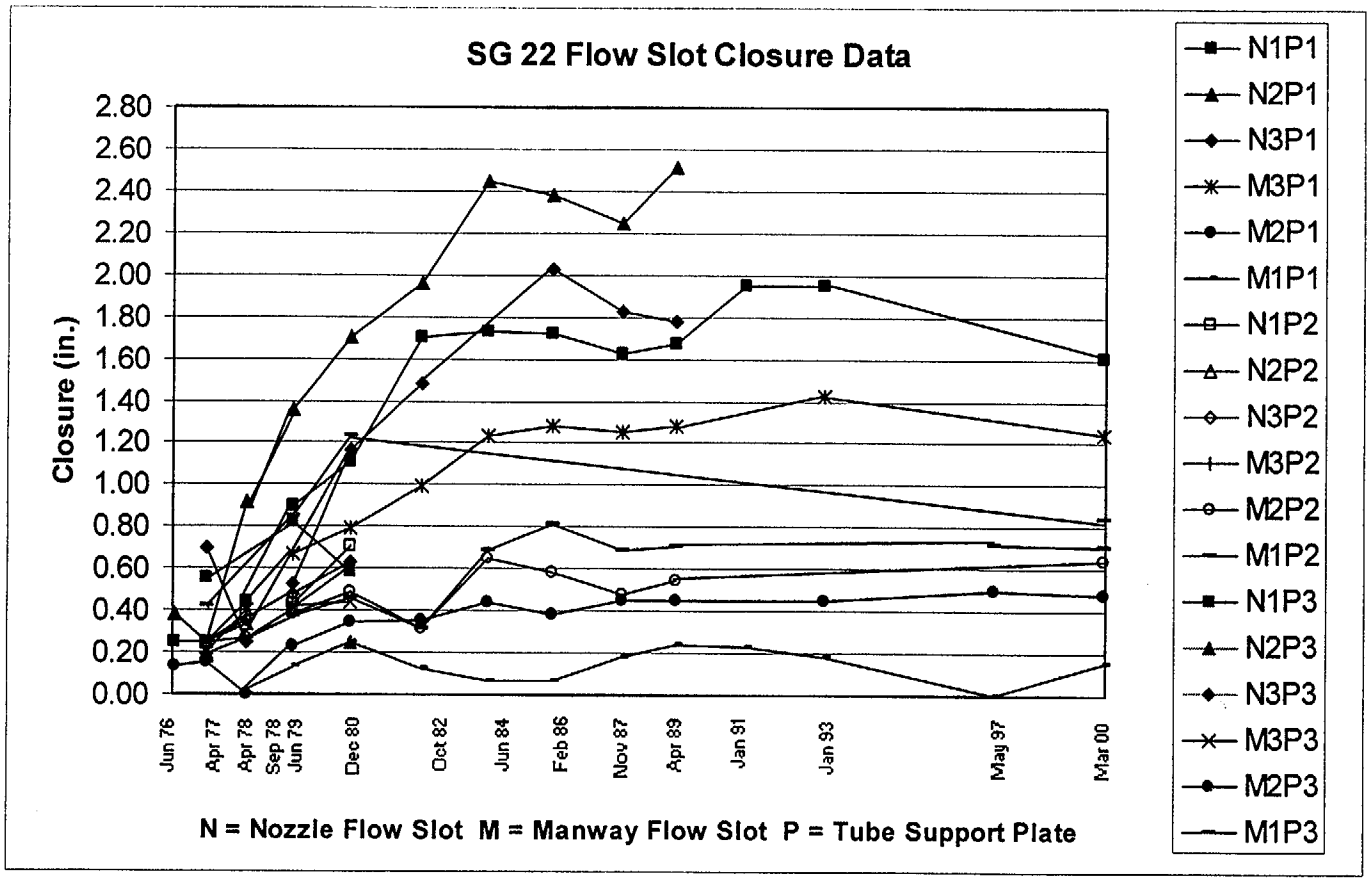

FIGURE 3.3: Updated SG 22 Flow Slot Closure History

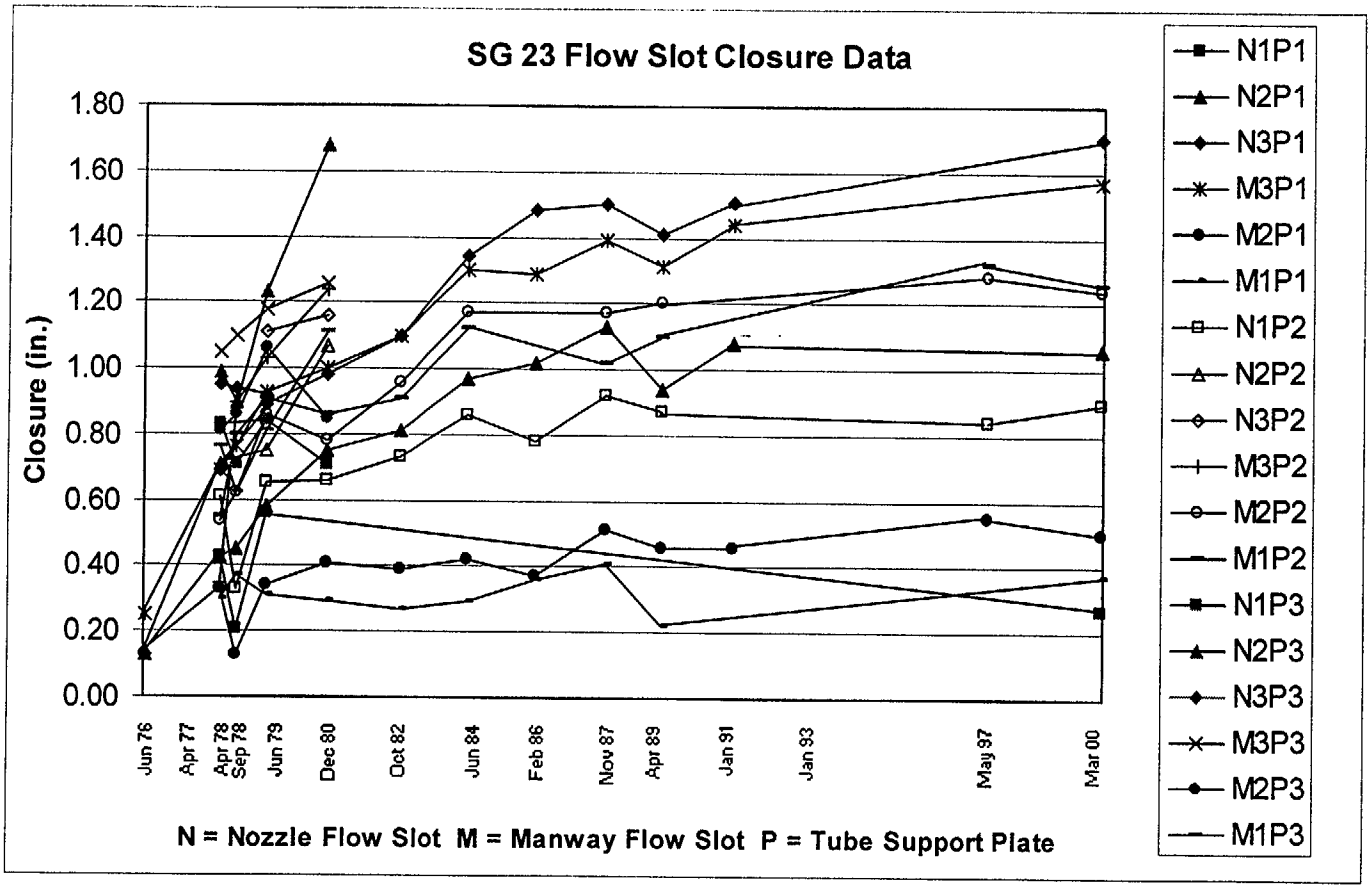

FIGURE 3.4: Updated SG 23 Flow Slot Closure History

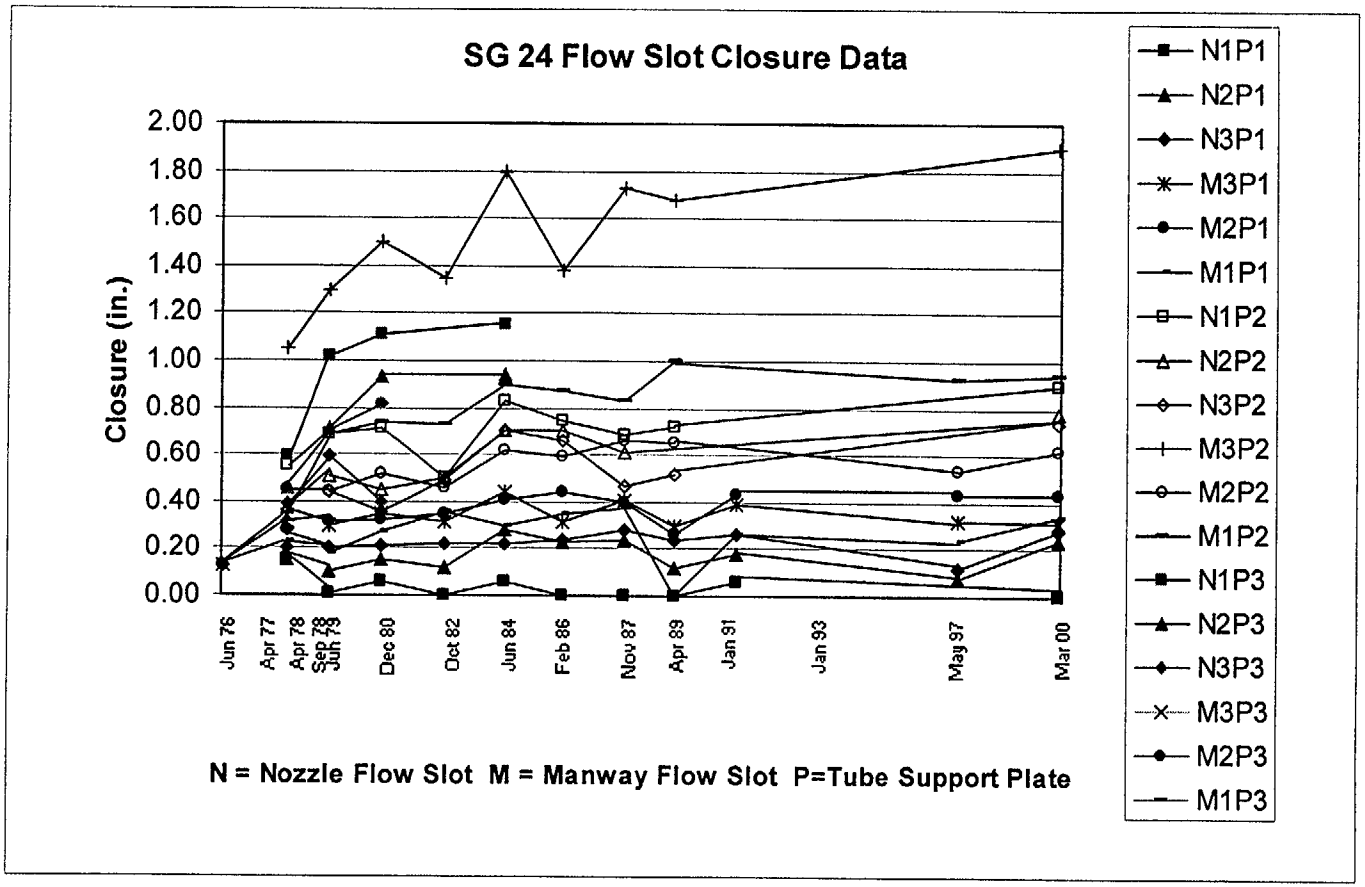

FIGURE 3.5: Updated SG 24 Flow Slot Closure History

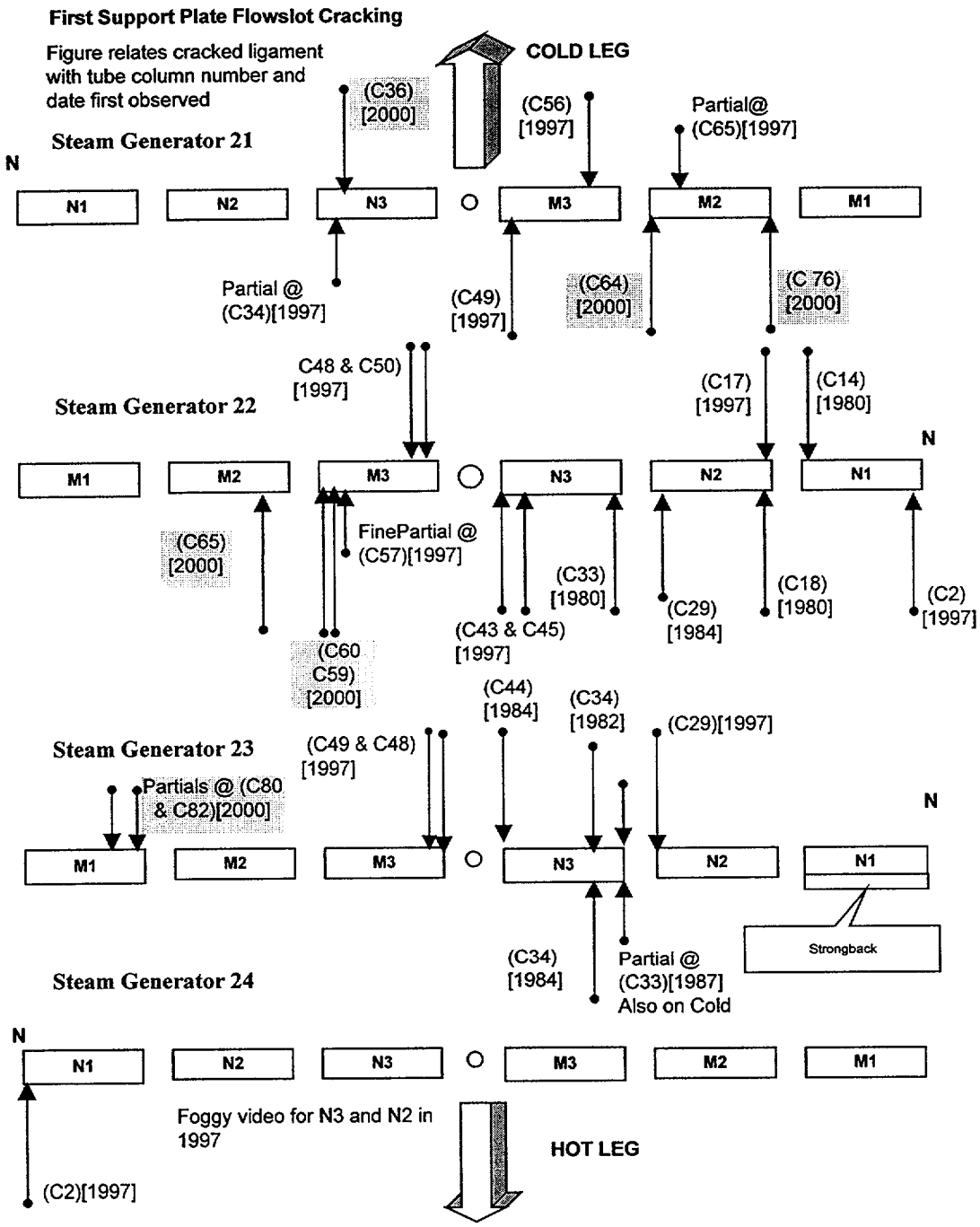

FIGURE 3.6: Flow Slot Cracking at First Support Plate

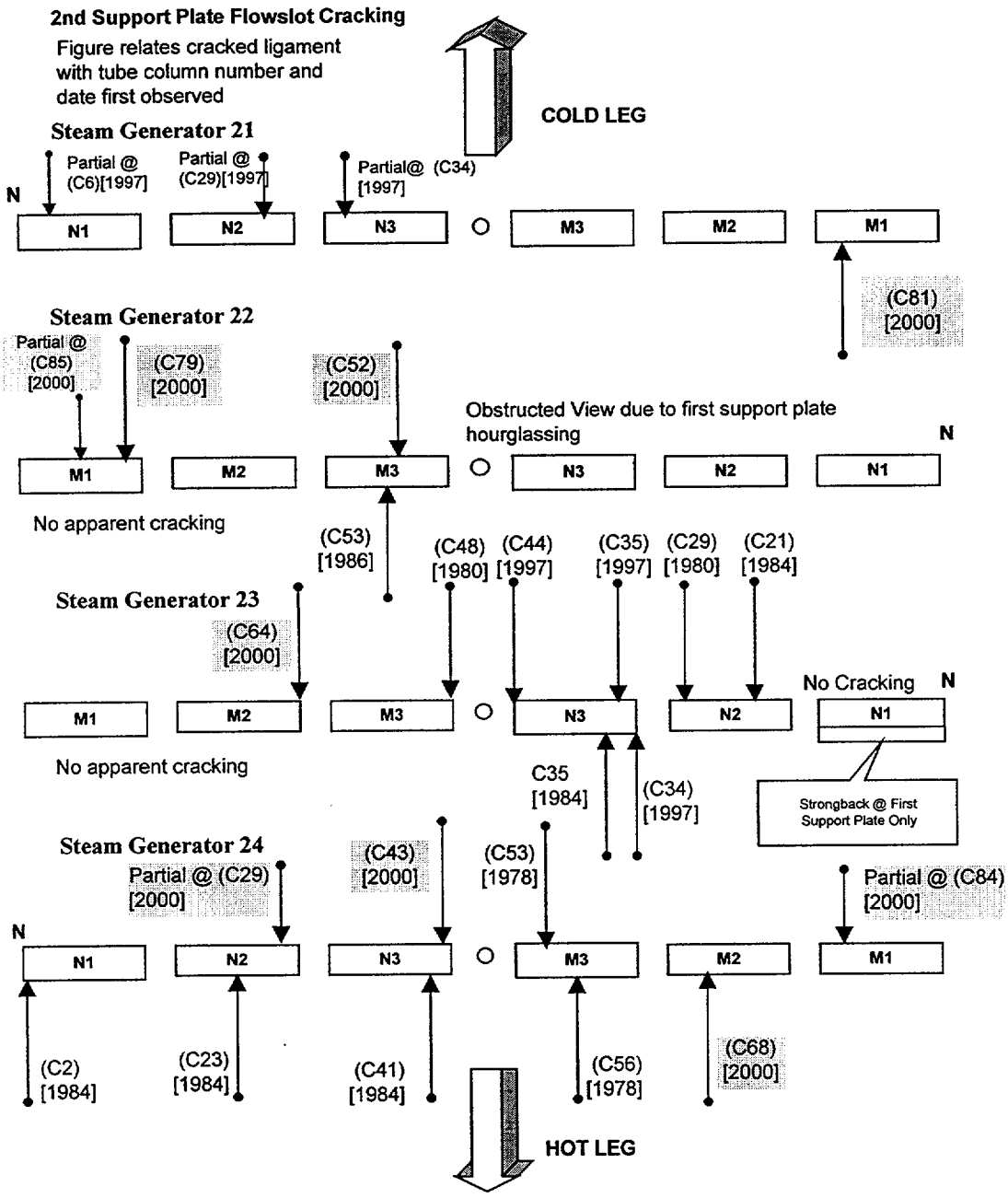

FIGURE 3.7: Flow Slot Cracking at Second Support Plate

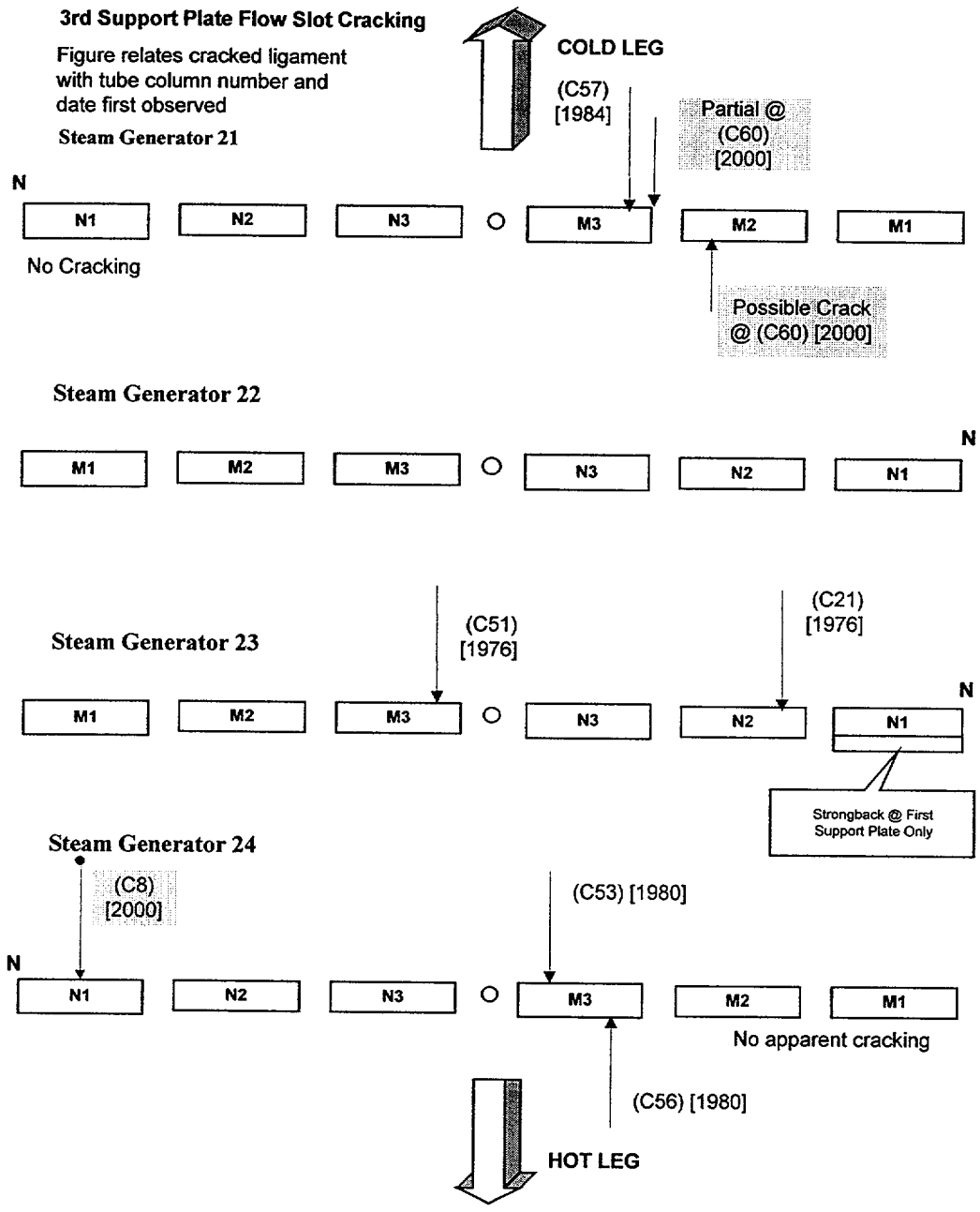

FIGURE 3.8: Flow Slot Cracking at Third Support Plate

Appendix B

Verification of Eddy Current Data

ATTACHMENT 1
EDDY CURRENT FINAL DATA TRANSMITTAL LETTER

Date: May 11, 2000
Site: Indian Point Unit 2
Owner: Consolidated Edison
Outage Date: February-May 2000
Lead Data Manager: Chris Marlis
Data Management System: ☒ ST2000
Transmittal Type: ☒ FINAL ☐ Change to Previously Transmitted File
File Names: IPP_21_FINAL_ALL_DATA_REV1.ZIP, IPP_21_FINAL_DENTS.ZIP
IPP_22_FINAL_ALL_DATA_REV1.ZIP, IPP_22_FINAL_DENTS.ZIP
IPP_23_FINAL_ALL_DATA_REV1.ZIP, IPP_23_FINAL_DENTS.ZIP
IPP_23_FINAL_ALL_DATA_REV1.ZIP, IPP_23_FINAL_DENTS.ZIP

First S/G: 21	File Size (In Bytes): 620,703	File Date: 05/11/00
Second S/G: 22	File Size (In Bytes): 591,917	File Date: 05/11/00
Third S/G: 23	File Size (In Bytes): 684,744	File Date: 05/11/00
Fourth S/G: 24	File Size (In Bytes): 598,212	File Date: 05/11/00

Location Of File(s) Transmitted: ANSER Server 10.1.1.1

File(s) Transmitted VIA: ☒ T-1 ☐ E-Mail ☐ FedEx ☐ Other: _____

Reason for and description of change:
Final edits have been made to the databases. This letter is transmitted with the understanding that engineering and eddy current analysts are performing a tube support plate integrity study that could result in further change to any or all of the files transmitted as specified by this document.

Lead Data Manager Signature	Date 5-11-00
Lead Analyst Signature	Date 5/11/00
Independent Verifier Signature	Date 5/11/00
Site EC Level III Or Designee Signature	Date 5/11/00
Westinghouse Engineering Signature	Date

Indian Point-2 U-Bend PWSCC Cycle 14 Condition Monitoring and Cycle 15 Operational Assessments

May 30, 2000

Prepared By

Westinghouse Electric Company
E-Mech Technology, Inc.

Indian Point-2 U-Bend PWSCC
Cycle 14 Condition Monitoring and Cycle 15 Operational Assessments

May 30, 2000

Authors:

T. A. Pitterle
Consulting Engineer

H. O. Lagally
Fellow Engineer

V. Srinivas
Senior Engineer

D. D. Malinowski
Consultant

A. Sagar
NDE Analyst

J. A. Begley
E-Mech Technology

Verified By:

W. K. Cullen
Senior Engineer

C. J. Begley
E-Mech Technology

Approved by:

W. B. Middlebrooks, Manager
Steam Generator Design & Analysis

Indian Point-2 U-Bend PWSCC
Condition Monitoring and Operational Assessment

Table of Contents

Section		Page
1.0	INTRODUCTION	1-1
2.0	SUMMARY AND CONCLUSIONS	2-1
2.1.	Overall Conclusions	2-1
2.2.	Summary of Additional Information Applied in This Report	2-5
2.3.	Open Items	2-7
3.0	U-BEND INSPECTION RESULTS	3-1
3.1.	Initial Mid-Range +Point Inspection	3-1
3.2.	High Frequency +Point Inspection	3-1
3.3.	Comparison of Mid-Range and High Frequency +Point Detection Sensitivity	3-4
3.4.	+Point Sizing of U-Bend Indications	3-5
3.5.	In Situ Test Results	3-7
4.0	DESCRIPTION OF ANALYSIS METHODS	4-1
4.1.	Axial Profile Analysis Methods	4-1
4.2.	Multi-Cycle Analysis Methods	4-3
5.0	INPUT DATA FOR TUBE INTEGRITY ANALYSES	5-1
5.1.	Indian Point-2 Operating Parameters	5-1
5.2.	Structural and Leakage Requirements	5-1
5.3.	Detection Threshold and Probability of Detection	5-2
5.3.1.	Detection Threshold for High Frequency +Point	5-2
5.3.2.	Probability of Detection	5-3
5.3.3.	Probability of Missed Row 3 Indications	5-5
5.4.	U-Bend PWSCC Growth Rates	5-5
5.4.1.	Indian Point-2 U-Bend PWSCC Growth Rates	5-6
5.4.2.	Comparisons with Other PWSCC Growth Rates	5-8
5.5.	+Point NDE Sizing Uncertainties	5-9
5.6.	Low Row U-bend Flow Stress	5-10
5.7.	New Indication Shape and Depth Distributions	5-14
5.8.	Maximum to Average Depth Ratio	5-15
5.9.	Crack Length Distributions	5-16
6.0	BENCHMARKING OF TUBE INTEGRITY ANALYSIS METHODS	6-1
6.1.	Axial Profile Analysis Methods	6-1
6.1.1.	Prediction of R2C5 Leakage from 1997 Inspection +Point Profile	6-1
6.1.2.	Prediction of Other EOC-14 U-Bend Indications from 1997 +Point Profiles	6-3
6.1.3.	Prediction of In Situ Test Results from EOC-14 +Point Profiles	6-3
6.2.	Multi-Cycle Analysis Methods	6-5

7.0 HISTORICAL TRENDS FOR ROWS 2 AND 3 U-BEND INDICATIONS 7-1
7.1. Introduction 7-1
7.2. Industry Low Row U-bend Indication History 7-1
7.2.1. Bend Radius Influence on Low Row Cracking 7-1
7.2.2. Effect of Operating Temperature 7-3
7.2.3. Recent History of U-Bend Indications 7-3
7.3. Stress Effects Resulting from TSP Hourglassing 7-4
7.3.1. Westinghouse Analyses 7-4
7.3.2. Altran Analyses 7-5
7.4. Manufacturing Issues 7-6
7.5. Conclusions 7-7

8.0 CONDITION MONITORING ASSESSMENT FOR U-BEND AXIAL PWSCC 8-1
8.1. R2C5 Assessment 8-1
8.2. Evaluation of In Situ Test Results for U-Bend Axial PWSCC 8-1
8.3. Condition Monitoring Assessment Conclusions 8-4

9.0 OPERATIONAL ASSESSMENT 9-1
9.1. Acceptable Row 3 Indication Sizes 9-2
9.2. Single Indication Analyses Based on Row 2 Indications 9-3
9.3. Reference Cycle 15 Operating Cycle Length Evaluation – Total SG Analyses Based on Row 2 Indications 9-4
9.4. Operational Assessment Applying Multi-Cycle Analyses 9-6
9.4.1. Row 3 Evaluation 9-6
9.4.2. Row 2 Evaluation for Cycle 15 9-7
9.4.3. Multi-Cycle Evaluation of Degradation Initiation Parameters 9-8
9.5. Recommended Operating Cycle Length 9-9
9.6. Recommended Leakage Monitoring Requirements 9-9
9.7. Recommendations for Development Activities 9-10
9.8. Operational Assessment Conclusions 9-11

10.0 REFERENCES 10-1

11.0 GLOSSARY OF ABBREVIATIONS 11-1

APPENDICES
A. C-Scans for 400 and 800 kHz A-1
B. C-Scans for Pre and Post In Situ B-1
C. NDE Profiles C-1

ATTACHMENTS
1. Altran Technical Report No. 00603-TR-005

1.0 INTRODUCTION

This report provides the condition monitoring and operational assessment (CMOA) for the Indian Point-2 axial PWSCC indications found in the U-bends of low row tubes following the March/April 2000 inspection. A SG generator leak in the U-bend of SG 4 tube R2C5 led to a forced outage in February 2000 with a subsequent steam generator (SG) inspection and end of cycle (EOC-14) refueling outage. The CMOA for other degradation mechanisms is provided in a separate report (Reference 10-1). A separate root cause evaluation report (Reference 10-2) has also been prepared that identified axial PWSCC at the extrados of the apex of R2C5 as the cause for the large leakage event leading to the plant shutdown.

The condition monitoring assessment evaluates the structural and leakage integrity of the tubes at the time of the inspection, and thus reflects EOC-14 conditions. The operational assessment is performed to determine an acceptable plant operating period up to the next SG inspection, and thus reflects a look-ahead evaluation. The principal objective of this report is to establish an operating period such that burst margin and accident condition requirements would be satisfied at the end of the operating period. All row 2 tubes have been plugged in the EOC-14 outage such that row 3 U-bend tubes are the limiting low row tubes left in service requiring an operational assessment for U-bend PWSCC indications. The tube integrity analysis methods applied in this report (two independent methods) are established techniques used in prior alternate repair criteria (ARC) analyses and/or operational assessments. Input data for the analyses are developed from Indian Point-2 data and supplemented by data from other evaluations.

Section 2 provides the summary and conclusions of this report. Results of the inspection and in situ testing for the U-bend indications are described in Section 3. The tube integrity analysis methods are described in Section 4 with benchmark analysis results given in Section 6 using input data developed in Section 5. Section 7 provides data on the historical trends for rows 2 and 3 U-bend indications. The EOC-14 condition monitoring assessment is given in Section 8. The operational assessment to determine an acceptable Cycle 15 operating period to the next SG inspection is provided in Section 9.

2.0 SUMMARY AND CONCLUSIONS

2.1. Overall Conclusions

Potential for Cracking in Row 3 U-bends

The potential for the occurrence of PWSCC at Indian Point-2 through Cycle 15 is considered to be negligible based on the following considerations:

- No indications were found in the 100% inspection of row 3 tubes including use of the high frequency +Point probe. If it is postulated that more than one indication is present and undetected, such as with average depths of 40% to 60%, the probability of missing about five indications with the high frequency probe is less than 0.01% and would be even smaller for larger indications.
- Only one row 3 PWSCC apex indication has been reported (SGs since replaced) in domestic SG inspections and none were found in tubes removed from SGs replaced due to severe denting. The single reported occurrence of apex PWSCC was found in a Model D2 SG (3/4 inch diameter tubing) without significant denting at TSP intersections. Row 3 U-bends have not been field heat treated due to the negligible occurrence of row 3 indications. The few row 3 indications found in other plants have been axial ODSCC.
- Based on analyses of the total stresses in the U-bends including hourglassing effects, it is concluded that cracks are not expected to be present in row 3. The differences between the row 2 and row 3 tube stress levels show that the time to crack initiation in row 3 would be approximately 2.5 to 4.0 times the time required for row 2 crack initiation. This is consistent with the fact that no indications were seen in row 3 at Indian Point-2.
- Even if row 3 crack initiation occurred during Cycle 15, the indication would not grow to challenge tube integrity by the end of the shorter planned operating period due to modest PWSCC growth rates (average depth growth rate at 95% probability = 12.9%/EFPY.

Leaking Indication R2C5 Evaluation

As previously identified in the root cause evaluation for the SG 4 R2C5 leakage event (Reference 10-2), the leaking indication was due to axial PWSCC located on the extrados at the apex of the U-bend. The length of the crack was estimated to be about 2.5 inches tip to tip with a throughwall length on the order of 2.2 to 2.5 inches. Crack opening was due to ligament tearing rather than a burst as the burst features of crack extension and fishmouthing of the opening cannot be identified by the visual or NDE examination. The crack appears to be the coalescence of several cracks that were separated by ligaments including at least five ligaments that can be seen by the visual exam to have spanned the crack faces prior to tearing. Based on ligament tearing models, it is estimated that the average crack depth of the indication prior to tearing of the ligaments (ligaments between cracks and remaining wall thickness ligaments) was about 90% throughwall. Plant

leakage prior to the event was only a few gpd. No firm conclusion can be drawn on the contribution of R2C5 to the operating leakage prior to the leakage event. One other indication (U-bend tube R2C71 in SG 4) was found during in situ testing to have a small leak (about 0.084 gpd) at normal operating pressure differentials.

A retrospective review of the 1997 inspection data showed that the indication was masked by signal distortion (noise) due to deposits on the tube including copper and geometry effects due to tube ovality. Expert review of the data concurred, based on the data utilized in 1997, that the indication would not have been called by accepted eddy current practices in 1997. The principal cause of the leakage event was the masking of the indication by deposits in the 1997 inspection. Based on the growth rate evaluation of this report, the growth of the indication between 1997 and 2000 was moderate and comparable to other PWSCC degradation mechanisms. Abnormally rapid growth was not a principal cause of the leakage event. Denting at the top TSP appears to have contributed to the row 2 cracking at Indian Point-2. The overall denting in the top TSP led to hourglassing of the plate in the flow slot region, which results in pinching (reduction in hot to cold leg spacing) of the U-bends and elevated hoop stress at the ID of the tube extrados near the apex.

Inspection Results

The initial EOC-14 U-bend inspection was performed using a midrange frequency (400 kHz) +Point probe and included 100% of the tubes in rows 2, 3 and 4. This inspection identified three tubes in row 2 with axial PWSCC indications including two in SG 4 and one in SG 1. However, the evaluation of the midrange coil inspection results identified a large number of tubes with eddy current signals consistent with the patterns that had been found in the 1997 SG 4 R2C5 response. This signals were classified as "bad data" due to noise signals potentially masking a flaw. In order to improve detection capability, the signal to noise ratio required improvement for indications similar to R2C5. Based on a review of alternate probes, a high frequency (800 kHz) +Point probe was selected for further inspection. The high frequency probe was selected because the increased frequency reduces OD deposit signals from magnetite and copper. A complete 100% reinspection of rows 2 and 3 tubes in all 4 SGs was performed with the high frequency probe. The high frequency probe was found to be very successful in improving data quality with the percentage of tubes with inconclusive data reduced from about 53% for the midrange probe to about 0.8% with the high frequency probe. Relatively small crack signals could be identified with the high frequency probe that had been masked by deposit signals with the midrange probe.

The high frequency probe identified PWSCC in four additional row 2 tubes including three in SG 4 and one in SG 3. Three of these indications were found in tubes classified as bad data from the midrange probe. One additional indication was found with the 620 mil diameter high frequency probe that was not inspectable with the 620 mil midrange probe due to inability of the probe to pass through the top TSP. A total of 14 indications were found in the 7 row 2 tubes. Small indications identified with the 800 kHz inspection included maximum depths sized at 38% and 44% and average depths sized at 14% and 23%. No indications were found in the row 3 inspection.

All U-bend indications were in situ tested. Two tubes in row 2 and one in row 3 that were NDD by +Point inspection were in situ tested followed by + Point inspection to assess the potential for small undetected indications. No indications were found by +Point inspection following pressurization of the tubes to 5500 psi. Pressurizing the tubes would be expected to open small cracks and increase detectability of the potential indications. While not a statistically based sample, these results suggest that widespread undetected indications are not present.

Condition Monitoring Assessment Conclusions

The following conclusions are developed from the condition monitoring assessment of this report:

- Condition monitoring requirements for Cycle 14 are not satisfied due to the large leakage event due to axial PWSCC in the U-bend of SG 4 tube R2C5.
- All other U-bend PWSCC indications found in the EOC-14 inspection satisfied condition monitoring structural and leakage requirements.
- All U-bend indications found in seven tubes were in situ tested. Six of the seven tubes did not leak at SLB conditions and the test pressures exceeded the operating temperature $3\Delta P_{NO}$ = 4617 psi burst margin requirement.
- For the R2C71 indication in SG 4 that leaked at SLB conditions, the indication did not burst at the maximum in situ test pressure of 4206 psi (adjusted to operating temperatures) and the expected burst pressure would exceed the $3\Delta P_{NO}$ burst requirement of 4617 psi. This conclusion is based upon the post in situ test, short ligament tearing lengths to throughwall and predicted pressure differences between ligament tearing and burst. The SLB leak rate of 0.024 gpm is also well below the allowable SLB leakage limit of 1.0 gpm/SG for freespan indications.

Operational Assessment Conclusions

All operational assessment analyses, which include independent single cycle axial profile and multicycle analysis methods, support Cycle 15 operation in excess of 1.0 EFPY. To provide additional structural and leakage integrity margin, the recommended operating interval to the next inspection is 0.85 EFPY (310 EFPD).

Acceptability of the 0.85 EFPY operating period is based upon:

- All row 2 tubes have been preventively plugged, and no indications were found in row 3 tubes during the EOC-14 inspection with either the midrange or high frequency +Point probes.
- Independent Monte Carlo analysis techniques (reference single cycle analyses using crack profiles and independent multi-cycle analyses based upon crack initiation rates) support Cycle 15 operation in excess of 1.0 EFPY. The analyses support the recommended cycle length even if it would be assumed that all row 2 tubes were not

preventively plugged (i.e., equivalent to assuming that the row 2 indications occurred in row 3).

- The reference cycle length analyses show that the $3\Delta P_{NO}$ = 4668 psi burst margin requirement for Cycle 15 is satisfied for a > 1.0 EFPY operating period between inspections. The projected limiting indication burst pressure is 4840 psi at 1.0 EFPY and 4937 psi at 0.85 EFPY. No SLB leakage is expected for cycle lengths in excess of one year. The projected SLB tube burst probability after 1.0 EFPY of operation is 3.2×10^{-3} compared to the EPRI tube integrity guideline of about 4.0×10^{-2}. Sensitivity analyses to growth, POD and NDE profile depths show that the limiting indication burst pressures do not change significantly when assumptions that are more conservative are made on these key parameters for cycle length evaluations. The 1.0 EFPY operating period is acceptable for a 25% increase in growth and the use of the more conservative 800 kHz +Point profiles rather than the 400 kHz profiles supported by benchmark analyses. The expected POD uncertainty is to improve the POD for which a 5% depth shift to improve the POD results in a limiting indication burst pressure increase of about 600 psi while a 5% depth shift to reduce the POD results in a burst pressure decrease of only about 345 psi.
- Independent analyses were performed with the multi-cycle methodology using parameters conservatively benchmarked against EOC-14 inspection results for row 2. If it is conservatively assumed that one indication was detected in row 3 at the EOC-14 inspection, the SLB and $3\Delta P_{NO}$ burst probabilities are 2.2×10^{-3} and 4.8×10^{-2}, respectively, and no leakage is predicted at SLB conditions even after 1.9 EFPY or full cycle operation. Under the very conservative assumption that row 2 tubes were not preventively plugged, the probability of burst after 1.0 EFPY of operation would be about 4.5×10^{-3} at SLB conditions and only 5.8×10^{-2} at $3\Delta P_{NO}$ compared to the EPRI tube integrity guidelines of about 4.0×10^{-2} and 8.0×10^{-2}, respectively. These results are consistent with the reference analyses. Benchmarking of the multi-cycle analyses against the EOC-14 inspection results required a low crack initiation rate over multiple prior cycles. An adequate benchmarking could not be obtained for a high initiation rate that could have resulted in a large number of undetected indications at EOC-14.
- As a defense in depth measure, the Indian Point-2 operating leak rate limit is being administratively set at 30 gpd to enhance the potential for detection of a large leaking flaw prior to the flaw growing to a structurally unacceptable size. Although the operating leakage at Indian Point-2 was only a few gpd prior to the R2C5 leakage event and this leakage level may not have been due to the R2C5 indication, the reduced leakage limit provides additional margin against an unexpected flaw size.

A laboratory test program is being initiated to develop +Point POD and NDE sizing uncertainty information for axial PWSCC in rows 2 and 3 U-bends. Accelerated cracking will be performed on prototypically fabricated U-bends. Differences in the time to crack between row 2 and row 3 U-bends will be evaluated as a part of this test program. NDE data will be obtained with and without deposits simulating the noise levels found in the Indian Point-2 U-bends. "Blind" (without knowledge of destructive exam results) analyses of the NDE data by field analysts will be used to develop POD and NDE uncertainty distributions. It is expected that these tests will demonstrate POD and NDE uncertainty distributions less conservative than the values used in this operational assessment. Due

to the extensive nature of this test program, the results are not expected prior to completion of the recommended operating cycle length of 0.85 EFPY.

2.2. Summary of Additional Information Applied in This Report

Historical Trends and Stress Analyses for Rows 2 and 3 U-Bends

Based on consideration of industry experience with low row U-bend cracking, stress analysis of the low row U-bends, and manufacturing considerations, the following conclusions have been made regarding susceptibility to apex axial PWSCC in the row 3 U-bends at Indian Point-2:

- Only one apex axial PWSCC indication in a non-dented SG and a few axial ODSCC indications have been observed in row 3 U-bends in Westinghouse SGs to date. Based upon stress analyses including hourglassing effects on reducing leg spacing, the time to crack initiation for row 3 is estimated to be about a factor of 2.5 to 4.0 longer than row 2. Stress analyses show that the final stress state due to flow slot hourglassing of the row 3 tubes is less than the final stress state of the row 2 tubes; hence, the susceptibility to cracking of the row 3 tubes is less than for the row 2 tubes. The principal factor limiting the stress is the greater flexibility of the larger radius U-bends, and the reduced strain hardening of the larger bends.
- The time to initial observation of row 2 cracking at Indian Point-2 has been greater than for other operating plants, consistent with the lower operating temperature of Indian Point-2. The lower operating temperatures at Indian Point-2 tend to increase time to crack initiation while the increased stresses from TSP hourglassing tend to decrease time to crack initiation. The two factors appear to have comparable effects on crack initiation time based on comparisons of times to crack initiation between plants. A like relationship is expected to apply for potential row 3 cracking.
- For stresses resulting from TSP hourglassing, a stress plateau (stress exceeds yield strength) is reached when the leg spacing at the TSP is reduced by about 0.15 inch. It is expected that all or most of the row 3 tubes reached this stress plateau many cycles ago when hourglassing was progressing. As a consequence of the plateau, stress levels would not increase even assuming modest progression of hourglassing, and stress driven PWSCC initiation and growth rates for Cycle 15 would be similar to Cycle 14.
- Any potential strain rate effect on crack initiation would be less than or equal to that in the prior cycle for which associated effects would be included in the growth rates derived from Indian Point-2 data. Strain rates in the range of 10^{-7}/sec to 10^{-8}/sec appear to be the most influential on SCC initiation as this range is most sensitive to the film breakdown/crack initiation/repassivation mechanism. At typical SG temperatures, strain rates > 10^{-7}/sec are more likely to lead to mechanical overload than SCC. A minimum strain rate for SCC initiation is not defined in the literature, which may be due to excessive test times required for evaluation. Multiple studies have indicated that only SCC initiation may be strain rate dependent and average crack growth rates are approximately independent of strain rate. Crack initiation, however, does not affect the acceptable operating cycle for U-bend degradation as new indications would not grow to structurally challenging indications over the

recommended operating cycle. Since strain rate effects have no apparent influence on crack growth rates, the influence of strain rates on the operating cycle evaluation is negligible.

- Manufacturing differences between the row 2 and row 3 tubes are believed to result in residual stress states that may enhance row 2 susceptibility to PWSCC while reducing the susceptibility of the row 3 tubes to cracking. Accelerated corrosion laboratory tests with prototypic U-bends in polythionic acid have shown that row 3 tubes did not crack in the time that row 2 U-bends cracked, indicating that the manufacturing process differences have significant influence on the cracking behavior of the low row U-bends.

Analysis Methods

Two independent analysis methods are used to establish an acceptable operating cycle length for the axial PWSCC U-bend indications. The reference analysis method is a single cycle methodology based on use of axial length versus depth profiles obtained from +Point NDE data. A multi-cycle analysis methodology, based on tracking indications from initiation through multiple inspection cycles, is applied herein as an independent check on the results of the single cycle analyses.

The single cycle Monte Carlo methodology is a relatively new method developed in the last two years and has been previously applied for a licensed ARC for axial PWSCC at dented tube support plate intersections as well as for multiple plant operational assessments. This method uses the plant outage specific +Point crack profiles to permit detailed crack shape analyses for leakage and burst. The application of this methodology evaluates the U-bend indications as freespan indications, which slightly differs from the constrained and freespan analyses for the ARC application. The multi-cycle analysis methodology utilizes crack initiation rates, burst effective average depth/length distributions and maximum to average depth ratios. These methods have also been used extensively for SG operational assessments over the last three to four years.

conditions. The tube material flow stress for burst and leakage analyses is defined for the U-bend regions reflecting the strain hardening from manufacturing bending of the tubes.

Benchmarking of Tube Integrity Analysis Methods

Benchmarking of the tube integrity analysis methods was performed for both the single cycle axial profile and multi-cycle analysis methods. For the axial profile methods, these analyses provide an integral check on the adequacy of the +Point profiles, NDE uncertainties and growth data as well as the analytical techniques. The benchmarking analyses include: predictions of the R2C5 leakage event from the 1997 depth profile for this indication; comparisons of 1997 burst pressure and leakage projections to EOC-14 with results from in situ tests and calculations using the year 2000 profiles; and comparisons of burst pressure and leakage analyses using the year 2000 profiles with in situ test results. Overall, it is concluded from these benchmark analyses for the axial profile analysis methods that the methodology applying the 400 kHz NDE profiles results in bounding analyses at the required lower 95% probability levels. These methods are applied for the operational assessments in Section 9. The use of the 800 kHz NDE profiles tends to be unnecessarily conservative.

For the multi-cycle analysis methods, the benchmarking analyses are used to compare predictions and inspection results for the EOC-14 indications including the large R2C5 indication and the depth distribution of the indications. This comparison guides selection of initiation rates and optimized prior cycle PODs and growth rates for application in the Cycle 15 projections.

2.3 Open Items

As of the date of issue for this report, the following items have not been completed. None affect the conclusions of this report or the length of the recommended operating cycle.

a) A computer code utilized for these analyses, AUTOAXPROFILE as described in Section 4, is a modification of a code documented in WCAP-15218 to increase the flexibility of input data compared to the original code. Although the changes to the code have been checked, final configuration control and documentation are in process at the time of this report.
b) The multi-cycle analyses described in this report were performed by E-Mech Technology, Inc. Verification signatures by E-Mech personnel on the title page of this report reflect verification of the E-Mech analyses and not the complete report. The Westinghouse analyses were verified by Westinghouse personnel. E-Mech is not currently on the Westinghouse qualified suppliers list. However, the process has been initiated to complete this qualification.
c) Computer spreadsheets were utilized in the preparation of some of the supporting data in this report, which have not been completely verified. These spreadsheets were used for the following information:
    a. Development of Figure 3-6

b. Development of Figures 5-1 and 5-2
c. Development of Figures 5-3, 5-4 and 5-8
d. Development of Figure 6-3 and data in Table 6-3 under the column title Ligament Tearing Pressure at 95/50

Although the spreadsheets have been checked, formal verification is necessary.

3.0 U-BEND INSPECTION RESULTS

3.1. Initial Mid-Range +Point Inspection

Following plant shutdown due to the leaking indication, the initial inspection focused on identification of the leaking tube and location of the flaw in the tube. Based on filling the secondary side of the SG, the leaking tube was identified as R2C5 in SG 4. A fiber optics visual exam from the ID was performed and identified the cause of the leakage as an axial indication at the apex of the U-bend on the extrados of the tube. Following characterization of the flaw in R2C5, the decision was made to proceed with a complete SG inspection as originally planned for the refueling outage scheduled for late April. In addition, refueling was performed during the outage so that the leaker outage represents EOC-14.

The initial inspection plan for the low row U-bends was to perform a 100% +Point inspection of the row 2 and row 3 U-bends in all 4 SGs. To establish confidence that cracking was limited to the expected row 2 conditions, the inspection was further expanded to include Row 4. A 620 mil, mid-range +Point coil on a flexible probe designed for the low radius U-bends was used for the inspection. This probe was EPRI Appendix H qualified for detection of axial and circumferential cracking in the low row U-bend region under ETSS #96511.

The midrange +Point inspection identified three axial PWSCC indications in Row 2 U-bends and none in row 3 or row 4. Two indications in SG 4 were found at R2C69 and R2C72. One indication was found in SG 1 at R2C87. R2C71 in SG 4, for which an indication was later identified, was found to be a restricted tube that would not pass the 620 probe and thus was not an inspectable tube with the midrange probe. However, the inspection with the midrange probe identified a large number of tubes (see discussion in Section 3.2 below) with inconclusive data due to noise signals in the U-bend (classified as "Bad Data" per NDE terminology). Data from these tubes could not be adequately analyzed. The bad NDE data was attributed to noise resulting from deposits of magnetite and copper on the tubes with additional contributions from coil lift-off due to tube ovality in the small radius U-bends. A tertiary review (additional primary, secondary, resolution process) of the U-bend data, supplementing the normal primary/secondary/resolution process, was conducted to further identify tubes with unacceptably noisy data and assess potential unreported indications. Repeat inspections of tubes with noisy data did not significantly reduce the number of tubes with such data. These inspection limitations led to an evaluation of alternate probes as described below.

3.2. High Frequency +Point Inspection

The detection of degradation using NDE techniques is dominated by the comparison of the degradation response to the response of other factors in the inspection environment or signal to noise (S/N) ratio. When the prior 1997 inspection data from R2C5 were reviewed, the signal to noise ratio was very low, and the indication would not have been expected to be called based on the probe and analysis guidelines in place. As a result of

the review of the 1997 data in which the R2C5 indication was identified, criteria were established to define unacceptable noise levels based on the signal characteristics of the R2C5 1997 +Point response. A large number of tubes were identified with unacceptable data. In order to improve the detection capability in the U-bend region under these circumstances, the signal to noise ratio for indications like that of R2C5 required improvement.

Several origins for the noise associated with the U-bend inspection were postulated. These were reduced to two main concerns 1) tube ovality and 2) OD deposits, where the nature of the OD deposits is a combination of copper and magnetite. Since the degradation associated with the indications found in the Indian Point-2 U-bends was found to be PWSCC originating on the inside surface of the tube, it was judged that increasing the eddy current test frequency would improve the S/N ratio when OD deposits are present. No improvement would be expected however for "noise" associated with tube ovality. The table below shows measurements of the mid-frequency +point coil response for a simulated copper deposit on the outside of a tube.

+Point Coil Response to Simulated Copper Deposits		
Frequency (kHz)	**Amplitude (Volts)**	**Phase (Deg.)**
600	0.6	79
400	1.2	36
300	1.8	10
100	5.0	-54

As the frequency of the inspection is increased, the deposit response decreases and its phase rotates in a clockwise direction. The impact of these two response characteristics is to allow separation of the response between the ID degradation and the OD deposits. The combined effect of the larger angle phase response of the deposits and an ID flaw (approximately 40° phase setup as throughwall) can be expected to increase the crack depth derived from the phase angle as a function of increased frequency.

It was concluded that a high frequency +Point probe offered the best available probe for inspection of the U-bends in the presence of deposits including copper. The high frequency probe was EPRI Appendix H qualified for detection per ETSSs #99997.1 and #99997.2 in order to support the Indian Point-2 inspection. Initially, the high frequency probe was used to inspect a few tubes to permit comparisons with the midrange +Point probe. The high frequency probe was found to have the best response, including reduction of the deposit noise levels at 800 kHz, and this frequency was applied for the inspection. A comparison of the midrange and high frequency probes is described below in Section 3.3. A complete 100% reinspection of Row 2 and Row 3 tubes in all four SGs was performed with the high frequency probe.

The high frequency inspection identified additional axial PWSCC indications in four tubes including R2C4, R2C71 and R2C74 in SG 4 and R2C85 in SG 3. The indication in R2C71, SG 4 identified with the 620 mil high frequency probe had been found to be a restricted or not inspectable tube with the 620 mil midrange probe. The remaining three indications

found with the high frequency probe were identified in tubes for which the U-bend midrange coil inspection data was classified as bad data (inadequate inspection). Sizing of the indications is described in Section 3.4.

Use of the high frequency +Point probe in the low signal to noise (BDA) tubes raised the issue of detectability of ODSCC due to the limited field extension of the high frequency coil at frequencies of 800 and 1000 kHz. First, it must be understood what BDA implied in the context of the Indian Point Unit 2 low row U-bend inspection. The mid-range probe exhibited a significant amount of data disregistry (such as irregularities in the indication contour due to probe slippage during rotation). This disregistry is typically caused by the mechanics of the probe rotation. A U-bend RPC is a coil riding against the tube surface in a shoe on the end of a cable (to achieve flexibility). The cable is rotated using a motor. The material of the shoe, its contact area and the length of the cable all contribute to friction, slowing of the motor and cable whipping (due to wind-up). This is a major source of the bad data reported for the mid-range probe. The high frequency probe exhibited a significantly improved data quality due to mechanical differences. The contributing factors were a smaller contact area due to the smaller coil and different shoe material leading to less friction, as well as a shorter cable length resulting in less of a wind-up effect.

In order to address the OD detection capability of the high frequency +Pt coil, a sampling of data was reviewed and compared to the mid-range +Pt coil at 300 and 400 kHz. The U-bend qualification data set included OD notches; however, they were not measured or recorded in the initial qualification. These signals were analyzed at Indian Point 2 after the qualification to determine the detectability of ODSCC using the high frequency probe. The graphics from the EPRI qualification data program clearly show a 36% OD circumferential notch and a 38% OD transverse notch at various frequencies. The calibration standard used to test those two tubes also clearly shows the 40% OD notch. Additionally, two tubes with sludge pile ODSCC axial indications in SG 2, tubes R33C51 and R35C51, were tested with the high frequency +Point probe and the indications were favorably compared with the 300 kHz midrange probe data on these tubes. Of the various frequencies of the high frequency +Point probe (1000, 800, 600, 400 and 300 kHz), 400 kHz shows the best response to the OD notches. The data analysts were required to scan and plot the 300 kHz and 400 kHz data for OD degradation in order to adequately detect OD indications with the high frequency probe at 400 kHz. Based on these studies, it was concluded that, the high frequency +Point provides adequate detectability with respect to OD degradation for the BDA tubes based on the similarity of the midrange probe 300 kHz and high frequency probe 400 kHz response of the calibration standard OD notches and two sludge pile ODSCC indications.

3.3. Comparison of Midrange and High Frequency +Point Detection Sensitivity

Reduction of Bad Data with High Frequency Probe

One of the objectives of the high frequency probe inspection was to reduce the number of tubes with bad NDE data in order to provide an acceptable inspection for these tubes. The "masking" of the R2C5 indication by deposits in the 1997 inspection was used to guide identification of "bad data" for evaluation of the EOC-14 inspection results. Table 3-1 compares the occurrences of bad data from the tertiary review of the midrange probe data with that for the high frequency probe. It is seen from the table that the bad data percentage was 53% in the low row U-bend tubes examined for the midrange probe and 0.8% for the high frequency probe. This result clearly identifies the inspection improvements obtained with the high frequency probe. The occurrence of bad data in the tertiary review did not show any dependence upon row number as shown in Table 3-2. Table 3-3 compares the U-bend cracks identified by the tertiary review of the midrange data with the indications found by the high frequency probe. The conclusions from the tertiary review of the midrange data and the high frequency probe are:

- The high frequency +Point probe proved very effective in improving data signal to noise ratios and essentially eliminated U-bends with bad data. The 0.8% of the tubes remaining with bad data are repaired due to inadequate inspection.
- The data quality criteria established for the tertiary review resulted in significant numbers of U-bend test results classified as bad data (BDA or BDN) for the midrange probe.
- While very conservative, the data quality criteria applied to the midrange +Point probe proved effective. No tubes exhibiting degradation with the high frequency probe were classified as acceptable (NDD) with the data quality requirements applied in the tertiary review. As shown in Table 3-3, three indications found with the high frequency probe were found in tubes with bad data from the midrange probe and one indication was found in a tube found to be restricted from U-bend access with the midrange probe.
- As a general rule, the midrange probe data quality did not improve significantly from the lower rows (row 2) to the higher rows (row 4). One exception is in SG 24.
- The high frequency +Point probe identified four more SAIs than the midrange probe and tertiary review, where they were classified as bad data (BDA) or restricted tubes (RST).

Detectability Improvements with the High Frequency Probe

Figure 3-1 shows the results of applying a high frequency inspection to a Row 2 U-bend. The C-Scan plot of the 400 kHz data for SG 4, R2C69 is compared to the same plot for the 800 kHz inspection. The bulk of the noise ridges in the 400 kHz data have disappeared in the 800 kHz data. In addition, three small indications while discernible in the 400 kHz data are clearly seen in the 800 kHz data. This result demonstrates the ability to detect small indications with the high frequency probe. Further a comparison of the 400 kHz and the 800 kHz strip chart traces demonstrate the impact of the higher frequency on the inspection capability. Since there is a significant change in S/N ratio as the frequency is

increased and careful review of the noise responses shows that they tend to rotate clockwise as the frequency is increased, the dominant "noise" source originates from deposits on the outside of the tube. Thus while tube ovality may contribute to the noise, it is not the most significant factor in this example.

Figures 3-2 and 3-3 compare the 400 and 800 kHz data for SG 4, R2C4 and R2C74. For R2C4, the 800 kHz data again show a substantial reduction in noise compared to the 400 kHz data and the small flaw can be clearly identified at 800 kHz. The 400 kHz data were classified as bad data due to the general noise level, and the flaw would be difficult to separate from the noise level. Given the knowledge of the flaw from the 800 kHz data, the flaw can be found in the 400 kHz data also. For R2C74, the very small flaw response near the center of the C-scan was identified in the 800 kHz data even though the data for this tube is relatively noisy for 800 kHz data. The improvement in data quality and flaw detection over the 400 kHz data is also apparent for this tube. No flaw can be identified in the 400 kHz data, which was classified as bad data due to limitations on detection of small flaws within the noise levels. Comparisons of the 400 and 800 kHz data for all U-bend flaws are given in Appendix A. These comparisons further support improvements in detection of small flaws for Indian Point-2 tube deposit conditions with the high frequency probe. Appendix A also includes C-scans from the 1997 U-bend inspection for the flaws detected in the 2000 inspection.

Appendix A also includes C-scans for the 400 kHz responses obtained with both the midrange and high frequency + Point coils. In general, the high frequency + Point responses show somewhat less noise than obtained with the midrange probe. This tends to indicate that the high frequency probe may reduce the effects of tube ovality in the responses. The high frequency probe has a different body and coil features which apparently improve the coil response.

It is concluded from the comparisons of the 400 and 800 kHz data herein and in Appendix A that the high frequency probe has eliminated the major influence of the OD surface deposits that masked detection of the flaw in R2C5 in the 1997 inspection. The visibility of small flaws in the high frequency data support a major improvement in detectability relative to the 400 kHz data used in the 1997 inspection.

3.4. +Point Sizing of U-Bend Indications

Capability to size axial PWSCC at dented TSP intersections has been demonstrated as documented in Reference 10-8. The PWSCC sizing in this report has been applied to support alternate repair criteria for axial PWSCC at dented TSP intersections. An NDE performance test of field analysts was conducted to develop NDE uncertainties to support application of the sizing techniques. As developed in Reference 10-8, the NDE uncertainties apply to the mid-range +Point coil evaluated at 300 or 400 kHz. Since the +Point coils are surface riding, the sizing techniques can be applied to the U-bend axial PWSCC with expected sizing accuracy comparable to that for the dented TSP intersections. To reflect some additional uncertainty for U-bend sizing in the absence of

direct destructive exam data for U-bend indications, the NDE uncertainties for sizing of U-bend indications have been increased as described in Section 5.5.

Since the + Point sizing techniques were demonstrated for the mid-range probe, it is important to establish the differences in the sizing results between 400 and 800 kHz. Sizing results for tube R2C69 at 400 and 800 kHz are shown in Figure 3-4. It is seen for this indication that the 800 kHz data are consistently higher than the 400 kHz data with the maximum depth increased from 74% to 89% and the average depth from 55.2% to 64.5%. The length is also increased, but only by 0.06" which is within the measurement uncertainty. A similar comparison is shown in Figure 3-5 for R2C71 with the 800 kHz data also higher than found for 400 kHz data. The results of sizing for the EOC 14 inspection are given in Table 3-5. The 800 kHz depths exceed those obtained at 400 kHz for all indications. Average depths and lengths are also given in the table for the burst effective lengths obtained by searching the depth profile for the segment with the lowest burst pressure. These lengths reflect the structurally significant lengths and eliminate the shallow tails of the indications. The burst effective results are also higher for the 800 kHz results. The EPRI ETSS#99997.2 for detection qualification of the high frequency plus point probes used at Indian Point-2 also shows the trend for the high frequency probe to overestimate crack depths.

As noted in Table 3-5, the indications in R2C85, R2C4 and R2C74 could not be sized with the 400 kHz midrange coil due to unacceptable noise levels, and were sized at 400 and 800 kHz using data from the high frequency probe. Since the high frequency probe is not optimized for data collection at 400 kHz, there may be more uncertainty in the sizing of these small indications. In particular, the indication in R2C74 was difficult to size due to very low signal to noise ratios of about 0.5 at 400 kHz and 1.2 at 800 kHz. Phase angle distortion was also significant for this indication. R2C4 also had a comparable signal to noise ratio but less distortion in the phase response and sizing would be acceptable for this indication. The remaining indications were larger with signal to noise ratios at 400 kHz ranging from about 1.3 for R2C87, 2.0 to 2.5 for R2C5 to 3.8 for R2C69 and sizing would be more reliable for these indications.

Based on the sizing qualification for 400 kHz data, the 800 kHz results would be expected to yield conservative tube integrity results. To increase conservatism in the cycle length evaluation for Cycle 15, the 800 kHz sizing results are included as sensitivity analyses to support the tube integrity assessments. Section 6 describes benchmarking of the overall analysis methods using both 400 and 800 kHz data. It is shown in Section 6 that the 400 kHz profiles generally provide improved agreement with in situ test results compared to the 800 kHz data. Only 400 kHz +Point data are available from the 1997 inspection for development of axial PWSCC growth rates for U-bend indications. For growth rate accuracy, the data for both cycles should be obtained using the same probe to avoid introducing probe variability into the growth rates. Therefore, the 400 kHz data for both cycles are applied in Section 5.4 to develop growth rate data.

All profiles for U-bend indications at both 400 and 800 kHz are given in Appendix C.

3.5. In Situ Test Results

All U-bend indications were in situ tested to eliminate any uncertainties on tube integrity that might be related to adequate sizing of the indications to select indications for testing. It remains informative to assess which indications would have required testing based on the requirements for in situ testing as given in the EPRI in situ test guidelines of Reference 10-3. The need for pressure testing is based on not satisfying condition monitoring requirements by analysis at 95% probability and 50% confidence. NDE uncertainties are included in the analysis by applying the PWSCC sizing uncertainties of WCAP-15128 (Reference 10-8) with a 25% increase in the standard deviation for the uncertainty. The uncertainties in NDE sizing, burst correlation and material properties are statistically combined by Monte Carlo analyses to develop a burst effective average depth versus length curve that defines the need for pressure testing. The resulting curve for row 2 U-bend indications is shown in Figure 3-6. For crack lengths less than about 0.6 inch long, the burst margin requirements would be satisfied even for throughwall cracks in row 2 U-bends, and NDE depth uncertainties would not have to be applied to define the test requirements. Since length of deep flaws are overestimated by +Point, a length uncertainty would also not be required below about 0.6 inch. The requirements curve of Figure 3-6 was extended down to 0.45 inch to conservatively bound any need for in situ testing. The burst effective sizing results at 400 kHz from Table 3-5 are shown as data points in Figure 3-6. Only 3 indications have lengths greater than 0.4 inch that could conservatively challenge structural integrity. Of these 3 indications, only R2C71 would require in situ testing by the requirements curve of Figure 3-6 with the indications at R2C69 and R2C72 lying just below the requirements curve. Thus only R2C71 would meet the requirements for in situ pressure testing. The requirements for in situ leak testing are that the maximum +Point voltage exceed 2 volts and that the maximum depth exceed 80% for PWSCC indications. Based on these requirements, R2C71 and R2C72 would have required leak testing. If the 800 kHz sizing results were conservatively applied, in situ testing would have been required for R2C69, R2C72, R2C71 and R2C87. The 400 kHz in situ guidelines for selecting indications for testing are supported by the test results described below in that only R2C71 leaked at SLB conditions and leakage prevented the test from reaching the target test pressure for structural confirmation.

Since the test mandrel cannot enter the U-bend, the indications were tested as whole tube tests with the seals located in the hot and cold leg tubesheet. For a whole tube test, the entire tube is filled with water and pressurized such that any indication in the tube can contribute to measured leakage. In addition, leakage can exceed the test system capacity (about 2 gpm) prior to reaching the desired pressure for the in situ test. The inability of the in situ test to reach the burst margin requirement due to high leakage does not directly imply failure to demonstrate burst margin requirements. The post test indication must be examined by NDE and/or visual exam to assess the crack opening and evaluation as a burst or ligament tearing. In addition, measured leak rates within the test equipment capacity at reduced pressures following the peak pressure test are used to estimate the throughwall length to support the ligament tearing or burst evaluation. In most cases, ligament tearing can be separated from a burst although for long cracks a clear separation may not always be possible by NDE. These evaluations must be performed to determine if a large leakage indication satisfied condition monitoring

requirements. For the U-bend indications that had leakage exceeding capacity, post test +Point inspection to size the indication and post peak pressure leak rate measurements to permit estimation of the throughwall length were performed. The evaluation of the in situ tests relative to satisfying condition monitoring requirements is given in Section 8.2.

The in situ test results for the U-bend indications are given in Table 3-6. Indications exceeding the $3\Delta P_{NO}$ burst margin with no leakage included: SG 4 indications at R2C69, R2C72 and R2C4; the SG 1 indication at R2C87; and the SG 3 indication at R2C85. The SG 4 indication at R2C74 exceeded the $3\Delta P_{NO}$ burst margin with a small initial leak rate of 0.035 gpm at 4800 psi and a leak rate of 0.112 gpm at a pressure margin of 5500 psi. None of these indications leaked at SLB conditions and all leakage requirements are satisfied for these indications.

The SG 4 indication at R2C71 had initial in situ leakage of 0.00024 gpm at 1741 psi and 0.102 gpm at 2841 psi, which exceeds the SLB pressure differential of 2560 psi adjusted to 2739 psi for a room temperature test. The 2739 psi value is based on the hot to cold material property adjustment factor of 1.07 for U-bend indications as discussed in Section 5.2. The leak rates versus pressure measurements for this indication, as adjusted to hot operating conditions, are shown in Figure 3-7. For comparison with the allowable leakage limits, the measured leak rate at room temperature must be adjusted to operating temperatures at ΔP_{SLB} = 2560 psi. The adjustment of the measured leak rates was performed following the EPRI adjustment procedure of Reference 10-6 with the results shown in Figure 3-7. The adjusted SLB leak rate at operating temperatures then becomes 0.024 gpm and the normal operating leak rate becomes 0.0084 gpm. This normal operating leak rate is less than the total SG 4 leak rate of a few gpd prior to the leakage event although this indication apparently contributed to the operational leakage. The SLB leak rate is much lower than the allowable freespan leakage limit of 1 gpm as discussed in Section 5.2 although this limit applies to the sum of the leak rates for all freespan indications. It is shown in Section 8 that the freespan leakage limit of 1 gpm is satisfied for Indian Point-2 for all indications except the R2C5 indication leading to the leakage outage. The R2C71 indication is further evaluated in Section 8.2 for satisfaction of the $3\Delta P_{NO}$ burst margin.

The in situ test results are also used in Section 6.1 to benchmark the analysis methods by comparing burst and leakage results from the in situ test results with values calculated from the +Point profiles.

Table 3-1. Review of Midrange vs. High Frequency Coil for Bad NDE Data				
Row	**Midrange Tertiary Review Results (Number of Tubes)**		**High Frequency Results (Number of Tubes)**	
	Acceptable Data	**Bad Data**	**Acceptable Data**	**Bad Data**
SG 21				
2	40	32	71	1
3	32	57	88	1
4	41	46	46	0
Totals	113	135	205	2
SG 22				
2	16	19	35	0
3	31	43	74	0
4	38	36	36	0
Totals	85	98	145	0
SG 23				
2	7	38	44	1
3	23	49	72	0
4	30	60	60	0
Totals	60	147	176	1
SG 24				
2	28	28	54	2
3	37	48	85	0
4	83	21	1	0
Totals	148	77	140	2
Overall Totals	406	457	666	5
Percent Bad Data		(53%)		(0.8%)

Table 3-3. Midrange Coil Bad NDE Data by Row			
SG	**Row 2**	**Row 3**	**Row 4**
21	32	57	46
22	19	43	36
23	38	49	610
24	28	48	1
Totals	117	197	143

Table 3-4. U-Bend Cracks Identified by Midrange and High Frequency Techniques			
SG	**Tube**	**Midrange Coil Tertiary Review**	**High Frequency Coil**
21	R2C87	SAI	SAI
23	R2C85	BDA	SAI
24	R2C4	BDA	SAI
24	R2C69	SAI	SAI
24	R2C71	RST	SAI
24	R2C72	SAI	SAI
24	R2C74	BDA	SAI

Table 3-5. Indian Point-2 U-Bend Indication +Point Sizing Results for 800 and 400 kHz Data

SG	Tube	Crack No.	+Point Sizing Results					
			Max. Volts	Max. Depth (%)	Avg. Depth (%)	Length (inch)	Burst Avg. Depth	Burst Length (inch)
	Leaking Indication		**400 kHz – 1997 Data**					
4	R2C5	1	2.24	92	63.0	2.43	73.6	1.26
		1	2.31	92	70.6	2.43	80.2	1.87
	New Indications		**400 kHz – 2000 Data**					
4	R2C69	1	2.71	74	55.2	0.91	58.3	0.79
		2	1.03	74	44.5	0.11	44.5	0.11
		3	0.94	54	38.2	0.23	42.0	0.20
4	R2C72	1	3.17	82	59.8	0.54	66.6	0.44
4	R2C71(1)	1	2.43	96	64.0	0.57	69.0	0.48
1	R2C87	1	1.68	55	42.8	0.30	48.0	0.25
		2	2.25	61	43.6	0.29	48.0	0.25
		3	2.28	53	41.6	0.35	44.3	0.31
3	R2C85(2)	1	1.20	50	38.9	0.25	46.0	0.18
4	R2C4(2)	1	0.86	44	23.2	0.17	32.3	0.10
4	R2C74(2)	1	0.97	38	14.4	0.19	19.4	0.11
	New Indications		**800 kHz – 2000 Data**					
4	R2C69	1	4.12	89	64.6	0.97	68.5	0.86
		2	1.03	68	48.8	0.27	48.8	0.27
		3	0.92	84	61.1	0.23	61.1	0.23
4	R2C72	1	3.60	82	62.8	0.56	69.9	0.47
4	R2C4	1	0.89	50	33.0	0.12	33.0	0.12
4	R2C71	1	1.77	95	75.6	0.58	75.6	0.58
		2	0.95	34	18.8	0.09	18.8	0.09
4	R2C74	1	1.42	53	39.4	0.16	39.4	0.16
1	R2C87	1	2.79	84	60.7	0.28	60.7	0.28
		2	2.91	79	65.1	0.35	65.1	0.35
		3	2.82	68	51.8	0.43	59.3	0.32
		4	1.81	58	46.5	0.23	48.2	0.21
		5	0.70	68	52.6	0.11	52.6	0.11
3	R2C85	1	1.41	68	44.5	0.28	47.9	0.25

1. Midrange probe was restricted and +Point inspection was not performed with midrange probe. Data at 400 kHz obtained by evaluating high frequency probe data at 400 kHz.
2. Bad data was obtained with midrange probe and U-bend region of flaw was not inspectable in region of flaw. Data at 400 kHz obtained by evaluating high frequency probe data at 400 kHz based on flaw detected at 800 kHz.

Table 3-6. Indian Point-2 U-bend Indication In Situ Test Results

SG	Tube	Test Pressure (psi)	Leak Rate (gpm)	Condition Tested	Comments
4	R2C69	2841 4940 5259 5173 300	0.0 0.0 0.0 > 2 2.5	>ΔP_{SLB} 3ΔP_{NO} Added Margin Max. Test ΔP Supplemental Leak Test	Sudden leakage at 5173 psi exceeded test system capacity following peak pressure of 5259 psi. Test pressure margin of 5259 psi exceeded 4940 psi 3ΔP_{NO} burst margin requirement. Leakage of 2.5 gpm at 300 psi follows plastic crack opening at 5173 psi.
4	R2C71	1741 2841 4500 1000	0.00024 0.102 1.99 0.77	>ΔP_{SLB} Max. Test ΔP Supplemental Leak Test	Test limited to 4500 psi when test system measurement limit of 1.99 gpm reached. Leakage of 0.77 gpm at 1000 psi follows plastic crack opening at 4500 psi. See Figure 3-6 for measured leak rates adjusted to operating temperatures vs. pressure.
4	R2C74	2841 4800 5000 5500	0.0 0.035 0.049 0.112	>ΔP_{SLB} >3ΔP_{NO} Added Margin Max. Test ΔP	Initial leakage of 0.035 gpm at 4800 psi. Test pressure margin of 5500 psi reached exceeding 4940 psi 3ΔP_{NO} burst margin requirement.
4	R2C72	2841 4992 5500	0.0 0.0 0.0	>ΔP_{SLB} >3ΔP_{NO} Added Margin Max. Test ΔP	Test pressure margin of 5500 psi reached exceeding 4940 psi 3ΔP_{NO} burst margin requirement.
4	R2C4	2841 4992 5500	0.0 0.0 0.0	>ΔP_{SLB} >3ΔP_{NO} Added Margin Max. Test ΔP	Test pressure margin of 5500 psi reached exceeding 4940 psi 3ΔP_{NO} burst margin requirement.
1	R2C87	2841 4992 5500	0.0 0.0 0.0	>ΔP_{SLB} >3ΔP_{NO} Added Margin Max. Test ΔP	Test pressure margin of 5500 psi reached exceeding 4940 psi 3ΔP_{NO} burst margin requirement.
3	R2C85	2841 4992 5500	0.0 0.0 0.0	>ΔP_{SLB} >3ΔP_{NO} Added Margin Max. Test ΔP	Test pressure margin of 5500 psi reached exceeding 4940 psi 3ΔP_{NO} burst margin requirement.

Figure 3-1. Comparison of R2C69 Inspection Results at 400 and 800 kHz

R2C69 400 kHz Inspection

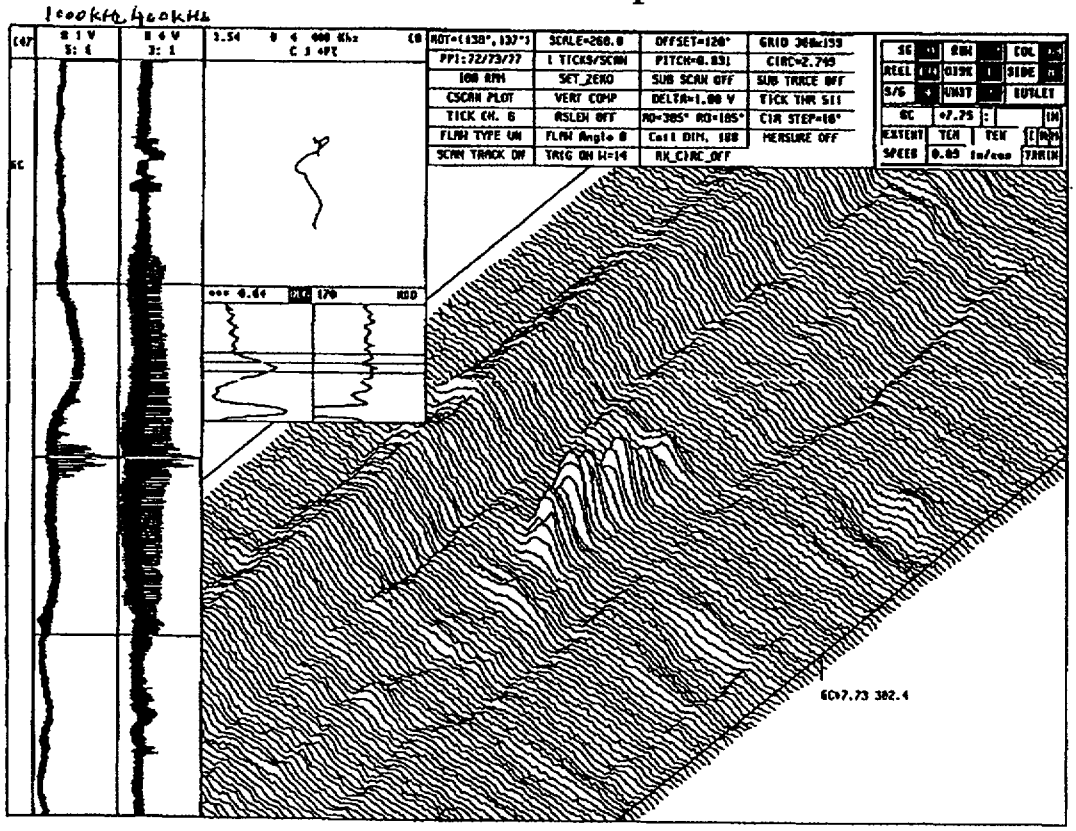

R2C69 800 kHz Inspection

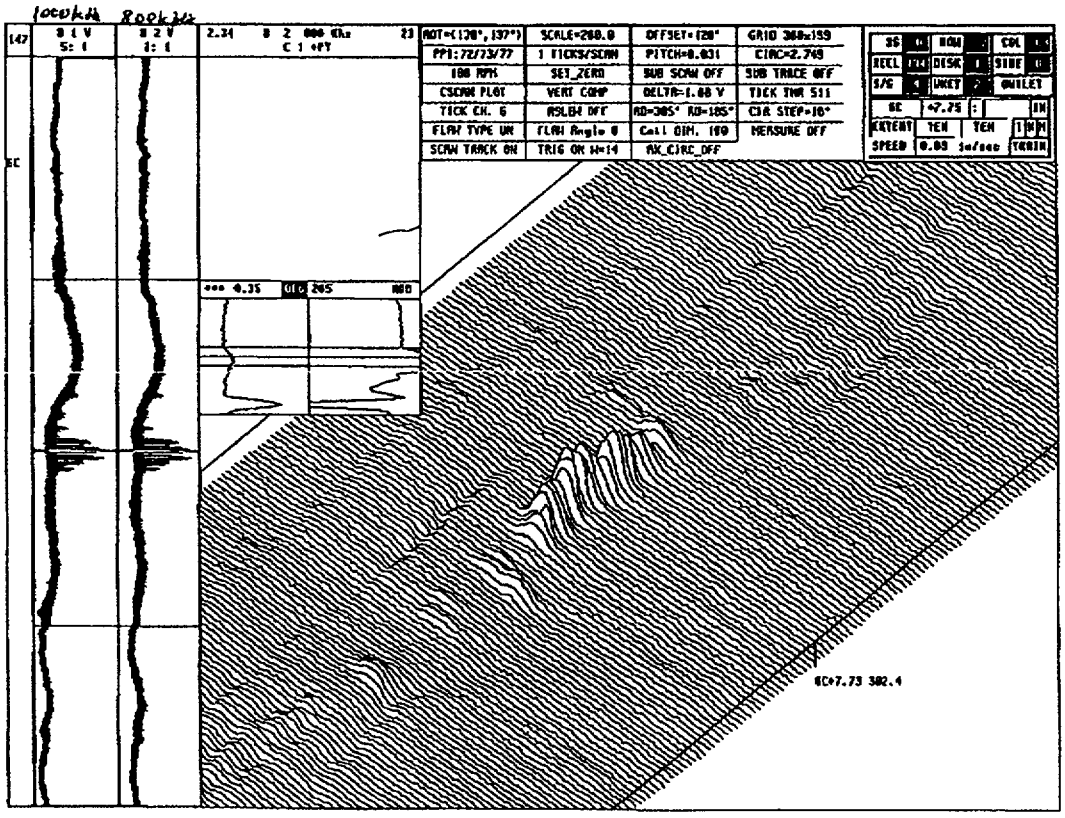

Figure 3-2. Comparison of R2C4 Inspection Results at 400 and 800 kHz

R2C4 400 kHz Inspection

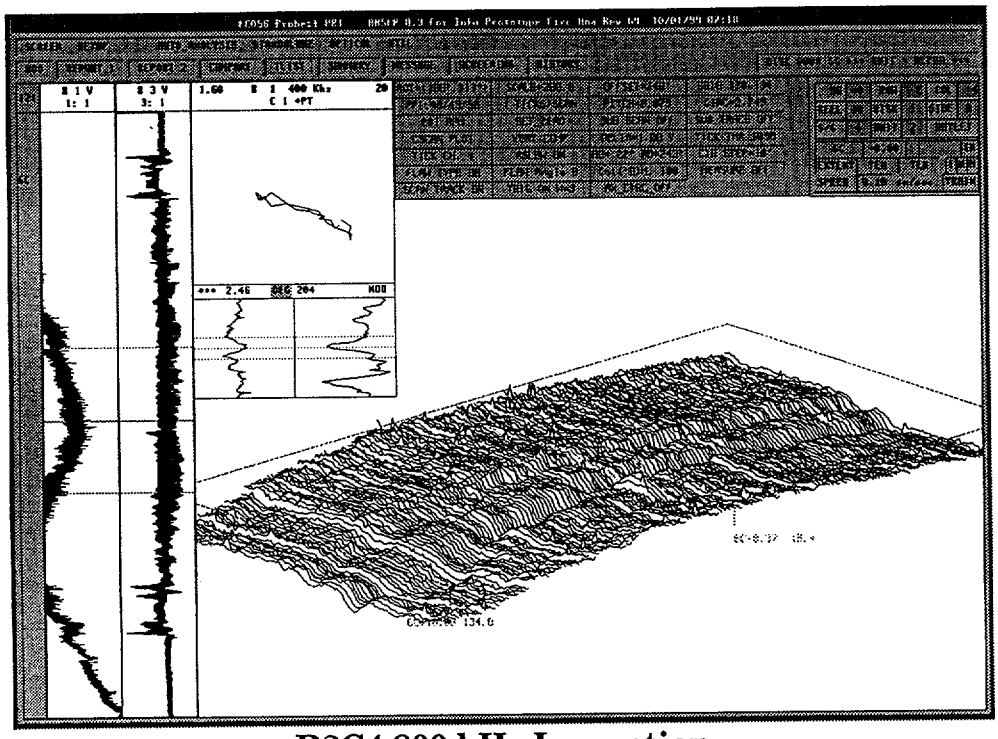

R2C4 800 kHz Inspection

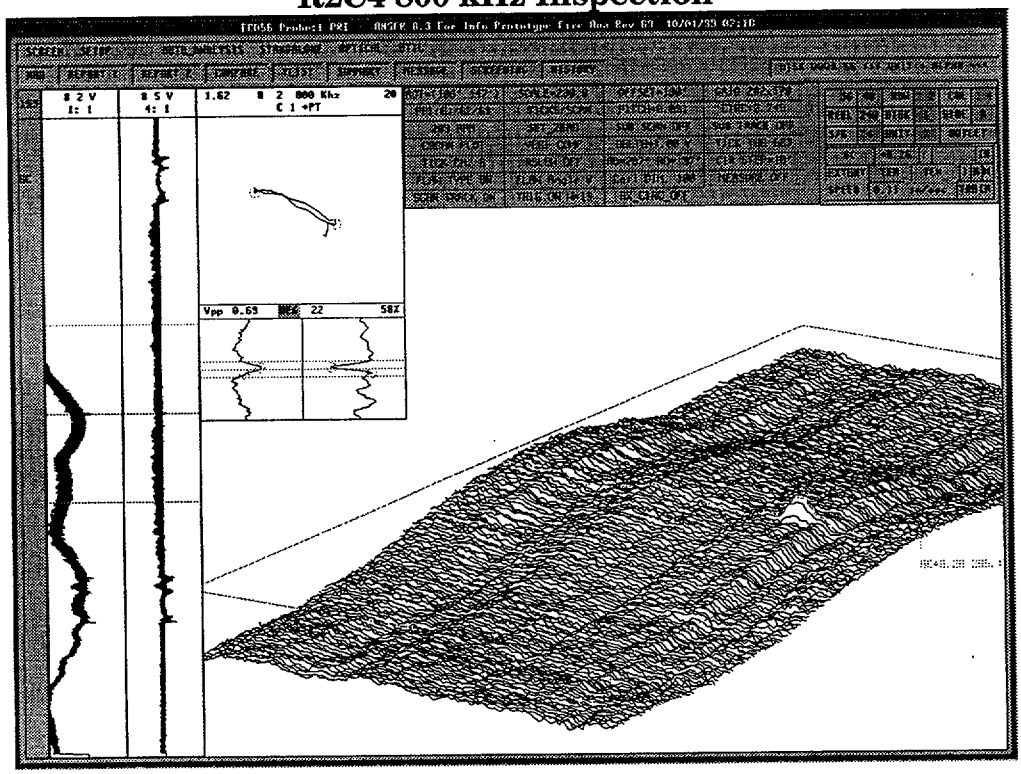

Figure 3-3. Comparison of R2C74 Inspection Results at 400 and 800 kHz

R2C74 – 400 kHz Inspection

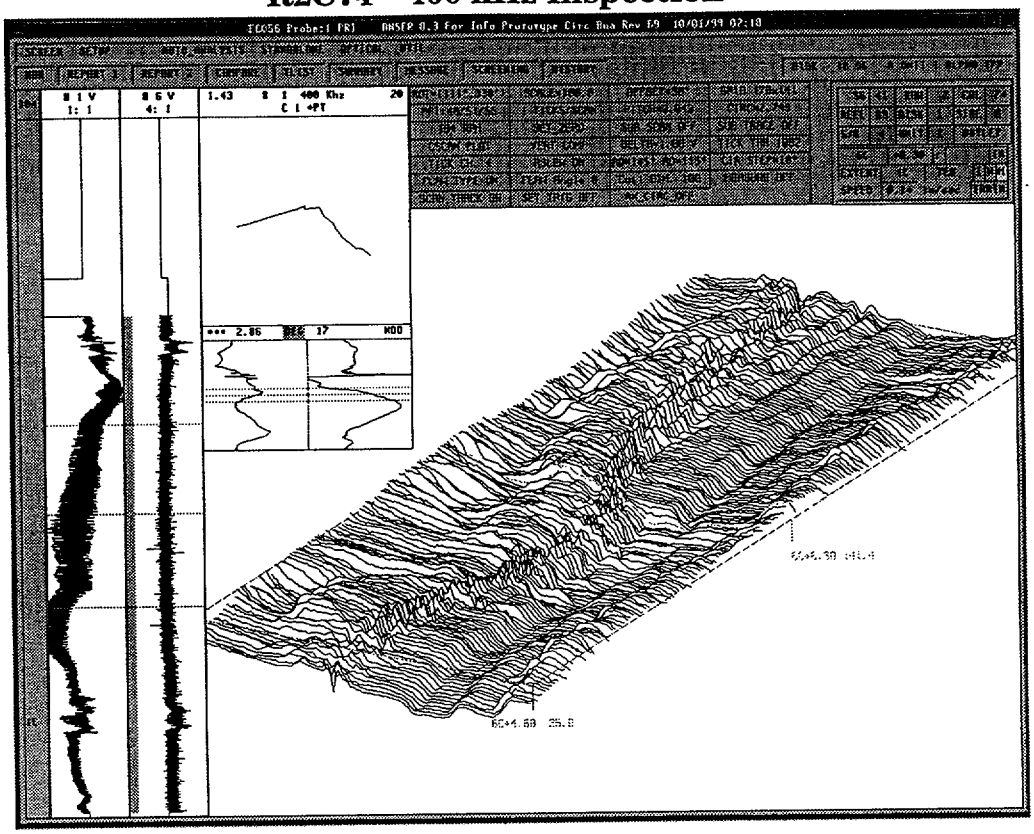

R2C74 800 kHz Inspection

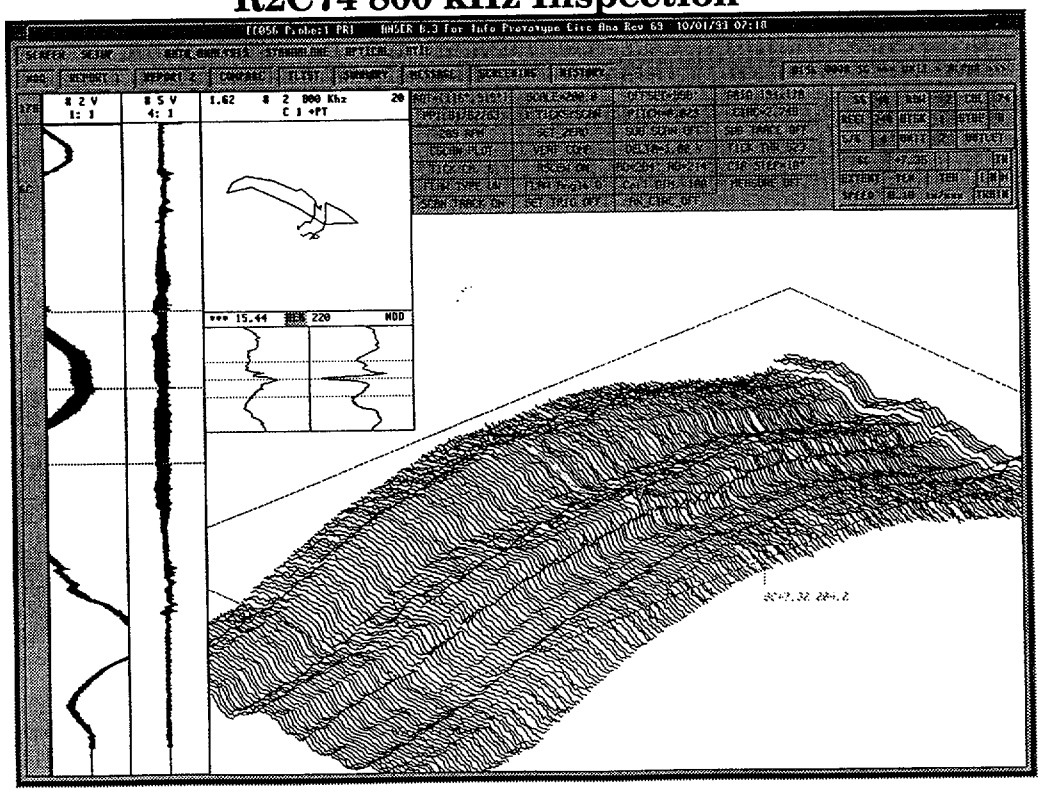

Figure 3-4. Indian Point-2: Comparison of SG 4 R2C69 400 and 800 kHz Depth Profiles

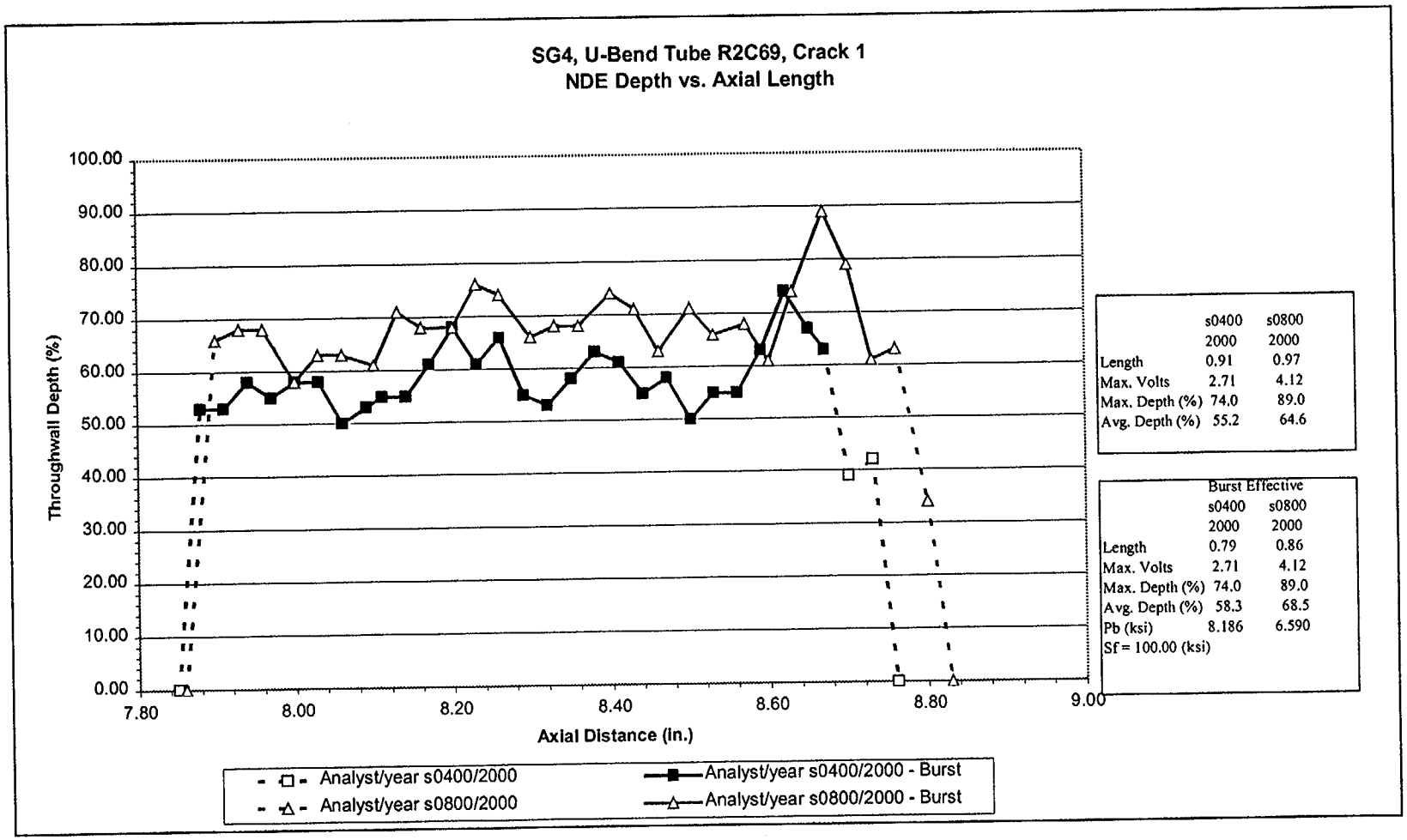

Figure 3-5. Indian Point-2: Comparison of SG 4 R2C71 400 and 800 kHz Depth Profiles

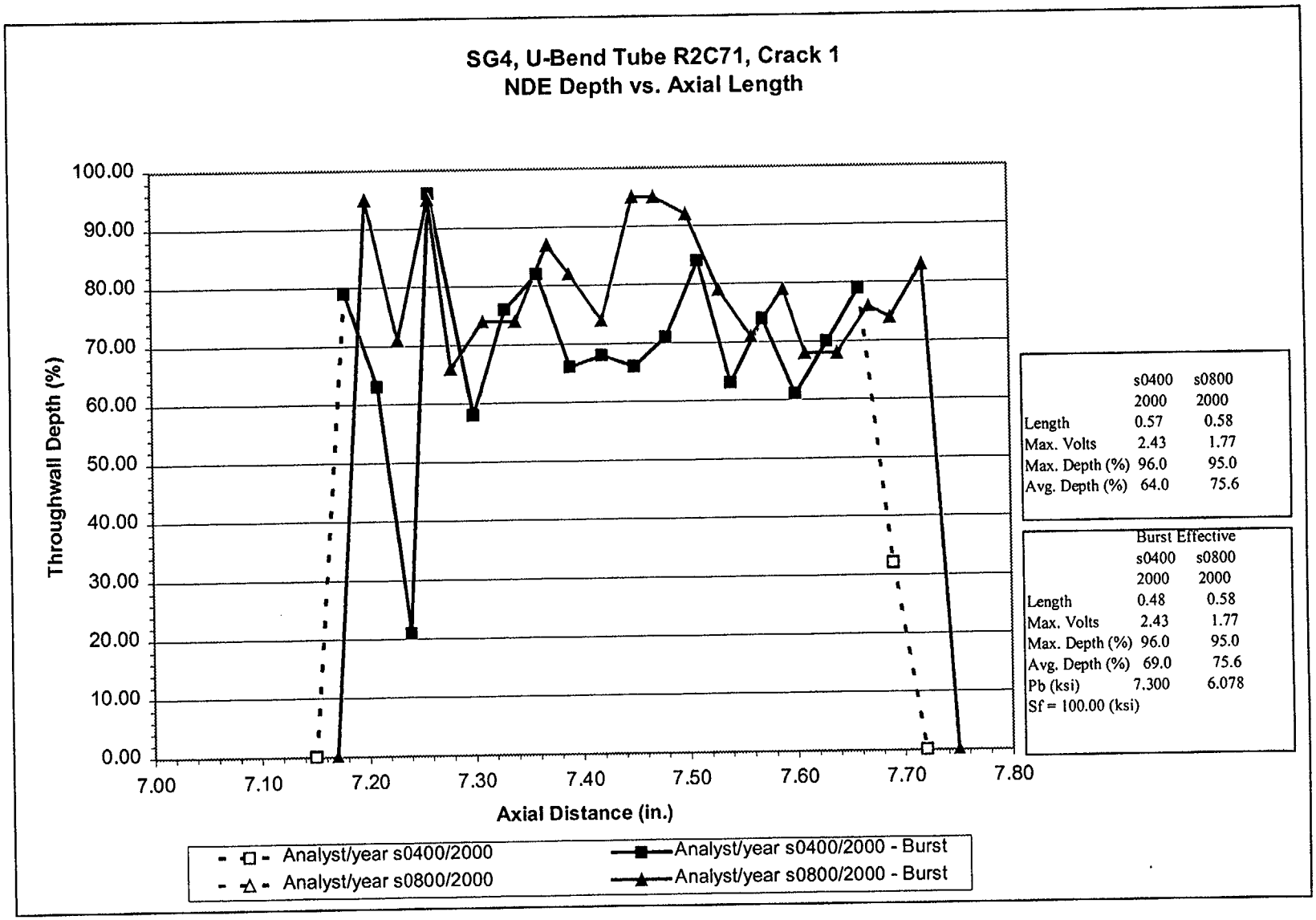

Figure 3-6.
U-Bend Row 2 Condition Monitoring Burst Acceptance Limits
PWSCC of 7/8" x 0.050" Alloy 600 MA SG Tubes at 650°F
3DPno = 4.665 ksi, 95/50 Probability/Confidence

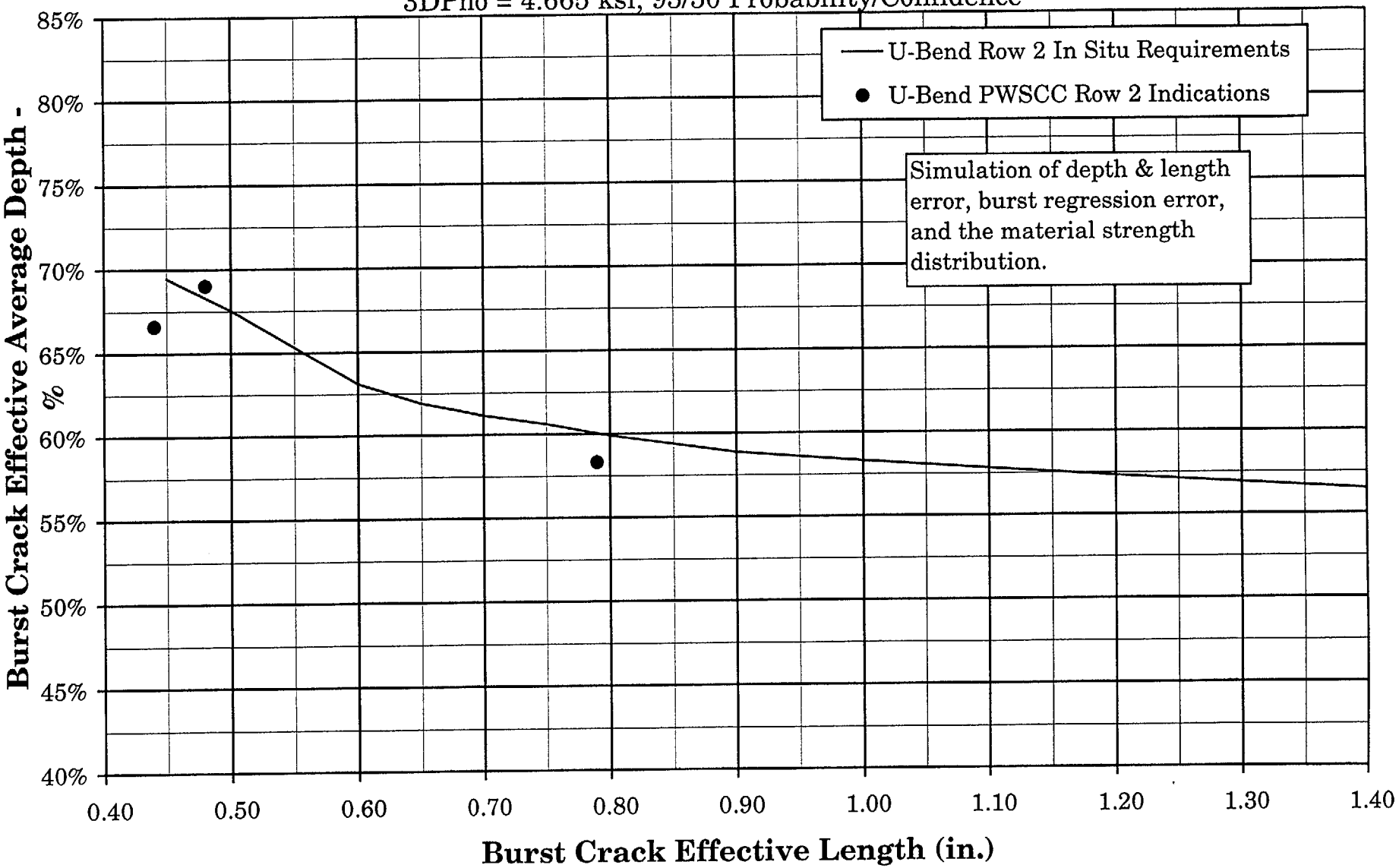

Figure 3-7
Indian Point -2 R2C71 In Situ Leak Test Data
Normalized to Tp= 590°F, Pp = 2575 psia and Ps = 15 psia - Reference SLB Conditions

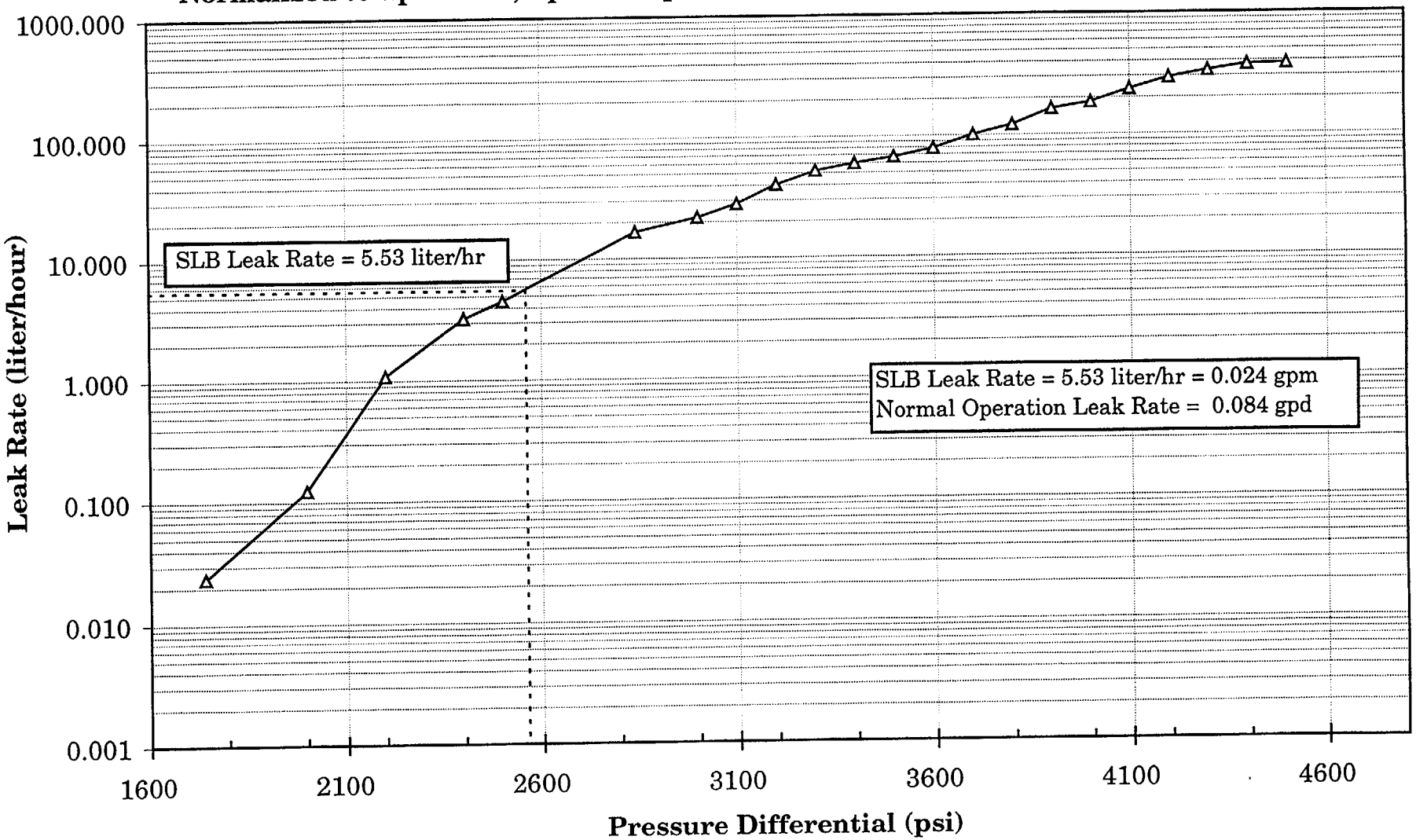

4.0 DESCRIPTION OF ANALYSIS METHODS

4.1. Axial Profile Analysis Methods

The axial profile probabilistic analysis methods are based on the use of crack depth versus length profiles obtained from + Point analyses of the axial indications. These methods are documented in Reference 10-8 for application to an ARC for axial PWSCC at dented TSP intersections. The computer code used for the analyses of this report is a modification of the Reference 10-8 code to increase the flexibility on input data compared to the original code. Although the changes to the code have been checked, final configuration control and documentation are in process at the time of this report. This methodology provides "first principle" analysis techniques in that burst and leakage are calculated from the crack profile rather than the more conventional simplifying assumptions of average depth or judgmental crack shapes. Since all +Point confirmed indications are repaired, the beginning of cycle (BOC) population is comprised of undetected indications and new indications (truly new indications and indications below the +Point coil detection threshold or smallest detected indication). The undetected population is obtained using the GL 95-05 methodology that leaves (1/POD – 1) indication in service for each detected indication, where the POD is depth dependent. Monte Carlo analyses are used to incorporate NDE uncertainties and growth for projecting the EOC indication size, burst pressures and leak rates.

The steps of the analysis process can be summarized as follows:

- BOC population for undetected indications
  - Each + Point indication is evaluated for average depth and maximum depth. PODs (developed as functions of average depth for burst and maximum depth for leak) are evaluated at the depths of the indication. For burst pressure analyses, the POD for average depth is applied and for leakage analyses, the POD for maximum depth is applied.
  - Application of (1/POD-1) to each indication leads to a fraction of an indication or more than one indication for each EOC detected indication. The undetected indications are assumed to have the same BOC crack profile as the EOC indication for which the POD is applied. Profiles with fractional indications from the POD correction are grouped from highest to lowest depth until the sum of the fractional indications totals unity to define a POD group number for burst pressure distribution calculations. In the Monte Carlo sampling for a POD group, the profiles comprising the group are sampled at the frequency of their contribution to unity for the group.
  - Separate populations of crack profiles are carried through the analysis for burst pressure and for leakage due to differences in PODs, NDE uncertainties and growth rates between average and maximum depth. This separation permits more direct application to the analysis of the parameters affecting leakage and can be expected to improve the accuracy of leakage predictions compared to applying PODs, NDE uncertainties and growth based only on average depth.
- BOC population for new indications
  - The total number of "new" indications is defined as an input to the analysis to reflect undetected indications below the detected indication threshold plus truly new

indications. Each new indication crack profile is obtained by sampling distributions of average depths, crack length and crack shape. The crack shape distributions used are examples from pulled tubes and field indications that have been selected to provide shapes varying from nearly flat profiles to profiles with one or more locally deep sections. A crack shape sample is adjusted by applying the samples for average depth and length.

- The sampling process defines BOC new indication crack profiles for each SG simulation.

- Application of NDE uncertainties
  - NDE uncertainties on average or maximum depth and crack length are applied to the BOC populations of undetected and new indications.
  - The NDE uncertainty on average depth (same process for maximum depth) is uniformly applied to each point in the crack depth profile. That is, the profile is assumed to grow in depth with the same shape as the initial profile.
  - The NDE uncertainty on crack length is applied by increasing or decreasing the spacing of profile points near both ends of freespan cracks since the length uncertainty occurs at the crack tips.
- Application of growth
  - For each indication, the cumulative probability distributions for growth in average depth and in maximum depth are sampled. The growth is then applied to each point in the crack depth profile.
  - Separate profile populations are evaluated using average depth growth for burst analyses and maximum depth growth for leakage analyses.
  - Growth in length is applied by uniformly scaling the spacing between profile points to reflect the change in length due to growth.
- Burst pressure calculations
  - The above steps lead to a projected EOC crack profile for each indication in the population. Profiles based on average depth PODs, NDE uncertainties and growth are used for the burst analyses. The crack profile is then searched for the lowest burst pressure between any two points in the profile. The predicted burst pressure is then obtained by sampling the burst correlation at the length and effective average depth for the indication.
  - The Westinghouse burst pressure correlation given in Reference 10-8 is used for the analysis of each Monte Carlo sample.
  - A burst pressure distribution is developed for each BOC indication or POD group. These distributions are searched after Monte Carlo sampling is completed to define the limiting burst pressure indication, evaluated at the required confidence level, for comparisons with the $3\Delta P_{NO}$ burst margin requirement. This process of per indication burst pressure distributions avoids more arbitrary definitions of the limiting indication for comparison with burst margin requirements.
  - The predicted burst pressure is also compared to the desired value for burst probability analyses (ΔP_{SLB}) to determine if the indication is a "burst" for inclusion in the burst probability analyses.
- Leak rate calculations
  - The above steps lead to a projected EOC crack profile for each indication in the population. Profiles based on maximum depth PODs, NDE uncertainties and growth are used for the leakage analyses. The ANL crack flow model of reference 10-18, as

described in Reference 10-8, is applied to the crack profile to determine if ligament tearing would occur to obtain a throughwall crack length for leak rate analyses. The crack profile is searched for the longest one or more ligaments that would tear to throughwall at SLB pressure differentials. The result of this analysis is one or more throughwall crack lengths for further leakage evaluation.

- Given the EOC "throughwall" length, the leak rate is calculated based on a correlation of corrosion specimen leak rates with calculated results from the Westinghouse "CRACKFLO" code. The correlation is developed for leak rates calculated for throughwall crack lengths. The CRACKFLO results adjusted to "truth" by the test to CRACKFLO regression curve represent the mean SLB leak rates and the uncertainties are obtained from the correlation of measured leak rates with the CRACKFLO results. The current analysis methods are very conservative for leakage as the leak rate correlation is based on throughwall corrosion lengths and the length used for leakage includes ligament tearing lengths that are longer than throughwall corrosion lengths.
- Leak rates are summed over all Monte Carlo sample indications in a SG population to obtain a sample of the total SG leak rate. The multiple SG samples then lead to a distribution of SG leak rates.

The ANL ligament tearing model is also applied separately from the SLB leak rate analyses in order to evaluate in situ test leakage at varying pressures. This model is used to either compute leakage at a given pressure or to compute the probability of ligament tearing or leakage as a function of pressure for comparisons with the onset of leakage from in situ tests. These analyses are used for benchmark analyses and the comparisons with in situ test results provide integral evaluations of the crack depth profiles and NDE uncertainties.

4.2. Multi-Cycle Analysis Methods

The multi-cycle analyses described in this report were performed by E-Mech Technology, Inc. Verification signatures by E-Mech personnel on the title page of this report reflect verification of the E-Mech analyses and not the complete report. The Westinghouse analyses were verified by Westinghouse personnel. E-Mech is not currently on the Westinghouse qualified suppliers list although this activity has been initiated.

The multi-cycle analysis methodology uses NDE inspection data obtained over several past outages to benchmark simulations of degraded tubing and project the evolution of this degradation through the current and upcoming operating cycles. A statistical representation of the physical properties of the flaw population is developed by repeatedly simulating the processes of flaw initiation, flaw growth, and tube inspection over several cycles. The simulated flaw geometries and tube properties are then used in conjunction with burst and leak rate equations to assess the structural integrity of the tube population at a given point in time.

The fundamental analysis parameters required as input to the multi-cycle model include the nominal tubing dimensions and flow strength distribution, the prescribed operating

and accident pressure differentials, the inspection scope and schedule, Weibull flaw initiation function, flaw growth rate distribution(s), characteristic flaw length distribution, and eddy current probe probability of detection curve(s). These parameters are derived from plant-specific operating conditions or directly measured data, where such data exists as applied in this report. The Weibull initiation function parameters are determined indirectly by assuming starting values and incrementally adjusting until the simulation output agrees reasonably with observed quantities, such as the number of detected flaws over several outages.

For each of thousands of steam generator trials, the multi-cycle model simulates an entire family of flaws assumed to be present in the tube population. The analysis tracks each of these flaws through its entire life, regardless of whether the flaw is numerically "detected" during a simulated inspection or not. Both detected and unseen flaws contribute to the integrity assessment of the tube population at a given outage simulation. Statistics accumulate for each operating cycle, over many steam generator trials. These statistics are used both to compare model output to observed data (in order to fine-tune the input parameters if necessary) and to calculate relevant tube integrity indicators, such as minimum projected burst pressure, probability of tube burst and estimated leak rate associated with an upcoming operating cycle.

The initiation of a flaw is simulated numerically by drawing a random "birth" time from a Weibull function. Again, the slope and scale parameters that define the Weibull function are determined on an iterative basis by adjusting these parameters until the model accurately predicts the actual number of flaws observed in past outages. The flaw initiation rate and the flaw detection rate are related, albeit indirectly as a function of flaw growth rate and inspection effectiveness. The use of a Weibull function in time-to-failure analyses is common.

The multi-cycle model idealizes each flaw using three parameters: average depth, maximum depth, and length. The average depth is defined as the average depth of the flaw profile, taken over the section of the profile that determines the burst pressure, which is called the burst effective length in this report. Maximum depth represents the deepest point of the flaw profile over its length. The maximum depth is assigned numerically in the multi-cycle model via a random draw from a distribution of max-to-average depth ratios. The parameters of this distribution have been determined by destructive examination of pulled tubes for several types of degradation and from the U-bend +Point analyses in this report.

At initiation, the flaw depth is defined to be zero. A random number is drawn from the growth rate distribution, allowing the flaw depth to increase over time. Growth rate distributions are often lognormal in nature, fit to measured data points. In the absence of measured data, a bounding growth rate distribution that is appropriate for the type of degradation being considered is used. Flaw growth in the length dimension may be included in a similar fashion.

An eddy current inspection is simulated at the end of each operating cycle for each flaw. A probability of detection (POD) curve must exist for each probe and/or inspection technique

relevant to the analysis. For this report, the +Point POD curve developed in Section 5 is applied for the EOC-14 inspection. The POD is a function of flaw geometry, most commonly flaw depth. In a simulated inspection, the POD for a given flaw depth is compared against a uniform random number between 0 and 1. If the random draw is less than the POD for the given flaw depth, that particular flaw is considered to be "detected." The flaw may then be removed from the simulation (for plug-on-detection schemes) or "sized" (for plug-on-sizing schemes.) To simulate flaw sizing, a random number is drawn from an assumed measurement error distribution and added to the simulated flaw depth and/or length. If the flaw is not detected, or if its apparent size is less than the appropriate plugging limit, the flaw remains in service and is present for the next operating cycle, where the growth and inspection process is repeated.

Regardless of whether a simulated flaw is detected or not, it is evaluated for structural soundness. A burst pressure is computed for every flaw using mathematical equations that are functions of the flaw average depth, length, and tube properties. If the computed burst pressure is less than the specified accident condition pressure differential, a tube burst event is recorded. Certain combinations of flaw length and depth lead to a situation where the applied pressure differential causes the flaw depth to "pop" through to 100% of the tube thickness over the entire flaw length, but the flaw length is not sufficient to cause a full tube burst. Such pop-through events (also called ligament tearing in this report) are discussed further in Section 6. Finally, a flaw with a maximum depth of 100% is considered to be leaking over some through-wall segment. The corresponding leak rate is computed using empirical leak rate equations that are a function of the mechanically derived crack opening area.

Statistics for each flaw are generated and recorded on a cycle-by-cycle basis. Many flaws are simulated for each steam generator trial, and many trials comprise a complete analysis. The results of the multi-cycle model include statistics that describe the simulated inspection results for several past operating cycles. This information is used to iteratively adjust the model input, particularly the initiation function parameters, to fully benchmark the model. The statistics generated for the current and upcoming operating cycles are then examined to assess the integrity of the tube population and provide data useful for condition monitoring and operational assessment purposes.

5.0 INPUT DATA FOR TUBE INTEGRITY ANALYSES

5.1. Indian Point-2 Operating Parameters

Indian Point-2 operates at a T-hot of 590°F based on previously lowering T-hot to reduce the potential for tube degradation. This temperature applies to Cycle 14 and is expected to be maintained for Cycle 15.

The measured steam pressure for Cycle 14 was 700 psia as corrected to a location in the SG dome. The steam pressures vary between SGs and were 702.3 for Loop 1, 701.3 for Loop 2, 699.4 for Loop 3 and 697.2 for Loop 4. The maximum pressure drop across the SG tubes occurs at the top of the tubesheet where the primary pressure including static head is about 2250 psia. The SG pressure drop from the top of the tubesheet to the dome of the SG is about 11 psi for the Indian Point-2 SGs. At the U-bend, the primary pressure drop from the tubesheet to the U-bend is larger than the decrease in the secondary side pressure. As a consequence, the use of the pressure drop across the tube at the top of the tubesheet is conservative for the U-bend and defines a ΔP_{NO} that can be applied for all SG tube degradation. The primary pressure drop from the top of the tubesheet to the top TSP is about 14 psi while the secondary side pressure drop is about 8 psi. Consequently, the pressure drop across the U-bend is about 6 psi lower than at the top of the tubesheet. Based on these considerations, a dome steam pressure of 700 psia can be conservatively applied for all SGs for tube integrity analyses. At the top of the tubesheet location, the maximum pressure drop across the tubes under normal operating conditions (ΔP_{NO}) at EOC-14 is 2250 – 711 = 1539 psi. This value is applied for the condition monitoring assessment.

For Cycle 15, the steam pressure is reduced due to plugging of additional tubes while maintaining T-hot at 590°F. Based on the increase in tube plugging of 6.1% for the EOC-14 inspection, the steam pressure would be reduced by about 17 psi. Then, ΔP_{NO} = 1556 psi for Cycle 15.

5.2. Structural and Leakage Requirements

The structural requirement for freespan indications is to satisfy a burst margin requirement of $3\Delta P_{NO}$ per the requirements of the EPRI SG integrity guidelines (Reference 10-3). For EOC-14, $3\Delta P_{NO}$ = 4617 psi at operating temperature for condition monitoring assessments. At room temperature for acceptance of in situ test pressures, the burst margin must be increased by 7% to correct for the changes in U-bend material properties (see Section 5.6), and $3\Delta P_{NO}$ = 4940 psi at room temperature. For Cycle 15 with reduced steam pressure due to tube plugging, $3\Delta P_{NO}$ = 4668 psi at operating temperature for operational assessments.

Under accident conditions, the freespan leakage limit as the sum of all leaking tubes in a SG must be less than 1 gpm/SG per the requirements of the EPRI SG integrity guidelines (Reference 10-3). The limiting accident condition is the steamline break (SLB) for which

the applicable pressure difference across the tubes is ΔP_{SLB} = 2560 psi at operating temperatures.

The above structural and leakage monitoring requirements must be satisfied at a specified probability and confidence level. Per the EPRI SG integrity guidelines, the required values are 90% probability and 50% confidence (referenced as 90/50) for both condition monitoring and operational assessments. Due to limitations on direct POD and NDE sizing data for U-bend indications, the more conservative requirements of 95/50 for condition monitoring and 95/95 for operational assessments are applied in the analyses of this report.

Since the deterministic $3\Delta P_{NO}$ burst margin requirement is applied for the condition monitoring and operational assessment analyses, no explicit requirements are necessary for burst probability at $3\Delta P_{NO}$ or ΔP_{SLB} conditions. Burst probabilities provide supplemental information on tube integrity due to their sensitivity to the entire population of indications rather than the single most limiting indication satisfying the deterministic $3\Delta P_{NO}$ burst margin. The EPRI SG integrity guidelines define satisfying a burst probability of < 0.1 for the burst of one or more tubes at $3\Delta P_{NO}$ pressure differential as equivalent to satisfying the deterministic burst margin requirement at 90/50 probability. The conditional probability of burst criterion at ΔP_{SLB} in the EPRI guidelines is $< 5x10^{-2}$ for the burst of one or more tubes. These burst probability should include known and unknown degradation mechanisms. Applying an allowance of 20% of the criterion for unknown degradation mechanisms, the burst probability guidelines become 0.08 for burst at $3\Delta P_{NO}$ and 0.04 for burst at ΔP_{SLB} at 90/50 probability when summed over all known degradation mechanisms. The $3\Delta P_{NO}$ guideline would generally be expected to be more limiting than the ΔP_{SLB} guideline for Indian Point-2. The two know freespan degradation mechanisms that could contribute significantly to a burst probability are the U-bend axial PWSCC indications and the sludge pile ODSCC axial indications.

5.3. Detection Threshold and Probability of Detection

This section addresses detection as a lower detection threshold and as a probability of detection (POD) as a function of depth. The detection threshold, as applied herein, is an estimate of the size of an indication that may represent the lower range of detection and may have been undetected and left in service. Since no destructive exam data are available to develop POD as a function of depth for the Indian Point-2 low row U-bends, a bounding POD is defined based on considerations of detection capability. Section 9 addresses a development program to determine PODs for low row U-bends.

5.3.1. Detection Threshold for High Frequency +Point

An application of a detection threshold is one element of the operational assessment, wherein an indication at the detection threshold is left in service and evaluated at the end of the planned operating cycle. This technique is one of the analysis methods applied in Section 9 for the operational assessment to demonstrate that indications below the detection threshold are acceptable for continued service. One estimate of the detection

threshold for potential indications not detected and left in service would be the magnitude of the smallest indication detected under the assumption that smaller indications were not detected. This detection threshold does not imply that all indications above the threshold are detected. Indications above the detection threshold and not detected are addressed in the tube integrity evaluations by application of a depth dependent POD in the analysis.

From the depth sizing results of Table 3-5, the smallest indications (400 kHz data for sizing) detected in terms of depth were R2C74, R2C4, R2C85 and R2C69 Crack 3 with average depths of 14.4%, 23.2%, 38.9% and 38.2%, respectively, maximum depths of 38%, 44%, 50% and 54%, respectively, and lengths less than about 0.25 inch. Due to low signal to noise ratio for R2C74, the depths of this indication appear to be underestimated based on comparisons with in situ test results. From considerations of NDE sizing uncertainty, the average depths would be expected to be more accurate than the maximum depths, which represent one point in the depth profile. The detected indications support an average depth threshold of 20% to 25% and a maximum depth threshold of <40% depth. Based on the detection of these indications in row 2 where a large number of indications would not be expected, it is reasonable to assume that the detection threshold is < 25% average depth and on the order of 40% maximum depth. Indications in this depth range and varying lengths are evaluated in Section 9 as part of the operational assessment. Indications less than this size are addressed as new indications in the tube integrity analyses based on the new indication distributions defined in Section 5.7.

5.3.2. Probability of Detection

Development of PODs as a function of depth depends upon the size of the sample population available to determine the POD (particularly shallow specimens), the type of degradation (PWSCC vs. ODSCC), the location of the degradation (U-bend, dented TSP, dented eggcrate, etc.) and the types of deposits on the tube. PODs for axial PWSCC have been developed for approximately symmetrical denting such as occurs at dented TSPs and for axially aligned denting such as occurs at flat surfaces. These PODs were developed from a combination of pulled tubes and laboratory specimens by field analysts "blind" to the destructive examination results. As shown below, these PODs differ significantly in terms of detection capability. The effects of denting on detection lead to the differences between these two types of denting. When the dents tend to approximate symmetrical conditions, the cancellation effects of the +Point probe function effectively to reduce the dent influence on the signal response. For axially aligned denting, the cracks are formed along the dent, the dents tend to be uniform axially, the +Point coil is not as effective in eliminating the dent signal, and the resulting PODs tend toward the poorer end of +Point detection capability. Without considerations of deposits including copper, detection in axial dents would be expected to be poorer than that for axial PWSCC in the U-bend. Consequently, the axial dent POD is a conservative POD for Indian Point-2 U-bend indications detected with the 800 kHz coil, which effectively reduces the effects of deposits. The evaluation of the 800 kHz data indicates that deposits such as copper are more influential on detection in the U-bend than ovality of the tubes. Currently, POD data for low row U-bend indications are not available. A development program is planned for obtaining POD data for low row U-bends as described in Section 9. For the operational

assessments of this report, a conservative POD for 800 kHz +Point detection is applied as described below.

Figures 5-1 and 5-2 show +Point average and maximum depth PODs for symmetrical dents (dashed curve to left of figure) and for axial dents (solid curve). These two curves tend to span the range of +Point detectability in the absence of deposits other than magnetite. Since the 800 kHz +Point probe effectively eliminates the effects of deposits for detection of axial PWSCC, the solid curves in the figures are expected to bound detection at Indian Point-2 for low row U-bends. The solid curves are applied as the Indian Point-2 POD for the 800 kHz inspection.

The average and maximum depth indications found in the EOC-14 inspection are shown at a POD = 1.0 in Figures 5-1 and 5-2, respectively, for the 400 kHz data and 800 kHz data where the indication was not detectable at 400 kHz (800 kHz used for R2C74 due to difficulty in sizing at 400 kHz for this indication). Comparisons of the detected indications with the POD show that most of the detected indications for both average and maximum depth are found where the POD is above about 0.5 as would generally be expected. Two average depth indications were found at about 19% and 23% average depth corresponding to a POD in the range of 0.20 to 0.35 POD. A few detected indications at this POD level would be expected. Of these small indications, the R2C4 indication with 23% average depth was a single indication in the tube while the 19% indication was a second indication in R2C71. The smallest detected maximum depth was 34% corresponding to a POD of about 0.30. These comparisons reflect the expected trend for detected indications based on the recommended POD. Overall, the detected indication depths support the consistency of the PODs with the inspection results, and adequacy of the recommended PODs for tube integrity assessments.

The POD for the 400 kHz inspection would have to reflect identification of unacceptably noisy data as discussed in Section 3.3 and Figures 5-1 and 5-2 would not be applicable to the 400 kHz inspection. For the EOC-14 inspection, criteria for defining unacceptable data for U-bend indications have been defined and indications with bad data, not eliminated by reinspection, are repaired. For the 800 kHz inspection, only a few tubes were found to have unacceptable data and required repair for this cause. At the 1997 EOC-13 inspection, criteria for defining bad data were not defined and the effective POD would not have been as good as the data of Figures 5-1 and 5-2.

EPRI ETSS 99997.1 providing Appendix H qualification data for the high frequency +Point probe in low row U-bends provides a POD of 0.91 at 90% confidence. The sample database is primarily EDM notches ranging from 27% to 100% depth. This POD is consistent with the better POD of Figure 5-2, and provides a U-bend estimate when deposits are not a strong influence on detection such as with the high frequency probe. These data indicate that the solid line POD curves of Figures 5-1 and 5-2 are very conservative estimates for the Indian Point-2 low row U-bend inspection with the 800 kHz probe.

5.3.3 Probability of Missed Row 3 Indications

The recommended POD for the high frequency probe can be used to estimate the probability of undetected row 3 indications. The probability of a single undetected indication at a given depth can be estimated as 1-POD and the probability of undetected multiple indications is the product of the 1-POD values for each indication. The probabilities of no detected indications, based on the average depth POD of Figure 5-1 for IP2 800 kHz, are given in the following table:

Postulated Number of Undetected Indications at Specified Average Depth					Prob. of No Detected Indication
40%	50%	60%	70%	80%	
2	2	1			0.005%
3	2	1			0.001%
2	1	1	1		0.001%
2	2	1	1		0.0001%
1	1	2			0.01%
3		1		1	0.0009%
2		1	1		0.01%

Indications would have to exceed 50% average depth to represent a challenge to tube integrity over the operating cycle to the next inspection. If it is assumed that an indication over 50% depth is present, it is very likely that more than one indication would be present. From the above table, it is seen that the probability of no detected indications would be very low when more than one indication >40% average depth is present. These results demonstrate a low likelihood for indications of significant depth being present in row 3 and not be detected.

5.4. U-Bend PWSCC Growth Rates

This section develops the U-bend PWSCC growth rates to be used for the Indian Point-2 operational assessment. Since the number of growth data points for Indian Point-2 is limited to 9 data points as described in Section 5.4.1, comparisons with other PWSCC growth rates are used to support the Indian Point-2 data as described in Section 5.4.2. The growth rates are developed for row 2 and very conservatively applied to row 3 U-bends. Row 3 U-bend growth rates can be expected to be smaller than row 2 due to the lower residual stresses from bending in row 3 and due to reduced effects from displacement of the tube legs at the top TSP due to hourglassing of the TSP. All row 2 tubes have been plugged and no row 3 indications have been identified in Indian Point nor reported in any other Westinghouse SG (see Section 7). The time to crack initiation is longer in row 3 together with the expected reduced growth rates.

5.4.1. Indian Point-2 U-Bend PWSCC Growth Rates

Growth rate data are obtained for the indications found in the leaker outage inspection, which is also the EOC-14 inspection. The 400 kHz data are used to develop the growth rates since only 400 kHz data are available from the 1997 section, and the 800 kHz data

result in significantly greater depth sizing than the 400 kHz data as seen in the Table 3-5 data. The 800 kHz data average about 19% greater average crack depths than the 400 kHz data. Use of the year 2000 800 kHz data together with the only available 400 kHz data from the 1997 inspection would lead to inconsistent and artificially high growth rates by more than a factor of two on the average depth growth. Of the 7 tubes with indications (Table 3-5, not including the R2C5 leaker), a total of 14 indications could be detected and sized with the 800 kHz data, and 11 indications were sized at 400 kHz including 3 indications sized at 400 kHz from the high frequency probe data. Of the 11 indications sized at 400 kHz at EOC-14, 8 of the indications could be sized in the 1997 midrange data given the knowledge of the flaw from the EOC-14 data. A probable precursor signal could be seen for the other 3 flaws (R2C85, R2C4 and R2C74) in the 1997 data, but the indications could not be sized to obtain growth rates. These three flaws are shallow in 2000 and the inability to size the indications for 1997 would not increase the large growth rates in the growth distribution. Inclusion of smaller flaws to increase the number of growth points would reduce the large growth tail of the distribution as the cumulative probability of the largest indication would increase based on the median rank ordering of the growth data given below.

The Indian Point-2 U-bend PWSCC growth rate data are given in Table 5-1. In addition to the 8 flaws found in the inspection, estimates of the R2C5 depths at the time of leakage are made to include this indication in the growth distribution. R2C5 is not sizeable in 2000 by NDE after the crack opening resulting in leakage. Ligament tearing of the part-throughwall R2C5 crack resulted in the leakage event. There are no indications that the crack burst to result in crack extension with fishmouthing of the crack opening by post leak eddy current or by visual examination. The visual exam from the ID shows crack face separation with tearing of ligaments between shorter crack segments to form the overall throughwall length estimated at about 2.2 to 2.4 inch. In addition to throughwall ligaments between crack segments, the remaining wall thickness ligament would have torn to cause the sudden leakage increase. Leakage prior to the event was a few gpd, which if assumed to be due to R2C5, would indicate a very short throughwall length. With ligament tearing as the expected cause for opening the R2C5 crack, the average depth to tear the ligaments of a 2.2 to 2.4 inch flaw would be about 90% at normal operating conditions (ΔP_{NO} = 1539 psi). As discussed in Section 3.4, the sizing of R2C5 in 1997 is defined as a range between two sizing analyses. The average depth growth rate for R2C5 applies the burst effective average depth of either 80.2% or 73.6% in 1997 since the burst effective length would approximate the throughwall length following ligament tearing to cause the leaker. As described in the condition monitoring assessment of Section 8.1, the deeper profile for R2C5 is more consistent with the predictions for the leakage event. Applying the 90% average depth at the time of the leakage event with the 80.2% or 73.6% average depth in 1997 leads to growth rates of 6.6%/EFPY or 11.1%/EFPY. Since the 11.1%/EFPY value results in the largest growth value for the Indian Point-2 indications, this value is assigned to R2C5 in Table 5-1. The maximum depth in 2000 is assumed to be throughwall since the local depth may have been close to throughwall.

The nine growth rate data points for the Indian Point-2 U-bends define the database for the growth rate evaluation. Burst effective average depths are used to define the growth rates as this practice reduces the sensitivity of the growth data to shallow tails of the

cracks which would have more sizing uncertainty than depths over the deeper part of the crack. As shown in Table 5-1, the average and maximum values for average depth growth are very similar for growth values developed for the burst effective length and the total crack length data. From Table 5-1, there is little difference between the growth data for average and maximum depth except that the largest growth value occurs for maximum depth. The largest maximum depth value occurs for the smaller Crack 2 in R2C69. This maximum depth value does not appear to be reliable, as the crack would have a maximum to average depth ratio of about 1.66 compared to the average and expected value of about 1.3 (Section 5.8). Also the average of 2.39% for the maximum depth values is less than the 3.09% for average depth. Maximum depths are more difficult to size accurately than average depths, and a more accurate estimate of the maximum depth growth distribution can be obtained by multiplying the average depth distribution by the maximum to average depth ratio of 1.30 from Section 5.8. Maximum to average depth ratios in the range of about 1.2 to 1.3 are found in successive outages for axial crack indications, which supports the use of a constant factor between average and maximum depth growth distributions unless sizing accuracy is well established. The 1.30 factor, as developed for the Indian Point-2 U-bend data in Section 5-8, is applied to the average depth growth distribution developed in this section.

The small number (9) of growth indications cannot be used directly to define a cumulative probability growth distribution since the cumulative distribution must be statistically adjusted for the small population. Bernard's median ranking of Reference 10-15 is applied to correct for the small population. The median ranking to define points of the cumulative probability distribution is defined by:

$$P = (i - 0.3)/(N + 0.4) \times 100\%$$

where i is the order ranking of the value and N is the sample size. After applying the median ranking, the Indian Point-2 average depth growth data are shown in Figure 5-3. Growth data can be generally fit by a log normal distribution. The negative growth values do not permit a direct fit to the data and the data must be corrected for NDE uncertainties. Monte Carlo analyses are performed to determine a growth distribution corrected for NDE uncertainties, which is sometimes called the 'true' growth distribution. The analyses are performed to obtain a log normal corrected distribution that has the same average growth rate when summed with the average NDE uncertainty as the growth measurements. To bias the corrected distribution toward the larger end of the measurements, a negative average NDE error is assumed in the analysis to maintain consistency with the measured average growth rate. The standard deviation for the NDE uncertainties and corrected distribution is permitted to exceed that of the measurements to support the bias of the corrected distribution. An acceptable corrected growth distribution is obtained when application of the NDE uncertainties to the corrected growth distribution yields agreement with the measured growth rates. The results of the analysis to obtain the corrected average growth distribution are shown in Figure 5-3.

As noted, the growth rate for maximum depth is obtained by multiplying the average depth distribution by a factor of 1.28. The Indian Point-2 growth in length was evaluated in the same manner as for average depth and the resulting distribution is shown in Figure

5-4. The Indian Point-2 growth distributions are compared to other data for axial PWSCC growth rates in the following section. As developed, the log normal distributions define conservative row 2 growth rate distributions, which are then applied as an even more conservative growth distribution for row 3 in the operational assessments. To address potential uncertainties in the growth distribution, the operational assessments of this report include sensitivity to increasing the growth rates by a factor of 1.25.

5.4.2. Comparisons with Other PWSCC Growth Rates

An accurate set of growth rate measurements for axial PWSCC depths were obtained as part of the dented TSP program documented in Reference 10-8. These growth data were obtained by applying sizing techniques demonstrated to correlate well with destructive exam data. The growth data from this program were adjusted to 590°F by applying the Arrhenius equation with an activation energy of 32.5 kcal/mole based on an average of Westinghouse and French data. This activation energy is consistent with the 32 kcal/mole obtained in Reference 10-9.

Figures 5-5 to 5-7 compare the Indian Point-2 growth distributions for average depth, maximum depth and length growth with the data obtained for dented TSP intersections. It is seen that the conservatively developed U-bend growth exceeds that found for dented TSP intersections for depth and length growth. In part, this difference may be due to the small population of growth values for the U-bend data. A larger population of small growth values would shift the probability distribution for the U-bends to the left and into closer agreement with the dented TSP data.

The growth distributions are applied for the Indian Point operational assessment given in Section 9. The operational assessments include sensitivity analyses for the bounding growth conservatively increased by a factor of 1.25. For average depth, the median growth rate (percent throughwall - % TW) is about 3.45% TW/EFPY and the 95th percentile is about 12.9% TW/EFPY. For maximum depth with a 1.30 factor on the average depth growth distribution, the corresponding values are about 4.48% TW/EFPY for the median 16.7% TW/EFPY at the 95th percentile.

A best estimate of the true growth rate for the Indian Point-2 U-bend PWSCC can be obtained by eliminating the bias toward large growth rates applied in Figure 5-3. In this case, the mean NDE error is assumed to be zero for the growth rates, which would generally be expected when the sizing for both years is performed with the same technique and analyst as applied for the Indian Point-2 data. In this case, the log normal growth distribution has the same average growth rate as the measured data. Figure 5-8 shows the resulting average depth growth distribution and the comparison of the predicted and actual measurements. The negative growth values for the measurements indicate that no adjustments have been made for NDE measurement errors. Each growth data point has two associated depth measurement errors, one for the EOC depth measurement and the other for the lookback depth measurement. At one extreme, negative apparent growth rates are obtained and, at the other extreme, very large apparent growth rates are obtained. Statistical techniques, such as Monte Carlo analyses applied here and above, account for sizing errors and develop a best estimate of the true crack growth rate

distribution. This process eliminates negative growth rates and reduces the frequency of very high growth rates. The solid line curve of Figure 5-8 shows the estimated true crack growth distribution for the measured Indian Point-2 growth data also shown in the figure. The true crack growth distribution, representing the measured data adjusted for NDE measurement errors, is shifted to the left of the measurements in Figure 5-8 and reduces the measured growth rates. The true crack growth distribution could be used in the operational assessment. However, to assure conservatism in the analyses, the biased average depth distribution of Figure 5-3, as also shown in Figure 5-8, is applied for the Indian Point tube integrity analyses. It is seen that the biased distribution is essentially the as measured distribution without NDE error corrections, and includes much larger growth rates than the best estimate distribution.

The growth rates of Figures 5-3 to 5-7 are developed from the Indian Point-2 data for row 2 U-bends. All row 2 U-bends are being plugged prior to the return to power for Cycle 15. As discussed in Section 7, both the initiation rates and growth rates for row 3 U-bends would be expected to be smaller than for row 2 U-bends. This reduced sensitivity to PWSCC is due to the lower residual stresses (larger bending radius, different bending process) and the reduced sensitivity to bending of the straight legs due to hourglassing of the TSPs.

Potential changes in primary chemistry were reviewed to assess the potential impact on PWSCC initiation and growth. The Indian Point-2 plan for RCS pH and lithium concentration control for Cycle 15 shows that in order to maintain a minimum pH_t=6.9, lithium will exceed 3.5 ppm for several days at the beginning of Cycle15. In Reference 10-20, a statistical analysis using multivariable modeling of the available PWSCC test data, it was stated that as lithium increases from 0.7 to 3.5 ppm resistance to PWSCC decreased by 10 to 35%, but the effect was only significant for long-term operation above 3.5 ppm Li. Also, from Reference 10-17, a review of available crack growth rate data with compact tension specimens show that for concentrations over the range of 0.73 to 3.2 ppm lithium, increasing lithium does not increase crack growth rates. Many plants have gone to 18-month fuel cycle operation with lithium concentrations above 3.5 ppm for much longer periods without any reported increase in PWSCC. It is concluded that the proposed Cycle 15 primary chemistry plan, because of the very limited exposure period above 3.5 ppm Li, is not considered to present a significant risk for an increase in PWSCC initiation or propagation.

5.5. +Point NDE Sizing Uncertainties

The +Point sizing techniques used in this evaluation are based on the methods applied for axial PWSCC at dented TSP intersections in Reference 10-8. These techniques are based on sizing indications at 300 or 400 kHz. The reference sizing applied for the U-bend indications is at 400 kHz with supplemental evaluations at 800 kHz. As shown in Section 3, the 800 kHz sizing analyses consistently yield higher depths than obtained at 400 kHz and can be expected to overestimate the crack depths based on the good correlations with destructive exam data found at 400 kHz in Reference 10-8.

Since the sizing techniques are based on surface riding coils and ovality does not appear to be a strong liftoff influence on rows 2 and 3 U-bends, the sizing accuracy for the U-bend indications would be expected to be similar between the dented TSP intersections and the U-bends. However, without direct U-bend sizing accuracy data and to account for potential differences in the influences of deposits on the tubes, the NDE uncertainties of Reference 10-8 are applied with the standard deviation increased by 25%.

As discussed in Section 9, a development program is planned to refine the U-bend data for POD and NDE sizing uncertainties. This program will include sizing uncertainties for both the 400 and 800 kHz data and will likely reduce the sizing uncertainties relative to the 25% increase in the Reference 10-8 data.

5.6. Low Row U-bend Flow Stress

The material flow stress for the U-bends is required for burst pressure and leak rate analyses. Due to strain hardening during bending to fabricate the U-bends, the yield and resulting flow stress (average of yield and ultimate strengths) for the tubing are increased relative to the straight length tubing. Row 2 flow stress values are required to support the condition monitoring evaluation since all detected indications are in row 2, and row 3 flow stress values are required for the operational assessment. This section develops the effective flow strength at the extrados of rows 2 and 3 U-bends in Westinghouse Model 44 SGs.

Introduction

An evaluation was performed to estimate the effective flow stress to be used in performing tube integrity calculations for row 3 U-bends in Westinghouse Model 44 SGs. The tubes are nominally 7/8" in diameter by 0.050" thick and were fabricated from Alloy 600 mill annealed material. The minimum radius of the U-bends in the SGs is 2.19" for row 1 and increases progressively by 1.234", the pitch dimension, for each row thereafter. The U-bend radius of row 3 tubes is then expected to be 4.66". The burst strength of the U-bend region of the tubes is expected to increase because of the strain hardening of the material during the forming process and because of geometry effects which may effectively increase the stiffness of local regions of the tube. For example, the resistance to burst on the intrados of the bend would be expected to increase because the axially adjacent material would resist deformation necessary for burst to occur. Burst testing of bent tubes with simulated axial throughwall cracks has demonstrated that there is an appreciable increase in the resistance to burst relative to similar degradation in the straight length portion of the tube. Consideration of the configuration of the bent tube leads to the speculation that there would be no appreciable geometry effect on extrados cracks, but that there could be an appreciable geometry effect on the strength when the cracks were located on the intrados or flanks of the bend. This has been confirmed by tests which demonstrated an increase in burst resistance of about 12% for axially oriented cracks located on the flanks or intrados of row 1 U-bends relative to cracks located on the extrados.

Background

In 1996, data obtained from a series of burst tests of 3/4" nominal diameter tubes performed in 1986 was analyzed, Reference 10-10. The conclusions drawn from the analysis of the data were that:

1) a minimum flow stress value of 100 ksi could be considered to be appropriate for the analysis of tubes with axially oriented linear degradation aligned along the flank or intrados of a row 1 tube U-bend, and
2) a minimum flow stress value of 90 ksi could be considered to be appropriate for the analysis of tubes with axial degradation aligned along the extrados of the U-bend.

The actual tests were performed on Alloy 690 tubes with 100% throughwall slots of various lengths machined in the tubes, Reference 10-11. The factors developed from the analysis of the results were based on test results from specimens typical of row 1 tubes, hence the maximum amount of thinning during the forming process was accounted for and extrapolation to larger row tubes would be expected to be conservative. For simulated degradation machined on the flanks or intrados of the U-bend tube specimens the measured burst pressures were 1.32, 1.33 and 1.40 times those for straight length specimens. For simulated degradation on the extrados of the U-bend specimens the measured burst pressures were 1.18, 1.21, 1.24 and 1.25 times their straight length counterparts. (Larger factors were reported for tests performed using 7/8" diameter tubes, Reference 10-12.) The flow strength of the tubing used for the tests was 77.4 ksi. Assuming a minimum flow stress of 100 ksi for the intrados or flank regions of the U-bends would lead to a strengthening factor of 1.29, which was noted to be less than the minimum value of 1.32 from the test data. Assuming a minimum value of the flow stress of 90 ksi likewise leads to an expected strengthening factor in the extrados region of the U-bend of 1.16, which was noted to be less than the minimum value of 1.18 from the test data.

Because of the significant amount of cold work performed in forming the row 1 U-bends, about 19% total axial engineering strain, it was postulated that the effective flow stress values derived from the test data would be invariant relative to the initial flow strength of the tube. This simply means that had the flow strength of the tubing been measured to be say 65 ksi, the effective flow strengths in the respective U-bend regions would have still been 100 and 90 ksi. This is based upon the large amount of cold work resulting in an elevation of the yield strength to the range of 80 ksi and above. Subsequent evaluations indicated that row 2 U-bends, where the strain-hardening is on the order of 12%, could be considered to be typified by a flow stress on the order of 85 ksi as a minimum. This result should be suspected of being an underestimate because significant strengthening occurs with the first few percent of cold work. This is illustrated on Figure 5-9, which is a representative stress-strain curve for Alloy 600 tube material at 600°F. There was no further work aimed at estimating the effect of the forming process on the strength of row 3 U-bend tube sections. The total strain in these bends is on the order of 9%.

Evaluation of Row 3 U-Bends

In order to utilize the prior results to estimate the effect at row 3, an alternative explanation of the test data was postulated based on the proposition that the work-hardening and the geometry combine to proportionally increase the strength of the U-bend region of the tube. The basis would be that the strength increase is proportional to the total strain in the U-bend from the bending process in addition to the strengthening effects of constraints associated with the geometry of the bend. The effect of geometry is manifest on the flanks and intrados because the flanks of a throughwall crack would be restrained in compression from bulging outward from the tube centerline. This is not the case on the extrados and only the work hardening would be expected to effect the demonstrated flow strength. Thus, the strengthening factor would be directly related to the total strain on the extrados.

An additional feature of the model postulated here is that the effective flow stress, S_f, of the material remains a constant fraction of the sum of the yield stress, S_y, and ultimate tensile strength, S_u, of the material regardless of the increase of the yield stress due to strain-hardening during the forming process. This is believed to be due to the anisotropy introduced by the forming process in that the strain hardening is in the axial direction while the strains associated with burst are in the hoop direction (the same is true of the plastic strains introduced by the tube straightening operation). Tests performed on non-degraded tubes have demonstrated that that fraction is about 0.6, however, the actual magnitude does not influence the outcome of predictions using the postulated model. Furthermore, it is assumed that the geometry of the U-bend does not increase the effective flow strength of the material on the extrados of the tube. Calculations of the effect of the forming process on the flow strength are then made based on the modeling the behavior of the material as being elastic to the yield point, followed by linear hardening. The assumption of linear hardening is illustrated by the dashed line on Figure 5-9, and is quite conservative relative to the actual hardening that takes place. Finally, the elastic strain is assumed to be negligible compared with the total strain to failure. This is also apparent from the stress-strain data on Figure 5-9. Using the linear model, the flow strength of low row U-bends may be simply calculated as a linear interpolation between the strain-hardened yield strength and the ultimate tensile strength using the ratio of the total axial strain of formation relative to the ultimate strain, estimated as the total elongation from a tensile test. This is illustrated as the dash-dot-dot line on Figure 5-9 (associated with the secondary ordinate axis). If the ratio of the yield stress to the ultimate tensile stress is taken as ξ, the increase in the flow strength due to the forming process is given by,

$$\frac{\Delta S_f}{S_f} = \frac{1-\xi}{1+\xi}\frac{\varepsilon_T}{\varepsilon_U},$$

where ε_T is the total axial strain and ε_U is the ultimate tensile strain. The calculated change in flow strength obtained from the actual yield strength is illustrated as the dash-dot line on Figure 5-9. It is noted that the linear approximation results in estimates

which are significantly less than those that are calculated from the actual yield strength (the difference between the dash-dot and the dash-dot-dot curves on Figure 5-9). A typical elongation for Westinghouse tubing is about 35%, and the yield stress is about 55% of the ultimate strength at room temperature and about 47% at operating temperature for tubes used in the fabrication of Westinghouse Model 44 and 51 SGs. The increase in the effective flow strength would be expected to be about 16% for row 1 tubes with a total axial strain of about 19%. This compares favorably with the aforementioned test result values of 18 to 25%. The increase in strength for row 2 tubes with a total axial strain on the order of 12% would be expected to be about 10%. This is the same as a historically recommended value to use 85 ksi for row 2 U-bends in tubes with a reported flow strength of 77.4 ksi. Finally, the expected increase in flow strength along the extrados in row 3 U-bends would be expected to be about 7.5% at ambient conditions and about 9% at operating conditions. This latter observation is in concert with additional information indicating that the reduction of flow stress with temperature is less for strain-hardened material than for non-strain-hardened material, Reference 10-13. The flow stress reduction with temperature can be obtained from cold rolled Alloy 600 tests for which the temperature reduction factor (70°F to 600°F) was found to be 7% (Reference 10-14). For some larger rows it may be expected that the strengthening effect of the U-bend is negligible. The predicted effects would be less than 4% for tubes in rows greater than 6 using the postulated model.

Discussion of the Effect of Strain-Hardening

The main postulate of the alternate model is that prior work hardening affects the flow stress as related to predictions of the structural integrity of the tube material. The effect is observable because one of the standard techniques for obtaining high strength tubing for test programs is to strain-harden the material using a straightening machine. In general, the burst process itself involves significant straining of the tube material, therefore, if strain-hardening results in an elevation of the flow stress, deformations associated with the burst process would be expected to increase the flow stress and the burst resistance of the tube section being tested. This means that prior strain hardening would not be expected to increase the flow stress beyond that which could be realized during the burst test itself. However, it does appear that prior strain-hardening does influence the subsequent rupture behavior of the material.

When a non-degraded tube is tested, the diameter increases and the material strain-hardens in response to the expansion of the diameter. Tubes are capped for the tests so the axial plastic strain is zero and the thickness plastic strain is simply the negative of the hoop plastic strain. Two things are happening, the diameter is getting bigger and the thickness is getting smaller. The engineering hoop stress is increasing only because of the diameter increase, and the true hoop stress is increasing due to both effects. Burst of the tube occurs due to excessive straining of the material in the hoop direction, but these strains are resisted if the material is not free to plastically deform in the axial direction. For a tube which has a reduced burst resistance due to the presence of a crack, the diameter may not increase, but the material at the ends of the crack plastically deforms until some critical value of the strain is reached. The burst behavior is usually predicted by considering a bulging factor to magnify the stress intensity at the crack tip or tips. The

governing strain for axial bursting is in the hoop direction. Strain-hardening in the axial direction increases the pressure required to develop the same magnitude of bulging factor that would be associated with a tube without strain-hardening. The increase in strength that could be expected from axial strain-hardening would be expected to be limited, however, the limit does not appear to have been reached by the strains associated with the formation of row 1 U-bends. The conclusion of this discussion is that it is reasonable to expect that cold-work or strain-hardening in the axial direction would increase the burst resistance of the tube relative to axial cracks and that such increase might be predicted from knowledge of the total strains introduced during the forming process.

Conclusions

Strain-hardening of tubes in the axial direction can be expected to result in an increased resistance to burst characterized by separation of the material in the hoop direction. It can also be expected that the degree of strengthening is correlated to the total strain applied in the axial direction. Comparisons with test results indicate that consideration of a one-to-one correlation is conservative for row 1 U-bends. Consideration of historical analysis practice and the evaluation performed indicates that considering the correlation to be linear is conservative. Finally, use of that correlation indicates that the flow strength used for estimating the strength of row 3 tubes with indications aligned along the extrados of the bend is about 7.5% at ambient conditions and about 9% at operating conditions greater than the value that would be used for calculations on the straight section of the tube. As discussed above, the reduction in flow stress from cold to hot conditions for strain hardened tubing is about 7% compared to almost 9% for straight leg tubing. The difference between the 7.5% and 9% flow strength increases is incorporated in the 7% cold to hot flow stress reduction factor. The level of conservatism associated with this evaluation is likely sufficient to assume that the linearly estimated values are invariant relative to the starting characteristics of the heat of material used to fabricate the tubes.

Based on the above, room temperature flow stress values of 85 ksi for row 2 and 81 ksi for row 3 are used in the tube integrity analyses of this report. These values are lower bound values such that variations in flow stress are not required, and a reduction of 7% is applied for operating temperatures.

5.7. New Indication Shape and Depth Distributions

The Monte Carlo analyses for the operational assessment include allowances for new indications below the detection threshold and newly initiated indications. The new indication crack profiles are obtained by sampling crack shape profiles, an average depth distribution and a length distribution. In the Monte Carlo sampling process, a sample for the shape is adjusted to the sample average depth obtained from the depth distribution and a sample length obtained from the length distribution. This section identifies the shape profiles and average depth distribution while the length distribution is developed in Section 5.8.

The shape profiles are obtained from the shapes found by NDE sizing of the Indian Point-2 U-bend indications. The shapes are selected to provide variations ranging from a nearly uniform profile to profiles with a locally deep length. The profiles selected to represent the new indication shapes and the basis for selecting the shape are:

- R2C69 crack 1, year 2000, 400 kHz: flat profile with a locally deep location
- R2C71 crack 1, year 2000, 800 kHz: irregular profile with two locally deep locations
- R2C72 crack 1, year 2000, 800 kHz: irregular shaped profile with varying depths
- R2C87 crack 3, year 2000, 400 kHz: uniform depth profile
- R2C69 crack 3, year 1997, 400 kHz: u-shaped profile with maximum depth at center of crack

Depth profiles for these indications are given in Appendix C.

In the analysis process, undetected indications are accounted for by the POD adjustment to detected indications wherein (1/POD-1) indications (applied with depth dependent indications and POD) are assumed to be undetected and left in service. This method accounts for undetected indications as small as the shallowest reported depth indication. The average depth distribution for the new indications addresses indications at depths less than found in the inspection. From Table 3-5, the smallest average depths, based on the 400 kHz data, were 14 and 23%. The new indication depth distribution is conservatively set to have a maximum depth of 25% to overlap the detected indications. The lower depth is set at 10% since shallower depths would have no influence on tube integrity considerations. A triangular distribution is assumed which results in a s-shaped distribution as shown in Figure 5-10. Leakage analyses are based on maximum depth POD, NDE uncertainties and growth. In this case, the new indication distribution is also based on adjusting the depth shapes to maximum depth. For the leakage analysis new indications, the average depth distribution of Figure 5-10 is increased by the maximum to average depth ratio of 1.28 developed below such that the upper end of the distribution is at 32% maximum depth.

5.8. Maximum to Average Depth Ratio

Pulled tube and NDE crack depth profiles have been shown to consistently result in maximum to average depth ratios of about 1.22 to 1.28. The average depth for this correlation must be the burst effective average depth to eliminate insignificant tails of the cracks, which can significantly change the total crack length average depth. Evaluation of this ratio for the Indian Point-2 data provides a general check on the consistency of the sizing analyses. This ratio is used in the analyses of this report to define maximum depth growth rates and new indication distributions, which have been evaluated for average depth data.

The maximum depth to burst effective average depth data for the Indian Point-2 U-bend profiles is shown in Figure 5-11. The ratio is in excellent agreement between the 800 and 400 kHz data with a ratio of 1.29 for 400 kHz and 1.30 for 800 kHz. These ratios are

slightly higher than the more common range of about 1.22 to 1.28, which could indicate some overestimation of maximum depths.

The maximum/average depth ratios for the 400 kHz R2C69 crack 2 and R2C74 are high compared to the remaining data, which could indicate that the maximum depths are overestimated for these indications.

5.9. Crack Length Distributions

The crack length distribution is applied in the operational assessment Monte Carlo analyses to sample a crack length for new indications. This distribution is developed in this section from the Indian Point-2 data. More indications were found with the 800 kHz data and length differences from the 400 kHz analyses are negligible. Therefore, the 800 kHz data are used to develop a log normal fit to the measured lengths to define the length distribution. Figure 5-12 shows the crack length measurements and the log normal distribution selected to represent the data. The selected distribution is biased toward longer lengths than found for the Indian Point data, which increases conservatism in the new indication lengths for the operational assessment.

Table 5-1. Indian Point-2 U-Bend Axial PWSCC Growth Rates (400 kHz Data)

			+Point - 2000 inspection Midrange Coil						+Point - 1997 Inspection Midrange Coil						Growth per EFPY 2000-1997 = 1.48 EFPY					
SG	Tube	Crack No.	Max. Volts	Max. Depth	Avg. Depth	Length	Burst Avg. Depth	Burst Length	Max. Volts	Max. Depth	Avg. Depth	Length	Burst Avg. Depth	Burst Length	Max. Volts	Max. Depth	Avg. Depth	Length	Burst Avg. Depth	Burst Length
	R2C5 Note 1	1		100			90		2.24	92	63.0	2.43	73.6	1.22		8.00	11.1		11.1	
									2.31	92	70.6	2.43	80.2	1.87						
4	R2C69	1	2.71	74	55.2	0.91	58.3	0.79	1.33	84	57.0	0.9	62.8	0.7	0.93	-6.76	-1.22	0.01	-3.04	0.06
			1.03	74	44.5	0.11	44.5	0.11	0.54	50	31.5	0.25	39.0	0.16	0.33	16.22	8.78	-0.09	3.72	-0.03
			0.94	54	38.2	0.23	42.0	0.20	0.61	50	33.8	0.16	37.7	0.13	0.22	2.70	2.97	0.05	2.91	0.05
4	R2C72	11	3.17	82	59.8	0.54	66.6	0.44	1.3	79	61.8	0.39	66.4	0.35	1.26	2.03	-1.35	0.10	0.14	0.06
4	R2C71	1	2.43	96	64.0	0.57	69.0	0.48	1.87	87	57.5	0.68	63.1	0.57	0.38	6.08	4.39	-0.07	3.99	-0.06
1	R2C87	1	1.68	55	42.8	0.30	48.0	0.25	1.05	63	40.8	0.15	40.8	0.15	0.43	-5.41	1.35	0.10	4.86	0.07
		1	2.25	61	43.6	0.29	48.0	0.25	0.76	53	36.4	0.19	40.8	0.16	1.01	5.41	4.86	0.07	4.86	0.06
		1	2.28	53	41.6	0.35	44.3	0.31	0.95	63	36.5	0.27	45.2	0.19	0.90	-6.76	3.45	0.05	-0.61	0.08
														Avg.	0.68	2.39	3.80	0.03	3.09	0.04
														Max.	1.26	16.22	11.1	0.10	11.1	0.08

Note 1. R2C5 not sizeable in 2000 by NDE after crack opening resulting in leakage. Maximum depth in 2000 is assumed to be throughwall. For ligament tearing, which is the expected cause for opening the R2C5 crack, the average depth to tear the ligament of a 2.2 to 2.4 inch flaw would be about 90%. The 90% depth value is applied with the smaller burst effective depth estimate for R2C5 in 1997 to assign a conservative growth value to R2C5.

Figure 5-1. Comparisons of +Point Average Depth PODs

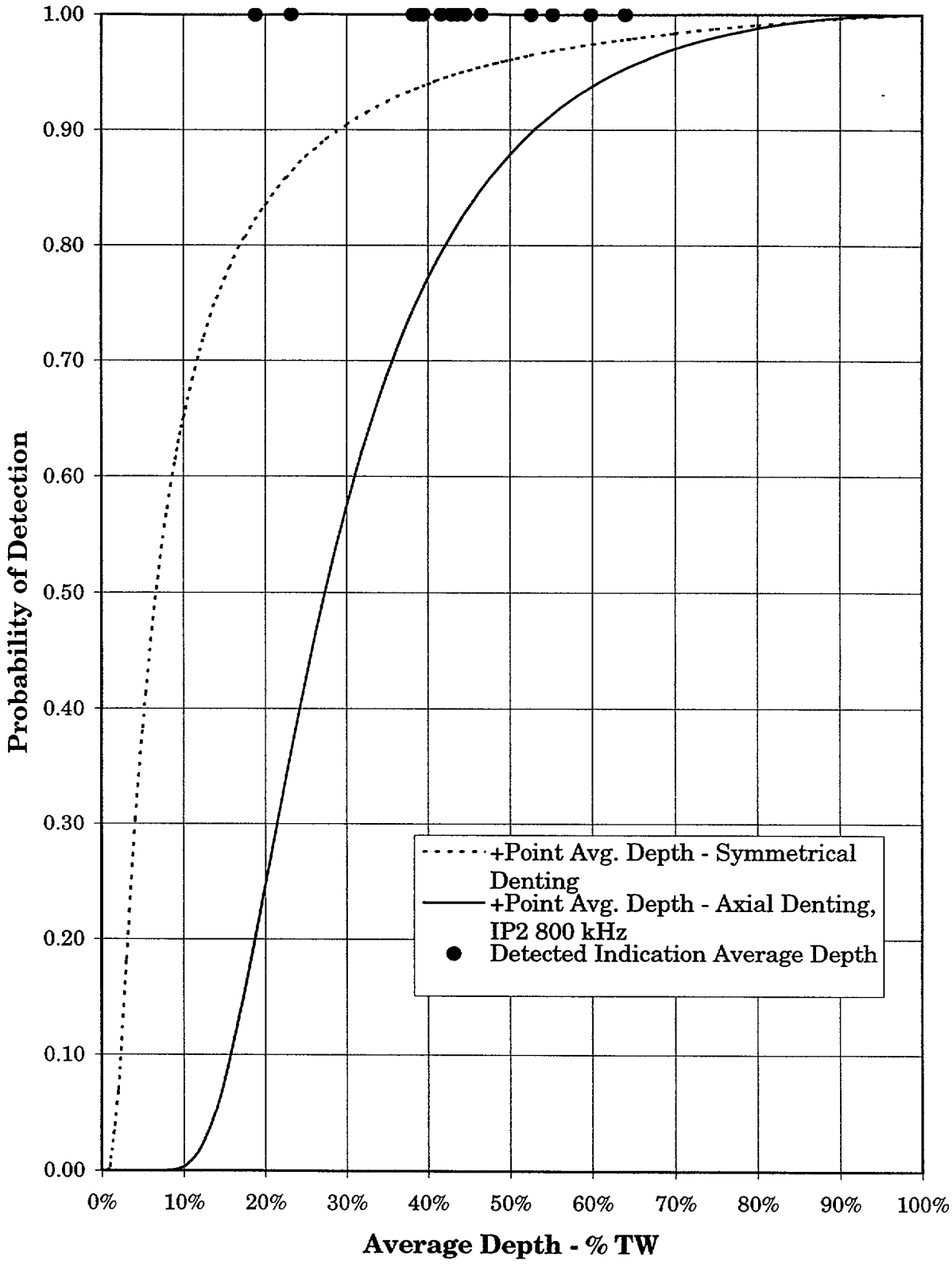

Figure 5-2. Comparisons of + Point Max. Depth PODs

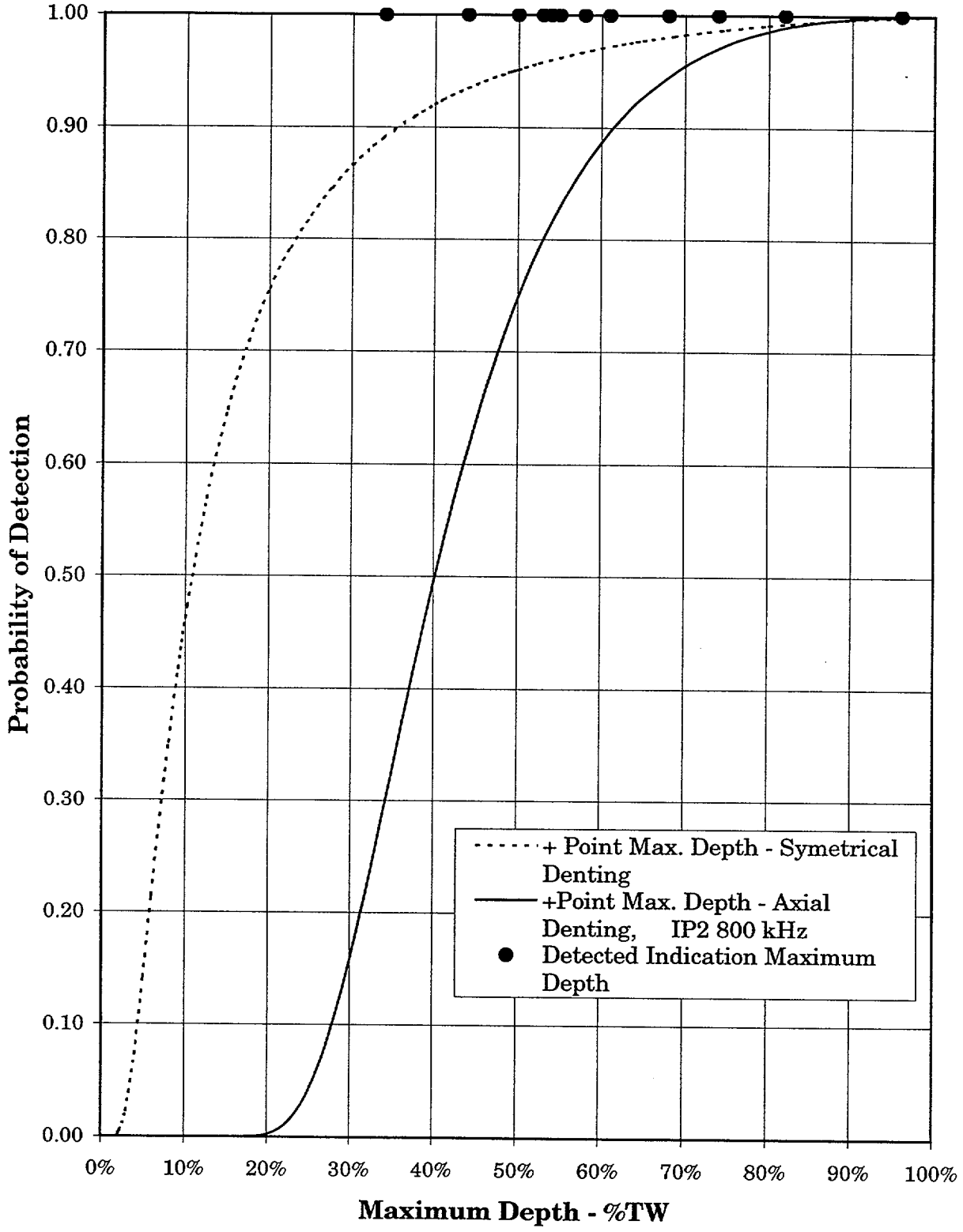

Figure 5-3. Indian Point-2 U-bend Average Depth Growth Data and Distribution

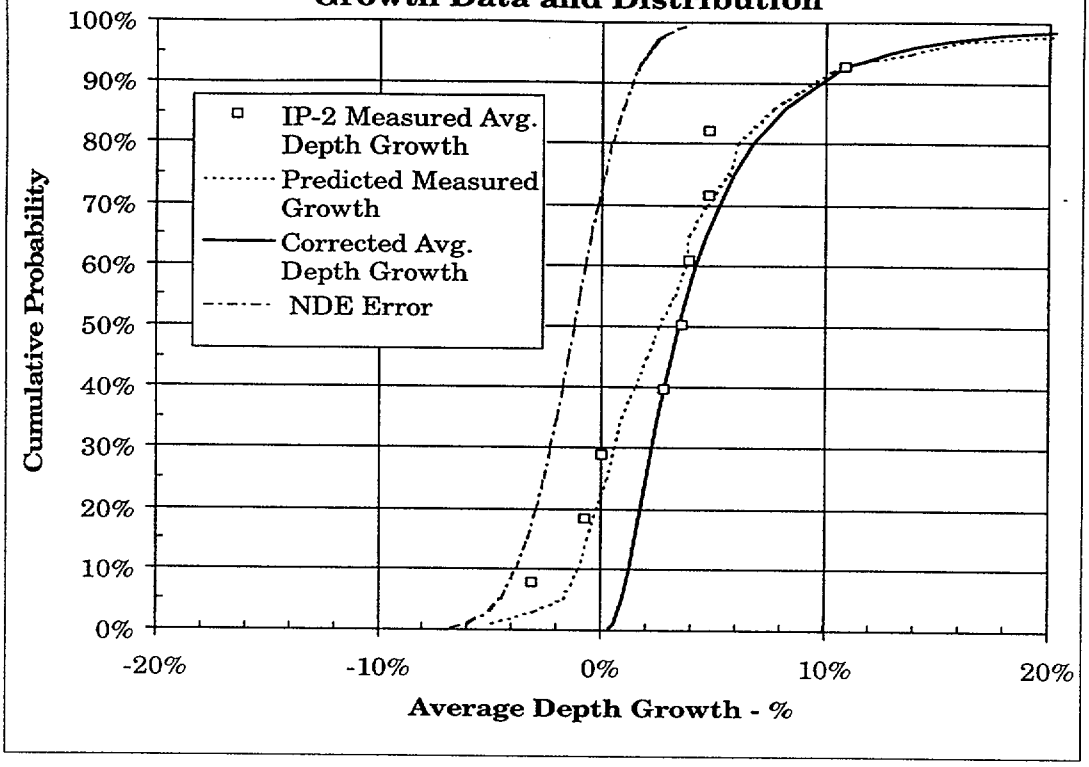

Figure 5-4. Indian Point-2 U-bend Length Growth Data and Distribution

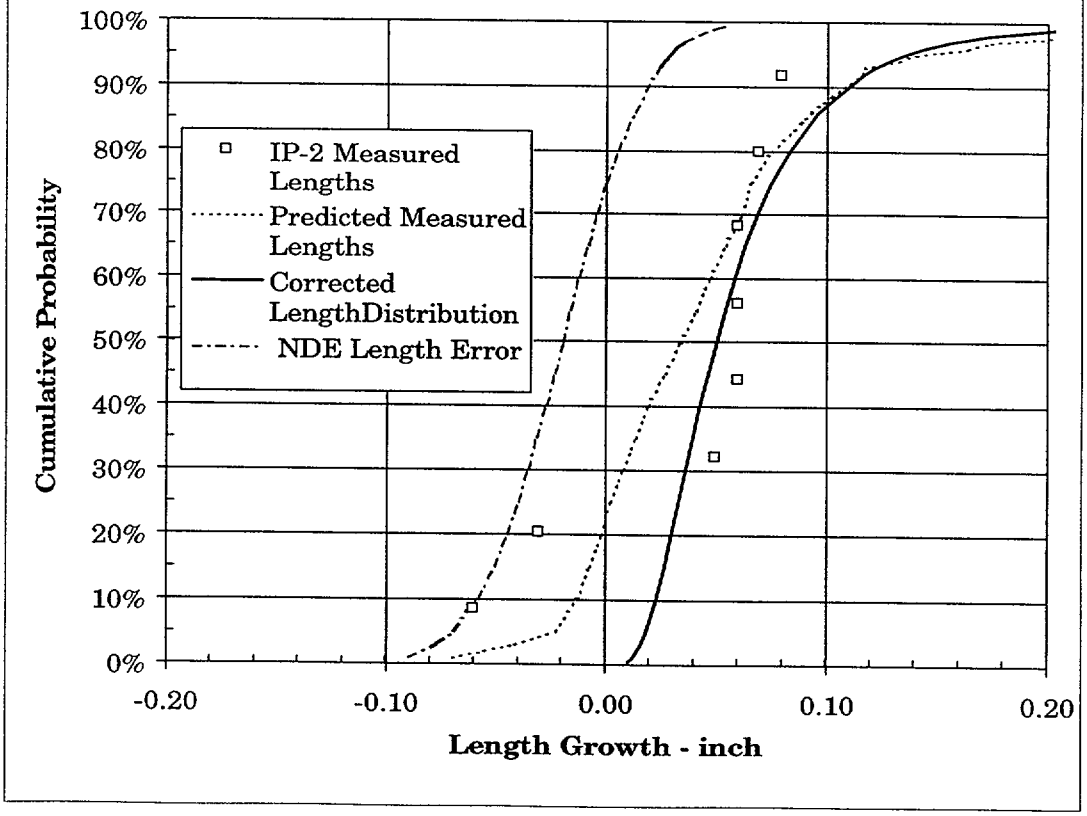

Figure 5-5.
Comparison of Indian Point-2 and Dented TSP PWSCC Growth at 590°F
Burst Effective Average Depth (%)

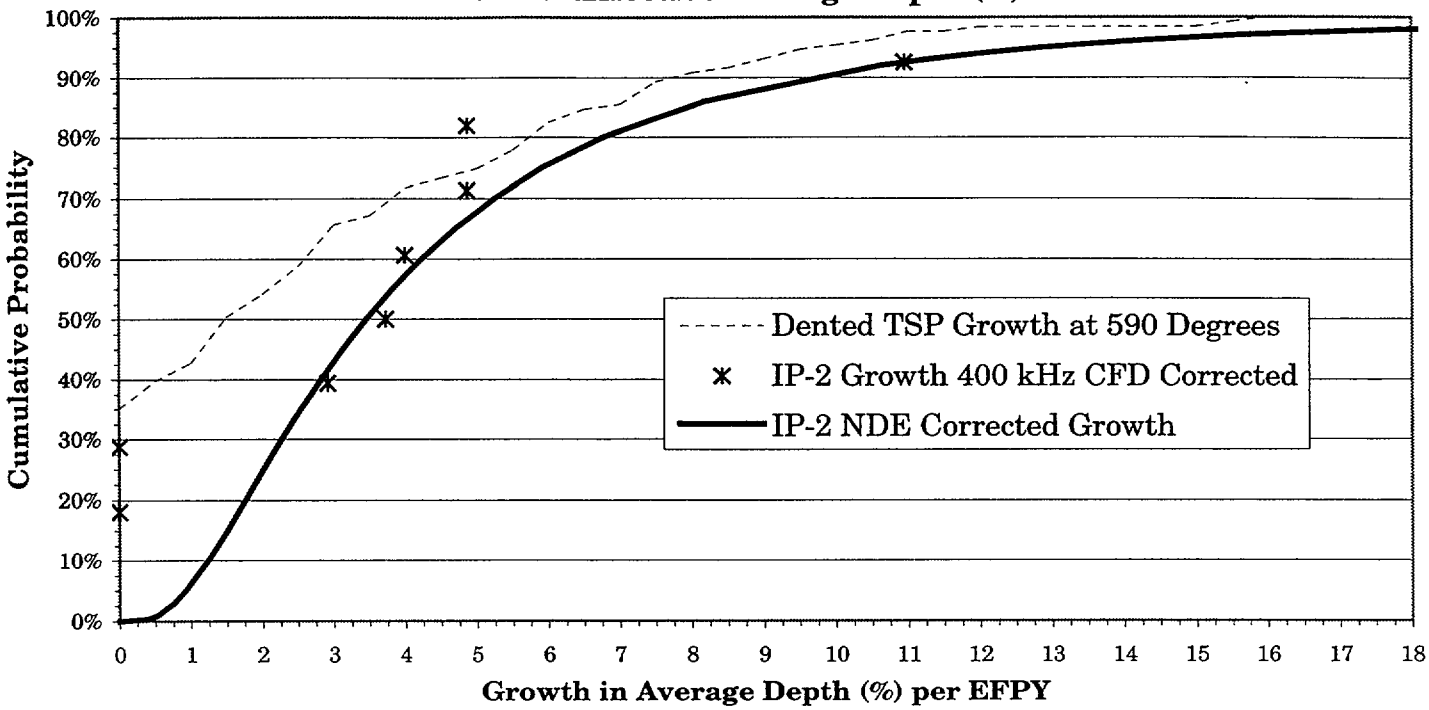

Figure 5-6.
Comparison of Indian Point-2 and Dented TSP PWSCC Growth at 590°F
Maximum Depth (%)

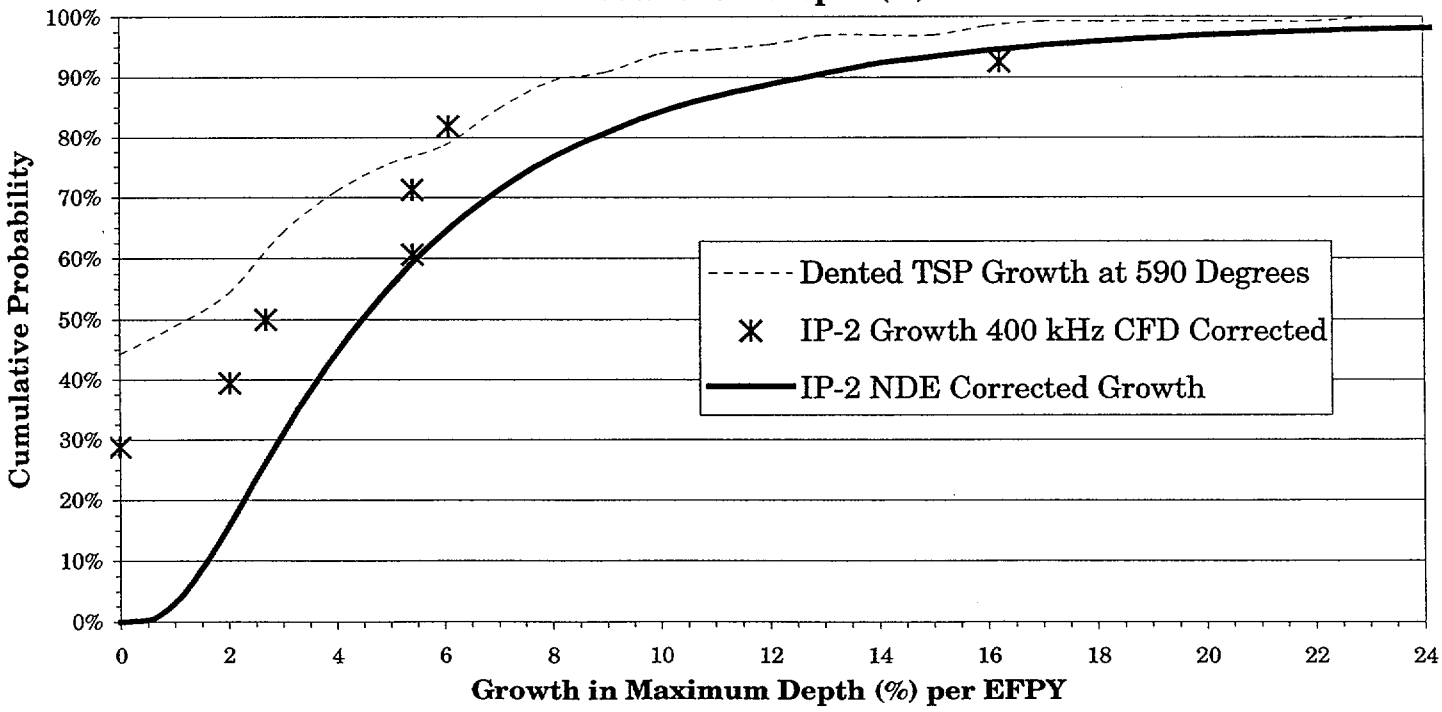

Figure 5-7.
Comparison of Indian Point-2 and Dented TSP PWSCC Growth at 590°F
Burst Effective Length (inch)

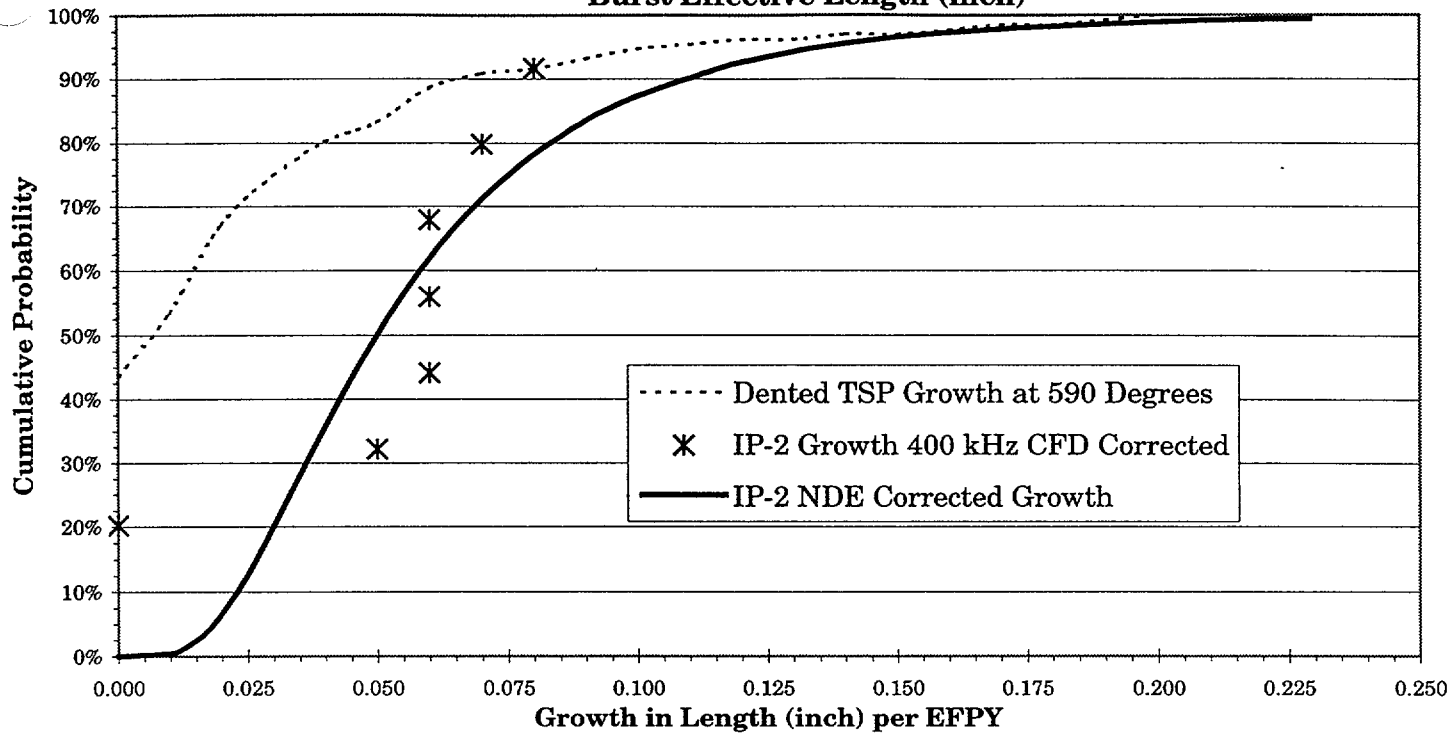

Figure 5-8. Comparison of Indian Point-2 Best Estimate "True" Growth with Distribution for Operational Assessment

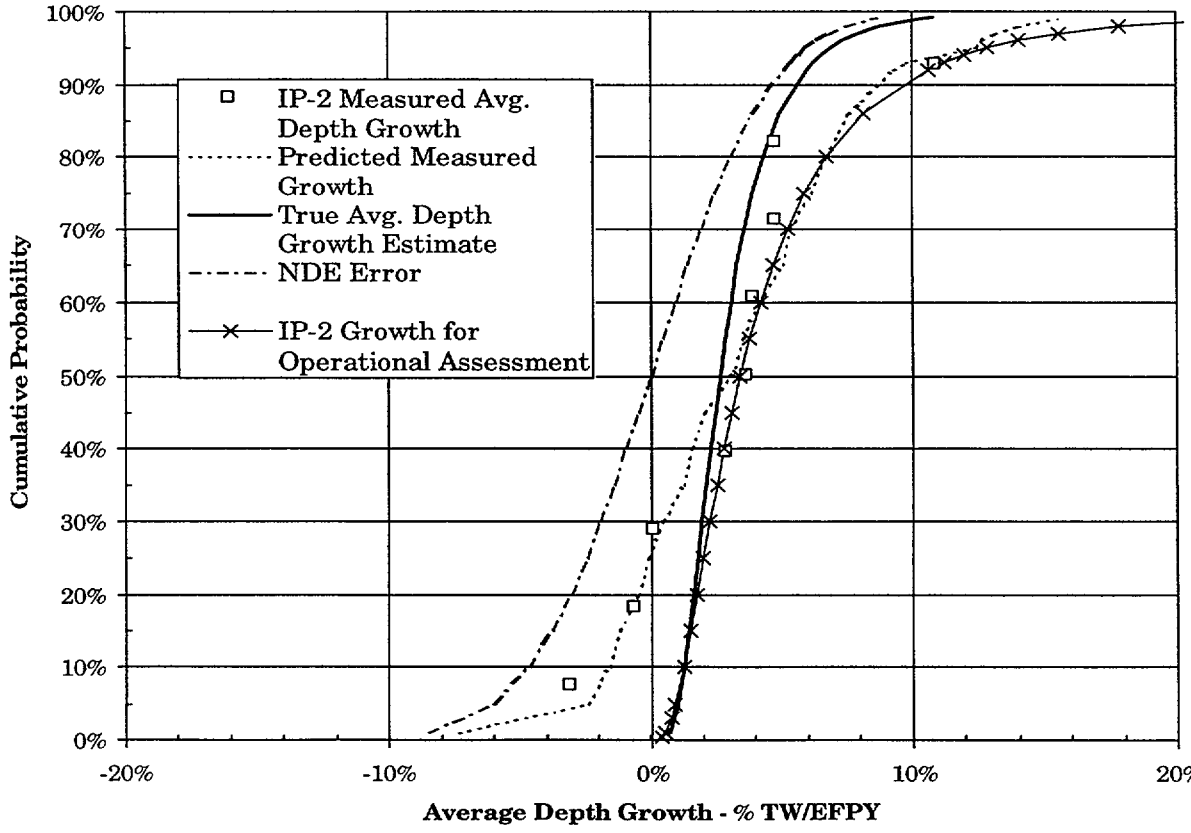

Figure 5-9

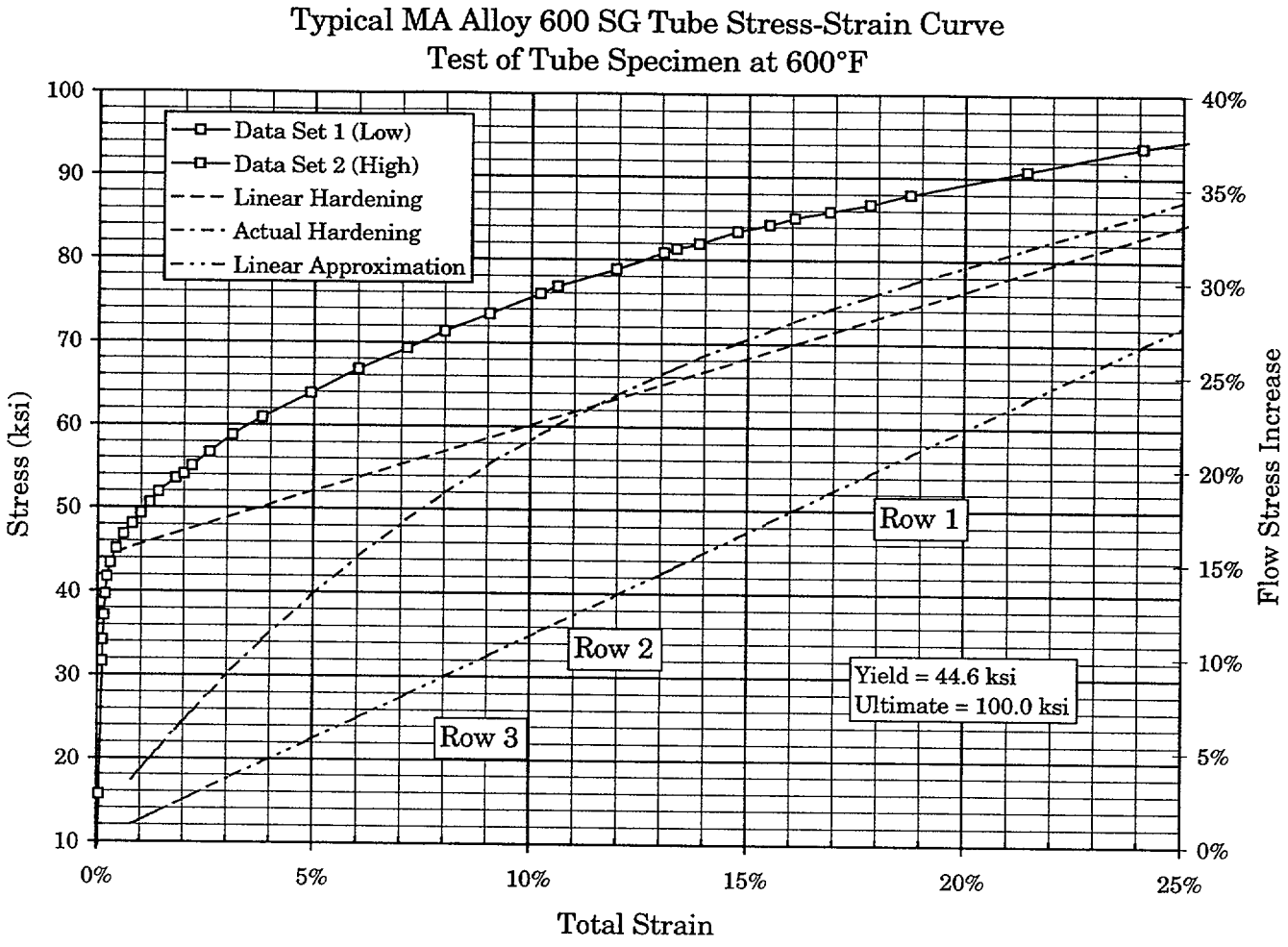
Typical MA Alloy 600 SG Tube Stress-Strain Curve
Test of Tube Specimen at 600°F
Data Set 1 (Low)
Data Set 2 (High)
Linear Hardening
Actual Hardening
Linear Approximation
Row 1
Row 2
Row 3
Yield = 44.6 ksi
Ultimate = 100.0 ksi
Stress (ksi)
Flow Stress Increase
Total Strain
100
90
80
70
60
50
40
30
20
10
40%
35%
30%
25%
20%
15%
10%
5%
0%
0%
5%
10%
15%
20%
25%

Figure 5-10.
Indian Point-2 New Indication Average Depth Distribution

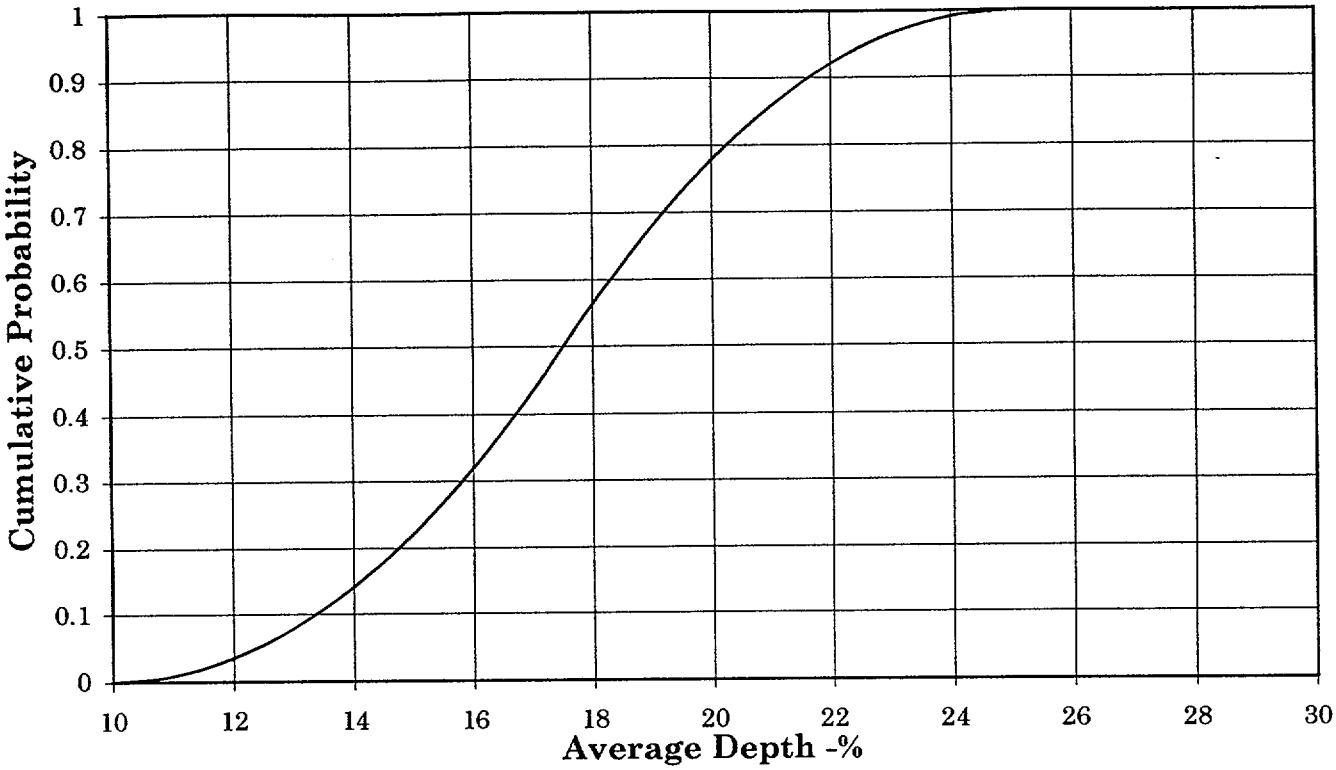

Figure 5-11
Indian Point-2 U-Bend PWSCC Ratio of Maximum to Burst Effective Average Depth

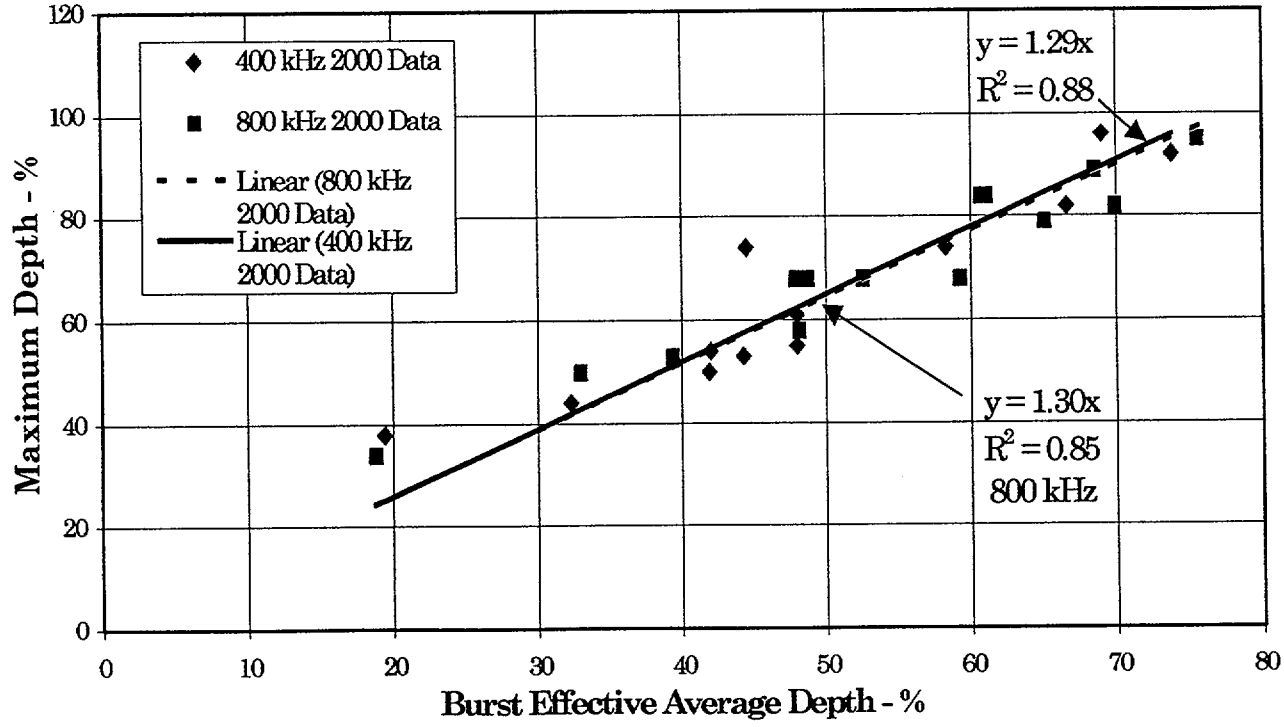

Figure 5-12. Indian Point-2 U-bend Crack Length Distribution

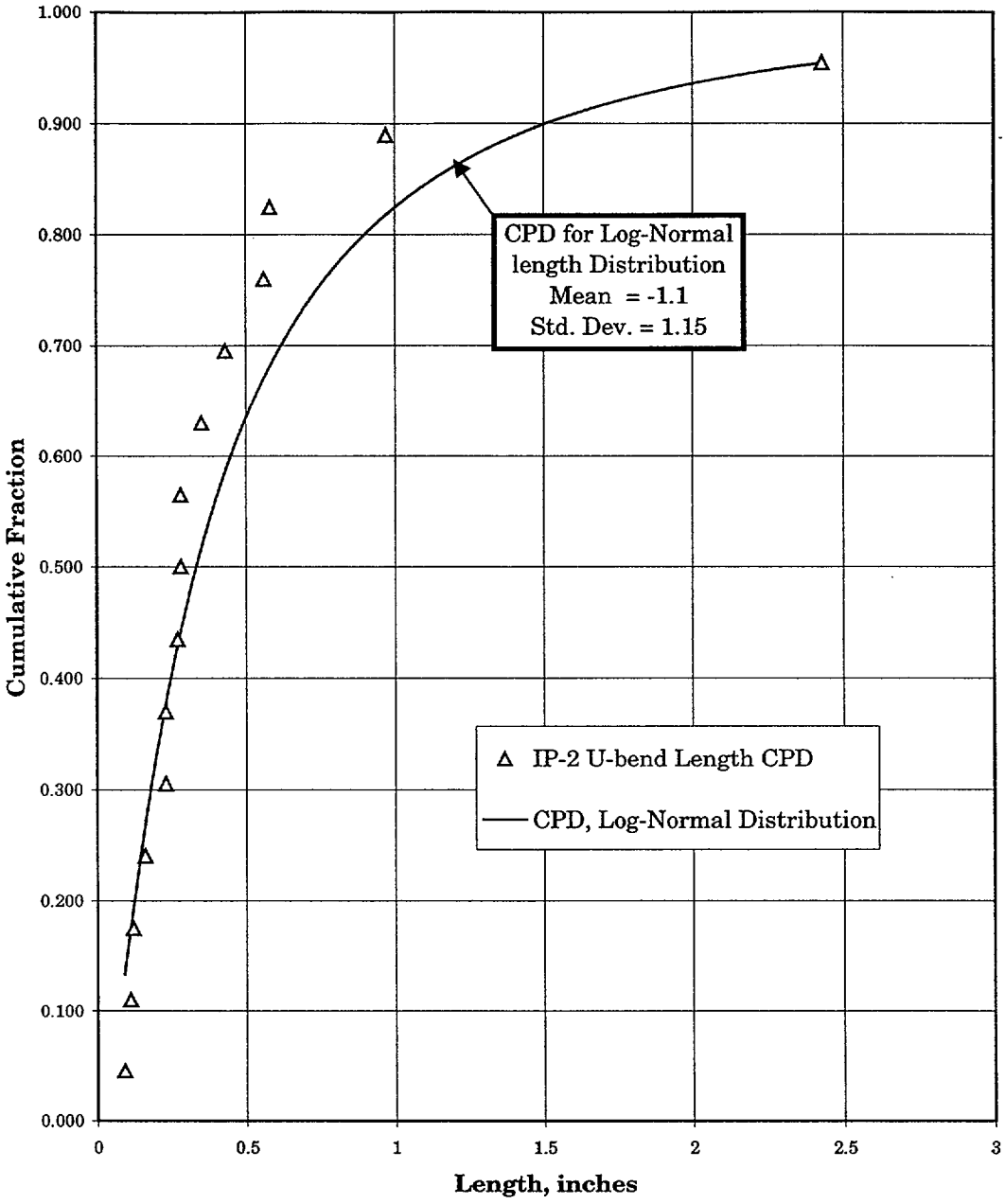

6.0 BENCHMARKING OF TUBE INTEGRITY ANALYSIS METHODS

This section provides benchmarking analyses for both the axial profile and multi-cycle tube integrity analysis methods. These analyses are performed to demonstrate that the methods provide adequately conservative predictions of structural and leakage integrity. The benchmarking analyses provide integral tests of NDE sizing techniques, NDE uncertainties and growth rates as well as the analysis methodology. Benchmarking of the axial profile analysis methods are described in Section 6.1 and the multi-cycle methods are given in Section 6.2.

The principal goal for the analysis methods and data is that the results at the required confidence levels (e.g., 95/95 for operational assessment) bound the actual data such as in situ test results. Ideally, all actual data are bounded by the 95/95 analyses. It is desirable as a secondary objective that the best estimate predictions provide a reasonable estimate of the actual data for condition monitoring assessments. EOC projections for the operational assessments should not be expected to predict the limiting indications at nominal or 50/50 confidence levels. The limiting indications typically have had the largest growth rates over the cycle and 50/50 confidence projections would only apply about the average growth rate. Consequently, assessment of the adequacy of operational assessment analyses from benchmarking analyses must be based on the 95/95 confidence levels to assure that the larger growth values are included in the comparisons.

6.1. Axial Profile Analysis Methods

This section provides benchmarking analyses for the axial profile tube integrity analysis methods. These analyses are performed to compare predictions of the R2C5 leakage event based on the 1997 +Point profiles with the operating experience, to compare predictions based on the 1997 +Point profiles with the year 2000 inspection and in situ results and to compare predictions using the year 2000 +Point profiles with the in situ results.

6.1.1. Prediction of R2C5 Leakage from 1997 Inspection +Point Profile

The flaw signal for R2C5 requires separation of the flaw signal from the background noise. The flaw signal can be distinguished from the noise by comparing the signal response with the indication to the deposit (C-scan ridge signal) response. The flaw signal represents the extension of the phase response beyond the characterized noise signal. The deposits on the tube also cause the +Point phase response for R2C5 to have a split phase angle. The +Point sizing guidelines of Reference 10-8, which are applied in this report, recommend that the depths for the two phase angles be averaged to determine the crack depth. This procedure was applied for the 1997 R2C5 data to obtain the best estimate depth profile shown in Figure 6-1. However, the split phase response for this indication is broader than typical and some positions for one of the phase angles lies in the OD plane. Averaging of ID and OD split phase responses is included in the qualification data of Reference 10-8, and is expected to result in the best estimate of the crack depth profile. An alternate depth profile can be obtained by sizing only the ID phase response. The resulting depth

profile is shown in Figure 6-1 as the alternate profile. The best estimate and alternate profiles of Figure 6-1 are expected to bound the R2C5 depth profiles in 1997. This section evaluates the two profiles relative to predicting the R2C5 leakage event.

The two 1997 profiles for R2C5 were projected to the leaker outage applying the NDE uncertainties and growth rates described in Section 5. The results are shown in Table 6-1. Results based on the single cycle analysis methods described in Section 4.1 are given for burst pressures and SLB leak rates at both 95/95 and 50/50 confidence levels. Also given are leak rates calculated for ligament tearing at normal operating condition pressure differentials. The R2C5 indication leakage event occurred as a result of ligament tearing at normal operating conditions rather than burst of the indication. Both SLB and normal operating condition leak rate analyses are included in this assessment as the SLB leak rate predictions are part of the operational assessment analysis results rather than normal operating leakage. For both profiles, ligament tearing is predicted at SLB conditions to result in leak rates exceeding 100 gpm at 95/95 confidence. The 95/95 burst pressure for the best estimate profile is less than the normal operating pressure differential while the alternate profile predicts a burst pressure above normal operation. The nominal 50/50 predictions show burst pressures of 3100 and 4070 psi and SLB leak rates of 3.89 and 0.0 gpm for the two profiles. In this case, the nominal predictions should not be expected to adequately predict the R2C5 leakage event. The nominal predictions apply the average growth rate and R2C5 growth defines the high growth tail of the distribution. The best estimate profile results in a predicted leak rate of 100 gpm at about 90% probability while the alternate profile reaches 100 gpm at about 94% probability. The best estimate profile of Figure 6-1 thus provides a slightly better prediction of the R2C5 leakage event than the alternate profile.

Predictions of ligament tearing leak rates at normal operating pressure differentials are also given in Table 6-1 to reflect predictions for the actual conditions for the R2C5 leakage event. At 95/95 confidence, the projected leak rate is about 12 gpm for both depth profiles with no leakage predicted for nominal 50/50 confidence levels. As noted above, nominal calculations for R2C5 should be expected to underestimate the leakage since the indication requires the high cumulative probability of the growth distribution to reflect the actual growth of this indication during Cycle 14. Thus the ligament tearing model predicts unacceptable leakage although not as large as the actual leakage event.

These analyses utilize the Cycle 14 growth distribution to predict the EOC-14 limiting indication. Consequently, these comparisons are primarily tests of the statistical methods and the +Point sizing applied for the 1997 indications. The results support the adequacy of the Monte Carlo methods applied at 95% probability to predict the limiting EOC indication and support the best estimate depth profile for R2C5 as representative of the condition of the tube in 1997.

Overall, the above evaluations support the best estimate profile for R2C5 as a better estimate of the 1997 depth than the alternate profile although the differences are not firmly conclusive. The single cycle analysis methods applying the 1997 +Point depth profiles and evaluated at the required 95/95 confidence levels predict a large leak rate for R2C5 consistent with the actual leakage event. The results indicate that it is necessary to

maintain a 95% probability on the predictions to assure that the large growth tail is included in the analytical predictions.

6.1.2. Prediction of EOC-14 U-Bend Indications from 1997 +Point Profiles

Burst pressures and leak rates from the 1997 +Point profiles projected to the 2000 outage can be compared with in situ test results and with burst pressures and leak rates calculated from the year 2000 +Point profiles. These results are given in Table 6-2.

It is seen that the 1997 95/95 projections for R2C69, R2C71 and R2C72 all predict burst pressures less than obtained in the in situ tests and less than predicted with the 2000 profiles at 95/50. The 1997 projections at 50/50 confidence for burst pressures are also less than obtained with the 2000 profiles at nominal conditions. The SLB leakage projections show significant leakage for R2C69, R2C71 and R2C72 at 95/95 confidence, where the 2000 NDE data for 400 kHz and the in situ tests show only a low leak rate for R2C71. The 1997 projections are conservative even in comparison with the 2000 data at 800 kHz.

Figure 6-2 compares burst pressure distributions at EOC-14 based on projections from the 1997 +Point profiles and calculated from the 2000 profiles at 400 kHz. Burst pressure distributions are shown for R2C69, R2C71 and R2C72. For each indication, the 1997 projections are more conservative than the burst pressures obtained from the 2000 profiles. In general, it would be expected that the 2000 profiles are more accurate than the 1997 profiles due to the larger indications for sizing in 2000. The 2000 profiles show adequate conservatism in comparison with in situ test results (see following section).

Thus, the methods based on the 1997 profiles are demonstrated to be conservative for projections to the 2000 outage. The analyses are primarily sensitive to the NDE profiles and growth rates, and support adequate or conservative sizing for the 1997 400 kHz data. The methods predict R2C69 and R2C71 to be the limiting indications in Table 6-2, which is consistent with the in situ test results.

6.1.3. Prediction of In Situ Test Results from EOC-14 +Point Profiles

The tube integrity analysis methods can be further benchmarked by comparing predictions of burst pressures and ligament tearing pressures for the EOC-14 +Point profiles with the in situ test results using the analysis methods described in Section 4.1. These condition monitoring analyses provide an integral benchmarking of the +Point depth profiles with additional influence from the NDE uncertainties, material properties and uncertainties in the burst or leakage correlations. Differences between best estimate and 95/50 predictions are indicative of the uncertainties included in the analyses. The best estimate for these comparisons is based on applying the NDE profile to calculate the burst pressure using the nominal burst correlation, and does not include any NDE uncertainty adjustments, thus increasing the sensitivity to the NDE profiles. For these comparisons, cumulative distribution functions (CDF) for ligament tearing as a function of the pressure differential are developed based upon the ANL ligament tearing model (Reference 10-18). The primary objective for the analysis methods is to provide sufficient

conservatism such that the analyses at the required 95/95 or 95/50 confidence levels bound the measured data.

Comparisons of the predicted burst and ligament tearing pressures with the in situ test results are given in Table 6-3. The calculated results are provided for both the 400 and 800 kHz +Point profiles described in Section 3.4. The burst pressures and ligament tearing predictions in the table are given at operating temperature material properties for best estimate and lower 95% probability confidence levels. With the exception of R2C71 for which the in situ test pressure was limited to 4206 psi by leakage, the nominal and lower 95% burst pressure predictions for the 400 kHz profiles and the test results exceeded the $3\Delta P_{NO}$ burst margin requirement of 4617 psi at operating temperatures. For the 800 kHz profiles, the lower 95% burst pressure predictions are less than the in situ test results and the burst margin requirement for R2C69, R2C71 and R2C72. These results tend to indicate that the 800 kHz profiles are unnecessarily conservative. The lower 95/50 burst pressure prediction for R2C71 is less than the burst margin requirement, and the maximum test pressure reached (limited by leakage) of 4206 is also less than the burst requirement. The R2C71 indication had initial leakage at 1627 psi and leakage reached the test system capacity of 1.99 gpm at 4206 psi (4500 psi room temperature). The R2C71 in situ results and estimated burst pressure are further evaluated in Section 8.2, where it is shown that the R2C71 indication burst pressure would exceed the $3\Delta P_{NO}$ = 4617 psi requirement. For R2C69, the in situ test resulted in leakage exceeding 2 gpm at about 4835 psi (above burst margin requirement). This condition is adequately predicted at 4851 psi by the lower 95% 400 kHz burst pressure, but is again unnecessarily underpredicted at 3749 psi for the 800 kHz profile. Based on the burst pressure comparisons of Table 6-3 between prediction and in situ tests, it is seen that the 400 kHz +Point profiles provide adequate conservatism and the 800 kHz results tend to be overly conservative.

An additional check on the analysis methods can be obtained by comparing the cumulative distribution function for ligament tearing pressure with the onset of leakage for the in situ tests. This distribution shown in Figure 6-3 for the R2C71 400 kHz profile is essentially a probability of leakage as a function of pressure. For this indication, the predictions show a 4% chance of leakage at low pressures, which is essentially the effect of NDE sizing uncertainties on the +Point profile. At 4500 psi, there is about a 30% probability of leakage. These analyses were performed for each indication. Table 6-3 includes the prediction of ligament tearing pressures at a lower 95% probability and the best estimate prediction obtained by applying the ANL ligament tearing model directly to the profile with no NDE uncertainties applied. For R2C71, the analysis results show the highest probability of leaking and this indication showed progressively increasing leakage with increasing pressure up to the maximum test pressure of 4206 psi (operating temperature). The R2C69 indication, which had ligament tearing at 4834 psi, is also predicted to have a significant probability of leakage (28%) at this pressure. The analyses over predict the likelihood of leakage for R2C72 and under predict leakage for R2C74 with had a small leak at 4486 psi. Since the ligament tearing pressures predicted for R2C74 are much higher than the 4486 psi for initial leakage, it is likely that the depth profile for this indication is underestimated as further discussed in Section 8. Overall, the analyses adequately predict the ligament tearing pressures for the larger indications, which

supports adequate NDE sizing for tube integrity assessments. The 800 kHz profiles result in overly conservative predictions of the probability of leakage. Leakage at the lower 95% probability is predicted for R2C69, R2C71, R2C72 and R2C87. R2C72 and R2C87 did not leak at the maximum test pressure of 5140 psi and R2C69 did not leak until 4834 psi. These analyses also show the same advantage of adequately conservative predictions found for the burst pressure analyses for the 400 kHz data compared to the 800 kHz data.

Overall, it is concluded from these benchmark analyses for the axial profile analysis methods that the methodology applying the 400 kHz NDE profiles results in bounding analyses at the required confidence levels. These methods are applied for the operational assessments in Section 9. The use of the 800 kHz NDE profiles tends to be unnecessarily conservative.

6.2. Multi-Cycle Analysis Methods

The multi-cycle Monte Carlo simulation approach can be benchmarked against notable observations in the service performance history of degraded steam generator tubing. Given successful benchmarking, confidence is obtained in any future projections using this approach. For U-Bends at Indian Point 2 the most notable benchmark is the occurrence of a normal operating pressure large leakage event at 1.48 EFPY into Cycle 14, which ended the operating cycle. The tube exhibiting this leak would have burst at differential pressures nominally postulated for SLB conditions. In situ testing of other Row 2 U-Bends at the EOC 14 outage led to leakage at test pressures exceeding 3ΔP. Leakage at these high test pressures serves to indicate the actual severity of degradation. During in situ testing, one tube had sudden large leakage at a test pressure 200 psi higher than the temperature corrected 3ΔP test pressure. Thus for benchmarking purposes, one tube (the leak event tube) failed the 3ΔP strength requirement and another tube was near the boundary of acceptability.

Extensive eddy current evaluations were performed at EOC 14 providing additional benchmarks, such as length versus crack depth profiles for the observed axial PWSCC degradation. The distribution of measured lengths is used as input to the simulation model. The history of occurrence of axial PWSCC U-Bend eddy current indications essentially determines the initiation function used in the simulation, so projections of the correct number of indications is not a difficult benchmark.

The distribution of measured indication depths is a good benchmark, since agreement between measurements and computer calculations provides assurance that the simulation is accurately representing the correct severity of degradation. Another key observation is that careful reanalysis of eddy current data from EOC 13 showed the presence of a large axial U-Bend crack in tube R2C5 in S/G 4. The structural length was 1.87 inches and the structural average depth was 80.4% TW. This crack then grew to lead to the NOP large leakage event. It is not difficult to show that this large crack at EOC 13 could grow to produce the observed leaker outage in Cycle 14. However, multi-cycle Monte Carlo simulations should predict a reasonable chance of occurrence of a large crack at EOC 13. The multi-cycle Monte Carlo simulation approach should project the degree of degradation

severity revealed by the NOP leakage event, in situ pressure testing and eddy current inspection results.

The multi-cycle simulation model used in this analysis is constructed to deal with all pertinent uncertainties and make projections of degradation severity on a best estimate basis. It is designed to provide the best estimate of actual degradation severity in operating steam generators including both detected and undetected degradation. Matching of multiple benchmarking parameters over multiple cycles of operation is naturally more difficult than keying to a single observation. Some degree of compromise is needed when using multiple benchmarks. This helps prevent unwarranted bias on a single variable. Good agreement of simulation results with multiple benchmarks provides confidence in similar applications of the simulation methodology.

The axial PWSCC degradation of Row 2 U-Bends was simulated over the last four cycles of operation. Benchmarking results are presented below for the reference set of input data. In this analysis, the reference crack growth rate distribution of Section 5 and the POD curve as a function of average depth was used as input. Section 5 does not define a POD for prior cycles and a prior cycle POD degraded from the recommended year 2000 POD was used. Table 6-4 lists various benchmarking parameters reflecting the severity of degradation of Row 2 U-Bends at Indian Point 2 at EOC 14 and associated multi-cycle Monte Carlo Simulation results. Computed results are matched to the observed numbers of indications in Row 2 U-Bends at EOC 13 and EOC 14. Since the NDE measured crack length distribution was used as input, the simulation results always match actual inspection results. In terms of other NDE observations, Figure 6-4 shows that the projected measured average depth distributions shows excellent agreement with actual NDE results. Figure 6-5 shows that the multi-cycle simulation is in very good agreement with the fact that a lookback NDE analysis found a 1.87 inch long, 80.4% TW average depth crack at EOC 13.

Multi-cycle Monte Carlo simulations point to a high probability of violating leakage integrity and $3\Delta P$ strength requirements at EOC 14. Simulation results using the reference input provide a good match with all observations of degradation severity. This simulation views the leakage event as essentially a 1 in 7 occurrence reflecting the unfortunate confluence of multiple parameters with extreme values.

Table 6-1. Summary of Predictions for R2C5 Leakage Event Based on 1997 Data

+Point Profile	Burst Pressure (psi)		SLB Leakage (gpm)		Ligament Tearing & Leakage at ΔP_{NO}[1] (gpm)		Estimated Event Leakage at ΔP_{NO} (gpm)
	95/95	50/50	95/95	50/50	95/95	50/50	
Reference Growth Rates							
Best estimate	1349	3100	166	3.89	12	0.0	140-160
Alternate estimate	1724	4070	118	0.0	12	0.0	
Growth Rates x 1.25							
Best Estimate	1295		195	6.31			
Alternate estimate	1535		145	0.0			

Notes:

1. Ligament tearing computed at ΔP_{NO} = 1569 psi for EOC-14. Leak rates adjusted from SLB leak rate correlation assuming a SLB to normal operating leak rate ratio of 5.0.

Table 6-2. Indian Point-2 U-Bend Indications: Comparison of Burst Pressures and Leakage for Projected and Actual EOC-14 Indications

Analyses & In Situ Results at Operating Temperatures - Requirements: $3\Delta P_{NO}$ = 4617 psi, SLB Leak Rate = 1 gpm

Indication			Calculation Parameters		Burst Pressure Predictions - psi				SLB Leak Rate gpm				In Situ Test Results	
					1997 NDE Projection		2000 NDE Data		1997 NDE Projection		2000 NDE Data		Burst Pressure psi	SLB Leak Rate gpm
SG	Tube	Crack No.	NDE Profile	Year Profile	95/95	50/50	95/50	50/50	95/95	50/50	95/50	50/50		
4	R2C69	1	400 kHz	1997	3313	5600	4851	6970	2.818	0.0	0.0	0.0	>4834	0.00
		2			6949	9750	8447	10000	0.0	0.0	0.0	0.0		
		3			7350	10000	7657	10000	0.0	0.0	0.0	0.0		
		1	800 kHz	2000	-		3749	5770	-	-	1.51	0.0		
		2			-	-	6589	9090	-	-	0.0	0.0		
		3			-	-	6099	8800	-	-	0.0	0.0		
4	R2C71	1	400 kHz	1997	3703	5860	4486	6430	1.047	0.0	0.04	0.0	>4206	0.024
		1	800 kHz	2000	-	-	3823	5570	-	-	0.60	0.0		
4	R2C72	1	400 kHz	1997	4283	6400	4888	6800	0.316	0.0	0.0	0.0	>5140	0.00
		1	800 kHz	2000	-	-	4432	6420	-	-	0.10	0.0		
1	R2C87	1	400 kHz	1997	6955	9580	6888	9380	0.0	0.0	0.0	0.0	>5140	0.00
		2			6888	9570	6968	9330	0.0	0.0	0.0	0.0		
		3			6391	8910	7048	9420	0.0	0.0	0.0	0.0		
		1	800 kHz	2000	-	-	5680	8240	0.0	0.0	0.0	0.0		
		2			-	-	5130	7490	0.0	0.0	0.0	0.0		
		3			-	-	5778	7900	0.0	0.0	0.0	0.0		

Table 6-3. Indian Point-2 U-Bend Indications: Comparison of Condition Monitoring Burst and Ligament Tearing Pressures with In Situ Test Results

Indication			NDE Profile Frequency	Burst Pressure Predictions psi		Ligament Tearing Pressure psi		In Situ Test Results	
								Burst Pressure psi	Initial Leakage Pressure psi
SG	Tube	Crack No.		95/50	Best Estimate	95/50	Best Estimate		
4	R2C69	1	400 kHz	4851	6503	2877	5796	>4834	4834 >2 gpm
		1	800 kHz	3749	5235	0.0	4580		
4	R2C71	1	400 kHz	4486	5799	0.0	5480	>4206	Steady Increase
		1	800 kHz	3823	4828	0.0	4096		
4	R2C72	1	400 kHz	4888	6219	2570	6022	>5140	>5140
		1	800 kHz	4432	5728	0.0	5466		
1	R2C87	1	400 kHz	6888	8838	6498	8835	>5140	>5140
		2		6968	8837	6553	8840		
		1	800 kHz	5680	7828	0.0	7665		
		2		5130	6834	2658	6688		
4	R2C4	1	400 kHz	9017	11314	9078	10664	>5140	>5140
			800 kHz	8879	11059	9041	10650		
4	R2C74	1	400 kHz	9850	12150	9470	11035	>5140	4486
			800 kHz	8035	10202	8487	10202		
3	R2C85	1	400 kHz	7456	9578	7580	9422	>5140	>5140
			800 kHz	6827	8846	6945	8862		

Table 6-4. Summary of Multi-Cycle Model EOC-14 Benchmarking Parameters	
Benchmark Parameter	**Reference Input**
Probability of Burst at Normal Operation	4.0%
Probability of Large Leakage at Normal Operation	8.1%
Probability of Burst at Steam Line Break	13.1%
Probability of Large Leakage at Steam Line Break	32.1%
Probability of Burst at 3 Times Operating Pressure, 3ΔP	57.2%
Probability of Large Leakage During In Situ Testing	94.5%
Median Minimum Degraded Tube Burst Pressure, psi	4501
95th Percentile Minimum Degraded Tube Burst Pressure, psi	1667
Chance of More Than 1 Burst at 3ΔP	19.4%

*Required Minimum Burst Pressure ($3\Delta P_{NO}$) is 4617 psi at Temperature

Figure 6-1
SG4, U-bend, Tube R2C5, Crack 1 - 1997
NDE Depth vs. Axial Length

PWSCC Version 2.0

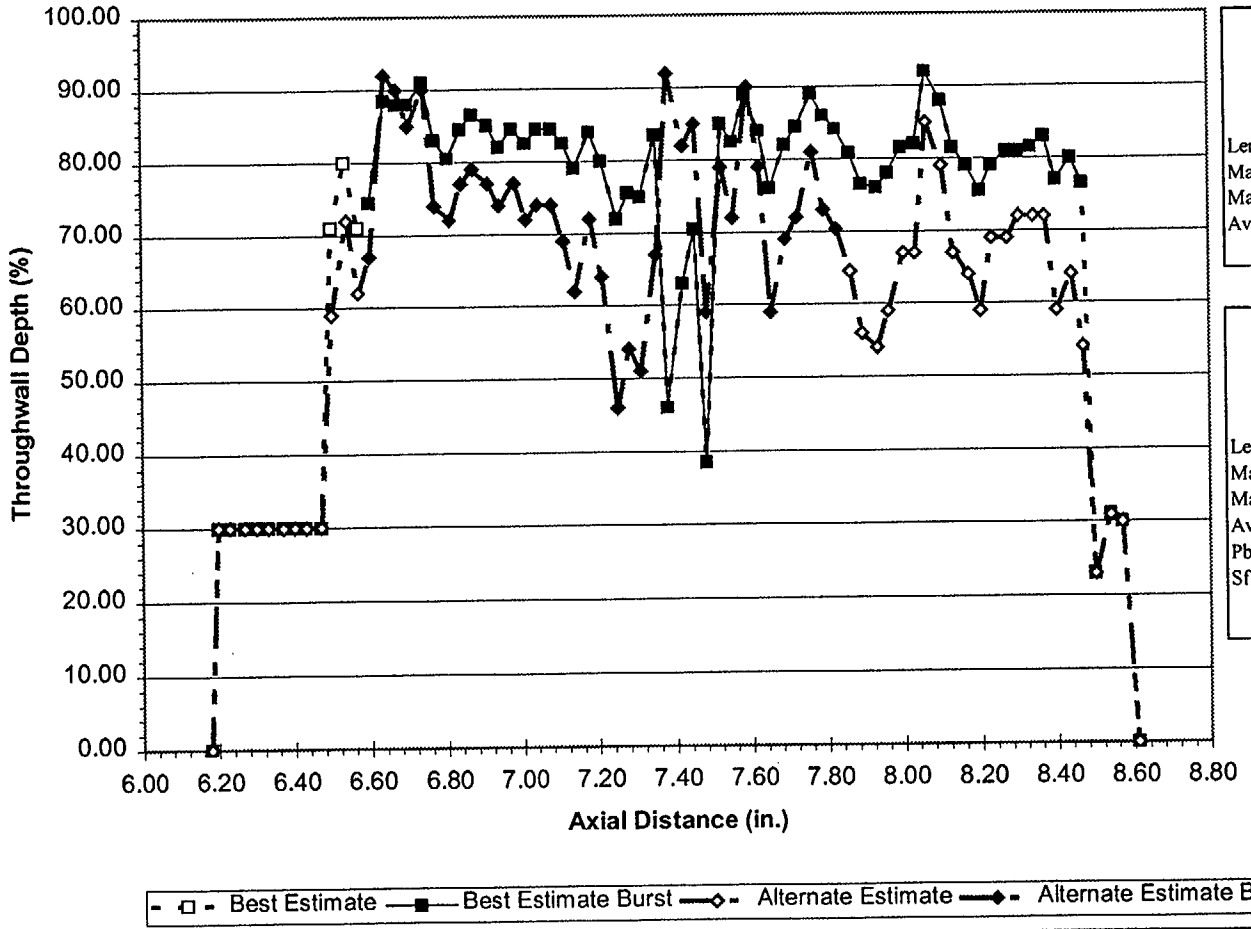

NDE Profiles

	Alternate Estimate 1997	Best Estimate 1997
Length	2.43	2.43
Max. Volts	2.24	2.31
Max. Depth (%)	92.0	92.0
Avg. Depth (%)	63.0	70.6

Burst Effective Profiles

	Alternate Estimate 1997	Best Estimate 1997
Length	1.22	1.87
Max. Volts	2.24	2.31
Max. Depth (%)	92.0	92.0
Avg. Depth (%)	73.6	80.2
Pb (ksi)	4.663	3.528
Sf =85.00 (ksi)		

Figure 6-2
Indian Point-2 EOC-14 Burst Pressure Predictions (400kHz)
Comparison of Projections from 1997 Profiles with 2000 Profiles

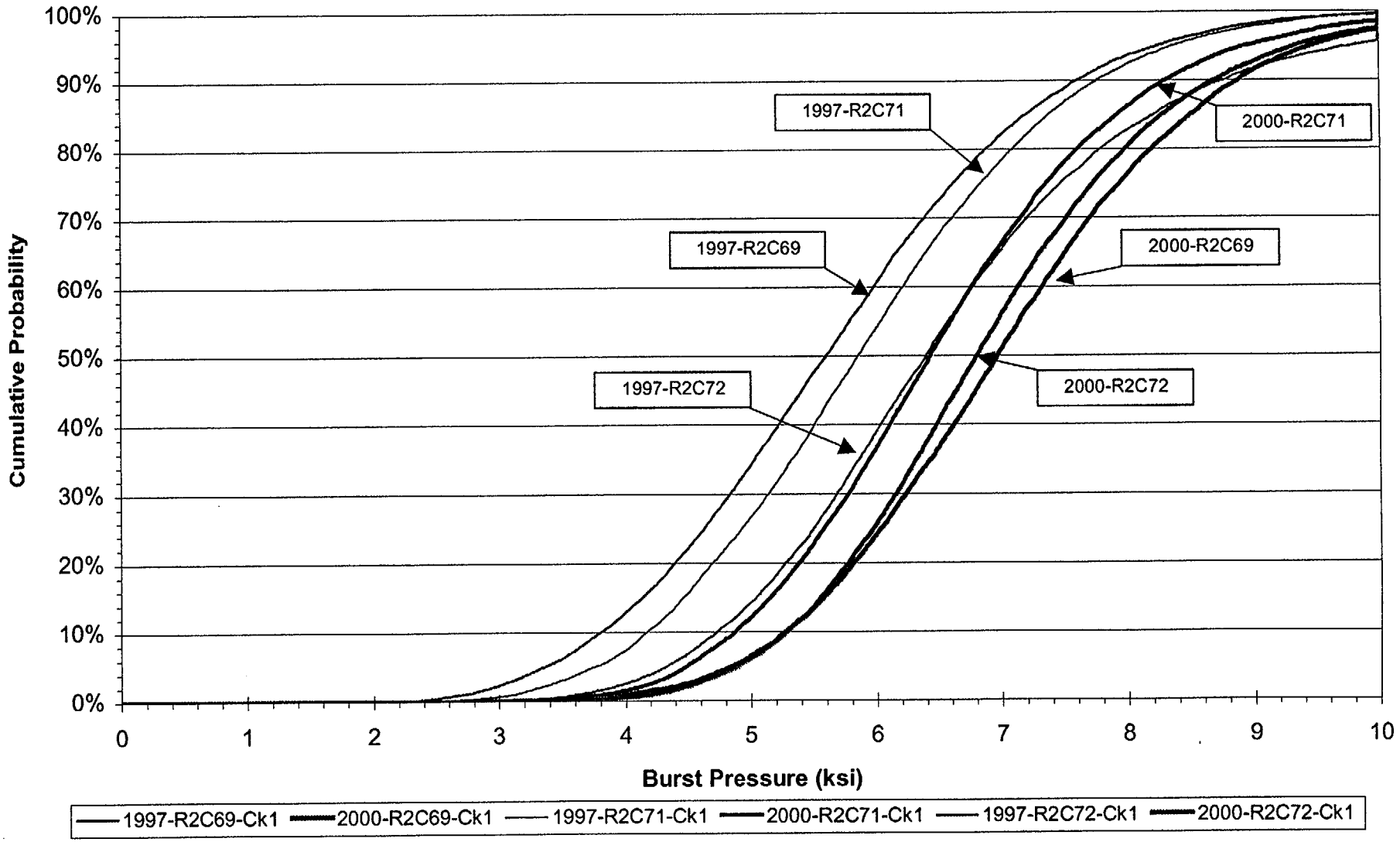

Figure 6-3. Indian Point-2: R2C71 400 kHz + Point, Distribution of Simulated Ligament Tearing Pressures

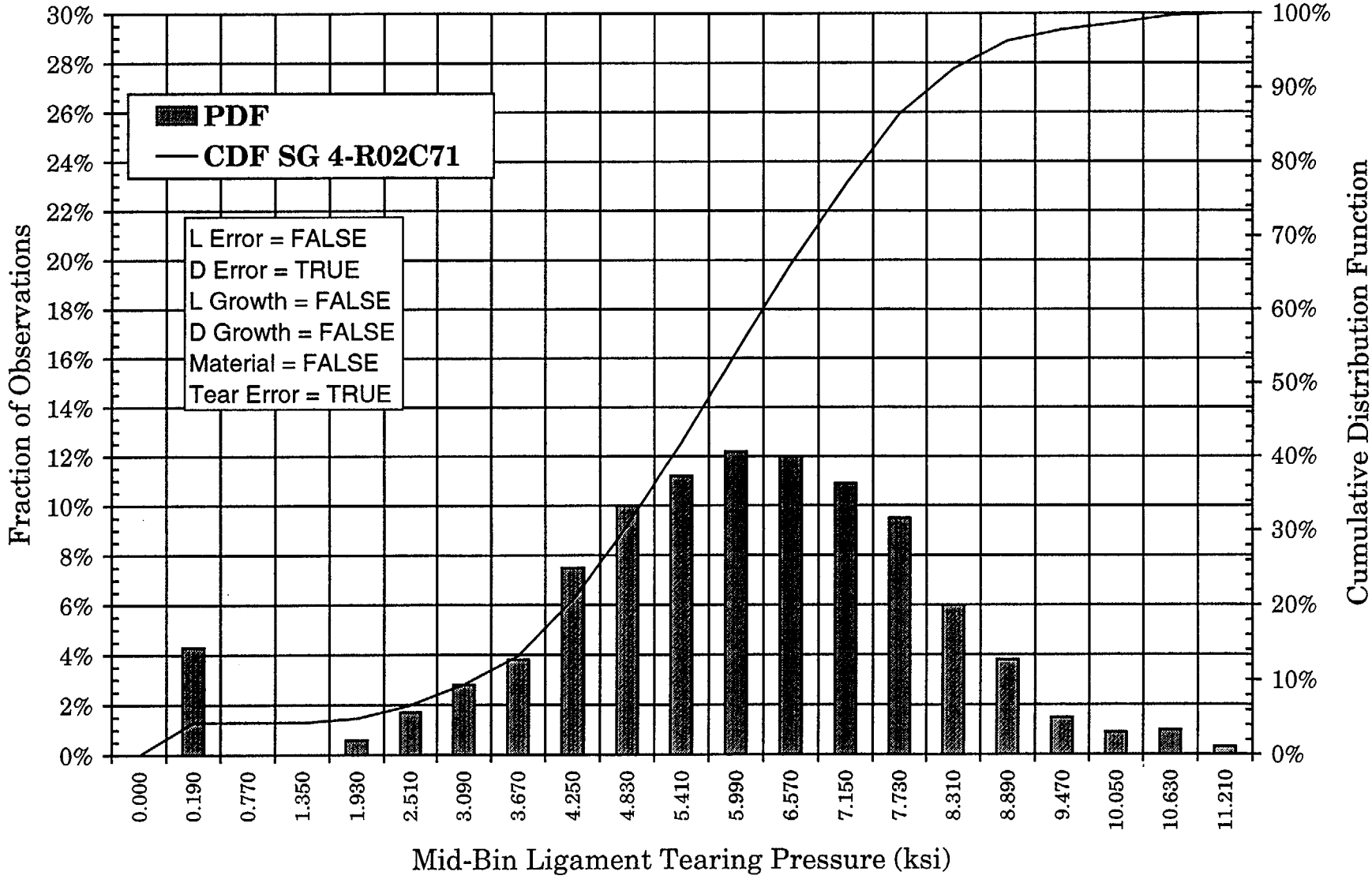

Figure 6-4
Comparison of Simulation Results and NDE Measured Depth Distribution at EOC 14

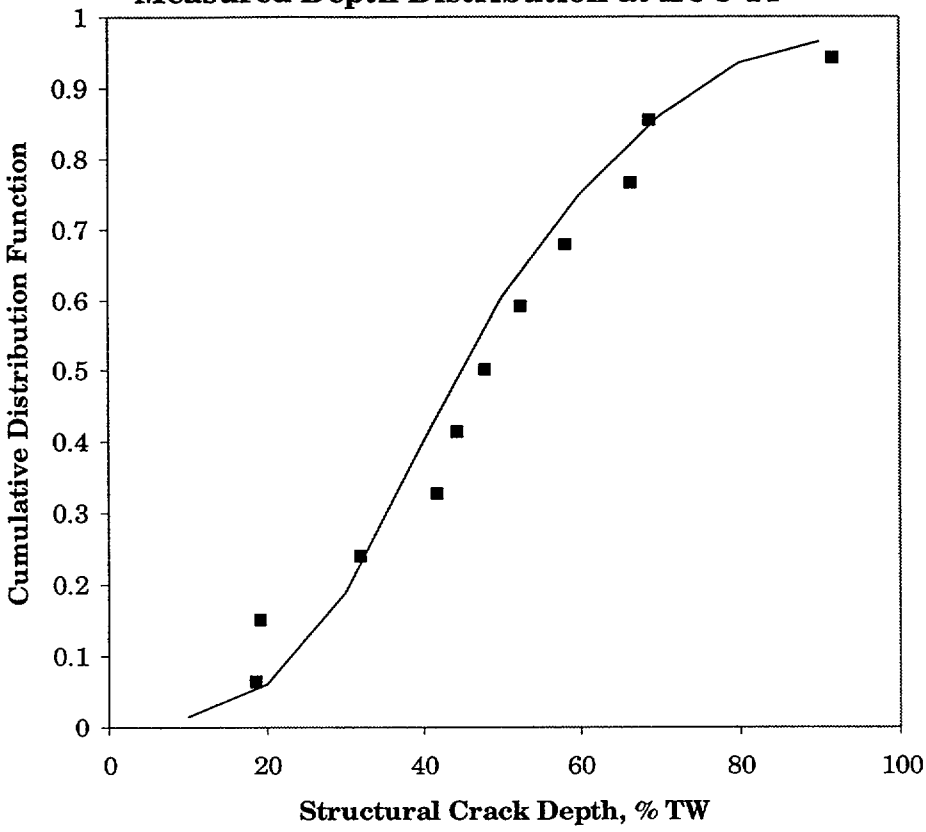

Figure 6-5.

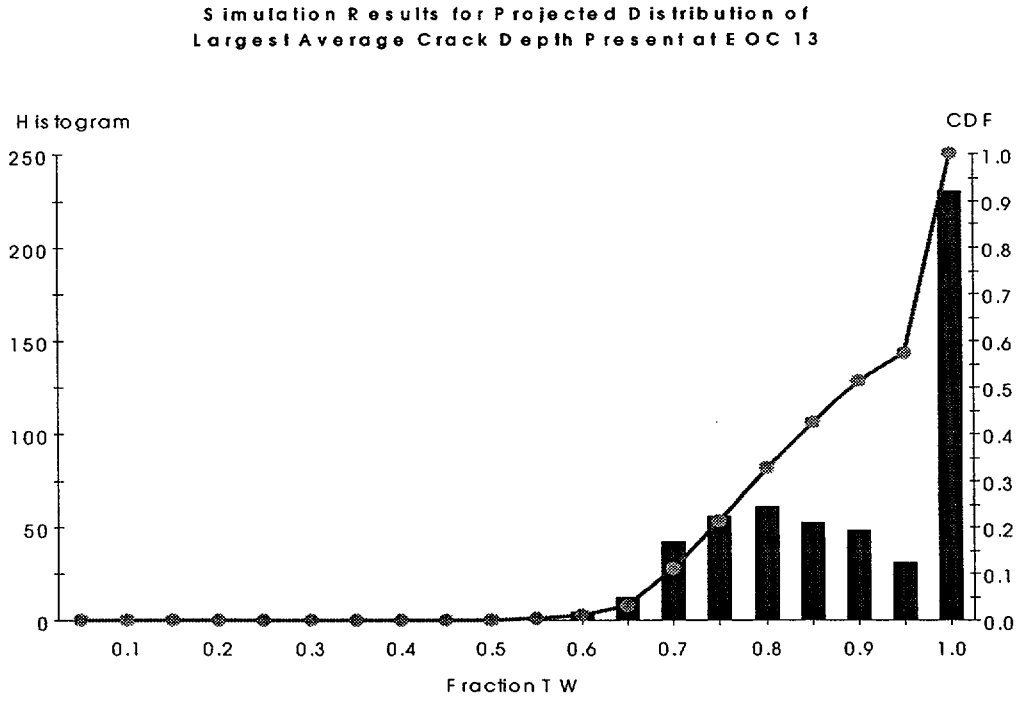

7.0 Historical Trends For Rows 2 And 3 U-Bend Indications

7.1. Introduction

Although low row cracking has been reported in operating SGs for many years, the incidence of PWSCC has been relatively low and has occurred dominantly in row 1 U-bends, and to a much lesser extent in the row 2 U-bends. The early incidence of cracking of the row 1 U-bends, and several large leakage events in row 1 U-bends, caused a number of the operating plants to preventively plug all of the row 1 tubes, or to apply thermal stress relief process to mitigate the residual stresses in the tubes. However, several plants with low T_{hot} continue to operate successfully with non-stress relieved row 1 U-bends in service. Very few cracks have been reported in the row 2 U-bends, and no large leakage events due to row 2 cracking had been reported until the Indian Point-2 leakage event. Only one axially oriented apex PWSCC indication has been reported in a row 3 tube. Axial ODSCC has been reported at a few plants in row 3 U-bends. This section provides a summary of key industry experience and analysis results to show that axial PWSCC in the row 3 tubes is extremely unlikely in the near term, in particular, during the term of the next operating cycle at Indian Point-2.

7.2 Industry Low Row U-bend Indication History

Cracking of low row U-bends, principally row 1, has been reported early in the operating life of operating Model 44 and Model 51 SGs. Two distinct modes of cracking have been observed: PWSCC at the apex of the U-bend, which has been associated with large leakage events, and tangent point leakage, which is characterized by small controlled leakage or no leakage. Tangent point leakage is the results of a characteristic of the Westinghouse bending process that results in an irregular transition at the end of the bend, and which has not been significantly observed in U-bends manufactured by Huntington Alloys, the manufacturer for the Indian Point-2 tubes. This section primarily addresses apex cracking, which was the cause of the leaking tube, R2C5, at Indian Point-2.

7.2.1 Bend Radius Influence on Low Row Cracking

In September 1976, a large leakage event, estimated by the NRC at 330 gpm (Reference 10-16), occurred at Surry 2. The leakage was traced to an apex crack in a row 1 U-bend, R1C7, SG-A (Figure 7-1). This leak was attributed to PWSCC arising from high stresses created by denting of the TSP and deformation of the tube straight legs via hourglassing. Examination of the top TSP of SG 2A showed that the flowslots had decreased from a nominal 2.75 inches to an average size of 1.46 inches; thus the average hourglassing was greater than 1.25 inches. Examinations of nine row 1 U-bends showed that the tubes adjacent to the flow slot (7 of 9) all had experienced PWSCC. Although the row 1 tubes were significantly affected by PWSCC, no indications were reported in the row 2 U-bends.

At approximately the same time, 31 low row U-bends were removed from Surry 1 with a denting condition similar to Surry 2. The 31 tubes removed included row 1, row 2 and a

single row 3 tube. Destructive examination of these tubes showed that only the row 1 tubes experienced PWSCC. No cracks were found in the row 2 tubes or the single row 3 tube.

Further in 1976, 31 low row U-bends were removed from Turkey Point 4, a plant that had also experienced denting. Fifteen were row 1, fifteen were row 2 and one was row 3. All of the tubes were examined visually and radiographically, from three different rotations. Dimensional measurements on leg spacing were also taken. Leg spacing measurements indicated a reduction of the nominal leg spacing of about 0.2 inch for the row 2 U-bends. Twenty-four of the tubes were examined, in some cases with eddy current, but in all cases with destructive examination techniques. Three of the examined row 1 U-bends showed degradation. None of the cracking was completely through-wall and the crack networks were not well established. Only row 1 tubes were observed to be cracked with no cracking detected in the examination of the row 2 tubes or the row 3 tube.

In 1979, Doel 2 experienced a large leak event (135 gpm) due to cracking at the apex of a row 1 U-bend (Reference 2). The leaking crack was characterized as a "relatively long axial crack". Ovalization of the tubes, measured by pushing various size ball bearings through the tubes, was identified as the cause of the cracking. The Doel 2 low row tubes were bent without using a ball mandrel to reduce ovality, and the resulting ovality is higher than obtained in tubes bent by Westinghouse or Huntington Alloys. The row 1 tubes with ovalization above the design limit were plugged, and the plant was restarted. No row 2 indications were reported. The operating period of the plant at that time was 3.20 EFPY. In 1994, when the plant had accumulated 14.9 EFPY operation, the first indication in a row 2 tube was reported.

The common observation among these examples of severe row 1 cracking is the absence of row 2 cracking. For all of dented plants examined, no row 2 cracking was observed at the time the row 1 tubes experienced cracking. This conclusion applies also to Doel 2 with significantly ovalized tubes that were judged the cause of row 1 cracking. The onset of row 2 cracking lagged the row 1 event by 11.7 EFPY operation. For the latter case, it is reasonable to assume that the row 2 tubes were manufactured similarly to the row 1 tubes, thus exhibiting similar ovalization trends as the row 1 tubes. Therefore, it is concluded that the propensity for axial PWSCC at the U-bend apex is strongly dependent on the bend radius of the U-bends.

Laboratory and analytical studies have been performed to investigate the cracking behavior of low row U-bends. Reference 10-19 presents the results of corrosion tests in polythionic acid of row 1, row 2 and row 3 U-bends of mill annealed Alloy 600 7/8"diameter by 0.05" wall thickness tubing. Two different bending techniques were evaluated: a) the technique typical of Westinghouse and Huntington Alloys manufactured tubing that utilized an internal bronze ball mandrel for bending rows 1 and 2 U-bends, and no mandrel for the row 3 U-bends, and b) a technique that utilized a plastic bullet-shaped internal mandrel for bending the rows 1 and 2 U-bends. A key conclusion from the corrosion test was that while the row 1 and row 2 U-bends were found to crack in the polythionic acid environment in about 25 to 75 hours, none of the row 3 U-bends cracked during the period of the tests. The locations of the cracks generated in these tests were

principally between the tangent point and the apex, although apex cracking was also observed. These tests confirm that the bending process difference between the row 2 and row 3 tubes significantly increases the time to cracking of the row 3 U-bends compared to the row 2 U-bends.

7.2.2 Effect of Operating Temperature

Operating temperature is an important factor in the initiation of PWSCC. This is demonstrated by Figure 7-2, which shows the initial observation of row 2 U-bend cracking as a function of the operating temperature, T_{hot}, of several operating plants. The trend of the data is consistent with the expected temperature relationship for PWSCC. Indian Point-2, because of its low operating temperature, exhibits the longest time to initiation of row 2 cracking among the plants for which data are available. The Indian Point-2 data point tends to be below the trend curve of Figure 7-2, which may be attributable to hourglassing of the top TSP. Initiation of row 2 PWSCC at Indian Point-2 may have been somewhat earlier than shown in the figure, but not detected until EOC-13.

The same temperature dependent trend is expected to apply for initiation of cracking in row 3 U-bends. The only row 3 PWSCC indication reported to date was reported in a SG operating near 620 °F or about 25 °F higher than Indian Point-2. Thus, among the operating plants, Indian Point-2 would be expected to have a long operating time increment between first incidence of row 2 cracking and expected incidence of row 3 cracking. The incremental time between initial row 1 and row 2 cracking observed at Doel 2 was approximately 11- 12 EFPY as noted above. This interval is consistent with expected times to initiation of row 3 relative to row 2 cracking developed from stress considerations as described in Section 7.3. The plants that are operating at T_{hot} greater than that for Indian Point-2 can be considered indicator plants for Indian Point-2, regardless of U-bend stress relief, since stress relief was applied only to the row 1 and row 2 tubes.

7.2.3 Recent History of U-bend Indications

NDE data for currently operating or recently replaced Westinghouse Model 44, Model 51 and selected Model D SGs were reviewed for low row U-bend indications. The results of this review are given in Table 7-1. In addition to Indian Point-2, axial PWSCC at the apex of row 2 U-bends has been found in only one SG. Only one PWSCC indication has been reported in row 3 for these SG models. This indication occurred in a Model D SG operating at high temperatures (near 620 °F), and with no significant TSP denting. These SGs have since been replaced. Two plants have reported axial ODSCC in row 3 with two of the indications reported at the apex of the tube. These inspection results support the low likelihood of finding row 3 axial PWSCC at Indian Point-2 in Cycle 15.

Inspection results for replaced SGs are not readily available for comparisons with the Table 7-1 data. For plants that had substantial denting and TSP hourglassing, tube plugging data cannot be used as a measure of potential row 3 indications. In the severely dented plants, tubes in two rows out from tubes found to have probe restrictions below acceptance values were plugged as a preventive measure for potential hourglassing

effects. Many row 3 tubes were plugged by this guideline for dent restrictions in rows 1 and 2.

7.3 Stress Effects Resulting from TSP Hourglassing

7.3.1 Westinghouse Analyses

Independent analyses of the low row U-bends (rows 2, 3 and 4) were performed by Westinghouse and ALTRAN (Reference 10-17) with the objective of evaluating the sensitivity of the tube stresses to pinching of the straight legs resulting from hourglassing of the TSP flow slots. An analysis was performed as described below that assumed no residual stresses resulting from the bending process. The objective of the analyses was to evaluate the relative stresses in the low row U-bends resulting from TSP hourglassing in order to assess the comparative sensitivity to cracking of the rows 2, 3 and 4 U-bends.

Finite element (FE) models of the U-bend tubes in rows 2, 3 and 4, above the upper most tube support plate (TSP #6), were developed. The FE model contains 1080 3D brick elements with elastic-plastic large strain and large displacement capabilities. A bilinear stress-strain law was assumed with kinematic unloading and a 2Sy Bauschinger effect. These models were used to make a comparison of the relative structural responses of the low row U-bends to the service loads and potential hourglass displacement of the adjacent TSP flow slot. The service loads consist of internal primary side pressure, external secondary side steam pressure, the throughwall temperature gradient and the thermal interaction of the tube with the TSP. The TSP hourglass displacements, measured at approximately 0.47 inch maximum at Indian Point-2, were expected to be sufficient to cause stresses in tube that exceed the expected elevated temperature yield strength of the tube.

Figure 7-3 shows preliminary results of the finite element calculated hoop stress on the inner surface of the tubes at the extrados of the U-bend apex. The maximum hoop stress at other locations along the U-bend axially removed from the apex is less than the stress at the apex, but follow the same trend as shown for the apex.

Figure 7-3 shows that a stress plateau is reached for a model that assumes no residual stresses in the tube, that is, the stress exceeds the yield strength, when the leg spacing at the TSP is reduced by approximately 0.15 inch. The maximum stress is respectively lower for the rows 3 and 4 tubes for the same assumed leg pinching, however, the yield point is reached with only a small increase in the straight leg pinching. For the same value of flow slot hourglassing, the row 3 straight leg pinching is estimated to be about 0.1 inch less than that for a row 2 tube in the same column. Similar results have been obtained by ALTRAN (Reference 10-17) in a separate analysis as described below in Section 7.3-2. The ALTRAN analysis also shows that the stress levels are reduced for ovalized tubes typical of the low row U-bends.

Attempts to model the residual stresses in the U-bends proved unsuccessful, largely due to the absence of consistent data against which to baseline the results. However, if the residual stresses at the ID of the extrados are assumed to be tensile in the hoop direction,

the critical value of TSP hourglassing displacement in Figure 7-3 would be shifted to the left (i.e., smaller displacement). Conversely, if the residual stresses are assumed to be compressive, the critical displacement would increase. Since the measured displacement is large compared to the critical displacement, the same final stress condition as show on Figure 7-3 would be attained for the Indian Point-2 tubes, regardless of the assumption of the direction of the residual stresses.

The results of the stress analyses show that the final stress state of the low row U-bends decreases with increasing bend radius, and thus, the susceptibility to PWSCC decreases commensurately. Although the displacement of the straight legs decreases with increasing row number for a constant hourglassing displacement, the principal factor limiting the stress is the greater flexibility of the larger radius U-bends, and the reduced strain hardening of the larger bends.

Current literature studies (summary of Reference 10-21, for example) on the effects of strain rates on crack initiation and growth do not permit a well-defined basis for evaluation. At typical SG temperatures, strain rates > 10^{-7}/sec are more likely to lead to mechanical overload than SCC. Strain rates in the range of 10^{-7}/sec to 10^{-8}/sec appear to be the most influential on SCC initiation as this range is most sensitive to the film breakdown/crack initiation/repassivation mechanism. A minimum strain rate for SCC initiation is not defined in the literature, which may be due to excessive test times required for evaluation. Multiple studies (Reference 10-21) have indicated that only SCC initiation may be strain rate dependent and average crack growth rates are approximately independent of strain rate. Separation of applied strain rates from creep related effects is also not clear in the literature. The applied strain rate for the U-bends would have to result from continued hourglassing of the TSPs, which is very low or zero. Strain rates in the next cycle for the row 3 U-bends cannot be quantified. Potential strain rates for row 3 U-bends should be less in Cycle 15 than Cycle 14 due to decreasing progression of hourglassing. A strain rate of 10^{-8}/sec corresponds to about 0.3 strain per year. This strain is two orders of magnitude higher than the total strain calculated in row 2 from TSP hourglassing to date and exceeds that in row 3. Any future applied strain rate would be much less than 10^{-8}/sec. It is concluded that any potential strain rate effect on crack initiation would be less than or equal to that in the prior cycle. Crack initiation, however, does not affect the acceptable operating cycle for U-bend degradation as new indications would not grow to structurally challenging indications over the recommended operating cycle. Since strain rate effects have no apparent influence on crack growth rates the influence of strain rates on the operating cycle evaluation is negligible.

7.3.2 Altran Analyses

As indicated in the secondary side condition monitoring assessment (Ref. 10-5), flow slot hourglassing has been leveling off over the recent years and any rate for continued hourglassing is very slow or zero. The existing extent of hourglassing that has been measured at TSP 6 in SG 4, has been shown both analytically and experimentally (see Attachment 1) to result in hoop stresses at the inside diameter of the apex extrados of the Row 2 tubes sufficiently high to be a major contributor to PWSCC at this location. Given that hourglassing progression has leveled off, the hoop stresses at the apex of Row 2 and

Row 3 tubes would have peaked to their present level several years ago. Any increase in hoop stress due to the present slow deformation of the top support plate will not substantially affect the relative susceptibility of Row 3 tubes as compared to the Row 2 tubes.

Conclusions from Attachment 1 based on analytical and experimental results, including support for the above observations, are:

- As indicated by the high ID hoop stress at the apex extrados resulting from the in-plane deformation of the U-bend tube legs, hourglassing in the top TSP appears to be a major contributor to PWSCC at the apex of the U-bends.
- As indicated by the lower ID hoop stress at the apex extrados for the Row 3 tubes as compared to the corresponding Row 2 tube, Row 3 tubes are much less susceptible to PWSCC than the Row 2 tubes. Also, based on the time to crack initiation study, PWSCC at the apex extrados of the mid flow slot Row 3 tube is expected to require a factor of 2.5 to 4.0 longer time for PWSCC to initiate compared to the corresponding Row 2 tube. .
- The residual stresses at the apex ID of a prototypically bent row 3 tube were measured to be compressive, thus reducing the potential for row 3 PWSCC.
- The behavior of the U-bend is such that future leg displacement, if it occurs, will not significantly increase the ID hoop stress at the U-bend apex and will not alter the relative susceptibility conclusion.
- Ovality resulting from the initial manufacturing of the tubes does not appear to have a significant effect on the ID hoop stress at the apex extrados for the Row 2 and Row 3 U-bends

7.4 Manufacturing Issues

Tube ovality has been implicated in the large leak events at Surry and at Doel, and has been studied in tubes removed from Surry and Turkey point. However, ovality alone is not an adequate indicator of the propensity for cracking in the U-bends. Unless ovality exceeds drawing requirements for Westinghouse SGs, other effects from manufacturing and TSP hourglassing are expected to be more important than ovality for crack initiation. The manufacturing process is thought to significantly affect the residual stress condition of the as-bent U-bends. Many studies have been performed on the residual stresses in low row U-bends; however, no firm conclusions on the exact nature of the residual stresses have been reached. Altran measurements (see Attachment 1) on row 2 tubes bent without a ball mandrel have indicated compressive residual stresses at the apex extrados ID and tensile on the OD. An additional consideration is the following qualitative scenario first proposed in 1978 in response to a RAI from the NRC to explain the absence of axial PWSCC in the Row 3 U-bends.

The row 1 and 2 U-bends were manufactured by using an internal mandrel to limit tube ovalization during bending. In contrast, the row 3 tubes were bent around a die without the use of an internal mandrel. This was common practice by both Westinghouse and Huntington Alloys at that time. The design ovality limit for all of these rows was the

same, i.e. 10%. During bending of the row 1 and row 2 U-bends, the tube naturally tends to ovalize; however, the internal mandrel forces the tube to return to a near circular condition. Thus, as the mandrel passes, the tube attains its equilibrium condition by an elastic springback toward the ovalized condition. This springback may result in a throughwall bending stress gradient in the hoop direction that is tensile at the ID of the tube and compressive at the OD. The operating pressure hoop stress is additive to the residual stress.

For U-bends bent without the use of an internal mandrel, the bending process results in ovalization of the tube cross section without restoration. When the bending process is completed, the elastic springback to achieve equilibrium is in the direction of restoration of the circular cross section. Consequently, the ID bending stress in the hoop direction is compressive, and the OD stress is tensile. The addition of operating ΔP hoop stress results in a reduced hoop stress condition at the ID of the tube compared to the row 2 and row 1 tubes that were bent using an ID mandrel.

7.5 Conclusions

Based on consideration of industry experience with low row U-bend cracking, stress analysis of the low row U-bends, and manufacturing considerations, the following conclusions can be drawn with regard to row 3 U-bend susceptibility to apex axial PWSCC at Indian Point-2:

1. Only one PWSCC indication has been reported in row 3 for Westinghouse SG models. This indication occurred in a Model D SG operating at high temperatures (near 620 °F), and with no significant TSP denting. A few plants have identified axial ODSCC in row 3 U-bends.
2. Based on analyses of the total stresses in the U-bends including hourglassing effects, PWSCC at the apex is not expected to be present in row 3. The difference between the row 2 and row 3 tube stress levels shows that the time to crack initiation in row 3 would be approximately 2.5 to 4 times the time required for row 2 crack initiation. This is consistent with the fact that no indications were seen in row 3 at Indian Point-2.
3. The behavior of the U-bend is such that future leg displacement, if it occurs, will not significantly increase the ID hoop stress at the U-bend apex and will not alter the relative susceptibility conclusion between row 2 and row 3 U-bends.
4. The time to initial observation of row 2 cracking at Indian Point-2 has been greater than for other operating plants, consistent with the lower operating temperature of Indian Point-2. The initiation of cracking in the row 2 U-bends as influenced by denting and hourglassing effects is compensated by the lower operating temperatures at Indian Point-2. A like relationship is expected to apply for potential row 3 cracking. Since none of the plants with mill annealed Alloy 600 tube have heat treated the row 3 and larger U-bends, plants operating at higher temperatures are indicator plants for potential row 3 cracking at Indian Point-2.
5. Accelerated corrosion laboratory tests with prototypic U-bends in polythionic acid have shown that row 3 tubes did not crack in the time that row 2 U-bends cracked,

confirming that the manufacturing process differences have significant influence on the cracking behavior of the low row U-bends.

6. Manufacturing differences between the row 2 and row 3 tubes may result in residual stress states that may enhance row 2 susceptibility to PWSCC while reducing the susceptibility of the row 3 tubes to cracking.

Table 7-1. Summary of U-Bend Rows 2 and 3 Indications
Westinghouse Originally Supplied Model 44 and Model 51 Steam Generators

Plant	Year Ind. Found	Heat Treat	Probe	Crack Type		ID or OD Crack		U-Bend Location	
				Axial	Circ.	PWSCC	ODSCC	Near Apex	Near Tangent
Row 3 Indications									
Farley-1	1997	No	+Point	1			1	1	
	1997	No	+Point	1			1		1
Farley-2	None	No							
Diablo Canyon-1	None	No							
Diablo Canyon-2	None	No							
Sequoyah-1	None	No							
Sequoyah-2	None	No							
Kewaunee	2000	No	+Point	5 tubes 11 ind.			5 tubes 11 ind.(1)	1 tube 1 ind.	4 tubes 10 ind.(2)
	None	No					3 MBMs '95, '96		3
Prairie Island-1	None	No							
Prairie Island-2	None	No							
Indian Point-2	None	No							
McGuire-1	1991	No	Pancake	1		1		≈1"from apex	
Row 2 Indications									
Farley-1	1991	Yes	Pancake	1 tube 2 ind.		1 tube 2 ind.			1 tube 2 ind.
	1994	Yes	Pancake	2			2		2
Farley-2	None	Yes							
Diablo Canyon-1	1992	Yes	Pancake	1		1			1
	1994		Pancake	1		1			1
	1997		+Point	1		1			1
Diablo Canyon-2	1996	Yes	+Point	1		1			1
	1998		+Point	1		1		1	
Sequoyah-1	None	Yes							
Sequoyah-2	None	Yes							
Kewaunee	1990	No	Bobbin/ Pancake		1				1
	2000	No	+Point	1 tube 2 ind.		1 tube 2 ind.(1)			1 tube 2 ind.
Prairie Island-1	None	No					1 MBM '81		1
Prairie Island-2	None	No							
Indian Point-2	1997	No	+Point	1		1		1	
	2000	No	+Point	8 tubes 15 ind.		8 tubes 15 ind.		8 tubes 15 ind.	

Notes:
1. New inspection results under review as potential MBMs. Indications were plugged.
2. Indications located between 1 inch above tangent and 1 inch below apex.

Figure 7-1. Radiograph of Tube R1C7 from Surry 2, SG A, 1976

Radiography Reveals Both Intrados and Extrados Cracking in Surry 2 U-Bend

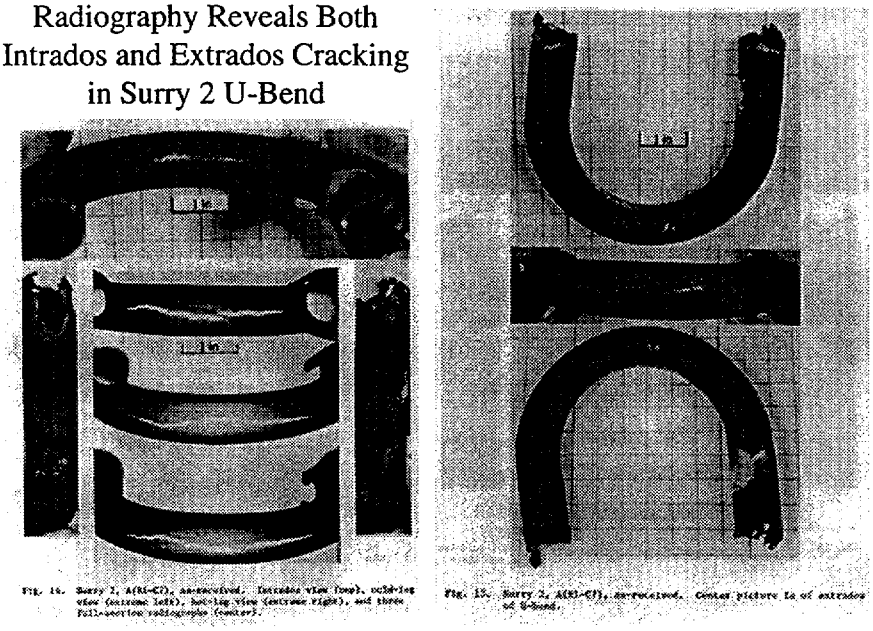

Figure 7-2
First Appearance of Row 2 U-bend PWSCC

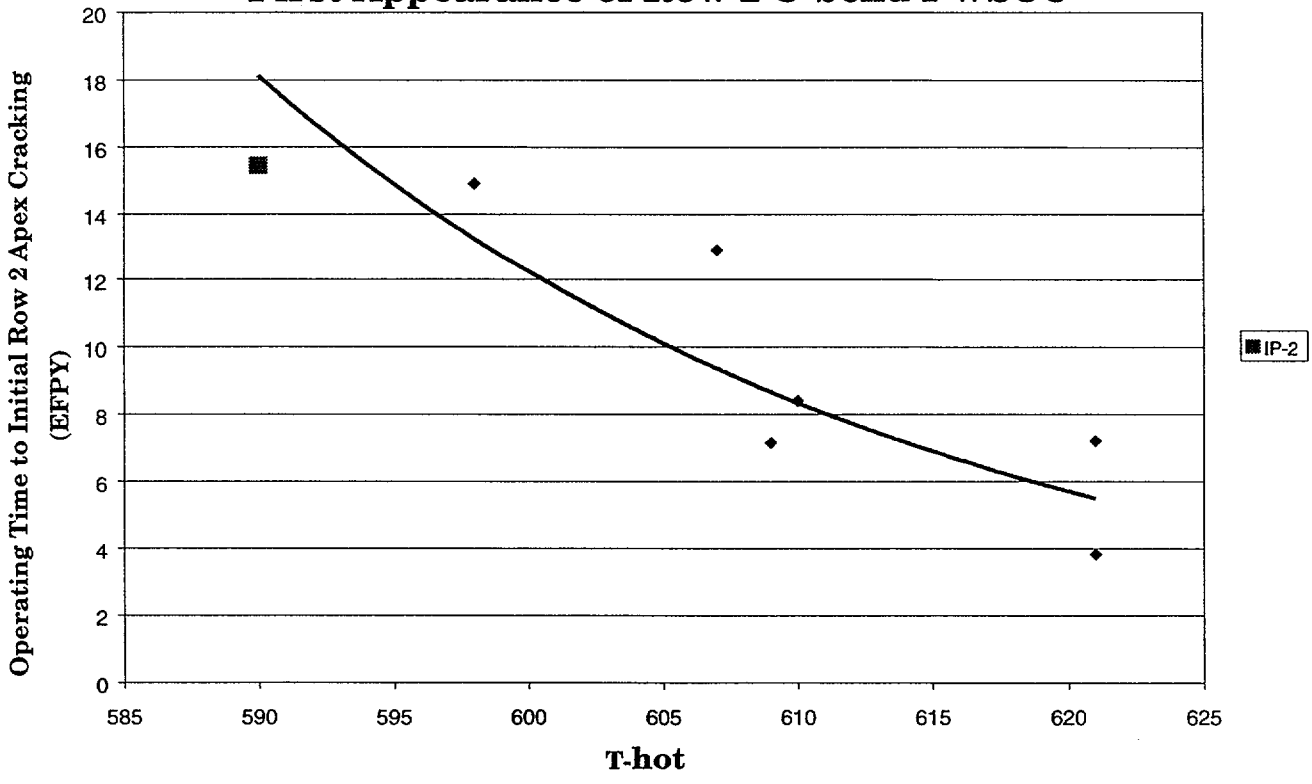

Figure 7-3
Finite Element Model Calculated Hoop Stresses
vs Reduction in Straight Leg Spacing from Nominal Dimension

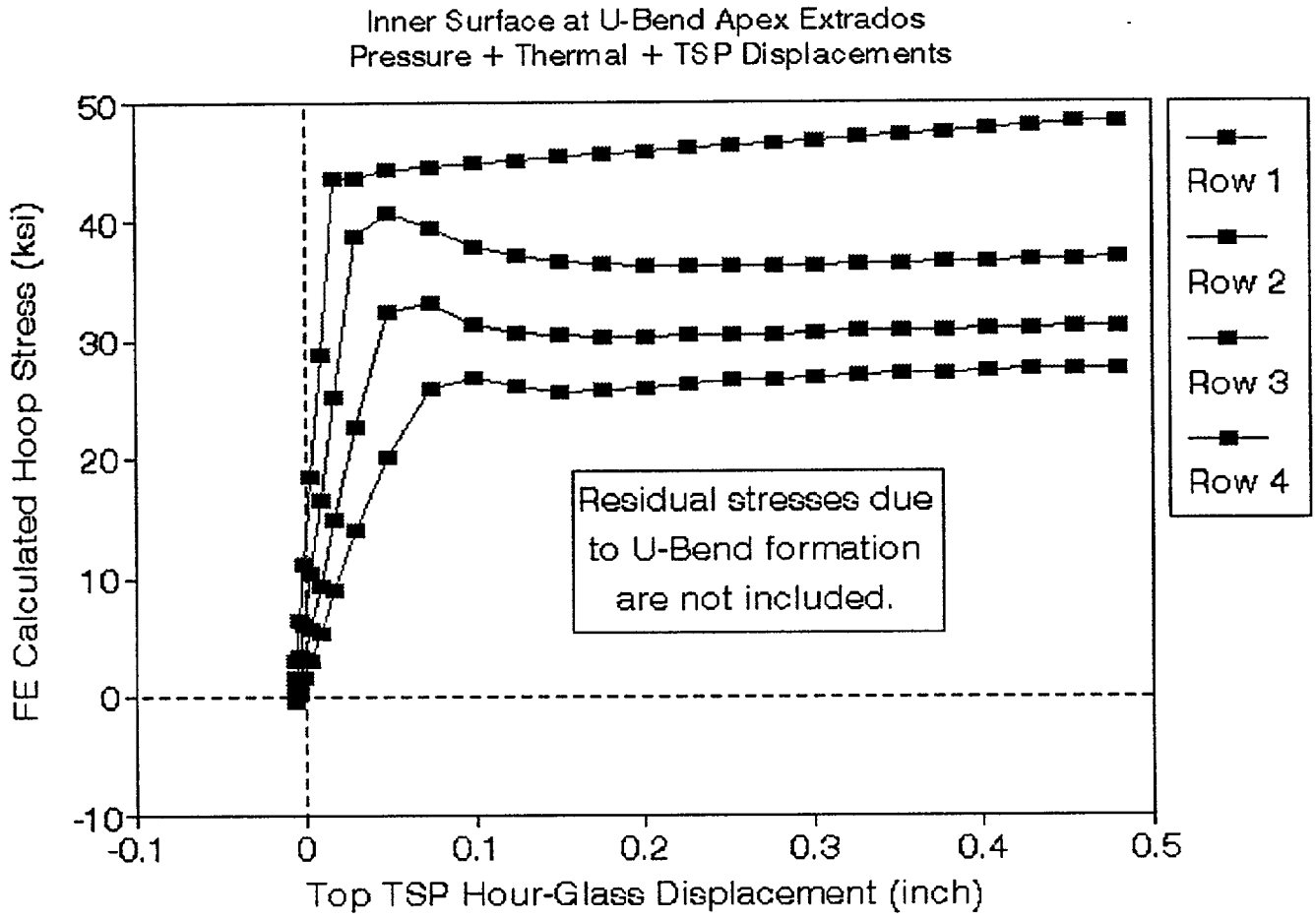

8.0 CONDITION MONITORING ASSESSMENT FOR U-BEND AXIAL PWSCC

8.1. R2C5 Assessment

As noted in the causative mechanism report of Reference 10-2, the cause of the leaker outage in March, 2000 was an axial PWSCC indication at the apex of the U-bend in tube R2C5. The indication was masked by deposits in the 1997 inspection and was not detected, which resulted in leaving a relatively large indication in service. Estimates of the depth profile for the R2C5 indication in 1997 were shown in Figure 6-1. The estimated leakage was 103 gpm leading to the forced outage.

Visual exam of the indication following the leakage event indicated a throughwall crack about 2 to 2.4 inches long as shown in Figure 8-1. It can be seen that at least five ligaments between crack sections were torn during the crack opening including a large ligament near the center of the crack. This large ligament may be the dip in crack depth seen in the Figure 6-1 profile. The crack opening length is about the same as found for the deep section in the 1997 profile. There is no indication of a tube burst that would have crack extension at the tips of the crack and fishmouthing of the crack opening. It is concluded that the leakage was caused by ligament tearing. As discussed in Section 5.4, the average crack depth of the indication at the time of ligament tearing would be about 90% throughwall based on the ANL ligament tearing model.

Since the allowable leakage limit for freespan indications is 1 gpm, the R2C5 leakage event represents a condition monitoring failure due to leakage exceeding requirements.

8.2. Evaluation of In Situ Test Results for U-Bend Axial PWSCC

The in situ test results were given in Table 3-2. As discussed in Section 3.5, the indications exceeding the $3\Delta P_{NO}$ = 4940 psi burst margin requirement at room temperature with no leakage were: SG 4 indications at R2C69, R2C72 and R2C4; the SG 1 indication at R2C87; and the SG 3 indication at R2C85. None of these indications leaked at SLB conditions and all leakage requirements are satisfied for these indications. The SG 4 indication in R2C71 had a small leak rate at SLB conditions and is separately evaluated in this section.

The R2C69 indication had no leakage up to 5172 psi and a ligament tear above this pressure that resulted in leakage exceeding 2 gpm. R2C69 was +Point inspected following the in situ test. However, the probe did not pass through the entire indication as the coil apparently became stuck in the crack opening. Figure 8-2 shows the pre and post in situ depth profiles including the partial length posttest profile. From the available data, it would appear that the ligament in the deepest part of the crack tore to throughwall. However, since the test pressure exceeded the $3\Delta P_{NO}$ = 4940 psi burst margin requirement and no leakage occurred at SLB conditions, all condition monitoring requirements were satisfied for this indication.

The SG 4 indication at R2C74 exceeded the $3\Delta P_{NO}$ burst margin with a small initial leak rate of 0.035 gpm at 4800 psi and a leak rate of 0.112 gpm at a pressure of 5500 psi. Thus, the in situ tests demonstrate that this indication also satisfied condition monitoring burst margin and SLB leakage requirements. The leak rate data were further evaluated to estimate the throughwall length resulting from ligament tearing for this indication above 4800 psi as discussed in Section 6.1.3. Based on calculations of the throughwall crack length to match the measured leak rates, tearing of the wall thickness ligament resulted in a throughwall length of about 0.16 inch at 4800 psi, which increased to about 0.18 inch at 5500 psi. The pre in situ length for R2C74 by +Point was 0.16 to 0.19 inch. The post in situ +Point data for this indication was distorted due to apparent probe slippage and length/depth evaluations for this short indication are approximate. The post in situ test length of 0.39 inch may be overestimated. Figure 8-7 compares the 800 kHz pre and post in situ depth profiles estimated for R2C74. This indication had the lowest signal to noise ratio of all the U-bend indications. The initial sizing evaluation, shown as "Pre In Situ" in Figure 8-7, is an apparent underestimate of the depth of this indication as is the 400 kHz sizing not shown in the figure. An effort was made to resize the indication by interpreting the maximum possible depth for the pre in situ +Point response. This evaluation is shown in Figure 8-7 as the "Pre In Situ Max. Depth Evaluation". This result would be more consistent with the leakage found at 4800 psi for this indication. Since there was no leakage at SLB conditions and the maximum test pressure of 5500 psi exceeded the $3\Delta P_{NO}$ = 4940 psi burst margin requirement, all condition monitoring requirements are satisfied for R2C74.

R2C71 Evaluation

The only remaining U-bend indication at R2C71 in SG 4 was limited in the in situ test to 4500 psi due to leakage reaching the test system measurement capability of 1.99 gpm. Based on adjusting the in situ test leakage measures to hot SLB conditions, the SLB leak rate for R2C71 was 0.024 gpm or well below the allowable limit of 1 gpm per SG. From the condition monitoring assessment of Reference 10-1 for other degradation mechanisms, no other leakage at SLB conditions would be expected. Thus, with the exception of the R2C5 leakage, all other indications would collectively satisfy condition monitoring leakage requirements.

The depth of the R2C71 indication after the peak in situ pressure of 4500 psi can be estimated from the post test +Point depth profile and by the throughwall length required to fit the measured leak rate at 4500 psi and the subsequent measurement of 0.77 gpm at 1100 psi. Figure 8-3 shows the pre and posttest +Point depth distributions obtained at both 400 and 800 kHz for the R2C71 indication. The agreement in depth shape between the three profiles is reasonable recognizing that the pressurization of the crack from the in situ test opens the crack faces which increases the signal to noise ratio for the indication. The post in situ 800 kHz profile indicates two throughwall lengths each about 0.05 inch with the possibility that the depths above 95% may also be throughwall as indicated by the 400 kHz data. For the 2 gpm leakage level reached in the test, the throughwall lengths would need to be longer than the 0.05 lengths indicated by the 800 kHz data. The post in situ results of Figure 8-3 show considerable remaining wall thickness within the

flaw and the burst pressure would be expected to be considerably higher than the test pressure of 4500 psi.

The calculated throughwall length for R2C71 using the Westinghouse CRACKFLO code is shown in Figure 8-4. To predict the post peak pressure leak rate of 0.77 gpm at 1100 psi, a single throughwall length of 0.37 inch or two lengths of about 0.34 inch are required. For the post test leak rate analyses, the plastic crack opening at 4500 psi is added to the elastic opening at 1100 psi to calculate the leak rate with the throughwall length iterated until the predicted and measured leak rates are in agreement. These throughwall lengths also yield good agreement with the measured leak rate of 1.99 gpm at 4500 psi. This leakage based estimate for the throughwall lengths following the 4500 peak pressure yields somewhat longer throughwall lengths than obtained from the +Point sizing results.

The posttest profile of Figure 8-3 and the estimated throughwall lengths of Figure 8-4 show that two or three ligaments of the profile have torn throughwall, but the indication has not burst at the room temperature maximum test pressure of 4500 psi (4206 psi at operating temperature). The required burst pressure at room temperature is $3\Delta P_{NO}$ = 4940 psi (4617 psi at operating temperature). The R2C71 in situ test pressure time history can also be used to assess the test results. Figure 8-5 shows the pressure and leak rate time history for the indication. The pressure reached 4500 psi but the test equipment could not sustain the pressure as the system leakage reached the limit of 2 gpm. If the indication was near the burst pressure, it would be expected that the slope of the pressure time history would decrease due to plastic deformation of the crack opening. Figure 8-6 shows the slope at each of the four step increases in pressure and at the maximum pressure of 4500 psi. The slope at 4500 psi is essentially the same as at the lower pressures, thus indicating that the indication has not had discernible plastic deformation at the peak test pressure. The pressure history thus also supports a higher burst pressure.

It is clear from the above assessments, that R2C71 has not burst at the 4206 psi (hot conditions) test pressure. The burst pressure would have to be 411 psi higher than the test pressure to satisfy the $3\Delta P_{NO}$ = 4617 psi burst margin requirement. From Figure 8-3, the R2C71 crack length is about 0.59 inch from the pretest measurements with a very local maximum depth of 96%. The post in situ NDE indicates about a 0.69 inch length with two or three short throughwall lengths. These data indicate that the crack opening has not yet reached the full ligament tearing length obtained deterministically from the ANL model. From the Monte Carlo analysis results given in Table 6-3, the expected (50% probability) ligament tearing pressures would be about 4605 and 5215 psi for the 800 and 400 kHz profiles, respectively. The corresponding expected burst pressures would be 4828 and 5799 psi. While these results indicate a difference of 200 to over 500 psi between ligament tearing and burst pressures, these results are not directly comparable due to differences in uncertainty evaluations. Direct deterministic calculations applying the Westinghouse burst correlation and the ANL ligament tearing pressure yield a burst pressure exceeding the ligament tearing pressure by about 320 psi where the analyses predict burst effective lengths of 0.48 and 0.51 inch. Given that the indication has not yet reached full ligament tearing and that the burst pressure would be a few hundred psi

above ligament tearing, it can be concluded that the burst pressure would be more than 411 psi above the test pressure and would exceed the 4617 psi requirement.

The R2C71 evaluation can be summarized as follows:

- The posttest NDE profile shows only short throughwall lengths resulting from ligament tearing.
- The leak rate measurements made following the peak in situ test pressure indicate that the throughwall length following the peak test pressure was about 0.37 inch.
- Both the posttest NDE and leakage measurements show that the full ligament tearing length per the ANL model has not been achieved.
- The pressure increases to reach full ligament tearing plus the estimated 320 psi that the burst pressure is predicted to exceed the ligament tearing pressure would exceed the 411 psi increase above the peak test pressure necessary to satisfy the $3\Delta P_{NO}$ = 4617 psi burst margin requirement.

Therefore, it is concluded based on the above assessments that all the U-bend indications found in the EOC-14 inspection would satisfy the burst margin requirement of 4617 psi.

8.3. Condition Monitoring Assessment Conclusions

The above evaluations lead to the following conclusions for the condition monitoring assessment.

- Condition monitoring requirements for Cycle 14 are not satisfied due to the large leakage event due to axial PWSCC in the U-bend of SG 4 tube R2C5.
- All other U-bend PWSCC indications found in the EOC-14 inspection satisfied condition monitoring structural and leakage requirements.
- All U-bend indications found in seven tubes were in situ tested. Six of the seven indications did not leak at SLB conditions and the test pressures exceeded the $3\Delta P_{NO}$ = 4617 psi burst margin requirement.
- For R2C71 in SG 4, the indication did not burst at the maximum in situ test pressure of 4206 psi and the expected burst pressure would exceed the $3\Delta P_{NO}$ burst requirement of 4617 psi. This conclusion is based upon the post in situ test, short ligament tearing lengths to throughwall such that the indication had not yet reached full ligament tearing, and the predicted pressure difference between ligament tearing and burst of more than 320 psi. The SLB leak rate of 0.024 gpm is also well below the allowable SLB leakage limit of 1.0 gpm/SG for freespan indications.

Figure 8-1. Photomontage of R2C5 U-bend Indication

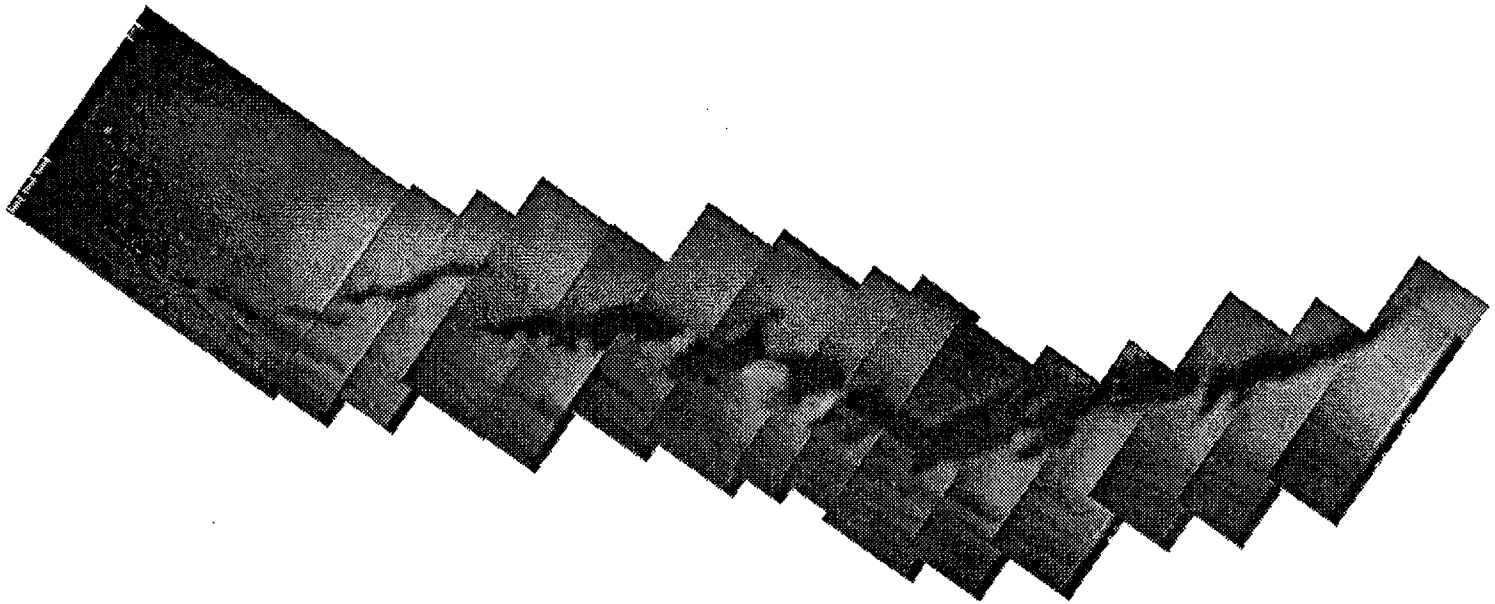

Photomontage of R2C5, SG24, Indian Point Unit 2 U-Bend Crack. Based on Images From the ID Video Inspection.

Figure 8-2
SG 4, U-Bend Tube, R2C69 Crack Depth Profiles
Comparison of Pre and Post In Situ
NDE Depth vs. Axial Length

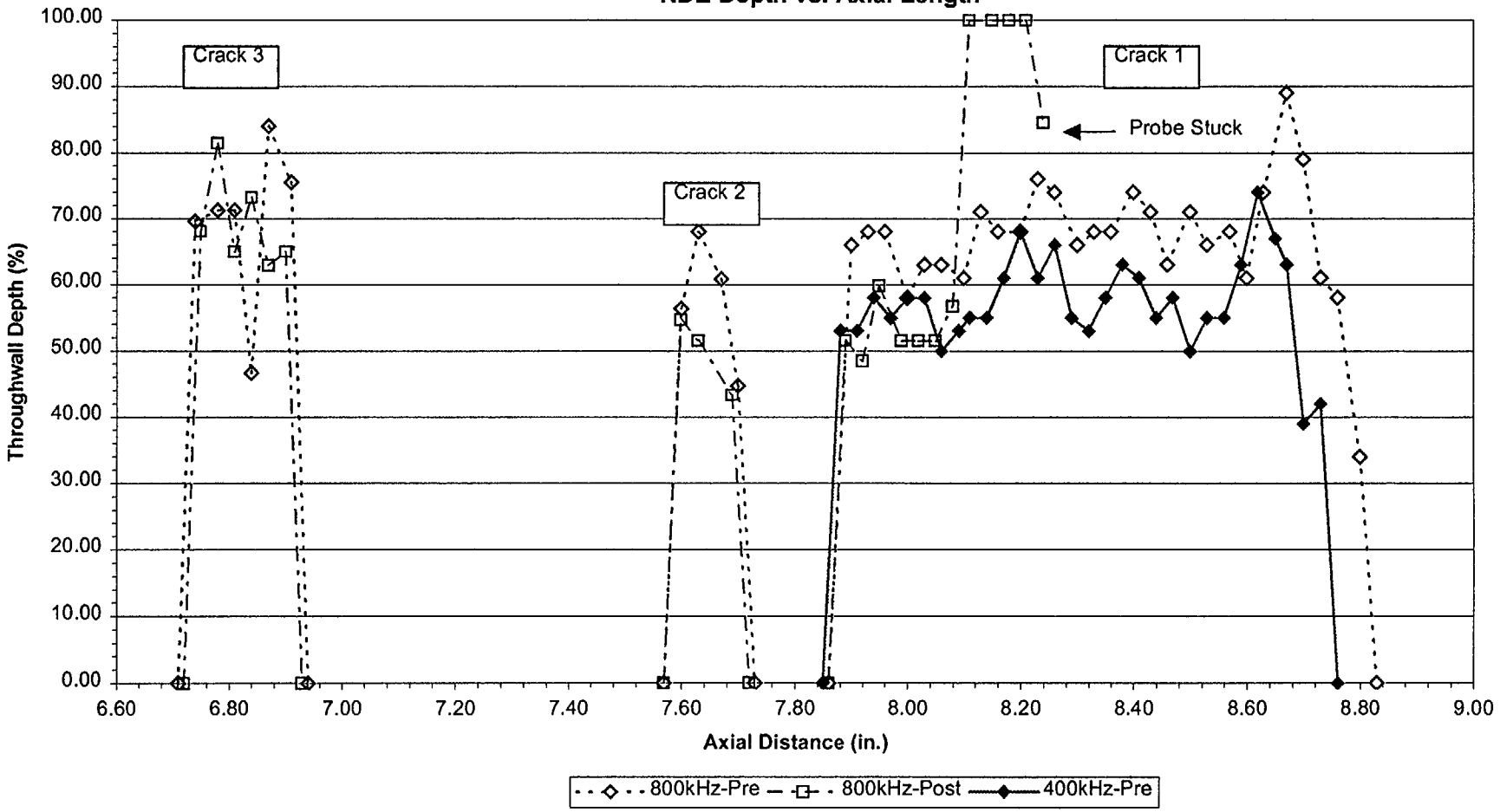

Figure 8-3
SG 4, U-Bend Tube R2C71, Crack Depth Profiles
Comparison of Pre and Post In Situ
NDE Depth vs. Axial Length

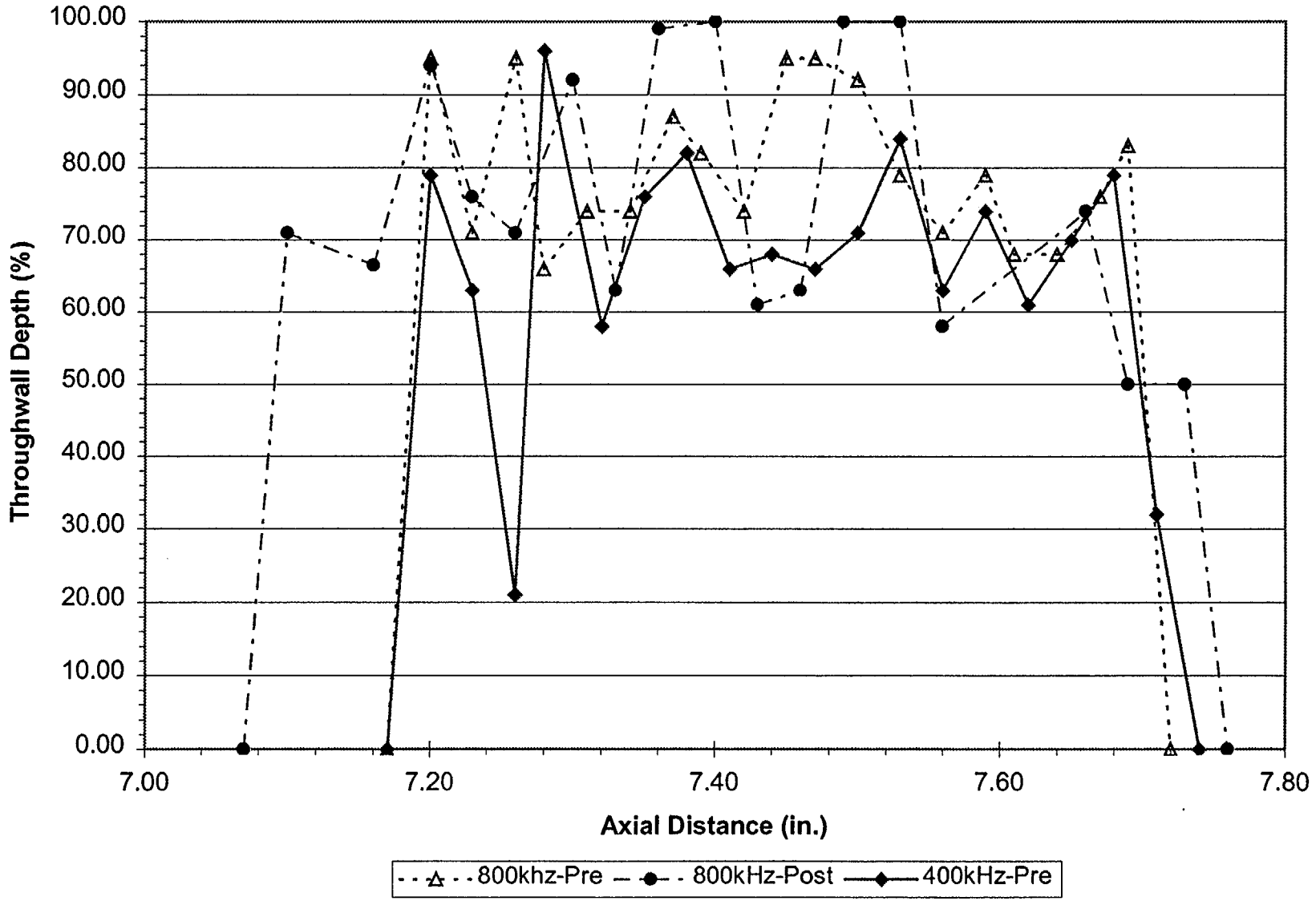

Figure 8-4. Indian Point-2 R2C71 Estimated Throughwall Length Following In Situ Test

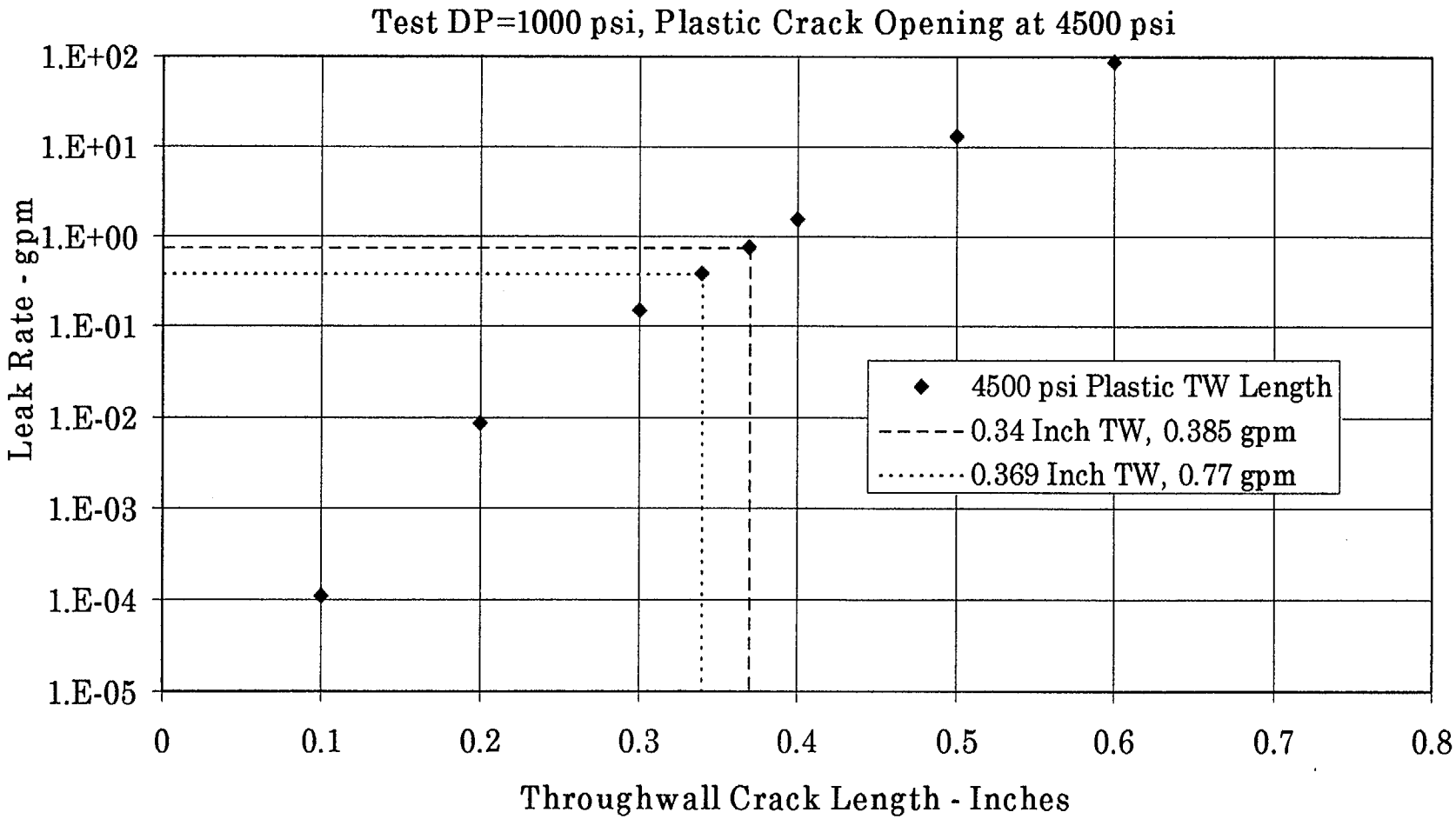

Figure 8-5. Indian Point-2 R2C71 In Situ Test Pressure and Leak Rate vs. Time

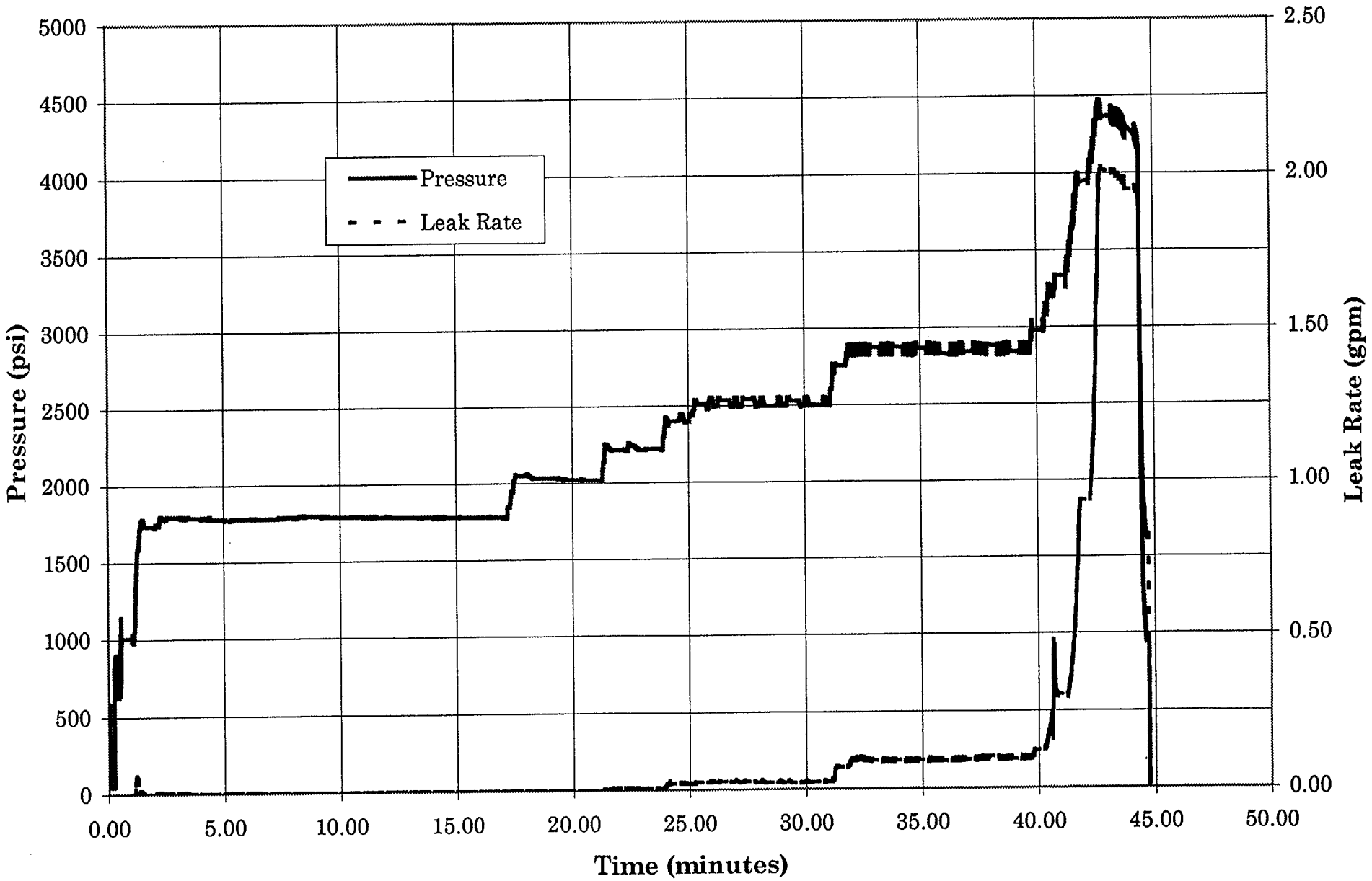

Figure 8-6. Indian Point-2 R2C71 In Situ Test Pressure vs. Time

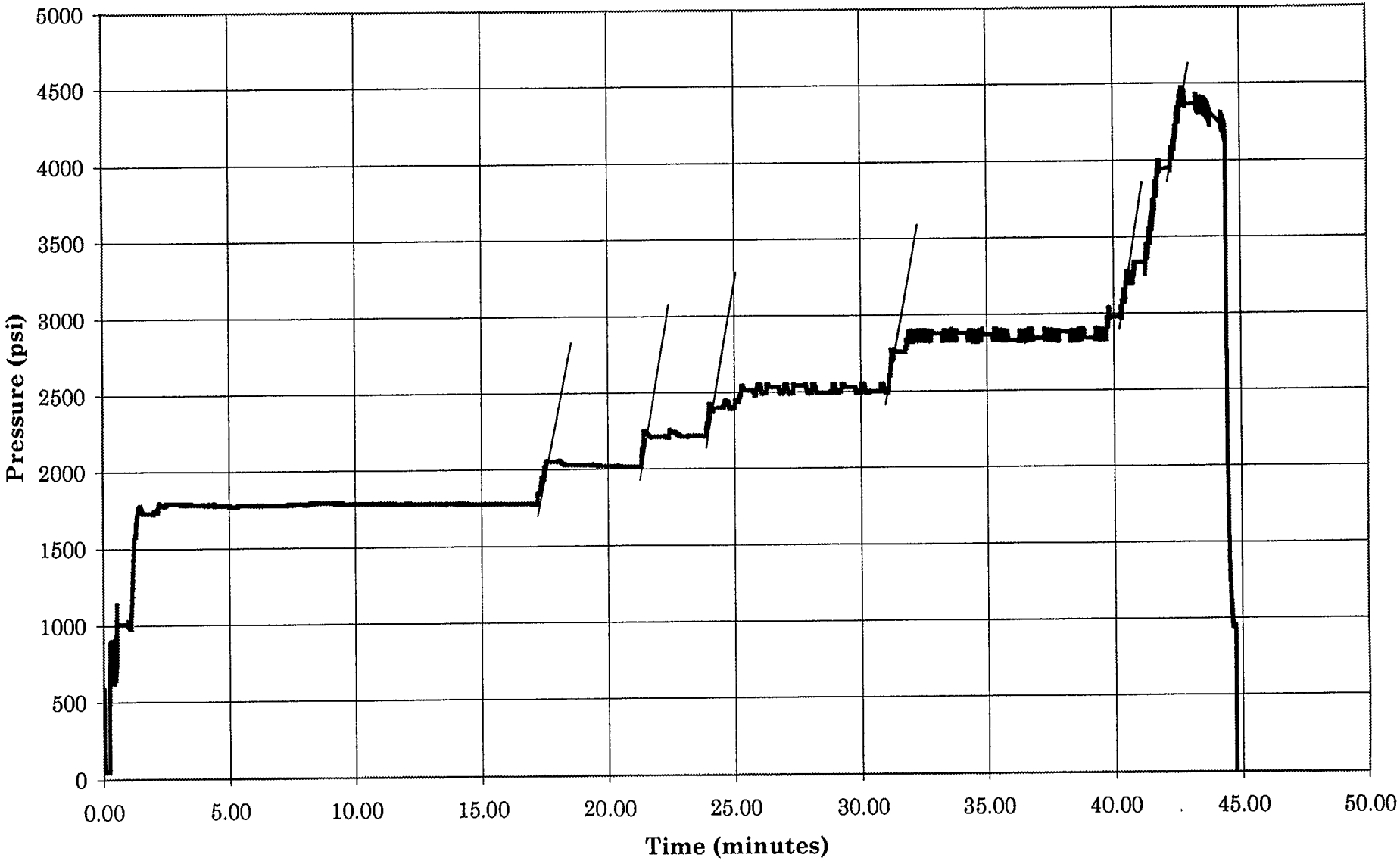

Figure 8-7
SG 4, U-Bend Tube R2C74, Crack Depth Profiles
Comparison of 800 kHz Pre and Post In Situ Test
NDE Depth vs. Axial Length

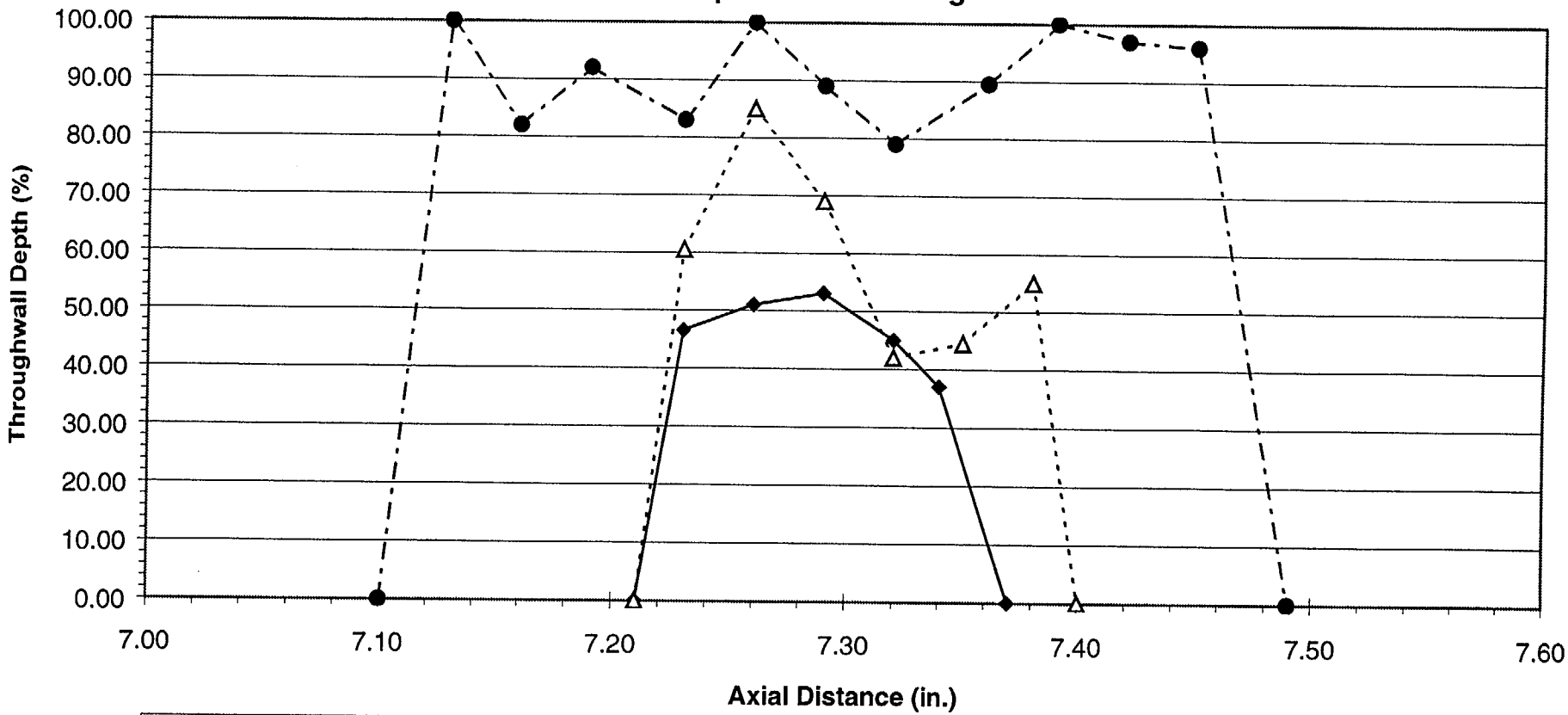

	Pre In Situ	Pre In Situ Max. Depth 2000	Post In Situ 2000
Length	0.16	0.19	0.39
Max. Volts	1.42	1.04	2.33
Max. D.(%)	53.0	85.0	100.0
Avg. D.(%)	39.4	53.2	83.1
Cal. Number	00240	00240	00245

9.0 OPERATIONAL ASSESSMENT

The overall objective of this section is to determine an acceptable operating period between inspections for axial PWSCC in the low row U-bends. Since all Rows 1 and 2 tubes have been plugged, the limiting low row U-bend would be Row 3. Since no indications were found in the row 3 U-bends in the EOC-14 inspection, no PWSCC indications would be expected based on historical plant operating experience for Westinghouse SGs as discussed in Section 7. The reduced stresses in the row 3 U-bends would be expected to extend the time to crack initiation in row 3 by about a factor of 2.5 compared to row 2 as noted in Section 7.3. Consequently, row 3 U-bend indications would not be a basis for limiting the Cycle 15 time between inspections. A very conservative approach is applied to define an acceptable operating period. That is, the operating period for the reference analysis is developed essentially as an acceptable period for row 2 by assuming that the indications found in row 2 were found in row 3.

Hourglassing of the TSPs due to denting with resulting reduction in the low row U-bend leg spacing leads to increased tensile hoop stresses at the apex of the U-bend. This effect is a contributor to the occurrence of apex PWSCC in the U-bends at Indian Point-2. These effects have been analyzed (Reference 10-5) including site measurements of leg displacements input to a TSP model to determine leg displacements by row and tube location. Results of these analyses support the conclusion that axial PWSCC in row 3 U-bends is not expected now or in the next cycle due to the lower stress levels in row 3. Based on historical monitoring of TSP hourglassing, Reference 10-5 concludes that denting and hourglassing are not significantly progressing at this time. Monitoring of tube restrictions to eddy current probes shows that the net number of restricted tubes did not change significantly in the EOC-14 inspection. The number of new restricted tubes is about equal to the number of previously restricted tubes that now pass the same size probe. This indicates that changes in the probe restrictions are a function of probe tolerances, probe pusher variations and operator variations, rather than denting progression. Based on the negligible denting progression, the following conclusions can be drawn relative to the analyses required for this operational assessment:

- Stress effects from leg displacement were present in the past cycles and are not changing significantly with time.
- Since denting progression is zero or small and decreasing with time, strain rate effects on the U-bend tubes are decreasing with time and would be the same or smaller in the next cycle compared to the last cycle. Consequently, strain rate effects on crack initiation would be the same or reduced for the next cycle. New indications, however, would not impact tube integrity at the end of the planned operating cycle due to modest growth. Literature data indicates that strain rate effects would not impact crack growth rates.
- Stress and strain rate effects due to denting are included in the crack growth rates developed from Cycle 13 U-bend indications. No further corrections to the growth rates for denting effects are required.
- New indications initiated in the next operating cycle would not challenge tube integrity in the next operating cycle as shown by the analyses of this report described below which include an assumption of an unexpected large number of

new indications. Thus, the operating cycle evaluation is independent of assumptions on new indication initiation related to denting effects or general corrosion rates.

Based on the above, the operational assessment can be performed without further considerations of denting effects beyond that included in the growth rate evaluations obtained from growth over the last operating cycle.

Row 3 indication sizes that could be undetected and be structurally acceptable after one EFPY of operation are discussed in Section 9.1. In Section 9.2, it is shown that the indications found by the high frequency probe in row 2, but not by the midrange probe due to noisy data, could be acceptably left in service if undetected in row 3. Section 9.3 provides the reference analysis for defining an acceptable Cycle 15 operating period. This reference analysis is based on a total SG structural and leakage assessment for row 3, assuming the row 2 indications occurred in row 3 and applying the conservatively developed high frequency probe POD given in Section 5. The assessments of Sections 9.2 and 9.3 are based on the Monte Carlo axial profile analysis methods described in Section 4.1 with benchmark analyses described in Section 6.1. Section 9.4 describes the operational assessment performed, as an independent analysis methodology, by applying the multi-cycle methods described in Section 4.2 with benchmark analyses described in Section 6.2. The recommended operating period to the next inspection is developed in Section 9.5. As a defense in depth measure, reduced operating leakage limits are described in Section 9.6. To demonstrate the conservatism applied for the bounding POD and NDE sizing uncertainties in this report, a laboratory program is planned, as described in Section 9.7, to develop a +Point POD and sizing uncertainty distributions utilizing corrosion induced cracks in rows 2 and 3 U-bends. Overall conclusions from this section are addressed in Section 9.7.

9.1. Acceptable Row 3 Indication Sizes

The sizes of indications that could be undetected in row 3 and acceptably left in service for Cycle 15 operation can be developed for BOC-15 by statistically combining the growth distributions, NDE uncertainties and burst correlation uncertainties. The growth rates and NDE uncertainties developed in Section 5 are used in these analyses. Acceptance limits for satisfying $3\Delta P_{NO}$ = 4668 psi on crack length versus depth are shown in Figure 9-1 for Cycle 15 operating periods between inspections of 0.85 and 1.0 EFPY. It is seen that the difference of 0.15 EFPY between these two cases has less than a 2% depth change in the acceptable values. That is, growth is not a strong influence for small changes in the cycle length. For short crack lengths less than 0.3 inch, the acceptable depths increase rapidly (not shown in figure) as short throughwall cracks would satisfy the burst margin requirements. In general, short cracks (<0.3 inch) would be more difficult to detect than long cracks. Since growth in length per EFPY is expected to be on the order of about 0.15 inch (95% probability in Figure 5-7), the short cracks could be throughwall at the end of the cycle and still satisfy burst margin requirements.

Figure 9-1, and the 400 kHz sizing data of Table 3-5 for indications found in the EOC-14 inspection can be used to estimate which of the indications would have been acceptable after 1.0 EFPY of operation even if not detected. The indications found in tubes R2C87, R2C85, R2C4 and R2C74 would meet structural requirements after 1.0 EFPY if not detected. This demonstrates that all indications found with the high frequency probe and not reported as flaws with the midrange probe due to bad data (R2C85, R2C4 and R2C74) would meet structural criteria. No leakage would be expected (see Section 9.2 for calculated burst margins and basis for no leakage). The indication in R2C71 was not inspected with the midrange probe due to probe restriction at the top TSP, but detection would have been expected if probe access would have been possible. It is seen in Figure A.3-9 of Appendix A that this indication was readily detectable by 400 kHz analysis of the high frequency probe data. Thus, the indications that would challenge structural integrity for one year of operation were detected with the midrange probe and the high frequency probe provided additional margin for longer periods between inspections.

From Table 3-5, 11 of the 14 indications found in the inspection had burst effective lengths ≤ 0.35 inch and the 3 longest indications had lengths ranging from 0.44 to 0.8 inch. From Figure 9-1, indications 0.8 and 0.44 inch long could have average depths of about 51% and 58%, respectively, for acceptable operation for one year. These depths and lengths would have a high probability of detection with the 800 kHz probe. The lower bound POD of Figure 5-1 shows a POD of 0.89 to 0.93 for indications with average depths in the range of 51% to 58%. Since row 3 is expected to have between no indications or at most a few indications, there is a very low likelihood of indications left in service that would not meet structural requirements after one year of operation.

9.2. Single Indication Analyses Based on Row 2 Indications

If it is assumed that indications near the detection threshold could be undetected and left in service, the structural margin for these indications can be estimated by analyses of the smaller indications found in the EOC-14 inspection. As noted above, these indications would satisfy structural margins after one year of operation based on Figure 9-1. To demonstrate the structural margin, the results of analyses for the indications found in R2C87 and R2C85 after 1.0 and 0.75 years of operation are shown in Table 9-1. The R2C87 indication was detected by the midrange +Point coil while the R2C85 indication was detected by the high frequency probe and identified as unacceptable data for the midrange probe. The indications found in R2C4 and R2C74 result in larger margins and are not included in the table. The indication in R2C74 is likely deeper than obtained from the NDE analyses based on in situ results, but would be unlikely to grow to leakage at SLB conditions after one year of operation. These indications exceed the Cycle 15 $3\Delta P_{NO}$ = 4668 psi requirement even if growth rates are increased by 25% over the growth distribution developed in Section 5. The 5887 psi burst pressure for R2C87 after one year of operation is reduced by only about 180 psi if growth rates are increased by 25%. For these short cycle lengths, the burst pressures are not strongly sensitive to growth distributions. Similarly, it is seen from Table 9-1 that reducing the operating cycle length from 1.0 to 0.75 year only increases the burst margin by about 160 psi, again demonstrating only a small dependence upon growth.

If indication sizes similar to the four smallest detected indications had been left in service for Cycle 15, it is concluded that these indications would have burst pressures > 5880 psi after one year of operation compared to the 4668 psi requirement. Any undetected indications in row 3, if any are present, would be expected to be smaller than or comparable to the smallest indications found at EOC-14 representing an upper bound to detection threshold capability for the 800 kHz +Point probe.

9.3. Reference Cycle 15 Operating Cycle Length Evaluation - Total SG Analyses Based on Row 2 Indications

The reference analyses for establishing an acceptable Cycle 15 operating cycle length are based on a total SG analysis applying the axial profile analysis methodology described in Section 4. This analysis applies Monte Carlo techniques to develop the limiting indication burst pressure distribution at the end of the period for comparison at 95/95 confidence with the $3\Delta P_{NO}$ = 4668 psi burst margin requirement for Cycle 15 (Section 5.2). The analysis methods also evaluate for SLB leakage including the ANL ligament tearing model in the analysis. The limiting SG for this analysis is SG 4, which had 5 of the 7 tubes with U-bend indications in the EOC-14 inspection. No U-bend indications were found in row 3 and, based on historical data showing no indications in other SGs operating at higher temperatures with no row 3 heat treatment, it is reasonable to expect that there may be no indications in the Indian Point-2 row 3 U-bends. A clearly conservative and worst case analysis for row 3 can be performed by evaluating row 2 indications to establish a lower bound operating interval for row 3. This worst case bounding approach is applied to establish an acceptable Cycle 15 operating period.

The input data for the total SG analysis are developed in other sections of this report as noted below:

- EOC-14 crack depth profiles at 400 kHz for reference analysis and 800 kHz for sensitivity analyses – Appendix C with the summary in Table 3-5.
- POD distributions as functions of average and maximum depth from lower bound IP2 800 kHz distributions of Figures 5-1 and 5-2 (Section 5.3).
- NDE uncertainties on average depth, maximum depth and length per Section 5.5 including 25% increase in uncertainty over values developed for 300 to 400 kHz data at dented TSP intersections.
- Growth rates for average depth, maximum depth and length per Section 5.4 and Figures 5-5 to 5-7.
- New indication shape, depth and length distributions per Sections 5.8 to 5.9 and Figures 5-10 and 5-11.
- U-bend material property flow stress of 75.7 ksi at operating temperature for row 3 U-bends per Section 5.6.
- Axial profile analysis methods, Westinghouse burst correlation and ANL ligament tearing model for leakage as described in Section 4.1.

The results of the reference analyses for acceptable operating cycle lengths are given in Table 9-2. For a 1.0 EFPY operating cycle, the limiting indication burst pressure at the end of the period is 4840 psi at 95/95 confidence compared to the $3\Delta P_{NO}$ = 4668 psi burst margin requirement for Cycle 15. No SLB leakage is expected over this operating period at 95/95 confidence, and the projected SLB tube burst probability is 3.23×10^{-3} compared to a guideline value of about 4.0×10^{-2} (Section 5.2) summed over all degradation mechanisms. Since the sludge pile SLB burst probability (Reference 10-1) after one year of operation is even smaller than the U-bend value, the combined burst probability would be about an order of magnitude less than the guideline value. Similarly, the probability of burst at $3\Delta P_{NO}$ of 4.2×10^{-2} at 95/95 or 4.1×10^{-2} at 90/50 is below the guideline value of 8×10^{-2} at 90/50, which also remains the case when combined with the sludge pile value (Reference 10-1). Consequently, operation in excess of 1.0 EFPY would be acceptable. The analyses for a 0.85 EFPY operating period show about a 100 psi increase in the burst pressure, which demonstrates that the limiting indication burst pressure is not strongly dependent upon growth for the operating cycles of about one year. An acceptable operating period for satisfying the burst margin requirement would be about 1.2 EFPY. It should again be emphasized that these results are worst case analyses for row 3 U-bends since the analyses demonstrate that the undetected indications, resulting from assuming the row 2 indications occurred in row 3, would satisfy burst requirements for more than one year of operation.

Analyses were performed to assess the sensitivity of the operating cycle length to growth rates, POD and the EOC-14 crack profiles. For growth rate sensitivity, a conservative increase in the growth rate distribution by a factor of 1.25 was evaluated. These results are given in Table 9-3. For a one year operating period, the 25% increase in growth reduces the limiting indication burst pressure by about 140 psi to 4701 psi, which still exceeds the $3\Delta P_{NO}$ = 4668 psi burst margin requirement for Cycle 15. For a cycle length of 0.75 EFPY, the burst pressure reduction for the growth increase would be only about 120 psi.

The +Point POD developed in Section 5.3 for Indian Point-2 +Point inspection with the high frequency probe was taken to be a lower bound POD distribution. The uncertainty on this POD would be in the direction of improved detection with the POD of Figure 5-1 shifted toward the left. This sensitivity to the POD distribution was evaluated by a –5% depth shift (improved POD) in the POD of Figure 5-1. For this expected improved POD, the limiting indication burst pressure increases form 4840 psi to 5434 psi, which demonstrates that the expected POD uncertainty significantly increases the burst margin. The NDE development program described in Section 9.7 is targeted toward determining the +Point POD for low row U-bend indications and is expected to demonstrate improvements in the POD relative to the bounding POD distribution of this report. As an extreme case for sensitivity analysis, a POD with a 5% depth increase (shift of distribution to deeper depths) was evaluated. This extreme conservatism results in a limiting indication burst pressure of 4496 psi. Although this burst pressure is slightly less than the $3\Delta P_{NO}$ = 4668 psi burst requirement, the burst pressure significantly exceeds the faulted condition burst margin requirement of $1.4\Delta P_{SLB}$ = 3584 psi. The results demonstrate that a shift in POD does not result in a large step change in burst pressures, and the results are considered acceptable for operation for 1.0 EFPY.

To assess the sensitivity of the acceptable operating to the +Point depth profiles, analyses were performed applying the 800 kHz depth profiles. The Section 6 benchmark analyses have shown that use of the 800 kHz profiles with NDE uncertainties obtained for 400 kHz data result in unnecessary conservatism in the tube integrity analyses. The results of the sensitivity analyses for the 800 kHz profiles are also given in Table 9-3. These results show a limiting indication burst pressure of 4740 psi for 1.0 EFPY operation, which also exceeds the 4668 psi requirement. The effect of the 800 versus 400 kHz profiles is only about a 100 psi decrease in the limiting indication burst pressure. With a 1.25 factor increase in growth, the limiting burst pressure is 4587 psi at 1.0 EFPY and 4698 psi at 0.85 EFPY. The 4587 psi value at 1.0 EFPY is about 81 psi below the burst requirement while the 0.85 EFPY results exceed the burst pressure requirement.

In summary, the reference analyses show that the $3\Delta P_{NO}$ = 4668 psi burst margin requirement for Cycle 15 is satisfied for a > 1.0 EFPY operating period between inspections. The projected limiting indication burst pressure is 4840 psi at 1.0 EFPY and 4937 psi at 0.85 EFPY. No SLB leakage is expected for cycle lengths in excess of one year. The projected SLB tube burst probability after 1.0 EFPY of operation is 3.2×10^{-3}, which is well below the guideline of 4.0×10^{-2}. Sensitivity analyses to growth, POD and NDE profile depths show that the limiting indication burst pressures do not change significantly with more conservative assumptions on these key parameters for cycle length evaluations. The 1.0 EFPY operating period is acceptable for a 25% increase in growth and the use of the more conservative 800 kHz +Point profiles rather than the 400 kHz profiles supported by benchmark analyses. The expected POD uncertainty is to improve the POD for which a 5% depth shift to improve the POD results in a limiting indication burst pressure increase of about 600 psi while a 5% depth shift to reduce the POD results in a burst pressure decrease of only about 345 psi.

9.4. Operational Assessment Applying Multi-Cycle Analyses

This section provides the operational assessment results applying the multi-cycle analysis methods described in Section 4.2. The multi-cycle analysis methodology is a best estimate technique with defined uncertainty levels, and tends to be less conservative than the single cycle axial profile analysis methods applied above and described in Section 4.1. With the multi-cycle statistically based methodology, the analyses do not directly compute the burst pressure distribution of the limiting indication for a direct comparison with the $3\Delta P_{NO}$ burst margin requirement. As an alternative, the methods compute the $3\Delta P_{NO}$ burst probability for comparison with the EPRI tube integrity guideline value of 8×10^{-2} (Section 5.2). The mean and lower 95/95 confidence values for the worst case burst pressure distribution are also reported. This value is more conservative than the limiting indication burst pressure, represents a high confidence on the "worst of the worst" burst pressures, and would not be required to satisfy the $3\Delta P_{NO}$ burst margin requirement.

9.4.1. Row 3 Evaluation

Multi-cycle Monte Carlo simulations of the evolution of axial PWSCC degradation were conducted for Row 3 U-Bends at Indian Point Unit 2. Analyses were performed using reference case input which gave excellent benchmark agreement with the observed behavior of Row 2 U-Bends. Results of the Row 3 analyses are presented in the following paragraphs.

Since axial PWSCC degradation of Row 3 U-Bends has not been observed to date, a conservative judgment of the expected time for the onset of such degradation was made. This was necessary in order to develop crack initiation input parameters. It was assumed that one NDE indication of axial PWSCC in a Row 3 U-Bend was found at EOC 14. The rate of progression of degradation was assumed equal to that of Row 2 U-Bends.

The best illustration of the projected structural and leakage integrity of Row 3 U-Bends is provided by repeating calculations of the benchmark parameters used to characterize the severity of degradation of Row 2 U-Bends. The results of such calculations are summarized in Table 9-4. The reference crack growth rate distribution of Section 5 was used as input along with the average depth POD curve of Section 5. Section 5 does not define a POD for prior cycles. A prior cycle POD degraded from the recommended year 2000 POD was used. Use of a well benchmarked analysis supports full cycle operation in Cycle 15. If the operating interval length is decreased to 1.0 EFPY, projected margins of structural and leakage integrity are substantial. The probability of burst at postulated SLB conditions of 2.2×10^{-3} and the probability of burst at $3\Delta P_{NO}$ of 3.9×10^{-2} are well below the Section 5.2 EPRI guidelines of 4×10^{-2} and 8×10^{-2}, respectively. The median projected worst case burst pressure is 8535 psi. The lower 95th percentile of worst case burst pressure projections, a worst of the worst criterion, is 6649 psi. This meets the required minimum burst strength of 4668 psi.

Figure 9-3 plots structural integrity figures of merit versus operating interval length for the row 3 analyses for cycle 15. These results are based on the reference input. Maintenance of acceptable structural and leakage integrity margins is expected for an operating interval of 1.0 EFPY and beyond. Recall that these calculations are based on the assumption that axial PWSCC of Row 3 U-Bends has already been observed. This is not the case since no row 3 indications were found. The recommended inspection interval is given in Section 9.5.

9.4.2. Row 2 Evaluation for Cycle 15

The conservatism of the multi-cycle Monte Carlo operational assessment for Row 3 can be illustrated by comparison with projected results for Row 2 even though Row 2 will be preventively plugged for the next operating cycle. Table 9-5 lists structural and leakage integrity figures of merit under the assumption of a 1.0 EFPY additional operating interval for Row 2. The probability of burst at postulated SLB conditions of 4.5×10^{-3} and the probability of burst at $3\Delta P_{NO}$ of 5.8×10^{-2} are below the Section 5.2 EPRI guidelines of 4×10^{-2} and 8×10^{-2}, respectively. For the best benchmark input, the projected 95/95 SLB leak rate is 0.0 gpm. The median worst case minimum burst pressure meets the $3\Delta P$ requirement. This requirement is met down to the lower 95th percentile worst case burst pressure. The Row 2 structural and leakage integrity figures of merit are less than those projected for Row 3 simply because there are more cracks (detected and undetected)

projected for Row 2 U-Bends. Acceptable integrity margins would be demonstrated for Row 2 U-Bends for an operating interval slightly more than 1.0 EFPY. Acceptable integrity margins are demonstrated for Row 3 U-Bends for an operating interval of 1.0 EFPY and beyond.

Row 3 analyses were performed with the multi-cycle methodology using parameters conservatively benchmarked against EOC-14 inspection results for Row 2 and further assuming one indication was detected in Row 3 at the EOC-14 inspection. Acceptable integrity margins are demonstrated for Row 3 U-Bends for an operating interval of 1.0 EFPY and beyond. This statement is supported by the fact that Row 2 U-Bend behavior clearly bounds that of Row 3, and a well-benchmarked Row 2 analysis would support operating in Cycle 15 for more than 1.0 EFPY even if Row 2 U-Bends are not preventively plugged. Additional analyses were performed with more adverse growth rates, POD curves and number of undetected indications. Conservative structural and leakage integrity margins were still maintained beyond an operating interval of 1.0 EFPY in Cycle 15.

9.4.3 Multi-Cycle Evaluation of Degradation Initiation Parameters

The multi-cycle Monte Carlo simulation approach uses a three parameter Weibull function to describe the distribution of times for the initiation of degradation. The observed service performance of Row 2 and Row 3 U-Bends at Indian Point allows the determination of the ranges of these initiation parameters that are realistic, that is, the range of initiation parameters which provide matches between computed results and observed performance. An evaluation of this type provides an independent check of the relative and absolute susceptibility of Row 2 and Row 3 U-Bends to axial PWSCC.

For Row 2 the observed performance is the severity of degradation observed in Cycle 14. For Row 3 the observed performance is no detectable indications at EOC 14. As a conservative measure, the number of computed Row 3 U-Bend axial PWSCC indications was set equal to 0.5 at EOC 14. No Row 3 indications were observed. A computed result equal to 0.5 implies that degradation has begun development but there is a less than 50% chance of finding any eddy current indications at EOC 14. Initiation parameters providing this computed result are conservative. Initiation of axial PWSCC in Row 3 U-Bends may occur at times later than those projected but not earlier.

Slope, scale and threshold time parameters in the Weibull degradation initiation function were systematically varied. Two versions of the multi-cycle Monte Carlo simulation code were utilized. One version resampled crack growth rates for a given degradation site for each cycle of operation. Another version sampled a growth rate for each degradation site only once, which assumes a constant growth rate for each indication over multiple cycles. Resampling of growth rates is arguably appropriate for ODSCC since there is no guarantee that the same concentrated environment will develop during successive heat up and cool down cycles. Primary side environments are relatively constant and the rationale for resampling is not as clear for PWSCC as for secondary side degradation. If stress and temperature are constant between cycles for PWSCC as would be expected for the Indian

Point-2 U-bend indications, the constant growth rate assumption over multiple cycles would be expected to better represent the indication history.

In terms of relative susceptibility of Row 2 and Row 3 U-Bends to axial PWSCC, all benchmarked cases using the multi-cycle Monte Carlo simulation approach show that it takes, as a minimum, a factor of 2 increase in operating time to create the same level of degradation severity in a Row 3 U-Bend as in a Row 2 U-Bend. This is true for both mild and severe levels of degradation.

The range of initiation parameters that are consistent with the observed service performance of Row 2 and Row 3 U-Bends show that the onset of axial PWSCC occurs at about 6 to 10 EFPY in Row 2. The corresponding early stage of development of axial PWSCC is projected to occur, as a minimum, at about 15 to 17 EFPY in Row 3 U-Bends. These results are approximately consistent with stress based evaluations, which show a factor of 2.5 in initiation times, of the relative and absolute susceptibility of Row 2 and Row 3 U-Bends to axial PWSCC.

When all types of analyses are equally well matched to benchmarks for observed Row 2 and Row 3 service performance, then projected structural and leakage integrity figures of merit in Cycle 15 for Row 3 U-Bends are essentially the same. The same statement holds true for projected Cycle 15 Row 2 results; acknowledging that this case is only hypothesized since Row 2 U-Bends will be removed from service. A broad array of initiation parameters and assumptions, when benchmarked to observed service performance, leads to the same qualitative and quantitative projections for Row 3 (and Row 2) structural and leakage integrity figures of merit for Cycle 15.

9.5. Recommended Operating Cycle Length

The operational assessments given in Sections 9.3 and 9.4 support Cycle 15 operation for a period exceeding 1.0 EFPY. Additional structural and leakage integrity margins can be obtained by limiting the inspection interval to about half of the planned operating cycle. To obtain additional margins, a mid-cycle inspection interval of about 0.85 EFPY (310 EFPD) is recommended.

If the development program described in Section 9.7 is completed prior to the mid-cycle inspection and demonstrates significant improvements in POD and NDE sizing uncertainties over the bounding values developed in Section 5 of this report, a revised operational assessment can be performed to potentially demonstrate longer acceptable operating periods between inspections than the recommended 0.85 EFPY.

9.6. Recommended Leakage Monitoring Requirements

Although the operating leakage at Indian Point-2 was only a few gpd prior to the R2C5 leakage event and this leakage level may not have been entirely due to the R2C5 indication, a reduced operating leakage limit provides additional margin against an

unexpected flaw size that could result in operational leakage. Ligament tearing of a remaining wall thickness ligament at an average crack depth of about 90% throughwall with minimal throughwall penetration was the apparent tube condition at the time of the leakage event. However, other cracks such as the R2C71 indication, which leaked at SLB conditions, may result in significant operational leakage if grown to unexpected depths. For this type of indication, which is more common than the breakthrough condition of R2C5, a reduced operating leakage limit can result in shutdown of the plant prior to the crack size growing to levels that could burst under postulated accident conditions. As a defense in depth measure, the Indian Point-2 operating leak rate limit is being administratively set at 30 gpd to enhance the potential for detection of a large leaking flaw prior to the flaw growing to a structurally unacceptable size.

9.7. Recommendations for Development Activities

A test program is proposed to develop the probability of detection of cracks and NDE sizing uncertainties in the U-bend apex region, to further develop the material properties for U-bends as compared to straight leg properties and to develop ovality data for Row 2 and Row 3 U-bends. An additional test objective is to assess differences in the time for crack initiation between row 2 and row 3 U-bends. Due to the extensive nature of this test program, the results are not expected prior to completion of the recommended operating cycle length of 0.85 EFPY.

The proposed test program as defined below will consist of approximately 50 to 80 U-bend tubes. The tentative plan is to provide a split of 45% fabricated as row 2 U-bends and 55% as row 3 U-bends. It is important to note that even though all of the row 2 tubes have been plugged, the operational assessment is based on Row 2 detection and sizing data. U-bends will be fabricated to perform the destructive examinations required to support the POD and NDE sizing uncertainty database, tensile tests of the extrados and flank material properties and burst tests to be performed in support of the material property testing of the U-bends with EDM slots. All POD and NDE sizing uncertainties will be developed in accordance with the EPRI ISI Guidelines TR-107569, Appendix H.

It is intended to obtain and use 7/8" by 0.050" wall tubing that is dimensionally equivalent to the tubing supplied in the Indian Point Unit 2 S/G's. Although the tubing heat numbers may be different, the mechanical properties of the tubing will be defined and documented. Final tube wall thicknesses may be slightly different than the original tubing but the tubing tolerances will remain within the limits of the original tubing.

Fabrication of the U-bends in support of this test program is being arranged through Huntington Alloys, who was the original manufacturer of the U-bend assemblies. The feasibility of using the original process is under review and appears to promising, if the manufacturer can recover the original tooling used to fabricate the U-bends. In order to control tube ovalization in the small radius U-bends during fabrication (i.e., rows 1 and 2), these U-bends were produced by the use of a bronze ball during the bending process, which restored the cross-section back into a configuration with considerably less ovality. The fabrication process for the bending of the Row 3 U-bends did not employ the use of the

bronze ball and therefore the tubes adopted the characteristic shape associated with the Von Karman flattening phenomenon.

All fabricated U-bends will be measured for ovality by documenting the dimensional differences of the measurements taken between the intrados to extrados and the measurements from flank to flank. These ovality measurement will be compared to the manufacturing drawing for the original tubing supplied for Indian Point Unit 2 SGs, and will be used to assess differences between row 2 and row 3 U-bends.

The PWSCC corrosion test program will utilize the fabricated U-bends produced as described above. U-bends will be configured within an autoclave environment where the corrosion process will be accelerated by providing high temperature steam containing hydrogen to the primary side of the U-bend tubing at approximately 1560 psig. Periodic NDE monitoring of the tubing will be performed to determine the point of crack initiation. Differences in the time to crack between Row 2 and Row 3 U-bends will be evaluated to assess probable differences in crack initiation times between those two rows.

Tests will be performed on U-bend specimens to determine the NDE effects of the presence of copper and sludge on detection by methods of copper plating, copper foil wraps and simulated sludge buildup. All U-bend specimens will be +Point inspected using standard midrange and high frequency probes throughout the complete testing processes. Following cracking of the specimens, +Point data will be obtained for the clean tube, for the tube with magnetite deposits and for the tube with copper and magnetite deposits. Additional +Point data will be obtained for tubes with these deposits, but without cracking to obtain "NDD" specimens for POD development. The number of "NDD" specimens will be approximately twice the number of crack specimens.

Evaluation of the data will be performed as "blind" NDE analyses wherein the analysts have no knowledge of the destructive examination results. A minimum of three field analysts will be used to develop the POD and NDE uncertainty data. The test results will be evaluated with the goal of meeting the established objectives for determining POD distributions and NDE sizing uncertainties. A report will be prepared documenting the test results.

9.8. Operational Assessment Conclusions

All of the above analyses, including the reference single cycle axial profile and the multi-cycle analysis methods, support Cycle 15 operation in excess of 1.0 EFPY. To provide additional structural and leakage integrity margin, the recommended operating interval to the next inspection is 0.85 EFPY (310 EFPD) corresponding to a mid-cycle inspection for Cycle 15.

Acceptability of the 0.85 EFPY operating period is based upon:

- All row 2 tubes have been preventively plugged.

- No indications were found in row 3 tubes during the EOC-14 inspection with either the midrange or high frequency +Point probes. Based upon analyses for the hourglassed TSP conditions at Indian Point-2, the time to crack row 3 tubes would be expected to be a factor of 2.5 to 4 longer than for row 2 crack initiation. Based on historical operating experience for other Westinghouse SGs, only one row 3 PWSCC indication has been found, and this occurred in a plant without significant denting. These results support the expectation that no PWSCC would be likely at Indian Point-2 during Cycle 15.
- Independent Monte Carlo analysis techniques (reference single cycle analyses using crack profiles and independent multi-cycle analyses based upon crack initiation rates) support Cycle 15 operation in excess of 1.0 EFPY. The analyses support the recommended cycle length even if it would be assumed that all row 2 tubes were not preventively plugged (i.e., equivalent to assuming that the row 2 indications occurred in row 3).
- The reference cycle length analyses show that the $3\Delta P_{NO}$ = 4668 psi burst margin requirement for Cycle 15 is satisfied for a > 1.0 EFPY operating period between inspections. The projected limiting indication burst pressure is 4840 psi at 1.0 EFPY and 4937 psi at 0.85 EFPY. No SLB leakage is expected for cycle lengths in excess of one year. The projected SLB tube burst probability after 1.0 EFPY of operation is 3.2×10^{-3} compared to EPRI guideline of 4.0×10^{-2}. Sensitivity analyses to growth, POD and NDE profile depths show that the limiting indication burst pressures do not change significantly when assumptions that are more conservative are made on these key parameters for cycle length evaluations. The 1.0 EFPY operating period is acceptable for a 25% increase in growth and the use of the more conservative 800 kHz +Point profiles rather than the 400 kHz profiles supported by benchmark analyses. The expected POD uncertainty is to improve the POD for which a 5% depth shift to improve the POD results in a limiting indication burst pressure increase of about 600 psi while a 5% depth shift to reduce the POD results in a burst pressure decrease of only about 345 psi.
- Independent analyses were performed with the multi-cycle methodology using parameters conservatively benchmarked against EOC-14 inspection results for row 2. If it is conservatively assumed that one indication was detected in row 3 at the EOC-14 inspection, the SLB burst probability is 2.2×10^{-3} and no leakage is predicted at SLB conditions even after 1.9 EFPY or full cycle operation. Under the very conservative assumption that row 2 tubes were not preventively plugged, the probability of burst at SLB conditions would be about 4.5×10^{-3} after 1.0 EFPY of operation and the probability of burst at $3\Delta P_{NO}$ is about 5.8×10^{-2} compared to the EPRI guidelines of 4.0×10^{-2} and 8.0×10^{-2}, respectively. These results are consistent with the reference analyses. Benchmarking of the multi-cycle analyses against the EOC-14 inspection results required a low crack initiation rate over multiple prior cycles. An adequate benchmarking could not be obtained for a high initiation rate that could have resulted in a large number of undetected indications at EOC-14.

As a defense in depth measure, the Indian Point-2 operating leak rate limit is being administratively set at 30 gpd to enhance the potential for detection of a large leaking flaw prior to the flaw growing to a structurally unacceptable size. Although the operating leakage at Indian Point-2 was only a few gpd prior to the R2C5 leakage event and this

leakage level may not have been due to the R2C5 indication, the reduced leakage limit provides additional margin against an unexpected flaw size.

A laboratory test program is being initiated to develop +Point POD and NDE sizing uncertainty information for axial PWSCC in rows 2 and 3 U-bends. Accelerated cracking will be performed on prototypically fabricated U-bends. Differences in the time to crack between row 2 and row 3 U-bends will be evaluated as a part of this test program. NDE data will be obtained with and without deposits simulating the noise levels found in the Indian Point-2 U-bends. "Blind" (without knowledge of destructive exam results) analyses of the NDE data by field analysts will be used to develop POD and NDE sizing uncertainty distributions. It is expected that these tests will demonstrate POD and NDE uncertainty distributions less conservative than the values used in this operational assessment. Due to the extensive nature of this test program, the results are not expected prior to completion of the recommended operating cycle length of 0.85 EFPY.

Table 9-1.
Indian Point-2 Cycle 15 Projected Single Indication Burst Pressures and Leak Rates(1)
Assumes Undetected Row 3 Indications Like Detected Row 2 Indications

Indication	Operating EFPY	Growth Rate Factor	NDE Profile (kHz)	Limiting Burst Pressure (psi)	SLB Leak Rate (gpm)
R2C87	1.0	1.0	400	5887	0.0
R2C85				6396	0.0
R2C87		1.25	400	5716	0.0
R2C85				6246	0.0
R2C87	0.75	1.0	400	6048	0.0
R2C85				6553	0.0
R2C87		1.25	400	5937	0.0
R2C85				6449	0.0

1. Acceptance criteria: $3\Delta P_{NO}$ = 4668 psi at operating temperature, SLB leak rate = 1 gpm summed over all degradation mechanisms.

Table 9-2. Indian Point-2 Cycle 15 Reference SG Cycle Length Analyses (400 kHz Profiles) for Projected Burst Pressures and Leak Rates(1)
Assumes Row 3 Indications Same as Detected Row 2 Indications

Operating EFPY	Limiting Burst Pressure (psi)	SLB Leak Rate (gpm)	SLB Burst Probability	$3\Delta P_{NO}$ Burst Probability
95% Probability/95% Confidence				
1.0	4840	0.0	3.23×10^{-3}	4.17×10^{-2}
0.85	4937	0.0	3.06×10^{-3}	3.61×10^{-2}
0.75	5001	0.0	3.20×10^{-3}	3.36×10^{-2}
90% Probability/50% Confidence				
1.0	5670	0.0	2.97×10^{-3}	4.07×10^{-2}

1. Acceptance criteria: $3\Delta P_{NO}$ = 4668 psi at operating temperature, SLB leak rate = 1 gpm summed over all degradation mechanisms. Burst probability guidelines: $\Delta P_{SLB} = 4 \times 10^{-2}$, $3\Delta P_{NO} = 8 \times 10^{-2}$ summed for all degradation mechanisms in limiting SG.

Table 9-3.
Indian Point-2 Cycle 15 SG Sensitivity Analyses for Growth, POD and NDE Profile Projected Burst Pressures and Leak Rates(1)
Assumes Row 3 Indications Same as Detected Row 2 Indications

Operating EFPY	Growth Rate Factor	NDE Profile (kHz)	POD	Limiting Burst Pressure (psi)	SLB Leak Rate (gpm)	SLB Burst Prob.	$3\Delta P_{NO}$ Burst Prob.
Sensitivity to Growth Rates							
1.0	1.0	400	Reference	4840	0.0	3.23×10^{-3}	4.17×10^{-2}
1.0	1.25	400	Reference	4701	0.0	3.72×10^{-3}	4.78×10^{-2}
0.75	1.0	400	Reference	5001	0.0	3.20×10^{-3}	3.36×10^{-2}
0.75	1.25	400	Reference	4881	0.0	3.24×10^{-3}	3.89×10^{-2}
Sensitivity to POD							
1.0	1.0	400	Reference	4840	0.0	3.23×10^{-3}	4.10×10^{-2}
1.0	1.0	400	Shift –5%	5434	0.0	1.36×10^{-3}	2.15×10^{-2}
1.0	1.0	400	Shift +5%	4496	0.0	6.35×10^{-3}	6.01×10^{-2}
Sensitivity to 800 kHz Profiles							
1.0	1.0	400	Reference	4840	0.0	3.23×10^{-3}	4.10×10^{-2}
1.0	1.0	800	Reference	4740	0.0	3.66×10^{-3}	4.68×10^{-2}
1.0	1.25	400	Reference	4701	0.0	3.72×10^{-3}	4.78×10^{-2}
1.0	1.25	800	Reference	4587	0.0	4.20×10^{-3}	5.32×10^{-2}
0.85	1.0	400	Reference	4937	0.0	3.06×10^{-3}	3.61×10^{-2}
0.85	1.0	800	Reference	4812	0.0	3.48×10^{-3}	4.42×10^{-2}
0.85	1.25	400	Reference	4816	0.0	3.52×10^{-3}	4.18×10^{-2}
0.85	1.25	800	Reference	4698	0.0	3.93×10^{-3}	4.85×10^{-2}
0.75	1.0	400	Reference	5001	0.0	3.20×10^{-3}	3.36×10^{-2}
0.75	1.0	800	Reference	4852	0.0	3.35×10^{-3}	4.24×10^{-2}
0.75	1.25	400	Reference	4881	0.0	3.24×10^{-4}	3.89×10^{-2}
0.75	1.25	800	Reference	4763	0.0	3.61×10^{-4}	4.58×10^{-2}

1. Acceptance criteria: $3\Delta P_{NO}$ = 4668 psi at operating temperature, SLB leak rate = 1 gpm summed over all degradation mechanisms. Burst probability guidelines: $\Delta P_{SLB} = 4\times10^{-2}$, $3\Delta P_{NO} = 8\times10^{-2}$ summed for all degradation mechanisms in limiting SG.

Table 9-4. Summary of Projected Row 3 Structural and Leakage Integrity Figures of Merit for Next Operating Interval(1)

Parameter	Reference Input 1.9 EFPY Operating Interval	Reference Input 1.0 EFPY Operating Interval
Probability of Burst at Normal Operation	nil(2)	nil
Probability of Large Leakage at Normal Operation	nil	nil
Probability of Burst at Steam Line Break	0.22%	0.01%
Probability of Large Leakage at Steam Line Break	0.33%	0.01%
Probability of Burst at 3 Times Operating Pressure, 3ΔP	3.9%	0.21%
Probability of Large Leakage During In Situ Testing	4.8%	0.25%
Median Minimum Degraded Tube Burst Pressure, psi	7557	8535
95th Percentile Minimum Degraded Tube Burst Pressure, psi	4881	6649
Chance of More Than 1 Burst at 3ΔP	nil	nil

1. Acceptance criteria: $3\Delta P_{NO}$ = 4668 psi at operating temperature, SLB leak rate = 1 gpm summed over all degradation mechanisms. Burst probability guidelines: $\Delta P_{SLB} = 4x10^{-2}$, $3\Delta P_{NO} = 8x10^{-2}$ summed for all degradation mechanisms in limiting SG.
2. nil = no occurrences in 10,000 simulations

Table 9-5. Summary of Projected Row 2 Structural and Leakage Integrity Figures of Merit for 1.0 EFPY Future Operation

Parameter	Reference Input 1.0 EFPY Operating Interval
Probability of Burst at Normal Operation	0.08%
Probability of Large Leakage at Normal Operation	0.26%
Probability of Burst at Steam Line Break	0.45%
Probability of Large Leakage at Steam Line Break	0.93%
Probability of Burst at 3 Times Operating Pressure, 3ΔP	5.8%
Probability of Large Leakage During In Situ Testing	7.8%
Median Minimum Degraded Tube Burst Pressure, psi	7047
95th Percentile Minimum Degraded Tube Burst Pressure, psi	4661
Chance of More Than 1 Burst at 3ΔP	nil

1. Acceptance criteria: $3\Delta P_{NO}$ = 4668 psi at operating temperature, SLB leak rate = 1 gpm summed over all degradation mechanisms. Burst probability guidelines: $\Delta P_{SLB} = 4x10^{-2}$, $3\Delta P_{NO} = 8x10^{-2}$ summed for all degradation mechanisms in limiting SG.
2. nil = no occurrences in 10,000 simulations

Figure 9-1. Indian Point-2 Cycle 15 U-bend Operational Assessment Burst Resistance Acceptance Limits

$3DP_{NO}$ = 4668 psi Acceptance Limit, 95/95 Confidence, Row 3 Flow Stress, PWSCC at 650°F

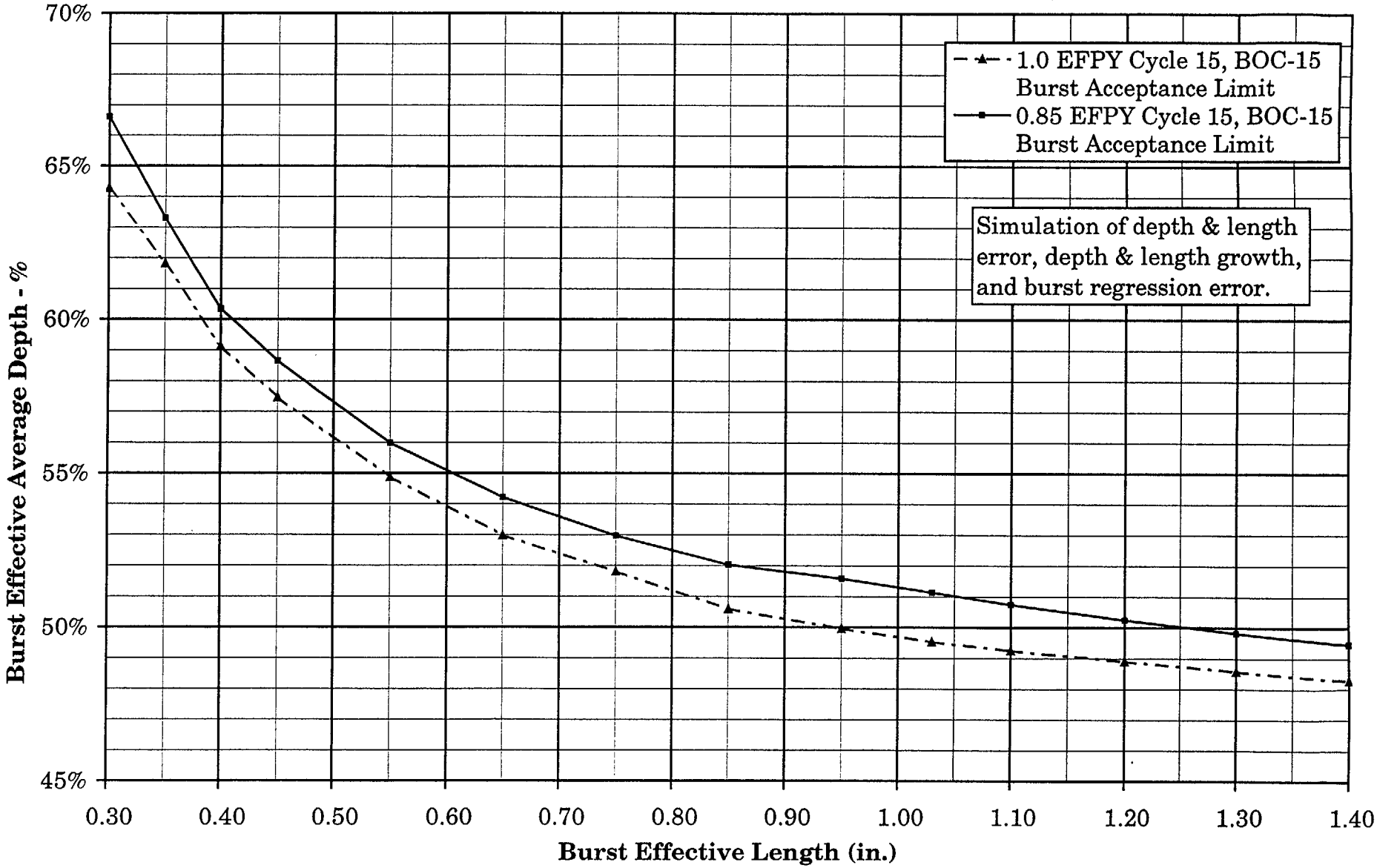

Figure 9-2. Indian Point U-Bend Operational Assessment
Limiting Burst Pressure and SLB Burst Probability Variation with EFPD

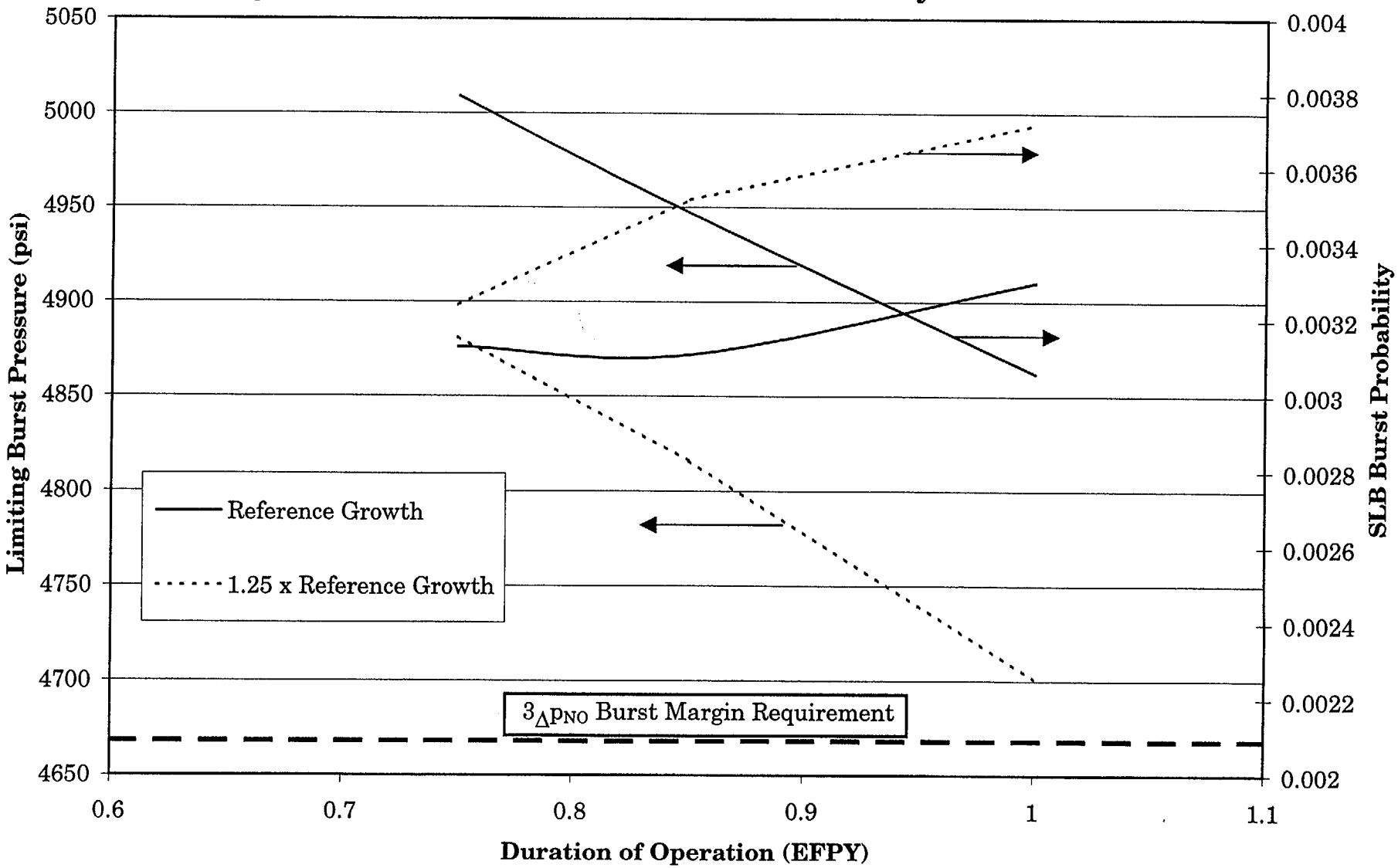

Figure 9-3
Projected Structural Integrity Figure of Merit of Row 3 U-Bends versus Operating Interval Length in Cycle 15

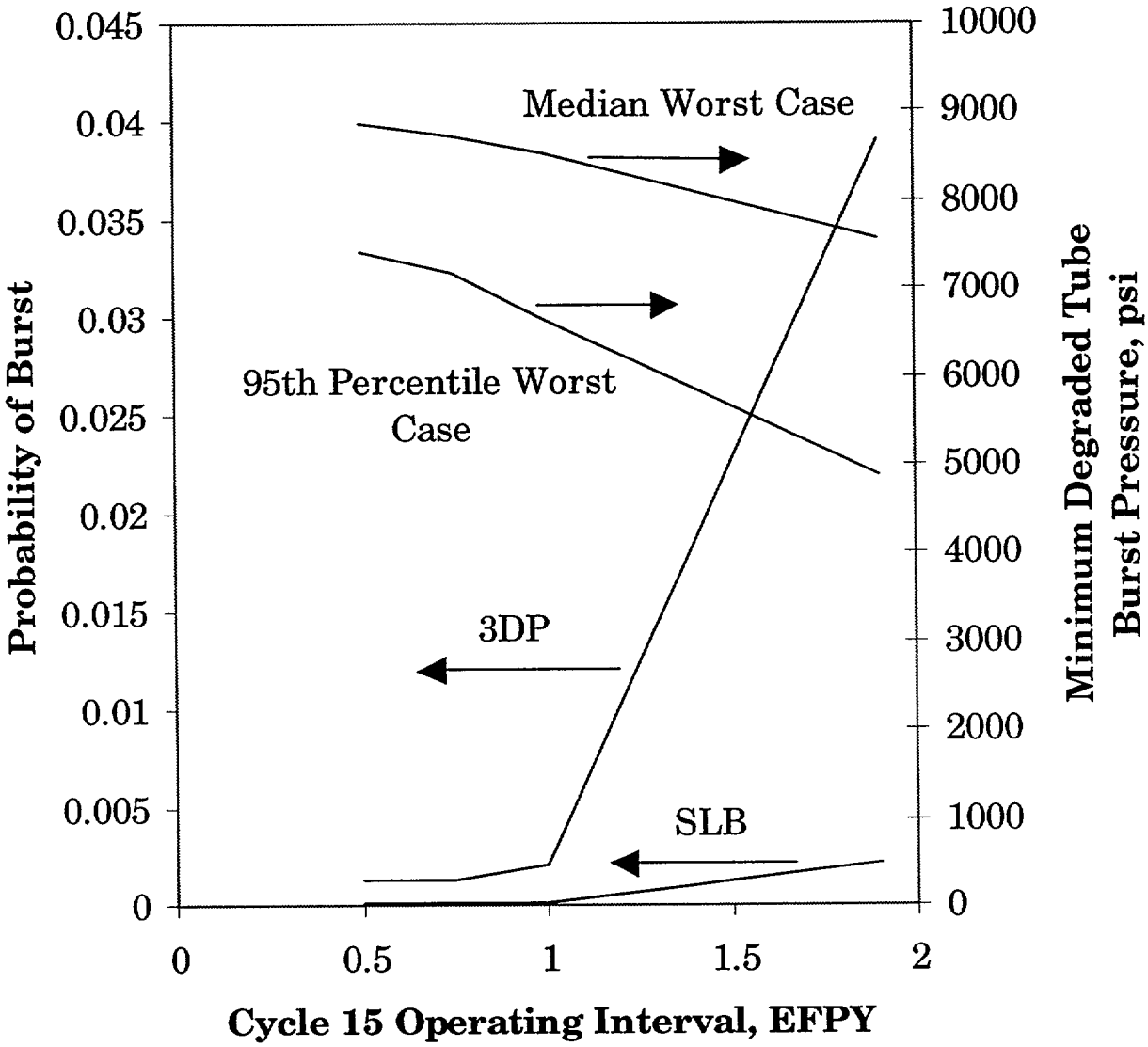

10.0 REFERENCES

10-1 Westinghouse Report SG-00-05-010, "Indian Point Unit 2, Cycle 14 Condition Monitoring Assessment for Degradation Mechanisms Other than U-bend PWSCC", May 30, 2000

10-2 "Indian Point-2 Root Cause Evaluation for SG-24, R2C5 Leakage Event", March 2000

10-3 EPRI Report TR-107620-R1, "Steam Generator In Situ Pressure Test Guidelines", June 1999

10-4 EPRI Report TR-107621, Rev. 0, "Steam Generator Integrity Assessment Guidelines; Revision 0", November, 1999

10-5 Altran Technical Report No. 00603-TR-004, "Secondary Side Condition Monitoring and Operational Assessment", included as appendix to Reference 10-1.

10-6 EPRI Report NP-7480-L, Volume 1, Revision 2, "Steam Generator Tubing Outside Diameter Stress Corrosion Cracking at Tube Support Plates Database for Alternate Repair Criteria: 7/8 Inch Diameter Tubing," June 1996

10-7 MRS-TRC-1088, Rev. 1, "Use of Appendix H Qualified Techniques at Indian Point Unit 2 Spring 2000 S/G Eddy Current Inspection," April 4, 2000

10-8 WCAP-15128, Revision 2, "Depth Based SG Tube Repair Criteria for Axial PWSCC at Dented TSP Intersections," March 2000, Westinghouse Electric Company LLC. Note: The databases used for the burst correlation in this report include updates transmitted to the NRC in TVA correspondence.

10-9 EPRI TR-109136, "Crack Growth and Microstructural Characterization of Nickel Alloy PWR Vessel Head Penetration Materials", December 1997

10-10 NSD-TAP-3136, "Sequoyah-2, Response to NRC Questions on SG Tube Integrity Assessment," Pitterle, T., Westinghouse Electric Company (September 4, 1996).

10-11 STD-7.2.4-7180 (Proprietary), "PWS 4.802 Final Report," Gowda, B., Westinghouse Electric Company (December 21, 1987).

10-12 MT-SGMCE-144 (Proprietary), "Burst Tests of Small Diameter U-Bends," Klein, A., Westinghouse Electric Company (June 16, 1982).

10-13 Personal communication between R. F. Keating (Nuclear Services Business Unit) and R. J. Jacko (Research & Technology Unit), Westinghouse Electric Company (April 10, 2000).

10-14 PD2-00-100, "Tension Test Results of Alloy 600 and 718 Screw Materials," Westinghouse Electric Company Proprietary Class 2, March 29, 2000.

10-15 "Reliability in Engineering Design," Kapur and Lamberson (1977), John Wiley and Sons, Inc., pp. 300.

10-16 P. E. McDonald, V. N. Shah, L. W. Ward and P. G. Ellison, "Steam Generator Tube Failures" NUREG/CR-6365, INEL-95-0383, April 1996.

10-17 EPRI Report TR-105958, "Crack Growth and Microstructural Characterization of Alloy 600 Vessel Head Penetration Materials", December 1995.

10-18 Majumbar, Saurin, "Predictions of Structural Integrity of Steam Generator Tubes Under Normal Operating, Accident, and Severe Accident Conditions," 24th Water Reactor Safety Meeting, October 21-26, 1996, Bethesda, MD.

10-19 S.Yashima, et al; "Stresses of Steam Generator U-tubes Affecting Stress Corrosion Cracking", ASME 82-NE-5.

10-20 EPRI Report TR-105656, "Multivariable Analysis of the Effects of Li, H_2, and pH on Primary Water Stress Corrosion Crack Initiation", May 1996.

10-21 NUREG/CR-5752 ANL-99/4, "Assessment of Current Understanding of Mechanisms of Initiation, Arrest, and Reinitiation of Stress Corrosion Cracks in PWR Steam Generator Tubing", February, 2000

11.0 GLOSSARY OF ABBREVIATIONS

ANL	Argonne National Laboratories
ARC	Alternate Repair Criteria
BDA	Eddy Current Data not useable due to low signal to noise ratio
BOC	Beginning of Cycle
CFD	Cumulative Distribution Function
Circ.	Circumferential
CL	Confidence Level
CM	Condition Monitoring
CMOA	Condition Monitoring and Operational Assessment
CMTR	Certified Material Test Report
Col.	Column
CPD	Cumulative Probability Distribution (same as CFD)
C-scan	Topographical Map Presentation of + Point EC Data
Dia	Diameter
EC	Eddy Current
EOC	End of Cycle
EDM	Electro-Discharge Machining
EFPD	Effective Full Power Days (24 hours at 100% power)
EFPY	Effective Full Power Years (365 EFPD)
EPRI	Electric Power Research Institute
ETSS	Examination Technique Specification Sheet
FEA	Finite Element Analysis
GPD	Gallons per Day
GPM	Gallons per Minute
HR	Hour
ID	Inside Diameter
IGA	Intergranular Attack
Ind.	Indication
IP2	Indian Point 2
ISI	In Service Inspection
Kcal	Kilo (one thousand) calories
kHz	Kilo (one thousand) hertz
Ksi	Thousands of Pounds per Square Inch
Loc.	Location
MA	Mill Annealed
MAI	Multiple Axial Indication
NDD	No Detectable Degradation
NDE	Non Destructive Examination
NOP	Normal Operating Pressure (also subscript NO)
NRC	Nuclear regulatory Commission
OA	Operational Assessment
OD	Outside Diameter
ODSCC	Outside Diameter Stress Corrosion Cracking
POD	Probability of Detection
PSI	Pounds per Square Inch

PSIA	Pounds per Square Inch Absolute
PWR	Pressurized Water Reactor
PWSCC	Primary Water Stress Corrosion Cracking
RAI	Request for Additional Information
R_C__	Row and Column in the SG Tube Bundle, R3C85 = Row 3 Column 85
RPC	Rotating Pancake Coil
RST	Restricted Tube
SAI	Single Axial Indication
SCC	Stress Corrosion Cracking
SG	Steam Generator
SLB	Steam Line Break
S/N	Signal to Noise Ratio
TSP	Tube Support Plate
TW	Through Wall (implies TWD)
TWD	Through Wall Depth
UTEC	Ultra Sonic Eddy Current (name for ultrasonic test equipment)
V	Volts
2R14	Indian Point 2 Refueling Outage Number 14

APPENDIX A

C-Scans for
400kHz and 800 kHz

APPENDIX A.1

Year 2000 C-Scans

Comparison of 400 kHz Mid-Range and 800 kHz High Frequency Probe

Figure A.1-1. Year 2000, SG1, U-Bend Tube R2C87 – 400 kHz Mid-Range

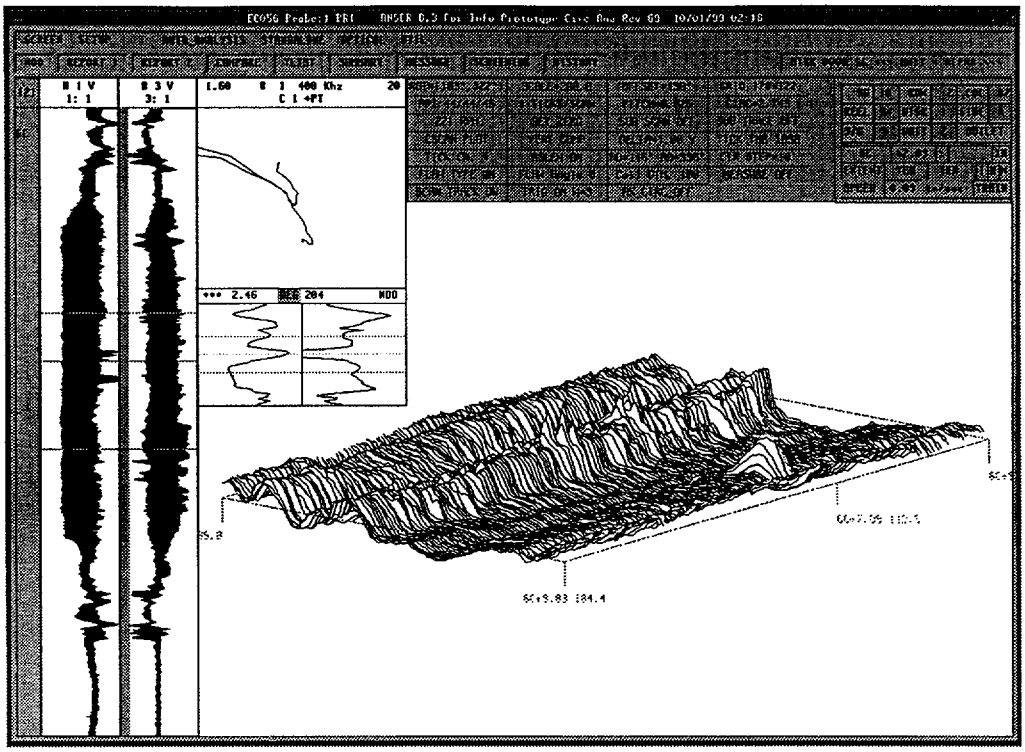

Figure A.1-2. Year 2000, SG1, U-Bend Tube R2C87 – 800 kHz High Frequency

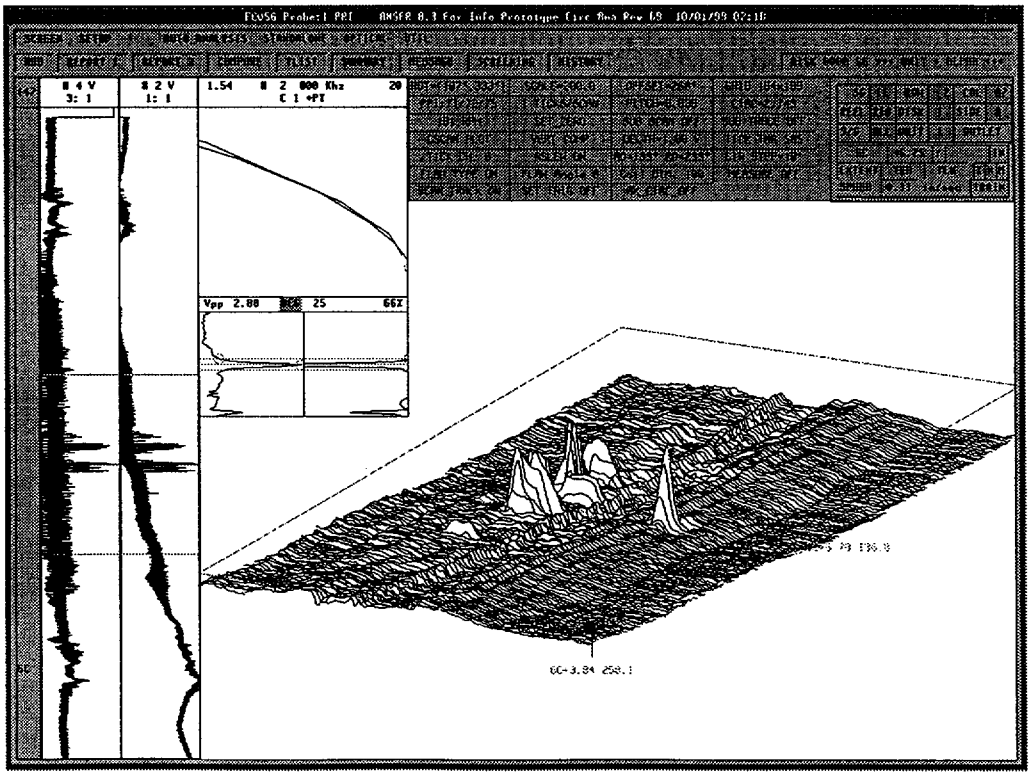

Figure A.1-3. Year 2000, SG 3, U-Bend Tube R2C85 – 400 kHz Mid-Range

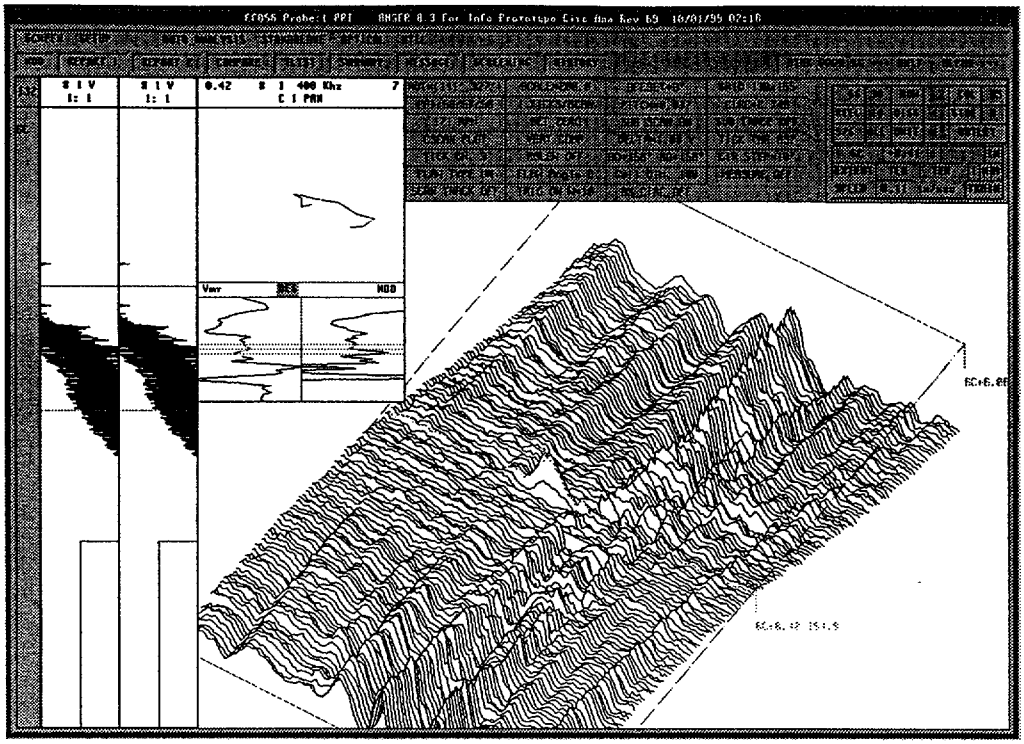

Figure A.1-4. Year 2000, SG 3, U-Bend Tube R2C85 – 800 kHz High Frequency

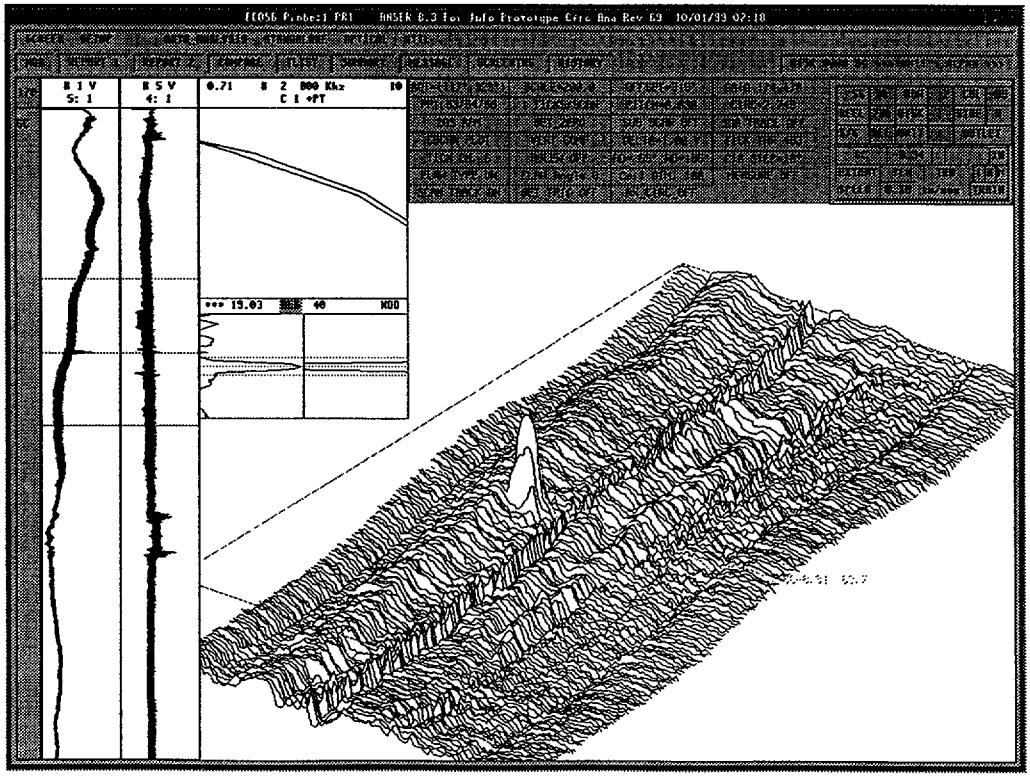

Figure A.1-5. Year 2000, SG 4, U-Bend Tube R2C4 – 400 kHz Mid-Range

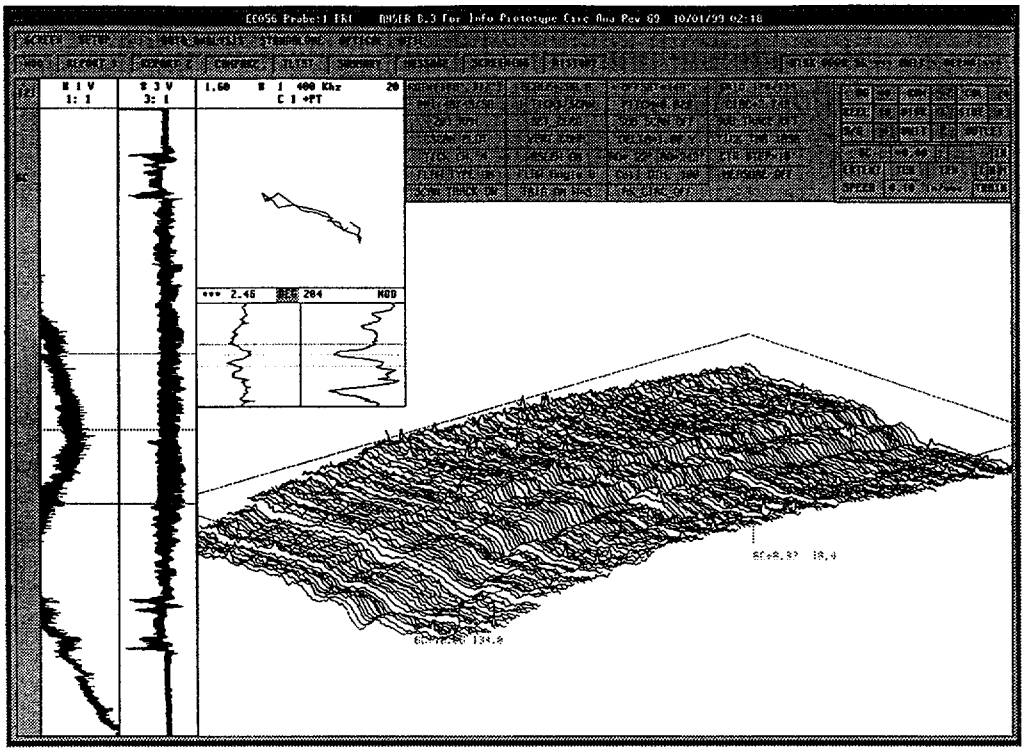

Figure A.1-6. Year 2000, SG 4, U-Bend Tube R2C4 – 800 kHz High Frequency

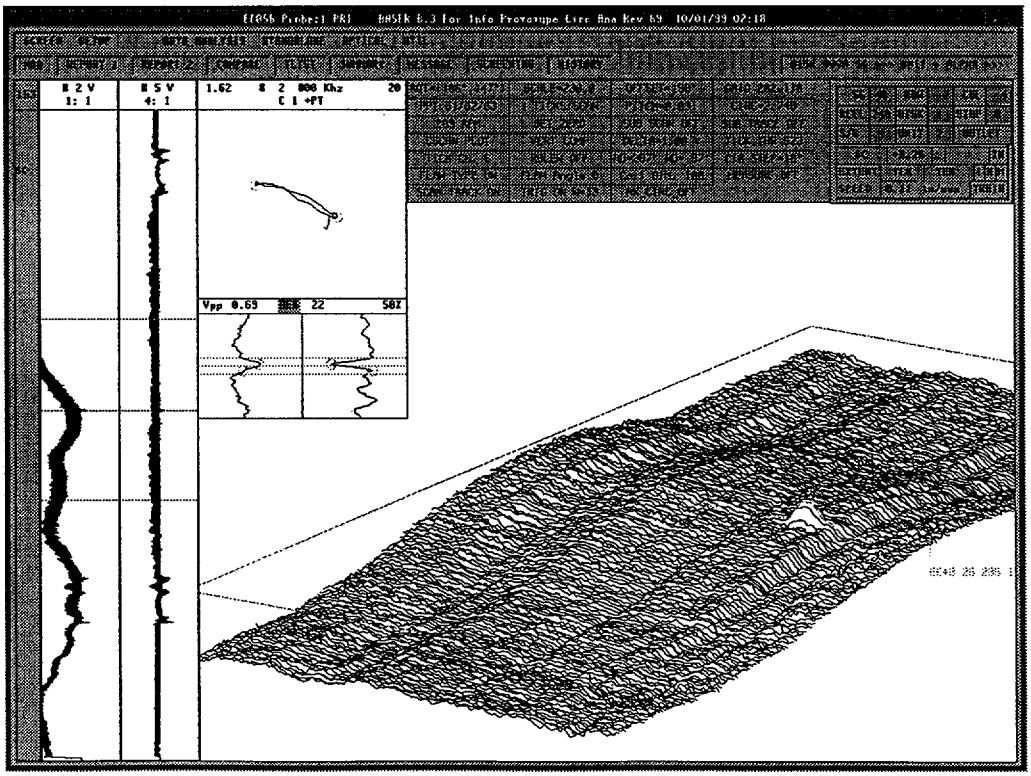

Figure A.1-7. Year 2000, SG 4, U-Bend Tube R2C69 – 400 kHz Mid-Range

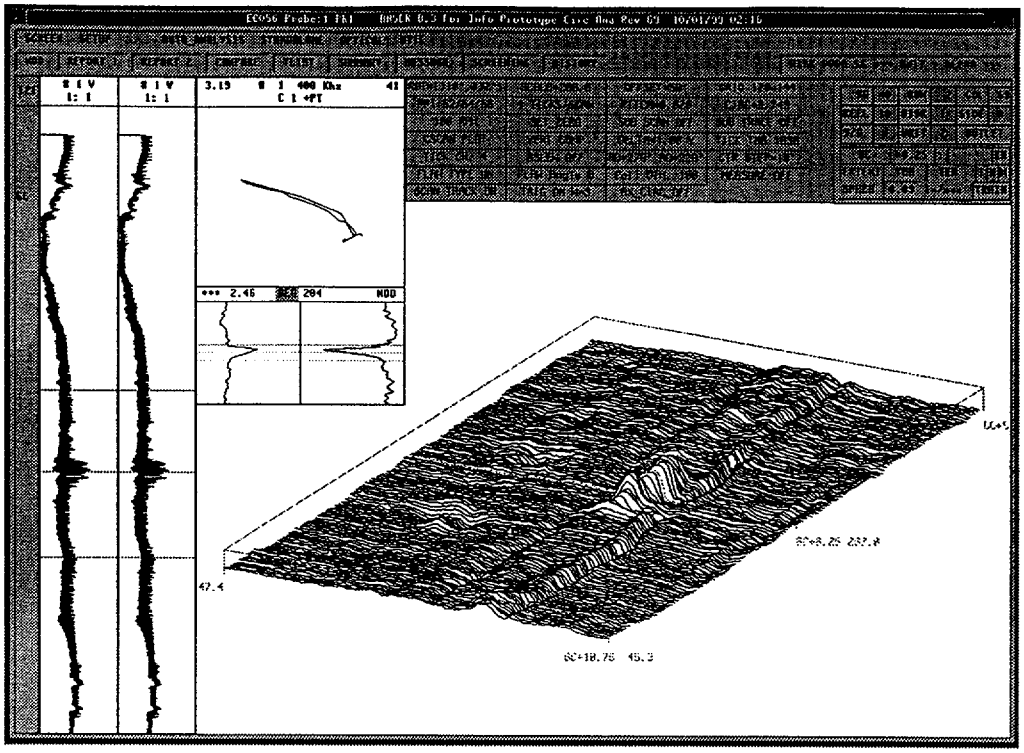

Figure A.1-8. Year 2000, SG 4, U-Bend Tube R2C69 – 800 kHz High Frequency

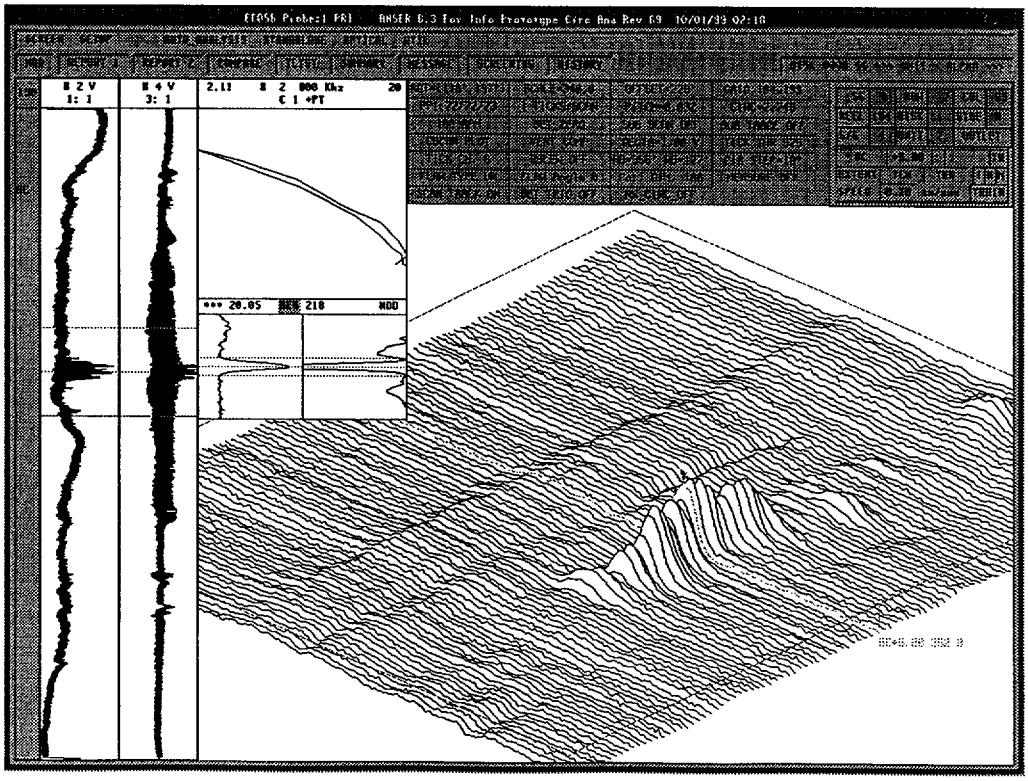

Figure A.1-9. Year 2000, SG 4, U-Bend Tube R2C71 – 400 kHz Mid-Range

(No C-Scan Available)

Figure A.1-10. Year 2000, SG 4, U-Bend Tube R2C71 – 800 kHz High Frequency

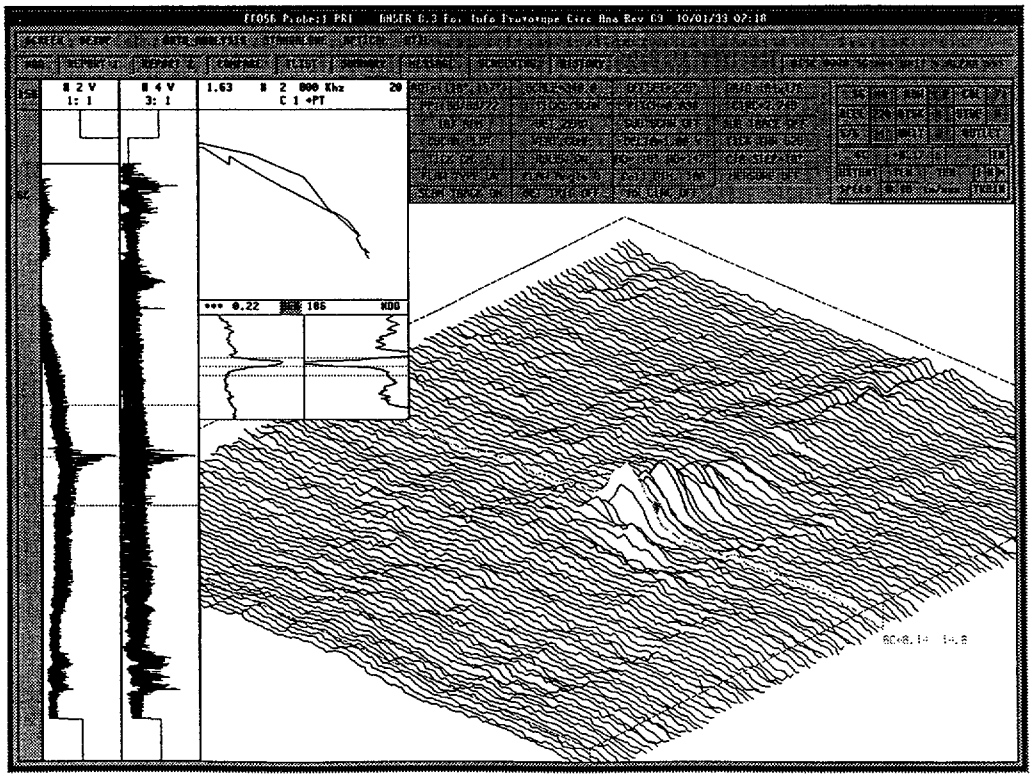

Figure A.1-11. Year 2000, SG 4, U-Bend Tube R2C72 – 400 kHz Mid-Range

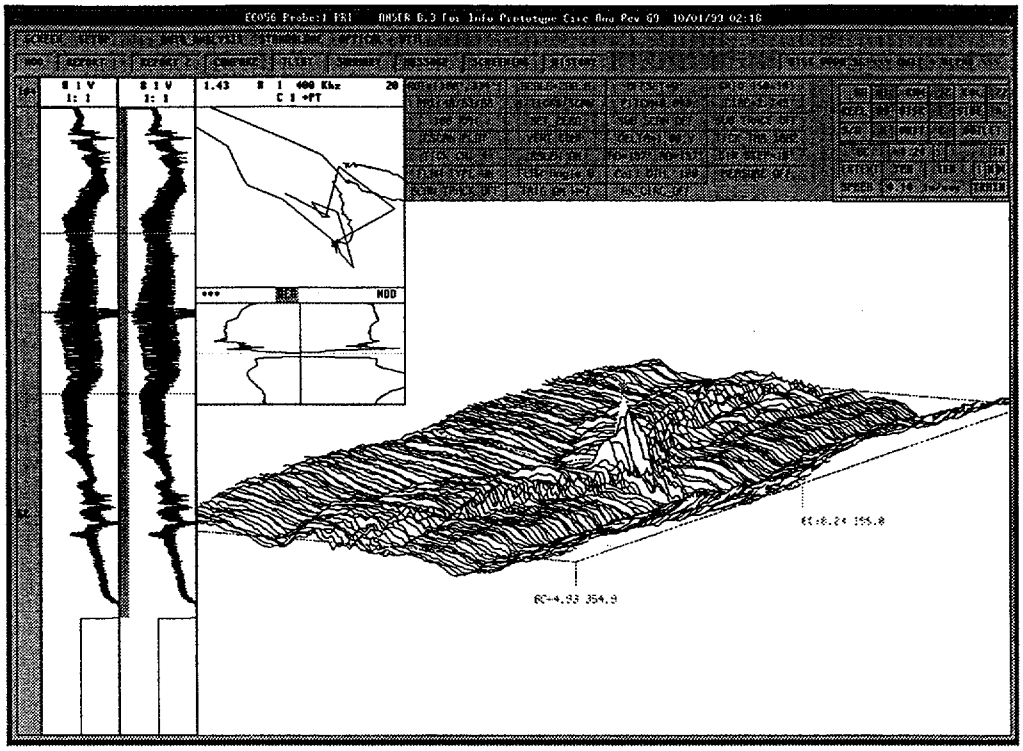

Figure A.1-12. Year 2000, SG 4, U-Bend Tube R2C72 – 800 kHz High Frequency

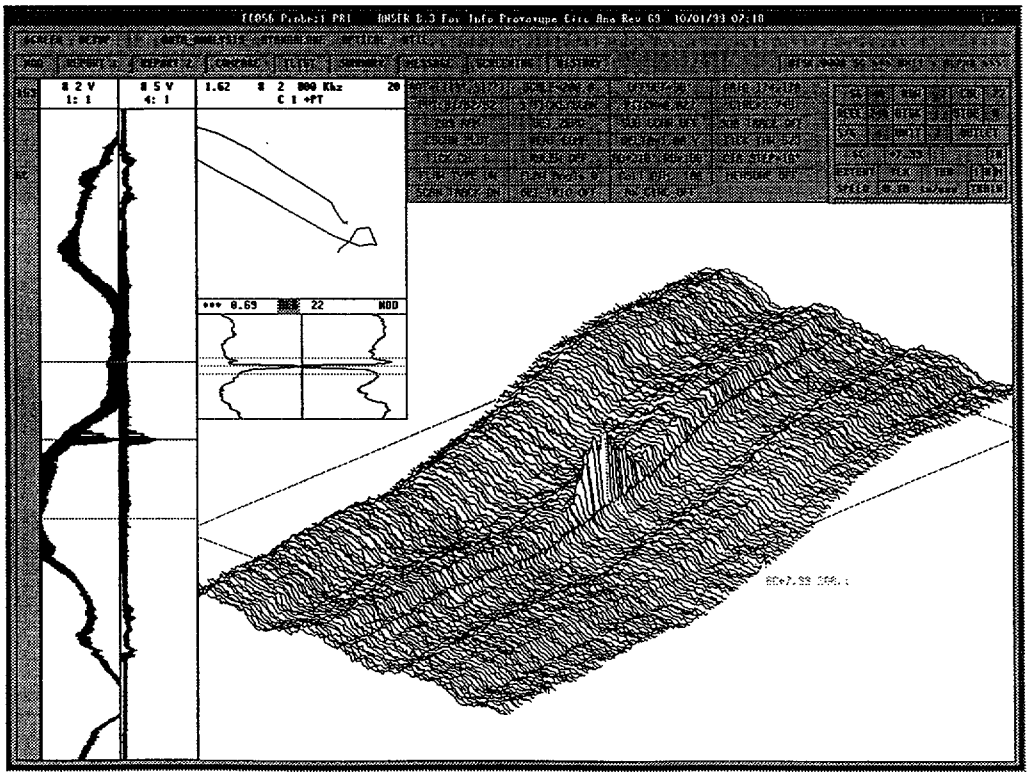

Figure A.1-13. Year 2000, SG 4, U-Bend Tube R2C74 – 400 kHz Mid-Range

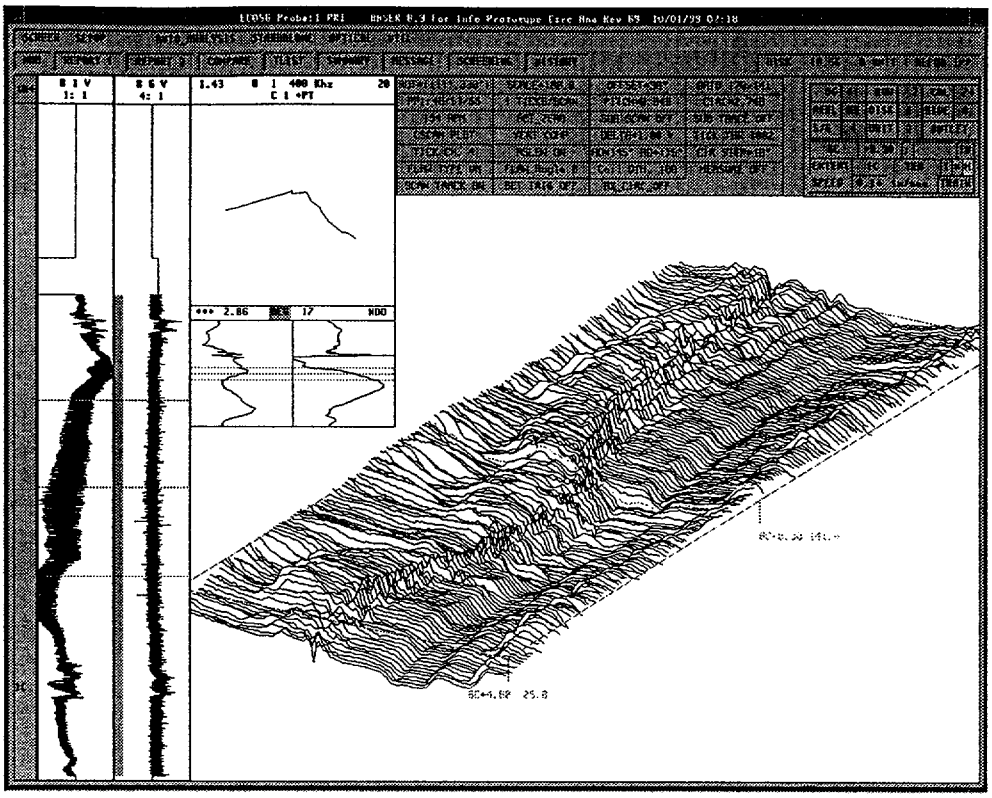

Figure A.1-14. Year 2000, SG 4, U-Bend Tube R2C74 – 800 kHz High Frequency

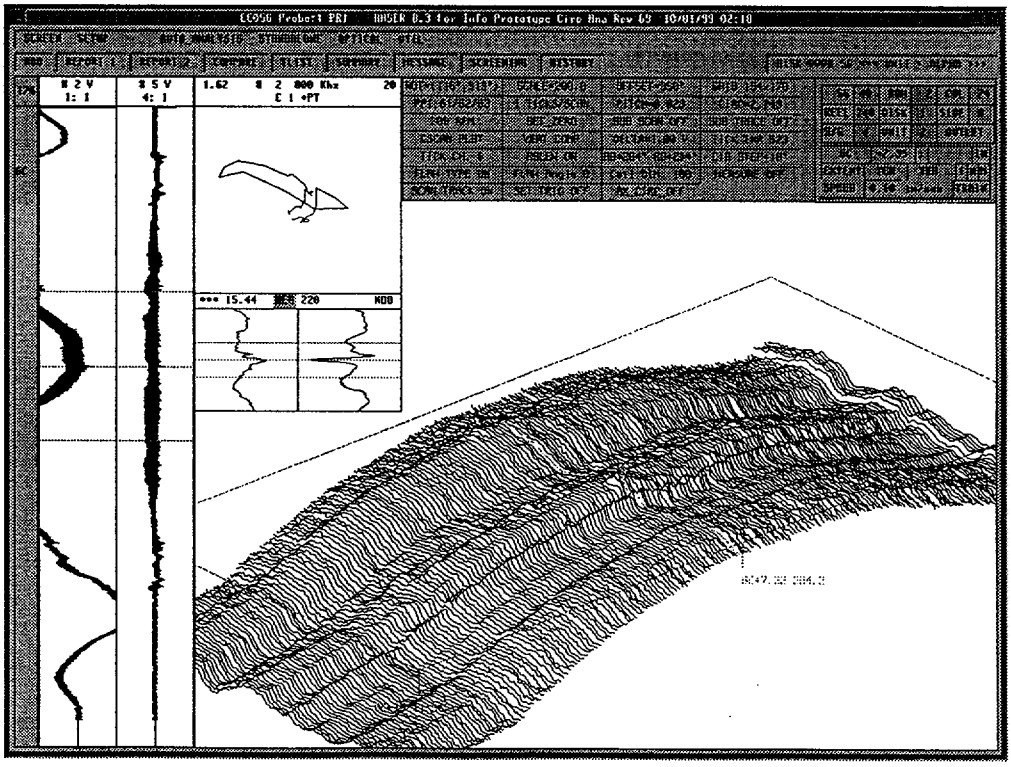

APPENDIX A.2

C-Scans for

1997

400 kHz

Figure A.2-1. Year 1997, SG 1, U-Bend Tube R2C87 – 400 kHz

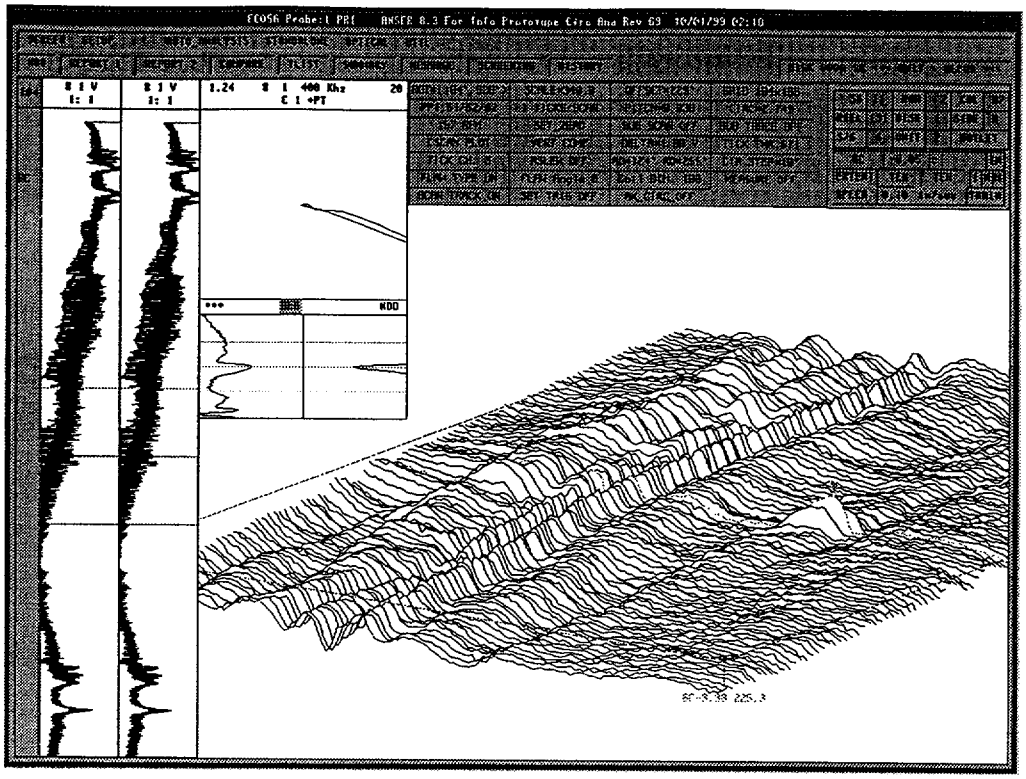

Figure A.2-2. Year 1997, SG 4, U-Bend Tube R2C5 – 400 kHz

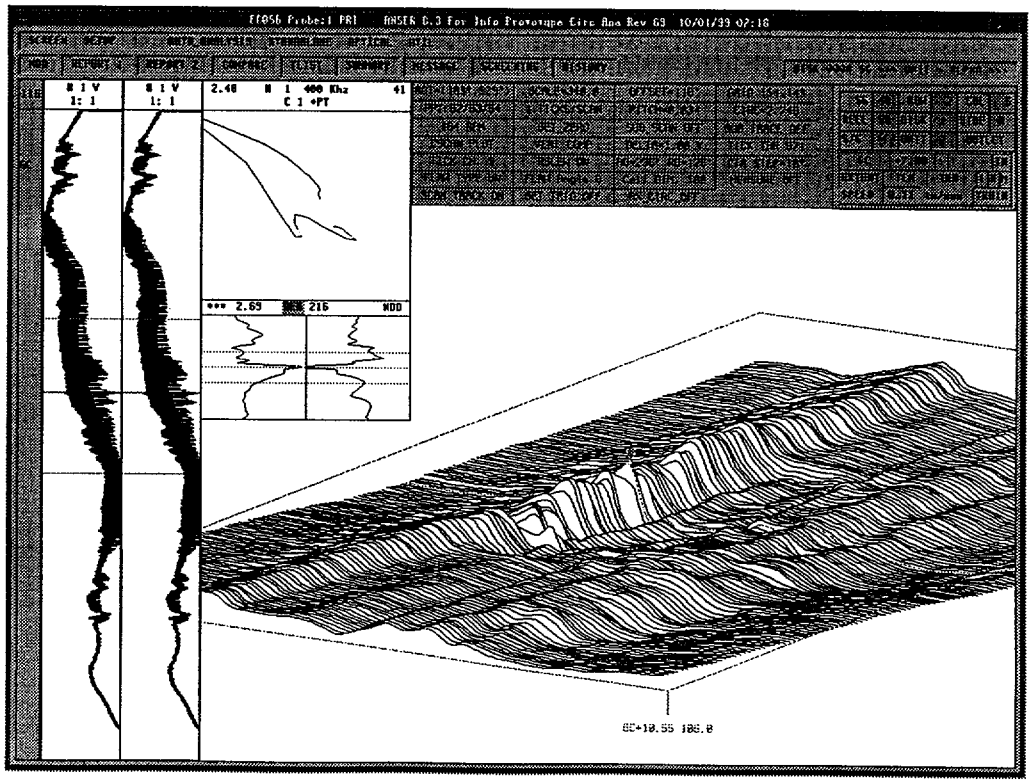

Figure A.2-3. Year 1997, SG 4, U-Bend Tube R2C69 – 400 kHz

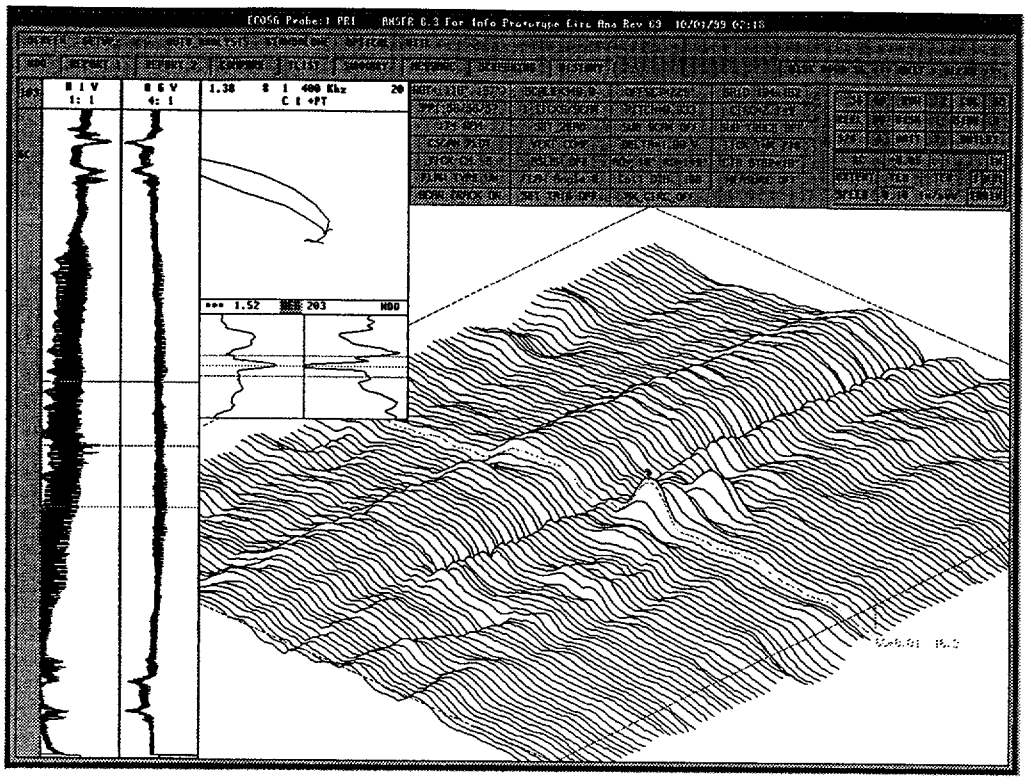

Figure A.2-4. Year 1997, SG 4, U-Bend Tube R2C71 – 400 kHz

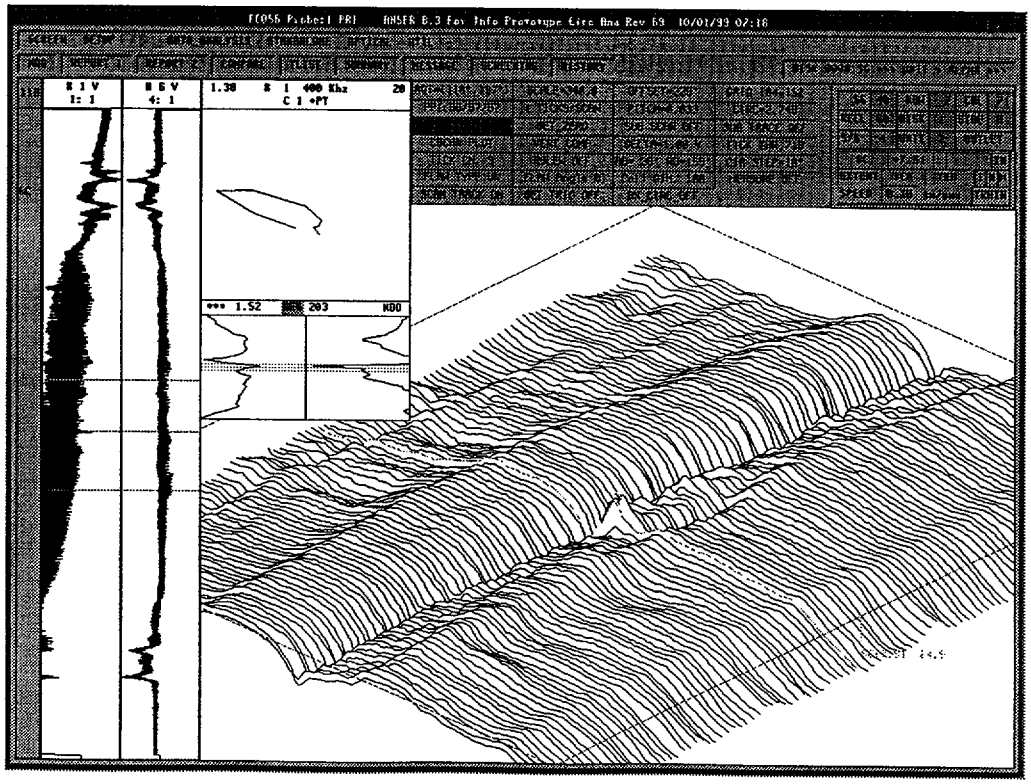

Figure A.2-5. Year 1997, SG 4, U-Bend Tube R2C72 – 400 kHz

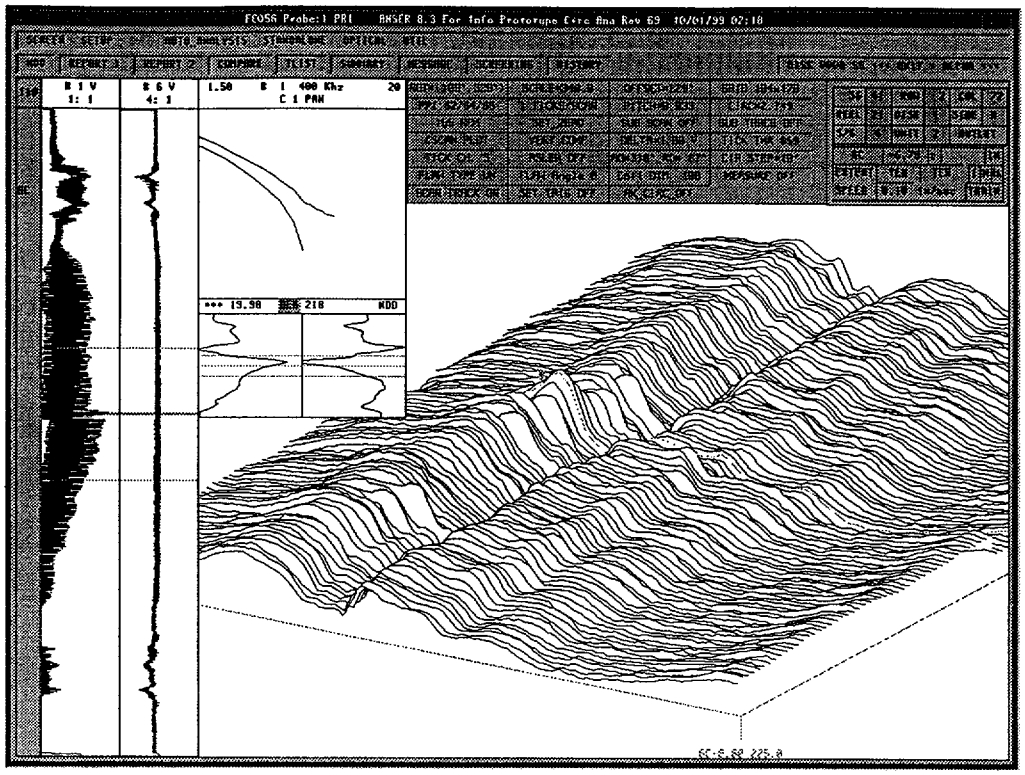

Figure A.2-6. Year 1997, SG 4, U-Bend Tube R2C74 – 400 kHz

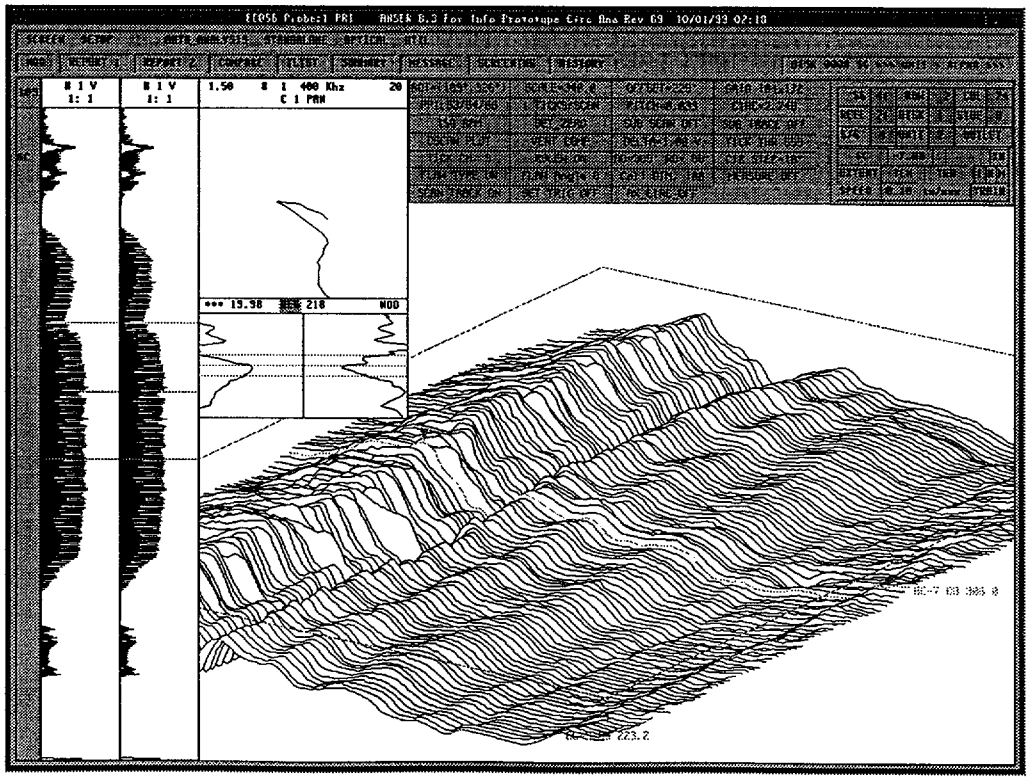

APPENDIX A.3

Year 2000 C-Scans

Comparison of 400 kHz Mid-Range and High Frequency Probe

Figure A.3-1. Year 2000, SG1, U-Bend Tube R2C87 – 400 kHz Mid-Range

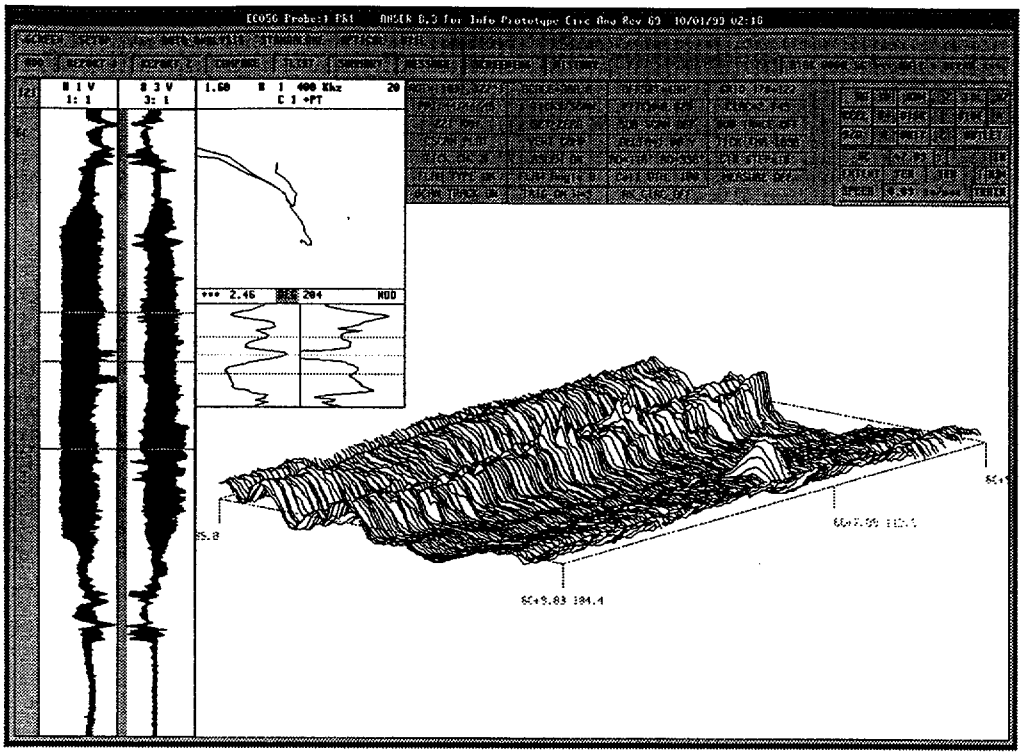

Figure A.3-2. Year 2000, SG1, U-Bend Tube R2C87 – 400 kHz High Frequency

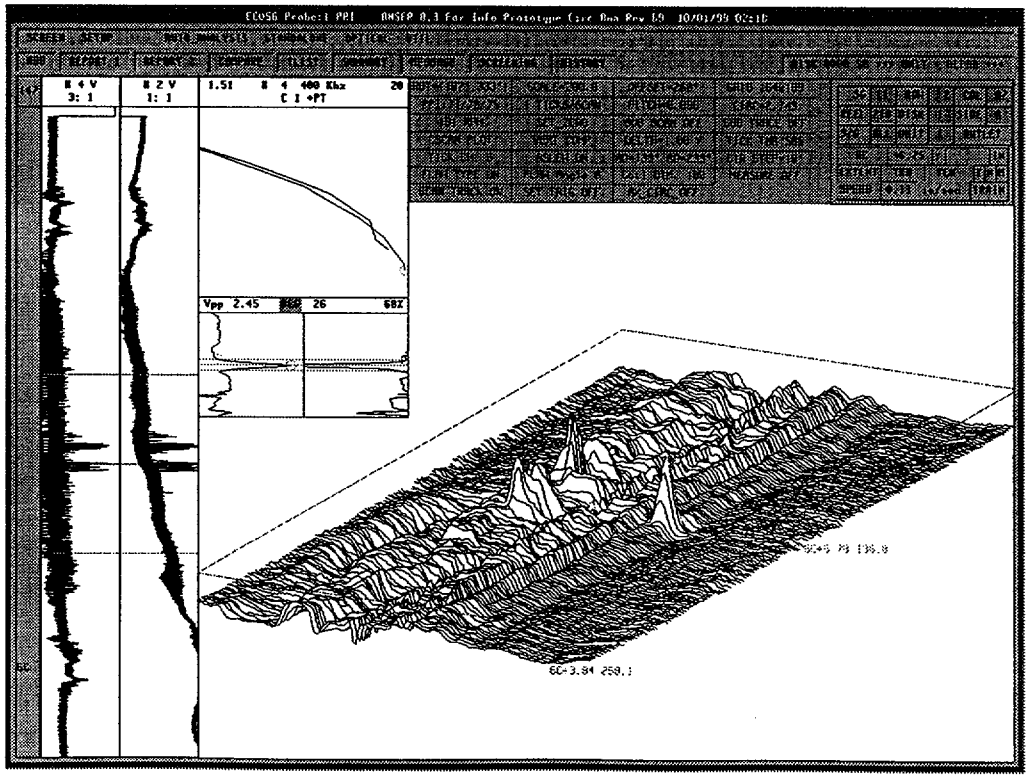

Figure A.3-3. Year 2000, SG 3, U-Bend Tube R2C85 – 400 kHz Mid-Range

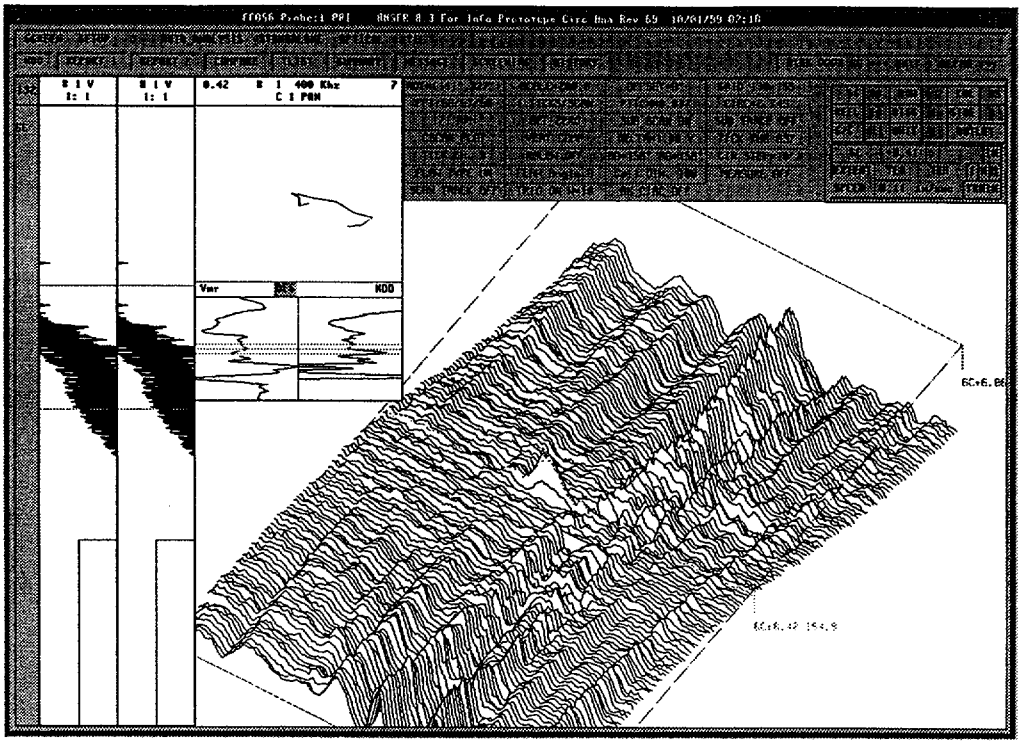

Figure A.3-4. Year 2000, SG 3, U-Bend Tube R2C85 – 400 kHz High Frequency

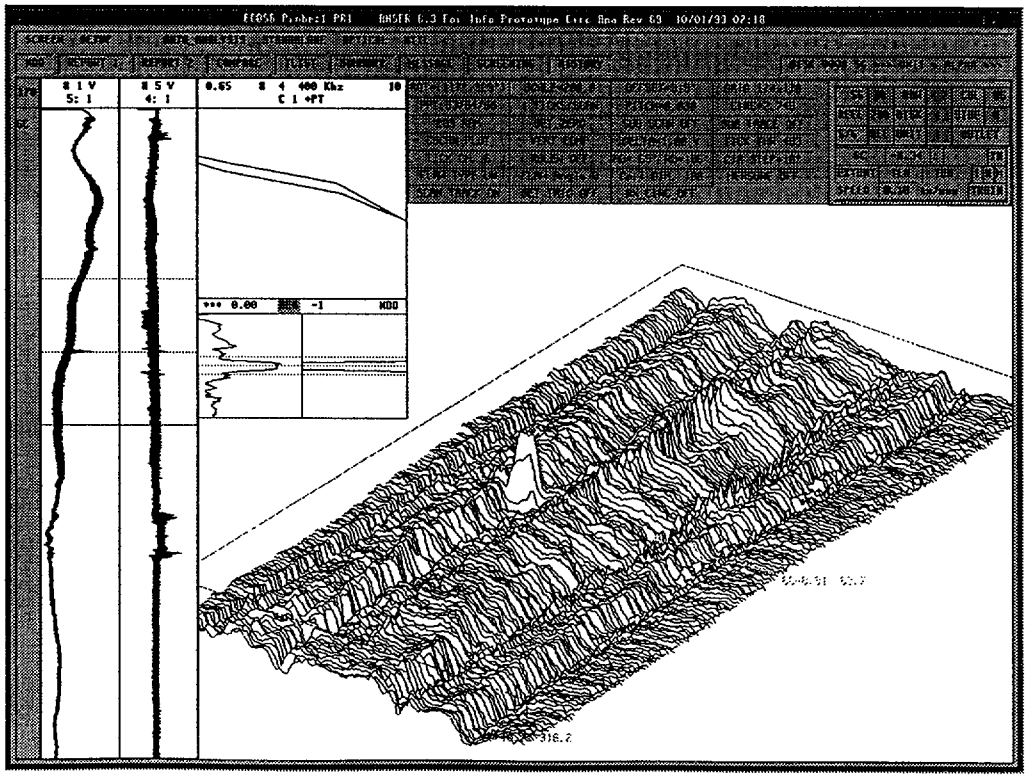

Figure A.3-5. Year 2000, SG 4, U-Bend Tube R2C4 – 400 kHz Mid-Range

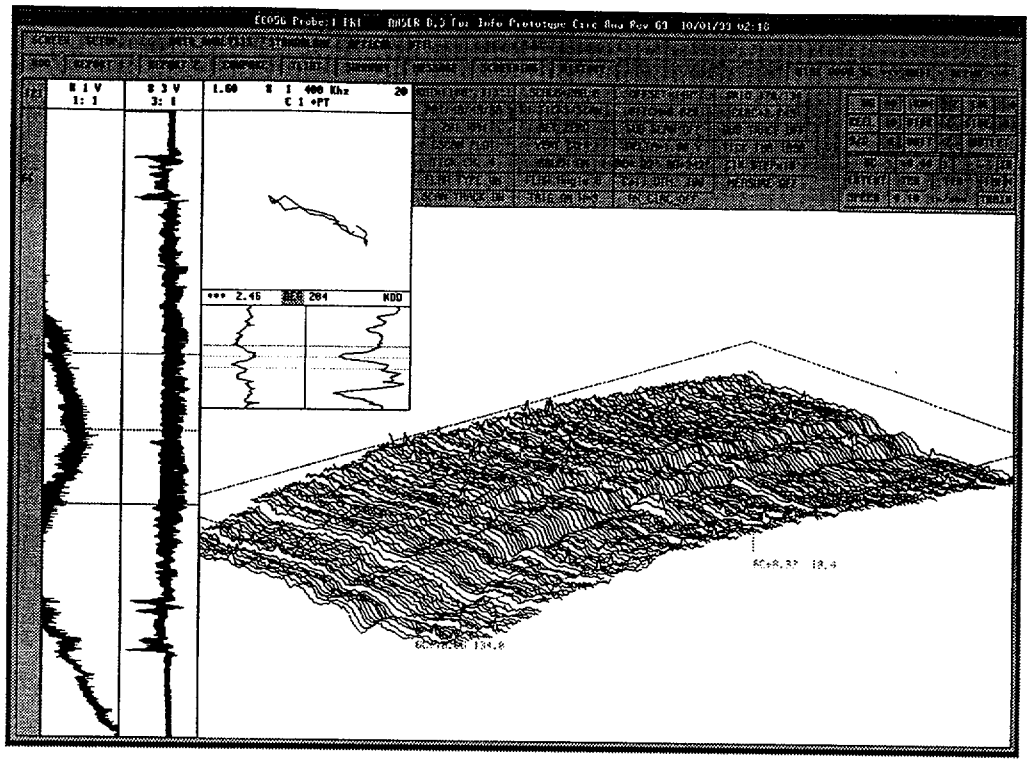

Figure A.3-6. Year 2000, SG 4, U-Bend Tube R2C4 – 400 kHz High Frequency

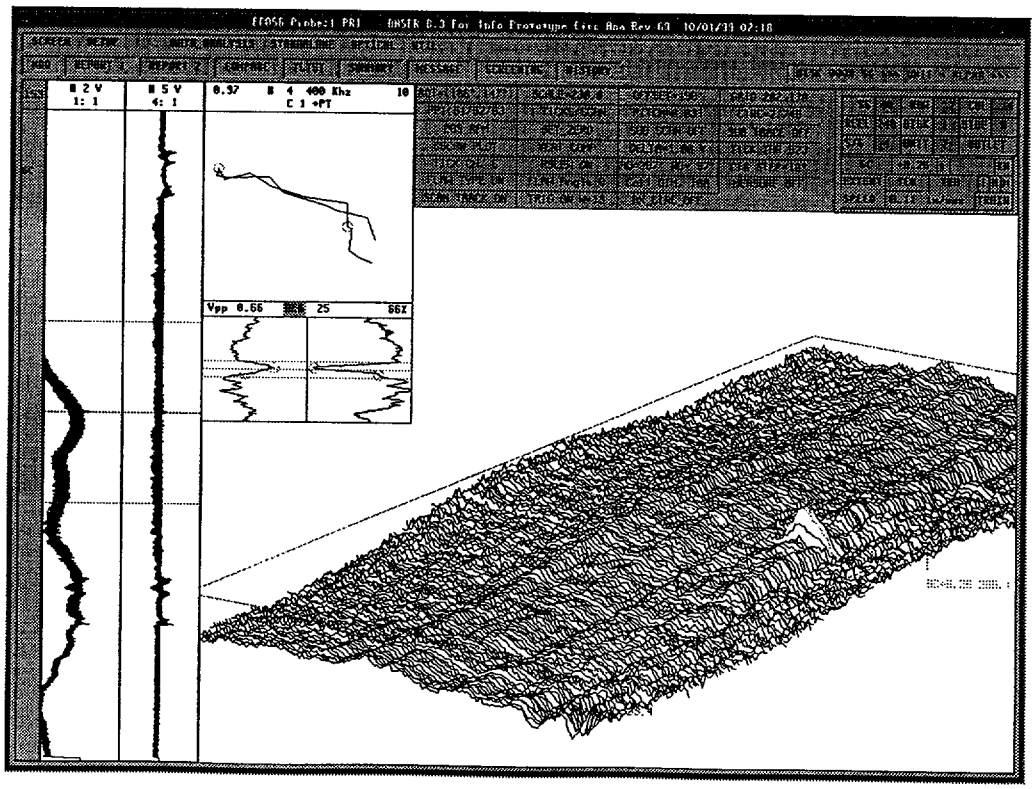

Figure A.3-7. Year 2000, SG 4, U-Bend Tube R2C69 – 400 kHz Mid-Range

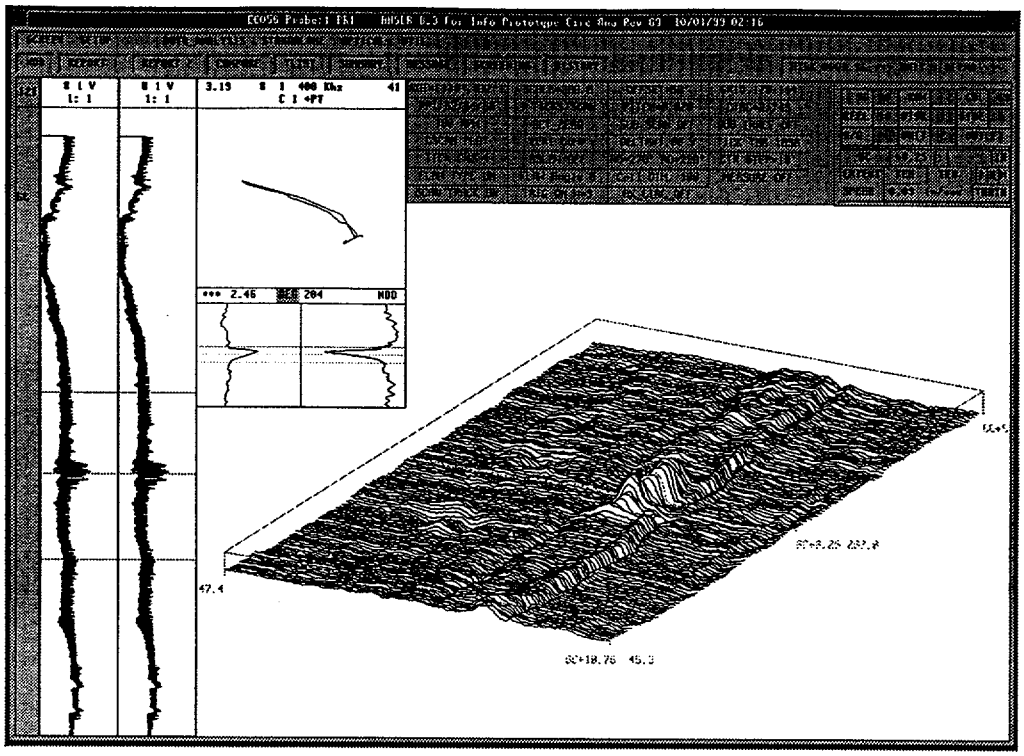

Figure A.3-8. Year 2000, SG 4, U-Bend Tube R2C69 – 400 kHz High Frequency

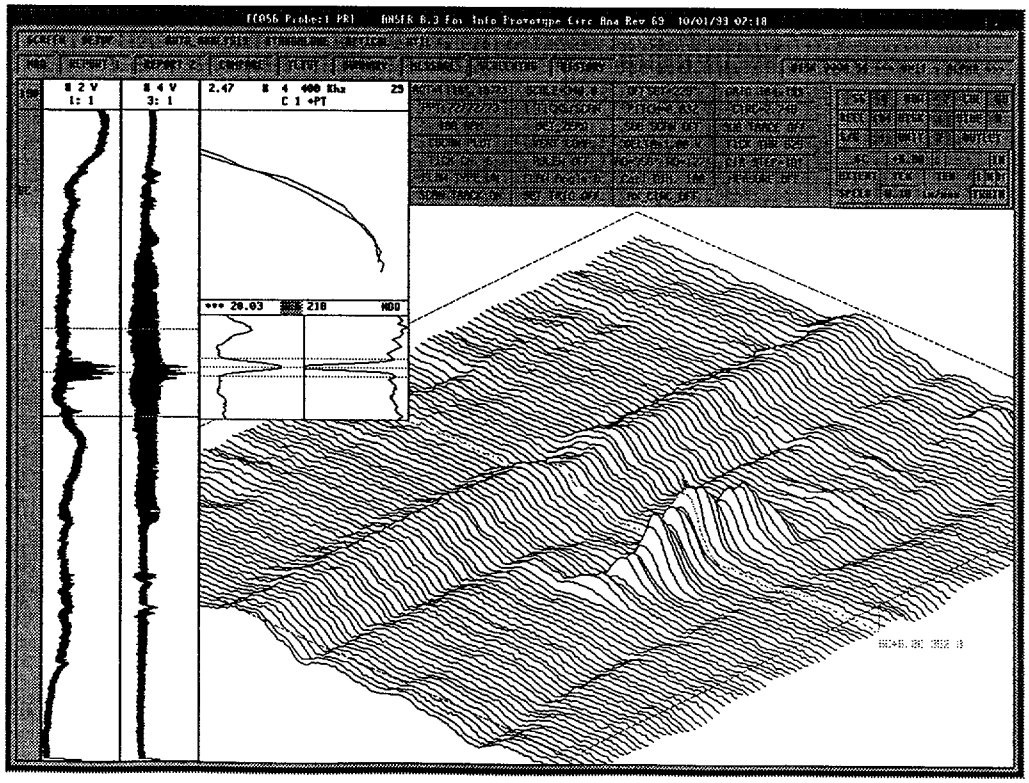

Figure A.3-9. Year 2000, SG 4, U-Bend Tube R2C71 – 400 kHz High Frequency

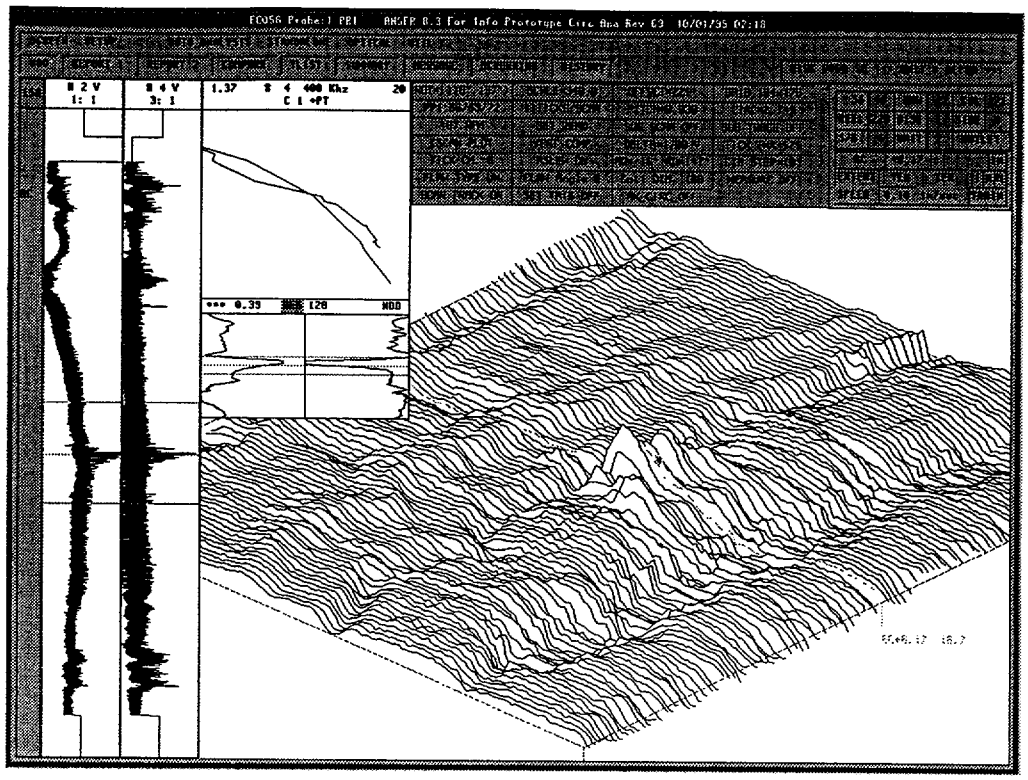

Figure A.3-10. Year 2000, SG 4, U-Bend Tube R2C72 – 400 kHz Mid-Range

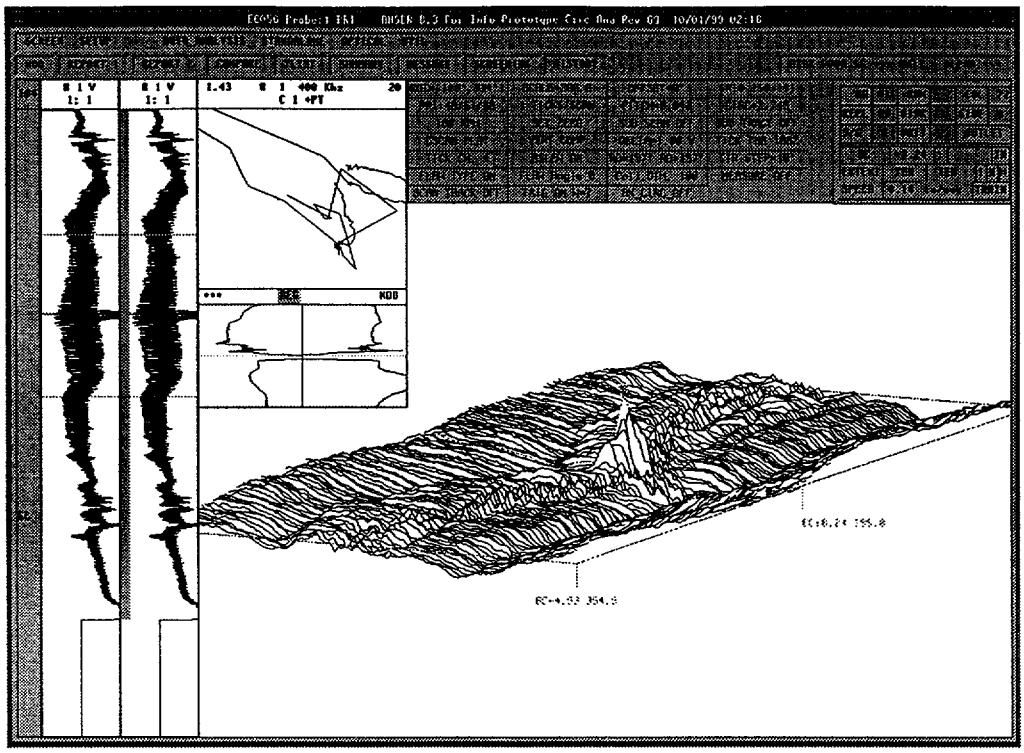

Figure A.3-11. Year 2000, SG 4, U-Bend Tube R2C72 – 400 kHz High Frequency

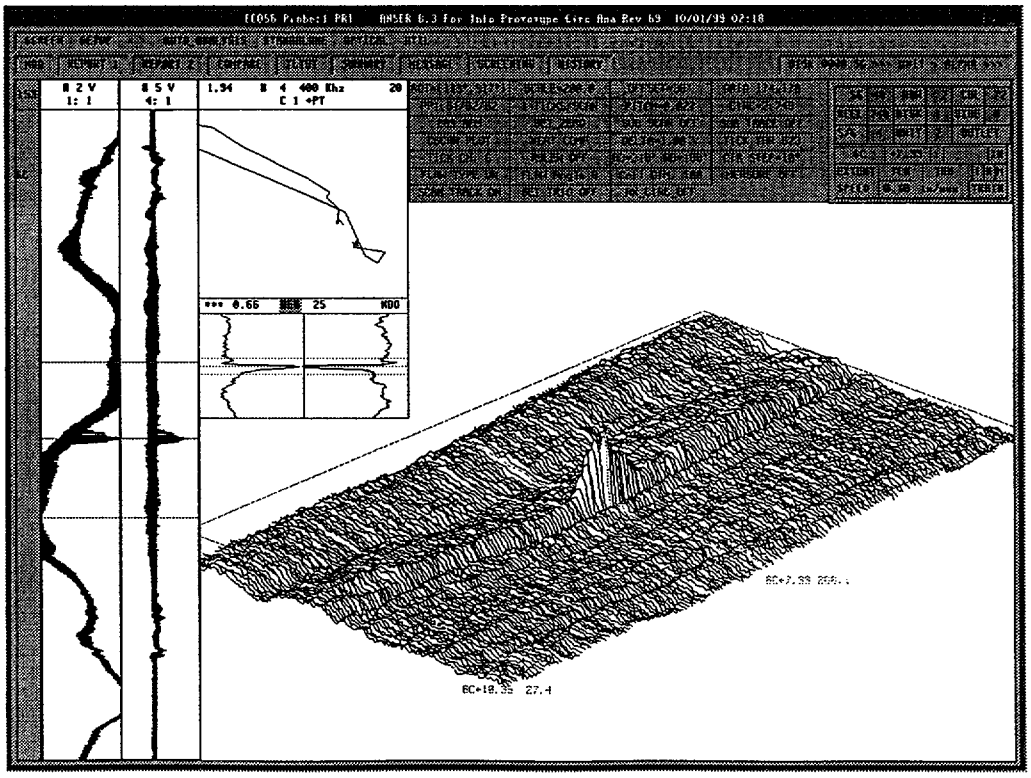

Figure A.3-12. Year 2000, SG 4, U-Bend Tube R2C74 – 400 kHz Mid-Range

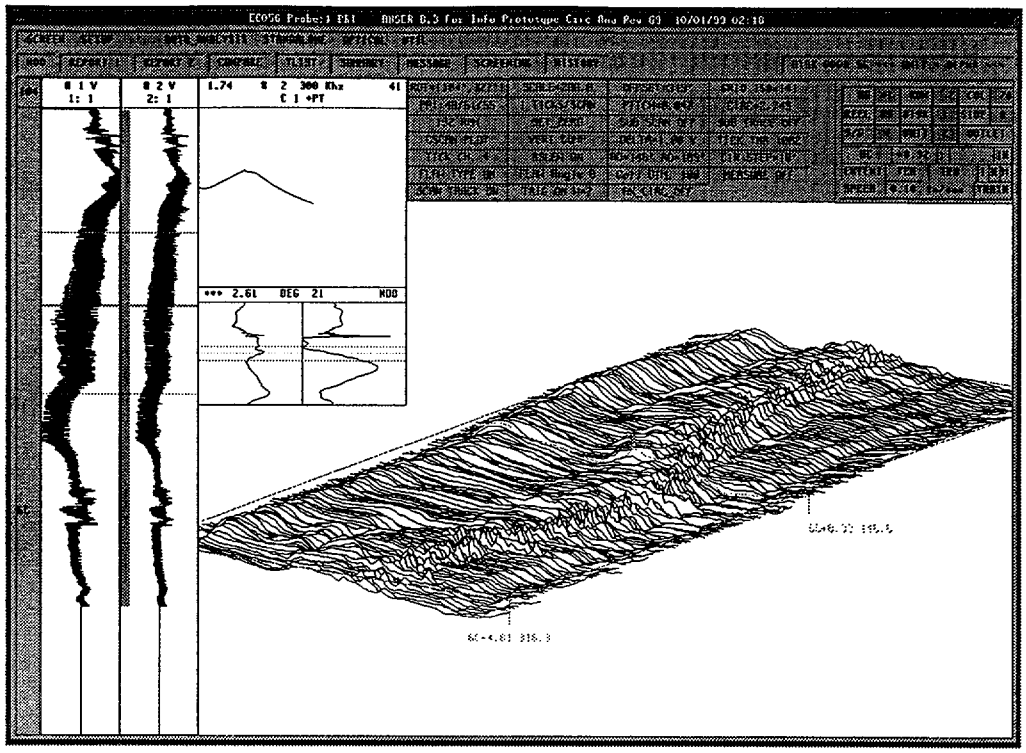

Figure A.3-13. Year 2000, SG 4, U-Bend Tube R2C74 – 400 kHz High Frequency

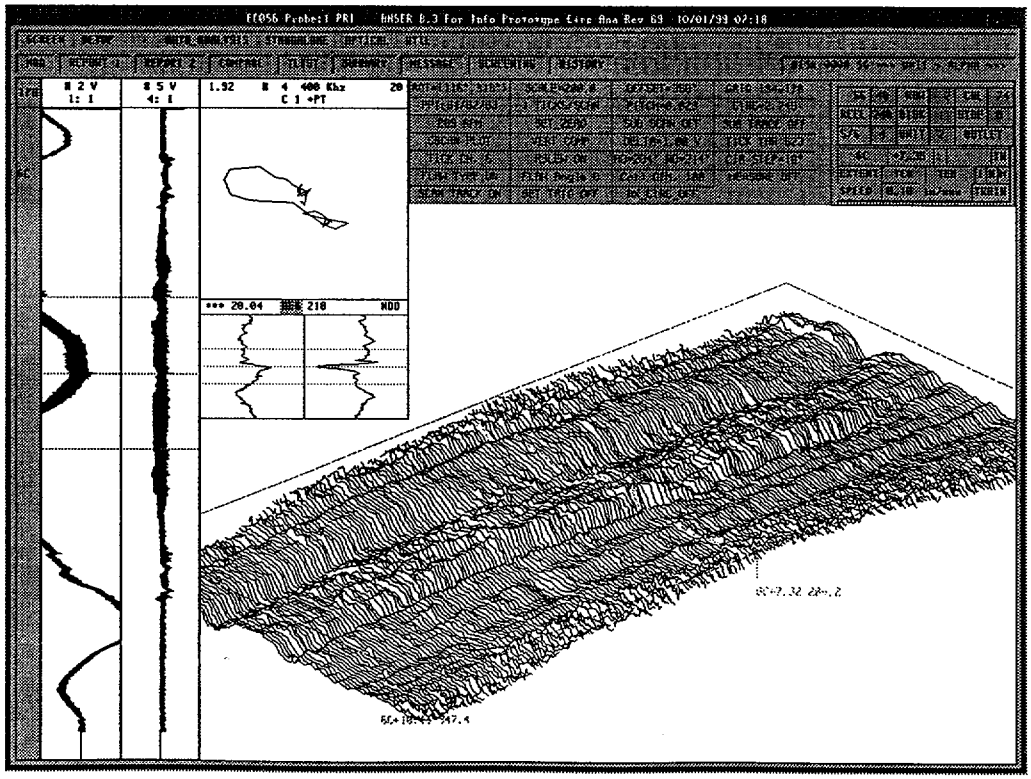

APPENDIX B

C-Scans for
Pre and Post Insitu

Figure B-1. Year 2000, SG 4, U-Bend R2C69 Pre-Insitu – 400 kHz HF

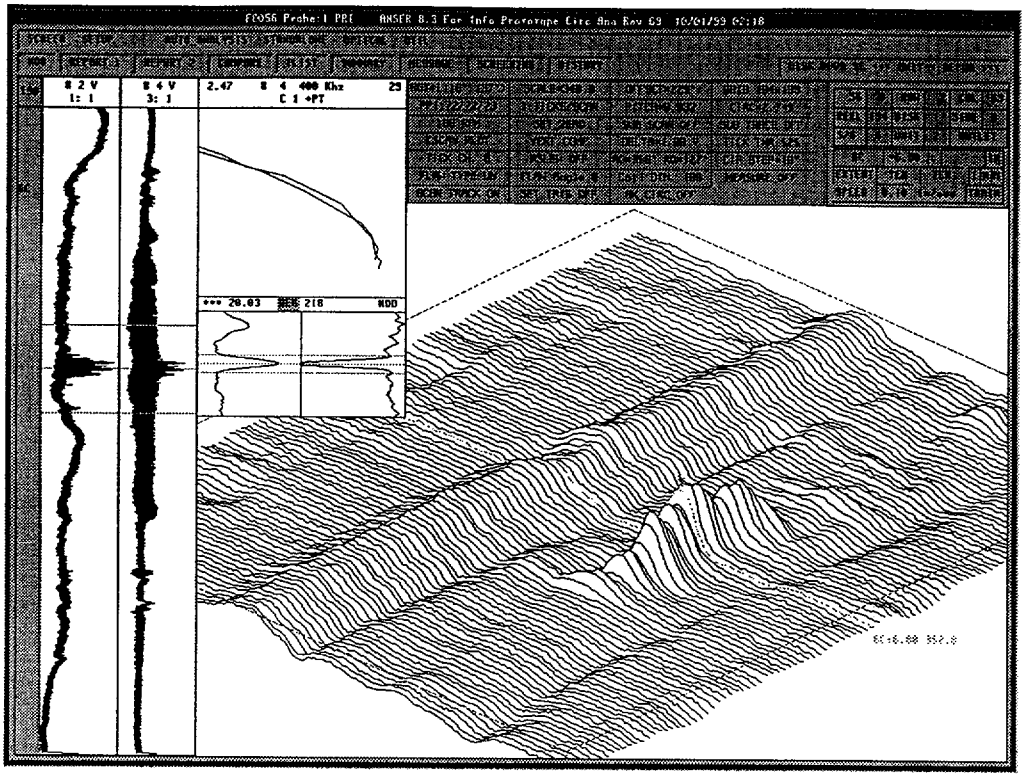

Figure B-2. Year 2000, SG 4, U-Bend R2C69 Post-Insitu – 400 kHz HF

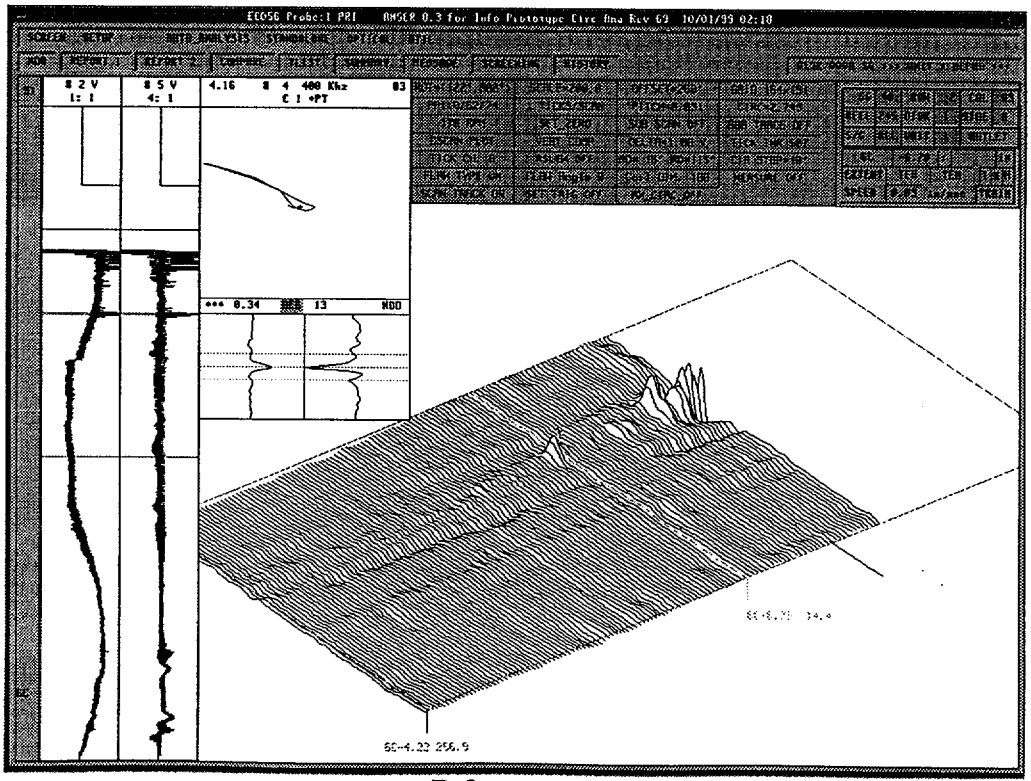

Figure B-3. Year 2000, SG 4, U-Bend R2C69 Pre-Insitu – 800 kHz HF

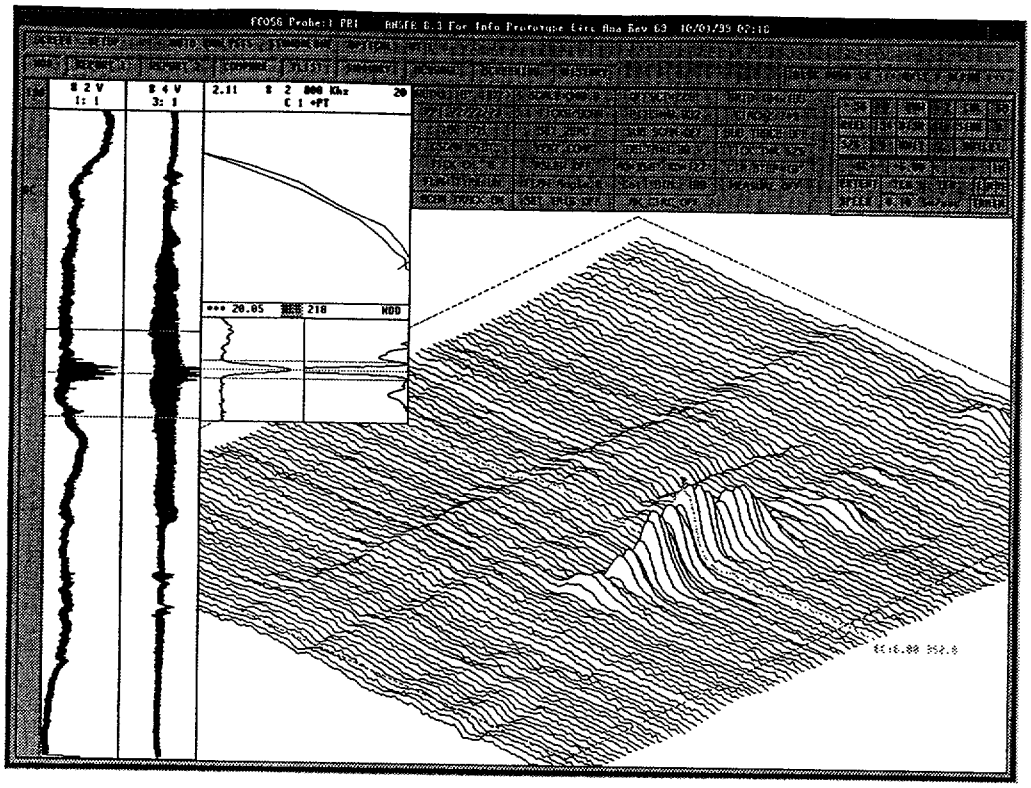

Figure B-4. Year 2000, SG 4, U-Bend R2C69 Post-Insitu – 800 kHz HF

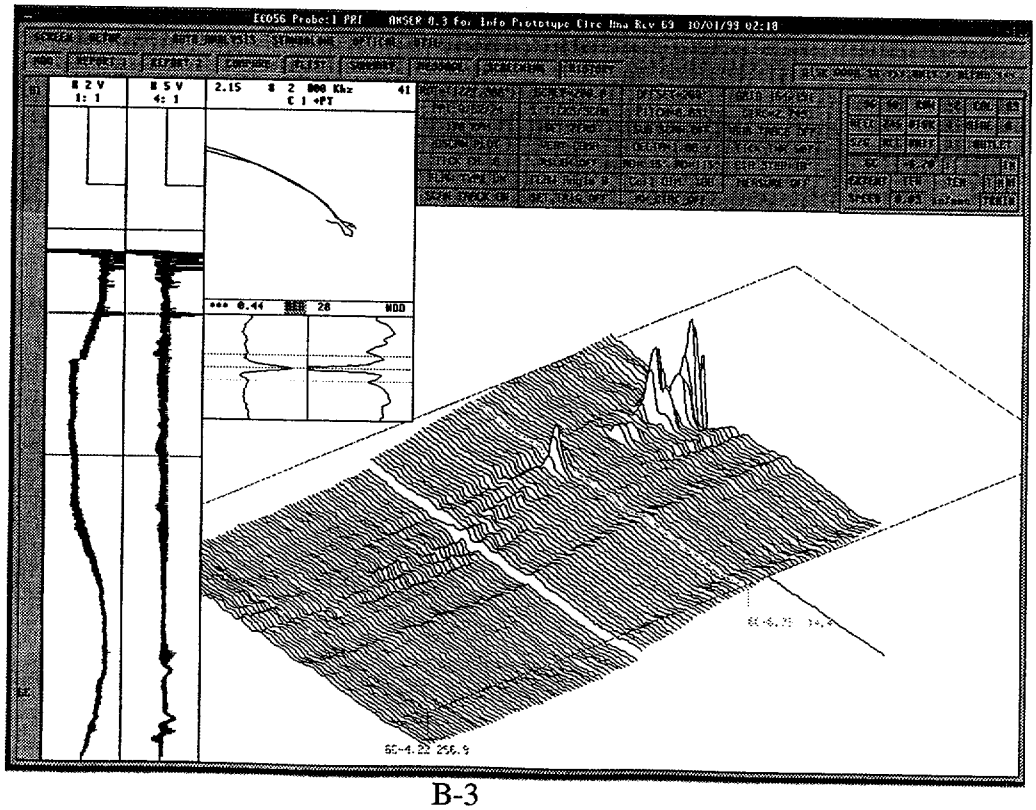

Figure B-5. Year 2000, SG 4, U-Bend R2C71 Pre-Insitu – 400 kHz HF

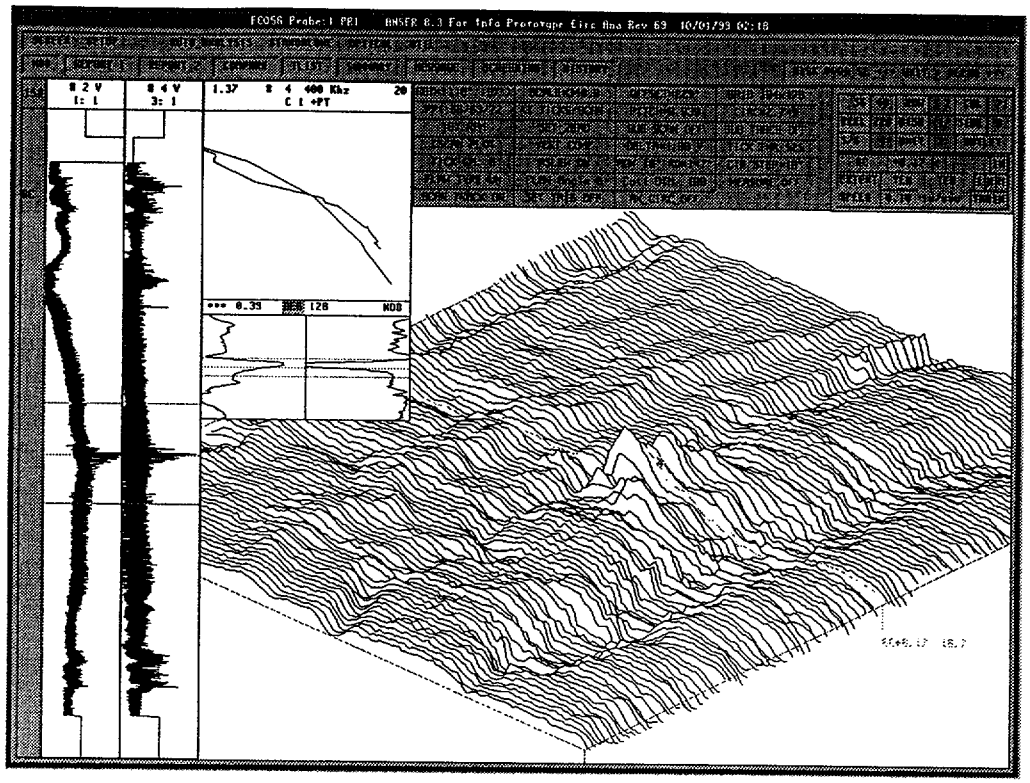

Figure B-6. Year 2000, SG 4, U-Bend R2C71 Post-Insitu – 400 kHz HF

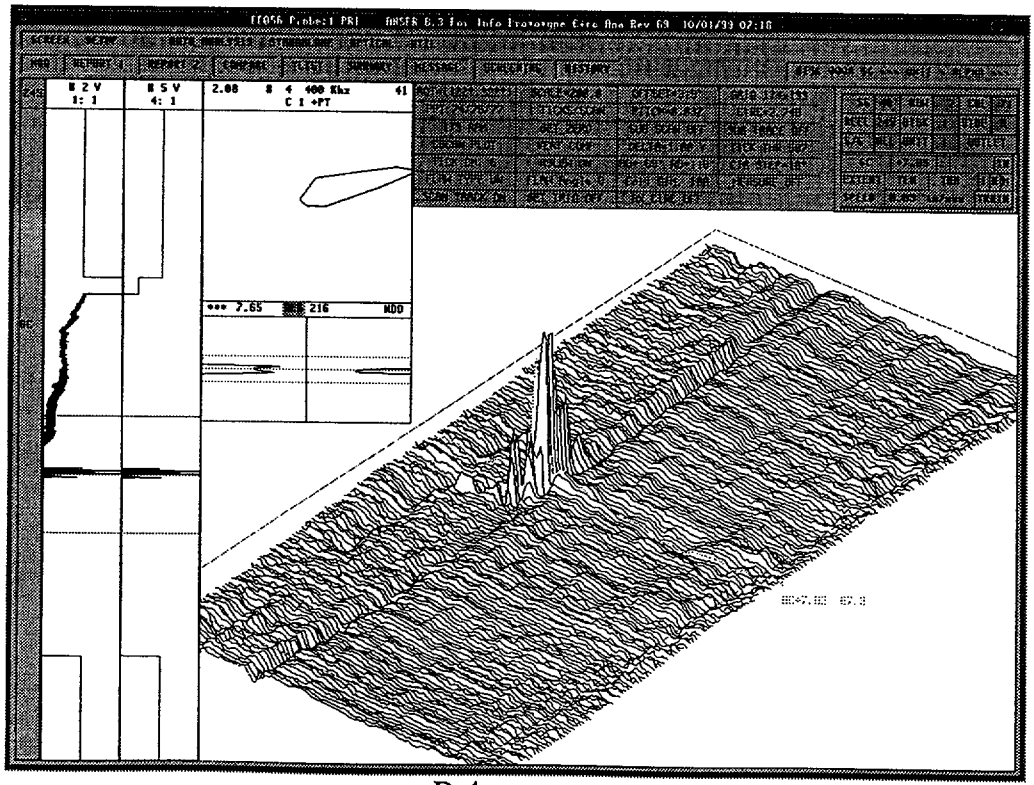

Figure B-7. Year 2000, SG 4, U-Bend R2C71 Pre-Insitu – 800 kHz HF

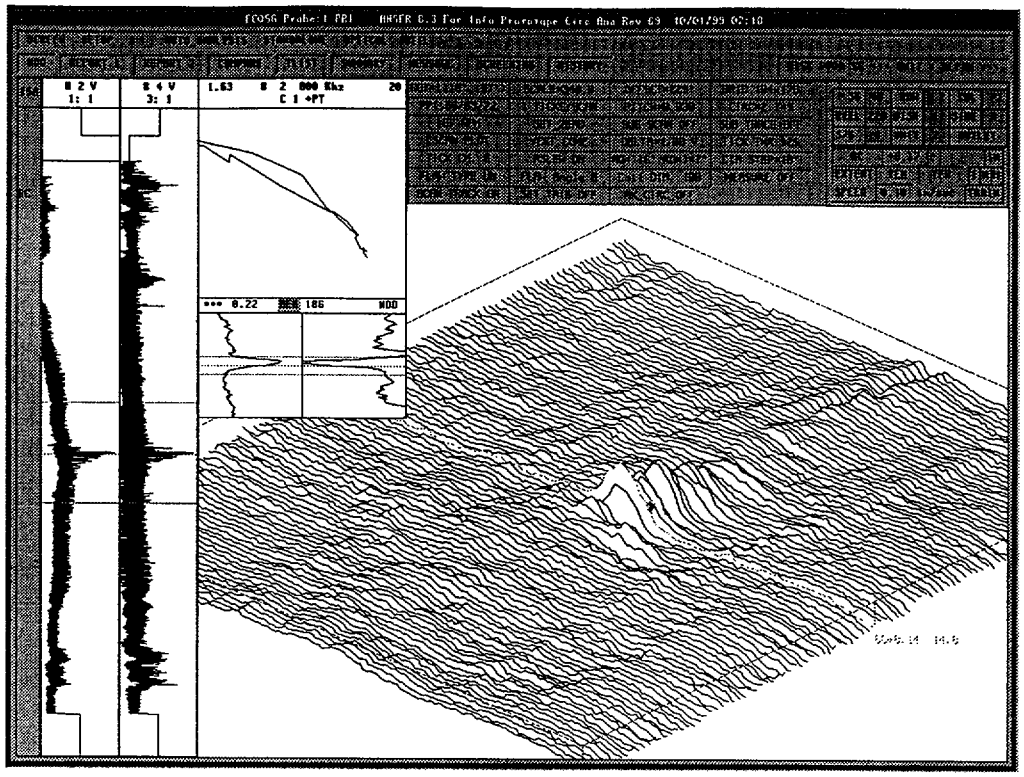

Figure B-8. Year 2000, SG 4, U-Bend R2C71 Post-Insitu – 800 kHz HF

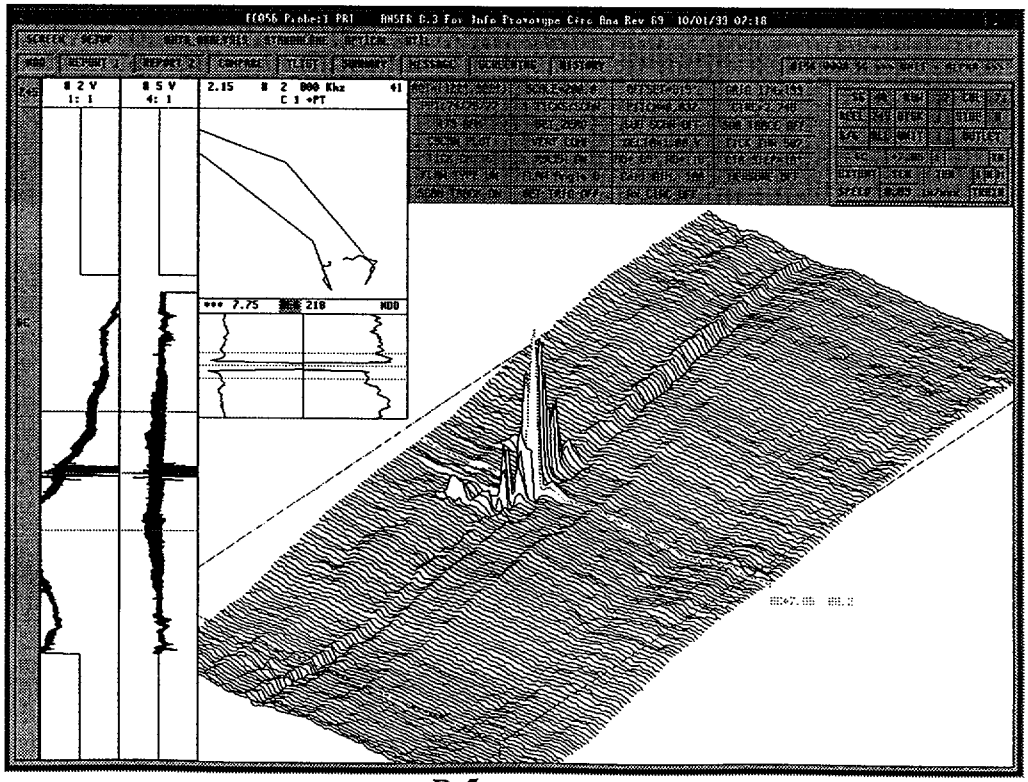

Figure B-9. Year 2000, SG 4, U-Bend R2C74 Pre-Insitu – 400 kHz HF

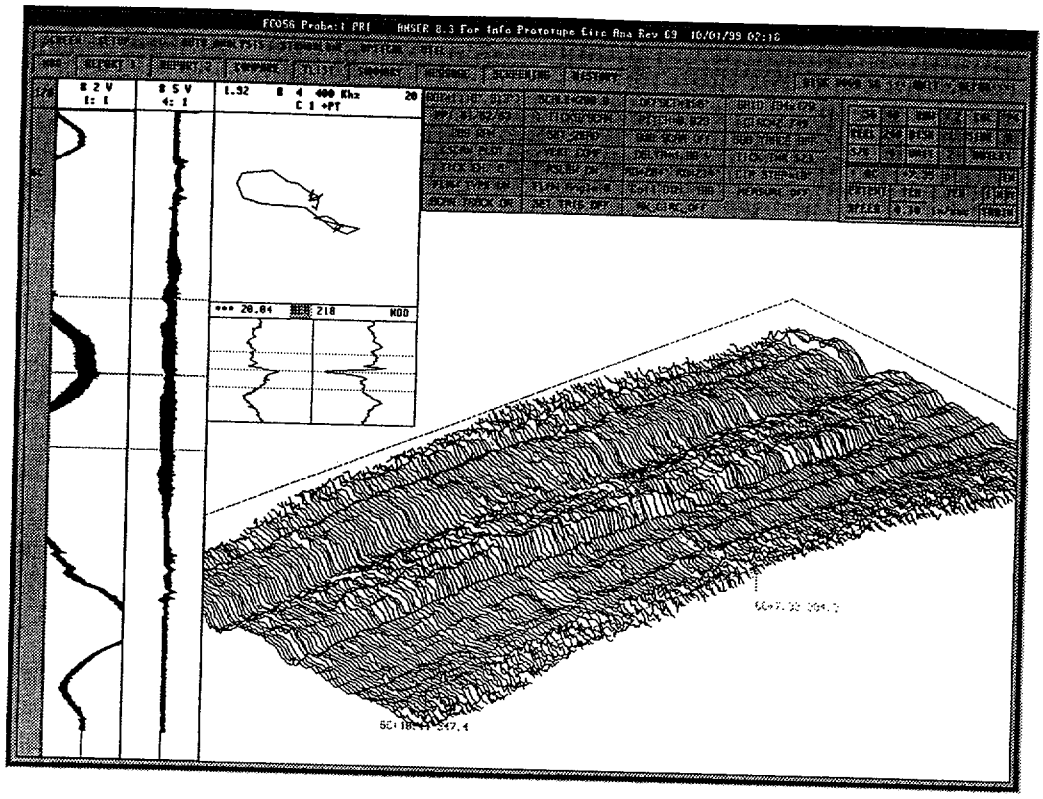

Figure B-10. Year 2000, SG 4, U-Bend R2C74 Post-Insitu – 400 kHz HF

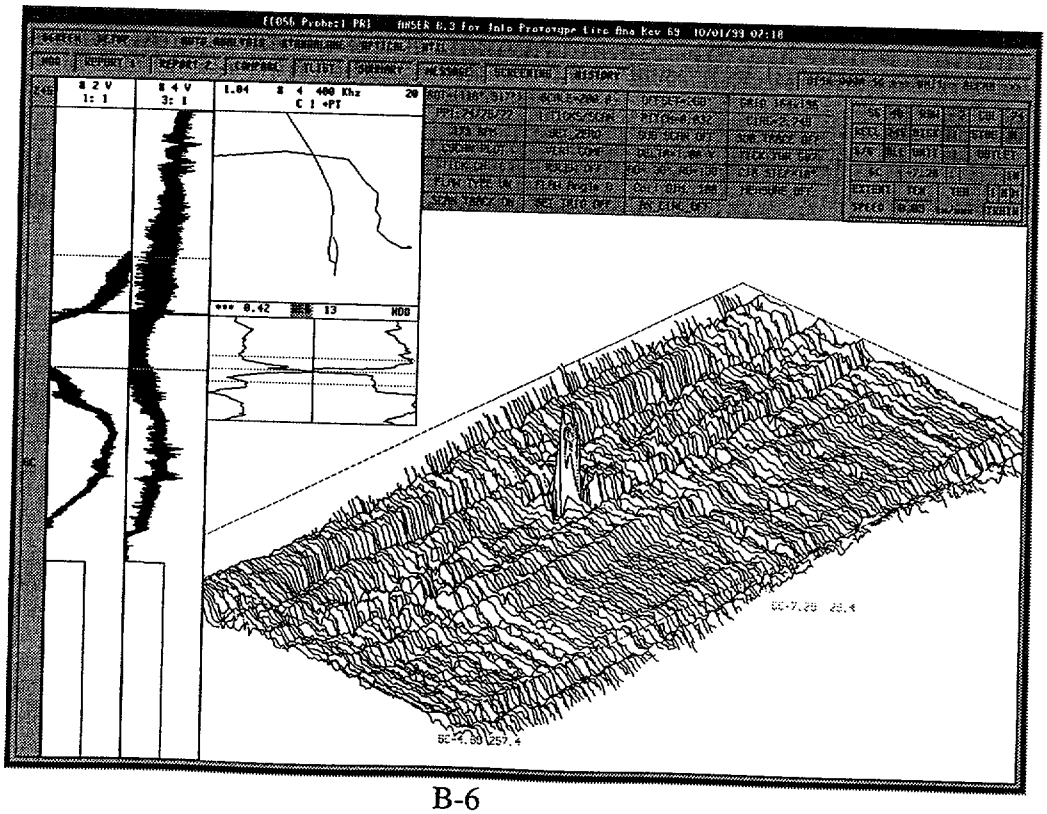

Figure B-11. Year 2000, SG 4, U-Bend R2C74 Pre-Insitu – 800 kHz HF

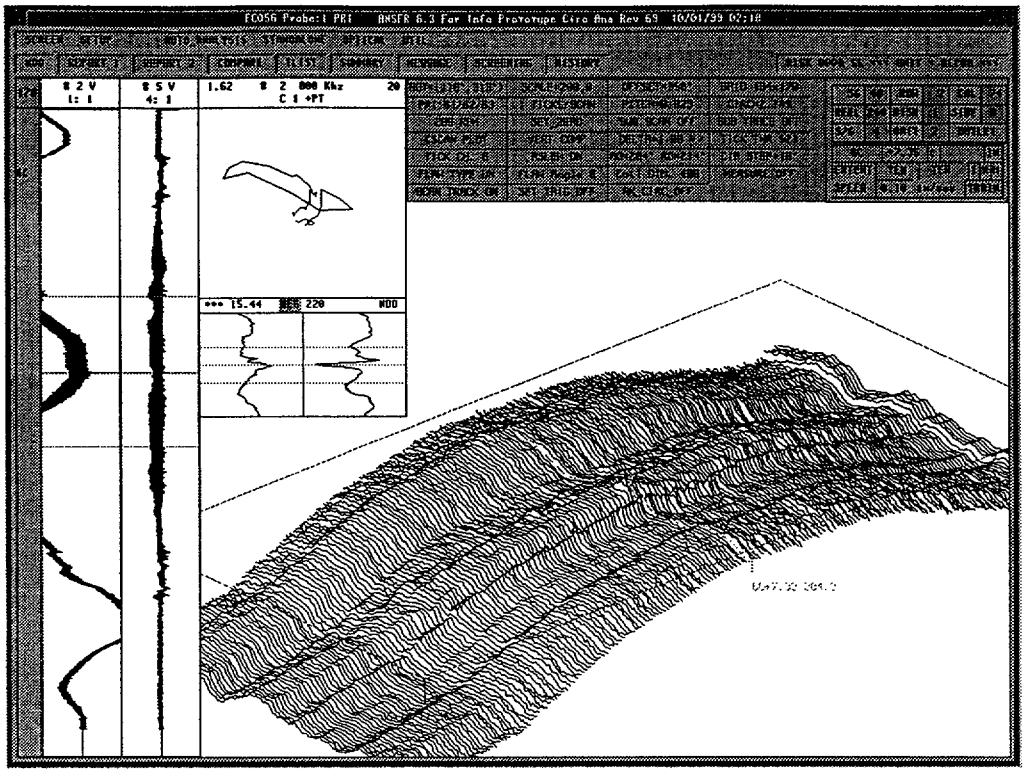

Figure B-12. Year 2000, SG 4, U-Bend R2C74 Post-Insitu – 800 kHz HF

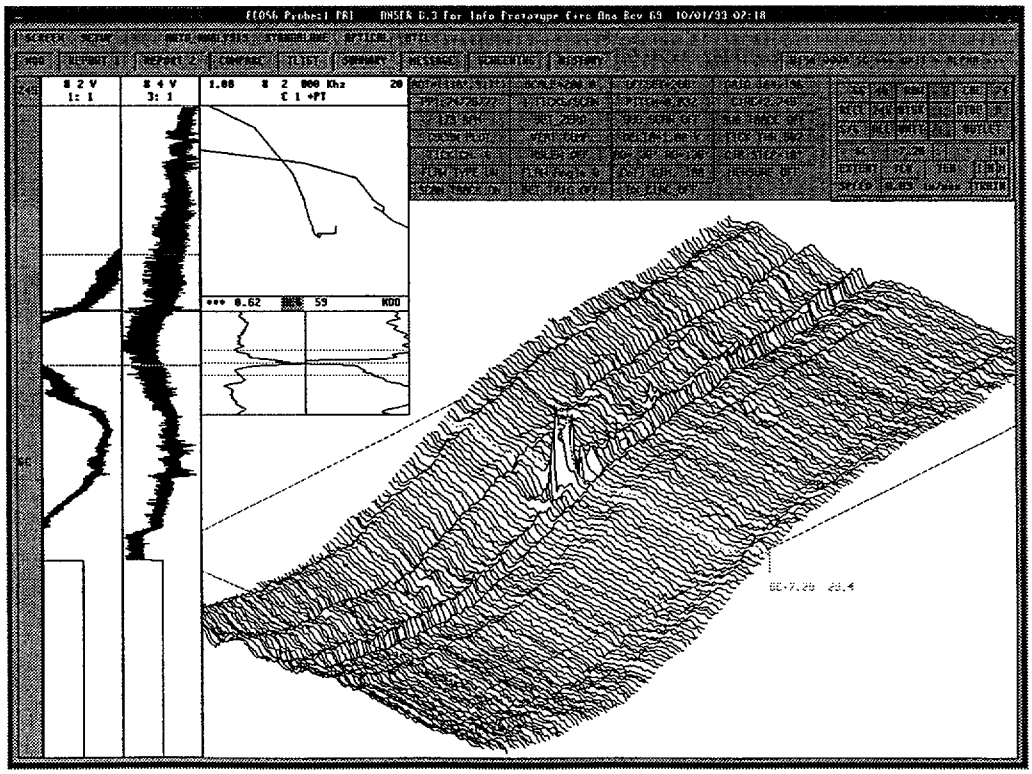

APPENDIX C

NDE Profiles

APPENDIX C.1

NDE Profiles for

2000

800 kHz vs. 400 kHz

Figure C.1-1

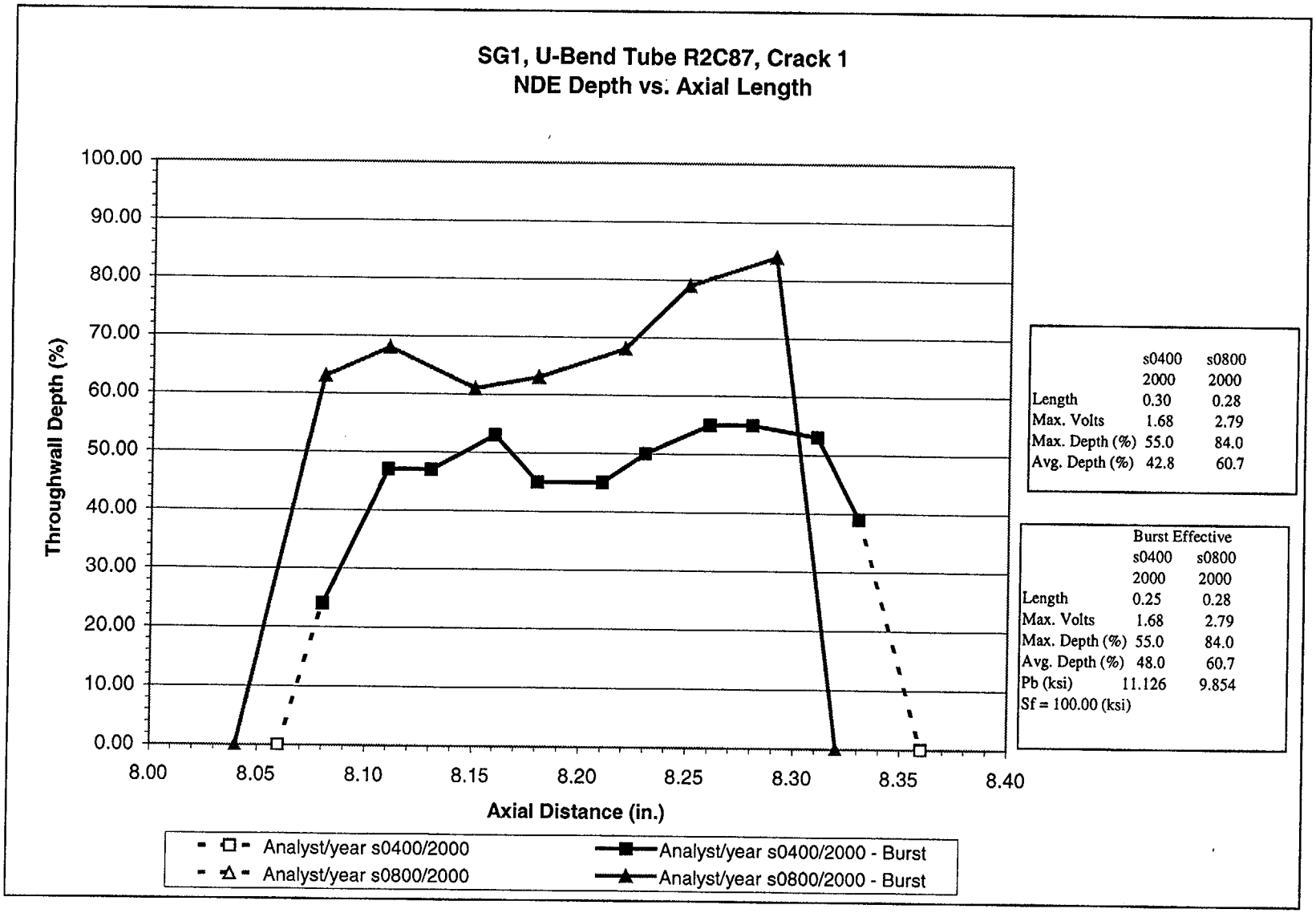
SG1, U-Bend Tube R2C87, Crack 1
NDE Depth vs. Axial Length
Throughwall Depth (%)
100.00
90.00
80.00
70.00
60.00
50.00
40.00
30.00
20.00
10.00
0.00
8.00
8.05
8.10
8.15
8.20
8.25
8.30
8.35
8.40
Axial Distance (in.)
Analyst/year s0400/2000
Analyst/year s0800/2000
Analyst/year s0400/2000 - Burst
Analyst/year s0800/2000 - Burst
s0400 2000
s0800 2000
Length 0.30 0.28
Max. Volts 1.68 2.79
Max. Depth (%) 55.0 84.0
Avg. Depth (%) 42.8 60.7
Burst Effective
s0400 2000
s0800 2000
Length 0.25 0.28
Max. Volts 1.68 2.79
Max. Depth (%) 55.0 84.0
Avg. Depth (%) 48.0 60.7
Pb (ksi) 11.126 9.854
Sf = 100.00 (ksi)

Figure C.1-2

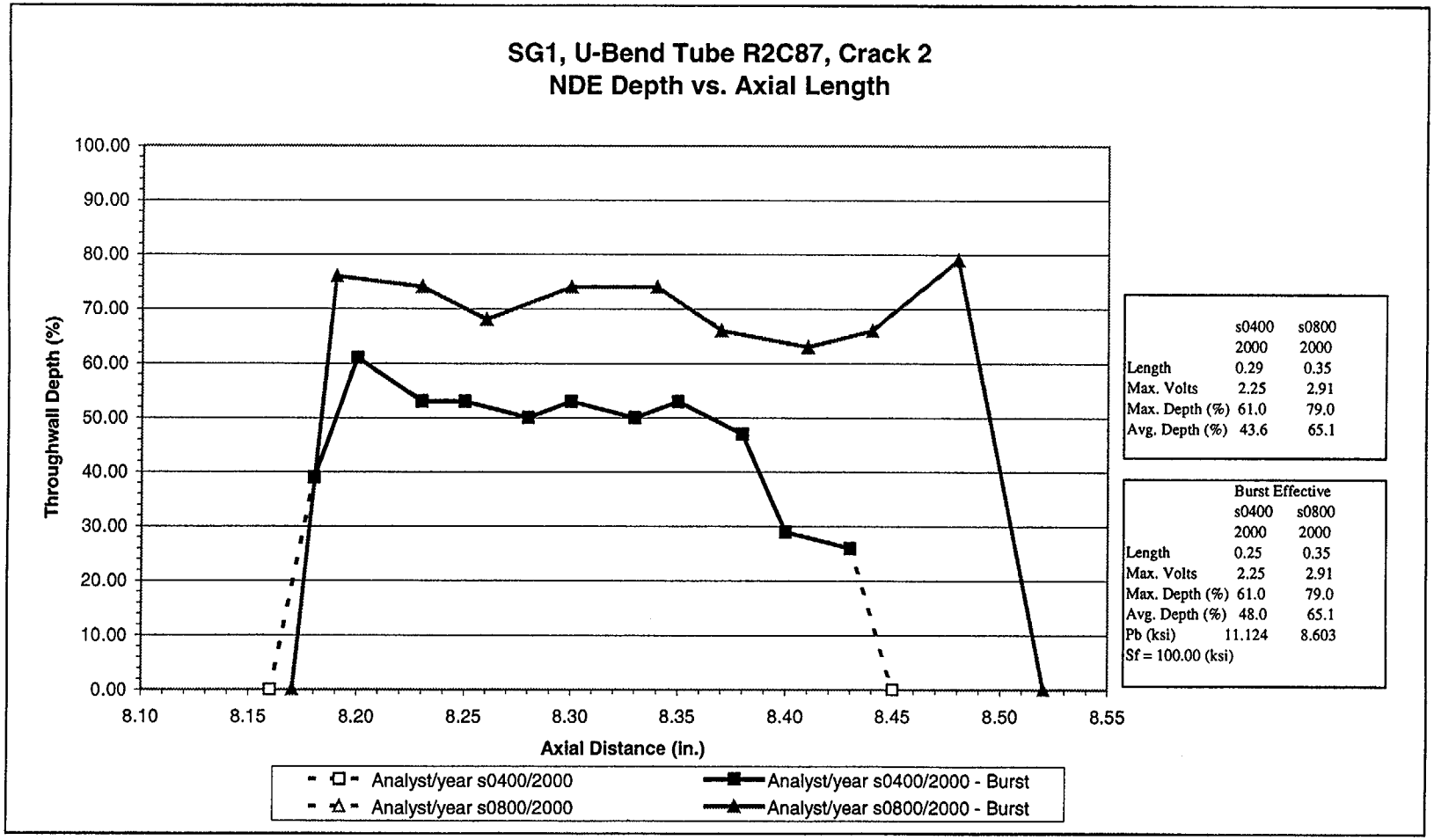
SG1, U-Bend Tube R2C87, Crack 2
NDE Depth vs. Axial Length
Throughwall Depth (%)
100.00
90.00
80.00
70.00
60.00
50.00
40.00
30.00
20.00
10.00
0.00
8.10
8.15
8.20
8.25
8.30
8.35
8.40
8.45
8.50
8.55
Axial Distance (in.)
Analyst/year s0400/2000
Analyst/year s0800/2000
Analyst/year s0400/2000 - Burst
Analyst/year s0800/2000 - Burst
s0400 2000
s0800 2000
Length 0.29 0.35
Max. Volts 2.25 2.91
Max. Depth (%) 61.0 79.0
Avg. Depth (%) 43.6 65.1
Burst Effective
s0400 2000
s0800 2000
Length 0.25 0.35
Max. Volts 2.25 2.91
Max. Depth (%) 61.0 79.0
Avg. Depth (%) 48.0 65.1
Pb (ksi) 11.124 8.603
Sf = 100.00 (ksi)

Figure C.1-3

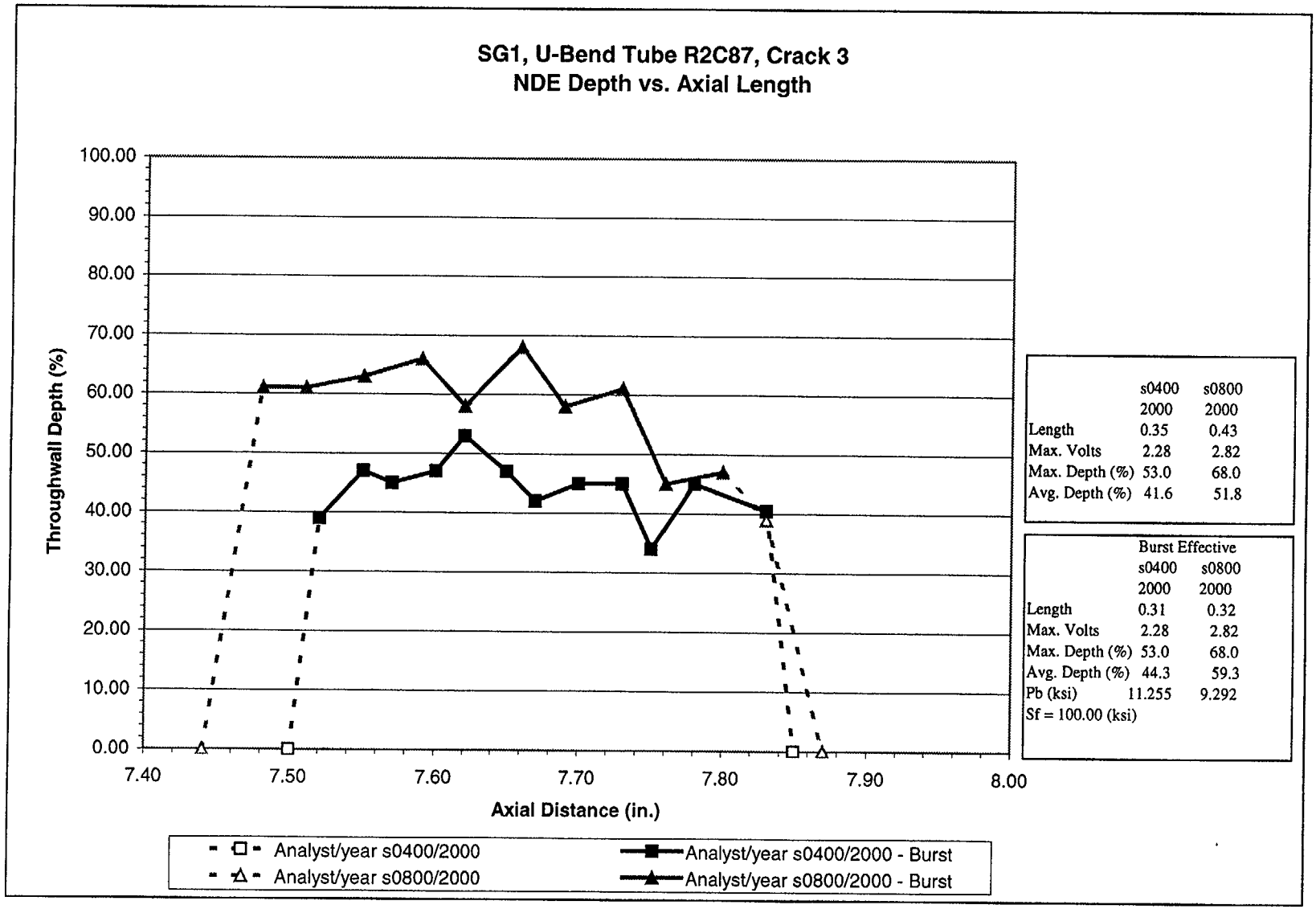
SG1, U-Bend Tube R2C87, Crack 3
NDE Depth vs. Axial Length
Throughwall Depth (%)
100.00
90.00
80.00
70.00
60.00
50.00
40.00
30.00
20.00
10.00
0.00
7.40
7.50
7.60
7.70
7.80
7.90
8.00
Axial Distance (in.)
Analyst/year s0400/2000
Analyst/year s0800/2000
Analyst/year s0400/2000 - Burst
Analyst/year s0800/2000 - Burst
s0400 2000
s0800 2000
Length 0.35 0.43
Max. Volts 2.28 2.82
Max. Depth (%) 53.0 68.0
Avg. Depth (%) 41.6 51.8
Burst Effective
s0400 2000
s0800 2000
Length 0.31 0.32
Max. Volts 2.28 2.82
Max. Depth (%) 53.0 68.0
Avg. Depth (%) 44.3 59.3
Pb (ksi) 11.255 9.292
Sf = 100.00 (ksi)

Figure C.1-4

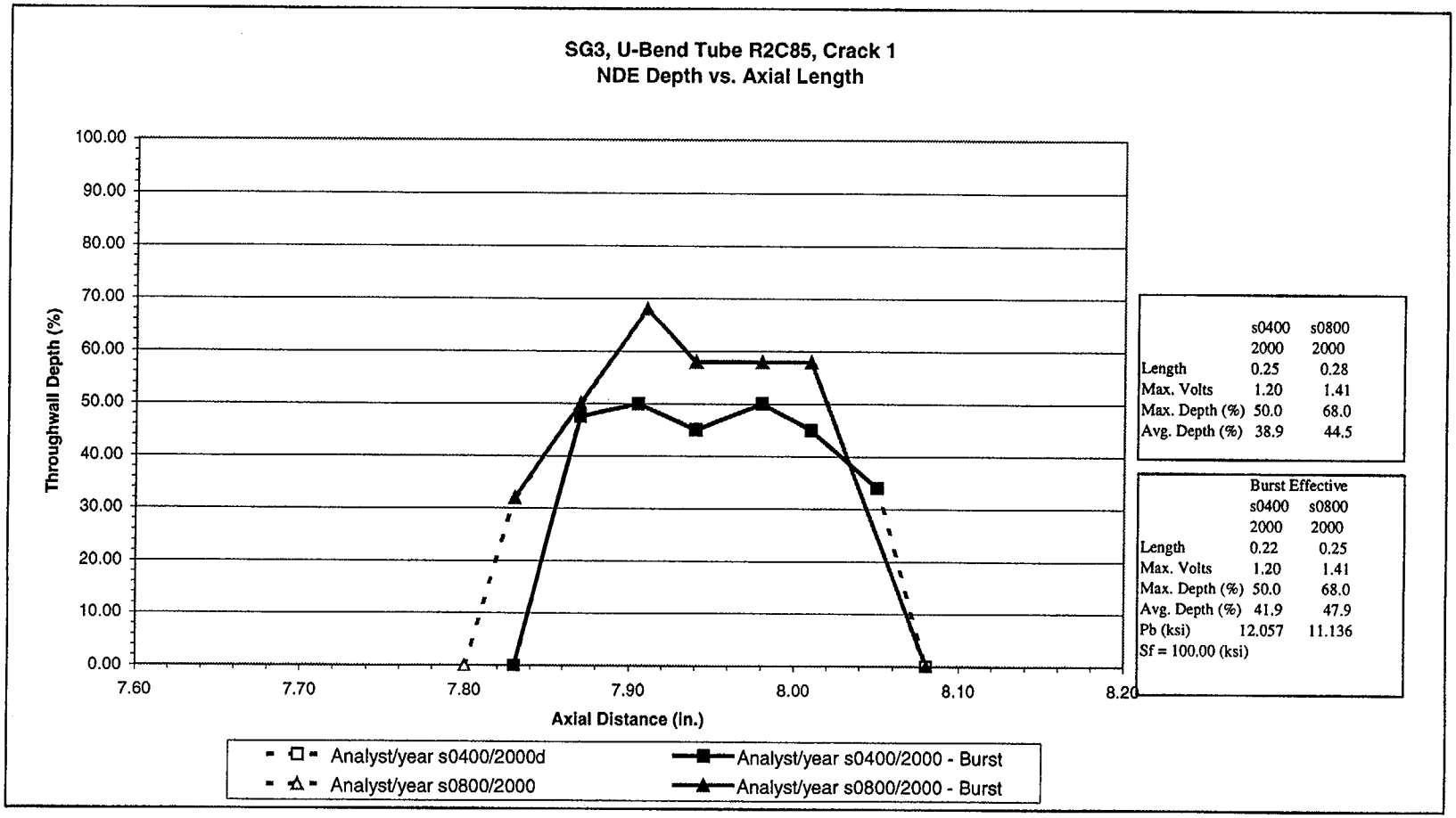
SG3, U-Bend Tube R2C85, Crack 1
NDE Depth vs. Axial Length
Throughwall Depth (%)
100.00
90.00
80.00
70.00
60.00
50.00
40.00
30.00
20.00
10.00
0.00
7.60
7.70
7.80
7.90
8.00
8.10
8.20
Axial Distance (in.)
Analyst/year s0400/2000d
Analyst/year s0800/2000
Analyst/year s0400/2000 - Burst
Analyst/year s0800/2000 - Burst
s0400 2000
s0800 2000
Length 0.25 0.28
Max. Volts 1.20 1.41
Max. Depth (%) 50.0 68.0
Avg. Depth (%) 38.9 44.5
Burst Effective
s0400 2000
s0800 2000
Length 0.22 0.25
Max. Volts 1.20 1.41
Max. Depth (%) 50.0 68.0
Avg. Depth (%) 41.9 47.9
Pb (ksi) 12.057 11.136
Sf = 100.00 (ksi)

Figure C.1-5

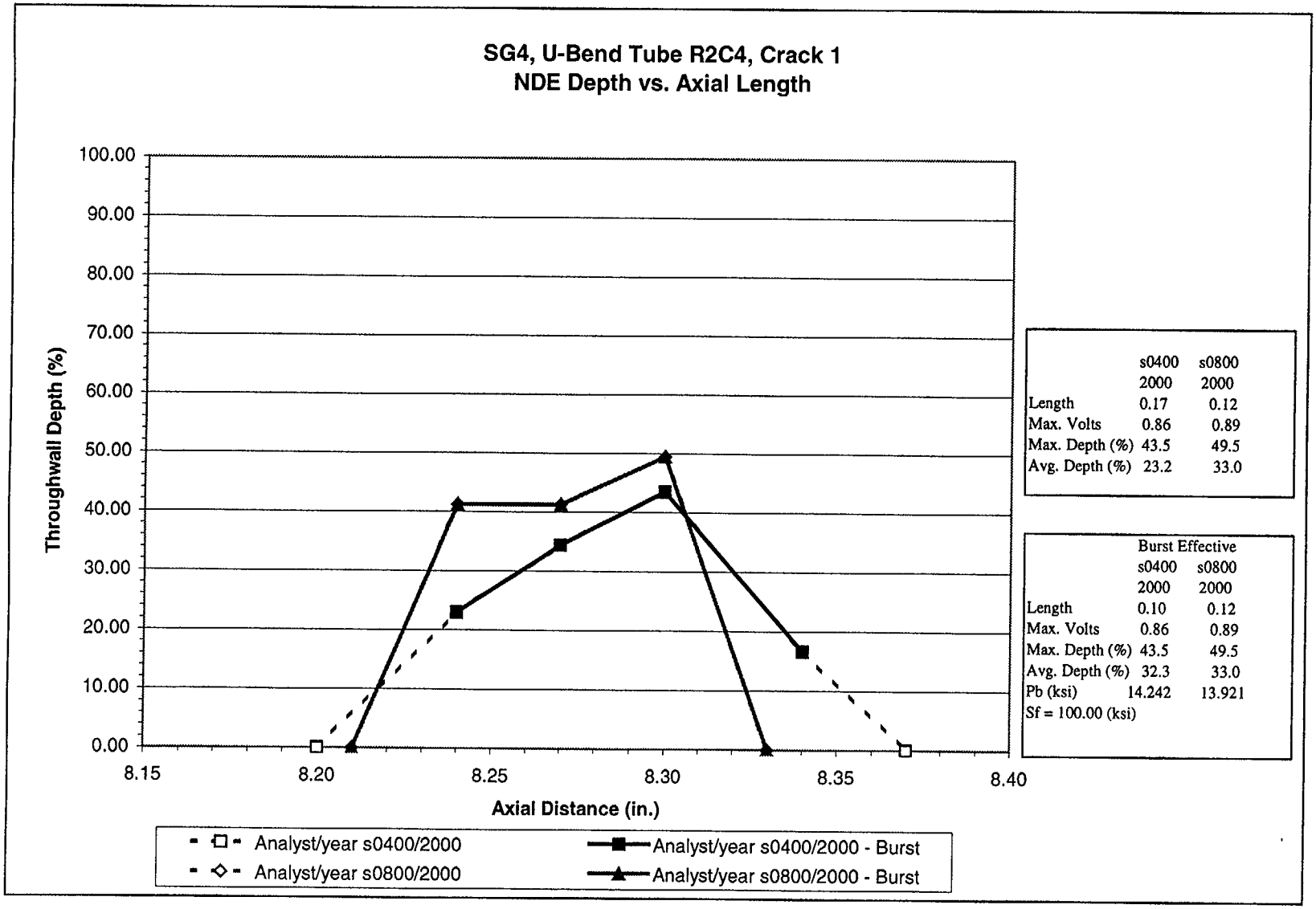
SG4, U-Bend Tube R2C4, Crack 1
NDE Depth vs. Axial Length
Throughwall Depth (%)
100.00
90.00
80.00
70.00
60.00
50.00
40.00
30.00
20.00
10.00
0.00
8.15
8.20
8.25
8.30
8.35
8.40
Axial Distance (in.)
Analyst/year s0400/2000
Analyst/year s0800/2000
Analyst/year s0400/2000 - Burst
Analyst/year s0800/2000 - Burst
s0400 2000 s0800 2000
Length 0.17 0.12
Max. Volts 0.86 0.89
Max. Depth (%) 43.5 49.5
Avg. Depth (%) 23.2 33.0
Burst Effective
s0400 2000 s0800 2000
Length 0.10 0.12
Max. Volts 0.86 0.89
Max. Depth (%) 43.5 49.5
Avg. Depth (%) 32.3 33.0
Pb (ksi) 14.242 13.921
Sf = 100.00 (ksi)

Figure C.1-6

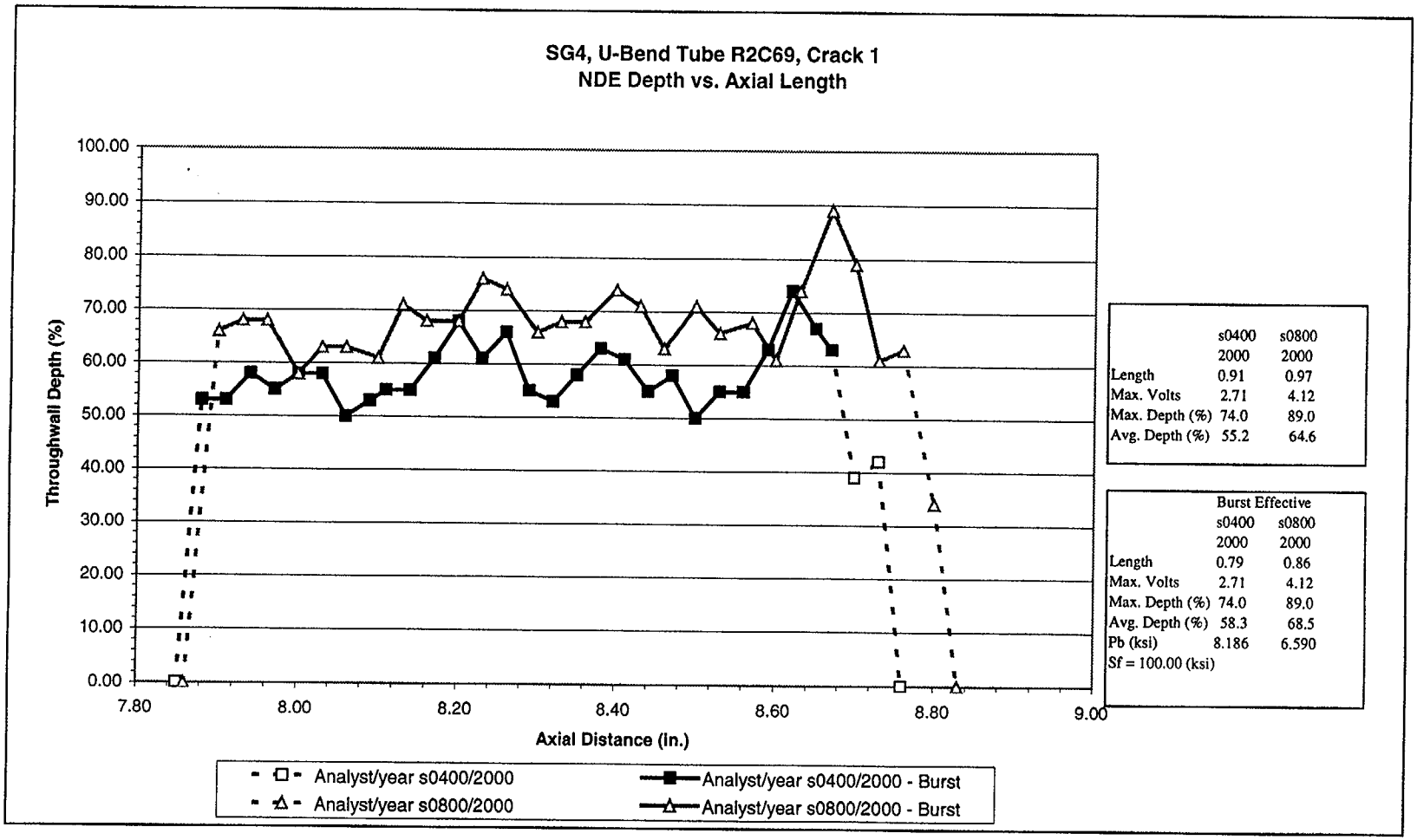
SG4, U-Bend Tube R2C69, Crack 1
NDE Depth vs. Axial Length
Throughwall Depth (%)
100.00
90.00
80.00
70.00
60.00
50.00
40.00
30.00
20.00
10.00
0.00
7.80
8.00
8.20
8.40
8.60
8.80
9.00
Axial Distance (In.)
Analyst/year s0400/2000
Analyst/year s0800/2000
Analyst/year s0400/2000 - Burst
Analyst/year s0800/2000 - Burst
s0400 2000
s0800 2000
Length 0.91 0.97
Max. Volts 2.71 4.12
Max. Depth (%) 74.0 89.0
Avg. Depth (%) 55.2 64.6
Burst Effective
s0400 2000
s0800 2000
Length 0.79 0.86
Max. Volts 2.71 4.12
Max. Depth (%) 74.0 89.0
Avg. Depth (%) 58.3 68.5
Pb (ksi) 8.186 6.590
Sf = 100.00 (ksi)

Figure C.1-7

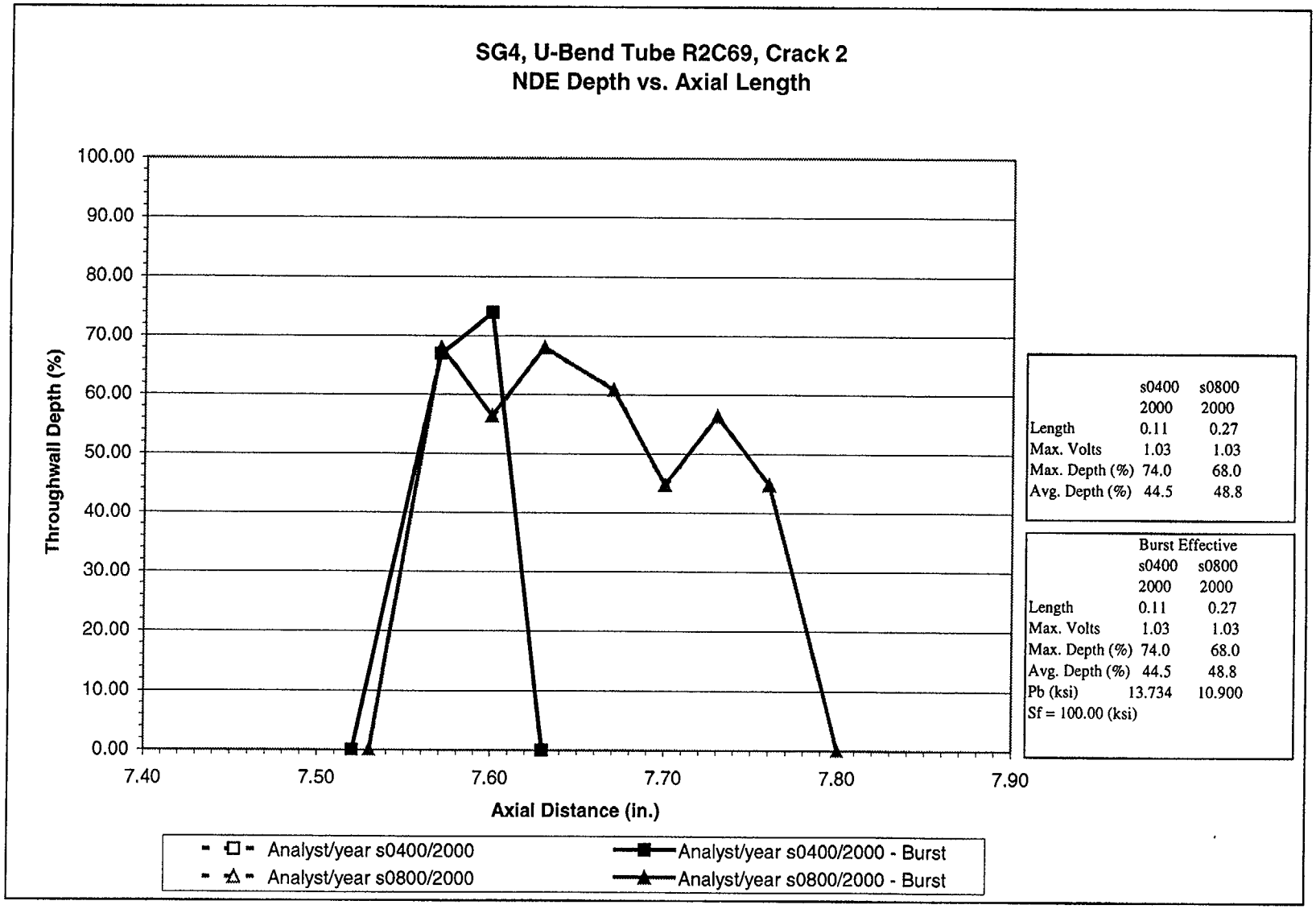
SG4, U-Bend Tube R2C69, Crack 2
NDE Depth vs. Axial Length
Throughwall Depth (%)
100.00
90.00
80.00
70.00
60.00
50.00
40.00
30.00
20.00
10.00
0.00
7.40
7.50
7.60
7.70
7.80
7.90
Axial Distance (in.)
s0400 2000 s0800 2000
Length 0.11 0.27
Max. Volts 1.03 1.03
Max. Depth (%) 74.0 68.0
Avg. Depth (%) 44.5 48.8
Burst Effective
s0400 2000 s0800 2000
Length 0.11 0.27
Max. Volts 1.03 1.03
Max. Depth (%) 74.0 68.0
Avg. Depth (%) 44.5 48.8
Pb (ksi) 13.734 10.900
Sf = 100.00 (ksi)
Analyst/year s0400/2000
Analyst/year s0800/2000
Analyst/year s0400/2000 - Burst
Analyst/year s0800/2000 - Burst

Figure C.1-8

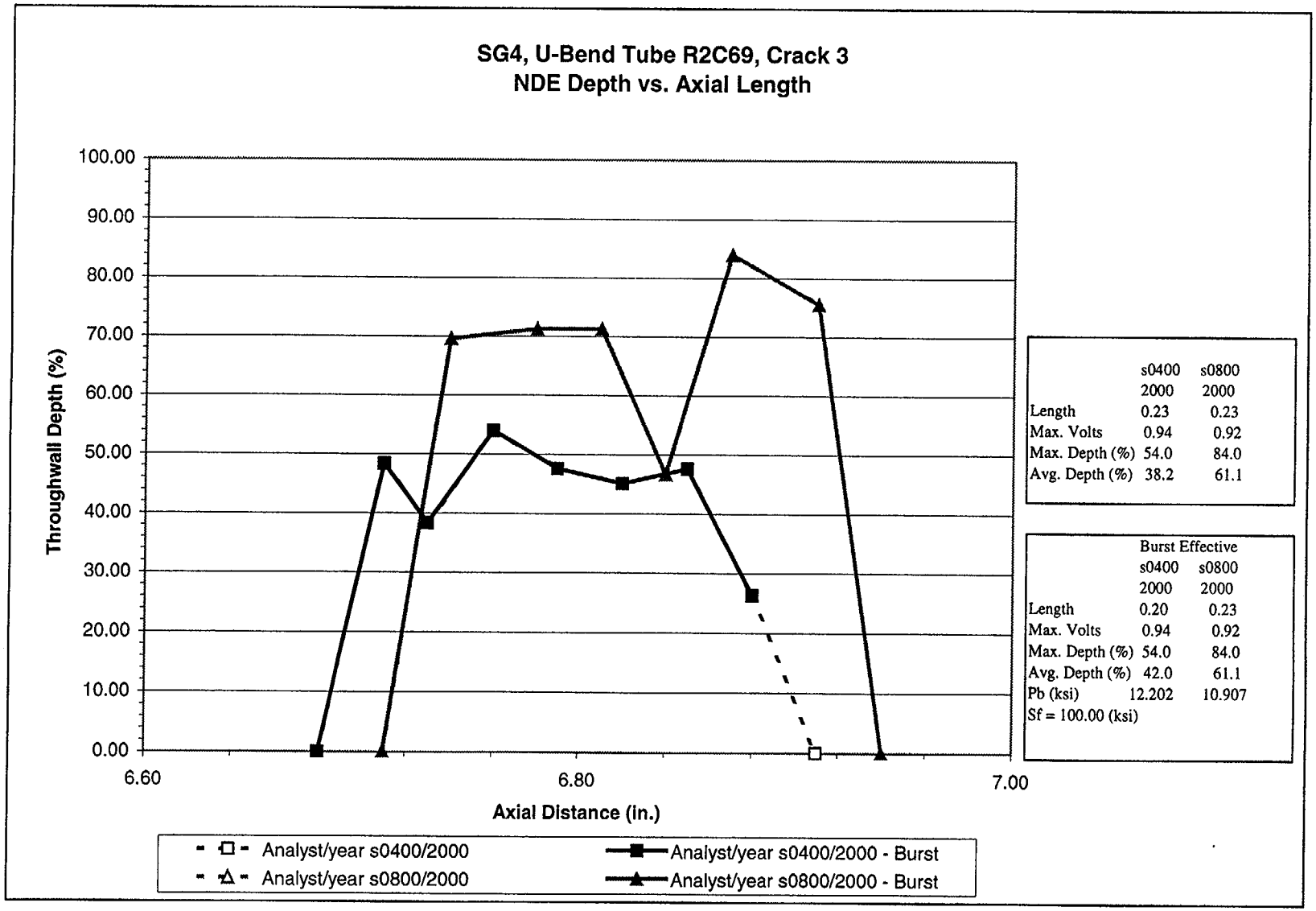
SG4, U-Bend Tube R2C69, Crack 3
NDE Depth vs. Axial Length
Throughwall Depth (%)
100.00
90.00
80.00
70.00
60.00
50.00
40.00
30.00
20.00
10.00
0.00
6.60
6.80
7.00
Axial Distance (in.)
s0400 2000 s0800 2000
Length 0.23 0.23
Max. Volts 0.94 0.92
Max. Depth (%) 54.0 84.0
Avg. Depth (%) 38.2 61.1
Burst Effective
s0400 2000 s0800 2000
Length 0.20 0.23
Max. Volts 0.94 0.92
Max. Depth (%) 54.0 84.0
Avg. Depth (%) 42.0 61.1
Pb (ksi) 12.202 10.907
Sf = 100.00 (ksi)
Analyst/year s0400/2000
Analyst/year s0800/2000
Analyst/year s0400/2000 - Burst
Analyst/year s0800/2000 - Burst

Figure C.1-9

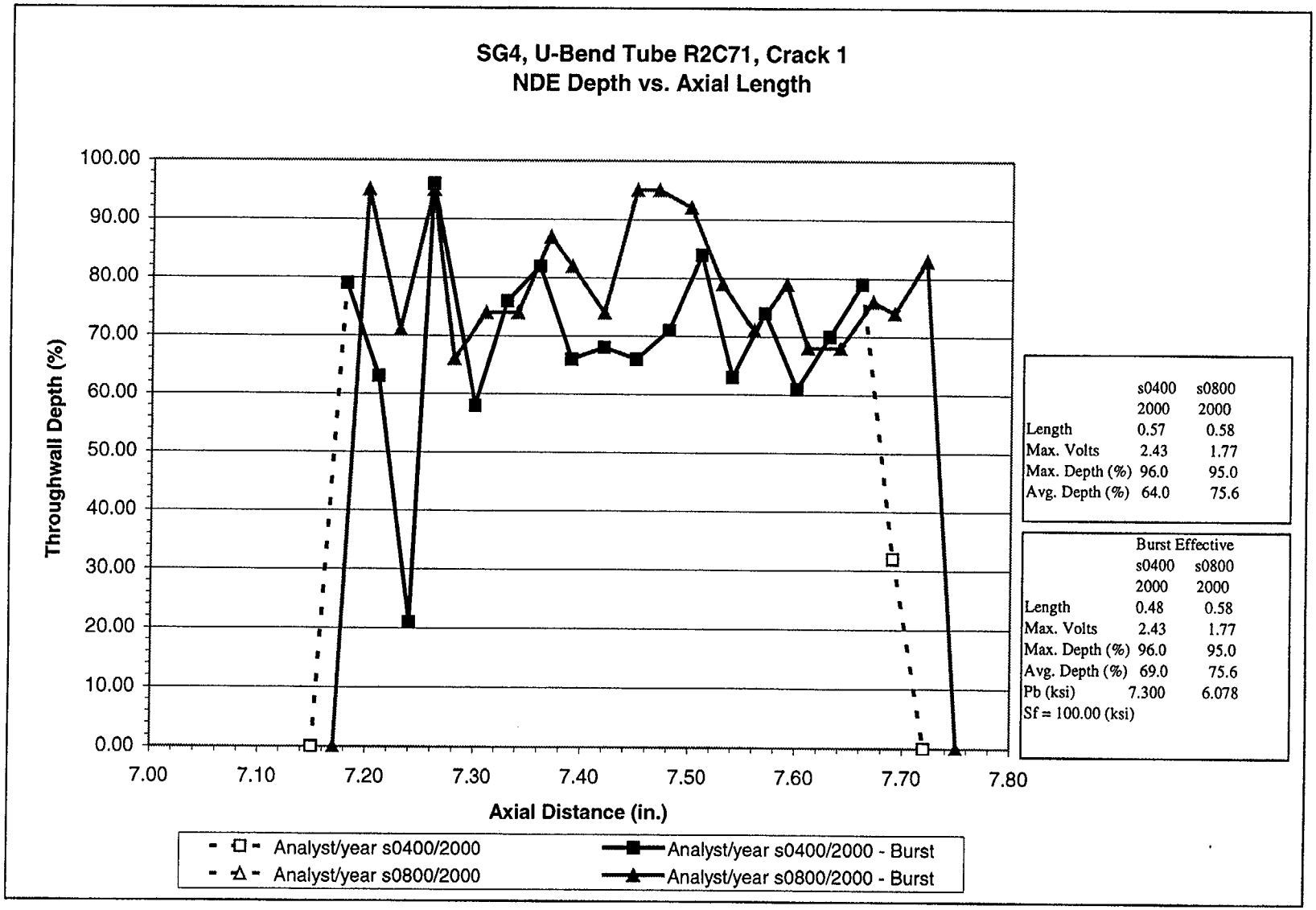
SG4, U-Bend Tube R2C71, Crack 1
NDE Depth vs. Axial Length
Throughwall Depth (%)
100.00
90.00
80.00
70.00
60.00
50.00
40.00
30.00
20.00
10.00
0.00
7.00
7.10
7.20
7.30
7.40
7.50
7.60
7.70
7.80
Axial Distance (in.)
Analyst/year s0400/2000
Analyst/year s0800/2000
Analyst/year s0400/2000 - Burst
Analyst/year s0800/2000 - Burst
s0400 2000
s0800 2000
Length 0.57 0.58
Max. Volts 2.43 1.77
Max. Depth (%) 96.0 95.0
Avg. Depth (%) 64.0 75.6
Burst Effective
s0400 2000
s0800 2000
Length 0.48 0.58
Max. Volts 2.43 1.77
Max. Depth (%) 96.0 95.0
Avg. Depth (%) 69.0 75.6
Pb (ksi) 7.300 6.078
Sf = 100.00 (ksi)

Figure C.1-10

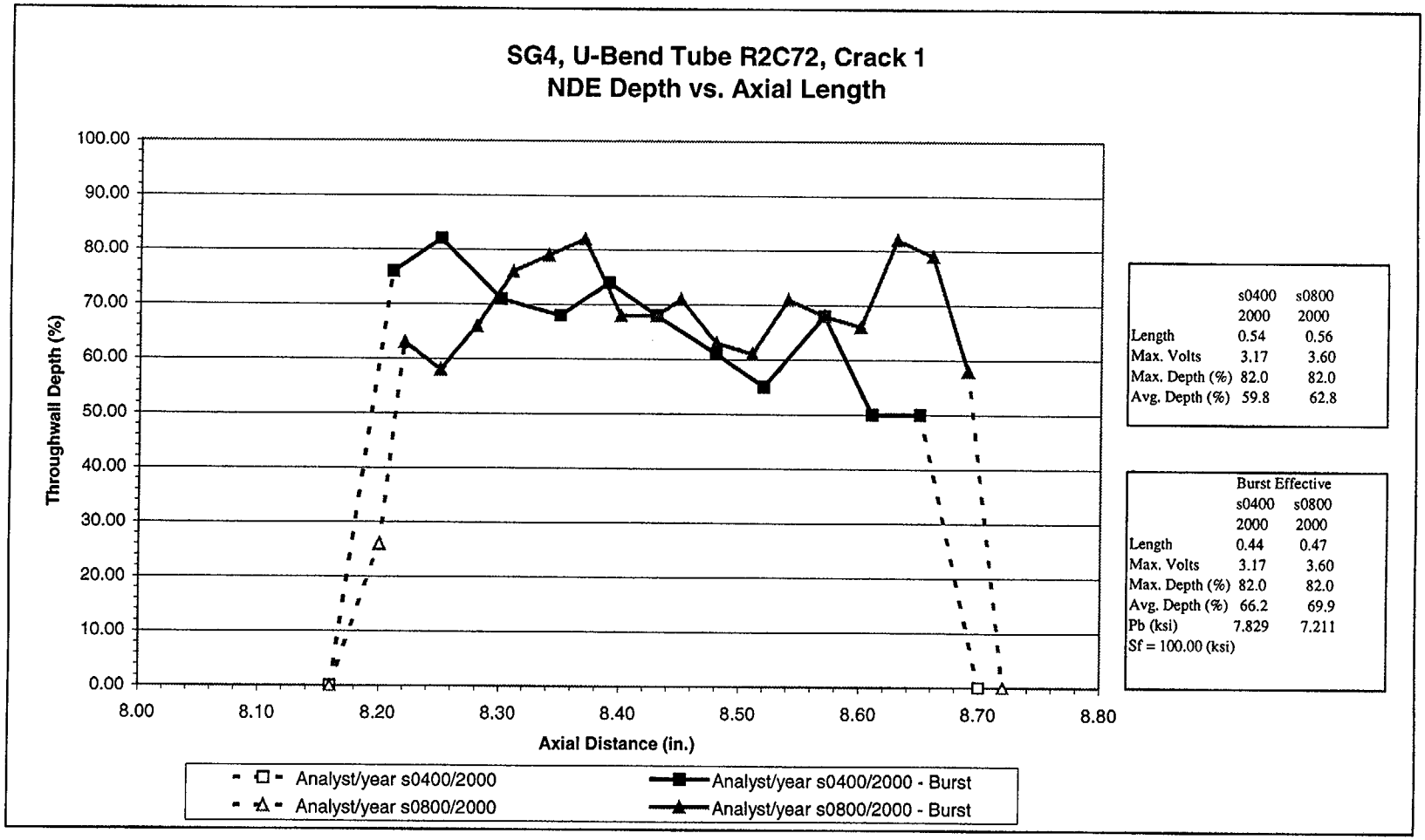
SG4, U-Bend Tube R2C72, Crack 1
NDE Depth vs. Axial Length
Throughwall Depth (%)
100.00
90.00
80.00
70.00
60.00
50.00
40.00
30.00
20.00
10.00
0.00
8.00
8.10
8.20
8.30
8.40
8.50
8.60
8.70
8.80
Axial Distance (in.)
Analyst/year s0400/2000
Analyst/year s0800/2000
Analyst/year s0400/2000 - Burst
Analyst/year s0800/2000 - Burst
s0400 2000
s0800 2000
Length 0.54 0.56
Max. Volts 3.17 3.60
Max. Depth (%) 82.0 82.0
Avg. Depth (%) 59.8 62.8
Burst Effective
s0400 2000
s0800 2000
Length 0.44 0.47
Max. Volts 3.17 3.60
Max. Depth (%) 82.0 82.0
Avg. Depth (%) 66.2 69.9
Pb (ksi) 7.829 7.211
Sf = 100.00 (ksi)

Figure C.1-11

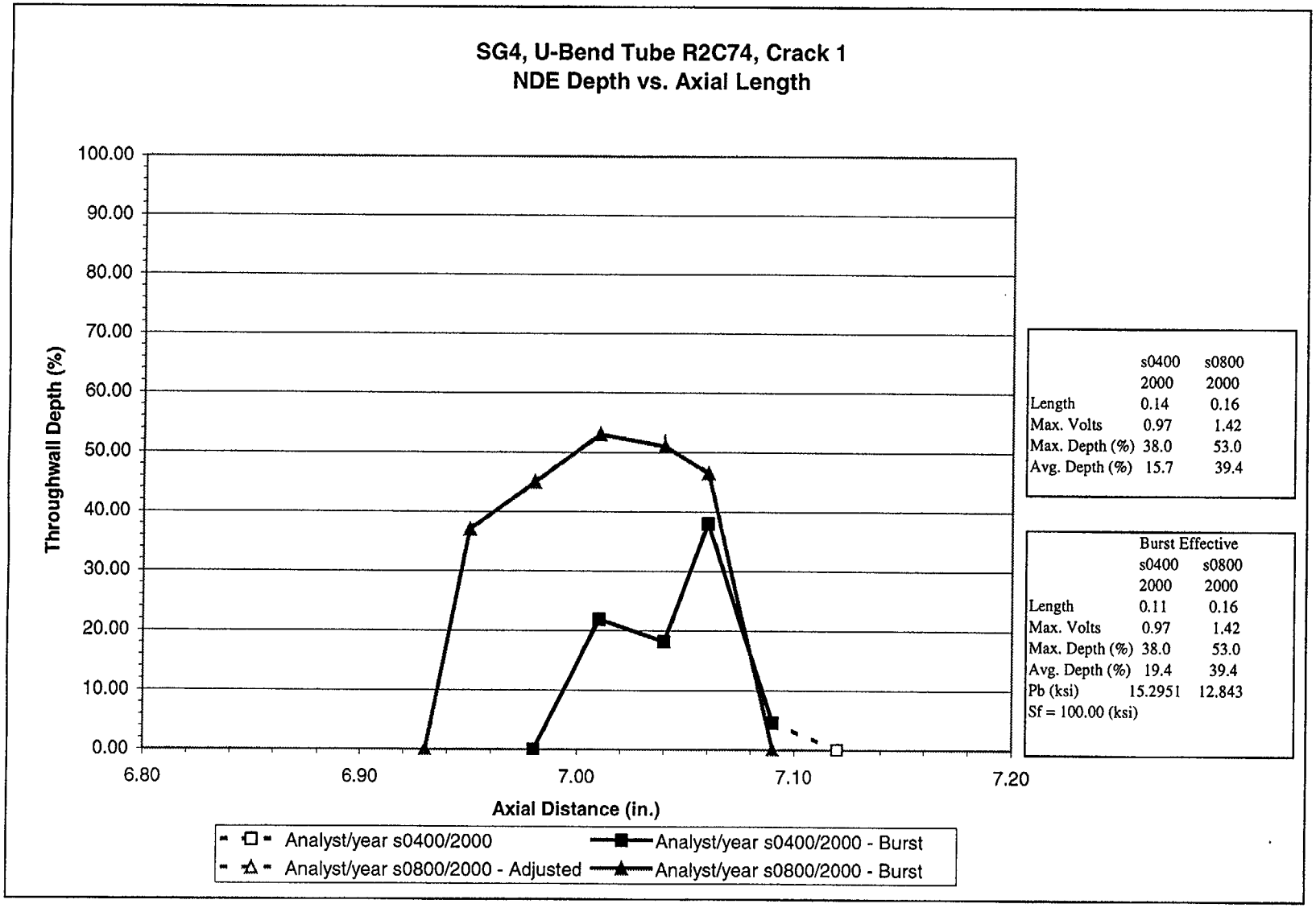
SG4, U-Bend Tube R2C74, Crack 1
NDE Depth vs. Axial Length
Throughwall Depth (%)
100.00
90.00
80.00
70.00
60.00
50.00
40.00
30.00
20.00
10.00
0.00
6.80
6.90
7.00
7.10
7.20
Axial Distance (in.)
Analyst/year s0400/2000
Analyst/year s0400/2000 - Burst
Analyst/year s0800/2000 - Adjusted
Analyst/year s0800/2000 - Burst
s0400 2000
s0800 2000
Length 0.14 0.16
Max. Volts 0.97 1.42
Max. Depth (%) 38.0 53.0
Avg. Depth (%) 15.7 39.4
Burst Effective
s0400 2000
s0800 2000
Length 0.11 0.16
Max. Volts 0.97 1.42
Max. Depth (%) 38.0 53.0
Avg. Depth (%) 19.4 39.4
Pb (ksi) 15.2951 12.843
Sf = 100.00 (ksi)

APPENDIX C.2

NDE Profiles for
1997 and 2000
400 kHz

Figure C.2-1

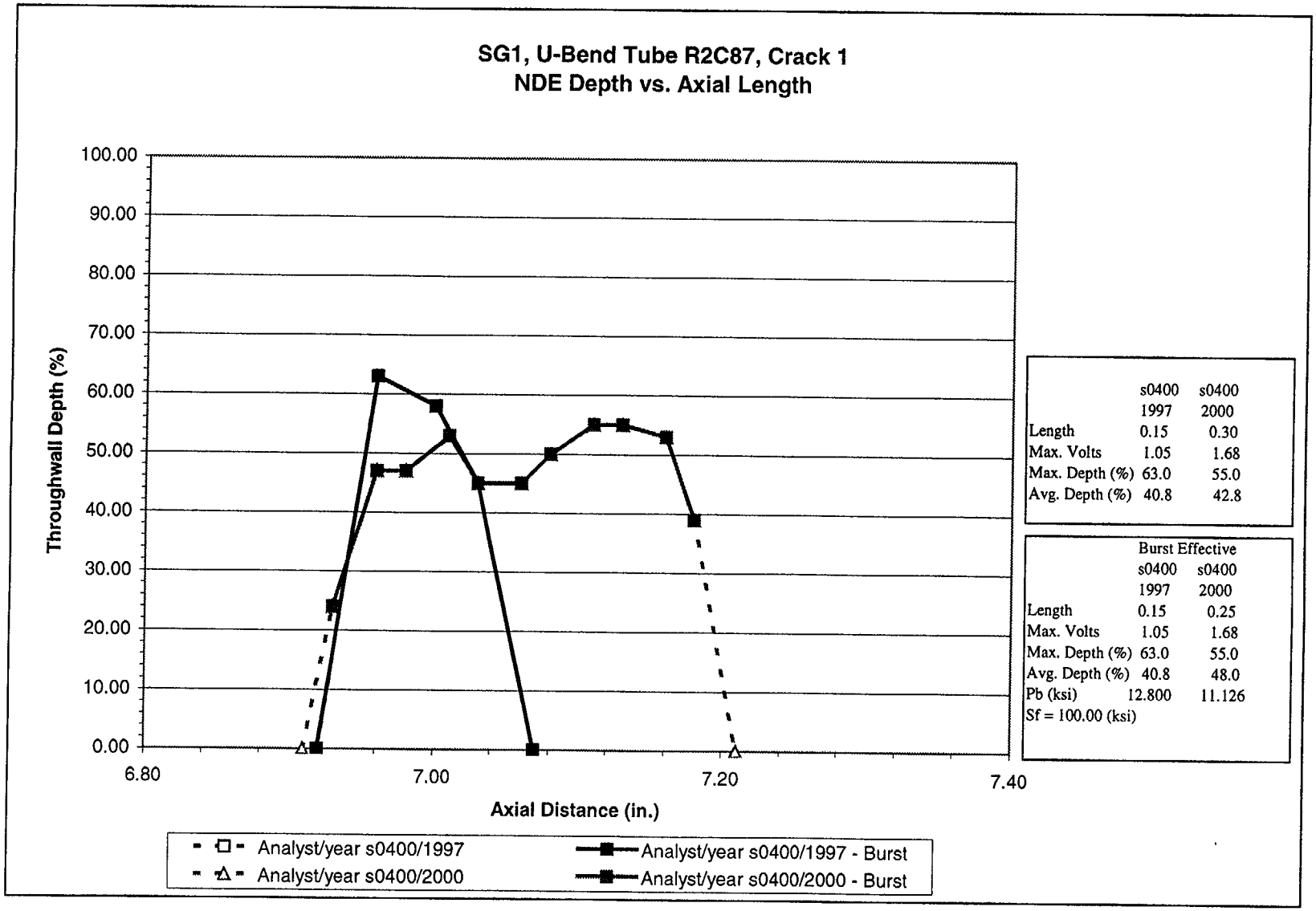
SG1, U-Bend Tube R2C87, Crack 1
NDE Depth vs. Axial Length
Throughwall Depth (%)
100.00
90.00
80.00
70.00
60.00
50.00
40.00
30.00
20.00
10.00
0.00
6.80
7.00
7.20
7.40
Axial Distance (in.)
s0400 1997 s0400 2000
Length 0.15 0.30
Max. Volts 1.05 1.68
Max. Depth (%) 63.0 55.0
Avg. Depth (%) 40.8 42.8
Burst Effective
s0400 1997 s0400 2000
Length 0.15 0.25
Max. Volts 1.05 1.68
Max. Depth (%) 63.0 55.0
Avg. Depth (%) 40.8 48.0
Pb (ksi) 12.800 11.126
Sf = 100.00 (ksi)
Analyst/year s0400/1997
Analyst/year s0400/2000
Analyst/year s0400/1997 - Burst
Analyst/year s0400/2000 - Burst

Figure C.2-2

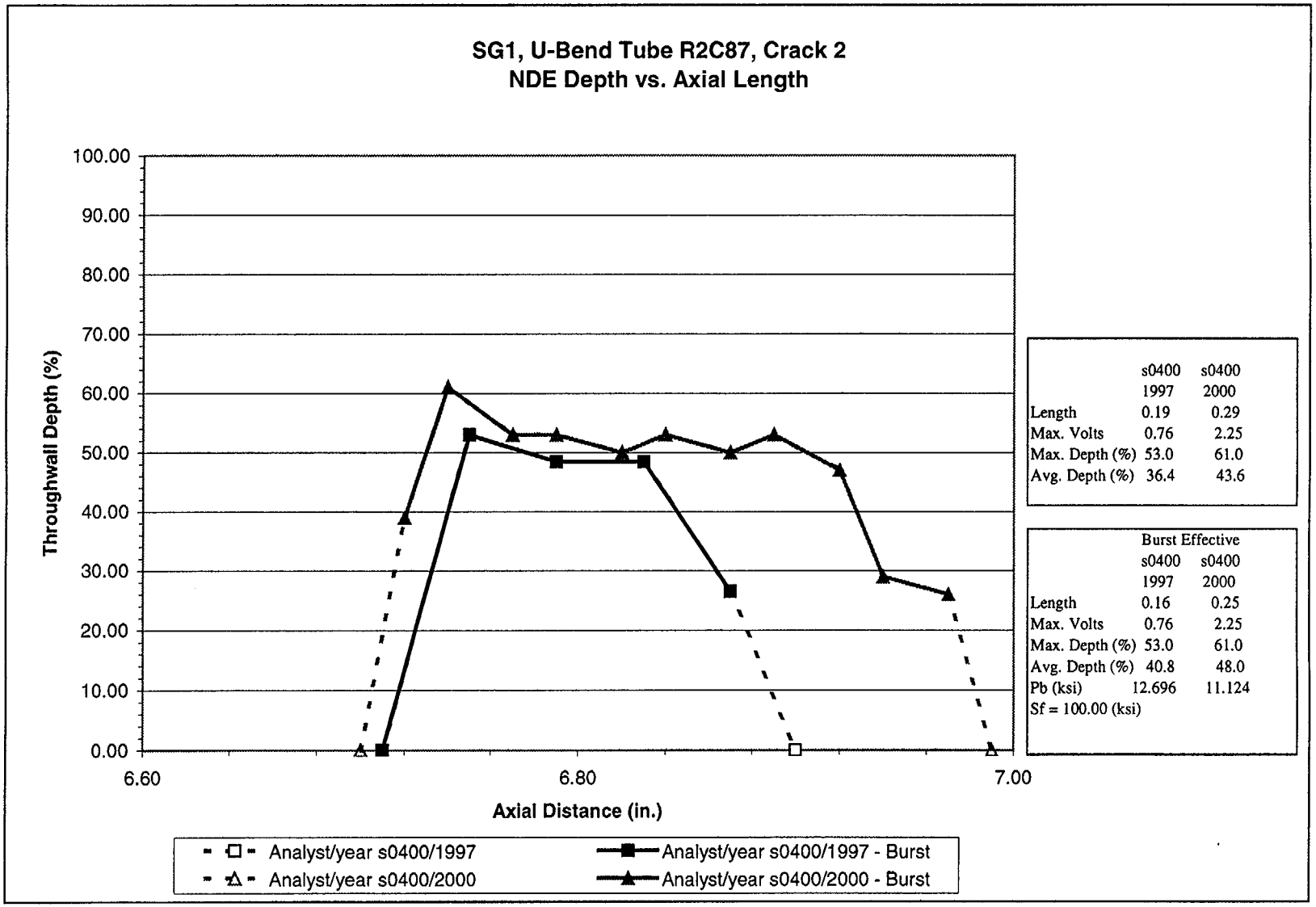
SG1, U-Bend Tube R2C87, Crack 2
NDE Depth vs. Axial Length
Throughwall Depth (%)
100.00
90.00
80.00
70.00
60.00
50.00
40.00
30.00
20.00
10.00
0.00
6.60
6.80
7.00
Axial Distance (in.)
s0400 1997 s0400 2000
Length 0.19 0.29
Max. Volts 0.76 2.25
Max. Depth (%) 53.0 61.0
Avg. Depth (%) 36.4 43.6
Burst Effective
s0400 1997 s0400 2000
Length 0.16 0.25
Max. Volts 0.76 2.25
Max. Depth (%) 53.0 61.0
Avg. Depth (%) 40.8 48.0
Pb (ksi) 12.696 11.124
Sf = 100.00 (ksi)
Analyst/year s0400/1997
Analyst/year s0400/2000
Analyst/year s0400/1997 - Burst
Analyst/year s0400/2000 - Burst

Figure C.2-3

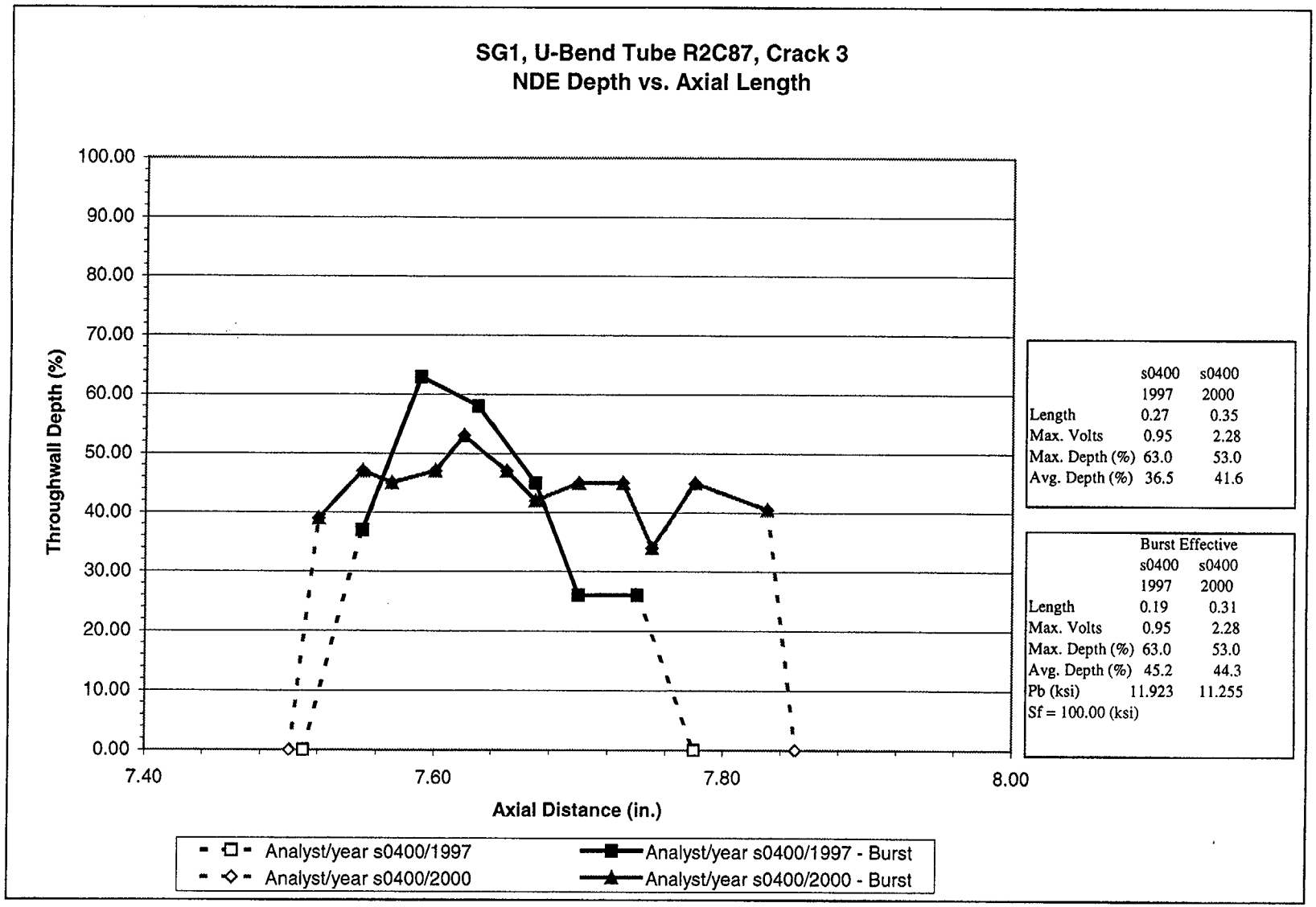
SG1, U-Bend Tube R2C87, Crack 3
NDE Depth vs. Axial Length
Throughwall Depth (%)
100.00
90.00
80.00
70.00
60.00
50.00
40.00
30.00
20.00
10.00
0.00
7.40
7.60
7.80
8.00
Axial Distance (in.)
s0400 1997 s0400 2000
Length 0.27 0.35
Max. Volts 0.95 2.28
Max. Depth (%) 63.0 53.0
Avg. Depth (%) 36.5 41.6
Burst Effective
s0400 1997 s0400 2000
Length 0.19 0.31
Max. Volts 0.95 2.28
Max. Depth (%) 63.0 53.0
Avg. Depth (%) 45.2 44.3
Pb (ksi) 11.923 11.255
Sf = 100.00 (ksi)
Analyst/year s0400/1997
Analyst/year s0400/2000
Analyst/year s0400/1997 - Burst
Analyst/year s0400/2000 - Burst

Figure C.2-4

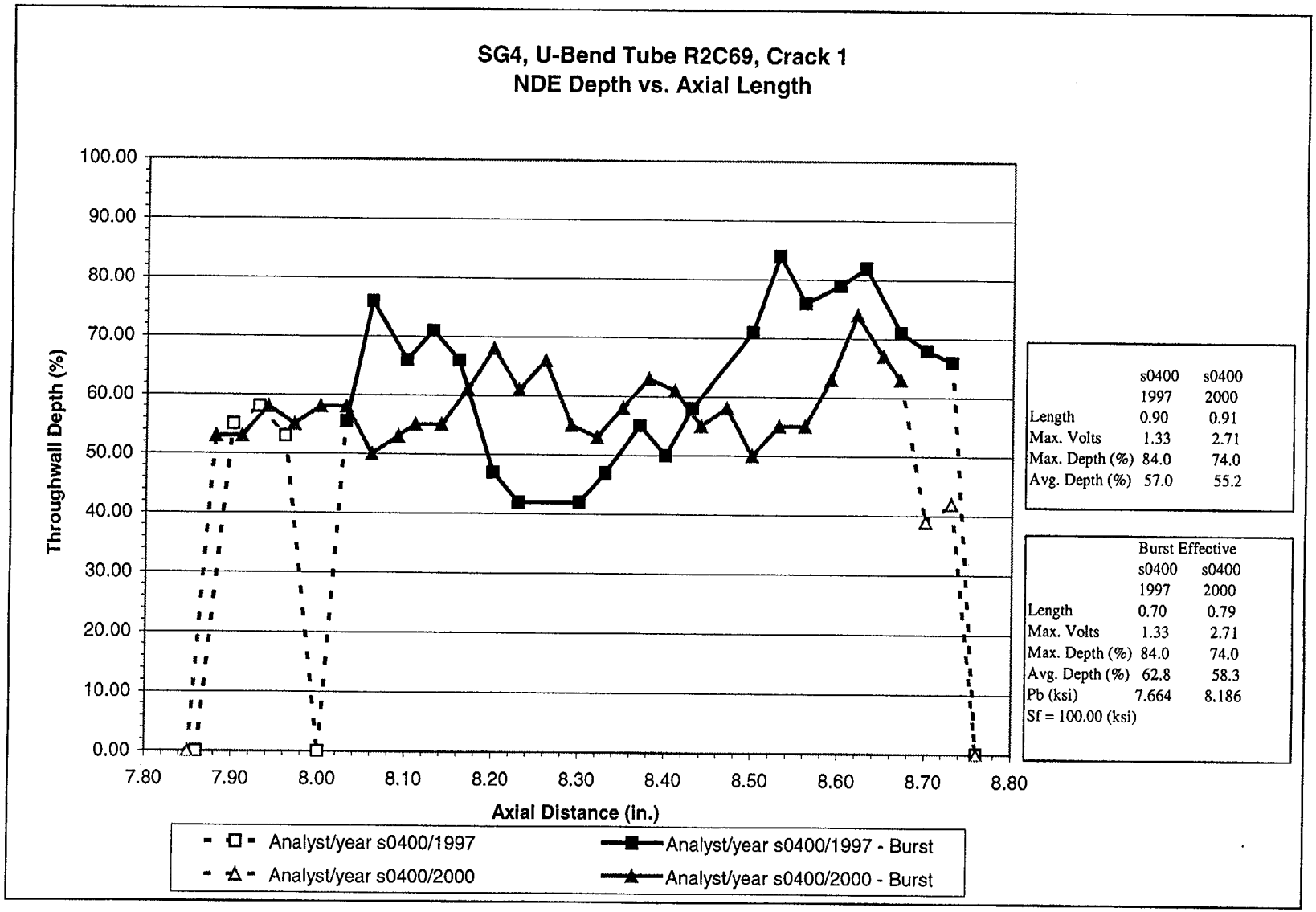
SG4, U-Bend Tube R2C69, Crack 1
NDE Depth vs. Axial Length
Throughwall Depth (%)
100.00
90.00
80.00
70.00
60.00
50.00
40.00
30.00
20.00
10.00
0.00
7.80
7.90
8.00
8.10
8.20
8.30
8.40
8.50
8.60
8.70
8.80
Axial Distance (in.)
Analyst/year s0400/1997
Analyst/year s0400/2000
Analyst/year s0400/1997 - Burst
Analyst/year s0400/2000 - Burst
s0400 1997 s0400 2000
Length 0.90 0.91
Max. Volts 1.33 2.71
Max. Depth (%) 84.0 74.0
Avg. Depth (%) 57.0 55.2
Burst Effective
s0400 1997 s0400 2000
Length 0.70 0.79
Max. Volts 1.33 2.71
Max. Depth (%) 84.0 74.0
Avg. Depth (%) 62.8 58.3
Pb (ksi) 7.664 8.186
Sf = 100.00 (ksi)

Figure C.2-5

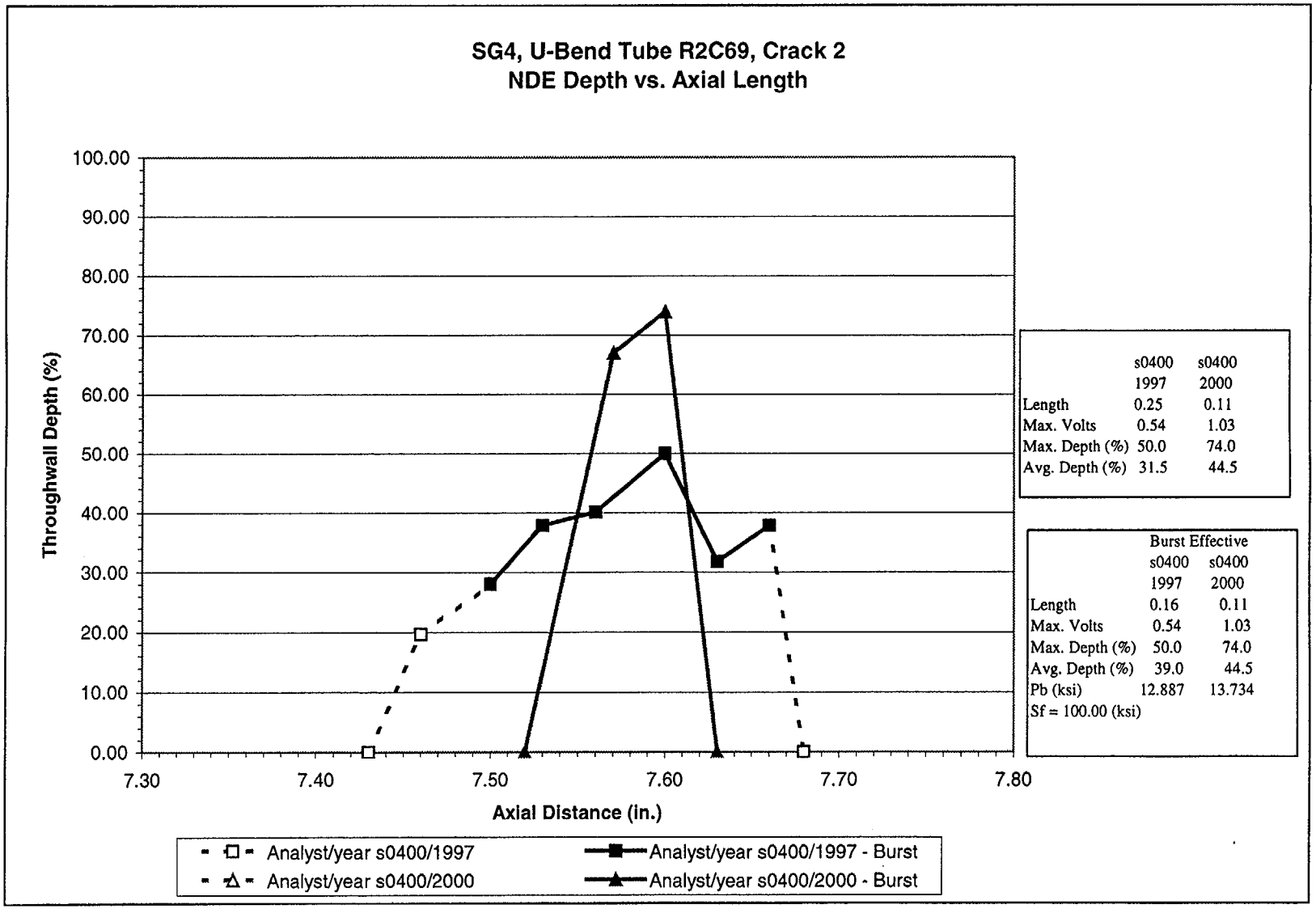
SG4, U-Bend Tube R2C69, Crack 2
NDE Depth vs. Axial Length
Throughwall Depth (%)
100.00
90.00
80.00
70.00
60.00
50.00
40.00
30.00
20.00
10.00
0.00
7.30
7.40
7.50
7.60
7.70
7.80
Axial Distance (in.)
Analyst/year s0400/1997
Analyst/year s0400/2000
Analyst/year s0400/1997 - Burst
Analyst/year s0400/2000 - Burst
s0400 1997 s0400 2000
Length 0.25 0.11
Max. Volts 0.54 1.03
Max. Depth (%) 50.0 74.0
Avg. Depth (%) 31.5 44.5
Burst Effective
s0400 1997 s0400 2000
Length 0.16 0.11
Max. Volts 0.54 1.03
Max. Depth (%) 50.0 74.0
Avg. Depth (%) 39.0 44.5
Pb (ksi) 12.887 13.734
Sf = 100.00 (ksi)

Figure C.2-6

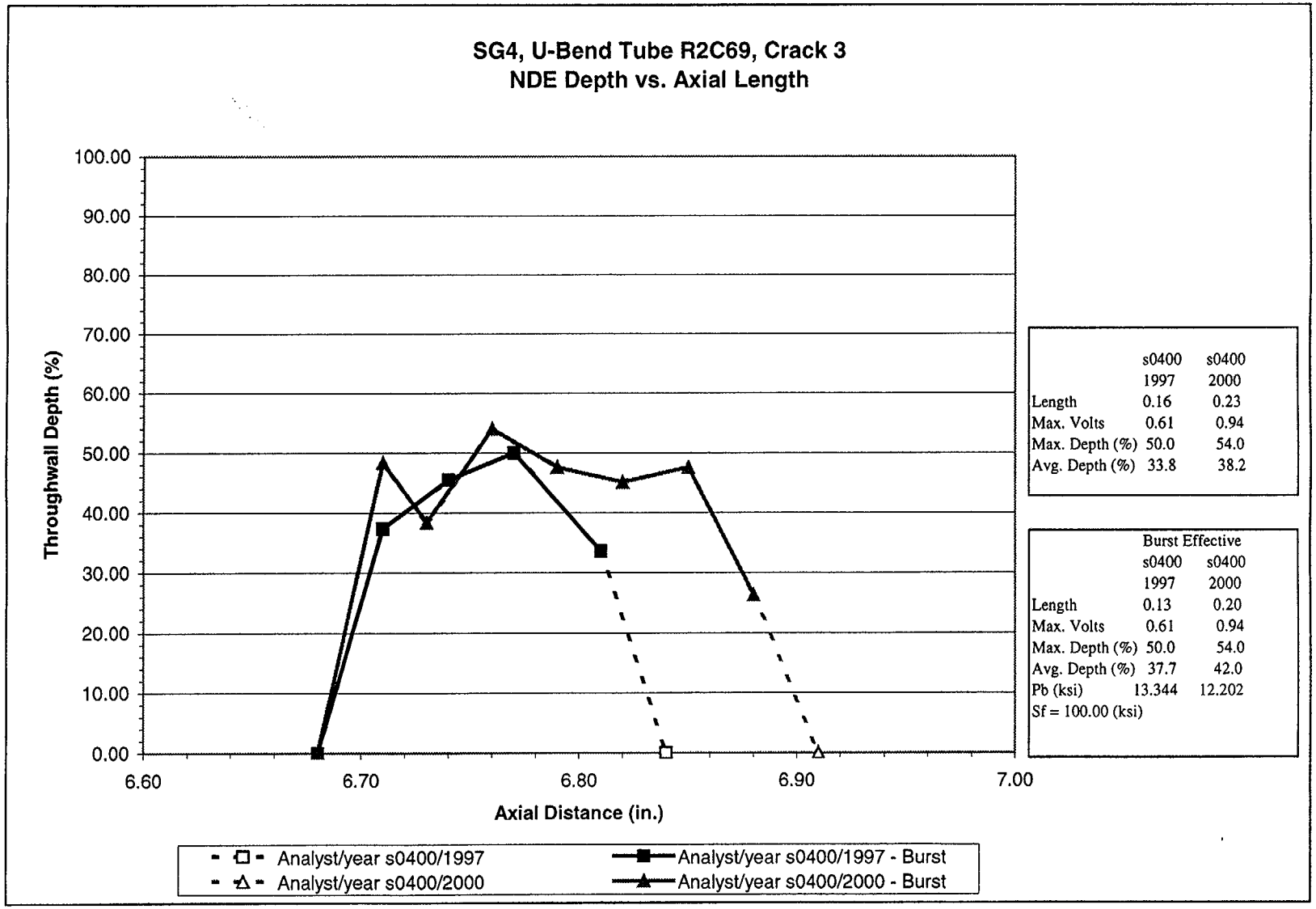
SG4, U-Bend Tube R2C69, Crack 3
NDE Depth vs. Axial Length
Throughwall Depth (%)
100.00
90.00
80.00
70.00
60.00
50.00
40.00
30.00
20.00
10.00
0.00
6.60
6.70
6.80
6.90
7.00
Axial Distance (in.)
s0400 1997 s0400 2000
Length 0.16 0.23
Max. Volts 0.61 0.94
Max. Depth (%) 50.0 54.0
Avg. Depth (%) 33.8 38.2
Burst Effective
s0400 1997 s0400 2000
Length 0.13 0.20
Max. Volts 0.61 0.94
Max. Depth (%) 50.0 54.0
Avg. Depth (%) 37.7 42.0
Pb (ksi) 13.344 12.202
Sf = 100.00 (ksi)
Analyst/year s0400/1997
Analyst/year s0400/2000
Analyst/year s0400/1997 - Burst
Analyst/year s0400/2000 - Burst

Figure C.2-7

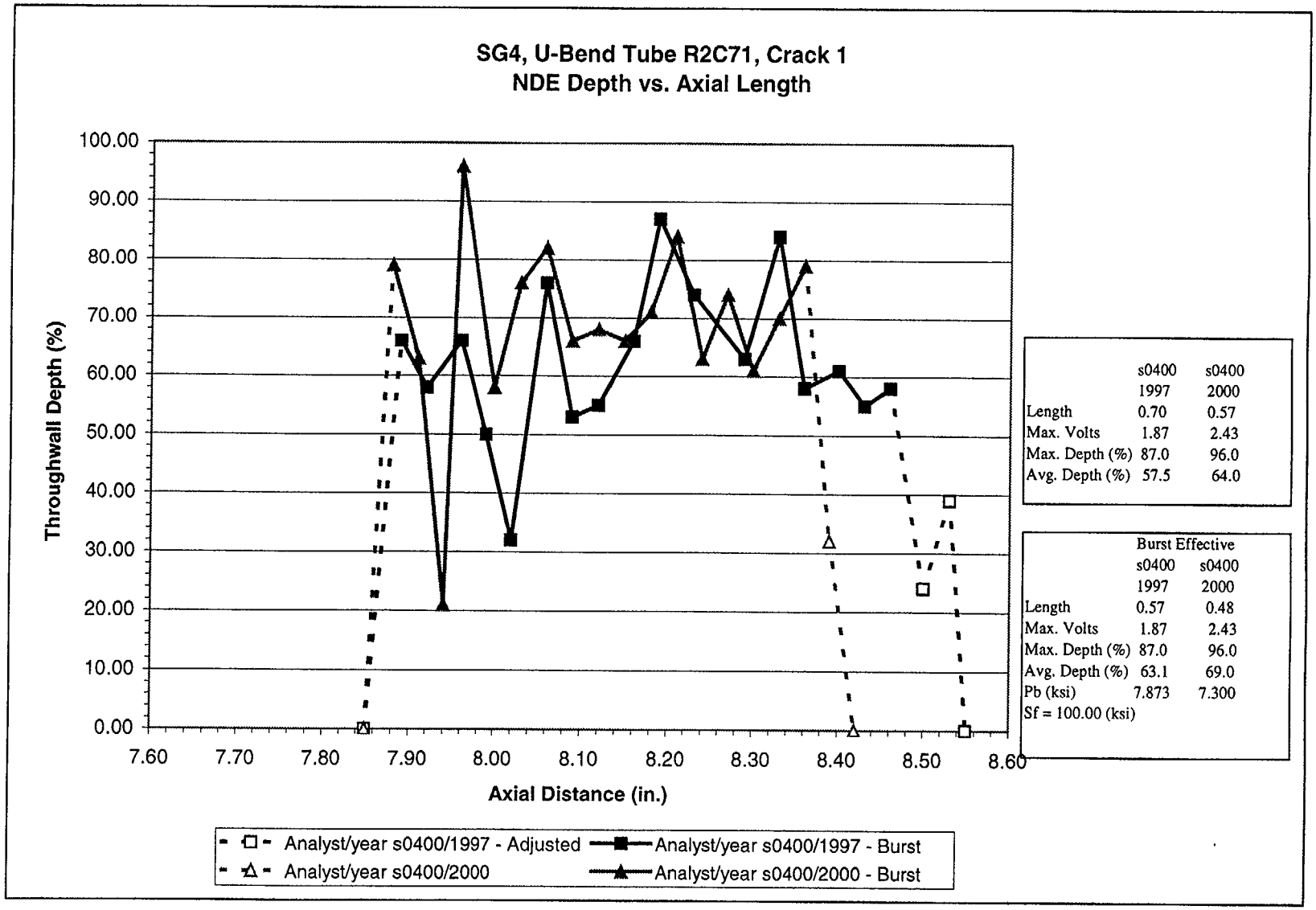
SG4, U-Bend Tube R2C71, Crack 1
NDE Depth vs. Axial Length
Throughwall Depth (%)
100.00
90.00
80.00
70.00
60.00
50.00
40.00
30.00
20.00
10.00
0.00
7.60
7.70
7.80
7.90
8.00
8.10
8.20
8.30
8.40
8.50
8.60
Axial Distance (in.)
Analyst/year s0400/1997 - Adjusted
Analyst/year s0400/1997 - Burst
Analyst/year s0400/2000
Analyst/year s0400/2000 - Burst
s0400 1997 s0400 2000
Length 0.70 0.57
Max. Volts 1.87 2.43
Max. Depth (%) 87.0 96.0
Avg. Depth (%) 57.5 64.0
Burst Effective
s0400 1997 s0400 2000
Length 0.57 0.48
Max. Volts 1.87 2.43
Max. Depth (%) 87.0 96.0
Avg. Depth (%) 63.1 69.0
Pb (ksi) 7.873 7.300
Sf = 100.00 (ksi)

Figure C.2-8

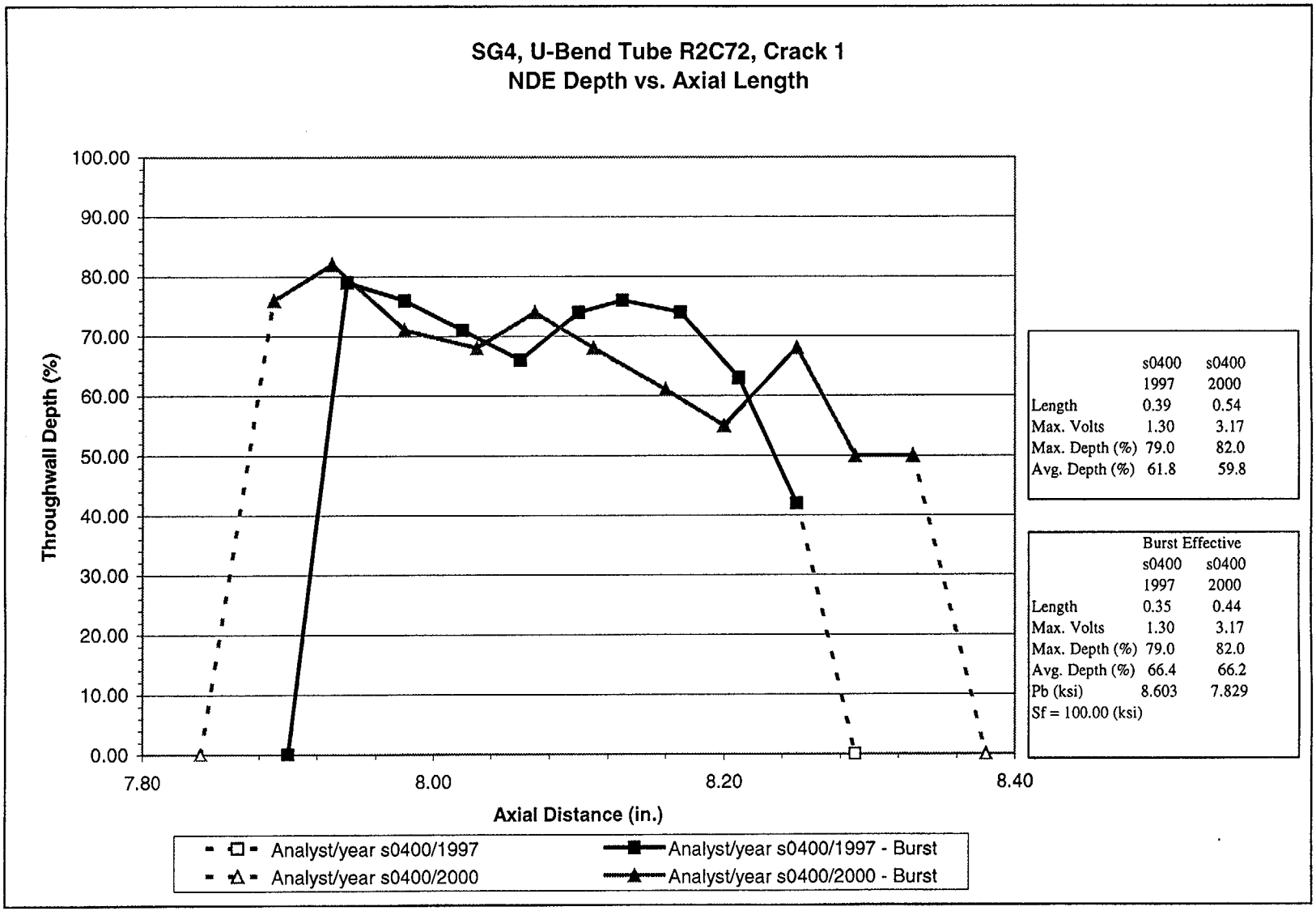
SG4, U-Bend Tube R2C72, Crack 1
NDE Depth vs. Axial Length
Throughwall Depth (%)
100.00
90.00
80.00
70.00
60.00
50.00
40.00
30.00
20.00
10.00
0.00
7.80
8.00
8.20
8.40
Axial Distance (in.)
Analyst/year s0400/1997
Analyst/year s0400/2000
Analyst/year s0400/1997 - Burst
Analyst/year s0400/2000 - Burst
s0400 1997 s0400 2000
Length 0.39 0.54
Max. Volts 1.30 3.17
Max. Depth (%) 79.0 82.0
Avg. Depth (%) 61.8 59.8
Burst Effective
s0400 1997 s0400 2000
Length 0.35 0.44
Max. Volts 1.30 3.17
Max. Depth (%) 79.0 82.0
Avg. Depth (%) 66.4 66.2
Pb (ksi) 8.603 7.829
Sf = 100.00 (ksi)

Attachment 1 to SG-00-05-008, Indian Point-2 U-Bend PWSCC Condition Monitoring and Operational Assessment

OVERVIEW OF SMALL RADIUS U-BEND TUBE SUSCEPTIBILITY TO PWSCC FOR INDIAN POINT 2 STEAM GENERATORS

Altran Technical Report No. 00603-TR-005
Revision 0

OVERVIEW OF SMALL RADIUS U-BEND TUBE SUSCEPTIBILITY TO PWSCC FOR INDIAN POINT 2 STEAM GENERATORS

Technical Report No. 00603-TR-005
Revision 0
Volume 1 of 1

Prepared for

Consolidated Edison Company of New York, Inc.
Indian Point Station, Unit 2

Prepared by

Altran Corporation
451 D Street
Boston, MA 02210

OVERVIEW OF SMALL RADIUS U-BEND TUBE SUSCEPTIBILITY TO PWSCC FOR INDIAN POINT 2 STEAM GENERATORS

Technical Report No. 00603-TR-005
Revision 0
Volume 1 of 1

Prepared for

Consolidated Edison Company of New York, Inc.
Indian Point Station, Unit 2

Originator: _____ Date: 5/26/00
Farid Elsabee/Ron Tomawski

Originator: _____ Date: 5/26/00
David Kalmanovitch

Verifier: _____ Date: 5/26/00
Bahaa Elaidi

Verifier: _____ Date: 5/26/00
Tom Esselman

Project Manager: _____ Date: 5/26/00
William McBrine

Overview of
Small Radius U-Bend Tube Susceptibility To PWSCC
for Indian Point 2 Steam Generators

TABLE OF CONTENTS

1.0	INTRODUCTION	3
2.0	ANALYTICAL AND EXPERIMENTAL INVESTIGATIONS	4
2.1	Top Support Plate Movement	4
2.2	Ovality Study	8
2.3	Experimental Investigations	9
3.0	STRESS ANALYSIS OF U-BEND TUBES	15
3.1	U-Bend Tube Geometry	15
3.2	U-Bend Tube Material Properties	16
3.3	Stress Analysis for Operating Conditions	17
4.0	RELATIVE TIME TO CRACK INITIATION	19
5.0	CONCLUSIONS	21
6.0	REFERENCES	22

Overview of
Small Radius U-Bend Tube Susceptibility To PWSCC
for Indian Point 2 Steam Generators

1.0 INTRODUCTION

Distortion of the Tube Support Plates (TSP) in the flow slot regions results in movements of the steam generator (SG) tubes from their original design locations. The effect of this movement is greatest at the top support plate (TSP 6), as it introduces bending stresses in the U-bend region of the first few rows of tubes. These tubes are most susceptible because of their small bend radii and the relatively small length between the top TSP and the transition region of the U-bend.

Primary Water Stress Corrosion Cracking (PWSCC) has been a problem in the U-bends and transition regions of steam generator (SG) tubes with small bend radii throughout the nuclear power industry. A requirement for PWSCC to occur is a tensile stress. An increase in the tensile stress resulting from flow slot distortion of the TSP will have a corresponding increase in the susceptibility to PWSCC in the U-bend region of the small radius tubes. This appendix investigates the relative susceptibility of small radius U-bends at Indian Point 2 (IP2) to PWSCC. The stress in the tube U-bends due to tube support plate and flow slot distortions are first determined. The increase in susceptibility to PWSCC is then quantified for the Row 3 tubes relative to the Row 2 tubes based on the calculated stress values for the Row 2 and 3 tubes. Since the leak in tube R2C5 in SG24 was from a longitudinal crack at the apex of the extrados (Ref. 1), the investigations reported herein concentrated on the hoop stress at the inside diameter (ID) at this location. This is the stress that would initiate and propagate such cracks.

The overall approach used in the investigation consisted of the following steps:

1. Determine the displacement of the tubes in the flow slot region of TSP 6 using a finite element model of the top support plate for a measured amount of hourglassing.
2. Investigate the extent and importance of the initial ovality resulting from bending during the manufacturing of the tubes.
3. Perform laboratory tests on similar U-bend tubes as those used in the IP2 SGs to determine material behavior, residual stresses from bending during manufacturing, and response to U-bend leg deformation.
4. Develop a finite element model of the Row 2 and 3 U-bend tubes, consistent with the results of the investigations of step 2, using appropriate stress-strain behavior and yield stress values, and benchmark it against the laboratory test results from step 3.
5. Using the U-bend model, determine the hoop stress at the inside of the apex extrados for the level of deformation of the top TSP calculated in step 1 and combine the normal operating stresses and the residual stresses derived experimentally.
6. Based on the resultant stress from step 5, assess the time to PWSCC initiation of Row 3 tubes relative to that of Row 2 tubes and assess susceptibility to the PWSCC mechanism observed in Row 2.

2.0 ANALYTICAL AND EXPERIMENTAL INVESTIGATIONS

To assess the susceptibility of the U-bend tubes to PWSCC initiation at its apex, the hoop stress at the inside of the extrados of the apex needs to be determined. A finite element model of the top TSP is first used to establish the amount of leg deformation the various tubes could experience. A tube U-bend model is used to calculate the stress level at the apex due to the deformation of the top TSP. The objective of these analyses is to quantify the Row 2 and Row 3 hoop stress at the apex of the tube due to the hourglassing of the top TSP.

2.1 Top Support Plate Movement

The movement of Row 2 and 3 tubes, resulting from a given amount of flow slot hourglassing, is determined using an ANSYS (Ref. 2) non-linear finite element model of the top TSP. The model, consisting of two dimensional elastic-plastic elements, is used to quantify the relative movement of the tube rows in the vicinity of the flow slots.

The model used for the analysis consists of one quarter of the plate with symmetry boundary conditions. The quarter model contains three flow slots, an elastic-plastic tube hole region of the first ten rows of tubes, a linear elastic tube hole region of the next thirteen rows of tubes, and an equivalent region for the remainder of the plate which is modeled without holes.

Figure 2.1.1 presents an overall view of the plate model comprised of the flow slot region, the tube holes, the flow holes, and the equivalent region without holes. Figure 2.1.2 presents a detailed view of the vicinity of the flow slot at the center of the plate with the symmetry boundaries.

Elastic elements inside all the tube holes are thermally expanded to simulate the in-plane pressure load applied by the corrosion products between the tubes and the TSP holes. This thermal load results in in-plane compression throughout most of the plate. The applied thermal expansion at the tube holes is adjusted to result in a target level of flow slot hourglassing of approximately 0.5 inch to simulate the measured deformation of 0.476 inch at the top TSP of SG24 (Ref. 1).

Evaluation of the results of the analysis concentrated on the X-horizontal displacement in the direction perpendicular to the tube lane. Figure 2.1.3 presents the X-displacement contours while showing an exaggerated deformation view of the flow slots. As noted during the visual inspections, the maximum flow slot deformation occurs at the center of the flow slot, characteristic of the hourglassing shape, with minimal deformation at the hard points between the flow slots.

The results were evaluated and a displacement profile of the tubes in the vicinity of the flow slot was developed. The displacement values are normalized to the maximum

displacement of the Row 1 tubes, which occurs at the middle of the flow slot. The displacement profile for the first three rows is presented in Table 2.1.1. As can be seen, the Row 2 tubes displace approximately 63% to 97% of the Row 1 tube with the maximum deformation. The Row 3 tubes displace approximately 63% to 92% of the Row 1 tube with the maximum deformation.

X-Displ. As a Percentage of R1C7			
Column No.	**Row 1**	**Row 2**	**Row 3**
3	67	63	63
4	85	81	76
5	93	90	85
6	98	94	90
7	100	97	92
8	100	97	92
9	99	96	91
10	96	93	88
11	91	88	83
12	83	79	74
13	67	63	62

Table 2.1.1
X-Displacement for the Tubes near Slot from the Quarter Model
(Values Normalized In Percentage to the Maximum Displacement of Tube R1C7 that was measured)

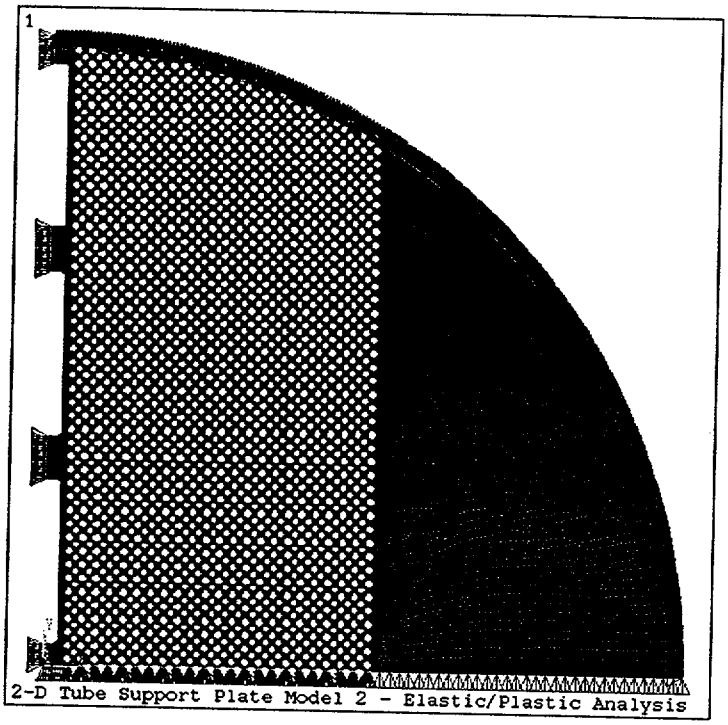

Figure 2.1.1
Quarter TSP Model

Figure 2.1.2
Quarter TSP Model
Detailed View of Flow Slot Region

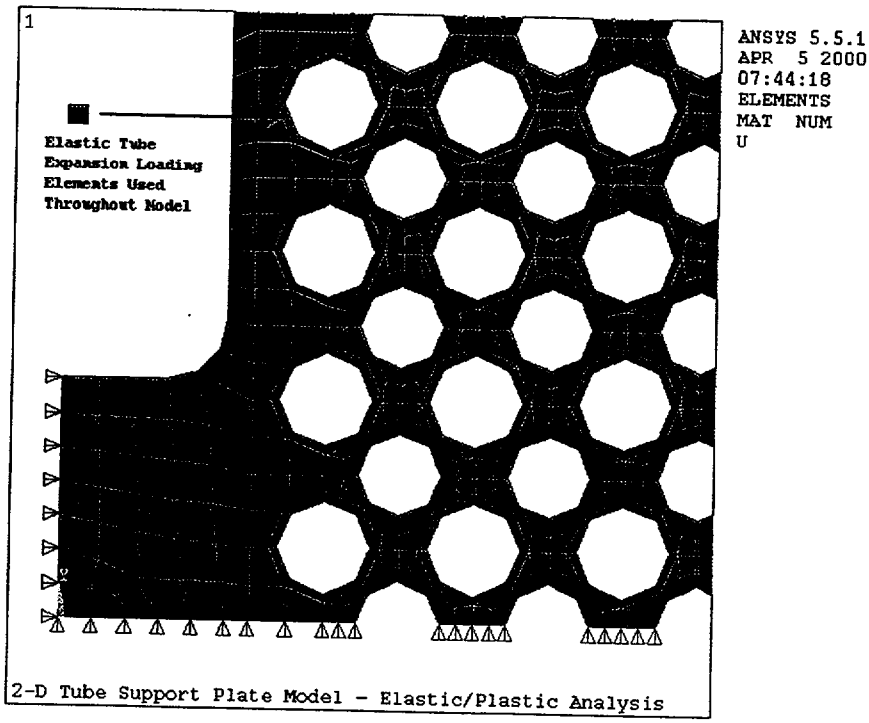

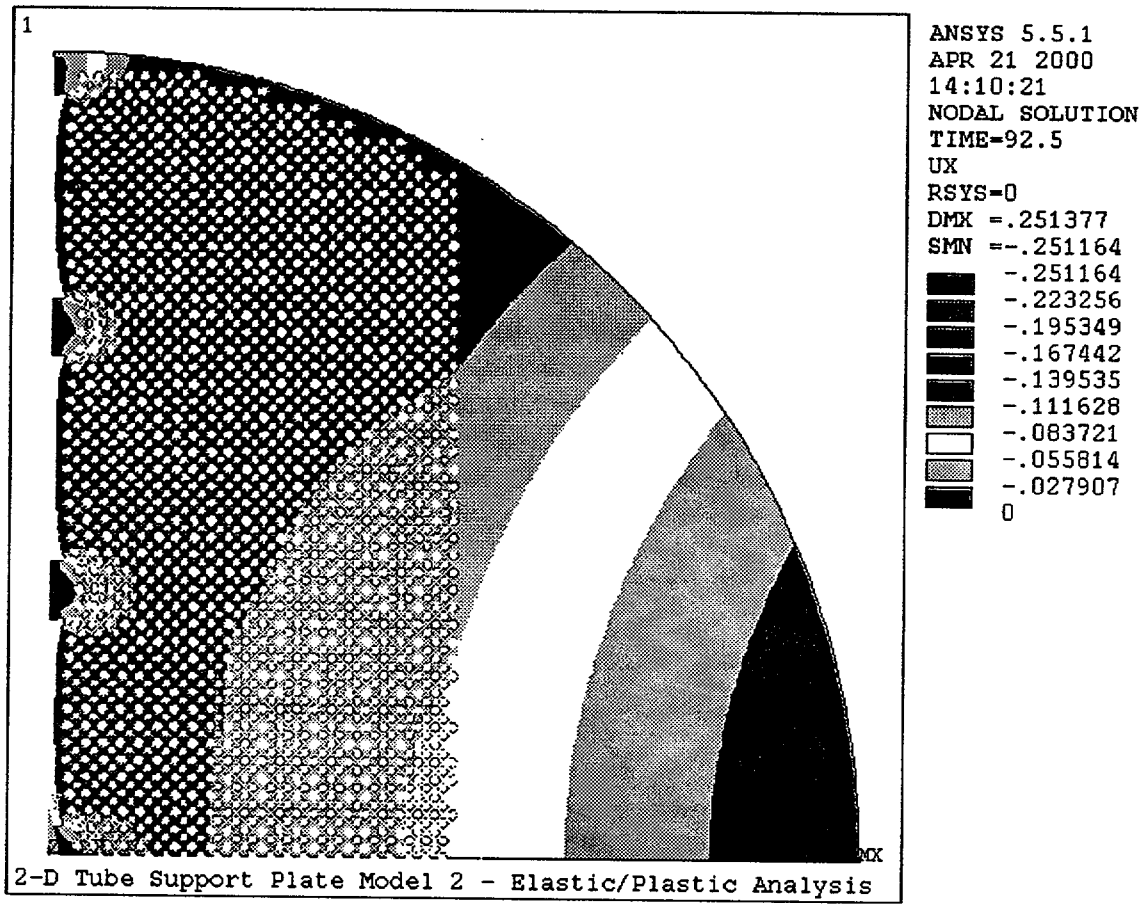

Figure 2.1.3
Quarter TSP Model
X-Displacement Contours
(With exaggerated deformation at flow slots)

2.2 Ovality Study

A parametric study of the effects of the "as-manufactured" ovality in small radius U-bend tubes on the stress at the apex of the U-bends was performed.

The study used an elastic-plastic finite element model of the tube U-bend that was assumed to be fully fixed at the top tube support plate. This boundary condition is imposed to represent the restraining at the existing oxide packed crevices. The loads imposed on the model consisted of an internal pressure, temperature differential, and a lateral displacement of the straight leg inward towards the center of the U-bend. The investigation considered Row 2 and 3 U-bend tubes with varying lateral displacement (from 0 to 0.5" of total flow slot hourglassing) and varying ovality (from 0 to 0.1). Figure 2.2.1 presents the calculated inside diameter hoop stress at the apex extrados for each case evaluated.

Based on this investigation, it is concluded that increasing the initial ovality of a U-bend tube decreases the inside diameter hoop stress of the extrados at the apex resulting from hourglassing. This investigation also indicates that the initial ovality of the tubes is not a major contributor to the stress environment at the extrados. Therefore, a U-bend analysis model that assumes a circular cross section will result in conservatively higher ID hoop stress values at the apex extrados.

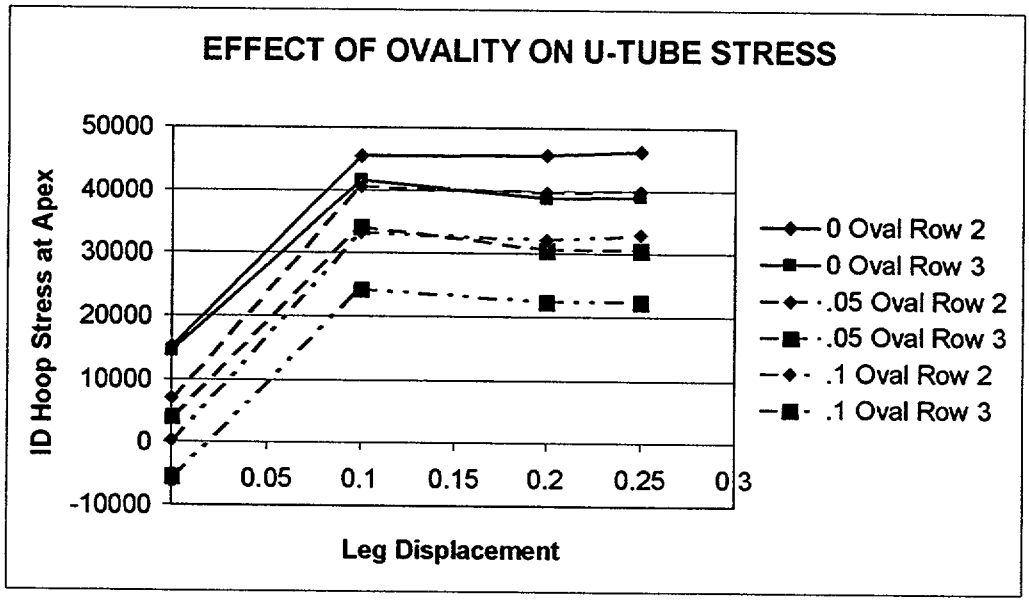

Figure 2.2.1
Comparison of ID Hoop Stress at the Apex Extrados

2.3 Experimental Investigations

The investigation of the susceptibility of the Row 3 tubes to PWSCC was also supported by means of experimental investigations. Samples of Inconel 600 U-bend tubes were located in the EPRI project archives and made available to Consolidated Edison of New York (ConEdison) for laboratory testing. These samples, consisting of three Row 2 and three Row 3 tubes, were identified to have been fabricated by Westinghouse for a previous project. The tubes have the same geometry and similar dimensions (7/8" OD with 0.050" nominal thickness) as the tubes used in the IP2 SGs. Five of the tubes were reported to have been bent without the use of an internal mandrel. The samples were used to obtain ovality, wall thinning, and yield stress measurements. Material stress-strain behavior and strain hardening at the apex region were also determined. Two tubes were also tested by imposing an in-plane deformation of the legs while monitoring the strain and the ovality in the apex region. Finally, residual strain resulting from the bending of the U-bends during the manufacturing process was also measured from two samples.

Wall Thinning and Ovality Measurements

Table 2.3.1 provides measurements made at the apex of the U-bend samples in the as-manufactured condition. Measurements of the as-manufactured ovality of the tubes bent without a mandrel at the apex of the U-bend resulted in values ranging from 4.99% to 5.65%, with an average of 5.24% for the Row 2 tubes and 5.31% for the Row 3 tubes. The ovality at the apex of the U-bend for a single Row 2 tube, reported to have been bent with a mandrel, was measured at 2.28%. These ovality measurements are calculated from the measured dimensions as the percent of the difference between the major and minor outside diameters (at the apex) to the original diameter of the tube (at the transition point or straight legs).

Table 2.3.1 also provides measurements of the as-manufactured wall thinning of the tube at the apex extrados. As indicated in the table, the values ranged from 0.002 to 0.004 inch with an average of 0.003" for both Row 2 and Row 3 tubes. A value of 0.004 inch was measured for the tube reported to have been bent with a mandrel.

Deformation of U-Bend Legs

A fixture was fabricated that allowed a U-bend pinching displacement to be applied at a location corresponding to the top TSP. Rotation at the restraint points was limited by the fixture to simulate the oxide packed TSP conditions. Two U-bend tube samples, one Row 2 and one Row 3 tube, were tested by applying an incrementally increasing closing deflection (by increments of 0.05") of the U-bend legs while monitoring the strain and ovalization of the cross section. The tubes were pressurized to 1600 psi during the test and the test was performed at ambient room temperature. Leg closure up to a maximum deflection of 0.55" for the Row 2 tube and 0.75" for the Row 3 tube was applied. The ovality of the tubes measured during the tests is presented in Figures 2.3.1 and 2.3.2. At the 0.5" deflection level, the measured ovality at the apex for both tubes was approximately

7%. This is compared to an initial value of approximately 2.5% for the Row 2 tube and approximately 5.5% for the Row 3 tube prior to the tests.

Mechanical Properties

Mechanical testing of four coupon specimens taken from two U-bends was also performed. Stress-strain curves from the four coupons are presented in Figure 2.3.3. Two coupon specimens (T1 and T2), taken from the legs of the same Row 2 sample that was previously tested by applying leg deformations, resulted in a 0.2% offset yield stress value of 45.5 and 44.2 ksi.

The other two specimens (T3 and T4) were taken from below the transition point and at the apex extrados of a different Row 2 sample manufactured from a different heat. The 0.2% offset yield value for T3 (from the straight portion) was 62.2 ksi while that for T4 (from the apex) was 92 ksi. These values demonstrate that the yield strength in the U-bend region of the tubes is higher than the nominal value and indicate a strain hardening of approximately 50% for the Row 2 U-bends.

Measurement of Residual Strains

Residual strains were also experimentally measured at the apex of one Row 2 and one Row 3 U-bend tube samples. These were measured on tubes that were fabricated without the use of internal mandrels. Strain gauges were applied at the outside diameter (OD) to the U-bend tubes and the "restraint" forces were relieved by cutting the tubes circumferentially. Inside diameter gauges were then applied and the tubes were cut axially to relieve the residual stress in the hoop direction. Strains were measured during all the cutting operations. Fabrication residual strains are then considered to be opposite in sign to those measured.

The test results indicate a compressive residual hoop strain on the inside diameter at the apex of the tube extrados and a tensile residual strain on the outside diameter. Figure 2.3.4 provides the strains determined from the tests along with a graphical representation of the equivalent elastic stress through the thickness of the tube wall at the apex extrados.

	As-Received U-Tube Samples		
Sample Number	Tube Row	Wall Thinning (in.)	Measured Ovality (in %)
00603-1	2	0.003	4.99
00603-2	2	0.003	5.48
Row 2 Average		**0.003**	**5.24**
00603-3	3	0.004	5.30
00603-4	3	0.004	5.65
00603-5	3	0.002	4.99
Row 3 Average		**0.003**	**5.31**
00603-6	2	0.004	2.28

Table 2.3.1
Wall Thinning and Ovality Measurements
at the Apex of U-Bend Tubes Received from EPRI

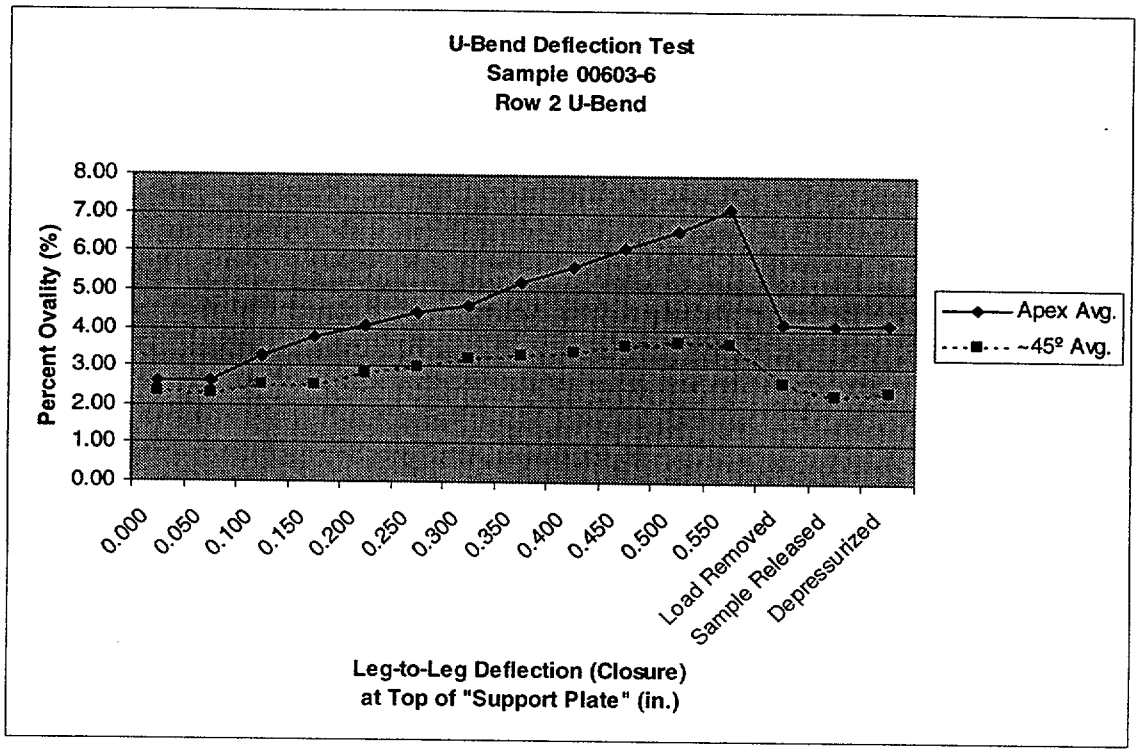

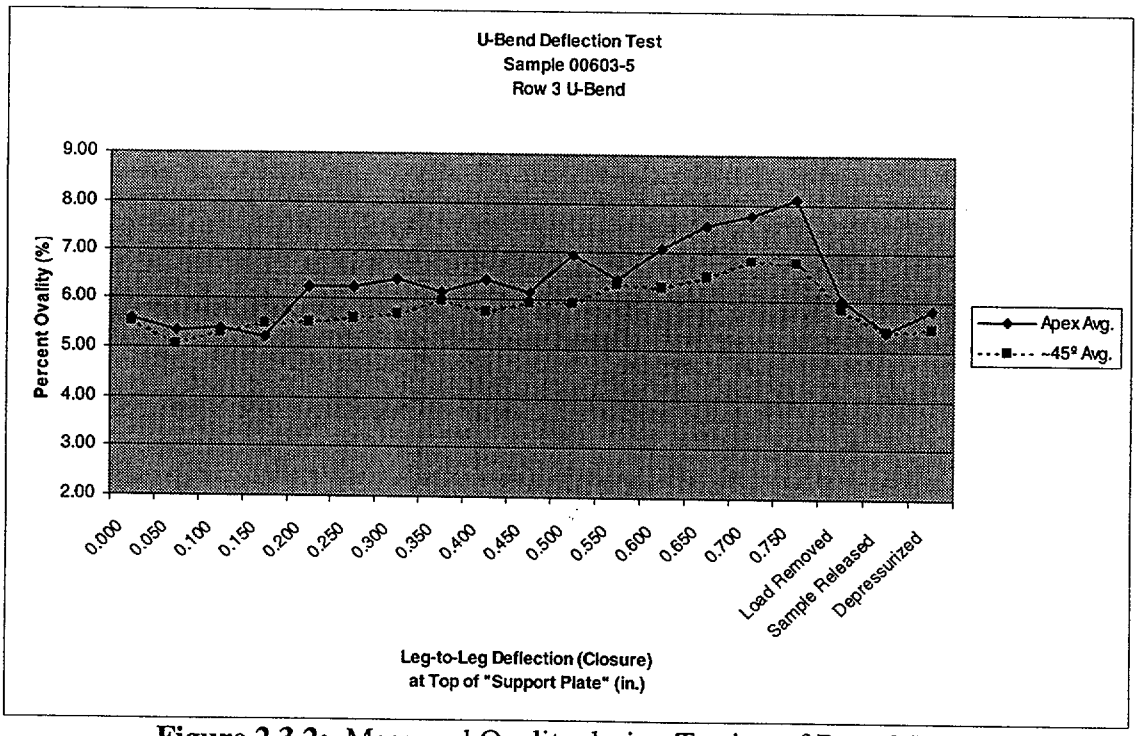

Figure 2.3.2: Measured Ovality during Testing of Row 3 Tube

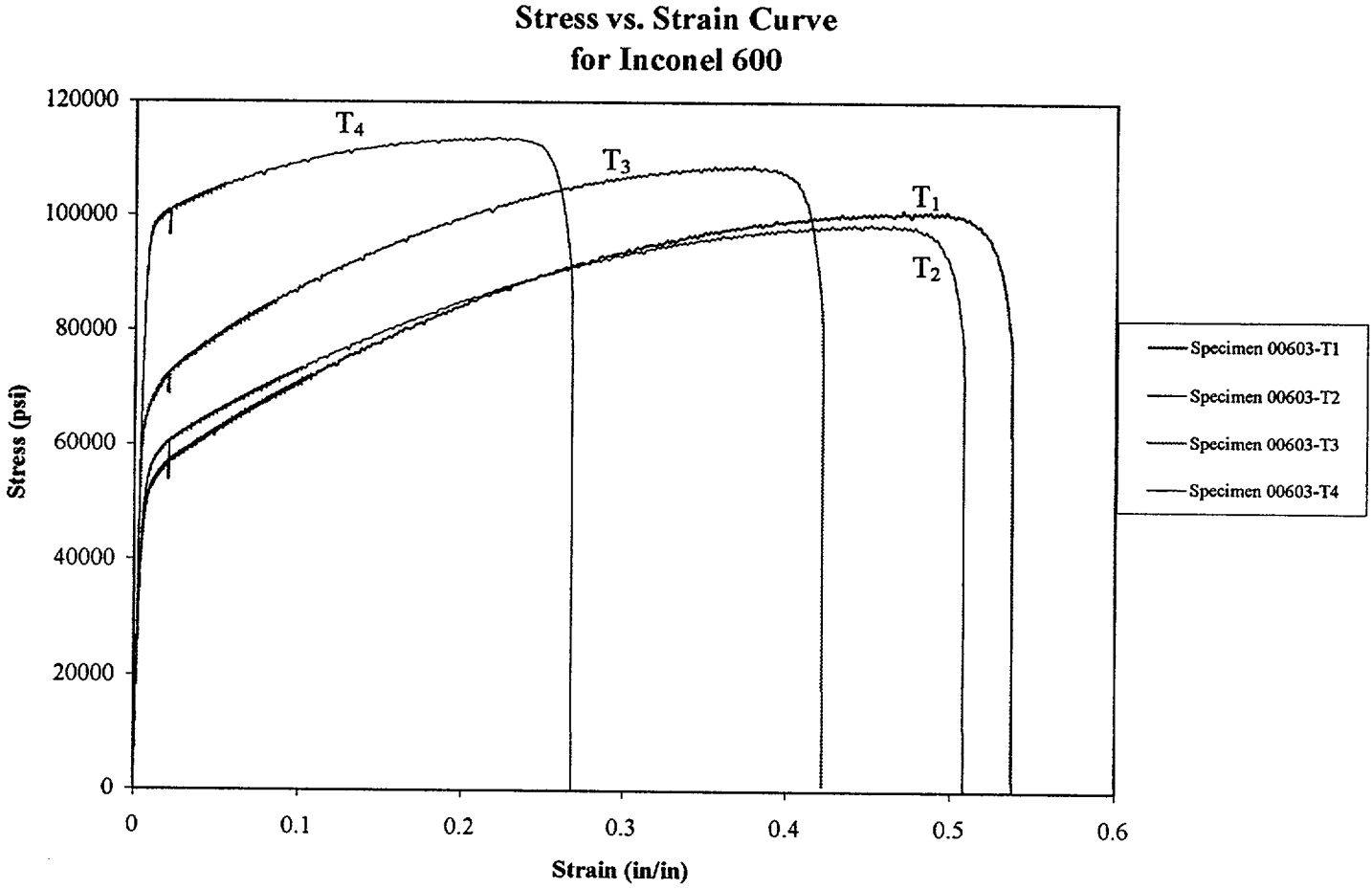

Figure 2.3.3
Stress-Strain Curves For Four Specimens
(T1, T2, and T3 coupons from straight legs;
T4 from apex)

Average Released (Measured) Hoop Strain in Rows 2 and 3 Samples at the Apex

Sample	Average Total ID Hoop Strain (in/in)	Average Total OD Hoop Strain (in/in)
Row 2	0.00038	-0.00030
Row 3	0.00036	-0.00029

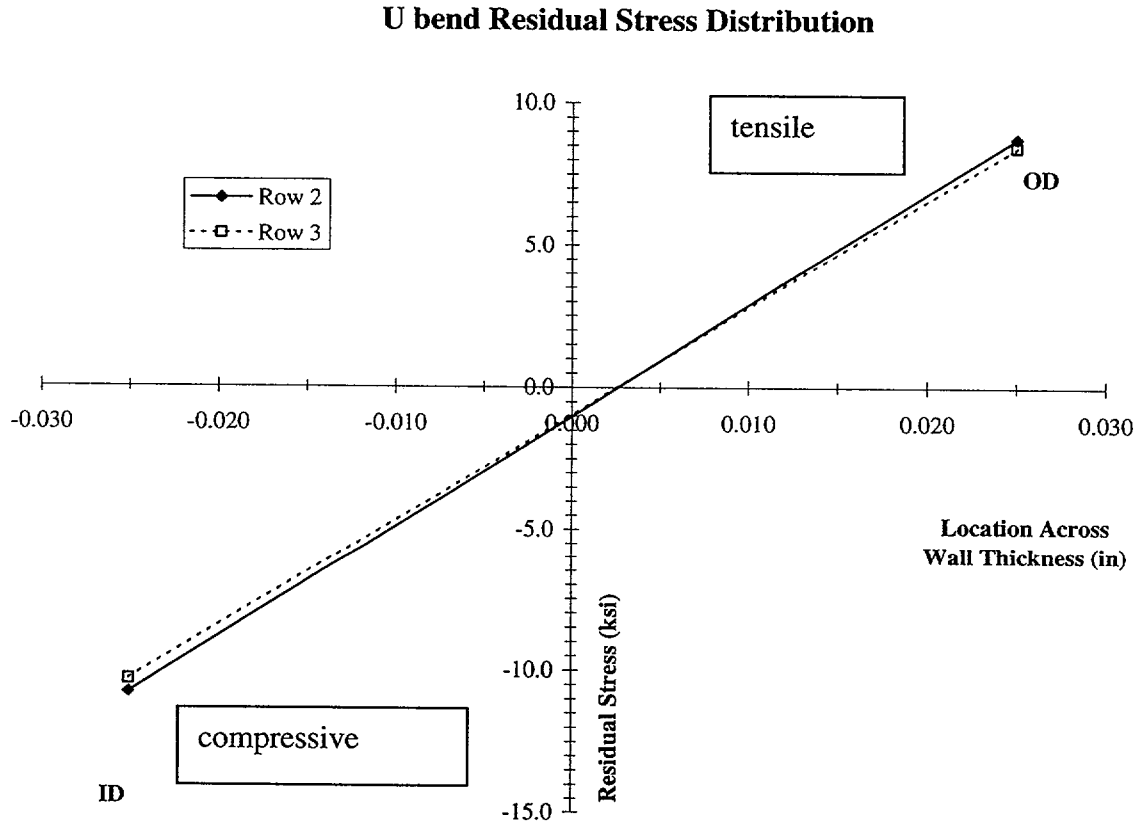

Figure 2.3.4
Average Residual Hoop Strain Determined Experimentally At the Apex Extrados of the U-Bend (Equivalent U-Bend Elastic Residual Stress Distribution using $E=28.7 \times 10^6$ psi/in/in)

3.0 STRESS ANALYSIS OF U-BEND TUBES

A series of non-linear finite element analyses were carried out to determine the stress states at the interior surface of the small radius tubes at the apex extrados of the U-bends located in rows 2 and 3. These analyses incorporated pressure and thermal conditions, tube leg displacements resulting from the TSP distortion, residual stresses, and nonlinear stress-strain properties. The stress states were determined for U-bends in rows 2 and 3 in the vicinity of a flow slot based on the plate deformation profile described in section 2.1.

3.1 U-Bend Tube Geometry

A three-dimensional elastic-plastic finite element analysis (FEA) model of the U-bend geometry (7/8" diameter and 0.050" thick) for a Row 2 and a Row 3 tube was developed using ANSYS (Ref. 2). The model, consisting of four 3-D solid elements through the thickness, used symmetry from the top support plate to the apex and one half of the tube diameter. Figure 3.1.1 shows a view of the model element geometry and boundary conditions. The model is fixed for all degrees of freedom at the surface intersection of the tube with the TSP except for the translation in the X-direction where the plate deformation is imposed on the model.

Based on the results of the study of Section 2.2, the FEA model does not incorporate any initial ovality that may have resulted from the original fabrication bending process of the U-bend tube. A circular cross section throughout the entire model is used (the tube will ovalize as the loads are imposed). A parameter was included in the model to account for 3 mils of apex thinning (see Section 2.3).

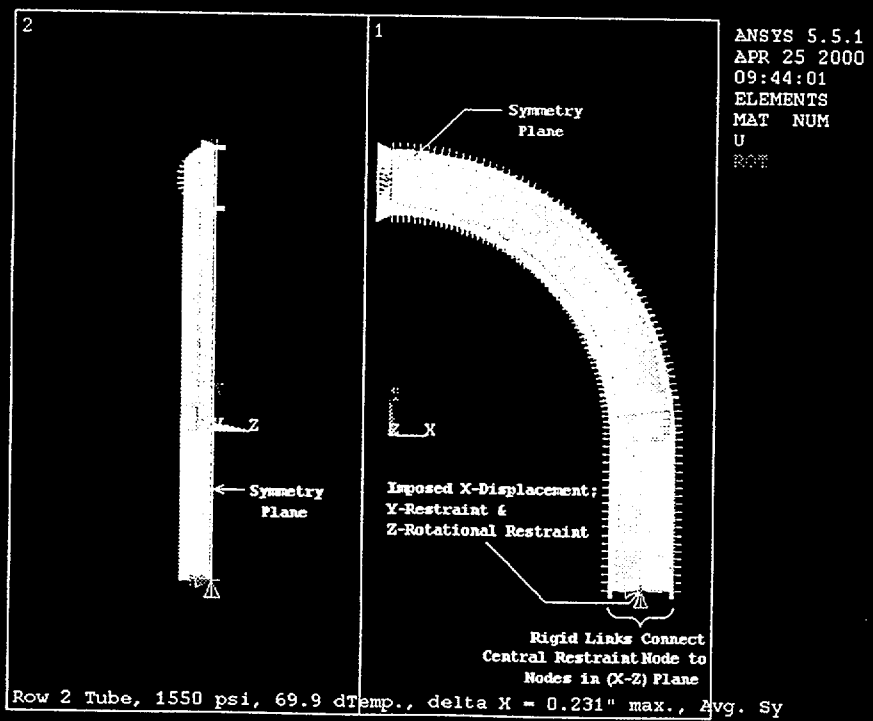

Figure 3.1.1 Typical U-Bend Tube Finite Element Model With Restraint/ Boundary Conditions

3.2 U-Bend Tube Material Properties

Certified Material Test Report (CMTR) records of the IP2 SG tubes were used to develop the material properties used in the FEA models. The CMTR records provided a range of values for the 0.2% offset yield strength at room temperature for the tubes in each row of the SGs. These values were used to define a maximum, a minimum, and an average yield strength value for each row. A reduction of 7 Ksi, based on values provided in ASME III Appendix I (Ref. 3), was applied to each value to correct the properties for the operating temperature of 590°F.

The corrected yield strength values were then used, in conjunction with the stress-strain behavior determined experimentally from coupon specimen T3 (shown in Figure 2.3.3), to obtain the tube material properties for the different areas of the U-bend tube FEA models. A linear elastic modulus of 28.7×10^6 psi/in/in, adjusted for the operating temperature of 590°F, was used based on ASME III Appendix I (Ref. 3).

The amount of strain hardening and the tangent modulus were adjusted for tubes in rows 2 and 3 based on the elongation along the extrados induced during the original as-manufactured bending of the tube. The induced elongation was taken as the ratio of the outside radius to the centerline radius of the U-bend. The strain hardening factor is then applied to the nominal yield strength determined from the CMTR data to obtain the strain hardened yield stress in the U-bend region of the tube FEA model. This strain hardening effect results in higher yield strength for Row 2 tubes than for Row 3 tubes. The unhardened and strain hardened yield stress values used in the FEA analyses are presented in Table 3.2.1.

	Yield Stress	Row 2	Row 3
Yield Stress @ Room Temp (ksi)	Low	37.0	36.0
	Average	48.5	49.3
	High	65.5	66.5
Yield Stress @ Oper. Temp (ksi)	Low	30.0	29.0
	Average	41.5	42.3
	High	58.5	59.5
Yield Stress w/ Strain Hard. (ksi)	Low	44.1	40.3
	Average	61.0	58.8
	High	86.0	82.6

Table 3.2.1
Summary of Yield Stress Values at the Apex Extrados

3.3 Stress Analysis for Operating Conditions

The modeling techniques described in Sections 3.1 and 3.2 were used to benchmark and validate the non-linear FEA model, including strain hardening, against the test results obtained during the leg deformation test of the Row 2 tube described in Section 2.3. Good correlation was obtained when the measured OD strain at the apex extrados was compared to the values obtained analytically.

Using the FEA models developed above, a series of non-linear analyses were carried out to determine the hoop stress at the interior surface of the Row 2 and Row 3 tubes at the apex extrados of the U-bends. The analyses were performed for the following loading conditions while varying the material properties to coincide with the low, average, and high yield strength values obtained from the IP2 CMTR data for each of the tube rows of interest:

- Internal pressure of 1550 psi
- Thermal differential expansion load to represent the difference between the tube temperature and the secondary side TSP temperature.
- Deformation of the U-bend tube model to reflects the TSP deformation profile provided in Table 2.1.1 multiplied by 0.238" (half of the measured value at TSP 6 of SG 24).

The ID and OD hoop stress values obtained from the FEA at the apex extrados of the U-bend tubes are combined with the experimentally measured hoop residual stress values. However, since the apex hoop stresses obtained from the FEA can be above the yield strength of the material, they are added on a strain basis to give the total strain. The total hoop stress on the ID and OD corresponding to the total hoop strain is then determined from the respective nonlinear stress-strain relationships used in the FEA model.

The use of the Row 2 residual strain measurement for a tube fabricated without an internal mandrel is considered appropriate. Any differences between the residual stresses in a tube with an internal mandrel and that measured will cause a minor difference in the final stresses and the conclusions of the analyses. The Row 2 tube stresses are above the yield stress and a different residual strain will have a much smaller effect than if the stresses were elastic.

Table 3.3.1 presents the resulting total ID and OD hoop stresses at the apex extrados obtained from the stress analyses with the effects of residual stresses. As noted from the table, the ID hoop stress values for Row 3 tubes are 70 to 80% of the values for Row 2 depending on the range of the yield stress of the material (i.e. low, average, or high).

	Yield Stress Case	Row 2		Row 3	
		I.D.	O.D.	I.D.	O.D.
Hoop Stress @ Col. 7 (psi)	Low	51,245	-35,169	40,743	-13,934
	Average	68,496	-48,952	52,711	-30,172
	High	92,378	-64,060	65,439	-37,204
Yield Stress w/ Strain Hard. (psi)	Low	44,100		40,300	
	Average	61,000		58,800	
	High	86,000		82,600	

Table 3.3.1
Summary of Hoop Stress Values at the Apex Extrados
From the Finite Element Analyses
(Including residual stress)

4.0 TIME TO CRACK INITIATION

Stress corrosion cracking occurs when a susceptible material is exposed to a particular environment while under a tensile stress. On the primary side, alloy 600 is susceptible to PWSCC in near neutral pH environments. PWSCC is strongly influenced by stress, microstructure (heat treatment & thermal-mechanical processing history), and local chemistry.

For a given microstructure and operating temperature, there is a significant stress dependence. As a result of the numerous microstructural and environmental parameters and their respective influences on the fracture mechanism, it is difficult to accurately determine the actual time to crack initiation. However, it is possible to estimate the relative time to crack initiation between the Row 2 and Row 3 tubes based on the relative magnitude of the stress in each row.

A simplified model for estimating crack initiation in A600 steam generator tubing is an inverse relationship between time for crack initiation, t_f, and the applied stress, σ, raised to the fourth power. This model, which has been presented and discussed in the literature (Ref. 4 and 5), is in the form:

$$\frac{1}{t_f} = C\sigma^4 \qquad (1)$$

Where C is a constant for the material and operational conditions. This model assumes the stress remains constant throughout this time. The expected time to crack initiation of tubes in Row 3, t_{f3}, relative to the time in a tube in Row 2, t_{f2}, with similar yield strength, is:

$$t_{f3} = t_{f2}\left[\frac{\sigma_2}{\sigma_3}\right]^4 \qquad (2)$$

Where σ_3 is the applied stress in Row 3 and σ_2 is the applied stress in Row 2. Note that this model conservatively does not consider the added potential difference in susceptibility due to the higher total plastic strain in Row 2 (Ref. 6). This relationship was used to define the expected crack initiation times of Row 3 tubes relative to the Row 2 tube.

Because of the range of the IP2 Row 2 and 3 yield strength values, it is considered appropriate to compare tubes with similar yield strengths in the work hardened condition in order to define an overall relative susceptibility to cracking. The time to cracking analysis was thus performed for several ranges of material yield strengths for each of the two rows and equation (2) applied within each range. This allows a relative susceptibility

comparison between Row 2 and Row 3 tubes of similar yield strength. This approach results in the following range:

Low Yield Strength Tubes Row 2/Row 3: Factor = $(51.2 \text{ KSI}/ 40.7 \text{ ksi})^4 = 2.5$

High Yield Strength Tubes Row 2/Row 3: Factor = $(92.4 \text{ KSI}/65.4 \text{ ksi})^4 = 4.0$

This evaluation of the data resulted in relative susceptibility factors for the time to crack initiation between Row 3 and Row 2 tubes of between 2.5 and 4.0.

5.0 CONCLUSIONS

Based on the above investigations, it is concluded that:

- Based on analytical investigations, ovality resulting from the initial manufacturing of the tubes does not appear to have a significant effect on the ID hoop stress at the apex extrados for the Row 2 and Row 3 U-bends.

- As indicated by the high ID hoop stress at the apex extrados resulting from the in-plane deformation of the U-bend tube legs, hourglassing in the top TSP appears to be a primary contributor to the PWSCC at the apex of the U-bends.

- As indicated by the lower ID hoop stress at the apex extrados for the Row 3 tubes as compared to the corresponding Row 2 tube, Row 3 tubes are much less susceptible to the PWSCC mechanism that affected the Row 2 tubes. Also, based on the time to crack initiation study, PWSCC at the apex extrados of the mid flow slot Row 3 tube is expected to take 2.5 to 4.0 times the amount of time for PWSCC to initiate as in the corresponding Row 2 tube.

6.0 REFERENCES

1. Westinghouse, "Indian Point 2 Root Cause Evaluation for SG-24, R2C5 Leakage Event," March 2000, Revision 2, 4/14/00.
2. ANSYS Computer Program, Version 5.5.1, ANSYS Incorporated, Canonsburg, PA.
3. American Society of Mechanical Engineering, Boiler and Pressure Vessel Code, Section III, 1989.
4. Bulischeck and Van Rooyen, "Effect of Environmental Variables on the Stress Corrosion Cracking on Inconel 600 Steam Generator Tubing", Nuclear Technology, Vol. 55, Nov 1981 pp. 383-93.
5. R. Bandy and D. van Rooyen, "Mechanisms of Intergranular Failures in Alloy 600 in High Temperature Environments," BNL-NUREG-34270, 1984.
6. "Assessment of Current Understanding of Mechanisms of Initiation, Arrest, and Reinitiation of Stress Corrosion Cracks in PWR Steam Tubing Generators", NUREG/CR-5752, ANL-99/4.

Attachment to NSBU-EDRE-RLE-00-165

Model 44 and 51 Steam Generator Tube Corrosion Performance Comparison to Indian Point Unit 2

May 2000

Prepared by:
Westinghouse Electric Company LLC

Model 44 and 51 Steam Generator Tube Corrosion Performance Comparison to Indian Point Unit 2

May 31, 2000

Authors

Gary W. Whiteman
Advanced Technical Engineer

J.N. Esposito
Consultant

Verified by:
J.T. Crane
Senior Engineer

Approved by:
E.P. Morgan
Manager, Chemistry Diagnostics and Materials Engineering

Model 44 and 51 Steam Generator Tube Corrosion Performance Comparison to Indian Point Unit 2

Table of Contents

Section		Page
1.0	Introduction	4
1.1	Background	4
1.2	Report Objectives	4
2.0	Model 44 and 51 Steam Generator Description	5
2.1	Design Description	5
2.2	Typical Operating Parameters	8
3.0	Model 44 and 51 Steam Generator Tube Integrity Operating Experience Discussion	8
3.1	Degradation Types	8
3.2	Forced Outages	11
3.3	Regulatory/Westinghouse Generic Communications	13
4.0	Operating Experience Comparison Considerations	16
4.1	Comparison Among Steam Generators at Different Plants	20
4.2	IP2 Response to Regulatory/Westinghouse Communications	26
5.0	Conclusions	28
5.1	Summary of Results	28
5.2	Degradation Management Assessment/NEI 97-06, Rev. 1B Program Impact	29
6.0	References	30

1.0 Introduction

1.1 Background

The steam generator (SG) tubes in pressurized water reactors have a number of important safety functions. These tubes are an integral part of the reactor coolant pressure boundary (RCPB) and are relied upon to maintain primary pressure boundary integrity. On February 15, 2000, a leak in the U-bend of SG 4 tube R2C5 led to a forced outage of Indian Point Unit 2. A root cause evaluation has since determined that the leakage was due to an axial primary water stress corrosion crack (PWSCC) located on the extrados of the apex of the U-bend. The resultant primary-to-secondary leakage rapidly progressed from less than 5 gpd to over 105 gpm [146 gpm from the NRC Augmented Inspection Team (AIT) report – Reference 8].

To place the Indian Point Unit 2 February 2000 leakage event in context, Westinghouse has compared the occurrence of steam generator tube degradation mechanisms in the Indian Point Unit 2 steam generators with other Westinghouse Model 44 and 51 steam generators which are comparable in design and have tubes which are metallurgically similar. The intent of the comparison is to provide additional data to better assess the adequacy of the steam generator program implemented to re-establish steam generator tube bundle integrity for Cycle 15 operation.

1.2 Report Objectives

The steam generator tubing in Model 44 and 51 steam generators has been subject to a variety of degradation mechanisms that occur throughout the industry. Steam generator tubes have experienced tube degradation related to corrosion phenomena, such as wastage, pitting, intergranular attack, stress corrosion cracking, as well as other mechanically induced phenomena such as denting and wear (Reference 1). The following report is intended to compare the extent of tube degradation occurring within the Indian Point Unit 2 steam generators with that which has occurred in other plants with Model 44 and 51 steam generators.

The report includes an overview of degradation mechanisms occurring in Model 44 and 51 steam generators as a function of time. This involves factoring in the effect of such key parameters as operating temperatures and pressures, manufacturing differences, and secondary side water chemistry. It provides a direct comparison of the extent of the degradation mechanisms occurring in the Indian Point 2 Model 44 steam generators and other Model 44 and 51 steam generators. The reasons for similarities and differences are highlighted. The report also identifies Indian Point Unit 2 licensing basis documents such as NRC generic communications (in the form of Information Notices, Generic Letters, Bulletins) and industry communications such as Westinghouse Communications (Technical Bulletins, Nuclear Safety Advisory Letters, etc.,) and Consolidated Edison's response to these items. Also, a discussion of steam generator replacement history is provided for information purposes.

2.0 Model 44 and 51 Steam Generator Description

2.1 Design Description

The functional requirements of a Model 44 and 51 steam generator are summarized below. A schematic of the Model 44 and 51 steam generators is provided in Figures 2.1.1 and 2.1.2, respectively.

Each loop of the reactor coolant system contains a vertically mounted U-tube steam generator. These generators consist of two integral sections: an evaporator section and a steam drum section. The evaporator section consists of a U-tube heat exchanger while the steam drum section is located in the upper part of the steam generator. The pressure boundary components of the Model 44 and 51 steam generators are designed and manufactured in accordance with applicable portions of Section II, III, and IX of the ASME Code.

High temperature and pressure reactor coolant flows into the channel head, through the Alloy 600 U-tubes, and back to the channel head. A partition plate divides the channel head into inlet and outlet sections. An access opening for inspection and maintenance is provided in each section of the channel head. Welding of the U-tubes to the tubesheet minimizes the potential for leakage across the tubesheet. Some steam generators have tubes that are expanded the full thickness of the tubesheet to minimize the annulus between the outside diameter of the tubes and the tubesheet. The methods of expansion are mechanical rolling and/or Westinghouse explosive tube expansion (WEXTEX). The Indian Point Unit 2 steam generators have received a partial depth roll expansion in the steam generator tubesheet region. The tubes are supported at intervals by horizontal, carbon steel support plates and by anti-vibration bars for the larger radius U-bends.

Feedwater enters the steam generator through a nozzle located on the upper shell and is distributed by a feedwater ring assembly into the downcomer annulus formed by the tube wrapper and steam generator shell. The feedwater mixes with recirculation flow from the moisture separators and enters the tube bundle near the tubesheet. Steam production increases as the bulk water rises in the tube bundle. The two-phase steam/water environment then enters a set of primary moisture separators, located above the tube bundle, removing most of the entrained water from the steam. Second stage steam dryers are employed to produce saturated steam of low moisture content.

Pressure containing parts, with the exception of Inconel tubes, are made of low alloy or carbon steel. Surfaces in contact with the reactor coolant are made of, or are clad with, stainless steel or Inconel. The secondary side internals are constructed of carbon or low alloy steel, stainless or Inconel materials.

Figure 2.1.1 Model 44 Steam Generator

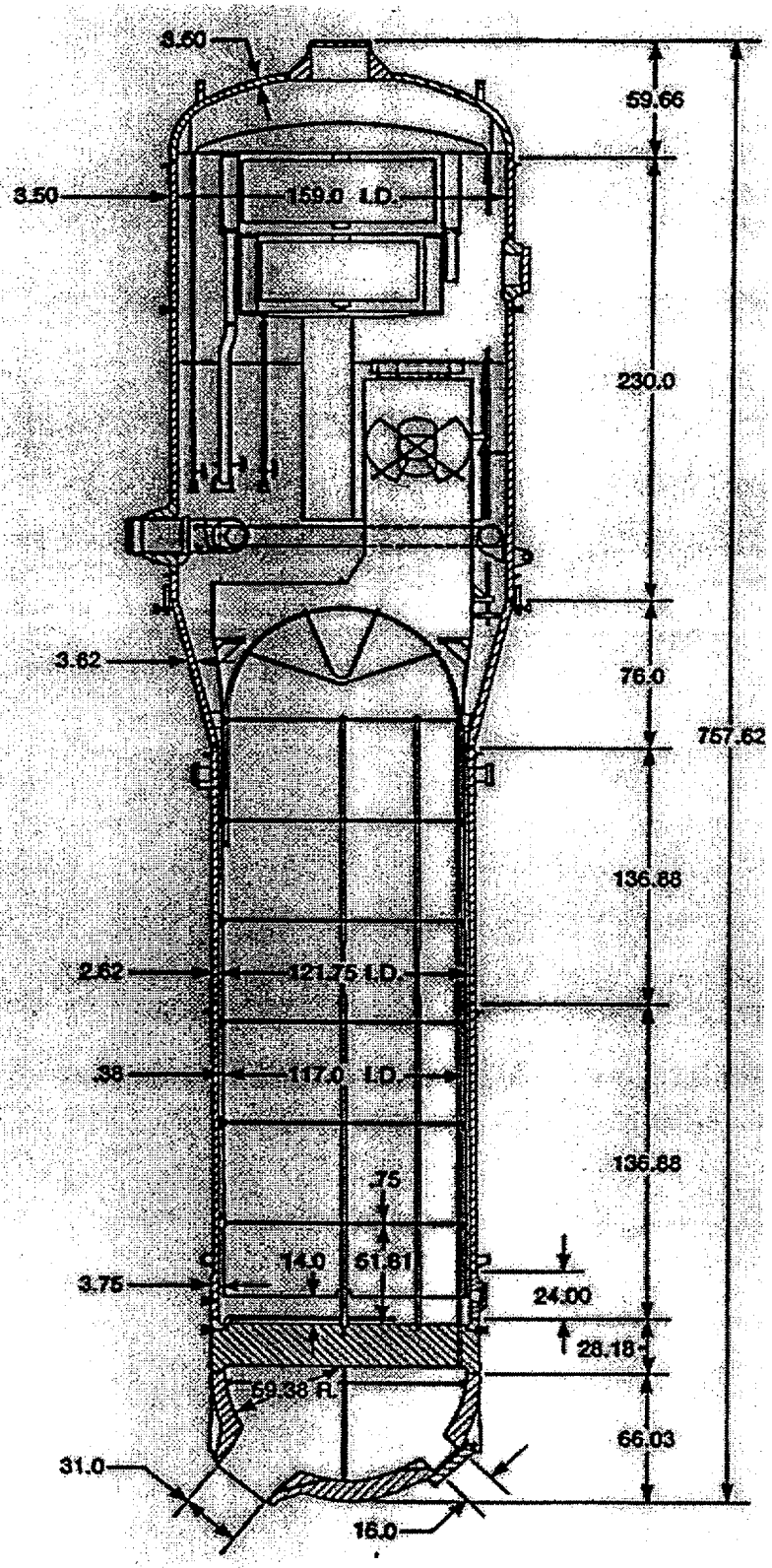

Figure 2.1.2 Model 51 Steam Generator

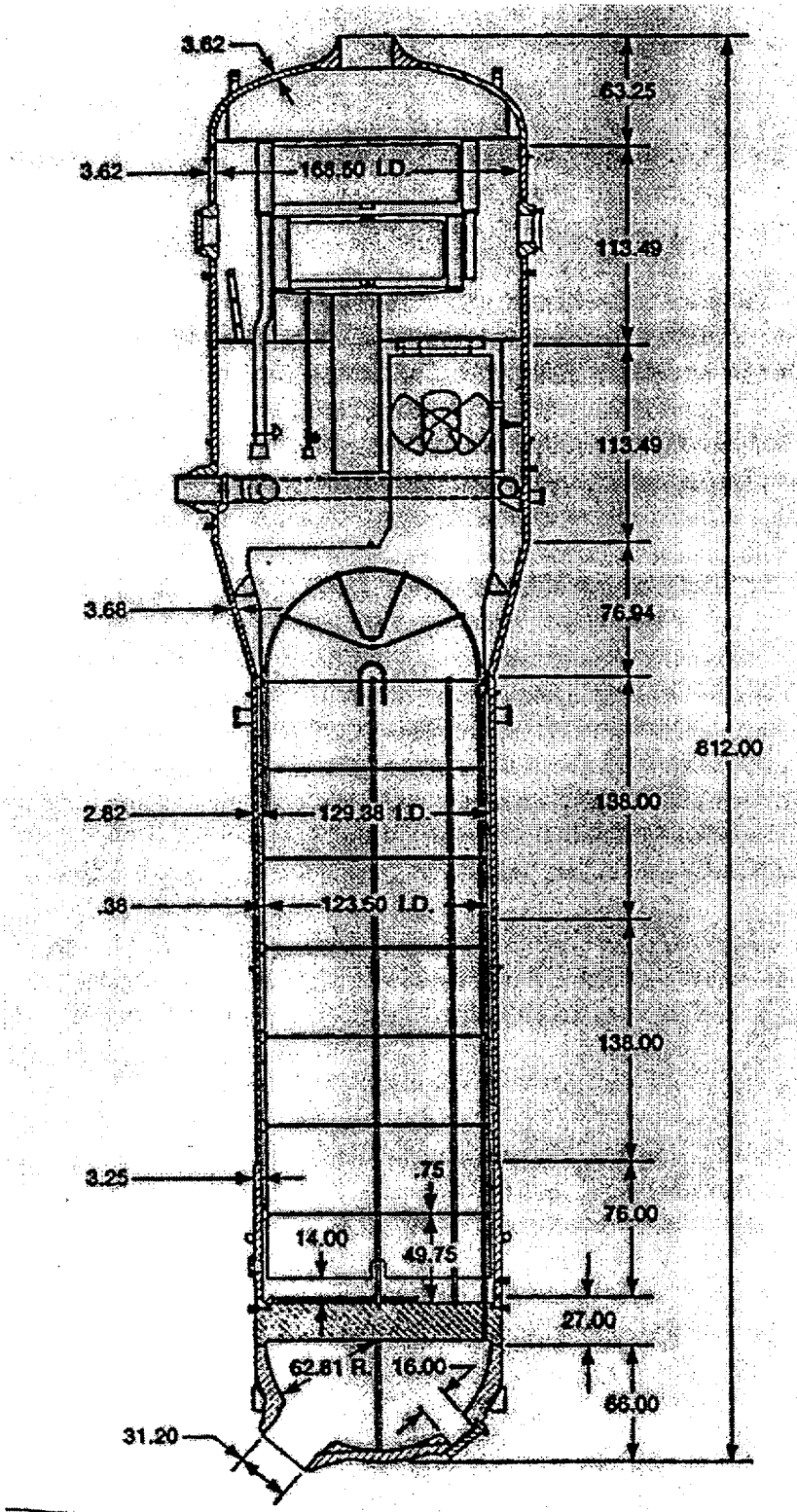

2.2 Typical Operating Parameters (Temperature Range, Chemistry Type)

The majority of plants with Model 44 and 51 steam generators came on line in the 1970's.

T-hot ranges from 587 to 621°F. Primary side pressure ranges from 2000 psia to 2250 psia. Steam side pressure ranges from 700 psia to 889 psia (References 2, 3 and 4).

All Volatile Treatment (AVT) is presently used as the method of secondary side chemistry control at most plants. The specifics of AVT chemistry operation have been the subject of much industry focus and continual refinements have been made in action levels, the specific volatile amine used, the methods and precision of analyses, operation of the water treatment plant, etc. In addition, some plants continue with the application of boric acid addition for additional corrosion control.

Boric acid was qualified for SG secondary side application on a case basis following extensive testing programs, which started in the late 1970's. The testing program showed that boric acid application was effective in reducing denting corrosion (acid chloride mechanism) and also tube support plate (TSP) ODSCC (caustic mechanism). More recently an extensive laboratory and field application program for zinc addition to the primary side of PWR units has been underway. The expected benefits include reduced PWSCC and lower radiation levels due to differences in the characteristics of protective deposits formed in the surface layers of materials such as Alloy 600.

3.0 Model 44 and 51 Steam Generator Tube Integrity Operating Experience Discussion

3.1 Degradation Types

The primary modes of steam generator tube degradation observed to date in Model 44 and 51 steam generators are described below. Degradation refers to any chemical or mechanical mechanism affecting steam generator tube integrity.

Denting: Plastic deformation of tubes resulting from the buildup of carbon steel support plate corrosion products (magnetite) in tube-to-tube support plate annuli.

Denting refers to the squeezing of tubes at support plate or tubesheet intersections caused by corrosion of the carbon steel support plates and tubesheet. The buildup of non-protective corrosion product oxides, consisting mainly of iron oxide (magnetite), leads directly to tube distortion and denting-

induced deformation of the tube support plate flow slots, which may result in U-bend deformation. The tube distortions have resulted in numerous instances of tube leaks caused by stress corrosion cracks, which initiated primarily from the inside surface of the dented tube in the tube support plate region or in the deformed U-bend of tight radius tubes.

Denting was first observed in 1975 when a number of plants changed from phosphate chemistry control to early versions of All Volatile Chemistry (AVT) chemistry control. In some cases, inspection probes could not be passed through the tubes, which indicated significant tube distortion.

In most cases, the corrosion mechanism occurs as an acid chloride environment that is related to the secondary side chemistry operation. Refinements in AVT chemistry, and the addition of boric acid as an inhibitor for the acid chloride mechanism, have reduced the onset and propagation of TSP denting corrosion in steam generators with ordinary carbon steel support structures (either grid or TSP).

Primary Water Stress Corrosion Cracking (PWSCC): PWSCC is an intergranular mechanism requiring at least the following conditions to be present:

- High applied or residual tensile stress or both (near the yield strength),
- A corrosive environment (high temperature water)
- Susceptible tubing microstructure

PWSCC occurs at locations on the inside surfaces of steam generator tubing with high residual stresses. These locations are primarily the expansion-transition regions in the tubesheets, the U-bend regions of the tubing inner rows, and any dent locations at the tube support plate, tubesheet or sludge pile. Under given conditions, the initiation of PWSCC increases with increasing temperature.

The denting process contributes to PWSCC in at least two ways. First, the deformation caused by denting results in increased stress levels at the subject locations. These locations are principally the TSP and also the tight radius U-bends, if significant hourglassing of the flow slots has occurred. Second, laboratory testing has shown that Alloy 600 materials will experience faster cracking rates if deformation occurs at operational temperatures.

In addition to stopping the denting corrosion, corrective field application measures for the PWSCC mechanism include reducing system temperature, stress reduction (e.g. peening and thermal stress relief) and the application of zinc to the primary system water chemistry.

Outer Diameter Initiated Stress Corrosion Cracking (ODSCC): ODSCC is a degradation mechanism that includes both intergranular stress corrosion

cracking (IGSCC) and intergranular attack (IGA) on the outside surfaces of tubing. IGSCC requires the same three general conditions as PWSCC. IGA is similar but unlike IGSCC, it can occur without large tensile stresses present. The cracks caused by IGSCC can be single cracks or networks of multiple cracks. IGA may be a precursor to IGSCC. Most outside diameter stress corrosion cracks are oriented in the axial direction, however, significant circumferential cracking has been observed in the expansion transition region of the tubing in some steam generators and is sometimes found near dents. ODSCC strongly depends on the presence of impurities, or contaminants, in the secondary side bulk water. Although these contaminants may be present in apparently low concentrations (ppb), localized thermal and hydraulic conditions in flow restricted regions (such as crevices or sludge piles) may increase concentrations to the percent levels by the physical process of boiling point elevation.

Corrective measures for ODSCC in operating units have included: improvements in AVT chemistry control, reduced temperatures, removal attempts of extant in-generator corrodents through soaking or chemical cleaning, deposit removal through sludge lancing or chemical cleaning, application of inhibitors such as boric acid and removal of synergistic corrosion mechanism materials, such as copper alloys.

Fatigue is material failure resulting from the initiation of cracks and/or the propagation because of cyclic loads. Mechanistically, some of the more significant SG tubing fatigue occurrences have been related to denting at the TSP. In the dented condition the tubes became 'fixed' at the tube support plates and, if the loading conditions on the tubing are appropriate, the tightly clamped TSP location becomes the 'hinge point' for the initiation of fatigue cracking. In some cases, the mechanism for fatigue cracking has been evaluated and preventive actions have been applied as in analyses related to NRC Bulletin 88-02.

Fretting: The loss of tube material caused by excessive rubbing of the tube against its support structure. This can be caused by either primary side or secondary side flow-induced vibration of the tubes.

Pitting: Localized attack on tubing resulting from non-uniform corrosion rates caused by the formation of corrosion cells. It is promoted mainly by the presence of chloride, and possibly sulfate, acids. Oxidizing conditions and the presence of copper species are probable accelerators. Pitting is not specifically related to operational temperature and often it is more prevalent on the cold leg side. Pitting rates may also be substantial at room temperature, if the chemistry conditions are appropriate.

Wastage: A localized secondary side corrosion of mill annealed Alloy 600 caused by chemical attack from acid phosphate residues concentrated in low flow areas

3.2 Forced Outages

Based on a review of NUREG/CR-6365 (INEL-95/0383), "Steam Generator Tube Failures", 5/15/96 (Reference 1), there have been a total of 10 "larger leakage event" forced outages at plants with Westinghouse Model 44 and 51 SGs. The approximate number of tube leak outage events in Model 44 steam generators is 62 (References 2, 3 and 4). A timeline of the occurrence of the more significant leakage is included in Figure 3.2.1 (the others are illustrated in Figures 4.1.1 and 4.1.2). The amount of leakage in the more significant events varied from 21 gal/hr to 760 gpm. The root causes of the larger leakage events in both the Model 44 and 51 steam generators have been: wastage (1), U-bend PWSCC (3), Loose Parts Wear (3), and High Cycle Fatigue (3). The root causes of the larger leakage in Model 44 steam generators have been: wastage (1), U-bend cracking (2), loose part wear (1), high cycle fatigue (2).

Figure 3.2.1
Model 44 and 51 Steam Generator Primary-Secondary Side Leakage

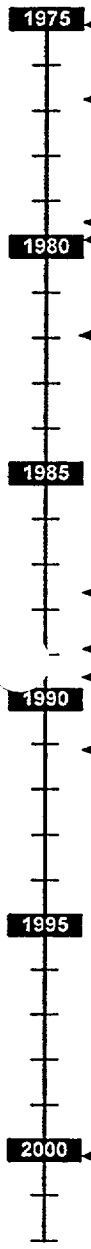

Plant	SG Model	Date	Leak Rate, gpm	Degradation
Point Beach 1	W44	2/26/75	125	Wastage - Sludge Pile
Surry 2	W51	9/15/76	330	PWSCC RIC7 U-Bend Apex
Doel 2	ACE-44	6/25/79	135	PWSCC RIC24 - U-bend PWSCC
Prairie Island 1	W51	10/2/79	336	Loose Part Wear
Ginna	W44	1/25/82	760	Loose Part Wear
North Anna 1	51	7/15/87	637	High Cycle Fatigue
Indian Point 3	44	10/19/88	120 gph	High Cycle Fatigue
Beaver Valley 2	51	6/21/89	21 gph	Loose Part - R31C16
Mihama 2	MHI-44	2/9/91	700	High Cycle Fatigue
Indian Point 2	W44	2/15/00	146	PWSCC - R2C5 U-bend Apex PWSCC

3.3 Regulatory/Westinghouse Generic Communications

There have been several generic communications from both Westinghouse and the NRC staff as a result of steam generator degradation mechanisms. A timeline of the topics addressed by both Westinghouse and the NRC staff is provided in Figure 3.3.1.

The NRC communications (since 1979) concerning tube integrity issues in the form of Information Notices, Generic Letters, and Bulletins are listed below. A majority of the communications from the NRC staff have been in the form of Information Notices which do not require any action by the utility. Topics range from: SG Tube Ruptures at two plants, loose parts in the secondary side of steam generators, intergranular attack leading to tube failure; detection and monitoring of sudden increase in steam generator primary-to-secondary leakage, stress corrosion cracking in steam generators tubes and results of steam generator tube examinations. Topics that required a response from utilities have been limited to: rapidly propagating cracks in steam generator tubes, circumferential cracking of steam generator tubes, and steam generator tube inspection techniques.

Westinghouse communications concerning steam generator tube integrity issues included the following topics: the occurrence of denting in steam generator tubes, localized steam generator tube diameter reductions, steam generator tube support plate cracking, steam generator sludge, PWSCC information meeting, fatigue cracking of steam generator tubes, eddy current detection of OD SCC (TSP elevation and free span cracking), tube deformation during a postulated LOCA + SSE event, and SG design ΔP change).

In addition to the written communications and the PWSCC Information Meeting mentioned above, there have been numerous symposia and workshops organized by Westinghouse for owners of Westinghouse plants. Some of these focused entirely or largely on steam generator issues and included presentations and discussion from utility personnel. The industry funded programs that were administered by the EPRI SGOG (Steam Generator Owners Group) and its successor organizations, and also sponsored many generalized and specialized meetings and programs related to steam generator issues.

Figure 3.3.1
Generic Communications Affecting Model 44 and 51 Steam Generators

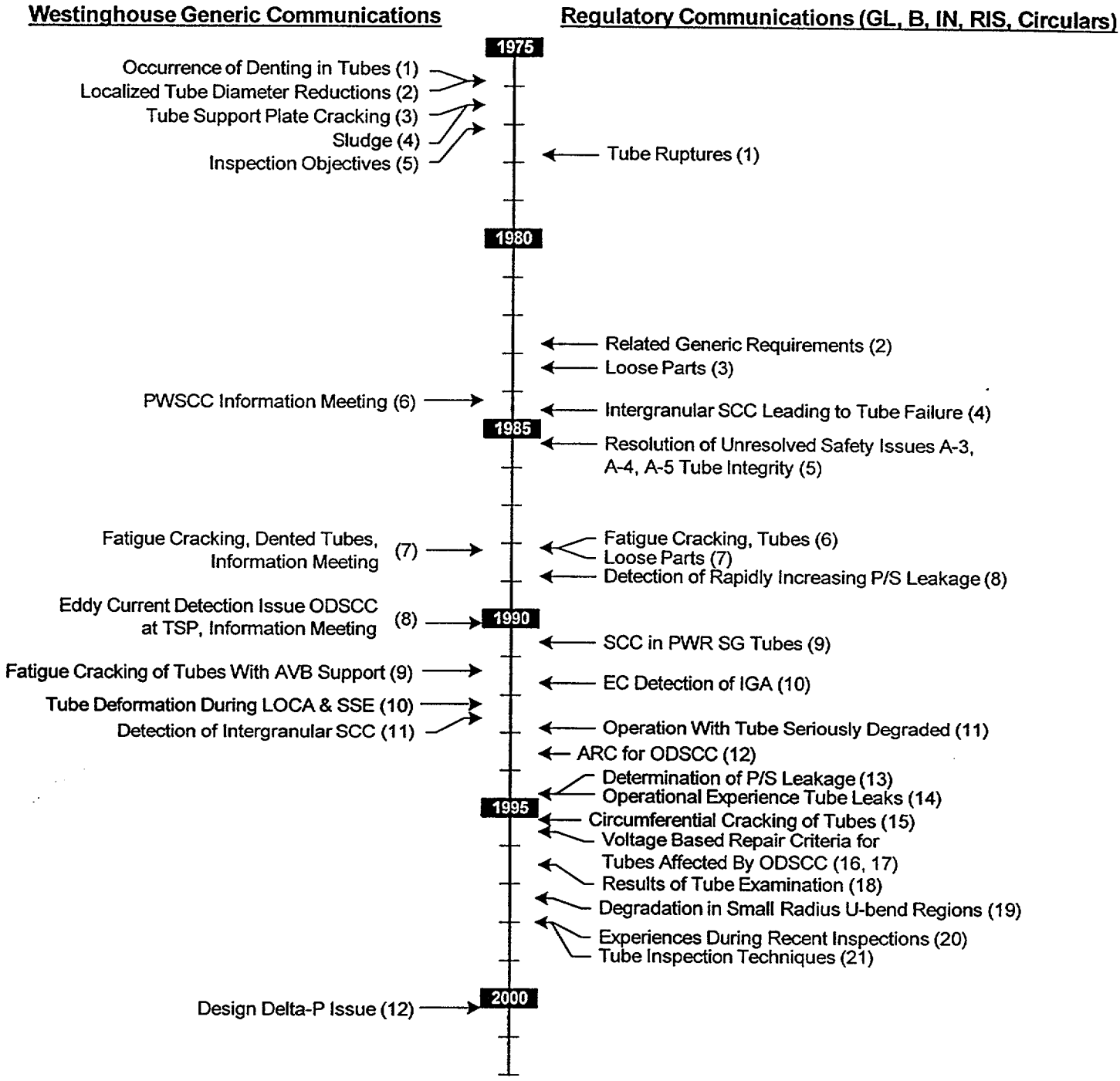

NRC GENERIC COMMUNICATION REFERENCES (FIGURE 3.3.1)

1. NRC Information Notice 79-27, "SG Tube Ruptures At Two PWR Plants", 11/16/71
2. NRC Generic Letter 82-32, "Potential SG Related Generic Requirements", 9/23/82
3. NRC Information Notice 83-24, "Loose Parts In The Secondary Side of SG's at PWRs", 4/28/83
4. NRC Information Notice 84-49, "Intergranular Stress Corrosion Cracking – Leading To SG Tube Failure", 6/18/84
5. NRC Generic Letter 85-02, "Staff Recommended Actions Stemming From NRC Integrated Program For The Resolution of Unresolved Safety Issues A-3, A-4, and A-5 Regarding SG Tube Integrity, 4/17/85
6. NRC Bulletin 88-02, "Rapidly Propagating Fatigue Cracks In Steam Generator Tubes", 2/5/88
7. NRC Information Notice 88-06, "Foreign Objects In SG's", 2/29/88
8. NRC Information Notice 88-99, "Detection and Monitoring of Sudden and/or Rapidly Increasing P/S Leakage", 12/20/88
9. NRC Information Notice 90-49, "Stress Corrosion Cracking in PWR SG Tubes", 8/6/90
10. NRC Information Notice 91-67, "Problems with the Reliable Detection Of Intergranular Stress Corrosion Cracking of SG Tubing", 10/21/91
11. NRC Information Notice 92-80, "Operation With SG Tubes Seriously Degraded", 12/7/92
12. NRC Information Notice 93-52, "Draft NUREG-1477, 'Voltage-Based Interim Plugging Criteria For SG Tubes'", 7/14/93
13. NRC Information Notice 94-43, "Determination of P/S SG Leak Rate", 6/10/94
14. NRC Information Notice 94-62, "Operational Experience on SG Tube Leaks and Tube Ruptures", 8/30/94
15. NRC Generic Letter 95-03, "Circumferential Cracking of SG Tubes", 4/28/95
16. NRC Generic Letter 95-05, "Voltage-Based Repair Criteria for Westinghouse SG Tubes Affected By ODSCC", 8/3/95
17. NRC Information Notice 95-40, "Supplemental Information to GL 95-03, Circumferential Cracking of SG Tubes", 9/20/95
18. NRC Information Notice 96-38, "Results of SG Tube Examination", 6/21/96
19. NRC Information Notice 97-26, "Degradation in Small Radius U-Bend Cracking In SG Tubes", 5/19/97
20. NRC Information Notice 97-88, "Experiences During Recent SG Inspections", 12/16/97
21. NRC Generic Letter 97-05, "Steam Generator Tube Inspection Techniques", 12/17/97

WESTINGHOUSE CUSTOMER COMMUNICATION REFERENCES (FIGURE 3.3.1)

1.	TB No. 75-12	10/15/75	Occurrence of Denting in SG Tubes
2.	TB No. 75-16	11/17/75	Localized SG Tube Diameter Reductions
3.	TB No. 76-06	5/14/76	SG Tube Support Plate Cracking
4.	TB No. 76-07	6/23/76	Steam Generator Sludge
5.	TB No. 77-04	2/25/77	SG Inspection Objectives
6.	PWSCC	1985	Informational Meeting
7.	Fatigue Cracking	10/87	Informational Meeting
8.	OD SCC	2/90	Informational Meeting
9.	ET-NSL-MFSL-91-286	8/30/91	Fatigue Cracking of SG Tubes with Support
10.	ET-NSL-MFSL-92-001	4/20/92	SG Tube Deformation
11.	NSAL-92-001	7/20/92	Detection of Intergranular SCC
12.	NSAL-00-007	5/5/00	SG Design Delta-P Issue

4.0 Operating Experience Comparison Considerations

The objective of this section is to offer a summary comparison of the experience of Indian Point 2 with other Model 44, and also Model 51, steam generators at other units. The scope of this comparison is limited to the steam generators actually manufactured by Westinghouse, as listed in Table 4.1.

This table shows that Westinghouse shipped twenty-three (23) Model 44 steam generators for operation at eight plants. These steam generators were manufactured beginning in the 1960's. The Model 44 designation indicated that there was approximately 44,000 square feet of heat transfer surface in the steam generator. Similarly, the Model 51 steam generators contained approximately 51,000 square feet of heat transfer surface and were also manufactured starting in the 1960's.

Many of the design features of the two models are similar. For example, both models were manufactured using Alloy 600 mill-annealed tubing that was supported by drilled hole tube support plates made of carbon steel. In this sense, it appears straightforward to offer a comparison among steam generators. Many details were changed, however, due to evolutionary design modifications that were intended to improve operational performance. For example, the earlier units were made with partially rolled tubes in the tube sheet.

This resulted in a nearly full tubesheet thickness crevice that later was shown to be a site for possible concentration of secondary side contaminants. Efforts to eliminate this crevice resulted in some units with explosive expansion (WEXTEX) that was applied to convert from partial to full depth expansion. Mechanical expansion, by step rolling throughout the tubesheet region, was applied in the factory and, subsequent to that, hydraulic expansion was applied in the Model F design. Such details of manufacturing make a simple comparison of the operating performance difficult. All of the original Model 44 steam generators were made with the partial roll resulting in the full depth crevice, but the Model 51 steam generators represent all three manufacturing modes; partial, WEXTEX and full depth.

Even tubing performance may exhibit subtle to significant differences depending on the manufacturing process. Tubing was supplied by a number of different vendors and the details of processing influenced the microstructure and subsequently the corrosion performance of the final product. This became clarified by extensive research into tube material processing during the qualification of thermally treated Alloy 600 (A600TT). The process specifications were changed to cause preferential carbide precipitation at the grain boundaries in the final tubing product. Corrosion testing established that this improved the corrosion resistance to both PWSCC and ODSCC and the process changes were incorporated into manufacturing and design depending on customer preferences and the design of new models. The same is true for A690TT material, which is included in some of the replacement steam generators for the original Model 44 and Model 51 units.

Operational chemistry is also of paramount importance, particularly with respect to secondary side corrosion phenomena such as thinning (or wastage), denting, pitting, and ODSCC. The evolution of water chemistry control, from the initial operation to present day experience, continues to be refined, resulting in higher levels of water purity. The early operation with phosphate chemistry was successful in providing a buffer to moderate the formation of excessively acidic or alkaline environments, but it was not as benign as originally accepted and soon resulted in a wastage phenomenon that produced tube wall thinning.

Following the change from phosphate chemistry, the implementation of AVT was itself evolutionary. Condenser leakage, resulting in both air and water contaminant ingress, was not well controlled on the switchover and high contaminant levels soon led to unusual and unexpected forms of corrosion, such as denting. Many development programs and much industry effort focused on the issue of operational chemistry and many laboratory and field programs were applied through the late 70's and 80's. Some key findings of these programs were the synergistic effect between copper oxides and chlorides to accelerate denting corrosion, the influence of copper oxides and alkaline species (NaOH) to accelerate ODSCC, the role of boric acid in mitigating both denting and ODSCC corrosion, and the benefit of lower contaminant levels. Many special laboratory

and field programs, such as molar ratio control and monitoring of denting produced hydrogen, were evaluated and implemented in the field. Obviously these innovations influenced the corrosion results and some plants more than others, depending on plant condition and the details of application.

Innumerable additional factors influence the corrosion performance of a particular unit. Seawater or brackish water ingress will generally hydrolyze to produce acid chloride environments, while fresh water ingress will generally result in alkaline environments. Thus seawater plants may be experiencing greater denting, and or pitting, while fresh water plants experience greater ODSCC or IGA. As water chemistry control improved, and contaminant water ingress from condenser in-leakage diminished, the details of the steam generator chemistry were dominated by the quality and control of the water make-up plant. For example, condensate polisher resin ingress, the purity of added chemicals and a rapid reaction to condenser in-leakage became even more significant.

These factors are important considerations in any detailed discussion and are mentioned here to indicate the potential complexity of a detailed evaluation and comparison among steam generators.

Table 4.1. Model 44 and Model 51 Steam Generators of Westinghouse Manufacture

		First	Last			Original Steam Generators						Replacement/Status					
PLANT	Alpha	Shipped	Shipped	ORIGINAL UTILITY	COUNTRY	Crit	Mfgr	Model	SGs	Tubing	HT	SGR	ship start	ship end	Year	Alloy	Mfgr.
Ginna	RGE	Lester HTD		Rochester Gas & Electric Corp.	US	1969	W	44	2	600	MA	Y			1996	690	BWI
Robinson 2	CPL	Lester HTD		Carolina Power and Light	US	1970	W	44	3	600	MA	Y	12/1/83	12/1/83	1985	600TT	W
Point Beach 1	WEP	9/1/83	9/1/83	Wisconsin Electric Power Co	US	1970	W	44	2	600	MA	Y			1984	600TT	W
Turkey Point 3	FPL	D-68	D-68	Florida Power & Light	US	1972	W	44	3	600	MA	Y	12/29/79	2/15/80	1982	600TT	W
Point Beach 2	WIS	Lester HTD		Wisconsin Electric Power Co	US	1972	W	44	2	600	MA	Y			1998	690	W
Turkey Point 4	FLA	J-70	J-70	Florida Power & Light	US	1973	W	44	3	600	MA	Y	6/20/79	6/20/79	1983	600TT	W
Indian Point 2	IPP	Lester HTD		Consolidated Edison	US	1973	W	44	4	600	MA	P	12/16/87	12/23/87		600TT	W
Indian Point 3	INT	Lester HTD		NYPA	US	1976	W	44	4	600	MA	Y	12/1/88	12/1/88	1989	690	W
Surry 1	VPA	9/16/69	11/1/69	Virginia Electric & Power Co	US	1972	W	51	3	600	MA	Y	2/15/79	10/21/79	1981	600TT	W
Zion 2	COM	7/8/71	8/4/71	Commonwealth Edison	US	1973	W	51	4	600	MA						CLOSED
Zion 1	CWE	7/16/70	9/3/70	Commonwealth Edison	US	1973	W	51	4	600	MA						CLOSED
Prairie Island 1	NSP	8/28/70	8/28/70	Northern States Power Co	US	1973	W	51	2	600	MA						
Surry 2	VIR	6/29/70	12/3/70	Virginia Electric & Power Co	US	1973	W	51	3	600	MA	Y	12/27/78	2/15/79	1980	600TT	W
Prairie Island 2	NRP	7/12/71	7/12/71	Northern States Power Co	US	1974	W	51	2	600	MA						
Takahama 1	TAK	8/16/72	8/31/72	Kansai Electric Power Co.	Japan	1974	W	51	3	600	MA	Y			1996	690	MHI
Kewaunee	WPS	9/24/70	9/24/70	Wisconsin Public Service Corp.	US	1974	W	51	2	600	MA	P				690	Ansaldo
Cook 1	AEP	10/8/70	10/20/70	Indiana & Michigan Electric Co	US	1975	W	51	4	600	MA	P				690	BWI
Beaver Valley 1	DLW	5/6/71	5/21/71	Duquesne Light Co	US	1976	W	51	3	600	MA						
Salem 1	PSE	3/21/70	6/2/71	Public Service Electric & Gas Co	US	1976	W	51	4	600	MA	Y			1998	600TT	W
Farley 1	ALA	9/12/72	10/12/72	Alabama Power	US	1977	W	51	3	600	MA	P			2000	690	W
Cook 2	AMP	4/18/72	5/22/72	Indiana & Michigan Electric Co	US	1978	W	51	4	600	MA	Y	6/24/88	7/8/88	1989	690	W
Kori 1	KOR	12/20/73	12/20/73	Korea Electric Power Corporation	Korea	1978	W	51	2	600	MA	Y			1998	690	W/Hanj
North Anna 1	VRA	1/5/72	1/26/72	Virginia Electric & Power Co	US	1978	W	51	3	600	MA	Y			1993	690	W
Salem 2	PNJ	5/12/70	6/2/71	Public Service Electric & Gas Co	US	1980	W	51	4	600	MA						
Sequoyah 1	TVA	9/11/71	11/23/71	Tennessee Valley Authority	US	1980	W	51	4	600	MA						
North Anna 2	VGB	2/20/73	5/18/73	Virginia Electric & Power Co	US	1980	W	51	3	600	MA	Y			1996	690	W
Farley 2	APR	6/22/74	8/7/74	Alabama Power	US	1981	W	51	3	600	MA	P			2001	690	W
Sequoyah 2	TEN	10/5/71	11/23/71	Tennessee Valley Authority	US	1981	W	51	4	600	MA						
Diablo Canyon 1	PGE	5/29/70	5/29/70	Pacific Gas & Electric Co.	US	1984	W	51	4	600	MA						
Diablo Canyon 2	PEG	11/2/72	11/2/72	Pacific Gas & Electric Co.	US	1985	W	51	4	600	MA						
Trojan	POR	6/27/72	7/18/72	Portland General Electric Co	US	1975	W	51A	4	600	MA						CLOSED
Ohi 1	OHI	4/6/73	5/10/73	Kansai Electric Power Co.	Japan	1977	W	51A	4	600	MA	Y			1995	690	MHI
Ringhals 2	SSP	4/5/72	4/5/72	Swedish State Power Board	Sweden	1974	W	51C	3	600	MA	Y			1989	690	KWU
Beaver Valley 2	DMW	10/25/78	10/25/78	Duquesne Light Co	US	1987	W	51M	3	600	MA						

4.1 Comparison Among Steam Generators at Different Plants

The plants with Westinghouse Model 44 steam generators are listed in Figure 4.1.1. In this figure, for example, the Ginna plant is identified by name in the first row. The steam generator outline symbols show that the plant contains two loops and produces 470 MWE, which represents an equivalent output of 235 MWE per steam generator. Higher values here would be consistent with higher temperatures and/or higher mass throughput, which may both influence the corrosion rate depending on plant specific conditions. The letter at the steam generator symbol represents the tubing vendor. All of the Model 44 steam generators listed had tubing supplied by Huntington, as symbolized by the 'H'.

The next entry in the row is the operational T-hot of the plant. If the plant has replaced steam generators, the entry immediately below represents the T-hot in the replacement. In the example of Ginna, the original T-hot of 601^{0}F was reduced to 589^{0}F following SG replacement.

Next is a time line, which indicates the year of initial plant operation in calendar time with the value for the effective full power years superimposed. For Ginna this value is 18.9 EFPY, until the steam generators were replaced in 1996. The time line continues on a lower level for the replacement unit, which for Ginna is manufactured with A690TT tubing. The circles imposed on the time line represent the six tube leak outages at Ginna. Also indicated below the time line is the first occurrence of sleeving at Ginna, which occurred in 1980.

At the far right, a pie chart indicates that 46% of the tubes at Ginna have been either plugged or sleeved. The major cause of this was stress corrosion cracking, with a variety of other lesser causes.

With this background in the content of Figure 4.1.1, it can be seen that the plant with the lowest operating temperature (Thot) of all of these Model 44 steam generators was Indian Point 2. The Thot history for Indian Point Unit 2 is (Reference 8):

5/22/73 to 6/25/75	-	593.5°F
6/25/75 to 2/28/77		581.5 °F
2/28/77 to 6/23/90		576°F
6/23/90 to 7/12/91		586.5 °F
7/12/91 to Present		589 °F

Indian Point 2 was also the first of only two plants to add boric acid, which had been established in laboratory testing to be an effective moderator of denting corrosion. It can further be seen that Indian Point 2 has had next to the fewest number of tube leak outages (including the year 2000 outage). It has the least number of tubes repaired, especially considering that row 1 tubes were

preventively plugged prior to operation because of primary side cladding manufacturing concerns.

Of the listed plants, Ginna, Robinson 2, Point Beach 1 and Point Beach 2 are fresh water plants. Note that the major modes of degradation at these plants was ODSCC. Turkey Point 3 and Turkey Point 4 are seawater cooled and both Indian Point plants are brackish water cooled. Both seawater and brackish water are acid forming. The Turkey Point plants were extensively dented and had many forced outages due to tube leaks, in comparison to the Indian Point 2 and Indian Point 3 plants. This is believed to be due to different water chemistry considerations and the timely addition of boric acid, which was intended to reduce denting rates. None of the Model 44 units experienced early apex cracking such as that experienced by Surry 2 (Model 51) in 1976.

As a final general factor relating to comparisons of degradation between units and over time consider the very important issue of the 'inspection transient'. This term is applied to the change in eddy current NDE reporting as a result of a step change having to do with the inspection and not representative of an actual corresponding change in the unit itself.

Inspection transients occur from two major causes. One of these is the application of a new sensitive probe, for example a surface riding probe in lieu of a bobbin probe in the tube expansion transition region. The new probe could identify degradation that may have accumulated over a number of different outages and this cumulative degradation may inappropriately be considered to have occurred only in the last cycle of operation, for example. The second cause is a change in the manner in which repeat data are analyzed. In this situation, for example, a surface riding probe may have been used for multiple outages but new criteria are given to the analysts. A lower threshold for signal calling will result in an increased number of indications reported; once again not necessarily related to the actual rate of degradation occurring in the field.

Figure 4.1.2 offers an overview of the Model 51 steam generator experience for the 26 plants with Westinghouse manufactured steam generators. The format of the table is similar to Figure 4.1.1 for the Model 44 steam generators. The letter designation below the steam generator indicates a 'W' for tubing of Westinghouse Blairsville manufacture and an 'H' if the tubing was supplied by Inco's Huntington mill. Among the earlier of the operational Model 51 steam generators were those at Surry 1 and Surry 2 which experienced numerous outages due to leakage resulting from denting in a manner similar to that occurring at the Turkey Point 3 and 4 units. More than half of the SG tube leak outages resulted from leakage in just four plants and most of these events occurred prior to 1985. Approximately 50% of the original Model 51 steam generators have been replaced. Many of the remaining steam generators have a relatively small percentage of tubes that have required plugging or sleeving.

Figure 4.1-1 - Overview of Westinghouse Model 44 Operating Experience

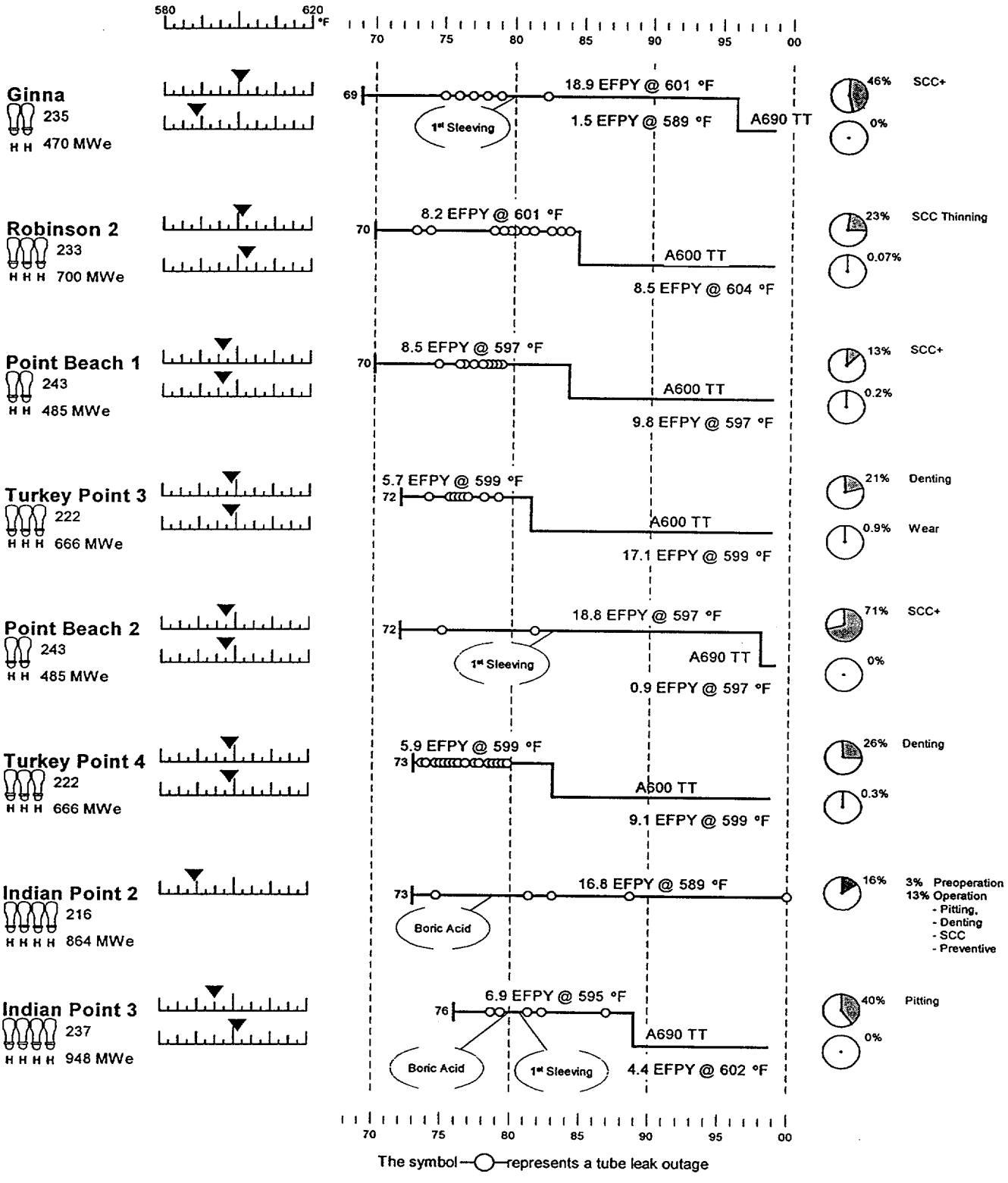

Figure 4.1-2 - Overview of Model 51 Operating Experience

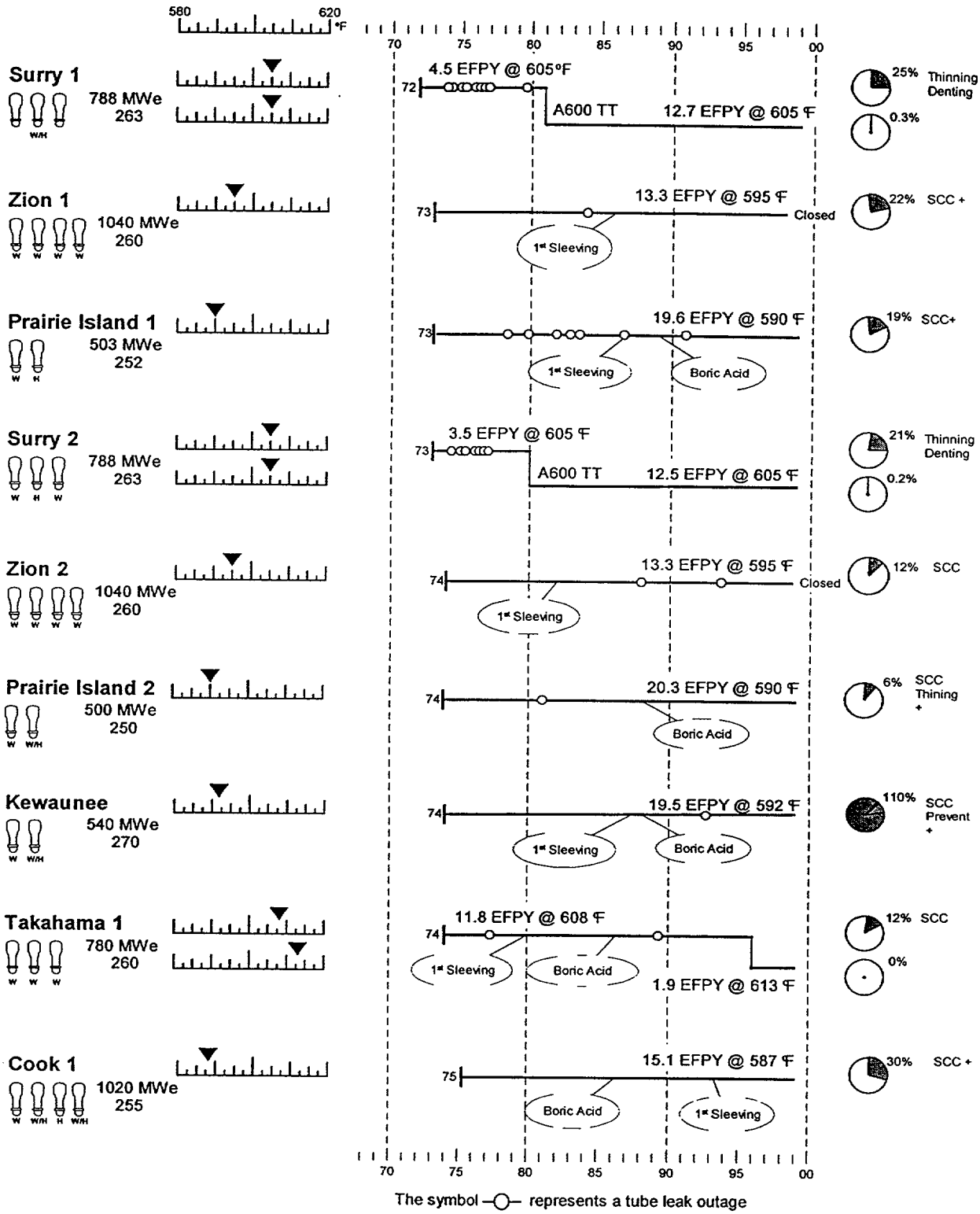

Figure 4.1-2 - Overview of Model 51 Operating Experience (continued)

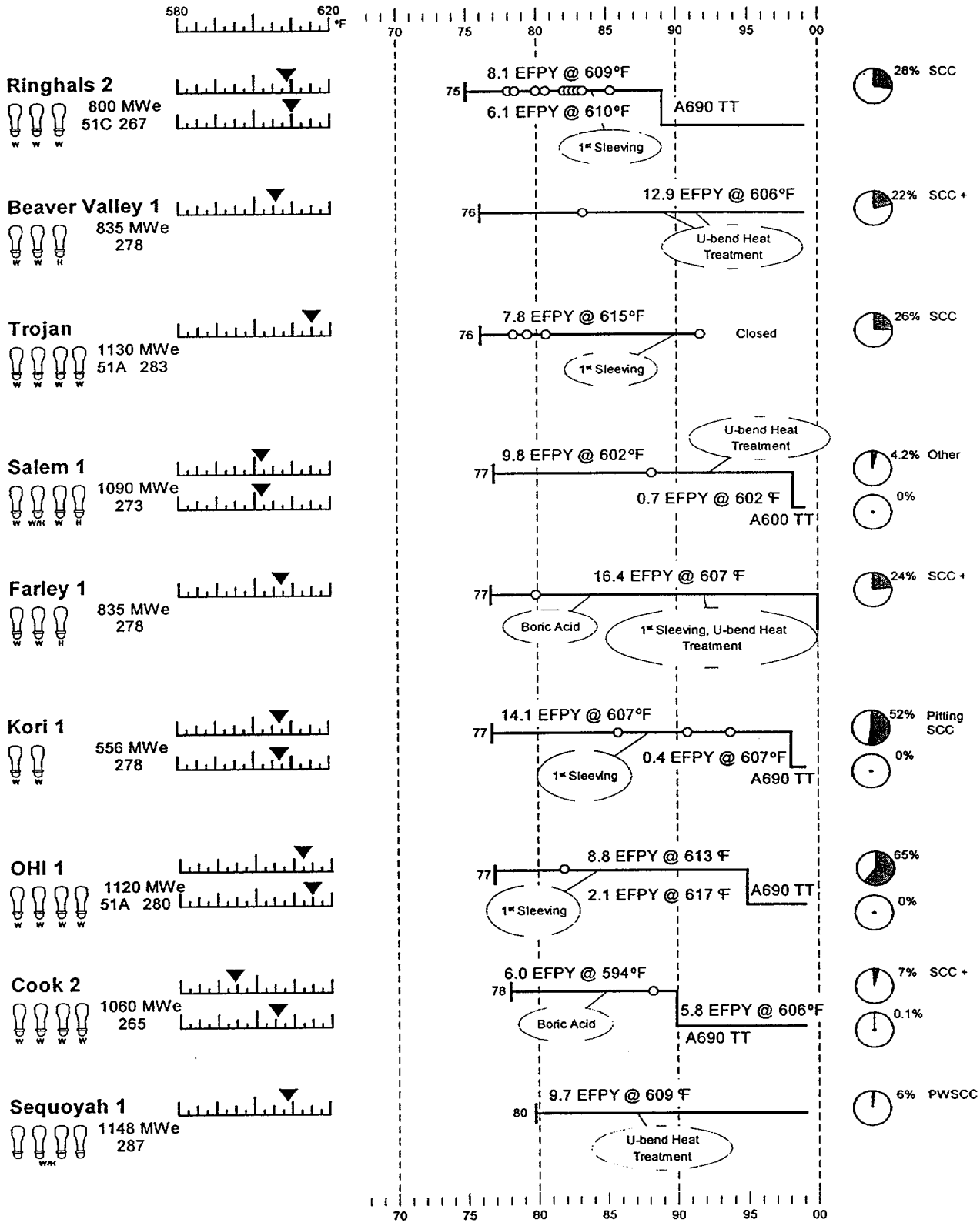

Figure 4.1-2 - Overview of Model 51 Operating Experience (continue)

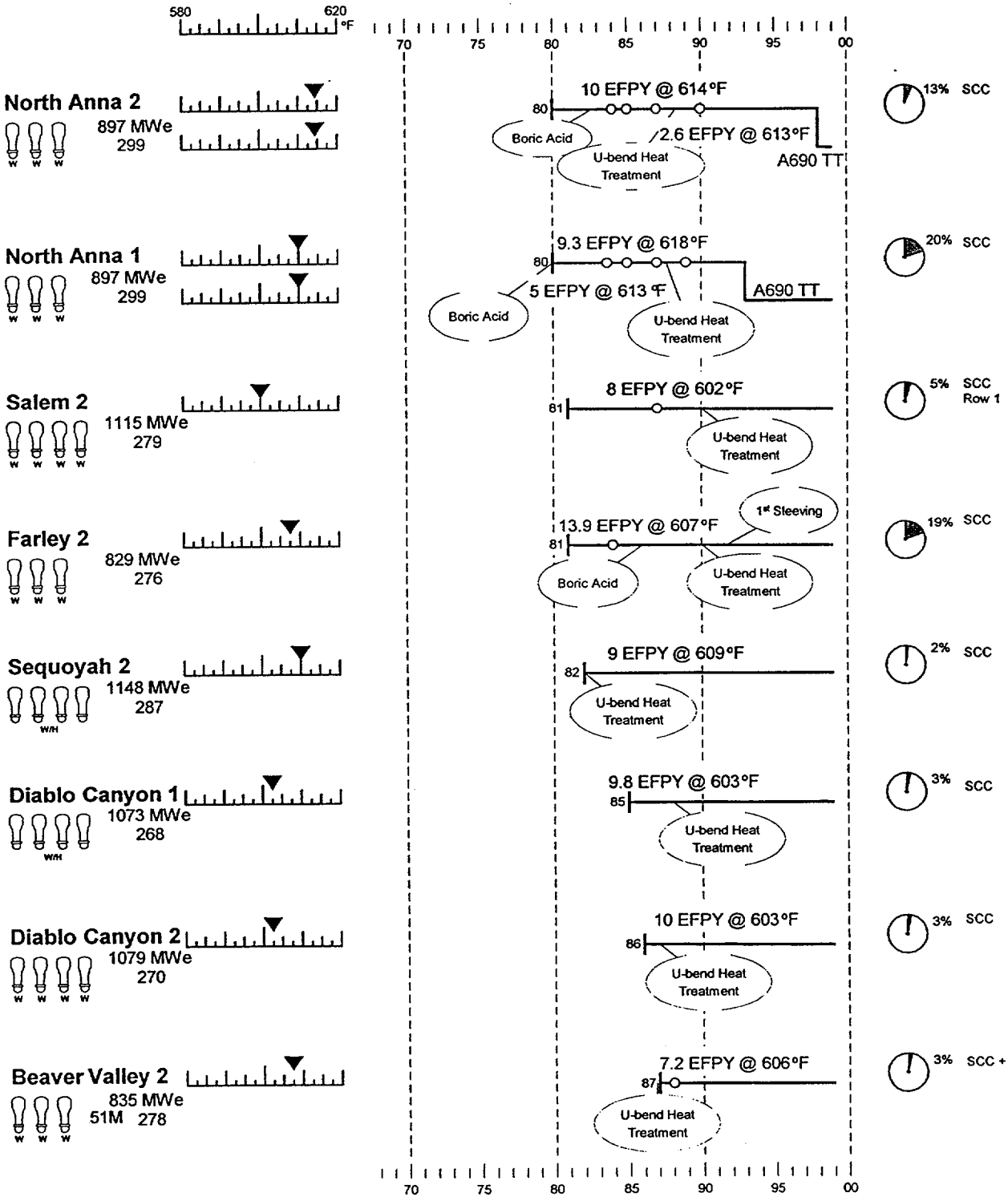

4.2 IP2 Response to Regulatory/Westinghouse Communications

Based on a summary of degradation found during 2R14 eddy current inspection, the degradation mechanisms occurring in the steam generator tubes at Indian Point Unit 2 can be prioritized based on frequency of occurrence as follows (Reference 5):

Tubesheet PWSCC
Tubesheet ODSCC
Above Tubesheet ODSCC
Pitting
Cecco Probe Indications at TSPs (SPIs)
Free Span PI Indications

This listing is consistent with the tube degradation mechanisms occurring in all Model 44 and 51 steam generators with the exception of the lack of occurrence of PWSCC or outer diameter initiated stress corrosion cracking at the tube support plate elevations. Based on a review of Figures 4.1.1 and 4.1.2, one possible explanation may be the addition of boric acid in the secondary side of the steam generators since 1978. Indian Point Unit 2 is the only brackish water site in operation that has added boric acid to the secondary water chemistry to minimize the occurrence of denting. The timing of the addition of boric acid, and the lower Thot of 589°F, represents a difference between the Indian Point Unit 2 steam generators and steam generators at other plants (fresh water or brackish water sites) that have experienced relatively extensive ODSCC or significant PWSCC at the tube support plate elevations.

Consolidated Edison has taken several actions to address NRC/Westinghouse generic communications as they affect the Indian Point Unit 2 steam generators:

1. As noted above, boric acid was added to the secondary water at Indian Point Unit 2 (1978) to control denting and the occurrence of IGA/SCC.

2. An alternate steam generator tube plugging criterion, an F* criteria, was implemented to address the occurrence of PWSCC within the hardroll region of the steam generators (via BAW-10195A).

3. In response to GL 88-02, the steam generator tubing at Indian Point Unit 2 was evaluated for susceptibility to fatigue-induced cracking of the type experienced at North Anna Unit 1 in July 1987. No modification, other than the preventive plugging of two tubes in steam generator 21 was required.

4. A series of 50.59 evaluations have been completed to address the safety significance of the presence of secondary side loose objects in steam

generators 21, 22, 23 and 24. The latest evaluation is SECL-00-058, Rev. 1 which was completed during the current outage.

During the current outage (February - May 2000) at Indian Point Unit 2, various foreign objects were evaluated as remaining in the steam generators (SGs) for the next operating cycle. The evaluation included various objects remaining in the tubesheet region following a foreign object search and retrieval (FOSAR) effort, and foreign objects (potential loose parts) discovered subsequent to FOSAR when eddy current analysts discovered indications of wear on two tubes in SG 22. The evaluation addresses the potential safety impact of subsequent operation of the Indian Point Unit 2 SGs for one additional operating cycle (of up to 24 months) with these foreign objects and tubes with potential loose part indications remaining in steam generators 21, 22, 23, and 24. An additional operating cycle is justified.

5. Consolidated Edison supported the WOG response (OG-99-55, June 26, 1995) to GL 95-03 addressing the occurrence of circumferential cracks.

6. Consolidated Edison supports the Generic SG License Change Package to implement the requirements of the Industry Initiative on NEI 97-06 "Steam Generator Program Guidelines". This license amendment request provides a programmatic framework for monitoring and maintaining the integrity of steam generator tubes consistent with performance criteria that, if satisfied, will provide reasonable assurance that tube integrity is maintained consistent with the plant licensing basis.

7. Westinghouse determined that the steam generator full-power primary-to-secondary side pressure differential at Indian Point Unit 2 (IP2) may have exceeded the 44 Series steam generator (SG) design pressure differential of 1550 psi specified in the SG Design Specification (NSAL-00-007). Con Edison provided confirmation that the maximum Cycle 14 full-power SG primary-to-secondary pressure differential (occurring in SG 24) was approximately 1553 psi. Therefore, a 50.59 safety evaluation was completed (SECL-00- 059) addressing the steps taken to confirm the IP2 SGs compliance with the ASME Code requirements concerning the design pressure differential. Specifically, the 44 Series SG design basis (design specification, stress calculations and stress report) has been revised to ensure compliance with the ASME Code requirements regarding the primary-to-secondary pressure differential and stress limits. In order to support continued operation of the IP2 SGs, Westinghouse revised the applicable SG design specification (by creating Revision 3), stress calculations, and stress report to include a design primary-to-secondary side pressure differential of 1700 psi. Also, the secondary side pressure in the IP2 steam generators will be monitored and determined to be greater than 650 psi. The stress calculations demonstrate that the

affected IP2 steam generator components (tubes, tubesheet and Westinghouse-supplied tube plugs) satisfy the stress limits of the ASME Code.

5.0 Conclusions

5.1 Summary of Results

As noted above, several factors affect the corrosion performance of all Model 51 and 44 steam generators. These factors include, but are not limited to:

- Steam Generator Design Differences
  - Geometry
  - Materials
- Plant Operating Parameters (Temperature and Pressure)
- Steam Generator Secondary Side Water Chemistry
- Primary Water Chemistry (e.g., Li concentration)
- Presence of Copper in the Secondary System
- Contaminant Ingress Events

Based on a review of operating experience in the Model 44 and 51 steam generators, the degradation mechanisms ongoing in the Indian Point Unit 2 steam generator tubes are similar to those which are occurring elsewhere. The types of corrosion experienced are largely axially oriented PWSCC and ODSCC in the tubesheet region, and pitting. The occurrence of Row 2 U-bend cracking is limited in number. No indications in the Row 3 U-bends have been detected. There is no confirmed indication of PWSCC and ODSCC at the tube support plates as might be expected based on industry experience. One explanation for the lack of SCC at the TSP intersections may be the early addition of boric acid to the secondary side of the steam generators. The occurrence of free span degradation has also been limited (which is comparable to other steam generators of similar design).

In general, the condition of the Indian Point Unit 2 steam generators compares favorably with all Model 44 and 51 steam generators. The IP2 steam generators have been in service for 16.8 EFPY. Referring to Figure 4.1.1, the longest length of service for a Model 44 steam generator prior to replacement was 18.9 EFPY and the next longest was 18.8 EFPY. Both of these plants replaced steam generators as a result of the occurrence of SCC with a significantly greater number of tubes either plugged or repaired than are currently plugged due to SCC at Indian Point Unit 2.

The occurrence of SCC in the Indian Point Unit 2 steam generators is less than the Model 51 steam generators remaining in service which have operated for a similar time period. NOTE: Figures 4.1-1 and 4.1-2 do not take into account the implementation of an alternate repair criteria at a given plant (e.g., voltage-based

plugging criteria at TSPs) to permit SCC tubes to remain in service. Twelve plants with Model 51 steam generators have been replaced. For these plants, the longest length of service to replacement was 16.4 EFPY. A total of 11 plants remain in service with Model 51 steam generators. Only three plants have operated longer than Indian Point Unit 2 without replacing steam generators. Each of these plants has added boric acid to the secondary side of the steam generators.

5.2 Degradation Management Assessment/NEI 97-06, Rev. 1B Program Impact

The most important element in maintaining steam generator tube integrity during plant operation is the performance of the steam generator tube inservice inspection process and the associated reliability of the nondestructive examination (NDE) systems. Current recommendations relative to ISI effectiveness are based on conformance to EPRI Report NP-6201, Revision 5, "PWR Steam Generator Examination Guidelines". These guidelines provide reliable NDE strategies for the diversity of degradation types occurring in the field to minimize the likelihood of forced outages due to tube leaks during each operating cycle, to ensure that established regulatory requirements are met relative to the maintenance of steam generator tube integrity, and to minimize unnecessary plugging and sleeving. As a general rule, the bobbin probe and plus point/CECCO-5 probe have been qualified for use at IP2. The ISI strategies implemented during the current outage either met or exceeded current EPRI-Guidelines to detect the presence of tube degradation mechanisms (Reference 6). Based on the inspection results obtained during the current outage, it is judged that the condition of the steam generator tube bundles at IP2 remain comparable to the 11 plant sites with Model 51 steam generators remaining in service (See Figures 4.1-1 and 4.1-2).

Consolidated Edison will continue to monitor both Westinghouse and NRC generic communications on steam generator tube corrosion performance concerns and react accordingly. In December of 1998, the NRC staff acknowledged that the Program Described by NEI 97-06, "Steam Generator Program Guidelines" and its referenced EPRI Guidelines provides an acceptable starting point for use in the resolution of differences between the the staff's proposed Generic Letter and the draft Regulatory Guideline (DG-1074). Consolidated Edison has committed to implement the requirements of this industry initiative which provides a programmatic framework for monitoring and maintaining the integrity of steam generator tubes consistent with Appendices A and B to 10 CFR Part 50 and the IP2 Licensing Basis (Reference 7).

Historically, control of the secondary side environment has a significant impact on corrosion behavior in steam generation and power turbine equipment. This concept of control is of major importance when AVT is used, as the volatile amines present in the system have no buffering capacity against contaminant species in the range of temperatures with PWR steam generator operation. It

appears that the boric acid addition program at IP2 was effective in mitigating denting and the rate of cracking initiation and progression in the IP2 steam generators.

6.0 References

1. NUREG/CR-6365, "Steam Generator Tube Failures", April 1996

2. EPRI Report TE-106365-R14, Steam Generator Progress Report, Revision 14, April 1999.

3. EPRI Report TR-106365-R13, Steam Generator Progress Report", Rev. 13, October 1997

4. EPRI Report, Research Project S405-3, Steam Generator Progress Report, Revision 4, December 1988

5. SG-00-05-010, "Cycle 14 Condition Monitoring Assessment and Cycle 15 Operational Assessment for Degradation Mechanisms Other than U-bend PWSCC", May 30, 2000

6. "Analyst Performance and Data Quality Indian Point 2 2R14", May 22, 2000

7. E-Mail, NEI (Dave Modeen) to Administrative Points of Contact, "Status of the Steam Generator Generic License Change Package", 3/31/00

8. E-Mail, Maris, James. R. to Ira, Steve M., Esposito, John. N, and Whiteman G.W., "FW:Model 44/51 Comparison", 5/28/00